



Ingrid Stober
Kurt Bucher

Geothermal Energy

From Theoretical Models to Exploration
and Development

Second Edition

Geothermal Energy

Ingrid Stober · Kurt Bucher

Geothermal Energy

From Theoretical Models to Exploration
and Development

Second Edition



Springer

Ingrid Stober
Institute of Geo- and Environmental Sciences, University of Freiburg
Freiburg, Baden-Württemberg, Germany

Kurt Bucher
Institute of Geo- and Environmental Sciences, University of Freiburg
Freiburg, Baden-Württemberg, Germany

ISBN 978-3-030-71684-4 ISBN 978-3-030-71685-1 (eBook)
<https://doi.org/10.1007/978-3-030-71685-1>

1st edition: © Springer-Verlag Berlin Heidelberg 2013

2nd edition: © Springer Nature Switzerland AG 2021

This work is subject to copyright. All rights are reserved by the Publisher, whether the whole or part of the material is concerned, specifically the rights of translation, reprinting, reuse of illustrations, recitation, broadcasting, reproduction on microfilms or in any other physical way, and transmission or information storage and retrieval, electronic adaptation, computer software, or by similar or dissimilar methodology now known or hereafter developed.

The use of general descriptive names, registered names, trademarks, service marks, etc. in this publication does not imply, even in the absence of a specific statement, that such names are exempt from the relevant protective laws and regulations and therefore free for general use.

The publisher, the authors and the editors are safe to assume that the advice and information in this book are believed to be true and accurate at the date of publication. Neither the publisher nor the authors or the editors give a warranty, expressed or implied, with respect to the material contained herein or for any errors or omissions that may have been made. The publisher remains neutral with regard to jurisdictional claims in published maps and institutional affiliations.

Cover illustration: Steam clouds from two wells of the Krafla geothermal power plant (N-Iceland)

This Springer imprint is published by the registered company Springer Nature Switzerland AG
The registered company address is: Gewerbestrasse 11, 6330 Cham, Switzerland

Preface

Geothermal energy is an inexhaustible source of thermal and electrical energy on a human time scale. Its utilization is friendly to the environment and supplies base-load energy. The energy source does not depend on weather, and the energy is supplied 24 hours per day during 7 days a week. Utilization of geothermal energy increases the regional and local net product. It relieves dependence from fossil fuels and helps to conserve the valuable fossil chemical resources. Deep geothermal resources provide thermal and electrical (converted thermal) energy, thus providing reliable and sustainable energy for the future.

Electrical energy from geothermal resources provides an important contribution to the base-load electrical energy supply and replaces large-scale power plants fired with fossil fuels. A particularly prominent ranking regarding the production of electrical energy holds the global high-enthalpy regions associated with active volcanism in dynamic tectonic areas. However, geothermal energy can be utilized worldwide and produced at various depths with different specific technical systems. Geothermal systems may be used for covering the heat demand of single buildings or entire districts. Solitary systems can be combined with large groups of systems, e.g., geothermal probes can be arranged to larger probe fields making it possible to heat and cool larger building complexes depending on actual needs.

Utilization of deep geothermal resources extracts hot fluid from thermal reservoirs. These hot waters are re-injected to the reservoirs, thus maintaining the natural balance and permitting a sustainable and economical management of the resource. Heat and electricity from geothermal sources have the potential to cover a substantial share of the worldwide base-load energy demand also outside the high-enthalpy regions. Fossil-fuel-fired power plants may be used covering peak period requirements only.

The utilization of geothermal energy from shallow resources for the production of energy at low temperature for heating and cooling applications made tremendous progress in the past decades.

Geothermal energy from deep sources and reservoirs can contribute significant base-load energy. The necessary technology of Enhanced Geothermal Systems (EGS) can be installed nearly everywhere. However, EGS technology needs further improvements and research. Successful demonstration projects would help to popularize EGS further.

Long-term concepts of energy politics integrate geothermal energy sources because it supplies base-load energy. Intelligent combination of geothermal systems with other sources of renewable energy can create diverse sustainable synergy benefits. For residential homes, for example, combining ground-source heat pump systems with solar-thermal systems proved to be highly energy efficient. Geothermal power from a deep hydrothermal system can be combined with a biogas installation improving the energy efficiency. The deep fluid reservoir can be used as a rechargeable aquifer storage facility for extracting heat in the cold season and recharging it in the warm season. Such combined systems strike out in a new direction ranging from heat management for single houses to large-scale city planning.

This book aims to offer the reader a general overview over the many different aspects of utilization of geothermal energy. We are looking forward to the further rapid development of this fascinating source of energy in the years to come. We wish all of us a reliable, safe and environmentally friendly supply of thermal and electrical power. We hope to contribute to the sustainable use of energy with this book.

Freiburg, Germany

Ingrid Stober
Kurt Bucher

Contents

1	Thermal Structure of the Earth	1
1.1	Renewable Energies, Global Aspects	2
1.2	Internal Structure of the Earth	3
1.3	Energy Budget of the Planet	7
1.4	Heat Transport and Thermal Parameters	9
1.5	Brief Outline of Methods for Measuring Thermal Parameters	14
1.6	Measuring Subsurface Temperatures	15
	References	18
2	History of Geothermal Energy Use	21
2.1	Early Utilization of Geothermal Energy	22
2.2	History of Utilization of Geothermal Energy in the Last 150 Years	27
	References	31
3	Geothermal Energy Resources	33
3.1	Energy	34
3.2	Significance of “Renewable” Energy	36
3.3	Status of Geothermal Energy Utilization	37
3.4	Geothermal Energy Sources	40
	References	42
4	Uses of Geothermal Energy	43
4.1	Near Surface Geothermal Systems	45
4.2	Deep Geothermal Systems	55
4.3	Efficiency of Geothermal Systems	69
4.4	Major Geothermal Fields, High-Enthalpy Fields	72
4.5	Outlook and Challenges	77
	References	77
5	Potential and Perspectives of Geothermal Energy Utilization	81
	References	84

6 Geothermal Probes	85
6.1 Planning Principles	86
6.2 Construction of Ground Source Heat Exchangers	86
6.3 Dimensioning and Design of Geothermal Probes	94
6.3.1 Heat Pumps	94
6.3.2 Thermal Parameters and Computer Programs for the Design of Ground Source Heat Pump Systems	99
6.4 Drilling Methods for Borehole Heat Exchangers	106
6.4.1 Rotary Drilling	111
6.4.2 Down-The-Hole Hammer Method	113
6.4.3 Concluding Remarks, Technical Drilling Risks	114
6.5 Backfill and Grouting of Geothermal Probes	118
6.6 Construction of Deep Geothermal Probes	123
6.7 Operating Geothermal Probes: Potential Risks, Malfunctions and Damages	125
6.8 Special Systems and Further Developments	127
6.8.1 Geothermal Probe Fields	127
6.8.2 Cooling with Geothermal Probes	130
6.8.3 Combined Solar Thermal – Geothermal Systems	131
6.8.4 Geothermal Probe: Performance and Quality Control	134
6.8.5 Thermosyphon, Heat Pipe: Geothermal Probes Operating with Phase Changes	139
References	143
7 Geothermal Well Systems	145
7.1 Building Geothermal Well Systems	147
7.2 Chemical Aspects of Two-Well Systems	150
7.3 Thermal Range of Influence, Numerical Models	151
References	154
8 Hydrothermal Systems, Geothermal Doublets	155
8.1 Exploration of the Geologic and Tectonic Structure of the Underground	156
8.2 Thermal and Hydraulic Properties of the Target Aquifer	160
8.3 Hydraulic and Thermal Range of Hydrothermal Doublets, Numerical Models	170
8.4 Hydrochemistry of Hot Waters from Great Depth	174
8.5 Reservoir-Improving Measures, Efficiency-Boosting Measures, Stimulation	179
8.6 Productivity Risk, Exploration Risk, Economic Efficiency	181
8.7 Some Site Examples of Hydrothermal Systems	188
8.8 Project Planning of Hydrothermal Power Systems	196
8.9 Aquifer Thermal Energy Storage (ATES)	199
References	201

9 Enhanced-Geothermal-Systems (EGS), Hot-Dry-Rock Systems (HDR), Deep-Heat-Mining (DHM)	205
9.1 Techniques, Procedures, Strategies, Aims	207
9.2 Historical Development of the Hydraulic Fracturing Technology, Early HDR Sites	209
9.3 Stimulation Procedures	211
9.4 Experience and Coping with Seismicity	217
9.5 Recommendations, Notes	218
References	223
10 Geothermal Systems in High-Enthalpy Regions	227
10.1 Geological Features of High-Enthalpy Regions	228
10.2 Development, Installation and Initial Commissioning of Power Plants	234
10.3 Main Types of Power Plants in High-Enthalpy Fields	238
10.3.1 Dry Steam Power Plant	238
10.3.2 Flash Steam Power Plants	240
10.4 Evolving Deficiencies, Potential Countermeasures	244
10.5 Use of Fluids from Reservoirs at Supercritical Conditions	250
References	254
11 Environmental Issues Related to Deep Geothermal Systems	257
11.1 Seismicity Related to EGS projects	259
11.1.1 Induced Earthquakes	261
11.1.2 Quantifying Seismic Events	264
11.1.3 The Basel Incident	265
11.1.4 The St. Gallen Incident (E Switzerland)	268
11.1.5 Observed Seismicity at Other EGS Projects	270
11.1.6 Conclusions and Recommendations Regarding Seismicity Control in Hydrothermal and Petrothermal (EGS) Projects	274
11.2 Interaction Between Geothermal System Operation and the Underground	278
11.3 Environmental Issues Related to Surface Installations and Operation	281
References	282
12 Drilling Techniques for Deep Wellbores	287
References	309
13 Geophysical Methods, Exploration and Analysis	311
13.1 Geophysical Pre-drilling Exploration, Seismic Investigations	312
13.2 Geophysical Well Logging and Data Interpretation	319
References	324

14	Testing the Hydraulic Properties of the Drilled Formations	327
14.1	Principles of Hydraulic Well Testing	328
14.2	Types of Tests, Planning and Implementation, Evaluation Procedures	338
14.3	Tracer Experiments	343
14.4	Temperature Evaluation Methods	347
	References	349
15	The Chemical Composition of Deep Geothermal Waters and Its Consequences for Planning and Operating	
a	Geothermal Power Plant	353
15.1	Sampling and Laboratory Analyses	355
15.2	Chemical Parameters Characterizing Deep Fluids	357
15.3	Graphical Representation of Deep Fluid Composition	362
15.4	Estimating Reservoir Temperature from the Composition of Deep Fluids	365
15.4.1	The Quartz Thermometer	366
15.4.2	The K-Na Exchange Thermometer	369
15.4.3	The Mg-K Thermometer	371
15.4.4	Other Cation Thermometers	373
15.4.5	The Ternary Giggenbach Diagram	374
15.4.6	Multiple Equilibria Models for Equilibrium Temperature	375
15.5	Origin of Fluids	376
15.6	Saturation States, Saturation Index	378
15.7	Mineral Scales and Materials Corrosion	379
	References	386

Chapter 1

Thermal Structure of the Earth



Island of Vulcano, southern Italy

1.1 Renewable Energies, Global Aspects

The term “renewable energy” is used for a source of energy from a reservoir that can be restored on a “short time scale” (in human time scales). Renewable energy includes geothermal energy and several forms of solar energy such as bio-energy (bio-fuel), hydroelectric, wind-energy, photovoltaic and solar-thermal energy. These sources of energy are converted to heat or electricity for utilization. An example: The “renewable” aspect of burning firewood in a cooking stove lies in the relatively short period of time required to re-grow chopped down forests with solar energy and the process of photosynthesis. In contrast, it will take much more time to “renew” coal beds when burning coal for the same purpose, although geological processes will eventually form new coal beds. The “renewable” aspect of geothermal energy will be explained and discussed in detail in this chapter.

The International Geothermal Association (IGA) wrote in the Status Report Ren21 (2017) on “Renewable Energy Policy Network for the 21st Century” that the global production of renewable energy increased by 168 GW_{el} (+9.1%) from 2015 to 2016. The total worldwide production of electricity from renewable resources in 2019 was 7028 TWh (1 Wh = 3600 J), corresponding to 26% of the global power production capacity. China registered the highest growth rate in the production of electricity from renewable resources (BP, Statistical Review of World Energy 2020). The growth in renewable energy consumption is larger than the increase in fossil fuel consumption in Europe and the US. Political and financial programs support the development and use of energy production from renewable resources in more than 60 countries.

Hydroelectric systems had the largest share in installed capacity for electricity power production from renewable energy sources in 2016 with 1098 GW_{el} followed by wind energy with 487 GW_{el}, photovoltaic systems (303 GW_{el}) and biomass conversion with 112 GW_{el}. Geothermal systems (13.5 GW_{el}) follow with a large gap, however, also increased by 35% from 2008. Thermal energy production from renewable sources is dominated by biomass (90%), followed by solar thermal systems (2%) and geothermal systems (2%) (Ren21 2017; U.S. Department of Energy 2016).

Geothermal energy has the potential to become a significant source of energy in the future because it is available everywhere and withdrawals are continuously replenished. From a human perspective the resource is essentially unlimited. Heat and electricity can be continuously produced and therefore it is a base load resource. The utilization is friendly to the environment and the land consumption for the surface installations is small. The coming years will show how the optimistic expectations and the positive perception of geothermal energy utilization will succeed in regions with low-enthalpy geothermal resources.

1.2 Internal Structure of the Earth

Geothermal energy is the thermal energy stored in the Earth body, geothermal energy is underground heat. 99% of the Earth is hotter than 1000 °C and only 0.1% is colder than 100 °C. The average temperature at the Earth surface is 14 °C. The surface temperature of the sun is about 5800 °C, which corresponds to the temperature at the center of the Earth (Fig. 1.1).

The Earth has a layered internal structure (Fig. 1.1) with a solid core of high-density material, an iron-nickel alloy surrounded by an outer core of the same material in a low-viscosity state. A thick internally layered, viscous magnesium silicate mantle encloses the core. The surface zone of the planet is build up of a thin rigid crust, whose composition is different on continents and oceans. This layered structure developed from a more homogeneous system by gravitational compaction and differentiation during the earliest history of the planet.

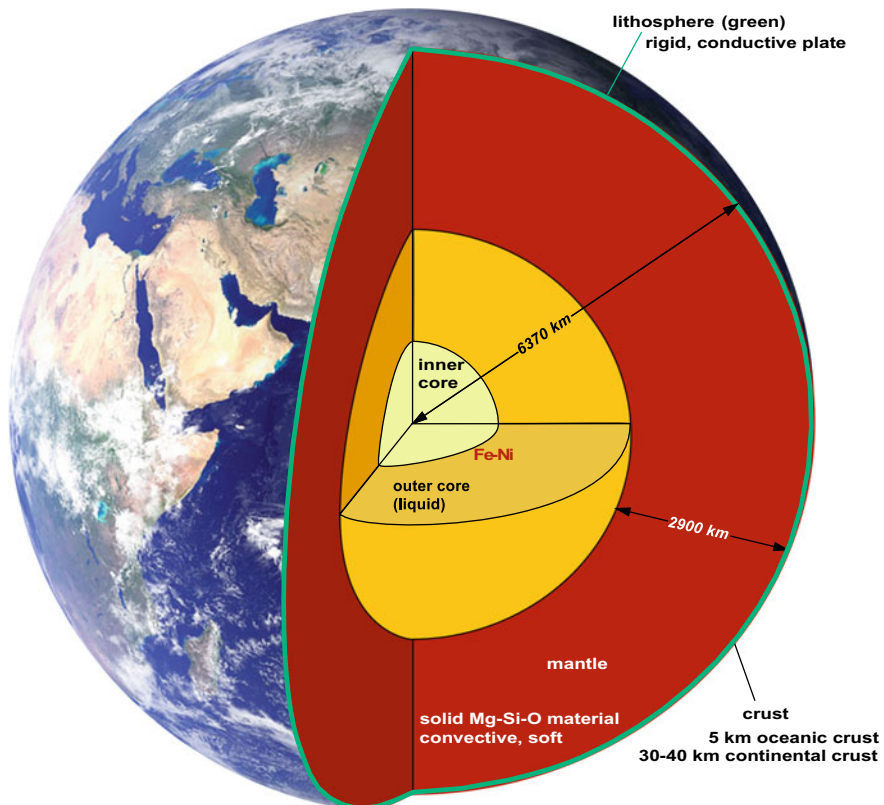


Fig. 1.1 Internal structure of the Earth

The total thickness of the core (Fig. 1.1) exceeds the thickness of the mantle. However, the core represents only about 16% of the volume of the Earth and, because of its high density about 32% of the mass of the planet.

At 6000 km depth the inner core temperatures are above 5000 °C and the pressure is about 400 GPa. Iron meteorites that arrive at the Earth surface occasionally from space consist of material similar to the Ni–Fe alloy of the core (Fig. 1.2). The molten Fe–Ni metal outer core (about 2900 °C) is together with the rotational movement of the planet responsible for the Earth's magnetic field. The core–mantle boundary is a zone of dramatic changes in composition and density where molten metal from the outer core and solid mantle silicate minerals mix. Beneath the lithosphere, the upper mantle reaches to a depth of about 1000 km. The boundary layer between lithospheric and convective mantle at 100–150 km depth is rheologically soft and melt may be present locally facilitating movement of the lithospheric plates. The solid but soft mantle is in a very slow convective motion driven by the heat of the core and transmitted through the core–mantle boundary (hot plate). A part of the heat given off to the mantle arises from the enthalpy of crystallization at the boundary between inner solid and outer liquid core in an overall environment setting of a cooling planet. The motor for mantle convection operates since the formation of the Earth.

The lithosphere is the rigid lid of the planet that is subdivided into a series of mobile plates that move individually as a result of pull and drag forces exerted by the convecting mantle (Fig. 1.3). The lithospheric mantle is separated from the crust by the petrographic MOHO and consists of the same rock types as the mantle as a



Fig. 1.2 Widmanstätten pattern made visible on an iron meteorite. The texture results from the intergrowth of the two minerals kamacite and taenite with different Fe/Ni ratios. Picture about 5 cm across

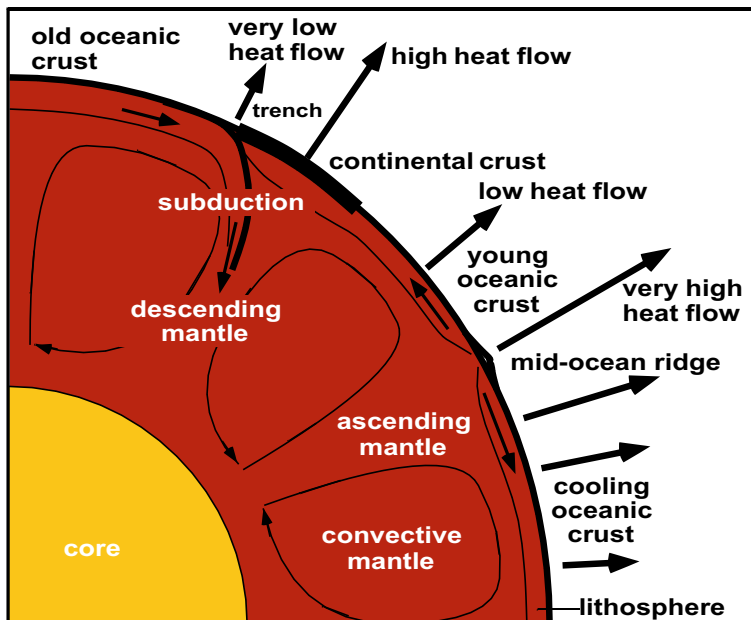


Fig. 1.3 Convection currents in the viscous mantle drive plate tectonics (movement of rigid lithospheric plates, the outermost shell of the planet) and controls large-scale heat flow (black arrows)

whole. The convecting mantle creates distinct thermal regimes at the Earth surface resulting from upwelling and subsiding hot mantle material and from the mechanical and thermal response of the lithosphere.

Convergent plate motions may create mountain belts such as the Alps and the Himalayas. The dense oceanic lithosphere of two convergent plates may be subducted and recycled into the mantle. Melting and release of H₂O from the subducting slab can generate massive amounts of melts in the overriding plate and the transfer of heat to shallow levels of the crust. Examples are the volcanic chain of the Cascades, parts of the Andes, Aleutian Islands, Japan, Philippines, Indonesia, North Island of New Zealand and many other volcanic areas of the world. Extending lithosphere creates rift and graben structures typically with a pronounced thermal response at the surface. Examples of this setting include the East African rift valley and the Basin and Range Province in the western USA.

Extensional oceanic plate margins are mid-ocean ridges and the sites of the most prominent volcanic activity on the planet. The Mid-Atlantic Ridge and the East Pacific Rise are examples of these settings (Fig. 1.4). Particularly spectacular large scale geologic structures are tied to focused upwelling systems of hot mantle, so called mantle diapirs or “hot spots”. A hot spot under oceanic lithosphere is causing intraplate volcanism on the Hawaii islands, a hot spot under continental lithosphere is causing extremely dangerous rhyolite volcanism in the Yellowstone area (USA) with all associated forms of hydrothermal activity such as geysers (Fig. 1.5), mud volca-



Fig. 1.4 Basaltic lava eruption from the Earth mantle at the mid-Atlantic ridge on Iceland (Krafla eruption 1984). Lava production follows an extensional fissure



Fig. 1.5 Different stages of an eruption of Echinus Geyser in the Norris Geyser Basin, Yellowstone National park, Wyoming, USA

noes, gas vents and others. The massive Yellowstone eruptions, that have devastated the whole Earth, have a periodicity of about 600 Ka. The last one occurred about 0.6 Ma ago. The crown of the hot spots is located underneath Iceland where it coincides with the extension of the mid Atlantic ridge causing an abnormally high volcanic activity and a massive heat transfer to very shallow levels of the crust. The ash cloud of the eruption of Eyjafjallajökull stopped all air traffic in Europe in 2010. The Italian volcanoes are classic examples of volcanism and associated hydrothermal and degassing phenomena (Fig. 1.6).

1.3 Energy Budget of the Planet

The average temperature at the Earth surface is 14 °C, at the core–mantle boundary the temperature is in the range of 3000 °C. This temperature difference between the surface and the interior is the driving force for heat flow, which tries to eliminate ΔT . The process is known as so-called Fourier conduction. Heat is continuously transported from the hot interior to the surface. The terrestrial heat flow is the amount of energy (J) transferred through a unit surface area of 1 m² per unit time (s) and is referred to as heat flow density (q). In its general form, the Fourier equation is:

$$q = -\lambda \nabla T \quad (\text{Js}^{-1}\text{m}^{-2}) \quad (1.1a)$$

where λ is a material constant explained below. The general form can be rewritten for the case of one-dimensional flow and along a constant temperature gradient as:

$$q = -\lambda \Delta T / \Delta z \quad (\text{Js}^{-1}\text{m}^{-2}) \quad (1.1b)$$

where $\Delta T / \Delta z$ is a constant temperature gradient in vertical (z) direction.

The average global surface heat flow density is about $65 \cdot 10^{-3}$ W m⁻² (65 mW m^{-2}). The planet loses heat because of this heat transfer from the interior to the surface. On the other hand, the planet gains some energy by capturing solar radiation. Electromagnetic solar radiation is created in the sun by nuclear fusion reactions that are ultimately converted to other forms of energy on the planet Earth such as coal, oil, gas, wind, hydroelectric, biomass (crop, wood), photovoltaic and solar thermal. The average global solar energy received by the Earth is 170 W m^{-2} , 2600 times the amount lost by heat flow from the interior. This corresponds to 5.4 GJ per year per 1 m² surface area, which is approximately the energy that can be extracted from one barrel of oil, 200 kg of coal, or 140 m³ of natural gas (source: World Energy Council). The total integrated heat flow of the planet corresponds to the impressive thermal power of 40 terra Watt ($4 \cdot 10^{13}$ W).

The measured surface heat flow density has several contributions. Only a small part of it is related to the Fourier heat flow from core and mantle as described above (about 30%). 70% is caused by heat generated by the decay of radioactive elements in the crust, mostly in the continental “granitic” crust. Specifically uranium (²³⁸U,

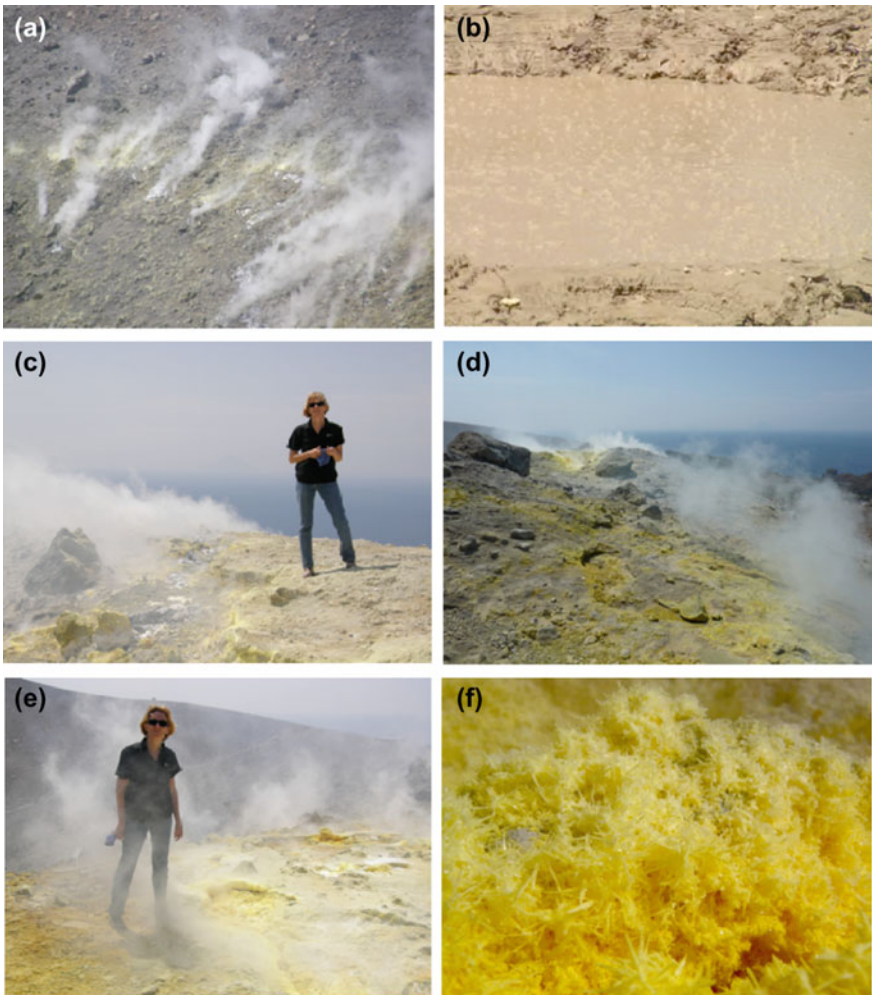


Fig. 1.6 Volcanic phenomena on the island of Vulcano (Italy): **a** Volcanic steam degassing from crater flank, **b** volcanic gasses bubble from hot water pond, **c** Steam degassing on the crater ridge, **d** Sulfur crusts on the crater ridge, **e** One of the authors submerged in poisonous volcanic gasses (photograph taken by the other author), **f** Sulfur crystals deposited from the oxidation of primary H_2S gas with atmospheric oxygen ($2\text{H}_2\text{S} + \text{O}_2 = \text{S}_2 + 2\text{H}_2\text{O}$)

^{235}U), thorium (^{232}Th) and potassium (^{40}K) in the continental crust produce $\sim 900 \text{ EJ a}^{-1}$ ($9 \times 10^{20} \text{ J a}^{-1}$). Together with the contribution of the interior of $\sim 3 \times 10^{20} \text{ J a}^{-1}$, the planet loses $1.2 \times 10^{21} \text{ J a}^{-1}$ (1.2 ZJ a^{-1}) thermal energy to the space. Most of it is restored in the crust continuously.

Heat production in the crust is thermal energy produced per time and volume ($\text{J s}^{-1} \text{ m}^{-3}$). The crust is composed very differently and its thickness differs considerably. Continental crust is typically thick, granitic and rich in radioactive elements, oceanic

crust is thin, basaltic and poor in radioactive elements (Mareschal & Jaupart 2013). Therefore heat production of crustal rocks differs over a wide range (Table 1.2). The total global radioactive heat production is estimated to be on the order of 27.5 TW (Ahrens 1995).

Surface heat flow q (W m^{-2}) composed of the heat flow from the interior and the heat production in the crust varies within a surprisingly narrow range of 40–120 mW m^{-2} . This is a factor of 3 only. The global average of 65 mW m^{-2} corresponds to an average temperature increase in the upper part of the Earth crust of about 3 °C per 100 m depth increase. Departures from this average value are designated to heat flow anomalies or thermal anomalies. The variation is caused by the different large-scale geological settings as outlined above and by the diverse composition of the crust. Negative anomalies, colder than average, are related to old continental shields, deep sedimentary basins and oceanic crust away from the spreading ridges. Positive anomalies, that are hotter than the normal geotherm, are the prime targets and the major interest of geothermal exploration. Extreme heat flow anomalies are related to volcanic fields and to mid ocean ridges. In low-enthalpy areas heat flow anomalies are often related to upwelling fluids (upwelling groundwater). The advection fluid flow also transports thermal energy to near surface environments.

Average heat flow density is 65 mW m^{-2} at the surface of continents (see above) and 101 mW m^{-2} from oceanic crust. The global average of 87 mW m^{-2} corresponds to a global heat loss of 44.2×10^{12} W (Pollack et al. 1993). A net heat loss of 1.4×10^{12} W (Clauser 2009) of the planet results from the difference between the heat lost to space and the heat production due to radioactive decay and other internal sources. The cooling process of the planet is very slow however. During the last 3 Ga (from a total of 4.6 Ga) the average mantle cooled 300–350 °C. The heat loss by thermal radiation from the interior is minimal (by a factor of 4000) compared with the thermal energy gained by solar radiation.

The total amount of heat (thermal energy) stored by the planet is about 12.6×10^{24} MJ (Armstead 1983). Therefore, the geothermal energy resources of the planet are truly enormous and omnipresent. Geothermal energy is everywhere available and can be extracted at any spot of the planet. Geothermal energy is friendly to the environment and it is available 24 h a day 365 days per year anywhere on the planet. Today it is used insufficiently but geothermal energy has a hot future.

1.4 Heat Transport and Thermal Parameters

A prerequisite for the design of geothermal installations is availability of data and information on the physical properties of rocks. Rock properties are required at sites of shallow geothermal installations and deep geothermal systems for heat and electricity production alike. Particularly needed are rock properties that relate to transport and storage of heat and fluids in the subsurface. Thermal properties include thermal conductivity, heat capacity and heat production; hydraulic properties embrace for

example porosity and permeability. Important properties of deep fluids are their density, viscosity and compressibility.

Geothermal heat can be transported by two basic mechanisms: (1) by heat conduction through the rocks and (2) by a moving fluid (groundwater, gasses), a mechanism referred to as advection. Conductive heat flow can be described by the empirical transport equation: $q = -\lambda \Delta T$ (Fourier law). It expresses that the heat flux (Watt per unit area of cross section) is caused by a temperature gradient ΔT between different parts of a geologic system and that it is proportional to a material property λ called thermal conductivity [$J s^{-1} m^{-1} K^{-1}$]. Thermal conductivity λ depicts the ability of rocks to transport heat. It varies considerably between different types of rock (Table 1.1). Rocks of the crystalline basement such as granites and gneisses conduct heat 2–3 times better than unconsolidated material (gravel, sand). Measured thermal conductivities for the same rock type may vary over wide ranges (Table 1.1) because of variations in the modal composition of rocks, different degrees of compaction, cementation or alteration, but also because of anisotropy caused by layering and other structures of the rocks. The thermal conductivity of stratified, layered or foliated rocks depends on its direction. It is generally anisotropic. In schists, for instance λ vertical to the schistosity can be only a third or less than λ parallel to the schistosity. Thick schist formations hamper vertical heat flux from the interior to the surface and thus have an insulating effect. The positive thermal anomaly at Bad Urach (SW

Table 1.1 Thermal conductivity and heat capacity of various materials

Rocks/fluids	Thermal conductivity λ ($J s^{-1} m^{-1} K^{-1}$)	Specific heat capacity ($kJ kg^{-1} K^{-1}$)
Gravel, sand dry	0.3–0.8	0.50–0.59
Gravel, sand wet	1.7–5.0	0.85–1.90
Clay, loam moist	0.9–2.3	0.80–2.30
Limestone	2.5–4.0	0.80–1.00
Dolomite	1.6–5.5	0.92–1.06
Marble	1.6–4.0	0.86–0.92
Sandstone	1.3–5.1	0.82–1.00
Shale	0.6–4.0	0.82–1.18
Granite	2.1–4.1	0.75–1.22
Gneiss	1.9–4.0	0.75–0.90
Basalt	1.3–2.3	0.72–1.00
Quartzite	3.6–6.6	0.78–0.92
Rocksalt	5.4	0.84
Air	0.02	1.0054
Water	0.59	4.12

Data for 25 °C 1 bar. Source VDI4640 2001, Schön 2004, Kappelmeyer & Haenel 1974, Landolt-Börnstein 1992

Table 1.2 Typical radiogenic heat production of selected rocks

Rock type	Heat Production ($\mu\text{J s}^{-1} \text{m}^{-3}$)
Granite	3.0 (< 1–7)
Gabbro	0.46
Granodiorite	1.5 (0.8–2.1)
Diorite	1.1
Gneiss	4.0 (< 1–7)
Amphibolite	0.5 (0.1–1.5)
Serpentinite	0.01
Sandstone	1.5 (0.2–2.3)
Shale	1.8

Source Kappelmeyer & Haenel 1974; Rybach 1976

Germany), for example, has been associated with the presence of thick shale series in the section (Schädel & Stober 1984).

All rocks contain a certain amount of voids in the form of pores and fractures. It is crucial for the heat transport properties of the rocks if the voids are filled with a liquid fluid (water) or gas (air). Air is an isolator with a very low λ value (Table 1.1). This is why in shallow geothermal systems the position and variation of the water table has a profound effect on the thermal conductance of unconsolidated rocks.

Thermal conductivity λ of air is 100 times smaller and the one of water is 2–5 smaller than that of rocks (Table 1.1). As a result the thermal conductivity of dry, air filled gravel and sand is about $0.4 \text{ J s}^{-1} \text{ m}^{-1} \text{ K}^{-1}$, however, for wet, water saturated gravel the thermal conductivity may be $2.1 \text{ s}^{-1} \text{ m}^{-1} \text{ K}^{-1}$ or higher. Knowing the water table and its temporal variation is critically important for determining the heat extraction capacity of a geothermal probe (subsection 6.3.2). This is extremely so in strongly karstified rocks.

The thermal conductivity (k) controls the supply of thermal energy for a given temperature gradient. The heat capacity (C) is a rock parameter that portrays the amount of heat that can be stored in the subsurface. It is the amount of heat ΔQ (thermal energy J) that is taken up or given off by a rock upon a temperature change ΔT of one Kelvin:

$$C = \Delta Q / \Delta T \quad (\text{JK}^{-1}) \quad (1.2a)$$

The specific heat capacity (c) also simply specific heat of rocks (material) is the heat capacity per unit mass. It characterizes the amount of heat ΔQ that is taken up per mass (m) of rock per temperature increase ΔT :

$$c = \Delta Q / (m \Delta T) \quad (\text{Jkg}^{-1} \text{K}^{-1}) \quad (1.2b)$$

If C is normalized to a constant volume (V) rather than mass, it is designated volumetric heat capacity also volume-specific heat capacity (s):

$$s = \Delta Q / (V \Delta T) \quad (\text{J m}^{-3} \text{K}^{-1}) \quad (1.2c)$$

The two parameters are connected by the equation ($c = s/\rho$), where ρ is the density (kg m^{-3}). Heat capacity and thermal conductivity depend on pressure and temperature. Both parameters decrease with increasing depth in the crust. As a consequence, for a specific material the temperature rises as depth decreases.

Table 1.1 lists specific heat capacities of common rocks. For solid rocks c typically varies between 0.75 and $1.00 \text{ kJ kg}^{-1} \text{ K}^{-1}$. The heat capacity of water $c = 4.19 \text{ kJ kg}^{-1} \text{ K}^{-1}$ is 4–6 times higher than c of solid rocks. Water stores many times more heat than rocks. Referred to the volumetric heat capacity water stores about twice the amount of heat than rocks. Consequently, highly porous aquifers of unconsolidated rock store more thermal energy than low-porosity aquifers with poor hydraulic conductivity consisting of dense rocks.

Heat flow density (q) and thermal conductivity (λ) reflect the temperature distribution at depth. The temperature gradient is the temperature increase per depth increment (grad T or ΔT) at a specified depth. Equation 1.3 shows that T at a specific given depth (for constant one dimensional gradients) is given by the heat flow density and the thermal conductivity:

$$\Delta T / \Delta z = q / \lambda \quad (\text{K m}^{-1}) \quad (1.3)$$

For example: With the average continental surface $q = 0.065 \text{ (W m}^{-2}\text{)}$, $\lambda = 2.2 \text{ (J s}^{-1} \text{ m}^{-1} \text{ K}^{-1}\text{)}$ for typical granite and gneiss (Table 1.1) a constant $\Delta T / \Delta z = 0.03 \text{ (K m}^{-1}\text{)}$ or $3 \text{ }^{\circ}\text{C}$ per 100 m depth increase follows from Eq. 1.3. The temperature increases in the upper kilometers of the central European continental crust with $2.8\text{--}3.0 \text{ }^{\circ}\text{C}$ per 100 m of Δz , consistent with the typical mean λ -values of crustal hard rock material (Table 1.1) and the typical measured surface heat flow density of 65 mW m^{-2} . Vice versa, Eq. 1.1b or 1.3 can be used to roughly calculate q for given T -gradients and rock material.

Temperature gradients, heat flow density and hence the temperature distribution in the subsurface is not uniform. If the deviation from average values is significant the features are termed positive or negative temperature (thermal) anomaly. There are numerous geologic causes of positive thermal anomalies including active volcanism (as described above) and upwelling hot deep waters in hydrothermal systems. Upwelling thermal waters are typically related to deep permeable fault structures often in connection with graben or basin structures or boundary fault systems of mountain chains. Hydrothermal waters commonly reach the surface and discharge as hot springs. Positive anomalies can also be caused by the presence of large volumes of rock with a high thermal conductivity such as rock salt deposits. Salt diapirs preferentially conduct more heat to the surface than other surrounding sedimentary rocks. So that high heat flow is channelized in the salt diapirs. Thick insulating strata in sedimentary sequences such as shales with low thermal conductivity (often strongly anisotropic as discussed above) may retard heat transfer to the surface. Unusually high local geochemical or biogeochemical heat production can also be a reason of heat anomalies. Positive anomalies are prime target areas

for geothermal projects because their exploration and development require smaller drilling depth (Chap. 5).

All rocks contain a certain measurable amount of radioactive elements. The energy liberated by the decay of unstable nuclei is given off as ionizing radiation and then absorbed and transformed to heat. In common rocks the heat production of the decay chains of the nuclei ^{238}U , ^{235}U and ^{232}Th and the isotope ^{40}K in potassium are the only significant contributions. Uranium and thorium occur in accessory minerals, mainly zircon and monazite, in common rocks such as granite and gneiss. Potassium is a major element in common rock forming minerals including K-feldspar and mica.

Total radioactive heat production of a rock can be estimated from the concentrations of uranium c_{U} (ppm), thorium c_{Th} (ppm) and potassium c_{K} (wt.%) (Landolt-Börnstein 1992):

$$A = 10^{-5} \rho (9.52 c_{\text{U}} + 2.56 c_{\text{Th}} + 3.48 c_{\text{K}}) \quad (\mu\text{Js}^{-1}\text{m}^{-3}) \quad (1.4)$$

where ρ is the density of the rock (kg m^{-3}). Some typical values for radiogenic heat production of selected representative rocks are listed in Table 1.2.

Because radiogenic heat production is related to the amount of K-bearing minerals and zircon in a rock, granite and other felsic rocks, they produce more heat than gabbros and mafic rocks (Sect. 1.3). Mantle peridotite and its hydration product serpentinite produce less than $0.01 \mu\text{W m}^{-3}$ (Table 1.2). A part of the radioactive elements can be mobilized by water–rock interaction and dissolve in hydrothermal fluids. Some thermal waters contain a considerable amount of radioactive components and are thus radioactive (Sect. 10.2).

The heat transport equation describes the variation of temperature in a rock in space and time (Carslaw & Jaeger 1959). Solutions to the equation depict the distribution of heat in the subsurface and its variation with time. The partial differential heat equation can be written as:

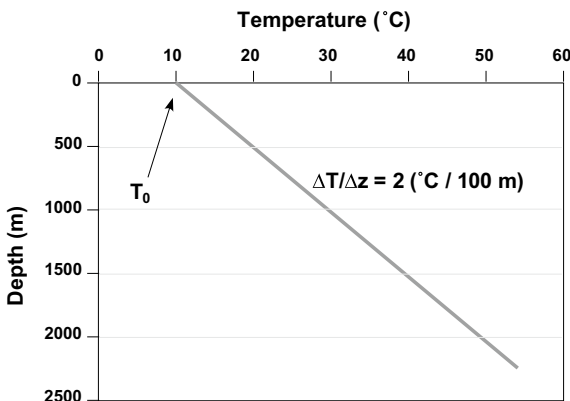
$$\partial(\rho c T)/\partial t = \nabla(\lambda \nabla T) + A - v \nabla T + \alpha g T/c \quad (1.5)$$

where the first term on the right hand side of the equation describes the heat conduction (see also Eq. 1.1a), A stands for the depth and material dependent internal heat production ($\text{J s}^{-1} \text{m}^{-3}$), the third term describes advective heat transfer (generally mass transfer) and the last term expresses the pressure effect with the density ρ (kg m^{-3}), v velocity (m s^{-1}), g acceleration due to gravity (m s^{-2}) and α (K^{-1}) the volumetric linear coefficient of thermal expansion defined by $\alpha = (1/V) \partial V/\partial T$. For most rocks $\alpha = 5\text{--}25 \mu\text{K}^{-1}$.

The analytical solution of Eq. 1.5 for one dimensional heat transport (along depth coordinate z), constant thermal conductivity (λ), constant radiogenic heat production (A), for a homogeneous isotropic volume of rock, no heat transport by mass flux and ignoring the pressure dependence is:

$$T(z) = T_0 + 1/\lambda q_0 \Delta z - A/(2\lambda) \Delta z^2 \quad (1.6)$$

Fig. 1.7 Computed temperature versus depth profile using Eq. 1.6 and the values for the parameters given in the text and on Table 1.1: $T_0 = 283$, $\lambda = 3.1 \text{ J s}^{-1} \text{ m}^{-1} \text{ K}^{-1}$ for granite, $q_0 = 65 \text{ mW m}^{-2}$, $A = 3 \mu\text{J s}^{-1} \text{ m}^{-3}$ for granite



where T_0 is the temperature at z_0 the top of the considered volume of rock, q_0 the heat flow density at z_0 and Δz the thickness of the considered rock volume. This simplified heat equation (Eq. 1.6) can be used to construct a thermal profile through the crust by adding layer by layer for the case of conductive heat transport and radiogenic heat production in the individual layers (Fig. 1.7).

1.5 Brief Outline of Methods for Measuring Thermal Parameters

Thermal conductivity of rocks can be measured on drillcores in the laboratory or in situ in boreholes directly. There are different methods and types of devices for measuring the thermal conductivity of rocks and soils on the market. All are based on the same principle: the sample is exposed to defined and controlled local heating and temperature sensors measure the temperature response to heating in space and time. The transient line source method is widely used in needle-type measuring instruments. A long and thin heating source is brought in contact with the sample and is heated with constant power, while simultaneously the temperature of the source is registered. The slower the source temperature rises, the higher is the thermal conductivity of the sample material.

Probably the most commonly used method for thermal conductivity measurements in geology is the use of so-called divided bar instruments. The instruments are commercially available also as portable electronic divided bar machines. Portable divided bars apply thermal gradient across a sample along with a substance of known thermal conductivity used as standard. Thermal conductivity of the sample is measured by the device relative to the standard.

Thermal conductivity measuring bars have differential temperature adjustment provisions and provide accurate results with a variance of only 2%. Portable divided bars can be easily calibrated and weigh only 8 kg facilitating easy transport. Divided

bar systems also generate less noise and can be used to measure thermal conductivity of fresh core samples even during remote drilling operations. Additionally, these rock thermal conductivity-measuring bars can provide readings for varying temperatures over a range of 20 °C. Portable thermal conduction measuring devices are very useful in geothermal energy explorations (web page: Hot Dry Rock, Australia).

The heat capacity of rocks is measured with a calorimeter in the laboratory. There are a large variety of calorimeters and the various instruments are used for very different purposes. The parameter C defined in Eq. 1.2a is measured with instruments that add or remove a defined amount of heat to the calorimetric system (sample plus embedding material, usually a liquid) and monitor the temperature response of the process.

The density of rocks in the form of drillcores is measured using Archimedes's principle. This means the mass of an irregularly shaped body like a piece of rock, is first measured by a balance. Then the mass of the body is submerged in a liquid of known density (e.g. water 1000 kg m⁻³ at about 25 °C and 1 bar) and measured by the balance. The volume of the sample follows from the difference of the two measurements, thus the density $\rho = m/V$ can be calculated from the data. The density of cuttings is measured with a pycnometer, a simple laboratory device for measuring densities of liquids and solids.

1.6 Measuring Subsurface Temperatures

A careful search for existing subsurface temperature data is one of the first and critical steps during the development of a new deep geothermal project. Compiled temperature data from existing old drillholes in the same region greatly facilitate the design of the new installation and dramatically increase the reliability of pre-drilling project forecasts. It is necessary to evaluate the reliability of the data and the exact reading depths.

In Central Europe, for example, the temperature increases with about 3 °C per 100 m depth in the near surface region. This is referred to as the "normal temperature gradient" for the region. This normal regional gradient may deviate in both directions, colder and warmer gradients. Departures from the normal regional gradient may occur in certain depth intervals of a borehole. The deviations from the normal gradient are caused by various local variations of the hydraulic and thermal properties of the geological material underground. The local temperature gradient is constant within a narrow range of near-surface depths. At greater depth the temperature gradient is given by the tangent to the temperature (T) versus depth (z) profile (T-z profile) at each depth (z). The detailed local temperature profile and the associated T-gradient at a site with a given geological structure results from conductive heat flow and from mass flow, which is flow of groundwater or flow of deep fluids. The T-gradient also varies with surface topography. With increasing relief, the T-gradient increases in the valleys and decreases along the ridges.

The SI unit for temperature is Kelvin (K). Derived from Kelvin is the unit Celsius ($^{\circ}\text{C}$). Other commonly used units are Fahrenheit ($^{\circ}\text{F}$) and Rankine ($^{\circ}\text{R}$, also R or Ra). At absolute zero temperature: $0\text{ K} = 0\text{ }^{\circ}\text{R}$. The temperatures can be converted using:

$$\text{T}_\text{K} = \text{T}_\text{C} + 273.16 \quad (1.7\text{a})$$

$$\text{T}_\text{F} = 1.8\text{ }\text{T}_\text{C} + 32 \quad (1.7\text{b})$$

$$\text{T}_\text{R} = 1.8\text{ }\text{T}_\text{C} + 491.67 \quad (1.7\text{c})$$

In deep boreholes the temperature of the liquid phase at the depth z is measured using a temperature sensitive device and the reading is in Ohm (Ω). The resistance is converted to temperature using a $\Omega - \text{K}$ calibration. The probes need a new calibration after some months in use.

Different types of temperature measurements are distinguished in boreholes:

- Temperature log
- Reservoir temperature or bottom-hole temperature (BHT)
- Temperature measurements during production tests (well tests).

Temperature logs are T data from continuous T measurements along the borehole profile. It is important to pay attention to the time of logging: During production, shortly after production or after a long downtime. The most useful data are produced after long downtime (Fig. 1.8). T-logs influenced by the production operation often provide meaningful T data only at the sites (depth) of water inflow points. T-logs can provide evidence of water inflow and outflow points (fluid sinks) (Fig. 6.19), leaks in the casing or vertical fluid flow (Fig. 13.5). Temperature data collected during production tests provide access to the vertical distribution of the hydraulic conductivity. (Fig. 14.10). Detailed treatment of hydraulic evaluation procedures can be found in Sects. 14.2 and 14.4.

BHT measurements are performed routinely immediately after completion of the industrial drill hole. Thus the data are commonly thermally disrupted by e.g. friction and circulation of drilling fluid. These BHT data can be corrected for these effects and reduced to the pristine situation, particularly because the influences of drilling fluid circulation on the temperature field are lowest at bottom hole. Commonly there are several BHT data available for most drill holes, often also for different depths that have been collected during an incremental drilling progress.

Different temperature extrapolation procedures are used depending on the downtime after completion of the drillhole, the duration of the flushing period, and the number of available temperature data:

- The “explosion cylinder source” (Leblanc et al. 1982)
- The “continuous line source” (Horner 1951)
- The “explosion line source” (Lachenbruch & Brewer 1959)
- The “cylinder source with statistical parameters” (Middleton 1982).

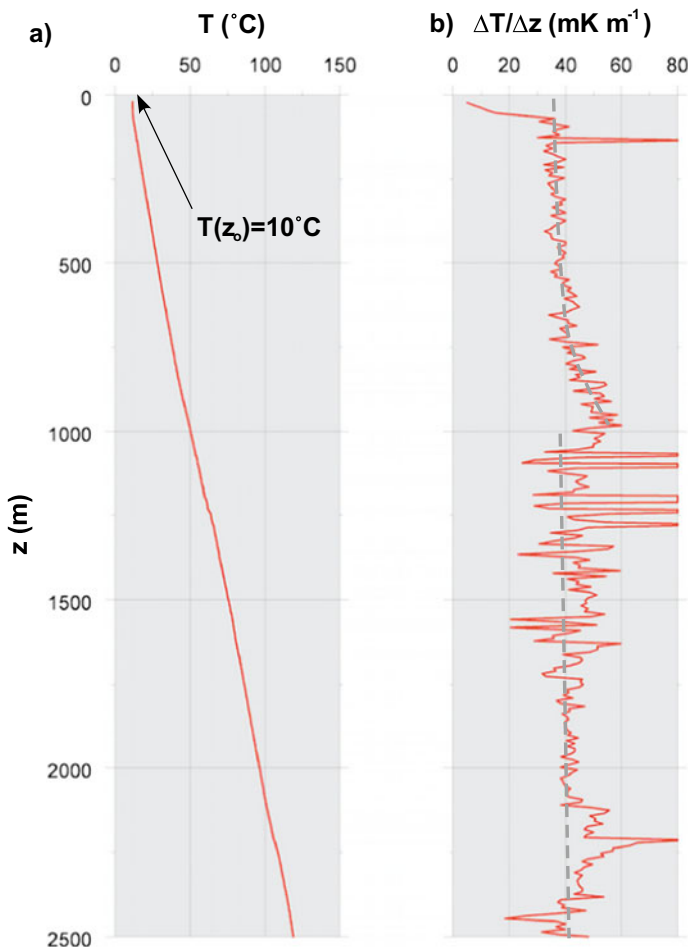


Fig. 1.8 Example of a T-log after a long downtime in the well Bühl in the upper Rhine rift valley (Germany) (Schellschmidt & Stober 2008): **a** T-profile; **b** T-gradient ($\Delta T/\Delta z$). Note that the striking gradient variations relate to small Δz between readings and thus are mostly caused by the technique and only to a minor extent related to the geology along the profile

Extrapolation of a single BHT measurement to the pristine pre-drilling temperature at bottom hole requires a derivation of statistical parameters from additional temperature data in the borehole.

The thermal conductivity of the formation can be derived from the temperature response of the probe installed during a production test. For this purpose the temperature is continuously recorded by the probe at a fixed position within the formation of interest. The procedure is analogous to the technique described in Fig. 6.8. The pristine temperature at the position of the probe can be deduced from the T data during the adjustment period using a so-called Horner Diagram (Horner 1951).

Temperature maps at a depth of interest can be constructed from interpolated temperature data in both horizontal and vertical direction. Different techniques exist for this purpose including the “gridding algorithm” (Smith & Wessel 1990).

For the computation of a three dimensional temperature model along the drill hole the temperature of the topsoil layer must be known. It defines the upper boundary limit of the model. The temperature (T_0) can be derived from long time annual averages of the local air temperature using data compiled by the local weather services or from the World Meteorological Organization (NCDC 2002). The average annual near ground surface temperature of the air corresponds is close to the soil or rock temperature at 13 m below the surface (in central Europe). At this depth the ground temperature does not vary with the season. Data interpolation for the model can be carried out utilizing a 3D universal Kriging method.

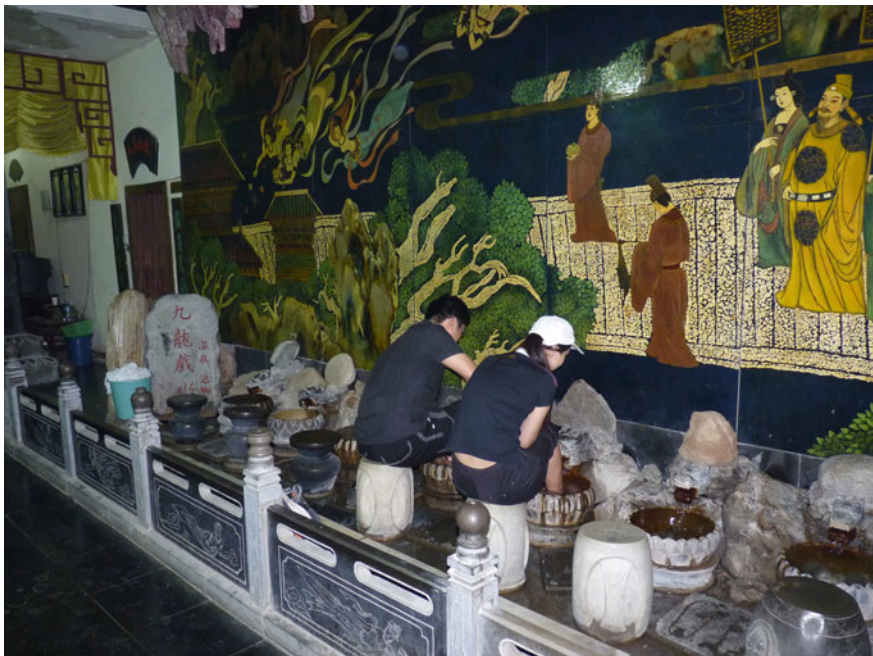
References

- Ahrens, T. J., 1995. Global Earth Physics: a Handbook of Physical Constants. Am. Geophys. Union, 376 pp.
- Armstead, H. C. H., 1983. Geothermal Energy. E. & F. N. Spon, London, 404 pp.
- Carslaw, H. S. & Jaeger, J. C., 1959. Conduction of Heat in Solids. Oxford at the Clarendon Press, Oxford, 342 pp.
- Clauzer, C., 2009. Heat Transport Processes in the Earth's Crust. Surveys in Geophysics, **30**, 163–191.
- Horner, D. R., 1951. Pressure Build-up in Wells. In: Bull, E. J. (ed.): Proc. 3rd World Petrol. Congr., pp. 503–521, Leiden, Netherlands.
- Kappelmeyer, O. & Haenel, R., 1974. Geothermics with special reference to application, pp. 238, E. Schweizerbart Science Publishers, Stuttgart.
- Lachenbruch, A. H. & Brewer, M. C., 1959. Dissipation of the temperature effect of drilling a well in Arctic Alaska. - Geological Survey Bulletin, 1083-C: 73–109; Washington.
- Landolt-Börnstein, 1992. Numerical Data and Funktional Relationships in Science and Technology. In: Physical Properties of Rocks, Springer, Berlin-Heidelberg-New York.
- Leblanc, Y., Lam, H.-L., Pascoe, L. J., & Johnes, F. W., 1982. A comparison of two methods of estimating static formation temperature from well logs. Geophys. Prosp., **30**, 348-357.
- Mareschal, J.-C. & Jaupart, C., 2013. Radiogenic heat production, thermal regime and evolution of the continental crust. Tectonophysics, **609**, 524-534.
- Middleton, M. F., 1982. Bottom-hole temperature stabilization with continued circulation of drilling mud. Geophysics, **47**, 1716-1723.
- NCDC, 2002. WMO Global Standard Normals (DSI-9641A), Asheville (USA) (Nat. Climatic Data Center).
- Pollack, H. N., Hurter, S. J. & Johnson, J. R., 1993. Heat Flow from the Earth's Interior - Analysis of the Global Data Set. Rev. Geophys., **31**, 267-280.
- REN21, 2017. Renewables 2017 Global Status Report.- Paris Ren21 Secretariat, <https://www.ren21.net>.
- Rybáček, L., 1976. Radioactive heat production in rocks and its relation to other petrophysical parameters. Pageoph (114), 309–317.
- Schädel, K. & Stober, I., 1984. The thermal anomaly of Urach seen from a geological perspective (in German). Geol. Abh. Geol. Landesamt Baden-Württemberg, **26**, 19-25.
- Schellschmidt, R. & Stober, I., 2008. Untergrundtemperaturen in Baden-Württemberg.- LGRB-Fachbericht, **2**, 28 S., Regierungspräsidium Freiburg.

- Schön, J., 2004. Physical properties of rocks, pp. 600, Elsevier.
- Smith, W. H. F. & Wessel, P., 1990. Gridding with continuous curvature splines in tension. *Geophysics*, 55: 293-305.
- U.S. Department of Energy., 2016. 2016 Renewable Energy Data Book, Energy Efficiency & Renewable Energy of the National Renewable Energy Laboratory (NREL) (<https://www.nrel.gov>).
- VDI, 2001. Use of subsurface thermal resources (in German). Union of German Engineers (VDI), Richtlinienreihe, 4640.

Chapter 2

History of Geothermal Energy Use



Huaqin Hot Springs near Xi'an, China

Geothermal energy, heat from the interior of the planet Earth, has been utilized by mankind since its existence. Hot springs and hot pools have been used for bathing and health treatment, but also for cooking or heating. The resource has also been used for producing salts from hot brines. For the early man the Earth internal heat and hot springs had religious and mythical connotation meaning. They were the places of the Gods, represented Gods or were endowed with divine powers. In many modern societies bathing in hot spring spas has still preserved the meaning of a divine ceremony.

Natural springs, where water emerges from the underground, have been symbols of life and power in all religions and civilizations. The mythical significance of springs producing hot and highly mineralized water from which minerals precipitate and form sinter, crusts and unusual mineral deposits was and still is immense.

Thermal springs had a religious and social function from early on. Godly healing power has been attributed to hot springs, where gods were near. Thermal springs and spas were centers of cultural and civilization development. In the Roman Empire, the middle Chinese Dynasties and the Ottoman Empires spas have been centers of balneological use of hot springs, where physical health and hygiene (modern term: wellness) have been combined with cultural and political conversation and progress of the time.

Natural hot springs (onsen) are numerous and highly popular across Japan. Every region of the country has its share of hot springs and resort towns, which come with them. There are many types of hot springs, distinguished by the minerals dissolved in the water. Different minerals provide different health benefits, and all hot springs are supposed to have a relaxing effect on your body and mind. Hot spring baths come in many varieties, indoors and outdoors, gender separated and mixed, developed and undeveloped. Many hot spring baths belong to a ryokan, while others are public bathhouses. An overnight stay at a hot spring ryokan is a highly recommended experience to any visitor of Japan.

Hot springs have been (and still can be) regarded as godly messengers of the immense energies stored in the subsurface of planet Earth.

2.1 Early Utilization of Geothermal Energy

Archeological finds prove that North American Indians utilized geothermal springs several thousands of years ago. Hot springs of South Dakota (USA) have been battle-fields among Sioux and Cheyenne tribes. Healing powers from the deep interior of the Earth have been attributed to the hot waters from the springs. A bathtub carved into the rocks at the spring witnesses the use of the waters by the Indians for therapeutic bathing. They also drank hot spring water to cure gastro-intestinal health problems. Later, white settlers started to use the hot springs for balneological purposes commercially. Today, the hot water is utilized for cooling and heating purposes with the assistance of heat pumps. Similar “Indian Hot Springs” are found along Rio Grande in Texas and in Mexico. The natives of North America have

also used them for therapeutic purposes and for bathing in rock pools since time immemorial. Several thousand thermal springs are known in the USA.

A peculiarity is Fishing Cone Geyser submerged in water near the Shore of Yellowstone Lake, which has been used for cooking fish by fishermen (Fig. 2.1). The small crater had been above water surface of the lake for some time and the fishermen held the rods with the still flouncing fish for cooking into the boiling and steaming small crater either from the boat or from the beach. Today Fishing Cone Geyser submerged in the lake water and the hot water eruptions stopped.

Historical written documents by the Romans, Japanese, Turks, Icelander, also from Maori in New Zealand describe the occurrence and utilization of hot springs for cooking, bathing and house heating. About 2000 years ago, bathing and treatment centers have been erected at the hot springs Huaqingchi and Ziaotangshan near Beijing in China.

About 3000 years ago, gods of Greek civilization have been associated with thermal and mineral waters and their healing power. In the 3rd to the first century B.C. Celts worshipped springs with healing power, e.g. the thermal springs of Teplice in Northern Bohemia. Bath in Southern England is associated with the cure of King Bladud, the father of King Lear, from leprosy in 863 B.C. Bath are the waters of Sul, the god of wisdom.

The Celts and then particularly the Romans demonstrably extensively utilized thermal springs in central Europe. Already more than 2000 years ago, the Romans

Fig. 2.1 Fishing Cone Geyser in Yellowstone lake (Yellowstone National Park, USA), (Photograph: US gov). The fisherman cooked fresh fish from the lake in the hot water of the hydrothermal cone



heated their baths with geothermal energy. It is proven that the Romans settled preferably in the vicinity of thermal springs from second century B.C. Examples are Aix-en-Provence (Aquae Sextiae), Bagnière de Luchon in the Pyrenees, Wiesbaden Germany (Aquae Mattiacorum), Baden-Baden Germany (Aquae Aureliae), Badenweiler (Aqua Villae) (Fig. 2.2) and many other places. No other epoch of the western civilization celebrated bathing and bathing culture with more delight than the classic Roman period. “Sanus per aquam” healthiness through water was the motto of the Romans. Bathing was the most important pastime of the Romans. Wellness has been a central aspect of their lifestyle; bathing was a feast for all senses. The bath was the place for social gathering, used for business affairs and for sports.

In Roman times established spas offered regular bathing programs, which were fundamentally related to believe in gods that were responsible for health. Liable for the success of a treatment were primarily the gods of the local springs such the Celtic-Roman god Apollo-Grannus and not so much the well-trained balneologists. In Roman spas cured patients donated sanctified platelets to express gratitude for the celestial accomplishment.

The hot springs of Badenweiler in the Black Forest (Germany), as an example, have been used by the Celts (known from coin finds). Shortly after the Roman conquest of the lands East of the Rhine River at the end of the first century A.C. the invaders raised a civil settlement and a bathing house (Fig. 2.2). During Roman



Fig. 2.2 Ruins of the Roman bathing facility at the thermal springs of Badenweiler in the Rhine rift valley (southern Germany)

times the water must have been significantly warmer than today's 26.4 °C, because the Romans built the large bathing halls without heating systems (Cataldi 1992). Also the mineralization of the water was probably higher than today even in the year 1560 according to the "spa travel guide" (Badenfahrtbüchlein) of Georgius Pictorius. After the withdrawal of the Romans the spa sunk into oblivion. It was rediscovered and unearthed in 1784.

The roman settlement Baden-Baden, Aquae Aureliae, in the foothills of northern Black Forest can be traced back to the first century. It developed into an important administrative town during the 2nd and 3rd Century. Aquae Aureliae was a flourishing town in the Roman province Germania Superior. The Roman city centered on the curative thermal springs, which were the source of the economic success and importance. The luxury imperial spa built by order of the roman emperor Caracalla is located underneath today's market square of Baden-Baden. The spa was destroyed in the year 260. The distinctly more frugal soldier spa is situated at some distance from the imperial spa. The extremely comfortable roman spas were technically highly sophisticated and very cultivated institutions. The spas were built with a so-called hypocaust system (hypocaustum) of central and underfloor heating, in other words with a geothermal heating system (Fig. 2.3). The Romans used the spas wearing wooden sandals protecting them from the hot floors.

Many of the spas have been abandoned after the retreat of the Romans from large areas of Europe. The early Christians preferred to build the first churches close to curative hot springs that have been used from ancient times. In central Europe of the Middle Ages thermal springs had such an enormous importance that e.g. Charlemagne (Charles the Great) expanded the imperial seat in Aachen to his palatinate and in the year 794 declared it to his permanent residence. The thermal springs of Aachen have already been used by the Celts and the Romans but have fallen into oblivion for several hundred years. The legend says Charlemagne was on a hunting trip in the vicinity of Aachen, in midst of overgrown remains of Roman times. The horse of the sovereign got stuck in a swamp. Charlemagne realized the sludgy water was hot and that steam emerged from the soil. Charlemagne has re-discovered the hot springs of Aachen.

The thermal spas southeast of Oradea in medieval Transylvania have been established at the hot springs of Peta River. The waters of Peta have later also been used as "defrost liquid" by directing them to the castle moat around the fortress of Oradea to prevent the water from freezing and to maintain the functionality of the moat.

In Chaudes-Aigues in central France, construction of the first district heating system, still functioning today, has been commenced in the fourteenth century (Lund 2007).

Most of the old roman spas were re-discovered in the thirteenth and fourteenth century. The big boom of the European thermal spas, however, started not before the eighteenth century. The spas developed to meeting places of the nobility, aristocracy and the rising bourgeoisie. The first scientific studies on the therapeutic use of thermal spas and the chemical composition of the waters have been written by the monk Savonarola and by the anatomist Fallopio in the fifteenth and sixteenth century.



Fig. 2.3 Thermal spa Baden-Baden, Roman soldier spa, underfloor heating system, first geothermal heating system

The first reports from China on thermal springs including therapeutic instructions and farming guides go back as far as the fourth to the sixth century. For example, the diversion of thermal water to the fields for rice crop permits the first harvest already in March and allowed for three harvests in the year. The pharmacologist Li Shizhen has written the first scientific review of mineral and thermal waters in China in the sixteenth century. In his book „Compendium of Materia Medica“ he classified the waters on the basis of chemical and genetic criteria.

In 1560 Georgius Pictorius published an account of the spas of southern Germany (“Badenfahrtbüchlein”) and instructions how to use them. It represents a first balneological treatise. Georgius Pictorius studied medicine at the University of Freiburg and was later regionally well known for his medical essays. He had studied all relevant experts on therapeutic bathing of the Antique and the Middle Ages. In his “Badenfahrtbüchlein” he described all classic spas in southwestern Germany that all are still in use today one by one.

Early experience with geothermal phenomena has also been reported from the mining industry. Agricola realized in 1530 already that the temperature in underground mines increases with depth. The first reported temperature measurements with a thermometer are probably those by De Gensanne in 1740 in a mine near Belfort France. Alexander von Humboldt measured a temperature increase of 3.8 °C per 100 m depth increase in the mining district of Freiberg, Saxony, in the year 1791. This was the first report on the concept of the geothermal gradient, a fundamental parameter in geothermal energy exploitation. Its existence and variation was rapidly confirmed by data from Central- and South-America. In Germany, temperature measurements in deep drill holes up to 1000 m depth were carried out in the years 1831 to 1863. A few years later, measurements down to 1700 m followed. An average temperature increase of 3 °C per 100 m emerged from the rapidly increasing volume of data, which is known today as the normal temperature gradient. The first measurement of the surface heat flow density has been achieved by Benfield ([1939](#)).

A surprisingly high temperature of 38.7 °C has been measured at the bottom hole of the 342 m deep drillhole Neuffen in Southern Germany in the year 1839. This corresponds to a geothermal gradient of 9 °C per 100 m. The first large geothermal temperature anomaly had been discovered.

2.2 History of Utilization of Geothermal Energy in the Last 150 Years

Using thermal water for energy conversion did not start before the second half of the nineteenth century related to the rapid development of thermodynamics. Thermodynamics helped to efficiently convert energy from hot steam first in mechanical energy and then into electrical energy with the help of turbines and generators.

The development of geothermal power generation is clearly associated with the Larderello region of Tuscany in northern Italy ([Tiwari & Ghosal 2005](#)). Until the early nineteenth century the thermal springs near Larderello have been used for the production of boron and other substances dissolved in the thermal water. In 1827 Francesco Larderel, the founder of the boron industry, installed the first plant for geothermal energy conversion. One of the hot water ponds has been covered with a brick cupola. The construction was the first low-pressure steam boiler heated naturally with geothermal water. It produced the heat needed to evaporate the boron-rich water for the production of boron and additionally also powered pumps and other



Fig. 2.4 Larderello 1904: The picture shows Principe Piero Ginori-Conti with his apparatus that converted geothermal to electrical energy for the first time in history. The installation had the power to light five light bulbs (Photograph: Unione Geotermica Italiana 2010)

machines. The installation saved large amounts of firewood and the deforestation of the region could be brought to an end. In the year 1904 the first electrical power was produced from a geothermal energy source by coupling a steam engine to a generator in Larderello (Fig. 2.4).

When the first Larderello power plant went into operation in 1913 it already had an electrical power of 250 kW. In 1915 the power station had power of 15 MW and was driven by saturated steam. From the year 1931 on, new deep drillholes produced superheated steam for the electrical power plant with a temperature of 200 °C. Superheated steam did not contain constituents that cause corrosion and scale formation in contrast to saturated steam. The installation of heat exchanger systems was therefore not necessary. In 1939 the total installed power of all Larderello power plants was up to 66 MW. The Italian geothermal fields were destroyed at the end of WWII but rebuilt after the war. Today 545 MW electrical power is installed at the Larderello plants, 1.6% of the total electrical energy production in Italy (2010).

The Larderello geothermal fields are caused by shallow level igneous intrusions at the convergent plate margin of the Apulian and Eurasian plates beneath Tuscany. Extremely high geothermal gradients result from the shallow magma chambers.

In 1890, early systematic geothermal heat utilization was accomplished in Boise, Idaho, USA by completing a district heating system. This system was copied in 1900 by Klamath Falls, Oregon, USA. Later, in 1926, Klamath Falls started to use

a geothermal well to heat greenhouses. The first private homes were geothermally heated from separate wells in Klamath Falls in 1930.

The utilization of thermal water for heating homes and greenhouses started in the Reykjavik, Iceland, on a large scale in the 1920s. The name Reykjavik, steaming bay, was given by the Vikings because of the visibly steaming thermal springs. The first wells were drilled into hot water reservoirs for heating buildings as early as in the middle of the nineteenth century. Geothermal heating of public buildings and entire city districts followed.

Today, Iceland is clearly number one in utilization of geothermal energy in the world. 79,700 TJ or 53% of primary energy is supplied by geothermal sources. Geothermal and hydroelectric energy provide 99.9% of the country's electrical energy demand. Low-enthalpy geothermal fields near Reykjavik supply water with temperatures of up to 150 °C, which can be used in house heating systems. More than half of the Iceland's population lives in the area. Geothermal fields provide heat and hot water for 90% of the Icelandic households. The high-enthalpy fields are located along the active volcanic belt that crosses the island. Typical temperatures are 200 °C and higher, but these waters are often highly mineralized and gas-rich and cannot be used directly. The diverse power plants produce typically some 10 s MW electrical power in steam turbines. The Hellisheiði plant in the southwest of Iceland is the largest electrical power plant on the island. It produces about 330 MW_{el} power. It uses the volcanic heat of the central volcano Hengill as well as the heat from springs and drilled wells (Fig. 2.5). The total installed electrical power of all geothermal plants in Iceland is 735 MW_{el} power (2019) (Chap. 10). The thermal waters of Iceland are utilized for many different industrial purposes.

Following the development in Italy and on Iceland, in 1958 New Zealand erected its first geothermal plant in Wairakei; in 1959 an experimental facility started in Pathe, Mexico, and in 1960 northern California initiated the project The Geysers. Today, The Geysers comprise 21 power stations with a total installed capacity of 750 MW electrical power. It is the largest geothermal installation in the world. The produced electricity is sufficient to supply a city of the size of San Francisco.

However, severe setbacks occurred too. The profitability of geothermal energy production is subject to general economic conditions, such as demand, supply and price of other forms of energy for instance crude oil. Changing laws and environmental regulations may cause increasing efforts and costs (Chap. 10). Greece and Argentina, for instance, shut down existing geothermal installations due to environmental and economic reasons. Germany's deep wells for geothermal installations were drilled in the 80ies of the last century following increased oil and gas prices. The further development of deep geothermal systems came to a halt during the economic crisis and the associated collapse of the oil price. Resumption of geothermal energy projects follows the price of dwindling fossil fuel resources. In the year 2003 the first electrical energy production from a geothermal source in Germany started in Neustadt-Glewe. 2007 the geothermal wells Landau and 2009 the wells in Bruchsal, which were drilled in the 1980ies already, started to produce electrical energy. Several geothermal installations followed, particularly in the Munich region in Southern Germany.



Fig. 2.5 Hellisheiði power plant on Iceland. Capacity in 2019: 330 MW_{el} electrical power, 133 MW_{th} thermal power used for district heating. Operated by ON Power

The earliest documented drilling for ground source heat pump systems in central Europe has been completed in the late summer of 1974 in Schönaich, southern Germany. For retrofitting an existing building (from 1965) with a ground source heat pump as the exclusive heating system five ground loops of 50–55 m depth have been installed with a distance of 4–5 m between the wellbores arranged in a linear array of five coaxial probes with thick-walled steel tubing (60 × 5 mm) and a coaxial plastic hose. The probes were loaded with a water–glycol mixture. Grouting of the annulus with a cement-bentonite suspension, a standard procedure today, had not been carried out at that time. Supply water temperatures in the probes were –3 to –4 °C for peak load periods (continuous outside temperatures of –15 to –20 °C during several weeks); return temperature was about +1 °C. The system was in operation for 30 years. One of the probes failed in 2005 probably because of a corrosion damage. Now the system runs with four probes and an oil-fired boiler.

In 1852, Lord Kelvin has invented the heat pump, a crucial piece of equipment for utilizing near surface geothermal energy. Heinrich Zoelly filed a patent application in 1912 to use a heat pump for extracting heat from the subsurface. The first successful implementation of a ground source heat pump system occurred not before the 1940ies. These first ground source heat pumps (GSHP) in Indianapolis, Philadelphia and Toronto had ground collectors that have been emplaced close to the surface. An experimental installation of the Union Electric Company in St. Louis used spiral pipes in 5–7 m deep drill holes as heat exchangers. Other early systems such as in an

administrative building in Zurich 1938 and the Equitable Building in Portland in 1948 used river- or groundwater as a heat source, thus they are not utilizing geothermal energy in a strict sense.

The US Department of Energy (DOE) maintains an excellent web page related to many aspects of geothermal energy: <https://www.energy.gov/eere/geothermal/geothermal-basics>.

The DOE published in 2010 a comprehensive series of four books downloadable as PDFs from their website on the history of geothermal energy development in the USA in the Geothermal Technologies Program: “A History of Geothermal Research and Development in the United States”. The series covers the years 1976–2006. A brief history of geothermal energy in the US can be found at: <https://www.energy.gov/eere/geothermal/history-geothermal-energy-america>.

References

- Benfield, A. E., 1939. Terrestrial Heat Flow in Great Britain. Proceedings of the Royal Society of London Series A: Containing Papers of A mathematical and Physical Character, 173(955), 428-450.
- Cataldi, R., 1992. Review of historiographic aspects of geothermal energy in the Mediterranean and Mesoamerican areas prior to the Modern Age. Geo-Heat Centre Quarterly Bulletin, 18, 13-16.
- Lund, J. W., 2007. Characteristics, Development and utilization of geothermal resources. Geo-Heat Centre Quarterly Bulletin, 28, 1-9.
- Tiwari, G. N. & Ghosal, M. K., 2005. Renewable Energy Resources: Basic Principles and Applications. 649 pp.

Chapter 3

Geothermal Energy Resources



Natural thermal water spring Da Qaidam, China

3.1 Energy

In physics, energy is the ability of a physical system to do work on other physical systems. There are many different forms of energy including mechanical (potential, kinetic), thermal, electric, chemical and nuclear energy. Thermal energy can be understood as the random motion of atoms and molecules.

The different forms of energy can be converted from one to another. E.g., chemical energy is converted to mechanical energy in a combustion engine. Solar heat radiation is converted in a photovoltaic system into electrical current.

The distinction between renewable and non-renewable forms of energy resulted from the increasing insight that natural energy resources are limited. Non-renewable kinds of energy, also called fossil energy resources, include coal, oil, gas and nuclear fuels (e.g. uranium). These forms of energy renew on time scales that are not interesting for the present day human economic system.

Solar energy is considered a typical representative of renewable energy. Radiation from the sun produced by solar nuclear processes is unlimited and last forever from a human perspective although the processes on the sun will stop when all nuclear fuel has been used up. The radiation energy reaching the Earth can be transformed into electricity (photovoltaic) or heat (solar thermic). Wind energy, hydroelectric energy and biomass (wood, energy plants) are also ultimately derived from solar energy. These forms of energy are limited only by the amount of radiation reaching the Earth from the sun provided they are used in a sustainable manner. The energy is renewable in the sense that the sun replenishes the energy consumed in the form of, for example fire wood and the potential energy of water in a reservoir every day and for “quite some time” (billions of years, although humans will not be able to enjoy this). Note that also the fossil “non-renewable” forms of energy such as coal and oil represent stored solar energy. Also these energy forms are renewed although at time scales not interesting to short lived human economic processes.

Geothermal energy, the heat in the interior of the Earth is an energy that is not related to the solar energy but ultimately has been created by gravitational energy and radioactive decay of unstable atoms. It is renewable in the sense that there is a very large amount of heat stored in the body of the planet and the human consumption cannot deplete the energy reservoir. Consumed geothermal energy is renewed and replenished from the internal planetary reservoir and is unlimited from a human perspective if used sustainably. Using renewable energy resources sustainably means that the rate of consumption is equal or smaller to the rate of the renewing process. Renewable energy is characterized by renewing processes that are fast in human timescales.

From the laws of physics (1. Law of thermodynamics) we know that energy cannot be created or destroyed. Energy can only be transformed from one form into one other. The total amount of energy remains constant and nothing is lost. Merely the usability value of one form of energy can be reduced during transformation and transport.

Many forms of energy cannot be directly used. For practical applications, they must be transformed into usable forms. Chemical energy, nuclear energy and radiation energy must be converted into mechanical, thermal or electrical energy.

Energy can be stored and it can be transported. Energy sources are stored in specific storage media. For example, typical fossil energy sources of the Earth including coal, oil and gas ultimately can be regarded as storage media for solar energy. In engineering the purpose of storing energy is to make it retrievable on demand and transportable. For example, chemical energy can be stored in transportable batteries and converted to electrical energy to drive an appliance when and where needed.

Heat that has been generated e.g. in a solar installation can be stored in a heat accumulator and utilized when the sun temporarily does not shine. Heat storage media are normally liquids (often water) or solids (typically rocks). Water is a preferred storage material because of its high specific heat capacity (Sect. 1.4). In order to prevent unwanted heat loss and rapid cooling the storage device needs to be thermally insulated. In addition to the conventional heat accumulators that operate at elevated temperature (sensible heat accumulators), latent heat accumulators utilize the latent heat associated with phase transitions to store thermal energy. The accumulator material begins to (e.g.) melt at the temperature of the phase transition. Further heating, however, continues to melt the substance but the temperature does not change until all solid is transferred to liquid (equilibrium melting). Latent heat accumulators store considerably more energy than sensible heat accumulators do. The property is referred to as a higher energy density.

For example, the energy required to heat water from 0 °C to 80 °C is equivalent to melting ice of 0 °C. The energy that must be invested to convert water to steam at 100 °C corresponds to 5.4 times the energy to heat the water from 0 °C to the boiling point of 100 °C at 1 bar.

Primary energy must be converted to net energy before the user can consume it. For the production of one kilowatt-hour electrical energy typically 3 KWh primary energy such as coal or petroleum is needed. A part of the losses during energy conversion is intrinsic and cannot be avoided. The ratio of usable net energy to spent primary energy characterizes the efficiency of the energy conversion (Sect. 4.2).

Conversion losses arise, for example, in industrial conversion of chemical energy into thermal energy such as in a coal fired power plant or a domestic oil heating system from incomplete reaction due to practical and technical conditions. Thermal energy is lost from a heat reservoir because of conductive heat flow. Therefore, heat cannot be stored in a home or a building for long periods. In this context, the thermal insulation of a house is a crucial construction feature. A typical home in central Europe without special thermal insulation requires more than 20 L heating fuel per m² per year. In insulated low-energy buildings heating fuel consumption reduces to 7 L m⁻² per year. A state-of-the-art passive house burns only 1.5 L fuel per m² and year for covering its heat demand.

Entropy and the second law of thermodynamics have the consequence that the directions of energy conversion processes are not equivalent. For example, mechanical kinetic energy can be completely converted into thermal energy. In the opposite direction, the conversion is always incomplete; the conversion of thermal energy

into mechanical energy has intrinsic conversion efficiency smaller than one. Energy conversion processes are anisotropic or asymmetrical.

Geothermal energy or geothermal heat is the thermal energy stored below the surface of solid earth. Geothermal heat recovered from different depths below the surface provides unique and different possibilities of utilization. Consequently, geothermal heat use is subdivided into near-surface geothermal systems and deep geothermal energy systems (Chap. 4).

3.2 Significance of “Renewable” Energy

The economic development of the energy sector depends also on factors that are not immediately discerned as relevant to the energy industry. The factors include population development, number of households, general economic trends, structural change and technological advance. In addition, economic parameters, legal framework and political environment further influence the growth of energy consumption and set guidelines for general development of energy use and consumption (Gupta & Roy 2006).

The known and proven global reserves of conventional energy commodities such as fossil fuels and nuclear fuels are in the order of 83 ZJ (1 Zettajoule ZJ = 10^{21} J; 1 Exajoule = 10^{18} J; 83 ZJ = 83,000 EJ; 2017 Estimate EIA 2020; excluding potential production from breeder reactors). The total global reserves correspond to about 200 times the annual consumption of primary energy in 2017 of 0.4 ZJ. Coal and lignite account for about 25% of the reserves. Dividing the reserves by the current production results provides the statistical range of a particular energy source. The estimated ranges using available data from 2007 are: 42 years for crude oil, 61 years for natural gas, 129 years for coal and 286 years for lignite (EIA 2020). The statistical range for nuclear fuel (uranium) for once-through reactors based on estimated reserves in 2017 is about 70 years. The reader is advised to regularly consult the EIA.gov web pages provided by the U.S. Energy Information Administration for current data and information regarding energy production and consumption.

The ranges given above represent snapshots and are, although afflicted by large uncertainties, meaningful only at the time of the estimate. The actual “true” range of a resource mostly depends on the price the consumer is willing to pay for it. It is a question of the market influenced by the price of competing resources and technologies among many other factors. The number of years until all oil etc. is “used up”, however, indicates that the commodity has a finite range because it is a fossil fuel that is formed by geological processes that are much slower than production and consumption by humans.

Total global energy consumption increased dramatically during the last 50 years parallel to the exponential growth of world population. Many competent sources predict an increase by three times in global energy consumption and an increase in world population from 8 in 2020 to 10 billion people in the next 30 years. In 2013, the total annual energy consumption per capita in the USA has been 290 GJ (290 ×

$\cdot 10^9$ J; EIA). If the future 10 billion inhabitants of this planet were allowed to use the same amount of energy as the US citizens used in 2013 then the 2017 reserves would be “used up” in about 30 years. This little exercise shows that “renewable” energy utilization must be dramatically developed in the near future if a high standard of living is a goal for all inhabitants of the planet. Parallel to the development of “renewable” energy, energy must be used more efficient, conversion losses must be reduced, energy saving must be made attractive. Energy efficiency requires new inventive technologies. Research and development of this knowledge calls for time and money.

In recent years, the change of global climate and the associated increase of the mean annual surface temperature has become a major concern. It is evident that the major cause of global warming is linked to the burning of fossil fuels and the release of carbon dioxide and other greenhouse gases to the atmosphere produced in the process. The greenhouse effects of anthropogenic CO₂ emissions contribute 50% of the observed global warming. There are many unwanted and on a long run very costly effects of global warming. The effects include displacement of vegetation zones, thawing of permafrost, melting of continental ice caps and associated sea level increase, melting of glacier ice in Alpine mountain ranges and associated effects on water and energy supply for large areas in mountain forelands, and predicted increase of extreme weather conditions.

The operation of electrical power plants and power producing systems utilizing “renewable” energies, such as photovoltaic, hydroelectric and geothermal systems is completely or nearly free of green house gas emissions. Thus, “renewable” energies are not only of vital importance for saving fossil fuel resources but also for preserving environmental conditions.

The declared goals of environmental politics of many countries include a significant increase in “renewable” energy utilization for electrical power production and in the total energy consumption (electrical power, heat, mobility). At the same time, major efforts are made to improve the energy efficiency of existing power plants. This leads to a reduction of imported energy and energy commodities, an improved flexibility of the energy supply system and an increased security of supply.

3.3 Status of Geothermal Energy Utilization

The USA has an installed capacity of 3.7 GW_{el} from geothermal sources and it is the leading country in geothermal energy utilization for electrical power production. Most of the U.S. geothermal power production is located in California (2.9 GW_{el}). In Europe, about 2.5 GW_{el} electricity is produced from geothermal systems (Bertani 2015; IEA-GIA 2020). At present more than 100 geothermal power plants are operational. About half of the plants run with “dry steam”, all of them in Italy and Iceland. About 20 plants operate with “flash steam” and 30% with “binary technologies” (Sect. 4.4). The specific situation differs from country to country depending on the available natural resources and the technology using these resources. In Iceland and

Table 3.1 Installed geothermal capacity in MW (2019). Top 10 countries. 14,900 MW total

USA	3653
Indonesia	1948
Philippines	1868
Turkey	1347
New Zealand	1005
Mexico	951
Italy	944
Kenya	763
Iceland	755
Japan	549
Other	1011

Source ThinkGeoEnergy.com

Italy deployed deep geothermal systems range from steam production from high enthalpy heat reservoirs, to direct use of hydrothermal reservoirs in deep sedimentary basins, that is reservoirs with a high content of energy in a kg of water. The top 10 countries regarding the installed geothermal capacity are listed in Table 3.1.

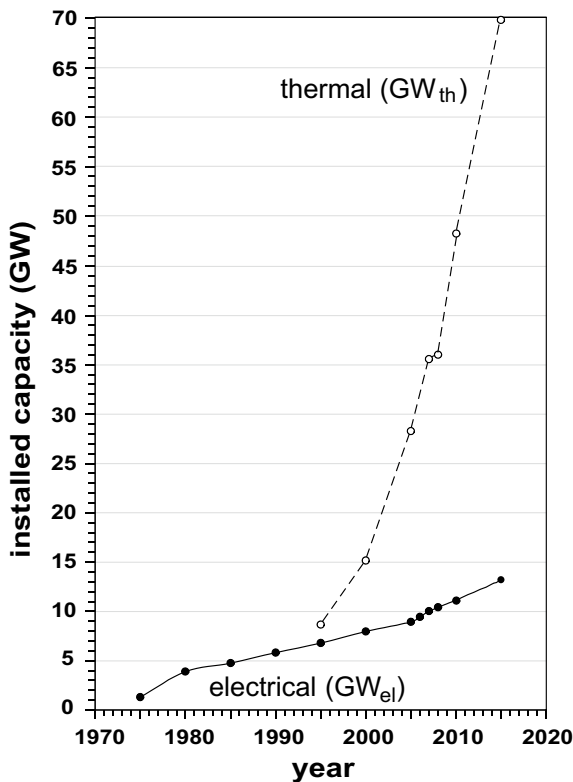
In the year 2019, geothermal energy has been used for the production of electrical power in 24 different countries. The total capacity installed amounted to 14.9 GW_{el} (Table 3.1) (IEA-GIA 2020). For the most part, dry steam and flash steam systems produce this electrical power from high enthalpy reservoirs that are characterized by high temperatures at shallow depth (very large geothermal gradients). These open systems use the produced geothermal aqueous fluid directly to drive a turbine for electrical power generation. Less common are closed systems that utilize heat from produced geothermal fluid to drive a turbine in a secondary loop in low-temperature reservoirs.

Dry steam and flash steam systems are for example installed in the following countries: USA, Philippines, Mexico, Indonesia, Italy, Iceland, Russia (Kamchatka, Kuril Islands), Turkey, Portugal (Azores) and France (Guadeloupe).

Electrical power production from low-temperature geothermal reservoirs using binary systems like organic ranking cycle plants (ORC) or Kalina plants started some years ago and is operative at a relatively small number of sites. The systems have a substantial potential and many locations are well suited for binary low-T systems. At present, many projects are in the development stage. If consistently extended, these systems have great ability to contribute significantly to the electrical power and heat production in the future.

After the year 1975, the utilization of geothermal energy continuously and markedly increased (Fig. 3.1). In the period from 1980 to 2005, the global installed capacity increased continuously by about 200 MW_{el} per year. After 2005, the annual growth boosted to 500 MW_{el}. In 2008, the USA had with 3040 MW_{el} the highest installed geothermal capacity worldwide. It was followed by Indonesia (992 MW_{el}), Mexico (958 MW_e), Italy (811 MW_{el}), New Zealand (632 MW_{el}), Iceland (575

Fig. 3.1 Worldwide installed electrical and thermal power capacity from geothermal energy sources since 1975 (Bertani 2015; IEA-GIA 2020)



MW_{el}) and Japan (535 MW_{el}). The 2012 number for the US is 3187 MW_{el} (GEA 2012).

These numbers vary between different countries and strongly depend on geological conditions. For example, utilization of deep geothermal energy is small in Germany compared with Iceland, USA or New Zealand, because of the absence of high enthalpy fields in central Europe. Nevertheless, also in Germany and other geologically less favorable countries deep geothermal energy is increasingly utilized and has a promising marked. Presently (2017), in Germany 10 geothermal plants with 37.1 MW_{el} total capacity produce electrical energy (www.geotis.de). The first plant was Neustadt-Glewe in 2003 followed by Landau in 2007. From 2012 Neustadt-Glewe is producing thermal energy for district heating only. 3 of the electricity producing plants are located in the northern Upper Rhine Rift Valley, 7 in the Bavarian Molasse Basin of the Munich region. The first geothermal heating plant was Waren an der Müritz (Eastern Germany). It was coupled to the district heating system in 1984. At present (2017), 21 geothermal heating plants are in operation in Germany producing a total of 313.5 MW_{th} district heating power. All uses of thermal energy from geothermal sources (direct heat use) including district heating, house heating and thermal spas adding up to 374 MW_{th} (www.geotis.de).

In contrast to deep geothermal systems, the near-surface geothermal systems, usually borehole heat exchangers or geothermal energy probes or ground source probes can be installed practically everywhere (Chap. 4). In 2016, geothermal energy was utilized for heating purposes in 73 different countries. The USA has highest energy production for heating purposes worldwide. In Europe, Sweden is leading followed by Germany and France. Sweden produces more thermal energy with heat pumps than Germany and France together. The global production is about 50.3 GW_{th} (IEA-GIA 2020) and doubles about every five years (Fig. 3.1).

In Germany near-surface geothermal installations produce about 4 GW_{th} from 315'000 ground source heat pumps. 23'000 new ground source heat pumps were installed in 2017. Ground source heating systems find a ready market today. Regrettably, the market share of ground source heat pumps is clearly behind the far less efficient air-air heat pumps.

3.4 Geothermal Energy Sources

Subsurface temperatures in the uppermost meters of the crust are mainly controlled by climate. In wintertime, the ground can be frozen to one meter depth in moderate climate zones and considerably warmed up during summer. Heat input occurs directly by solar radiation and indirectly by heat exchange with air and infiltrated precipitation water.

The seasonal ground temperature variations decrease with depth. In moderate climate zones, the annual cycle disappears at 10–20 m depth. At this depth, temperature is constant throughout the year and its value corresponds closely to the local long-term average surface temperature (Fig. 3.2). Climatic effects at extended time scales such as ice ages are perceptible to greater depths (e.g. 200 m in central Europe). The consequences of the ice ages for the local geothermal gradients are still visible today. With increasing depth, temperature increases because of terrestrial heat flow and according to the local geothermal gradient. A large portion of the geothermal energy stored in these increasingly hot rocks is generated in the crust itself (Sect. 1.5).

Geothermal industry distinguishes between near-surface and deep geothermal energy utilization (Chap. 4). A notional boundary at 400 m depth and 20 °C separates the two quite different fields of geothermal energy uses. Deep geothermal energy utilization distinguishes furthermore between high enthalpy and low enthalpy reservoirs. The thermodynamic potential enthalpy reflects the heat content of material. Its symbol H stands for heat content (unit: Joule J). The distinction between the two types of reservoirs is at an imaginary dividing temperature of 200 °C.

Electrical power can be produced with high efficiency directly from steam turbines where steam is produced from high enthalpy reservoirs (in high enthalpy fields) (Chap. 10). High temperatures of more than 200 °C are required for the necessary steam pressure using water as heat transfer material. Producing electrical power from low enthalpy reservoirs is only possible with heat transfer substances with higher vapor pressure. Organic Rankine Cycle (ORC) plants use e.g. pentane and Kalina

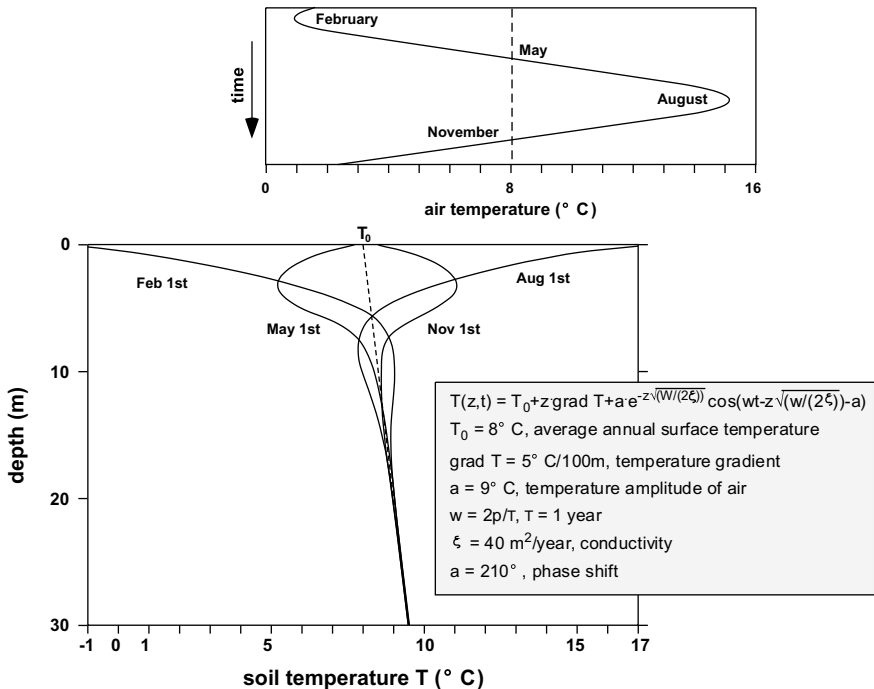


Fig. 3.2 Annual air and ground temperature variation in temperate zones (Lemmelä et al. 1981)

cycle plants ammonia-water mixtures as heat transfer substances (Sect. 4.2). The electrical efficiency of such plants varies between 10 and 15% depending on transfer material and operation temperature.

The high enthalpy fields of the planet are typically located along volcanic belts related to tectonic plate boundaries (Sect. 1.2) but also to intraplate volcanic fields related to mantle plumes (or combinations thereof like on Iceland). Some high enthalpy fields are also related to hydrothermal convection linked to shallow level magma chambers and near-surface igneous intrusions in the crust. Many plutonic rocks indicate crystallization pressures of 50–100 MPa corresponding to intrusion depths of 1.5–3 km and crystallization temperatures in excess of 650 °C. Geothermal gradients in such regions can be extremely high and temperatures of up to 400 °C can be reached at very shallow depth of a few hundred meters below surface. In high enthalpy regions, the production of electrical power from geothermal sources is mature technology and well established. The electrical power consumption of San Francisco is supplied by geothermal power plants by nearly 100%. On Iceland the electrical power production from geothermal sources exceeds local consumption leading to the establishment of new power consuming industries. Even export of electricity from Iceland to Europe via subsea cables is considered a viable project.

In deep geothermal systems, high and low enthalpy fields, the geothermal fluid that transports heat from the reservoir to the surface is natural liquid water or steam

depending on the temperature and pressure conditions. The water is usually rich in dissolved solids and gasses e.g. CO₂ and H₂S (Giroud 2008). In high enthalpy fields, the aqueous fluid can be in a state of vigorous convection because of strong density contrasts caused by the very high temperature gradients. The convection cells are characterized by zones of upwelling hot water and descending cooler water.

Deep geothermal systems can be water-dominated (liquid-dominated) or gas-dominated (H₂O steam). In water-dominated systems liquid water is the pressure controlling fluid phase, although it may contain some dissolved gas, however below the saturation condition. Such systems are very common in a temperature range of 125–225 °C. These systems produce hot liquid water, a two-phase mixture of liquid water and steam, wet steam or occasionally also dry steam depending on prevailing pressure and temperature conditions. In gas-dominated systems, most commonly liquid water and steam coexist in a two-phase system with a gas (steam) continuum and gas as pressure controlling phase. Such geothermal systems are less common (e.g. Larderello Italy, The Geysers USA) than liquid water dominated systems. Gas dominated systems are characteristic of high enthalpy fields and produce dry superheated steam, that is steam at temperatures considerably higher than the condensation point (on the boiling curve).

In regions with normal or slightly elevated geothermal gradients, low enthalpy systems produce warm or hot water depending on the depth of the borehole that can be used for heat or electrical power supply. If permeability of the reservoir is too low for fluid extraction heat can be extracted directly at depth by deep ground source probes (Chap. 4).

References

- Bertani, R., 2015. Geothermal Power Generation in the world—2010–2014 Update Report. Proceedings of the World Geothermal Congress in Melbourne, Australia.
- EIA, 2020. International Energy Outlook. US Energy Information Administration, <https://www.eia.gov>.
- GEA, 2012. Annual US Geothermal Power Production and Development Report. GEA Geothermal Energy Association, 35 pp.
- Giroud, N., 2008. A Chemical Study of Arsenic, Boron and Gases in High-Temperature Geothermal Fluids in Iceland. Dissertation at the Faculty of Science, University of Iceland, 110 p.
- Gupta, H. K. & Roy, S., 2006. Geothermal Energy, an alternative resource for the 21st century. Elsevier Science and Technology, 279 pp.
- IEA-GIA, 2020. IEA Geothermal, 2019 Annual Report. International Energy Agency, Weirakei Research Center, 171 pp., Taupo, New Zealand.
- Lemmelä, R., Sucksdorff, Y. & Gilman, K., 1981. Annual variation of soil temperature at depth 20 to 700 cm in an experimental field in Hyrylä, South-Finland during 1969 to 1973. *Geophysica*, 17, 143–154.

Chapter 4

Uses of Geothermal Energy



Enhanced geothermal system Soultz-sous-Forêts, Alsace, France

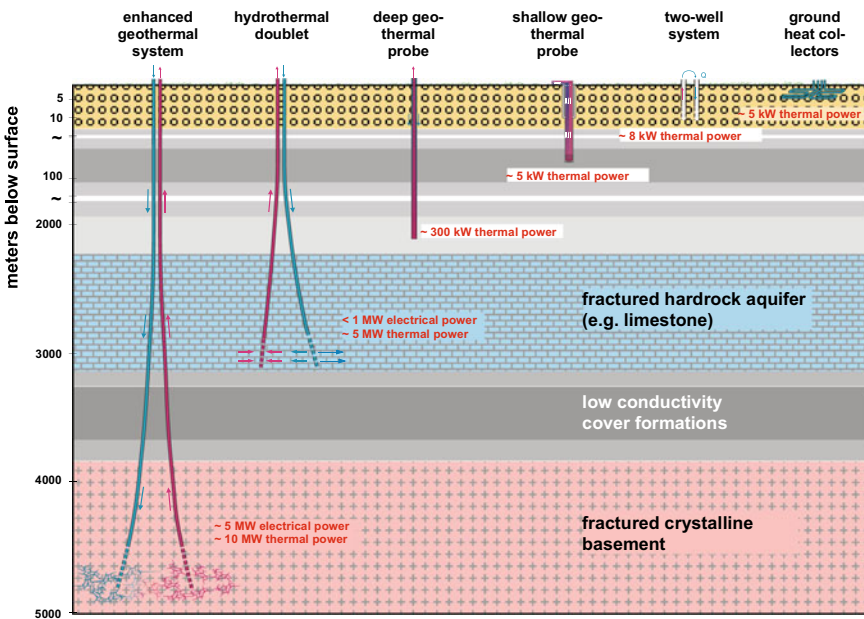


Fig. 4.1 Schematic illustration of different geothermal systems and their characteristic power output. Not shown are high enthalpy systems of active volcanic regions

Utilization of geothermal energy from high-enthalpy reservoirs, typical of active volcanic regions is treated in Chap. 10 separately from the deep geothermal systems presented in this chapter. In high-enthalpy fields very high temperatures are reached at shallow depths permitting the production of large quantities of electrical energy. Geothermal gradients in these fields are typically extremely large whereas deep geothermal systems described in this chapter produce geothermal energy from low-enthalpy fields characterized by somewhat above normal geothermal gradients.

The distinction between near surface and deep geothermal systems follows from the different depth levels of the geothermal reservoirs and different techniques of utilization (Fig. 4.1). Yet, the transition between the two worlds is smooth. Distinguishing the two main fields of geothermal energy utilization is useful, because their specific techniques for energy production require different geological and geophysical parameters for the description of the systems.

Deep geothermal systems exploit geothermal energy by means of deep boreholes. The mined thermal energy can be used directly and does not require further transformation.

Near surface geothermal systems, extract thermal energy from the uppermost layer of the earth crust. In most cases a depth of about 150 m is of interest. It may extend to a maximum of 400 m. Typical systems include: ground heat collectors, borehole heat exchangers, boreholes into groundwater, and geothermal energy piles (Sect. 4.1; Chap. 6). The exploitation is indirect and requires conversion with e.g. heat pumps.

Direct use in the very low temperature range via heat pipes is under development. Railroad switch heaters and deicing of roads are typical potential applications.

With this definition of the boundary between shallow and deep systems, deep geothermal methods are employed at depth of 400 m and below. However, deep geothermal low-enthalpy systems in the proper and real sense are those at depth more than 1000 m and above 60 °C (Fig. 4.1). One needs to keep in mind, however, that in high enthalpy fields high temperature fluids can be produced from boreholes in the range of hundreds of meters rather than thousands of meters as in the low enthalpy deep geothermal fields.

4.1 Near Surface Geothermal Systems

Near surface geothermal techniques distinguish between open and closed systems with respect to the surrounding ground. A closed system exchanges thermal energy with the ground only. The following presentation concentrates on closed loop systems, where the thermal energy is extracted from the ground by a fluid circulating in closed tubing. The systems range from a few meters depth to some tens of meters, rarely more than 150 m deep boreholes. Therefore, the temperature normally does not exceed about 25 °C.

Typical systems include ground source heat collectors, borehole heat exchangers, and geothermal energy piles (Fig. 4.1). Also thermosyphons, geothermal baskets, geothermal groundwater well systems, and energetic geostructures are near surface geothermal systems. At suitable temperatures, the utilization of wastewater, mine water and tunnel waters also belong to near surface geothermal energy uses. In Switzerland, a number of road and rail tunnels produce warm water that is used for heating purposes. Examples include the Gotthard road tunnel, the rail tunnels Furka, Ricken and Lötschberg (Table 4.1). Utilization is made possible by means of heat pumps (www.geothermie.ch). A specialty of the Lötschberg base tunnel is its unconventional use of the warm groundwater flowing into the tunnel. The about 85 l s^{-1} of 19 °C warm water leaving the tunnel at the village of Frutigen on the N tunnel portal. The thermal energy is used in a “tropical house” for farming

Table 4.1 Swiss tunnel water uses (Rybáček et al. 2003)

Tunnel	Discharge (L s^{-1})	Temperature (°C)	Thermal power (kW)
Gotthard	7200	17	4520
Furka	5400	16	3756
Grenchenberg	18,000	10	11,693
Rawyl	1200	24	1503
Lötschberg	85	19	6830
Ricken	1200	24	1503

permanently 80,000 sturgeons (caviar) and breeding 1 million perch type fish. After this first step the water cooled to 14 °C but thermal energy can be further extracted using two heat pumps ($2 \times 500\text{ kW}$) for heating the “tropical house” and provide other users with thermal energy. The greenhouses in Frutigen produce 2 tones exotic fruits and spices. The “tropical house” Frutigen uses also other renewable energy sources including hydro, solar thermal, photovoltaic, and biogas in addition to geothermal energy.

The thermal energy contained in mine water of deep underground mines, active and abandoned, is used at many locations worldwide as a useful geothermal resource (e.g. Jessop et al. 1995; Hall et al. 2011; Limanskiy and Vasilyeva 2016; Bao et al. 2018). During the operation of deep underground mines large quantities of mine water must be pumped to the surface. An active mine may produce up to some million m³ warm water per year. This geothermally heated water can be used for house heating or for heating commercial buildings. For this purpose the use of heat pumps and typically also heat exchangers is necessary. The direct usage of the thermal energy for cooling purposes is possible, however.

A unique application of geothermal energy has been established at the salt mine Riburg near Rheinfelden (High Rhine region, Switzerland). The NaCl salt mine is active since more than 150 years. The process: Freshwater is pumped into the salt reservoir and after salt dissolution in the underground deposit the salt brine can be produced from the deep wells. NaCl salt of different grade is gained by evaporation of the brine. Recently a shrimp farm has been installed at the site that uses the salt and the waste heat of the Riburg mine (swissshrimp.ch).

It can be worthwhile using the thermal energy contained in waste water for bigger buildings at a certain maximum distance to a sewage plant or a main sewer. The heating or cooling application can be installed before or after the sewage plant. However, heat exchangers and heat pumps are mandatory for this kind of usage. A well-known geothermal system that uses wastewater is the Olympic Village in Beijing, China. Waste water pumps heat and cool a total living space of 410,000 m².

Ground source heat collectors are near surface geothermal systems (Fig. 4.1) that extract thermal energy from the ground to about 5 m depth. The tubes of the respective probe loops of the collector may be up to several hundred m long. The tubing can be arranged in very different geometries. If arranged in a horizontal pattern the installation is called a horizontal ground heat collector (closed loop horizontal ground source heat collectors). These systems are also known under the terms: Horizontal heat exchanger, horizontal ground heat collector, horizontal brine pipes, horizontal surface collectors, and others. In the following, we use the term horizontal ground heat collector. The pipes can also be arranged in spirals forming a geothermal basket. Heat collectors use solar energy stored by the top soil layer supplied by direct radiation or heat transfer from the air or precipitation (strictly, these collectors utilize not geothermal but rather solar radiation heat). Therefore the collector field should not be developed close to residential or industrial buildings.

Horizontal ground heat collectors consist of numerous horizontally installed plastic pipes of up to several hundred meters length at about 1–2 m depth (Fig. 4.2). The pipes must be mounted below the maximum penetration depth of winter frost.

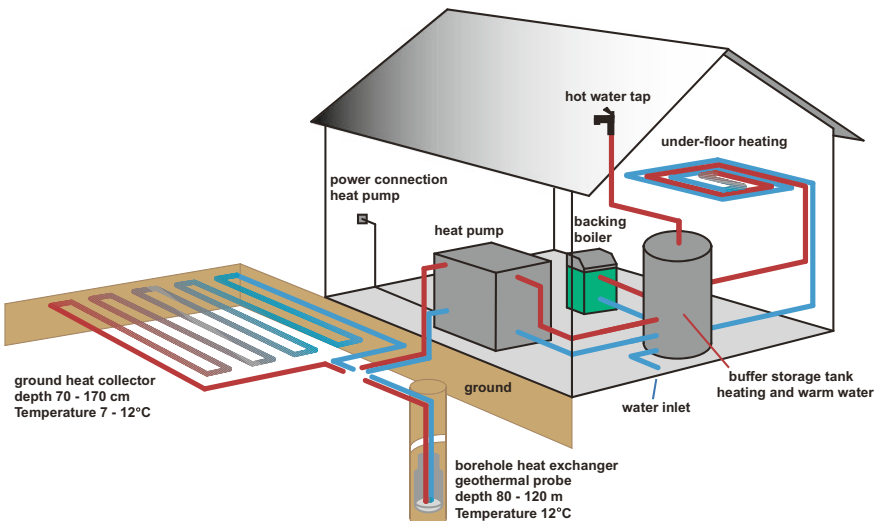


Fig. 4.2 Schematic illustration of a horizontal ground heat collector in combination with a borehole heat exchanger for house heating and hot water supply (redrawn from AEE Agentur Erneuerbare Energien)

Also, the system needs to be above the level of solar regeneration in the summer. In the pipe system a circulating fluid (liquid) extracts heat from the ground. The fluid is identical to the heat transfer fluid of the heat pump making a heat exchanger superfluous.

The most significant parameters controlling the thermal extraction output of such systems are the heat conductivity and specific heat capacity of the ground. The water and air content of the pore space and the ground temperature are important as well because of their effect on the key parameters heat conductivity and specific heat capacity. High porosity and void content of the ground typically reduce the heat conductivity.

If the groundwater table is low and the ground is in the vadose zone instead of the saturated zone, the voids are filled with air instead of water and the heat conductivity of the entire system is considerably lower (Sect. 1.4). Consequently, highly permeable sand and gravel and water tables below 2 m below surface are problematic with respect to the efficiency of ground source heat collectors.

The land required for horizontal ground source heat collectors is large. The collector field cannot be further developed or covered because the system uses the solar heat input to the ground. If the groundwater table is temporarily low, irrigation of the ground heat collector field may increase its efficiency. The systems require a considerable effort, which should not be undervalued, particularly if irrigation should be necessary. The efficiency of the total system increases if the collector field can be used for cooling in addition to heating.

Starting point for planning of horizontal ground heat collectors are ground and soil maps and sections containing data on the structure of the near surface ground. These primary data are needed as input parameters for computer codes and techniques that model the heat conductivity structure of the ground as a function of soil compaction and water content (soil moisture). The computed models are essential for the final system design. Several computer models of variable complexity are presently available. However, no specific procedures for field tests have been developed so far. This is in marked contrast to thermal response tests for borehole heat exchangers. In addition, the computation tools cannot deal with heterogeneities of the ground. Furthermore, potential daily and annual variations of ground temperature and groundwater table are ignored in the system design. Nevertheless model computations are helpful and allow a generous dimensioning of the collector field and ensure that the spacing of the tubing is sufficiently wide, because of the potential for extensive icing of the ground.

The specific heat extraction power depends on the annual operating time and the local climatic conditions (sun, shadow). The extraction power ranges from 10 to $40 \text{ W}_{\text{th}} \text{ m}^{-2}$ ($5\text{--}15 \text{ W m}^{-2}$ direct cooling). Horizontal ground heat collectors produce during e.g. 1800 h annual operation time about $10 \text{ W}_{\text{th}} \text{ m}^{-2}$ in dry non-cohesive soil, $20\text{--}30 \text{ W}_{\text{th}} \text{ m}^{-2}$ in moist cohesive soils and $40 \text{ W}_{\text{th}} \text{ m}^{-2}$ in water saturated sand or gravel. The distance between the extraction tubes depends on these three soil types and must be >0.8 , >0.6 and $>0.5 \text{ m}$ respectively. With increasing operation time the extraction power decreases accordingly.

Icing is an intrinsic system property of ground heat collectors; therefore, the systems cannot be operated with pure water. The system design must prevent massive freezing of the ground. The ground cools by operating the facility with the consequence of a retarded and shortened vegetation period. The biochemical activity of the soil biota including the production of humic and fulvic acids and other decomposition products of biomass may be altered. These chemical effects on the soil chemistry may trigger further chemical effects on the composition of seepage and groundwater.

A further reason why ground heat collectors cannot be run with pure water as a heat transport medium follows from its proximity to the surface. In wintertime, the system extracts heat from the ground at a low temperature level. Consequently, return temperatures commonly decrease to freezing conditions. Therefore, ground heat collectors need to be operated with special heat transfer liquids. For the approval and use of these liquids, detailed regulatory requirements must be obeyed, especially in groundwater protection fields.

A variant of the horizontal ground heat collector uses coiled tubing arranged in many loops of horizontal tube spirals (Fig. 4.3). These systems are also known as horizontal “slinky”® loop geothermal systems in the USA (IGSHPA 1994).

Vertical ground heat collectors (closed loop vertical ground source heat collectors) consist of numerous tubes vertically installed in trenches. Thermal power of the tubes ranges between 400 and 1000 W depending on size.

Ground heat collector systems are popular in e.g. Sweden and the USA where plots for family homes are typically larger than in e.g. densely populated central Europe and conform better to the space requirements for collector systems.

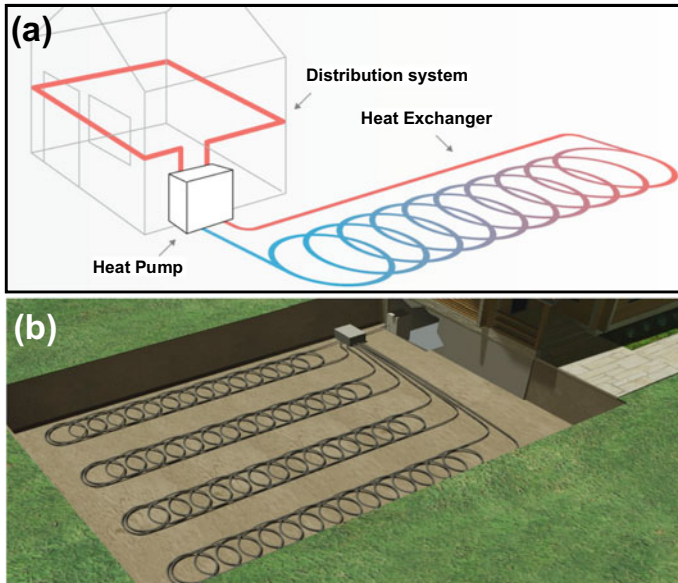


Fig. 4.3 Horizontal ground heat collector: **a** General system design (from pdp.services/renewables/ground-source-heat-pumps), **b** Example layout (from a-1team.net/geothermal/green-loops/slinky-loop/)

Geothermal tube baskets or conic baskets heat exchanger (Fig. 4.4) are 1.5–3 m high conical-shaped baskets made of spiral exchanger tubes. The baskets are buried up to 4.5 m underground depending on size. The essential property of the baskets is that they take hold of the annual cyclic seasonal temperature variation underground, with a temperature maximum before the beginning heating season and a temperature minimum before summer. The diameter at the top of the basket is about 2–3 m. The

Fig. 4.4 Geothermal tube basket



typical length of the exchanger tube is 100–200 m. The heat extraction capacity of a small basket is about 0.5 kW_{th}. The heat extraction power of large baskets is in the range of 1.5–2.0 kW_{th}. Baskets can be installed in groups with 4 m distance between them for small baskets and larger distances for big baskets. Usually several baskets are necessary for heating a single-family house. Massively increased extraction power is possible if the baskets can be installed in an aquifer. Placed in dry sediments the geothermal extraction power of the baskets is drastically reduced.

Geothermal structures use the ground contact of the groundwork of large buildings but also for residential houses for the extraction of geothermal energy for heating and cooling. **Geothermal piles** combine pile foundations with closed-loop ground source heat pump systems. For the purpose pipe loops are integrated into the pile foundations. The systems are also known under the terms energy piles, energy geo-structures, energy foundation, thermal piles and others. Any structural component in contact with the ground (soil) can be used for energy extraction, including piles, wall and ground plates. Because of its high thermal conductivity and storage capacity concrete is an ideal material for the extraction of thermal energy from the ground. These energy foundations serve as geothermal heat exchangers in addition to the static function. For the exchange of thermal energy between the ground and the building the energy piles are equipped with plastic pipes for the circulation of a heat transfer fluid. In diaphragm walls or foundation plates the pipes are installed two-dimensional. Concrete elements in contact with both the ground and the building interior, the pipes are installed at the outer parts in contact with the ground (soil). The bundled tubing connects to one or several heat pumps. Proper hydraulic balancing increases the efficiency of the system. The foundation of the building serves as heat exchanger and geothermal system.

Energy piles or thermo-active piles are piles of reinforced concrete containing double or quadruple plastic U-tube heat exchanger or a network of polyethylene tubes. The tubes are completely embedded in concrete (Fig. 4.5). The heat transfer medium cycles between the pile and the heat pump in a closed loop. Depending on the energy demand of small or large industrial buildings, the installed thermal power of such systems ranges from 10 to 800 kW_{th}. The specific thermal extraction rate of an energy pile of >0.6 m in diameter ranges between 20 and 80 W_{th} m⁻² depending on the conditions underground. Foundation plates may transfer 20–50 W_{th} m⁻². Thermal activation of almost all types of foundation is possible unrelated to the dimension of the construction project. Energy geo-structures belong normally to the group of so-called bivalent systems because an additional separate heating system (boiler) must be installed.

Geothermal probe, closed-loop borehole ground heat exchanger: A very popular and widespread utilization of near surface geothermal energy is the use of borehole ground heat exchangers so called geothermal probes (Fig. 4.6). The systems are technically mature and the installation is routine work for specialized commercial suppliers. The heart of the system is a borehole of typically about 100 m depth (Fig. 4.1). The deepest drill holes for geothermal probes reach 400 m. For many installations, more than one drill hole is used for energy exchange with the ground. In the plastic tubes of closed-loop borehole heat exchanger water or another

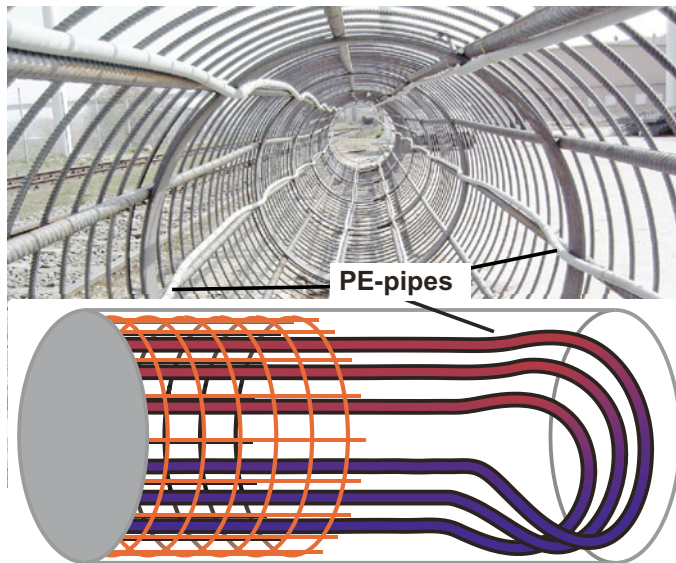


Fig. 4.5 Schematic illustration of an energy pile. In the indicated PE tubing a heat transfer liquid is cycled in a closed system

heat transfer liquid such as water-anti freeze mixtures or also gases extract heat from the ground. The fluid circulates between a heat pump and the ground in a closed loop. The space in the borehole between the ground and the tubing must be grouted with a thermally conductive and impermeable filling. The backfill may not be necessary in boreholes entirely drilled in highly permeable gravel. Geothermal probes are also used for cooling in summer time. If so, the warm water must be provided by another technical system. Geothermal borehole heat exchangers are particularly efficient in combination with solar-thermal installations. These systems store excess heat in the warm season for meeting the demand in the cold season. In Chap. 6, the combined systems will be presented in detail.

Heating and cooling of large commercial buildings or industrial complexes with geothermal energy requires a multitude of geothermal probes. Such installations are called geothermal probe fields (Sect. 6.8.1). The probes are normally installed in the excavation pit before the construction of and deeper than the foundation slab of the building. The geothermal probe field must be adequately dimensioned and configured, which requires appropriate computation tools (e.g. Kavanaugh and Rafferty (1997), ASHRAE Handbook (2007)).

The geological structure and the ground properties are multifaceted and vary from place to place. The thermal properties of the ground differ from site to site accordingly. It is very important for the dimensioning of a geothermal installation to take the variability of the geological properties of the ground into account. The thermal properties of some important types of rocks are compiled on Table 1.1. Highly permeable aquifers and aquifers with high groundwater flow velocities such

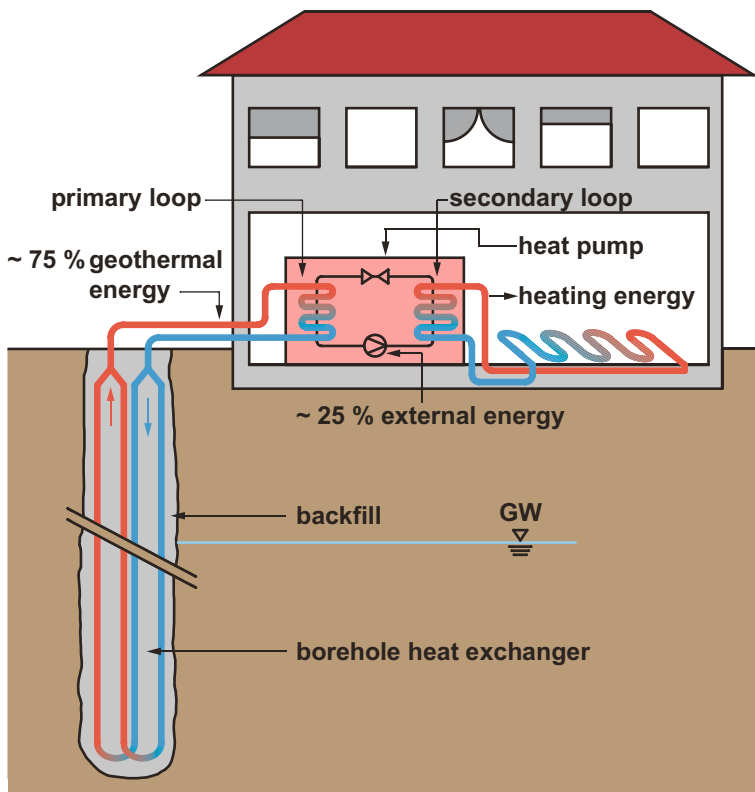


Fig. 4.6 General design of a borehole heat exchanger system

as in karst areas are environmentally vulnerable. Drilling and casing of bores can be accompanied by mud losses, turbidity and chemical and microbial contamination and pollution of flowing groundwater. Drilling of a geothermal probe potentially intersects layers with different permeability, hydraulic situations and hydro-chemical properties. Tight grouting of the annular void and sealing of the annulus conserves the layer separation. This is mandatory for any geothermal probe system. It is required by the matters of groundwater protection and for the prevention of damage and hazards (Sect. 6.7). Furthermore, it is essential for the efficiency and the economic lifetime of the installation.

Ideal sites are characterized by a uniform medium or low hydraulic conductivity. Areas with highly permeable karst aquifers or fractured hard rock aquifers are less favorable because of possible technical problems with drilling and casing. Drilling is often troubled by mud losses and can be associated with groundwater contamination. Moreover, it is often difficult to seal the annulus tight because of losses of cement slurry in the highly permeable voids. In such areas, higher costs must be expected for a professionally proper installed borehole heat exchanger. Occasionally the drilling is not successful and the wellbore must be abandoned and sealed.

In addition to the restricted potential of an area resulting from unfavorable geology, site-specific difficulties may trouble a geothermal energy project: Past losses, previous pollution, natural hazards, neighboring risks, adjacent bodies of water, protected areas, underground gas reservoirs, and others. Drilling into over- or under-pressured aquifers, or into layers of highly water-soluble minerals such as rock salt, gypsum or anhydrite may be potentially hazardous or cause technical drilling difficulties (Sect. 6.7). For these reasons gathering of detailed knowledge of the local stratigraphy is a pre-drilling effort of utmost importance.

Thermosyphon: A thermosyphon is a widely used method of passive heat exchange without the need of an electricity-consuming pump. It is based on convective transport performed by the circulation of a fluid undergoing boiling in the temperature range of operation of the system (two-phase closed thermosyphon). In geothermal applications a thermosyphon transfers the thermal energy from the ground to the user without consuming external energy. The heat transfer efficiency of a well-designed thermosyphon can be somewhat higher than that of other near-surface geothermal systems. Most geothermal thermosyphons operate with CO₂ as heat transfer fluid. The systems utilize the liquid-gas transition of the refrigerant and operate at elevated pressure. Liquid cold CO₂ flows downwards along the probe walls and extracts heat from the ground until it starts boiling. The evaporated CO₂ gas ascends in the center to the probe head. There the thermal energy is transferred to a secondary closed loop where it can be used for HVAC applications. The CO₂ gas condenses in the heat exchanger at the probe head during the heat transfer and starts a new cycle as liquid CO₂. Geothermal thermosyphons are normally made of stainless steel pipes.

A classical use of thermosyphons is the Trans-Alaska-Pipeline where the technology is used to cool and stabilize the pylons in permafrost ground (Fig. 6.28).

Near surface geothermal energy can also be extracted directly from groundwater by means of an open two-well system (Fig. 4.1). Heat is extracted from water of a production well and the cooled water re-injected and returned to the aquifer in a second well (injection well). If such systems are planned for larger buildings the design may require several production and injection wells. If used for heating the thermal energy is extracted from the produced water and the cooled water is returned to the aquifer via the injection well. The inverse process can be used for cooling applications. It is important that the wells do not influence each other thermally and hydraulically. E.g. the cool water must not be injected upstream from the production well.

Furthermore, the chemical composition of the groundwater can be critical because of the potential to precipitate scales. The scales and mineral deposits tend to clog well screens, pipes or the heat exchanger. Detailed description of such systems is given in Chap. 7.

Operation of a near surface geothermal system for heating and heat production usually requires a heat pump, which increases the temperature of the circulated heat transfer fluid. A heat pump is a device that transfers heat from a source at relatively low temperature to a heat sink at higher temperature by means of mechanical work. The mechanical work is provided by a pump driven typically with external electrical

power. The device can be used for cooling (refrigerators and freezers are typical heat pump household devices) or heating (used in building space heating). Reversible cycle heat pumps are typically used for geothermal applications. The devices are equipped with a reversing valve so that the direction of heat flow may be reversed. The machines are evaporation-condensation systems and utilize the latent heat of condensation of a heat transfer fluid for space heating. Section 6.3.1 explains the technical characteristics of a heat pump. The efficiency of a heat pump system using a specific heat source and operating at a particular temperature is characterized by the annual performance factor (APF). The ground source heat pump (GSHP) systems should operate at a minimum annual performance factor of four (Sect. 6.3). This means that per unit of invested energy to drive the pump four units of energy should be extracted from the ground source. Investment costs, annual running costs, the primary energy requirement and the CO₂ emissions are the decisive criteria assessing the economical performance, the energy efficiency, and the environmental effects of ground source heat pump systems.

The legal and regulatory requirements for building and operating near surface geothermal systems vary from country to country (also between states and districts within countries). Normally they are based on groundwater and mining regulations. Typically, the authorities provide investors with guidelines and recommendations with detailed descriptions of all legal requirements for the building of the system of interest. Such guidelines also inform about existing restrictions for building a specific system. Potential restrictions include: groundwater protection areas, areas of unfavorable and difficult aquifer structure, drilling risks, and others. The guidelines may also assist developers and clients with recommendation procedures to follow in case of drilling into an artesian aquifer or under- or over-pressured confined aquifers, drilling into strata with gas over-pressure, drilling into large cavities or karst and into strata with soluble salts or with swelling minerals.

The utilization of geothermal energy for heating purposes requires significant initial investments. Prior to planning the system, potential and possible reductions of heating needs must be implemented. Highly recommended are thermal insulation measures, which directly reduce the need for heating. Included are masonry and façade insulation, thermally insulated high-quality windows and the like. Floor and wall heating systems significantly improve the economic viability of the heating system. Floor heating systems operating with supply temperatures of 35 °C or with concrete core temperatures of walls as low as 25 °C are far more economical than radiators running at 55 °C supplied by the heat pump. Economic and efficiency requirements also consider the hot water needs of a building (shower, washbasin, and the like). Expert advice and competent qualified planning of the total system assures an economic and enduring operation friendly to the environment.

4.2 Deep Geothermal Systems

Deep geothermal systems in low-enthalpy regions include with increasing depth of the heat source, deep geothermal probes, hydrothermal doublets and enhanced geothermal systems (EGS) (Fig. 4.1). The three types of systems use the heat stored in warm or hot water of natural aquifers. The heat reservoir is exploited directly, generally employing a heat exchanger, occasionally also via a heat pump. The produced thermal water can be fed into the local and district heating networks or directly used in spas, heating of industrial complexes and heating of green houses.

Each deep geothermal project requires a carefully developed and well-founded heat and energy concept. Requirements and availability of heat transport networks for district heating, needs of energy supply and plant operation conditions must be cautiously coordinated. Proactively, the future role and task of the planned geothermal plant within the existing regional energy infrastructure must be farsightedly examined. It must be clear, which existing conventional heat or/and energy supply should be taken over by the new plant and when. It is important to stress again that geothermal energy is well suited for base load energy supply and less so for peak demand requirements. It is also strongly recommended that the public be continuously informed with clear particulars regarding the new plant during planning, installation and later operation.

Conversion of the heat to electrical energy with **binary cycle power plants** based on the **Organic Rankine Cycle** or the **Kalina Cycle** is possible if the produced water is above about 80 °C. However, economically feasible efficiency requires 120 °C or more (ORC Figs. 4.7 and 4.8; Kalina Fig. 4.9).

Organic Rankine Cycle (ORC) plants work with an organic heat transfer fluid with a relatively low boiling temperature. Typical transfer fluids include hydrocarbons (e.g. n-butane and isopentane) and fluorinated hydrocarbons (e.g. 1,1,1,2-Tetrafluoroethane, Freon). Environmental concerns motivate the search for alternative refrigerants with a low Global Warming Potential (GWP). Currently refrigerants with GWP < 1 such as R1233ze and R1234ze (Solstice) are increasingly used in geothermal applications. In the ORC plant a pump compresses the transfer fluid in a first step thereby increasing its temperature. In the pre-heater unit the fluid takes up thermal energy from the produced thermal water and reaches boiling temperature. In the downstream boiler further heat transfer from the thermal water provided by the production well transfers the fluid to the gas phase. Geothermal heat is therefore transferred in two steps in two different units, the pre-heater and the boiler. The produced vapor of transfer fluid expands in a gas turbine and drives electricity production in an alternator downstream. The subsequent condenser unit cools and liquefies the vapor using air or water as cooling media. The liquid transfer fluid is then ready for the next process cycle. The residual heat after the turbine is transferred in a recuperator to the liquid leaving the condenser. Different detailed technical designs are realized for different plants at different locations depending on the requirements at the site. ORC plants produce electrical energy ranging from about 2–20 MW_{el}. The

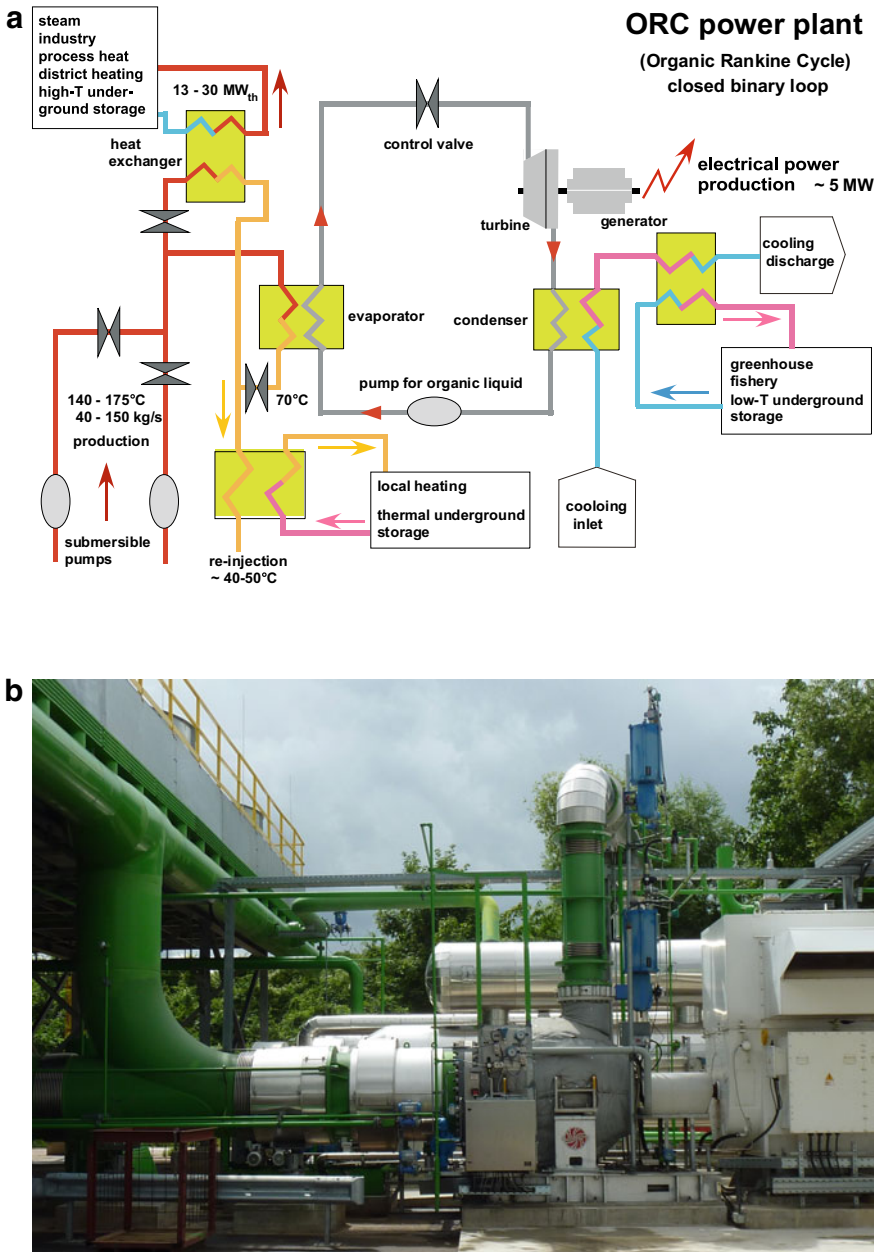


Fig. 4.7 Organic Rankine Cycle power plant: **a** Concept and design (modified from Stadtwerke Bad Urach, Germany); **b** ORC cooling system; **c** ORC turbine (photographs b and c from Soultz-sous-Forêts, France)



Fig. 4.7 (continued)



Fig. 4.8 The hydro-geothermal ORC power plant of Holzkirchen near Munich (Germany). Produces electrical power ($5.6 \text{ MW}_{\text{el}}$) and heat for the district heating network from geothermal water at 140°C (from Turboden S.p.A.)



Fig. 4.9 Wet cooling tower of the Kalina binary cycle power plant at Bruchsal in the upper Rhine river valley (Germany)

performance roughly relates to the temperature of the produced geothermal water, which stretches from 110 to 170 °C.

Kalina installations are an alternative to the ORC process. Kalina plants use an ammonia—water mixture as a heat transfer fluid. The non-isothermal boiling of two-component fluid is a characteristic process of most fluid mixtures, excluding azeotropes. This property is used in the so-called Kalina cycle used in geothermal applications (Kalina 1984, 2003; Ibrahim 1996; Henry and Mlcak 2001; Ahmad and Karimi 2016).

Electricity production in **binary power plants (ORC, Kalina)** from low-enthalpy geothermal sources is associated with substantial energy losses. A significant portion of the produced thermal energy is re-injected unused into the aquifer or lost as waste heat in the condenser. Also losses by the turbine and the power consumption of the

plant itself reduce the overall yield. International programs are currently working on the optimization of the plant design for increasing the energy efficiency.

The most popular kind-of-use of hydro-geothermal resources is the **hydrothermal doublet** (Chap. 8). The system is based on two wellbores drilled into a hot water aquifer, one of which is used as a production well where hot water is pumped from the aquifer to the surface, whereas the second well of the doublet is used for injecting the cooled water back into the subsurface reservoir (Fig. 4.10). At the surface, the thermal energy of the hot water is transferred to a suitable fluid by means of a heat exchanger. The heat energy cannot be completely transferred and converted to electrical power. The hot water is typically cooled to about 55–80 °C only and, accordingly, much of the thermal energy remains in the thermal water. The residual heat has the potential to be utilized if appropriate customers and demand exist and the proper infrastructure can be installed. The economic success of a power plant depends much on selling the residual or “waste” heat. Efficient and resourceful waste heat recuperation is the key to profitable operation of the plant. However, plant development must also acquire potential buyers of the thermal energy and secure access to existing district heating grids. This also extends to enhanced geothermal systems (EGS) formerly known as hot-dry-rock (HDR) systems (Chap. 9).

The cooled water with its residual heat is recycled to the aquifer from an injection well. The screens (filter sections) of the two wells of the doublet are at an exactly defined distance from each other (Fig. 4.10). Depending on the geological situation, injection may require a pump (Figs. 4.11 and 12.16). The need for recycling the produced hot water in a closed loop has several reasons. It is necessary to contribute to the recharge of the aquifer, because natural recharge of deep aquifers is a very slow process. Since a hydro-geothermal plant pumps large amounts of water it is simply necessary to make sure that the extracted water is replaced. Re-injection of cool water is also worthwhile for economical and practical reasons, because the waters contain typically high concentrations of dissolved solids and gases. For reasons of waste management, it is advantageous to dispose the waters in the original reservoir.

An example of a hydro-geothermal doublet is the plant of Riehen near Basel (Switzerland), which continuously supplies residential units in Switzerland and nearby Germany with thermal energy for heating (Fig. 4.12) since start-up in 1994. The two wells located at a distance of one kilometer tap thermal water from the Muschelkalk aquifer at 1547 and 1247 m depth, respectively.

Production and injection well of a hydro-geothermal doublet can be bored from one drilling site as inclined bores (Fig. 4.13). This greatly reduces the area requirement of the surface installation of the plant. In the subsurface, bottom hole of the bores in the hot water reservoir are typically 1000–2000 m away from each other. The optimal distance of the wells must be determined pre-drilling by numerical modeling of the system. If the wells are too close to each other a thermal short-circuit is at stake. This means that the cooled re-injected water may reach the production well after a relatively short time of plant operation, cooling therefore the produced water. On the other hand, the wells should not be too far apart, because in this case the production well does not receive hydraulic support from the injection well. However, production

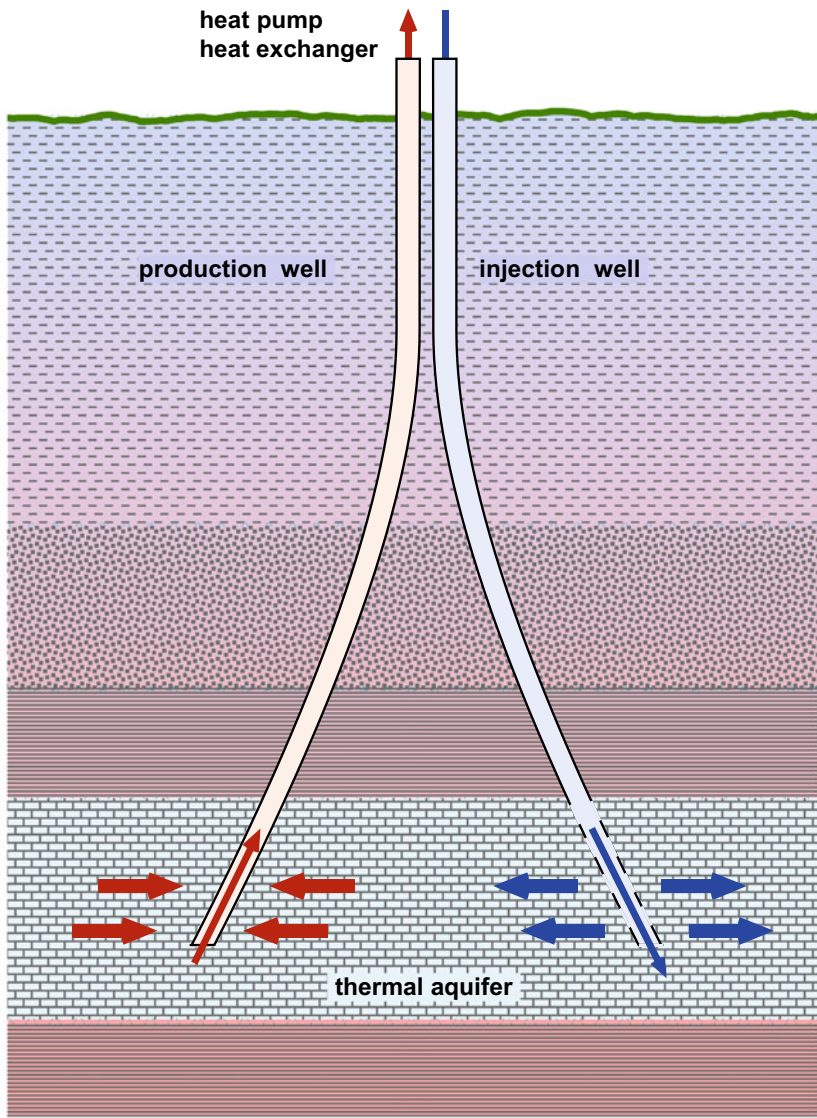


Fig. 4.10 Underground design of a deep geothermal open system installation (doublet, 1 producer, 1 injector)

Fig. 4.11 Fitting an electric submersible pump (ESP) into a production well of a hydro geothermal doublet (2500 m deep borehole Bruchsal, Upper Rhine River Valley)



depends on an intermediate time scale on the recharge of the aquifer by cooled water re-injection.

The pumped hot water and, after cooling, reinjected water circulate in a system that allows keeping the fluid under a defined pressure. This is necessary to prevent or minimize scales and mineral precipitations from highly mineralized and gas-rich fluids in the installations caused by pressure drop and gas loss. Ca-carbonates (calcite and aragonite) are among the most typical and widespread scales. Degassing of CO₂ from pumped hot water causes carbonates to precipitate in the pipe system even though the carbonates are more soluble in cold water, because CO₂-loss outweighs the temperature effect. In closed pipe systems, the pressure can be adjusted in such a way as to prevent degassing and scale formation. At some sites, small additions of a strong acid (e.g. hydrochloric acid) or other chemicals (organic inhibitors) may be needed to prevent scales (Sect. 15.3). The same applies to the EGS systems described in Sect. 9. The cooled fluid can be recycled to the reservoir by free flow or by pumping depending on the hydraulic properties of the reservoir rocks. Typical

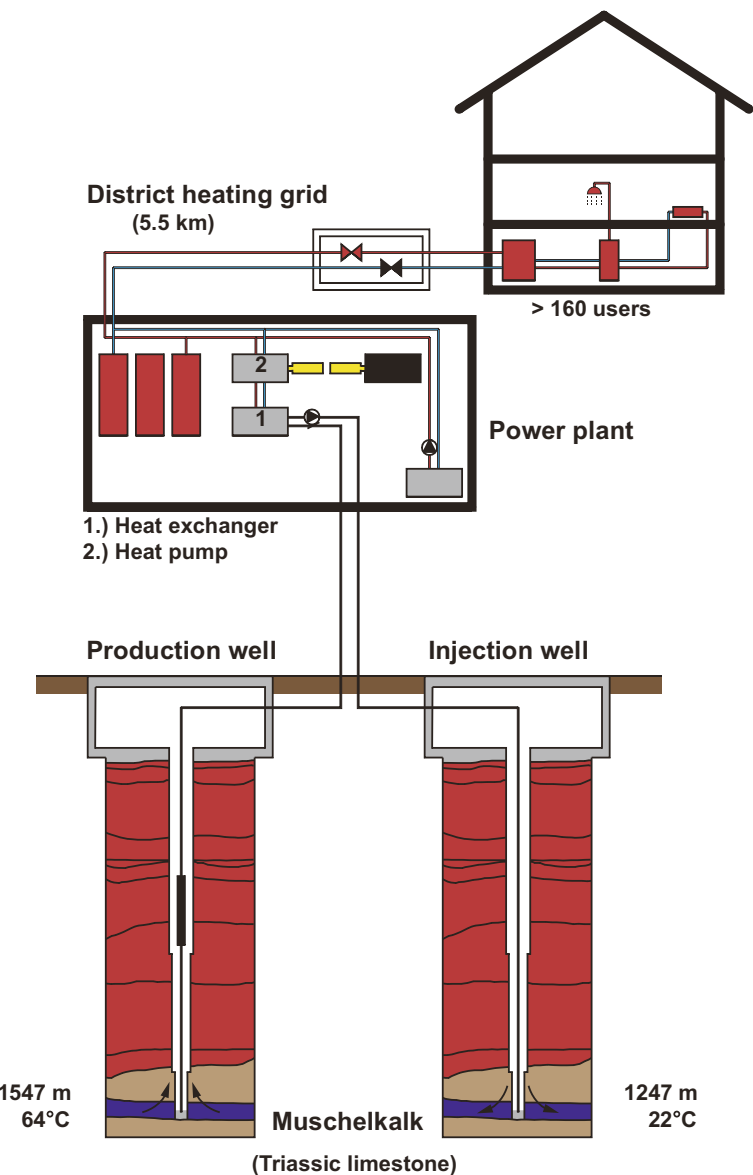


Fig. 4.12 The hydro geothermal doublet system at Riehen (Basel, Switzerland), redrawn from documents of Gruneko Corporation

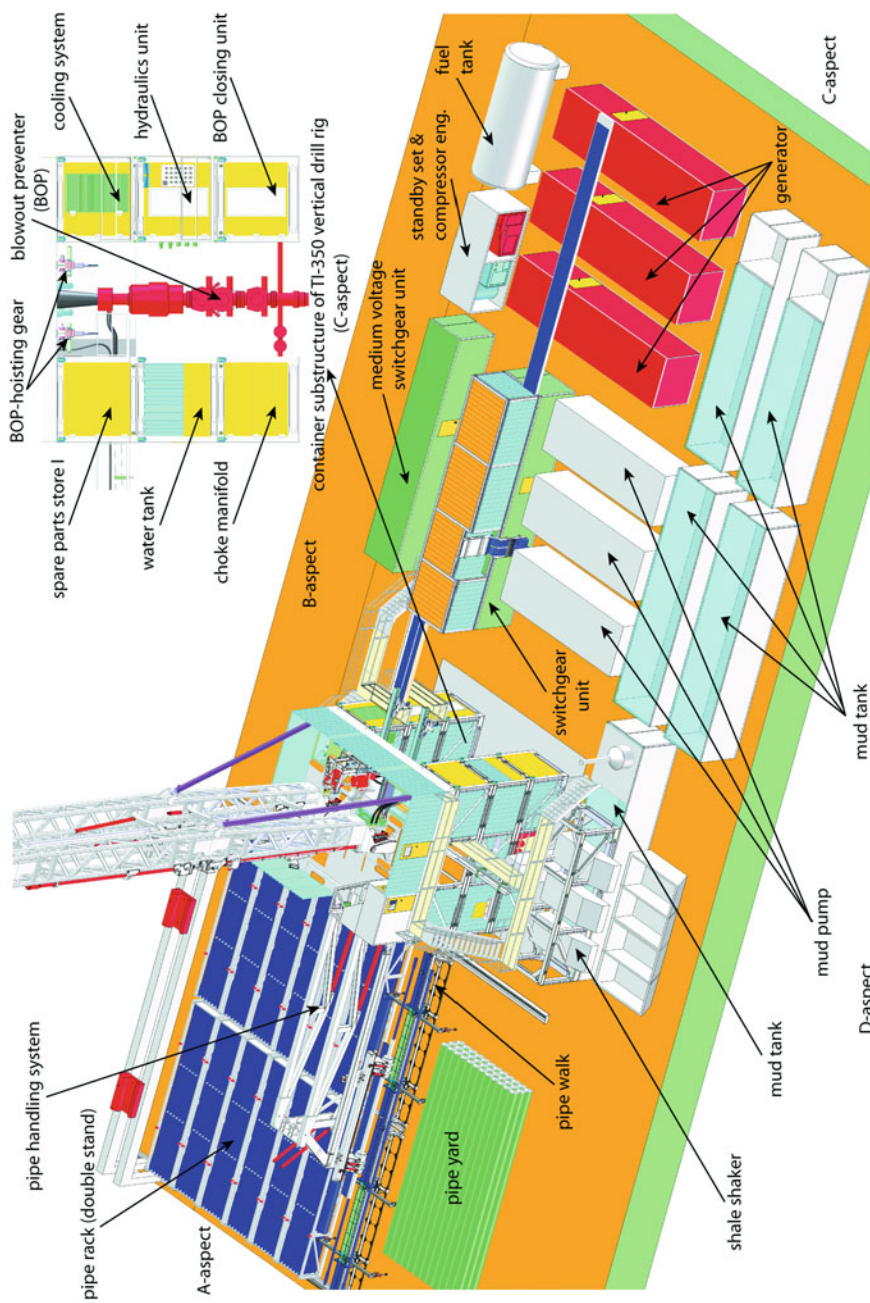


Fig. 4.13 Schematic illustration of a modern drilling site (the figure has been generously provided by Herrenknecht Vertical)

reinjection pumps are multistage, single-entry centrifugal pumps in modular design with axial inlet and radial outlet.

Geothermal energy installations typically use two kinds of fluid production pumps: Line shaft pumps (LSP) operated at the surface and electric submersible pumps (ESP) (Fig. 4.11). The pumps for lifting hot fluids to the surface must resist high temperatures, high pressures and chemically aggressive and corrosive fluids thus belonging to the most stressed components of a geothermal power plant (Sect. 15.4). ESPs lift the hot fluid with centrifugal force to the surface, where it is directed to a heat exchanger. The extracted thermal energy can then be converted to electrical power or directly fed into a district-heating grid. Combined heat and power improves energy efficiency and reduces emissions. These are particularly environmentally friendly and economical schemes.

Favorable fields for hydro-geothermal plants are above deep aquifers with high natural hydraulic conductivity and high temperatures. If the natural conductivity is too low for extracting hot water from the aquifer at the required rate the hydraulic structure of the aquifer needs to be improved by measures of artificial conductivity enhancement. Improvement measures include well shocking by sudden pumping, acidifying carbonate rocks, stimulation with high water pressures as well as combined stimulation and acidifying by pumping acid solutions with high pressure into the aquifer. Following the knowhow of the oil industry, improved extraction rates can be achieved by side tracking the well. For more on improvement measure see Sect. 8.5.

Utilization of thermal water by means of hydrothermal doublets for heating purposes is for the most part a mature technique. Hydrothermal installations that have been operating for dozens of years are currently in service worldwide. In the Munich region (Germany) a number of hydro-geothermal plants for heat and electrical power generation went into operation in recent years (Fig. 4.8). After 2013, OCR plants based on geothermal energy produced from hydrothermal doublets went into operation in many countries worldwide, including Germany, France, Turkey, Croatia, Japan, and the USA. In the Paris basin (France) geothermal systems provide thermal energy for district heating since the 1960s. Presently (2020) 35 geothermal doublets make heat available for more than 200,000 households.

Aquifer Thermal Energy Storage (ATES) systems (Sect. 8.7.2) stand for a further use of hydrothermal energy. ATES is an interesting possibility for the temporary storage of process heat from cogeneration units, gas and steam turbines, power plants or any other heat-producing device. ATES utilizes highly conductive deep aquifers. The process heat is stored in and later retrieved from the aquifer by means of deep wells using water as a heat transfer fluid. ATES can also be used for storing seasonal solar excess heat for later use in the cold season. The ATES technique can likewise be combined with cogeneration systems that produce excess heat in the warm season. In principle, shallow aquifers can correspondingly be used for cooling purposes (ATES reads then as Aquifer Thermal Energy Sink).

The heat deposited during the months of the warm season can be retrieved from the aquifer when needed by pumping warm water from the well. Because the flow velocity of groundwater in deep aquifers is low thermal losses are negligible. The efficiency of the heat reservoir increases with operating time of the system because

the temperature of the rock matrix gradually increases and with it the temperature of the entire reservoir. The warm water produced from the aquifer can be kept at constant temperature using heat exchangers and heat pumps. The ATES systems, therefore, produce thermal energy in water at constant temperature ideal for district heating purposes.

Special cases of hydro-geothermal installations are balneological spas utilizing thermal deep waters. In addition to the use of hot water in the bathing pools, the pumped thermal water is also used for the heating of buildings in the local area. After use, the raw sewage is cleaned but not reinjected into the aquifer.

Hydro-geothermal systems may also utilize thermal water in highly permeable fault and fracture zones underground. However, it is geologically challenging to identify water-conducting fault zones during pre-drilling exploration. Seismic exploration, analysis of the local stress field and numerical geomechanical modeling may help to identify mechanically damaged zones in solid rocks. However, the hydraulic conductivity and the presence of transferable thermal water cannot be demonstrated with certainty before drilling (Sect. 11.1).

Enhanced-Geothermal-Systems (EGS): The future core systems of deep geothermal energy utilization are petrothermal systems that extract heat from hot rocks characterized by relatively low hydraulic conductivity (Fig. 4.1). The systems are known under a variety of names reflecting the historical development of deep petrothermal techniques. The names include: Hot-Dry-Rock (HDR), Deep-Heat-Mining (DHM), Hot-Wet-Rock (HWR), Hot-Fractured-Rock (HFR) and Stimulated- or Enhanced-Geothermal-Systems (SGS, EGS). The original name HDR reflects the erroneous concept that basement rocks at great depth are dry and devoid of an appreciable permeability. After a large number of deep wells were drilled, it became evident that deep basement rocks (granites and gneisses) at several km depths are generally fractured and that the fracture porosity contains hot and usually salty water. The hydraulic conductivity of the hot rocks at depth is relatively large. In this book we will use the name Enhanced Geothermal Systems (EGS) for these techniques. EGS extract thermal energy stored in the rock mass, in contrast to hydro-geothermal systems that use the thermal energy of water stored in the pore space of rocks. Therefore EGS do not require a heat reservoir with aquifer properties in the hydrogeological sense. EGS primarily have electrical power production in mind, whilst heat is a secondary byproduct. Consequently target temperature is 200 °C and beyond. The hot rocks, usually crystalline basement (granites and gneisses), function as a heat exchanger. Heat transfer to the surface is achieved by natural formation water present in the fracture pore space of the basement (Stober and Bucher 2007; Bucher and Stober 2010). In crustal sections with average geothermal gradients, 5–7 km deep wellbores are necessary to reach the required rock temperatures (Chap. 9). In recent years EGS technology has also been applied to compact sedimentary rocks such as sandstones. In the following, the basics of EGS in crystalline basement are briefly outlined. A detailed treatment is given in Chap. 9.

The crystalline basement of the continental crust is generally fractured in its upper part. The fractures are the result of failure of stressed rocks in the brittle deformation regime in the uppermost about 12 km thick layer of the Earth. The fractures are

flow paths for advective water transport. The hydraulic properties of the fractures depend on fracture aperture, surface roughness of fracture surfaces, connectivity and frequency of fractures and other parameters (Caine and Tomusiak 2003). The hydraulic behavior of the fractured basement corresponds to an infinite homogeneous low-conductivity aquitard.

Usually a wide range of stimulation techniques are applied to the target volume of fractured rocks. Developing an artificial heat exchanger consisting of fractured hot rocks of sufficient hydraulic bulk conductivity is the objective of the efforts. The stimulation methods include hydraulic and chemical methods. High-pressure injection of water into the borehole increases the aperture of natural fractures and unlocks partly sealed fractures therefore improving the hydraulic conductivity. Chemical stimulation removes mineral coatings on fracture surfaces, remains of drilling mud and remnants of grout in the near borehole environment. The measures aim at improving the hydraulic properties of the heat reservoir and enhancing the hydraulic contact to the wellbore in particular. The target interval of the well for stimulation can be separated using packer systems. Successful stimulation permanently improves the hydraulic properties of the heat reservoir. After stimulation displaced faults and fracture surfaces may undergo some stress relaxation causing thereby measurable microseismicity (Sects. 9.4 and 11.1). Quartz sand and proppants can support open conductive fracture systems (Stober 2011).

Once the reservoir is established injected water passes the fractured rock heat exchanger at depth and scavenges heat from the rock mass. In addition, EGS use natural formation water as the heat transfer medium. Heat extraction at depth takes place in a nearly closed water cycle. The extracted thermal energy reaches the surface via a production well and can be converted to electrical power and also used directly for district heating.

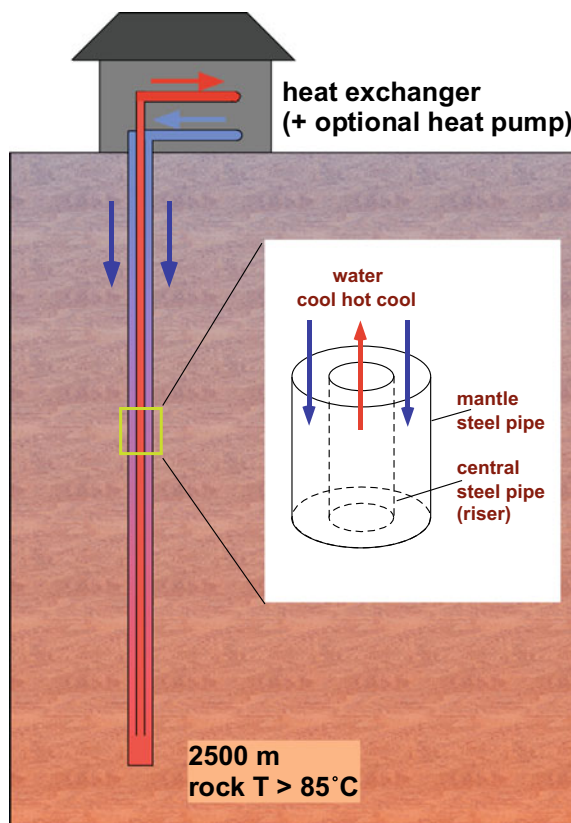
The EGS concept uses deep hot fractured rocks with relatively low permeability and does not depend on high-yield aquifers. In principle, an EGS project can be realized anywhere. However, valuable projects aim for locations with raised geothermal gradients and a suitable tectonic setting. In 2011, only one single EGS plant was operational worldwide. The plant is located in Soultz-sous-Forêts (France) in the upper Rhine rift valley and is in continuous operation since 2007. The yield of the production well GPK2 increased during operation of the plant as a result of flushing of fractures and pore space and because of chemical fluid-rock interaction (Schmidt et al. 2018). Although other long-term experience does not exist, EGS will probably play an important role for the electrical power production in the years to come. Their fundamental advantage over other environmentally friendly energy systems is the supply of base load electric power.

Deep geothermal probes (DGP): Deep geothermal probes are, in principle, also a form of petrothermal systems (Fig. 4.1). Here, a probe extracts thermal energy from any kind of rock or rock sequence using a closed loop of heat transfer fluid in a deep probe. Deep geothermal probes are used exclusively for heat supply. Because of the relatively low process temperature of the probes, electrical power cannot be generated with presently available technology.

The technology of deep geothermal probes is comparable to that of near surface probes, either coaxial vertical heat probes or double U-tube probes. In a deep probe a heat transfer fluid is circulated in a single borehole to depths of up to 3000 m (Fig. 4.14). The system does not require permeable rocks at depth and thus can be installed wherever. Particularly well suited for installation of deep geothermal probes are existing old abandoned deep wellbores (e.g. from the oil industry). If an old well is planned to be reused as deep geothermal probe the location of the consumer of the thermal energy should be close to the old well (<1 km). Because of the closed loop, deep probes do not chemically interact with the deep heat reservoir. The utilization of the deep probes combines other heat producing facilities in an integrated heating central. The heat production of a deep geothermal probe can be in order of 300 KW_{th} depending on the local conditions. Examples of deep geothermal probes include the following locations: Prenzlau, Aachen, Arnsberg (Germany); Newcastle (UK).

Heat transfer from the hot rocks occurs by heat conduction through the grouting of the probe and the casing to the advecting fluid. Ammonia is a commonly used heat transfer fluid. The cool fluid slowly flows downward in the annulus of a double-containment pipe system and is gradually heated by the surroundings by conductive

Fig. 4.14 Schematic drawing of a deep geothermal probe. It operates as a single borehole heat exchanger. The probe extracts heat at depth and transfers it to the surface heat exchanger (in combination with an optional heat pump) in a closed loop



heat transfer from the ground. The descend velocity is typically in order of 5–65 m min⁻¹. The steel casing should have a diameter of more than 7" (18 cm). In a thermally insulated central pipe thermal energy is taken to the surface by the heated fluid (Fig. 4.14). The central pipe is typically made of polypropylene. An optimal insulation of the central pipe minimizes heat losses and significantly improves the efficiency of the probe. At the surface, heat is extracted from the hot fluid by a surface heat exchanger supplemented by an optional heat pump depending on the preferred temperature level on the end user side. The cooled fluid (15 °C) is pumped back to the annulus. The heat extraction process cools the underground in the vicinity of the probe.

The amount of effective heat produced by a deep probe depends primarily on the temperature of the ground. Thus areas with a positive thermal anomaly are economically particularly gainful. Further parameters controlling the productivity of a deep probe include the thermal properties of the ground, particularly the thermal conductivity, the total time of operation, the technical layout of the probe, and the thermal properties of the casing and screen materials used. Long and large-diameter probes have evidently a large heat exchange surface. Research has shown that coaxial deep probes (Fig. 4.14) extract more total thermal energy than double U-tube probes. A thermally insulating grouting is used for the upper sections of a DGP, whilst the middle and deep section are grouted with highly conductive cement.

The deep geothermal probe of the urban district Triemli in Zurich (Switzerland) may serve as an example of a DGP system (Keiser and Butti 2015). Originally an unsuccessful 2708 m deep thermal water well has been fitted with a DGP in 2011. The probe extends to 2371 m and temperature at its base is 94 °C. The existing wellbore is fitted with steel pipes. However, the lower part of the bore (below 2371 m) has been grouted because its diameter was too small for the installation of an inner pipe. The 10 cm diameter inner pipe consists of glass fiber reinforced plastic (FRP) and extends to 2350 m depth. The average temperature of the heat transfer fluid is 43 °C. A heat pump at the surface increases this temperature. After initial startup, the heat transfer fluid circulates without using a pump solely driven by gravity and temperature difference. The DGP produces 300 KW_{th}. 28 geothermal probes and a natural gas boiler in addition to the DGP produce the energy for space heating and hot water preparation for 200 households. 80% of the thermal energy is produced by the geothermal installations in this bivalent system.

Further fields of use of deep geothermal energy sources include: Heat from deep underground mines, rock caverns and storage of thermal energy in deep geological structures (see comments on thermal use of mine water in Sect. 4.1).

The structure of thick rock sequences is often characterized by properties that are transitional or mixed between hydro-geothermal and petrothermal systems. It became evident in recent years that there is a lower limit for the natural hydraulic conductivity of the target reservoir formation in order to run an EGS system cost-effective. Stimulation methods may improve bulk conductivity by a factor of 5 at most, but a factor of 100 cannot be achieved. Fault zones possibly have a high local hydraulic conductivity potentially supporting high circulation rates for both hydrothermal and EGS plants. However, fault zones always must be seen in context

with the local geology and the undamaged host formation. Fault zones are never stand-alone utilization options. Fault zones typically show a complex internal structure of dense impermeable fault cores and damaged zones of high permeability. The detailed structure decides whether or not a given fault zone is suitable for a geothermal installation.

The different types of deep geothermal systems presented in Sect. 4.2 can be regarded as “end-member” systems. Often systems are combined hybrid systems reflecting the geological complexity of the ground and economical requirements in an optimal manner.

Besides the low-enthalpy hydro-geothermal and enhanced geothermal systems introduced above, high-enthalpy steam or two-phase systems are used for electrical power and thermal energy production mostly in active volcanic areas (Table 3.1; Sect. 4.4 and Chap. 10).

4.3 Efficiency of Geothermal Systems

Efficiency characterizes the degree of conversion of primary thermal energy to mechanical and finally electrical energy. Efficiency is the ratio of output to input, or benefit to effort. Because of the second law of thermodynamics, this ratio is always smaller than one. The Carnot efficiency η describes the maximum possible efficiency for any heat engine. It relates the maximum of work that can be produced by the system to the amount of heat put into the system. It is the theoretically possible maximum efficiency for an ideal heat engine. The efficiency of real systems is related to the Carnot efficiency η . The system design aims to reach efficiencies as close as possible to η . The Carnot efficiency η is defined by Eq. 4.1:

$$\text{The Carnot efficiency } \eta = 1 - (T_c/T_h) = W/Q_{\text{th}} \quad (4.1)$$

where T_c corresponds to the temperature of the cold side, the outlet T of the fluid, and T_h the temperature of the hot side, the inflow T of the heat carrier fluid (both in Kelvin). This can also be expressed by the ratio of work done by the system (W) to the thermal energy added to the system (Q_{th}). The Carnot efficiency η of a system with, for example, an inlet $T_h = 100^\circ\text{C}$ (373 K) and $T_c = 20^\circ\text{C}$ (293 K) has a theoretical maximum of 0.21 (21%) (Fig. 4.15).

The physical upper limit of thermal efficiency for power stations driven by thermal water (hydro-geothermal or EGS plants) of 100–200 °C is about 12–22%. In this temperature range, electricity production is feasible only with binary loop plants (Fig. 4.16). Two different systems are available on the market, systems based on the Organic Rankine Cycle (ORC) and systems based on the Kalina Process. ORC systems use organic fluids, typically isobutane, as heat transfer fluid. Kalina systems work with a zeotropic mixture of ammonia and water. Zeotropic mixtures boil over a certain temperature interval called temperature glide (in contrast to azeotropic mixtures where the liquid and the gas phase have identical compositions). The power

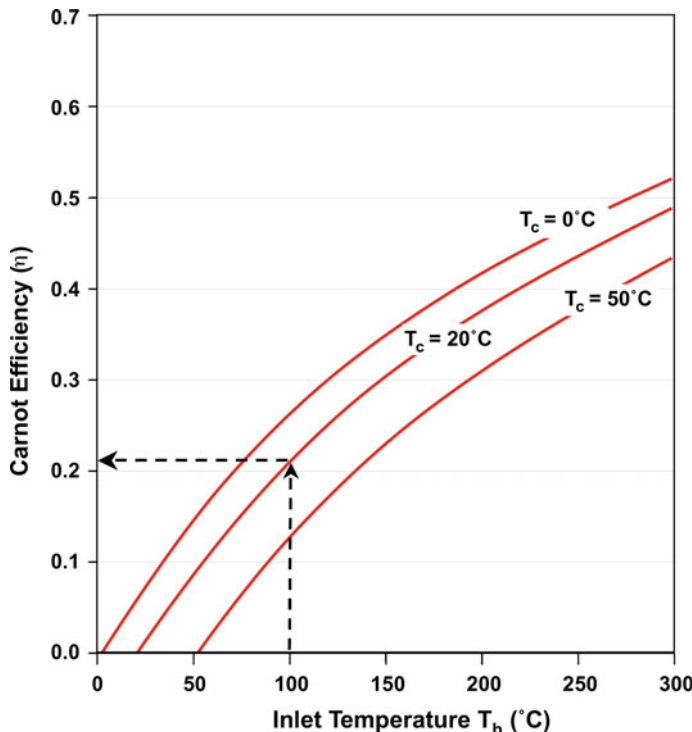


Fig. 4.15 Diagram showing the Carnot efficiency η (Eq. 4.1) as a function of the inlet temperature T_h (here in °C) for three different outlet temperatures T_c (also in °C)

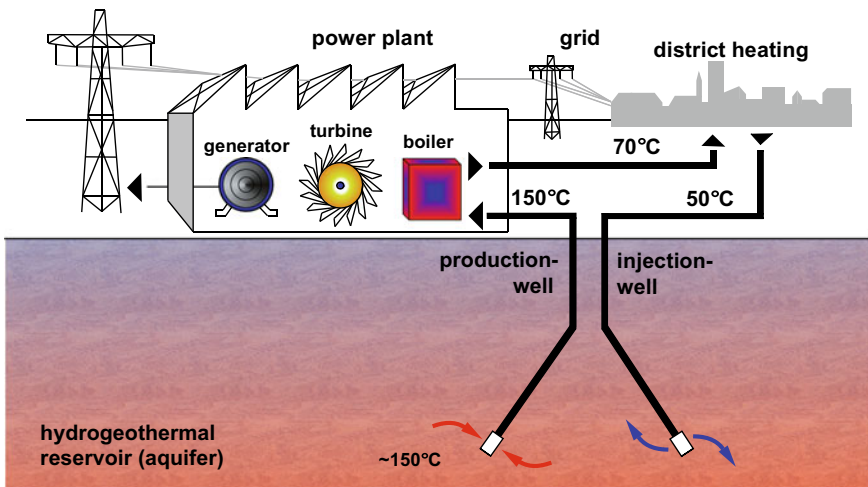


Fig. 4.16 Schematic diagram of a hydro-geothermal system with a binary system power plant converting the produced thermal energy to electricity and utilizing the process or waste heat for district heating

output to the grid of air-cooled Kalina systems tends to be higher than that of ORC systems at low input temperatures, whereas ORC plants tend to be better performers at higher input temperatures. Kalina systems withdraw less thermal energy from the thermal water than ORC systems but convert it to electrical power with higher efficiency. In the low temperature range ORC systems suffer from low thermal efficiency that follows from a high auxiliary power requirement of the cooling system, especially when air cooled (Park and Sonntag 1990). However the difference between the two systems is relatively small. An unbiased direct comparison of the overall performance of the two systems is difficult because ORC systems are widely used in many plants in contrast to very few Kalina plants presently still in operation. The other is that ORC use widely different normally organic heat transfer fluids but even including NH_3 and CO_2 (plants using these inorganic fluids are thus not ORC systems in a strict sense). Furthermore, some ORC plants operate in a two-stage mode with a high- and a separate low-temperature cycle. The thermal performance of geothermal power plants based on the Kalina cycle is very similar to that of ORC plants. The pros and cons of the two binary cycle systems have been hotly debated in the literature for geothermal applications (e.g. Kalina 2003; Mlcak 2002; DiPippo 2004; Guzović et al. 2010, 2014; Ahmad and Karimi, 2016; Deepak and Gupta 2014) and also for waste heat recovery (e.g. Nemati et al. 2017). However, a large number of ORC geothermal power plants are currently in operation worldwide and only a handful of Kalina based plants if any are currently operational (see below).

The first Kalina geothermal plant went into operation in 2000 in Húsavík, Iceland (Henry and Mlcak 2001; Mlcak 2002; DiPippo 2004). It produced 2 MW_{el} and 20 MW_{th} from geothermal water at 122 °C with a flow rate of 90 kg s⁻¹. The plant is no longer operational and has been dismantled because of severe corrosion problems. The geothermal plant in Unterhaching (near Munich, Germany) produced 3.4 MW_{el} from a Kalina system and 38 MW_{th} for district heating after commissioning in 2009. The heat reservoir is in upper Jurassic limestone (Malm) at 3350 m depth. The formation water has a temperature of 122 °C in the first well and 133 °C in the second well, respectively. In the mean time the Kalina plant has been decommissioned and the system is entirely used for district heating today. The district-heating grid is 47 km long and the geothermal system supplies 7000 households with 108 GWh thermal energy per year (2017). A geothermal power plant in Bruchsal (Upper Rhine Valley, Germany) produces 580 kW_{el} work with a Kalina system since 2009. Kalina Cycle geothermal plants are also in operation in Russia, Japan and in PR China. The many EcoGen Units in Japan are miniaturized devices working with the Kalina Cycle designed for the Japanese hot spring industry. The typical performance of the units is 50 kW_{th}.

All geothermal power plants produce heat in addition to electrical power (Fig. 4.16). This heat needs to be used in combined heat and power systems. The optimal use of the byproduct heat determines the economic success of a geothermal power plant. Moreover, production of electrical power only and pointlessly wasting the co-produced heat would be ecologically insensitive and ignorant.

The efficiency of electrical power production is relatively low. Taking the auxiliary power requirement of the production pump and the cooling loop into consideration,

the typical efficiency of the total system is about 5–7%. However, it is economically and ecologically feasible using the residual heat of the thermal water after electrical power production for district heating (Fig. 4.16) and other purposes. The environmental benefit of the total system is determined by the quantity of supplied heat. Geothermal energy systems can also be combined with other heat sources including biogas plants and hybrid plants thus improving the environmental balance.

The conversion of thermal energy to mechanical or electrical energy in thermal plants inherently produces waste or process heat that needs to be discarded. If the process heat can be transferred to lake or river water a very low temperature T_c (Eq. 4.1) and a corresponding high efficiency can be attained. However, at many sites potential environmental degradation or lack of cooling water in sufficient quantities requires cooling by means of cooling towers. Wet cooling towers (Fig. 4.9) and dry cooling towers (Fig. 4.7) transfer process heat to the atmosphere.

4.4 Major Geothermal Fields, High-Enthalpy Fields

The annual global production of electrical power from geothermal sources is about 13.5 GW_{el} (2016) (Chap. 1). Most of the geothermal electricity is produced in high-enthalpy fields that reach high temperatures at shallow depths. The electricity is generated in dry-steam and flash-steam power plants. Examples are the Coso geothermal field at the western edge of the Basin and Range geologic province in eastern California (USA), the Wairakei geothermal field in the Taupo Volcanic district in New Zealand, the Mori geothermal field in Hokkaido (Japan), the Hatchobaru geothermal field in central Kyushu (Japan) and many other similar systems worldwide.

These power plants of high-enthalpy fields function as open system geothermal installations. The systems use steam produced by decompressing the thermal heat transfer fluid to drive turbines for electrical power production (Fig. 4.17a–c). The minimum operation temperature in flash-steam plants is 175 °C. The turbine converts geothermal energy into mechanical energy that is converted to electrical energy by a generator. A part of this electrical energy is consumed by pumps and other machinery of the power plant; the net power is fed into the grid.

Electrical energy production from geothermal sources in closed binary-loop low-enthalpy systems such as ORC and Kalina cycle plants (Figs. 4.7, 4.9, and 4.17c) is a technology that has been installed at relatively few locations worldwide although suitable locations are far more frequent than high-enthalpy fields. There is an enormous potential for future development and expansion of deep low-enthalpy systems. A major disadvantage of high-enthalpy fields is their limited occurrence in volcanic and tectonically active areas along plate boundaries or extensional basins. A major breakthrough for increased geothermal energy utilization must come from petrothermal EGS systems in addition to further development of hydro-geothermal systems.

In Europe, Italy has the highest installed power of 944 MW_{el} and is well ahead of Iceland with 755 MW_{el} (2019). In Tuscany (Italy) favorable geological settings,

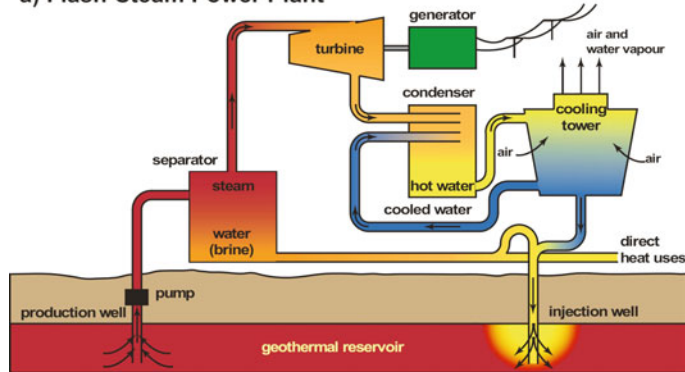
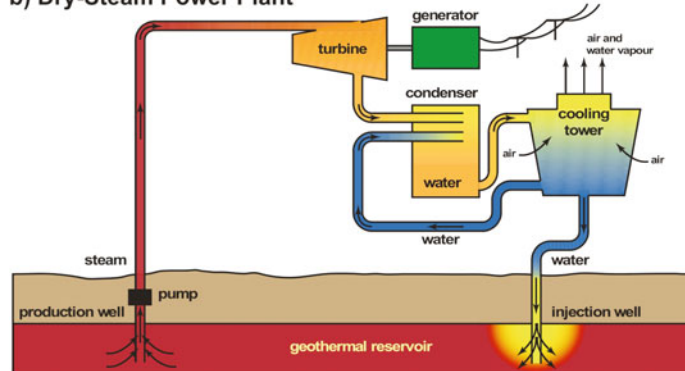
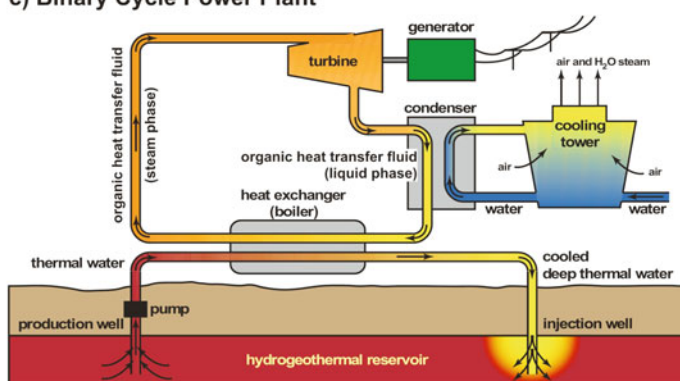
a) Flash-Steam Power Plant**b) Dry-Steam Power Plant****c) Binary Cycle Power Plant**

Fig. 4.17 Process diagrams for three common types of geothermal power plants used for electricity production: **a** Flash steam plant, **b** Dry steam plant, **c** Binary cycle power plant (inlportal.inl.gov/portal and geothermal.nau.edu)

very early development and the resulting experience led to a steady growth of the geothermal energy industry. However, the big five in the world are: USA, Indonesia, Philippines, Turkey, and New Zealand with a capacity greater than 1 GW_{el} each (Table 3.1). Other major producers of electrical power from geothermal resources include Mexico, Kenya and Japan. Much of the power of the high-enthalpy fields in these countries is produced by dry-steam plants (Fig. 4.17a).

Iceland uses mostly geothermal resources from high-enthalpy fields related to the volcanic mid-ocean ridge and the Iceland mantle plume. However, the country also installed some binary loop plants in low-enthalpy fields in recent years. The important Russian high-enthalpy fields and the associated geothermal plants are all situated in Kamchatka and on the Kuril islands. The total installed capacity is 82 MW_{el}. Turkey has an enormous geothermal energy potential. Geothermal resources have been rapidly developed in recent years and catapulted the country into the big five league (>1 GW_{el}, 2019). 10 high-enthalpy fields are on the list of identified 170 geothermal heat reservoirs. Some of the boreholes reach 200 °C already at 800 m depth. A very rapid growth of the geothermal industry has been experienced by Kenya in recent years. The installed capacity passed Iceland in 2019 (Table 3.1). The plants are located in the East African Rift Valley (e.g. Olkaria at Hells Gate). The high-enthalpy fields are associated with a geologically very dynamic continental rift system with active volcanism. The rift has the potential for producing more than 20 GW_{el} from geothermal power plants including also Kenya's neighbors (United Nations Environment Program). The Olkaria power plants are dry-steam power plants (Fig. 4.17a) fed by more than 300 about 2000–3000 m deep wells and typically produce about 100–200 MW_{el}. The power company Kenya Electricity Generating Company (KenGen) recently opened a geothermal spa similar to the famous Blue Lagoon in Iceland. A pioneering specialty of the Kenya geothermal power utilization is the installation of small power producing units directly at the wellheads. The cost effective and quickly installed devices produce between 2.5 and 7.5 MW_{el} each.

The most important and largest high-enthalpy geothermal field in the world is “The Geysers” in California (USA). The field has 1517 MW_{el} installed capacity and uses a 300 °C dry steam reservoir at 600–3000 m depth (deepest well: 3900 m). The power is produced from 100 km² drilled area, 424 production and 43 reinjection wells. Average steam temperature is 235 °C (at 12.4 bar) and the average flow rate per well 5 kg s⁻¹. The steam is produced from a sandstone and graywacke reservoir that is heated by a magma chamber at greater depths.

As a result of the power production and the associated reduction of steam pressure the ground became seismically active after about 1975. Seismic events reached magnitude M_L = 4 (Sect. 11.1). Seismic tremors correlate with the power production and the related rate of steam extraction from the reservoir even though a part of the condensed and cooled steam is reinjected to the reservoir. The steam pressure in the reservoir is decreasing by about one bar annually since 1966. The increased seismicity relates to reservoir compaction because of reduced pore pressure due to withdrawal of fluid and thermal contraction resulting from cooling (Nicholson and Wesson 1990).

“The Geysers” reached peak production of 1900 MW in the year 1989. After that, maximum continued steam withdrawal resulted in aging of the reservoir and a decrease of steam pressure. In the last decade additional water injections partly compensate the withdrawals. In 2011, about 800 kg/s cleaned municipal wastewater from Clear Lake and Santa Rose props up the reservoir. The measures slowed down reservoir degradation and total power output resumed.

The second largest geothermal field is Cerro Prieto, Mexico with 820 MW_{el} and 149 production and 9 reinjection wells. The liquid fluid reservoir at 2800 m depth is in the temperature range of 300–340 °C. At Cerro Prieto 13 dry steam power plants produce the electrical power. The facility is located in south Mexicali, Baja California, in Mexico.

The Malitbog Geothermal Power Station on the Philippines is the largest single geothermal power plant with a capacity 233 MW_{el}.

The history and development of the high-enthalpy field Larderello in Tuscany (Italy) is separately described in Sect. 2.2. In the high-enthalpy geothermal field of Larderello the heat flow density is very high and locally reaches 1000 mW m⁻². Two different geothermal reservoirs are currently used by the geothermal industry. The shallow reservoir extends from 700 to about 1000 m depth and a deep reservoir located in fractured metamorphic basement rocks ranges from 2000 to 4500 m depth. The highest measured temperature in wellbores was 400 °C (Bellani et al. 2004).

Today (2019), the total installed capacity of the Larderello geothermal dry steam plants is 795 MW_{el} equivalent to the power of a modern coal-fired power plant. Like with all other plants in high-enthalpy fields, the production costs for the unit of electrical power output is low because there are no fuel costs (coal, oil, fuel rods). Some of the production wells produce up to 350 t h⁻¹ (100 kg s⁻¹) steam at a temperature of 220 °C. The installations at Larderello inject all water not used in the cooling loop back into the reservoir. However, the losses or unbalanced difference between extraction and reinjection caused deterioration of the steam pressure and, as a result, a decline in power production. In the reservoir, the thermal energy is still there but the heat transfer fluid, here steam, is lacking or no longer present in sufficient amounts.

The plant operator ENEL (Ente Nazionale per l’Energia Elettrica) designed a program to revitalizing the high-enthalpy field. The exploited steam reservoirs are replenished with water from neighboring fields. New deep wells replace older shallow wells. This new technique permits to increase the working pressure from presently 4.5 to 5.0 bar to 12 bar. New 60 MW power blocks replace the array of old 20 MW turbines.

Because of the geologic position of Iceland on the Mid-Atlantic Ridge and above the Iceland mantle plume, a multitude of volcanoes is presently active on the island. The geothermal fields associated with the volcanoes are extensively utilized and Iceland is the leading geothermal country (Sect. 2.2). 53% of the used primary energy is geothermal energy. Six larger geothermal power plants produce 26% of the island’s consumption of electricity and 90% of the households are supplied with heat. The installed geothermal capacity of the plants on Iceland is about 735 MW_{el} including the first development stage of the Theistareykir (Þeistareykir) geothermal field in

northern Iceland (hydroelectric systems 1986 MW_{el}, fossil fuel plants 114 MW_{el} and wind energy 2 MW_{el}). Several geothermal plants mainly of the flash steam type (Fig. 4.17b) produce electrical power. The Hellisheiði Power Station in southwestern Iceland 30 km East of Reykjavik uses the geothermal power of the Hengill volcanic field. With its 303 MW_{el} and 133 MW_{th} used for Reykjavik district heating. The plant is operated by ON Power of Reykjavik Energy and is the third largest single geothermal power station in the world (The Sarulla plant in Indonesia and the Tiwi plant on the Philippines have a design capacity of 330 MW_{el} each. Global Energy Observatory).

The hot water for the capital city of Reykjavik with its 120,000 inhabitants, including the hot water for deicing installations for sidewalks and roads, is supplied by warm water reservoirs, the so-called Perlan at an elevated height above the city making pumps unnecessary. The reservoir consists of five single tanks with 4000 m³ capacity of 85 °C hot water each. The hot water is produced from 70 drilled wells in the city. In addition, the power stations at Hellisheiði and Nesjavellir East of Reykjavik provide hot water to the city that has been geothermally heated to 80 °C.

The hot waters produced from high-enthalpy fields in Iceland, like in any other area, typically contain a large amount of dissolved solids. The hot waters are normally not in chemical equilibrium with the minerals of the reservoir rocks. Therefore, the waters react with the rock matrix in complex hydrothermal reactions. The total mineralization increases with temperature because for many substances and minerals the solubility increases with temperature and since the kinetics of mineral dissolution reactions increases with temperature (Chap. 15). Because of the water-rock interaction, the waters regularly contain high concentrations of dissolved silica. At low temperature, only small amounts of silica can stay in water under equilibrium conditions. Thus, precipitation of silica sinter and silica scale is a common occurrence and problem in high-enthalpy fields. The rate of silica precipitation depends on the temperature and the composition (salinity) of the water, which allows to partly controlling the site of precipitation in the system to some degree. The efficient pressure-controlled separation of steam and liquid (Fig. 4.17a–c) is crucial to avoiding silica scales in surface installations, such as turbines or heat exchangers (Sect. 15.3). The expanded steam from high-enthalpy reservoirs on Iceland contains 5 mg kg⁻¹ dissolved solids only in contrast to the separated liquid phase that contains 45,000 mg kg⁻¹ total dissolved solids (Giroud 2008). The major components in most thermal fluids are sodium, potassium and calcium and the associated anion is normally chloride. Dissolved silica is typically in the range of 600–700 mg kg⁻¹ SiO₂ (this compares to the equilibrium concentration of 6 mg kg⁻¹ at 25 °C). Boron, fluoride, barium, mercury and other trace elements can be significantly enriched. The high TDS of the produced fluid and solutes that are partly difficult to cope with are a serious challenge to the high-enthalpy geothermal plants. Some of the reservoir fluids also contain high concentrations of dissolved gasses, which are not condensable like CO₂ and H₂S. Degassing of high CO₂ concentrations promote calcite scale formation and CO₂ is corrosive. High H₂S concentrations may cause metallurgical problems, react with metal surfaces, cause corrosion, fatigue and cracking (Sect. 15.3).

The Iceland Deep Drilling Project (IDDP) with several international partners drilled a wellbore into a hot-fluid reservoir containing H₂O in its supercritical state. Reservoir conditions are T > 375 °C at P ~ 225 bar. The critical point of H₂O (CP) is at the coordinates T = 374 °C and P = 221 bar. It is planned to utilize the supercritical fluid for power production. The development and utilization of supercritical fluid reservoirs appears attractive because the system efficiency may be improved by a factor between 5 and 10 in relation to the produced fluid volume.

Wells on Iceland may reach 360 °C at a depth of only 2200 m in some places, meaning that *P-T* conditions are close to the critical point of H₂O. The fluids are often toxic and very corrosive. Further challenges are scales that are difficult to control and problematic to remove and dispose without harm to the environment.

The development of very deep high-enthalpy reservoirs for industrial use is presently not workable due to technical reasons. At temperatures of 400 °C and more, the temperature resistance of materials, of drilling mud and geophysical instruments, the materials strength and limited hook load (<500 t) of drilling rigs pose serious difficulties.

4.5 Outlook and Challenges

Projections predict a total installed world capacity of geothermal electricity production of 140 GW_{el} for the year 2050 (Fridleifsson et al. 2008). This ambitious goal can only be reached if the EGS systems, which are relatively independent on location in contrast to high-enthalpy plants, are being further industrially developed. Additionally, existing geothermal fields must be further developed with increasing numbers of production and reinjection wells. Systems with production wells only are not environment friendly and economically not profitable. Geothermal reservoirs must be backed, that is to say they must be replenished and renewed. Reinjection recycles the highly mineralized fluids to the original reservoir, which also helps to prevent dislikable subsidence of the ground, reduction of reservoir permeability and an associated decrease of power production. The development of a geothermal field must be inclusive and integrate all potential users from the beginning of the planning stage: In addition to electricity production, this includes the utilization of the produced heat in industry, district heating, sports facilities, green houses and other secondary heat users.

References

- Ahmad, M. & Karimi, M. N., 2016. Thermodynamic analysis of the Kalina Cycle. International Journal of Science and Research, 5, 2244–2249
ASHRAE Handbook, 2007. “HVAC Applications,” SI Edition, Atlanta (USA).

- Bao, T., Liu, Z., Meldrum, J. & Christopher Green, Ch., 2018. Large-Scale Mine Water Geothermal Applications with Abandoned Mines. In Zhang, D., & Huang, X. (Eds.): GSIC 2018, Proceedings of GeoShanghai 2018. International Conference: Tunneling and Underground Construction, pp. 685–695, 2018. Springer Nature Singapore Pte Ltd. 2018.
- Bellani, S., Brogi, Lazzarotto, A., Liotta, D. & Ranalli, G., 2004. Heat flow, deep temperatures and extensional structures in the Larderello Geothermal Field (Italy): constraints on geothermal fluid flow. *Journal of Volcanology and Geothermal Research*, 132, 15–29.
- Bucher, K. & Stober, I., 2010. Fluids in the upper continental crust. *Geofluids*, 10, 241–253.
- Caine, J. S. & Tomusiak, S. R. A., 2003. Brittle structures and their role in controlling porosity and permeability in a complex Precambrian crystalline-rock aquifer system in the Colorado Rocky Mountain Front Range. *GSA Bulletin*, 115(11), 1410–1424.
- Deepak, K. & Gupta, A.V. S. S. K. S., 2014. Thermal performance of geothermal power plant with Kalina cycle system. *International Journal of Thermal Technologies*, 4, 61–64.
- DiPippo, R., 2004. Second Law assessment of binary plants generating power from low-temperature geothermal fluids. *Geothermics*, 33, 565–586.
- Fridleifsson, I. B., Bertani, R., Huenges, E., Lund, J. W., Ragnarsson, A. & Rybach, L., 2008. The possible role and contribution of geothermal energy to the mitigation of climate change. In: PCC Scoping Meeting on Renewable Energy Sources, Proceedings (ed Trittin, O. H. a. T.), pp. 59–80, Luebeck, Germany.
- Giroud, N., 2008. A Chemical Study of Arsenic, Boron and Gases in High-Temperature Geothermal Fluids in Iceland. Dissertation at the Faculty of Science, University of Iceland, 110 p.
- Guzović, Z., Lončar, D. & Ferdelji, N., 2010. Possibilities of electricity generation in the Republic Croatia by means of geothermal energy. *Energy*, 35, 3429–3440.
- Guzović, Z., Rašković, P. & Blatarić, Ž., 2014. The comparision of a basic and a dual-pressure ORC (Organic Rankine Cycle): Geothermal Power Plant Velika Ciglena case study. *Energy*, 76, 175–186.
- Hall, A., Scott, J.A. & Shang, H., 2011. Geothermal energy recovery from underground mines. *Renew. Sustain. Energy Rev.* 15, 916–924.
- Henry, A., & Mlcak, P. E. 2001. Design and Start-up of the 2 MW Kalina Cycle® Orkuveita Húsavíkur Geothermal Power Plant in Iceland. European Geothermal Energy Council 2nd Business Seminar EGEC 2001.
- Ibrahim, O. M., 1996. Design Considerations for Ammonia-Water Rankine Cycle. *Energy*, 21, 835–841.
- IGSHPA, 1994. Closed-Loop Geothermal Systems—Slinky Installation Guide #21050. (Fred Jones), Oklahoma State University, ISBN-13: 9780929974040
- Jessop, A. M., MacDonald, J. K. & Spence, H., 1995. Clean energy from abandoned mines at Springhill. *Energy Sources* 17, 93–106
- Kalina, A. L., 1984. Combined-Cycle System with Novel Bottoming Cycle. *Journal of Engineering for Gas Turbines and Power*, 106, 737–742.
- Kalina, A., 2003. New binary geothermal power system. International Geothermal Workshop, Sochi Russia. *Geothermal Energy Society*, 1–11.
- Kavanaugh, S. P. & Rafferty, K., 1997. Ground source heat pumps—Design of geothermal systems for commercial and institutional building. *ASHRAE Applications Handbook*, Atlanta, USA
- Keiser, U. & Butti, G., 2015. Ökonomische Analyse der Tiefen Erdwärmesonde Triemli vom EWZ.- Schlussbericht energieschweiz, Bundesanstalt für Energie BFE, 35 S., Bern/Schweiz.
- Limanskiy, A. & Vasilyeva, M., 2016. Using of low-grade heat mine water as a renewable source of energy in coal-mining regions. *Ecol. Eng.*, 91, 41–43.
- Mlcak, H.A., 2002. Kalina cycle® concepts for low temperature geothermal. *Geothermal Res. Council Trans.*, 26, 707–713.
- Nemati, A., Nami, H., Ranjbar, F. & Yari, M., 2017. A comparative thermodynamic analysis of ORC and Kalina cycles for waste heat recovery: A case study for CGAM cogeneration system. *Case Studies in Thermal Engineering*, 9, 1–13.

- Nicholson, C. & Wesson, R. L., 1990. Earthquake Hazard associated with deep well injection—a report to the U.S. Environmental Protection Agency, pp. 74, U.S. Geological Survey Bulletin.
- Park, Y. M. & Sonntag, R. E., 1990. A Preliminary Study of the Kalina Power Cycle in Connection with a Combined Cycle System. International Journal of Energy Research, 14, 153–162.
- Rybäch, L., Wilhelm, J. & Gorhan, H., 2003. Geothermal use of tunnel waters—a Swiss speciality. International Geothermal Conference, Reykjavík, Sept. 2003, S05 Paper 051, 17–23.
- Schmidt, R.B., Bucher, K. & Stober, I., 2018. Experiments on granite alteration under geothermal reservoir conditions and initiation of fracture evolution. Eur. J. Mineral., 30, 899–916. <https://doi.org/10.1127/ejm/2018/0030-2771>.
- Stober, I., 2011. Depth- and pressure-dependent permeability in the upper continental crust: data from the Urach 3 geothermal borehole, southwest Germany. Hydrogeology Journal, 19, 685–699.

Chapter 5

Potential and Perspectives of Geothermal Energy Utilization



Drill bits

Geothermal energy is renewable energy in the sense that heat extraction by technical systems is replenished by heat flow from the heat reservoir of the Earth. The latter is virtually inexhaustible at human time scales (Sect. 1.3). Although the ultimate heat reservoir is in effect everlasting, the question of sustainability of geothermal energy utilization must be answered for each individual site, plant and location separately because it depends on the system design and the dimensioning of the installation.

At almost all sites, terrestrial heat flow is too low to balance the heat extracted for use in the power plant. Normally the geothermal system uses heat stored in a reservoir, which consequently cools for a certain period of time before it is replenished by heat flow from depth again. The heat flow density is insufficient in supplying the bore-hole heat exchangers for heating buildings alone. Because of this, the sustainability of the utilization of near surface geothermal energy is controversial. The removal of heat in shallow ground layers employing geothermal probes may overexploit a limited resource and may lead to continuous temperature decrease of the soil, which would eventually not be economically meaningful. The plausible fears and concerns, however, overlook the significant external heat supply to the ground by solar radiation. The solar contribution to the total of removed ground heat is typically distinctly larger than the amount provided by the heat flow from the interior. All borehole heat exchanger systems gradually approach a steady state where the removed heat is balanced with the recharge heat with its solar and terrestrial components. Along the path to the steady state the soil cools, initially fast then slower and finally approaches a constant steady state temperature. After a few years operating the installations, the annual temperature decrease is minimal (Eugster 1998).

Advectional heat transfer by groundwater flow, not considered in the analysis above, may have an additional and often significant effect on the heat budget of a geothermal installation. If borehole heat exchangers intersect groundwater-bearing strata (aquifers) then a large portion of the extracted heat is directly replenished by the advecting groundwater. Advectional heat transfer may dramatically increase the efficiency of the ground source heat exchanger (Sect. 6.3.2). Direct use of geothermal energy from groundwater wells draws on groundwater advection (Sect. 7.3).

In deeper ground, outside the reach of solar heat input, the situation is different and the extraction of ground heat mines a heat reservoir that is sluggishly replenished (Sect. 8.3). In open systems, the cooled thermal water must be returned to the reservoir via an injection well for sustainable operation. Depending on local conditions, system design and extraction rates, and the temperature of the produced thermal water may continuously decrease after a certain operation time. If production rate is too high, the distance between production and injection well is too small and/or the temperature of the re-injected fluid is too low, then the economic efficiency of the geothermal system is at stake. The production could be forced to be reduced or even discontinued until the reservoir temperature recovers. Therefore, deep geothermal systems should not be planned and designed without appropriate numerical modeling of the heat and fluid transfer under various conditions of operation. During operation, modeling must be continued and accompanied with appropriate monitoring programs providing the appropriate data (Sect. 8.8). The total lifetime of the installation can be estimated

from simulation of the reservoir response to plant operation and sound prognosis of system progression may be possible if quality data are available.

Today, the global production of electrical energy from geothermal sources is absolutely dominated by the high-enthalpy fields (Sect. 4.4; Chap. 10). The geodynamic setting of high-enthalpy fields results in high geothermal gradients and correspondingly require typically short shallow level drill holes to reach the reservoirs with hydrothermal fluids of 300 degrees centigrade and above (Sect. 1.4). Depending on the *P-T* conditions at the reservoir, the systems can be steam or liquid (water) dominated. State-of-the-art also in high-enthalpy fields is the reinjection of the cooled liquid-phase to the reservoir. The condensed steam phase is often non-hazardous and it could be discharged into surface waters. However, it is recommended to inject this water also for safeguarding the reservoir (Sect. 4.4).

Because of the small temperature difference between supply and return flow in low-enthalpy installations, the maximum efficiency of these systems is intrinsically lower than that of high-enthalpy systems. The secondary loops used in low-enthalpy plants (ORC, Kalina) presently consume up to 25% of the produced electricity for pumps and other equipment (Sect. 4.2). However, low-enthalpy geothermal plants have a great potential and probably an excellent economic future because of their relative insensitivity to the local geological setting.

Direct use of geothermal energy for local and district heating networks is widely used today (2020). We expect that geothermal energy utilization will further expand particularly on the heat supply market. The geothermal heat will save fossil fuels for more valuable products. The development and perspectives of geothermal heat utilization depends strongly on political programs for supporting or subsidizing geothermal energy in the different countries.

The use of near-surface geothermal energy, particularly by borehole heat exchangers and groundwater well systems substantially increased during the past years. There is a rapidly growing market for installations for heating and cooling of buildings, both for private homes and for business and office buildings. A further rapid development is seen in systems that combine geothermal energy extraction from the ground with solar-thermal systems including storage of excess heat in the ground during summer for retrieval during the cold season. Because these systems operate with electrically driven heat and fluid pumps, energy efficiency and ecological value are determining factors for the economic benefit also.

Increasingly difficult political conditions for the use of fossil energy resources trigger an enlarged demand for geothermal heat energy from sources that are available everywhere at any time. This is particularly obvious on the background of the fact that about one third of the total energy consumption in areas of middle latitudes goes into heating. Cities and metropolitan areas will revise heat supply concepts and develop efficient district heating systems. Annual and seasonal municipal heat energy management will require new concepts for ground utilization as a heat energy storage reservoir. Geothermal energy utilization techniques will be central and indispensable in the future energy industry.

References

- Eugster, W. J., 1998. Longterm behavior of the geothermal probes at Elgg (Zurich, Switzerland) (in German). In: Projekt 102, Polydynamics, pp. 38, Schlussbericht PSEL, Zürich.

Chapter 6

Geothermal Probes



Drilling equipment for shallow wells

6.1 Planning Principles

The basic condition of near-surface geothermal energy utilization is the low temperature of the thermal reservoir. The temperature is typically lower than the working temperature of house heating. The heat transfer fluid in house heating systems requires a minimum temperature of about 20–30 °C, whereas ground temperatures are typically in the range of 5–15 °C. Therefore, in order to use the geothermal energy for the heating of buildings the transfer fluid temperature must be increased by means of a heat pump system. The highest reservoir temperatures are accessible to geothermal probes. Depending on the depth of the probe, drillhole heat exchangers may provide fluid temperatures of 10–12 °C depending on the local conditions (Central Europe). The temperature increase needed by the house heating system is then done by the heat pump. Most heat pumps are driven electrically. Electricity is expensive and produced with large losses from fossil energy resources in most countries.

For this reason in the run-up of geothermal energy utilization, a project should make each effort to reduce the heat demand of the planned building or object. This includes thermal insulation measures such as façade and roof insulation, high quality insulating and heat absorbing glass windows.

The economic efficiency of the system and its environmental value depends critically on the required heating temperature. The temperature for underfloor heating systems is typically about 35 °C, active cover or concrete core activation requires about 25 °C only, whereas heating with the classical hot-water radiators craves 45–65 °C flow temperature. These considerations can be easily integrated in the planning of new buildings leading finally to an economically and ecologically optimal heating system. More problematic are restorative measures in existing buildings.

To promote sustainability and long term operation of the heating system it is important to limit the withdrawal of thermal energy from the ground during the annual house heating period to the natural heat influx to the reservoir. Heat extraction must be balanced by natural regeneration.

Still, the optimal layout of a geothermal probe depends on a detailed and correct description of the drilled geological layers independent of the drilling method used.

6.2 Construction of Ground Source Heat Exchangers

Geothermal probes are liquid-filled tubes installed in a borehole. There are different types of geothermal probes including single U-tube probes, double U-tube probes and coaxial probes (Fig. 6.1). Single U-tube probes are closed seamlessly drawn plastic tubes with a U-shaped foot. Double U-tube probes are two independent single U-tubes installed in the borehole. Cool liquid flows downward in the tubes and accumulates heat from the surrounding ground. The warmed liquid turns around in the U-shaped foot at bottom hole and flows back to the heat pump at the surface. The heat pump uses the extracted ground heat to increase the fluid temperature of a secondary cycle so that it can be used for heating purposes. Coaxial probes contain the return tube

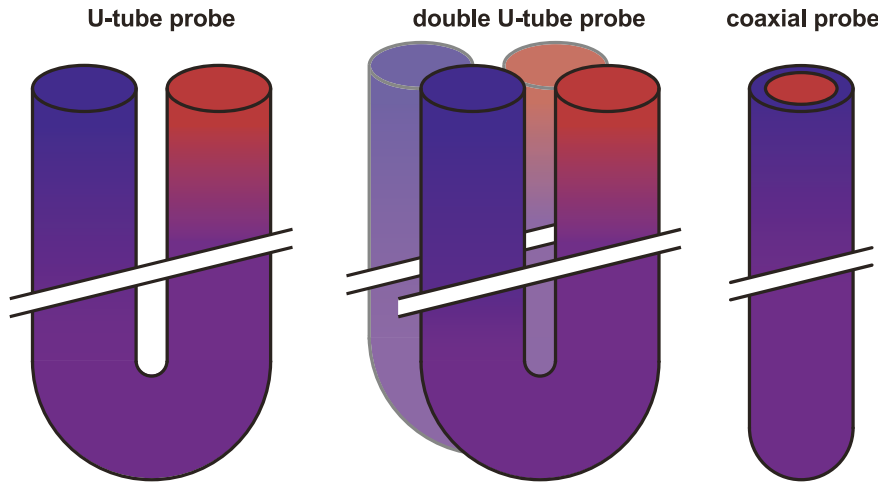


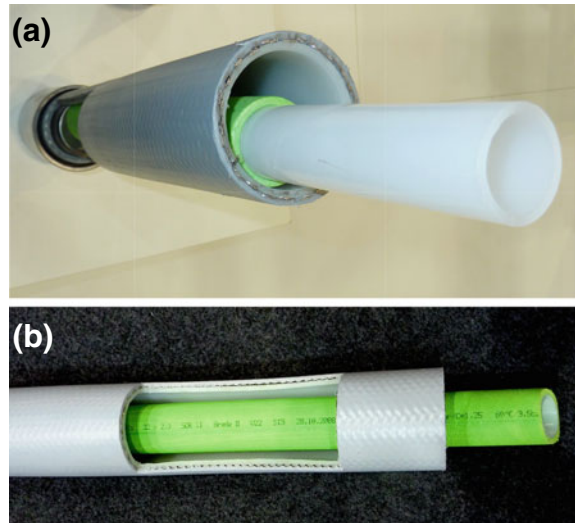
Fig. 6.1 Schematic illustration of types of probe tube design

to the heat pump in the center of the tube for the descending liquid of the probe (Figs. 6.1 and 6.2).

Double U-tube probes are most commonly used. The advantage is that in case of a tube damage the borehole is not completely lost but can be used as a single U-tube probe with the second tube.

Coaxial probes (Fig. 6.2) have a superior performance potential and are increasingly used as geothermal probes. In the heating mode, the cold working fluid flows downward in the annulus, takes up thermal energy from the ground and returns

Fig. 6.2 Coaxial probe:
(a) the reinforced outer tube has an outer diameter of 63 mm. The white inner tube of 40 mm brings the hot/warm water to the surface. It is thermally insulated (green Styrofoam mantle) Manufacturer: **(b)**



through inner tube as warm fluid to the heat exchanger at the surface. In the cooling mode the warm working fluid gives off heat to the ground. Coaxial probes with a wide range of specific technical designs and complex layouts can be found on the fast growing market. An advantage of coaxial probes is that they can be constructed like convectional groundwater monitoring wells, which is routine work for drilling companies. A potentially damaged backfill can be located with geophysical tools because of the large diameter of the probe (Sect. 6.8.4). The inner tube can be removed for restoration measures if necessary. The annulus between the wellbore and the outer tube of the probe should be sufficiently large so that sealing measures can follow the routines used in conventional groundwater well construction. However, installation of large-caliber coaxial probes can be difficult or impossible in some geologically difficult ground e.g. moraine or conglomerates with very coarse pebbles.

The U-tube probes typically have tubes with 32 mm in diameter. Rarely tubes with 40 or 25 mm are also used. Coaxial probes have an outer diameter of 50–140 mm or more, rarely also 40 mm and a corresponding inner tube of 30, 40 or 25 mm.

The geothermal probe extracts heat from the ground and cools the vicinity around the probe. The resulting thermal cone is analogous to the drawdown cone in groundwater hydraulics (Fig. 6.3). The geothermal probe receives its heat supply from the surroundings and the efficiency depends on the thermal conductivity of the underground system.

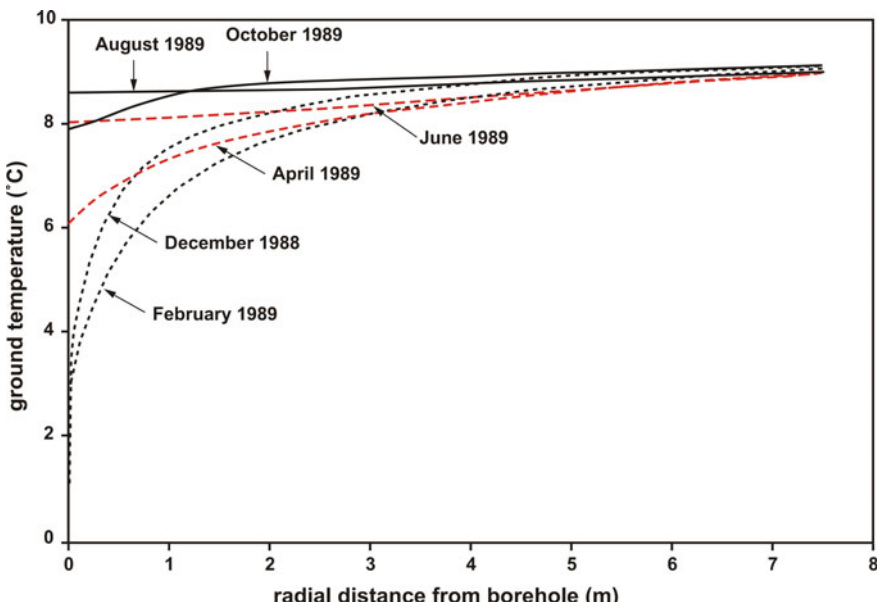


Fig. 6.3 Dynamic temperature decrease around a geothermal probe (measured data and model calculation for a specific installation in Elgg, Switzerland, Eugster 1998). Deepest thermal cone in February 1989, thermal recovery after shutdown of installation until August 1989, renewed development of cone after reactivation until October 1989

The length of a probe depends mainly on the system design and the thermal properties of the ground. Essential properties are the thermal conductivity of the individual strata, the temperature distribution in the subsurface and the climatic situation of the area. Also important are the thermal properties of the probe, of the grouting material (backfill) and of the heat transfer fluid.

A special probe design, called heat pipes or thermosyphon, works with phase changes of the heat transfer fluid along the fluid flow path in the probe thus making use of the latent heat of vaporization and condensation. In contrast to the conventional probes heat pipes are typically made of metal (Sect. 6.8.5).

The outside diameter of standard probe U-tubes is normally 32 mm, rarely 40 mm or even 25 mm. Coaxial probes have commonly outside diameters of 63 mm or 50 mm, occasionally also 40 mm. The central pipe has a smaller diameter of 32, 40 or 25 mm respectively.

The probe pipes are usually made of polyethylene (PE 100). The pipes specification conforms to a nominal pressure of 16 bar (1.6 MPa). This means that probes of more than about 160 m vertical length require special measures and care for correct installation, particularly if the groundwater table is low (Sect. 6.6).

Nearly all probes consist of polyethylene, which is a poor heat conductor with a low thermal conductivity of about $0.4 \text{ W m}^{-1} \text{ K}^{-1}$. Due to this fact the heat transfer from the ground to the heat transfer fluid is not particularly efficient. New probes have been developed using raw material of increased thermal conductivity of up to $1.0 \text{ W m}^{-1} \text{ K}^{-1}$ and launched on the market recently.

The polyethylene U-tubes come factory-welded, they are not welded at the construction site. Cross-linked polyethylene pipes have a warm-bent probe foot from the manufacturer and do not require welding. Cross-linked polyethylene pipes have a superb resistance to stress cracking and other mechanical damages compared to simple tubes. Probes made from cross-linked polyethylene are also thermally durable and resist long-term exposure to temperatures up to 95 °C. Therefore probes made from this material can be used for transferring heat to the ground for instance in combination with a solar thermal installation. This way excess heat can be transferred to the ground for storage during the warm season. This helps to thermally restore the underground and permits even storage of additional thermal energy. Combining solar thermal and geothermal installations has the further advantage of saving probe length.

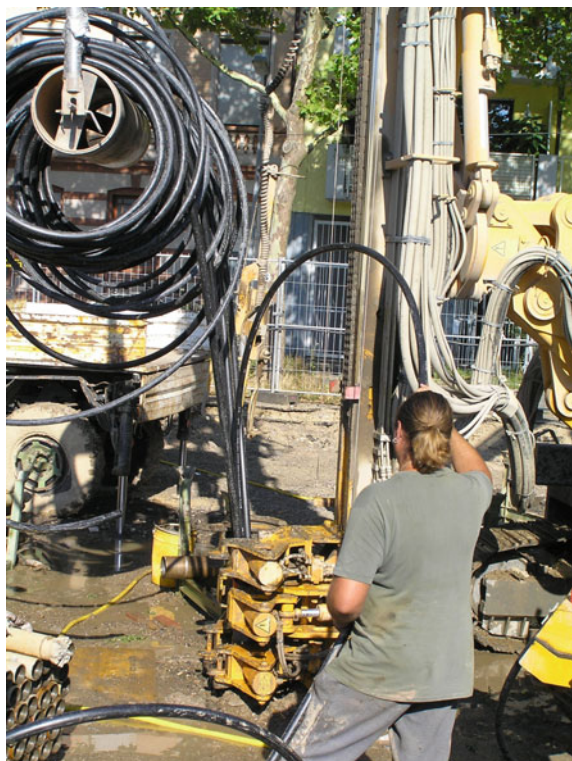
The probe foot is mantled with mechanical protection for borehole installation. A heavy weight at the base of the probe (Fig. 6.4) facilitates mounting of the probe into a groundwater-filled borehole. If the borehole is water-filled, it can be necessary to fill the probes with heat transfer fluid (or water) prior to inserting them into the borehole to avoid buoyancy and excessive pressure onto the probe tubes. At the construction site the probe comes in the necessary length wound onto a reel ready for installation into the borehole (Fig. 6.5). The probe is wound off the reel and together with a grouting hose inserted into the borehole.

Ground source heat probes are closed systems containing a circulating heat transfer fluid. A number of different chemical compounds and mixtures are used as heat transfer fluids. Most common are aqueous solutions of organic anti-freeze



Fig. 6.4 Geothermal probe with installation weight

Fig. 6.5 Installation of a geothermal probe from the reel into the borehole



chemicals that depress the freezing temperature of pure water. Thus, the system can be operated over a larger temperature range than with pure water. Consequently, the heat pump can extract more heat from the fluid that is eventually returned to the ground with a lower temperature. Accordingly, the lower inflow temperature extends the cone of thermal depression in the ground and increases the temperature gradient towards the probe. However, a certain danger for damages that compromise the durability of grouting and sealing occurs during the first series of freezing thawing cycles.

Table 6.1 Isothermal (25 °C) hydraulic and thermal properties of heat transfer fluids commonly used in geothermal probes (Zapp and Rosinski 2007)

Working fluid	Dynamic viscosity μ (kg/m s)	Heat capacity c_p (J/kg K)	Density ρ (kg/m ³)	heat conductivity λ (W/m K)
Water	0.0018	4217	1000	0.562
Ethylene glycol 25%	0.0052	3795	1052	0.480
Ethanol 25%	0.0046	4250	960	0.440
Propylene glycol 30%	0.0108	3735	1038	0.450
Calcium chloride 20%	0.0037	3050	1195	0.530
Methanol 25%	0.0040	4000	960	0.450

Color code: red = best values, green = worst values for system efficiency

It may have negative effects on the long-term efficiency and may cause conflicts with groundwater protection regulations (Sects. 6.5 and 6.7).

Hydraulic and thermal properties of commonly used heat transfer fluids in their typical mixing proportions with water show that pure water has optimal properties. Pure water is the ideal heat transfer fluid (Table 6.1). In addition to the fluids listed in Table 6.1, other substances are used in mixtures with water including potassium carbonate, potassium formate, bataine, magnesium chloride or sodium chloride. We strongly discourage using sodium or potassium carbonate or any other high-pH working fluids because of their severe corrosion potential. Ethylene glycol—water mixtures is probably the most commonly used heat transfer fluid.

Low dynamic viscosity and low density of the fluid increase the efficiency of a probe because of savings in pump power consumption. High specific heat capacity means high heat storage and high thermal conductivity implies efficient heat transfer. A high thermal capacity of the working fluid (product of density σ in kg m⁻³ and specific heat capacity c_p in J K⁻¹ kg⁻¹) means that less fluid must be pumped to transport equal amounts of thermal energy. This follows from the equation for the thermal capacity $c_{th} = \sigma c_p$ (J m⁻³ K⁻¹). Thus the amount of fluid necessary for heat transfer is proportional to the inverse of c_{th} : V_{Fluid} (m³) $\sim 1/c_{th}$.

It follows from the data listed on Table 6.1 that, as already mentioned, pure water is the ideal heat transfer fluid. However, geothermal probes that are operated with pure water must be precisely dimensioned to avoid freezing conditions during operation. A very positive side effect of water-based systems is that the system avoids damage to the backfill and the adjacent soil caused by freezing (Sects. 6.5 and 6.7). An integrated T-sensor switches the system to purely electrical heating if the geothermal system approaches freezing.

Hydraulic and thermal properties of different heat transfer fluids (Table 6.1) depend on temperature and vary during circulation of the fluid in the probe. Especially the viscosity of the fluid changes strongly with temperature. The viscosity of

ethylene glycol (25%) at -8°C is twice as high as at $+12^{\circ}\text{C}$, thus operation of the probe at freezing conditions requires considerably more electrical power for the pump than at temperatures above freezing conditions. Consequently, for economical reasons a geothermal probe should not be operated at freezing conditions. Otherwise the overall efficiency of the entire system is compromised.

Heat transfer fluids also often contain special additives that prevent development of bio films in the probe or to prevent corrosion. Many of these chemicals are toxic and problematic from a legal point of view. Using preventive groundwater protection as guiding principle water is the recommended working fluid. The next best alternative is pure ethylene glycol or propylene glycol without any additives (e.g. glycol—water mixtures with glycol > 90 vol. %).

The drilling diameter must be chosen big enough to easily accommodate probe and grouting hose and leaving enough space for the sealing backfill. The total cross-sectional area of the probe pipes and the grouting hose should be less than 35% of the cross-sectional area of the borehole ($r^2\pi$). This permits a tight backfill with an excellent thermal connection to the ground. A 32 mm diameter double U-tube probe requires at least a 120 mm drill hole, 40 mm geothermal probes must have a borehole at least of 150 mm in diameter. The drilling diameter depends additionally also on the planned drilling technique and the geological details of the ground. The recommended drilling diameters above refer to down-the-hole-hammer drilling used typically for hard rock drilling. For rotary drilling (wash drilling) in loose rock the boreholes must have a larger diameter. An overview over commonly used drilling techniques for ground source heat probes is given in Sect. 6.4.

The probe tube is directly unwound from the reel and is carefully placed into the bore together with the grouting hose. For safety reasons motor-driven reels should be used for installing long probes that permit machine-controlled braking. The grouting hose must be attached to the probe before lowering the pipe and hose together into the wellbore. After the installation of the probe pipe it is virtually impossible to put the grouting hose in place separately. In a next step, the grouting material is pumped through the hose to fills the space between the probe pipes and the borehole wall from bottom hole to the wellhead (Tremie method, contractor procedure). This method ensures best thermal connection of the probe to the ground and optimal sealing. Before injecting grouting material the ground probe pipes must be liquid-filled and pressurized to avoid damaging the pipes. Deep wellbores or difficult geological structures may require the insertion of two grouting hoses.

Prior to grouting and after binding, complete pressure tests assess if the probes are leak-proof. A flow test verifies the permeability of the geothermal probe.

Directly touching probe pipes have a significantly lower heat transfer capacity compared to separately guided pipes (Acuña and Palm 2009). The ascending and descending probe pipes at different temperature should be separated in the borehole. This is practically achieved using inner spacers. Outer spacers or centering aids help to install the probe centrically in the borehole in order to reach the best thermal connection to the ground and optimal sealing. Numerous centering aids and spacers in a short distance are necessary to keep the pipes centered in the borehole and separated from each other. The heat conductivity of the material used for these aids



Fig. 6.6 Combined centering aid and spacer used for geothermal probes (blue pipes). Central blue pipe: Grouting pipe

is low and increases the thermal resistivity in the borehole. Improved combined spacers are relatively easy to handle and may help to improve the efficiency of the installation (Fig. 6.6). The usefulness of centering aids and spacers is under debate, especially because the current models often slip during installation of the pipes in the borehole. The tools may also obstruct the ascending grouting material, particularly of course when slipped, thus creating blowholes or air-filled cavities.

Several new instruments and methods for automated sealing control are presently under development and testing. The procedures record and digitally document the quality of the grouting. One of the techniques measures the rising pressure during grouting with a pressure sensor directly in the injection hose or with sensors being left in the well. The method requires precise knowledge of the density of the grouting material, which can directly be gauged at the same time. However, the thermal contribution from the hydration heat, groundwater influx or thermal behavior of the PE-tubes cannot yet be considered. Another technique is based on measuring the susceptibility of dotted grouting slurry with a tool from the inside of the tube. Several methods are currently (2019) in a state of development and some can detect large cavities or massively defective grouting only.

Plastic pipe material tends to be stiff and vulnerable to mechanical damaging in cold weather. During construction work under cold weather conditions, the probe should be stored at a warm place prior to installation or flushed with warm water at the construction site.

6.3 Dimensioning and Design of Geothermal Probes

The design of borehole heat exchangers is made on the basis of the heat demand of the building that should be supplied by the geothermal probe. The heat extraction rate of the probe depends on several factors including the geological and thermal structure of the subsurface at the site, the type of the probe, the heat transfer fluid and the grouting. The hydraulic coupling of the geothermal probe with a heat pump creates an additional interrelationship. A geothermal probe can be operated reliably, efficiently and economically for long periods of time only, if all relevant parameters have been considered and optimized. For the optimization of the geothermal probe the planning must include the architect and the planner of the building services.

Geothermal installations often have considerable total pipe lengths. Numerous branching, bows and fittings cause an increasing flow resistance with increasing distance from the heat pump and gradually reduce fluid flow and heat transfer. Therefore, it is important to know the flow properties in the system and keeping flow resistance low by optimized dimensioning of all system components. Only a flow-optimized installation has the potential to become an efficient system. The flow resistance of the supply (feeder) lines and in the connecting blocks should be as low as possible. However, in vertical probe pipes underground fluid flow should be turbulent for best heat extraction rates. Laminar flow would cause much lower flow losses but the heat transfer from the pipe wall to the heat transfer fluid is much better with turbulent flow.

If probe pipes and lines to the heat pump are of exceptionally different lengths hydronic balancing of the system preceding the heat pump improves the heat extraction efficiency.

Vital for the success of heat pump heating systems are the failure-free long-term operation and low electrical power consumption. The technical parameters of the heat pump, the source temperature and the heat requirement of the heating system mutually influence each other. It is difficult to reliably predict the operating behavior and the economic viability of the heating system without computer simulation (modeling).

6.3.1 Heat Pumps

Heat pumps are devices that transfer thermal energy from a source at a low temperature to a drain at a high temperature by means of mechanical work (ASHRAE Handbook 1997; Puttagunta et al. 2010). The fluid at the high-temperature side can then be used, for example, for house heating. Heat pumps make it possible to use a relatively low-temperature heat source such as the near surface ground, soil or groundwater for house heating purposes.

Technical types of heat pumps:

- Compressor heat pumps

- Sorption heat pumps, subdivided in adsorption- and absorption heat pumps
- Vuilleumier heat pumps.

Other existing technical solutions for heat pumps may not have potential for being used in house heating and warm water supply in the near future.

Compressor Heat Pumps are considered state-of-the-art and most widely used. Depending on the type of motor one distinguishes between electric motor and gas motor driven compressor heat pumps. Near-surface geothermal energy installations almost exclusively use electric motor compressor heat pumps. Therefore its technical principle is briefly explained below. However, compressor heat pumps can also be driven with natural gas, petroleum, or biofuel (biogas, rapeseed oil). In such devices the compressor is driven by a combustion engine. The use of gas-driven compression heat pumps has the advantage that the heat of the exhaust can also be used for heating and thus the primary energy input is used more efficiently than with electric heat pumps.

Sorption Heat Pumps Sorption is a physical–chemical process where a substance in one state becomes attached another substance in another state. Solids for example zeolite minerals can capture liquids or gases by absorption. Dissolved components in a liquid or gas can be removed from the phase and attached to the surface of a solid (Adsorption). Sorption processes are driven by changing external physical parameters such as temperature and pressure and can be reversed if the parameters are rearranged (reversible processes). Sorption heat pumps convert retrieved geothermal energy to warm working fluids for heating purposes or in the reversed cooling mode transfer heat to the ground loop. The sorption process in sorption heat pumps is based on pairs of an absorption medium and a heat transfer fluid. Commonly used pairs are: (1) LiBr (absorption medium) and water (heat transfer fluid). (2) Water (absorption medium) and ammonia (heat transfer fluid). Sorption heat pumps have a long tradition being used in refrigerators but they can be efficiently used in geothermal applications.

Vuilleumier Heat Pumps Work according to the principle of a thermally driven regenerative gas-cycle process comparable to the Stirling process.

Geothermal probes most commonly use electric motor compressor heat pumps for the heat transfer at the ground surface. Thus it will be simply referred to as the heat pump in the following. It also works also like in a refrigerator, however, with the difference that heat production of the condenser is the desired power output and not the cooling power of the evaporator (Fig. 6.7).

The fluid of the internal circuit of a heat pump extracts heat from a heat source in a first heat exchanger (the evaporator). The fluid undergoes a phase change from liquid to gaseous. The gaseous fluid reaches the compressor unit driven by an electric motor where the fluid pressure is increased. The resulting associated temperature increase permits the extraction of the heat transferred to the working fluid (also called refrigerant) from the original heat source (here the heat from the ground source) in a second heat exchanger, the condenser unit. The high pressure of the gaseous fluid is reduced in an expansion valve cooling the fluid below condensation and it returns

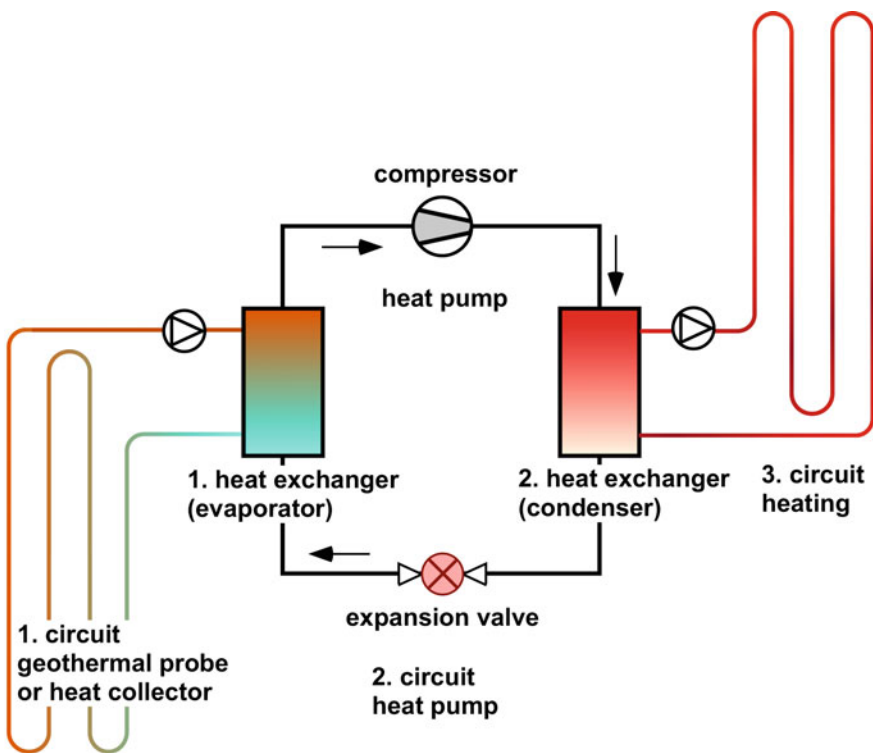


Fig. 6.7 Schematic diagram of a heat pump system utilizing geothermal energy for house heating

to the liquid state. The liquid fluid returns to the evaporator where it is reloaded with thermal energy from the ground source.

Many different heat transfer fluids are used in heat pumps including pure or mixtures of liquids such as partly fluorinated hydrocarbons, pure hydrocarbons (propane, butane) and carbon dioxide. Ammonia is not approved in many countries because of its hazard potential.

The primary undisturbed temperature of the ground heat source is given by the thermal and hydraulic properties of the subsurface and the climatic conditions at the location of the probe. During operation of the geothermal probe, heat extraction cools the vicinity of the probe pipe. The effective temperature of the transfer fluid entering the evaporator is still lower than the cooled ground because of unavoidable physical heat transfer losses.

The heat pump needs to produce the required thermal power at the expected lower limit of local conditions. For example, probe systems are typically designed to work at -12°C surface temperature in Central Europe. They will have problems to heat a house if the temperature falls to -25°C . For efficiency reasons it is essential to reduce the heat demand of a building by thermal insulation measures prior to planning a geothermal probe heating system. In addition, the supply water temperature of

the heating system should be as low as possible. Ideally, the temperature difference between the fluid from the ground source (1. circuit) and the supply water (3. circuit) should be small, saving electrical energy for the heat pump (Fig. 6.7). Typical traditional radiator heating in buildings requires 55 °C warm supply water. Underfloor heating can be operated with 35 °C warm water. Large area wall heating requires even lower supply water temperatures.

Invariably, the geothermal probe or the ground source heat exchanger should be generously dimensioned. The source temperature is then high and causes an increased efficiency of the heat pump. The geothermal probe should always be operated at temperatures above freezing.

The dimensioning of the geothermal probe must be adapted to the evaporator capacity of the heat pump. The heat source, specifically the total length of the probe is tailored to the heat demand, the desired extraction rate and operating life. A geothermal probe is not characterized by a defined and constant power at a certain operating point, as it is often specified on heat pumps. A probe may extract high power for a short period of time or lower power for an extended period (Basetti et al. 2006). Therefore, defined extraction profiles (e.g. 1800 h of thermal performance, monovalent per year) should be verified in advance. The design of a geothermal probe system must also consider the dimensioning of the circulation pump for the heat transfer fluid in the probe (Sect. 6.3.2).

It is generally economically worthwhile using the heat pump for hot water preparation also. However, in this case the system is in operation throughout the year and the time for a certain thermal regeneration of the soil is short. For the hot water preparation the output temperature must be increased to 60 °C, which is higher than for heating. Combining the geothermal probe with a solar thermal installation may give the best economical and energy solution (Sect. 6.8.3). The excess heat produced by the geothermal probe during summer can be stored in the ground for supporting house heating during winter. The solar thermal system produces the hot water for the user during the warm season. During the summer, waste heat from house cooling also can be brought to the subsurface with the geothermal probe (Sanner and Chant 1992).

The so-called coefficient of performance (COP) number facilitates the evaluation of the quality of heat pumps. The COP number is the ratio of electrical power of the compressor plus auxiliary power and the thermal capacity of the condenser (both in kW). COP values increase with increasing efficiency of the heat pumps. COP also increases with decreasing temperature difference between ground source and supply water of the heating system. The COP value, however, does not include the energy demand of the circulation pumps of the geothermal probe and the heating circuit. It is evident that efficient operation of the heating system correlates with high ground source temperature and low flow temperature.

For the complete heat pump heating system the seasonal performance factor (SPF) is the most significant and relevant parameter characterizing the performance of the system. SPF is the ratio of the total amount of thermal energy transferred to the heating and hot water production per year and the total amount of electrical energy taken up by the system during the same time (both numbers in Joules, or kWh). SPF

= 4 means that 1 kWh electricity produced 4 kWh heat output. The energy efficiency of the entire system is the better, the higher the seasonal performance factor is. The SPF and, hence, the performance of the system can only be controlled if an electronic heat meter is installed and measures the thermal energy produced by the heat pump.

COP is a device performance factor that characterizes the heat pump as a machine. It depends on the operating conditions. In contrast, the seasonal performance factor (SPF) is an economical and energy political significant parameter, which depends not only on the installed machine but also on the habits of the user, the climatic situation, operating conditions and other factors.

If the heating system ought to be beneficial from the viewpoint of primary energy consumption, then the seasonal performance factor of an electrically driven system must be clearly higher than the equivalent SPF calculated with the primary energy needed for the production of the electrical energy to run the system. Energy conversion efficiency is different from country to country. In Germany for example, nearly 3 kWh primary energy (from a blend of differently operated power plants and other energy sources) is needed on average for the production of 1 kWh electrical power. Therefore, the legislator requires a minimum SPF of 4 for water-based heat used for house heating. If used also for hot water preparation SPF must be better than 3.8.

In practice, minimizing the temperature difference between evaporation and condensation (heat source and heat output) represents a significant optimization potential for the system engineering of heat pump systems. Each extra Kelvin temperature difference means an excess energy consumption of the compressor of 3.5%. Thus the hot water part of the building (bath, hot water) reduces the SPF of the entire installation.

For efficient operation every heating system must be hydraulically balanced. Particularly important is this for heating systems with heat pumps. Hydronic balancing is done on the house/building side of the system right after the heat pump. The installer of the heating system adjusts the flow volume of hot water individually for each radiator of heating circuit of a panel or under floor heating to where the flow volume in each room covers the heat requirement of the room for a given supply water temperature. Thus each room receives exactly the amount of heat needed to reach the desired room temperature. After successful hydronic balancing the heating system can be operated with an optimal system pressure, an optimally low volume of water and the lowest possible supply water temperature, or in other words with the best possible system efficiency.

We recommend considering the following advice for installation of heat pumps:

- Thorough design of the entire system, adjusting the different components (heat source, reservoir, heat sink...) to work as a part of a well orchestrated total system and an integral trade-spanning multidiscipline object specific planning,
- Check and verification of loading strategies of the reservoirs, particularly of combination storages, and monitoring the supply water temperature,
- Careful hydronic balancing and gapless insulation of pipes and components,
- Avoid overly complex hydraulic and reservoir systems,

- Properly designed systems do not require auxiliary electrical heating (heating rod), except perhaps during construction drying.

For high output ranges above about $100 \text{ kW}_{\text{th}}$, gas-absorption heat pumps become an interesting alternative to the electric compressor heat pumps. The advantage of the absorption technology is, heat and cold can be used in chorus thus increasing the total efficiency of the system significantly.

6.3.2 Thermal Parameters and Computer Programs for the Design of Ground Source Heat Pump Systems

A broad-brush dimensioning of a geothermal probe is useful for a cost estimate at best. A ground source heating system must be skillfully planned and professionally dimensioned. An undersized system may cause significant damages to components (Sect. 6.7). If probes have been installed which are too short, the mistake can only be repaired with the installation of a new probe in an additional borehole. We strongly discourage installing electrical heating rods to compensate for the lack of power on economical and ecological reasons. Short-term operation of auxiliary heating rods can possibly be justified in certain emergency situations (Sects. 6.3.1, 6.5, 6.7).

A rough estimate of the necessary length ($l \text{ m}$) of the geothermal probe to cover the heating requirement ($H [\text{W}]$) of the object to be heated is normally based on the so-called specific heat extraction rate ($E [\text{W m}^{-1}]$). The specific heat extraction rate of a geothermal probe is normally related to the thermal properties of the different ground layers (E_i) that have been intersected by the borehole, specifically to the thermal conductivity of these layers. This is common usage, although the specific heat extraction rate depends on many other factors as well (e.g. grouting material, heat transfer fluid). Strictly speaking, the specific heat extraction rate of a geothermal probe does not exist but merely a potentially recoverable, however, intrinsically variable cooling or heating power of the ground.

In any case, of prime importance is a detailed and precise description of the drilled layers and a verification of the geological profile and thus of the credibility of the assumed heat conductivities in model calculations.

The thermal conductivity laboratory data often fail to precisely characterize the real situation in the subsurface for various reasons. The used samples may not representatively reflect all the heterogeneity including fractures and local variability of a certain layer. Laboratory data also do not characterize the effects of stagnant or flowing groundwater in the pore space or the thermal consequences of air-filled pore space in the vadose zone. Therefore, it is important and recommended to acquire data by direct in-situ measurements using so-called Thermal Response Tests (TRT) (Sect. 6.3.2).

The thermal properties of a particular rock (thermal conductivity, specific heat capacity) may vary widely depending on its detailed local structure and water-content (Table 6.2). To be on the save side, it is recommended to work with the pessimistic

Table 6.2 Compilation of thermal conductivity λ , heat capacity s and formal heat extraction rate data for various types of rocks (VDI 2001).

Ground, rock	Thermal conductivity ($\text{W m}^{-1} \text{K}^{-1}$)	Heat capacity ($10^6 \text{ J K}^{-1} \text{m}^{-3}$)	Extraction rate (W m^{-1})
Gravel, sand dry	0.4	1.4–1.6	20–30
Gravel, sand moist	0.6–2.2	1.2–2.2	30–50
Gravel, sand wet ^a	1.8–2.4	2.3–3.0	55–70
Moraine	1.7–2.4	1.5–2.5	40–55
Clay, loam moist	0.9–2.2	1.6–3.4	30–50
Limestone dense	1.7–3.4	2.0–2.6	45–65
Marl	1.3–3.5	3.0	40–60
Sandstone	1.3–5.1	1.6–2.8	40–70
Conglomerate	1.4–3.7	2.1	40–65
Granite	2.1–4.1	2.1–3.0	50–70
Basalts	1.3–2.3	2.3–2.6	35–55
Andesite	1.7–2.2	2.4	45–50
Quartzite	3.6–6.0	2.1	65–92
Breccia	2.2–4.1	2.1	50–70
Schist	1.5–2.6	2.2–2.5	40–55
Gneiss	1.9–4.0	1.8–2.4	50–70

^aWater saturated

The data for the specific heat extraction rate E refer to a single geothermal probe and for an operating time of 1800 h per year. The values are prone to the reservations made in the text

lower parameter values if any ambiguity on the true values exist during the planning stage of the project. The listed values for the potential extraction rates (Table 6.2) should be considered as rough estimates for orientation. However, it follows from the compilation that the potential extraction rate varies by a factor of three depending on the material present underground.

Also note that the extraction rate for a specific geological unit may vary from place to place and cannot be safely predicted using Table 6.2, or any other fixed compilation. The parameter cannot be transferred from site to site. Remember that the true achievable extraction rate also depends on local climatic factors, the installed system, the heating habits of the residents and other factors. It does not exclusively depend on the properties of soil and rock. Here it is used as a parameter for rough verification of the system design. The parameter should never be used as the only tool for the dimensioning of the system without any further critical reflection.

In practice, for a specific heat demand of an object (H [W]) the necessary length of the geothermal probe is commonly estimated from the known stratigraphy and thicknesses of the individual layers (h_i [m]) by adding together the contributions of the individual strata to the total extraction rate:

Single layer case:

Probe length h [m] = heat requirement of the object H [W] / specific extraction rate E [W m^{-1}]

Multilayer case:

$$\sum (E_i \bullet h_i) = H \quad [\text{W}] \quad (6.1a)$$

$$\text{Probe length } h \text{ [m]} = \sum h_i \quad (6.1b)$$

The heat extraction rate of geothermal probes varies between 20 and 90 W per meter probe length, with outliers in both directions. The indicated variation is large and may be even larger under unfavorable circumstances.

The definition of one heat extraction rate that characterizes a geothermal probe is only sensible if it does not fluctuate much in the building/object (Sect. 6.3.1). Large-scale plants but also small units (< 20 kW) with high power variations need to be designed with dedicated expert tools. The same holds true for bivalent systems, systems that include hot water production or swimming pools, for integrated geothermal fields and combined systems for heating and cooling. Furthermore, geothermal probe projects in areas where the average annual surface temperature is below about 10 °C should be planned with special dimensioning tools. At such low surface temperatures, which is equivalent to average temperature of the near surface soil layer, the extraction rate of the probe rapidly decreases.

The extraction rate of a geothermal probe, as described above, depends on many factors including (Eskilson 1987; Kohl and Hopkirk 1995; Signorelli 2004):

- the conductive and convective heat transfer power of the ground and of individual layers (thermal conductivity, flow rate, ...),
- the temperature distribution in the subsurface, the climatic situation at the building site,
- the duration of heat extraction from the ground (annual operating hours),
- the diameter of the drill hole,
- the thermal properties of the grouting (backfill) material,
- the type of heat transfer fluid used, the type of the probe, material of the probe, position of the pipes in the borehole (Sect. 6.2),
- design and geometry of the probe field: Distance of the probes from each other, number and arrangement of the probes.

It follows from the diversity of the listed factors how complex the assessment of the true extraction rate of a geothermal probe really is (Sect. 6.3.1). Therefore, the planning engineer relies on computer codes and tools for the optimal dimensioning of a system. Some of the more popular tools are:

- the application EWS by Huber (2008), (hetag.ch/index_en)
- the application EED (Earth Energy Designer) by Sanner and Hellström (1996), (buildingphysics.com)

- the application TRNSYS18 by The University of Wisconsin Madison (sel.me.wisc.edu/trnsys/)
- the code PILESIM (Version 2, 2007) by Pahud ([1998](#)).

These applications compute and model the expected temperature evolution in the heat transfer fluid at the entry point to the heat pump as a function of time. The programs are of variable complexity and some do not consider all listed factors that may influence the heat extraction rate. Thus under detrimental circumstances the programs may produce erroneous results. Some of the programs also handle simultaneous computation of multiple probes or of entire ground source heat exchanger fields. The number of geothermal probes, their arrangement and length can be varied and selected to where the target settings for the temperature course can be achieved with the lower and upper limits. Applications such as EWS, EED (Hellström and Sanner [2000](#)) or PILESIM also consider the heating requirements of the building, which is the monthly energy heating and cooling requirement and the heating and cooling load. An example of a modeling program for heat pump heating systems is WP-OPT[®] (wp-opt.de). It permits planning and optimization of heating systems using heat pumps (Sect. [6.3.1](#)).

Because of variable pumping temperatures from site to site and different types of uses it is evident that a standardized geothermal probe does not exist. Thus a professional dimensioning of the geothermal probe is of vital importance for its later successful operation. Dimensioning of geothermal probes with rule-of-thumb values such as 45 W per running meter of probe that do not consider specific particularities of site and building is unfortunately widespread practice. Such an unprofessional approach may lead to irreversible damages to the system (Sect. [6.7](#)).

Fundamental research on complex systems requires three-dimensional models such as the 3-D finite element program FRACTURE (Kohl and Hopkirk [1995](#)). Using FRACTURE Signorelli ([2004](#)) has demonstrated for example that the temperature of the top soil layer may have a larger effect on the dimensioning of geothermal probes than the thermal conductivity of the underground.

Numerical modeling using different programs consistently suggest that if two geothermal probes are placed at a distance of 10 m and more no significant mutual interference ($> 1^{\circ}\text{C}$) will occur even after many years of operation. Most commonly a distance of about 7 m is sufficient (e.g. Eugster [2001](#)). But again, these specific distances should not be generalized as they vary with the number of ground source heat exchangers to be installed, their arrangement in space, their depth, if the probes are placed in flowing ground water or if the ground consists predominantly of clayey sediments with low thermal conductivity.

The thermal range of geothermal probes used for heating is principally larger if the ground is predominantly clayey and silty compared to aquifers consisting of sand and gravel. This is because of the low hydraulic conductivity of clay and silt, which results in extremely low groundwater flow velocities even if hydraulic gradients are high. Numerical experiments have shown that the thermal range, defined as effects greater than 1°C after year-long operation, may exceed 10 m for soils with low

hydraulic conductivity. The findings have been confirmed by observations in the test-field Elgg near Zurich (Eugster 1998).

Guidelines for the design distance of borehole heat exchangers are based on the assumption that the boreholes are accurately vertical. In practice, it is not always feasible to drill perfectly vertical for justifiable expense. Placing a standpipe in the upper meters of the borehole helps to accomplish relatively vertical drilling. In addition, also the plastic probe pipes do not run strictly vertical but are coiled in the drill hole. Taking all this into account it is wise to observe a recommended minimum distance for the probes of 10 m.

Thermal Response Tests (TRT) are well-established tools for the in-situ measurement of the thermal properties of the ground (Mogensen 1983; Gehlin and Nordell 1997; Gehlin 2002; Sanner et al. 2000). The tests inject a defined amount of heat energy into one end of the loop of the probe over a period of several days and measure the outflow temperature at the other end of the loop. The temperature of incoming and outgoing heat transfer fluid, the flow rate of the fluid, and the thermal energy input are the principal parameters measured during a test. The particulars of the temperature increase provide information on the thermal properties and structure of the underground in the vicinity of the borehole analogous to the hydraulic properties with a pumping test (Sect. 14.2) (Fig. 6.7). Instead of the hydraulic conductivity and the specific storage coefficient, which are measured with hydraulic pumping tests, Thermal Response Tests provide thermal conductivity and the specific heat capacity of the ground. The hydraulic effects of the wellbore, skin and wellbore storage (Sect. 14.2) have their equivalents in thermal tests and are lumped to effects of the “inner zone”. This structurally damaged area around the borehole shows a complex sequence of thermal resistances between circulating groundwater and intact ground, heat transfer to the probe pipe, the grouting material and other structural elements. The “inner zone” thermal structure depends also on the type of probe (single U-pipe, double U-pipe, coaxial pipe) and the diameter of the borehole. The thermal borehole resistance R_b (K m W^{-1}) is the sum of all effects of the “inner zone”.

The comprehensive hydraulic computation tools that have been mostly developed by the oil and gas industry during the last decades are ultimately based on analytical solutions of the line source problem (Theis 1935). Originally the mathematical solution for the line source stems from the subject matter of heat conduction (Carslaw and Jaeger 1959) and has been adapted by Theis (1935) to the evaluation of pumping tests. Today highly developed and sophisticated hydraulic evaluation tools can be modified for thermal evaluation methods such as the Thermal Response Test (Sect. 14.2).

Numerical models for the interpretation of Thermal Response Test data have been presented for example by Wagner and Clauser (2005) and by Gustafsson (2006). The advantage of using numerical models is that they allow considering simultaneously any kind of boundary conditions and spatially heterogeneous ground properties (e.g. Diersch 1994). In practice, however, algorithms based on analytical solutions still dominate the daily working routine (e.g. Yu et al. 2016).

In order to access the undisturbed original rock and its thermal properties and the inhomogeneity of these properties beyond the near field of the borehole (“inner zone”)

with a Thermal Response Test, the test must be of adequate duration by analogy to a pumping test. Otherwise the TRT is useless and the obtained pseudo-data should not be used as basis for the system design. As a general rule, a successful TRT typically lasts for several 10 s of hours. On-line recording of the data stream and continuous evaluation of the data allow for stopping the test as soon as the data can be implicitly modeled. The interpretation of TRT data is usually based on the analytical solution of the line source equation with the asymptotic solution for sufficiently long periods in analogy to hydraulic pumping tests (Cooper and Jacob 1946). The temperature T ($^{\circ}\text{C}$) at distance r (m) from a thermal line source with a constant heat output Q (W) in an infinite homogeneous and isotropic ground with a thermal conductivity λ ($\text{Wm}^{-1} \text{K}^{-1}$) and a volumetric heat capacity s ($\text{Wsm}^{-3} \text{K}^{-1}$) can be computed from Eq. 6.2:

$$T_{(r,t)} = T_0 + Q/(4\pi\lambda H) \cdot [\ln(4\lambda t/\text{sr}^2) - 0.5772] \quad (6.2)$$

where H (m) denotes the length of the geothermal probe (test length), T_0 is the original undisturbed ground temperature. Equation 6.2 does not consider the thermal borehole resistance.

The effect of the thermal borehole resistance R_b can be approximated by adding the following term to Eq. 6.2 (Hellström 1999):

$$\Delta T_{iz} = QR_b/H \quad (6.3)$$

This approximate description is sufficiently accurate for $t > 4\text{sr}^2/\lambda$, that is for long periods of time. Temperature changes tend to become proportional to the logarithm of time $\ln(t)$ at large t . This correlation is used to describe the effective thermal conductivity of the volume of ground around the borehole and includes effects of groundwater flow. The thermal conductivity of the “inner zone” is expressed as an average parameter value for the total length of the geothermal probe H (m). The effective thermal conductivity λ_{eff} follows from the slope α (Ks^{-1}) of the straight line through the data points representing the undisturbed ground in Fig. 6.8 after conversion of the logarithms from \ln to \log ($\log x = \ln x/\ln 10$):

$$\lambda_{\text{eff}} = 2.303 Q/(4\pi H \alpha) \quad (6.4)$$

A set of TRT data is shown as an example in Fig. 6.8. In this example, the average effective thermal conductivity of the drilled formations is $\lambda_{\text{eff}} = 2.75 \text{ Wm}^{-1} \text{ K}^{-1}$ using the parameters given in Fig. 6.8. The graph clearly shows the thermal regime during the first period of about 8 h of the experiment is strongly influenced by processes other than heat transfer through undisturbed rock matrix. During this initial experimental phase effects of the “inner zone” that correspond to wellbore storage in hydraulics and other effects prevail and the criterion for the asymptotic approximation ($t_c = 4\text{sr}^2/\lambda$) not yet applies. Beyond that critical time t_c the thermal response of the undisturbed ground dominates. It can also be seen in Fig. 6.8, that a meaningful interpretation of TRT data requires a test lasting for about 33 h (1.5 days) in this particular example.

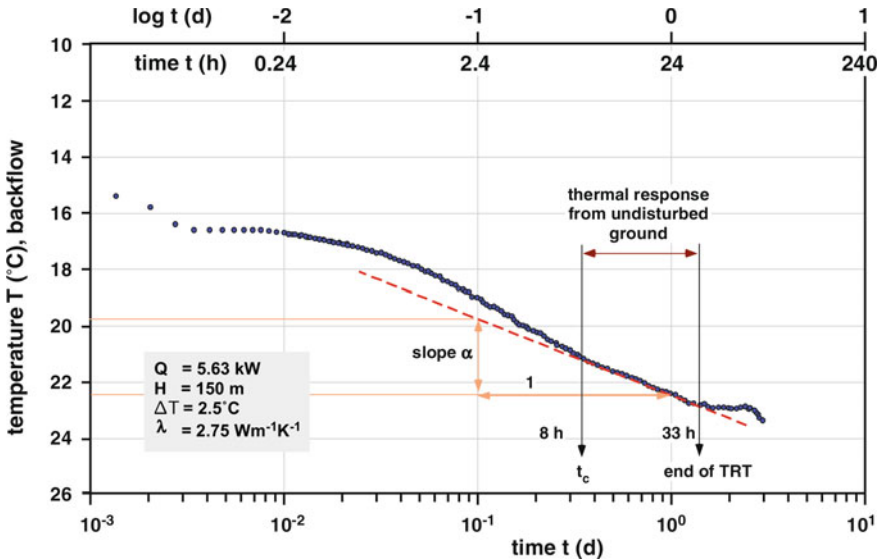


Fig. 6.8 Interpretation of thermal response test data: Temperature of the heat transfer fluid versus logarithm of time. The slope of the straight line through the thermal response of the infinite homogeneous matrix provides the average effective thermal conductivity. Slope $\alpha = \Delta T / \Delta t$, [K d⁻¹]

After determination of the thermal conductivity λ , the thermal resistance of the borehole R_b is obtained by rearranging Eq. 6.2:

$$R_b = H/Q(T_{(r,t)} - T_0) - 1/(4\pi\lambda) \cdot [\ln(4\lambda t/s^2) - 0.5772] \quad (6.5)$$

The heat capacity s is very similar for different kind of rock materials and thus has not much effect on R_b . For the example made here, $R_b = 0.15 \text{ K m W}^{-1}$ using the same parameters as above and an assumed heat capacity of $s = 2.7 \cdot 10^6 \text{ J m}^{-3} \text{ K}^{-1}$.

The range of temperature changes in the ground is estimated from:

$$r = \sqrt{2.25\lambda t/s} \quad (6.6)$$

It follows from Eq. 6.6 that the range of temperature changes is independent of the heat input. Using the example parameters given above, Eq. 6.6 predicts that after one year of operation the zero influence line has reached a distance of 8.5 m from the borehole. A noticeable temperature effect at this distance, however, may not be expected before 10–30 years of operation.

The results of the described interpretation practice for TRT data are average values for the total test interval. It means that all derived thermal properties of the subsurface

and the thermal resistance of the borehole integrated averaged values across all drilled layers for the total depths of the geothermal probe.

It is possible to record a vertically resolved temperature profile with an improved TRT technique. Special tools can measure temperature profiles inside the borehole. But also external fiber-optical temperature measurements from fixed devices outside the geothermal probe produce depths-resolved temperature data. These data can be used to identify thermal effects of groundwater flow. Hydraulically active aquifers can be discerned. If data from multiple temperature measurements has been collected, thermal conductivities of individual layers can be derived and separated from the thermal resistance. For this extended type of TRT fiber-optical temperature measurements proved to be beneficial. The depth-connected thermal parameters of the ground gained with this method can be correlated with the local stratigraphy known from drilling. If additional advective heat transport resulting from groundwater flow occurs at the site then the derived thermal properties for that layer are effective system properties not representing the rock only.

Fiber-optical temperature measurements at different depth in the wellbore performed in the context of an enhanced TRT can detect defective grouting (Sect. 6.8.4).

TRT is a relatively costly analytical method and is typically used for larger projects such as borehole heat exchanger fields or for larger development projects where it is planned to drill many geothermal probes. The dimensioning of a geothermal probe for heating a single-family home is done in practice on the basis of a predicted stratigraphy and the climatic situation at the site with the methods described above. Typical thermal conductivities are attached to the rock layers underground, the heat extraction rates and the dimensioning of the geothermal probe modeled with programs described above resulting in an estimate for the required length of the probe to be installed. Therefore, it is important that the drilled geology is determined and documented carefully, and the predicted or assumed stratigraphy is verified.

6.4 Drilling Methods for Borehole Heat Exchangers

Drilling methods are established routine and typically the client may choose from many competing service providers (Fig. 6.9). Drilling the borehole for a geothermal probe should go on fast and at low cost. However, fast and cheap should not compromise the long-term durability of the system. The probes installed in the borehole are the foundation for the yearlong sustaining functioning of the heating system.

Legal regulations and guidelines for well drilling and well engineering vary from country to country. It is necessary to get acquainted with the details of these local regulations during planning of the system and making sure that the contractor follows the regulations during the constructing phase.

The boreholes must be drilled with the required diameter, the correct caliber, and straight vertical to the needed depths (Sect. 6.3). The required diameter of the borehole depends on the size of probe pipes, the type of ground to be drilled and the

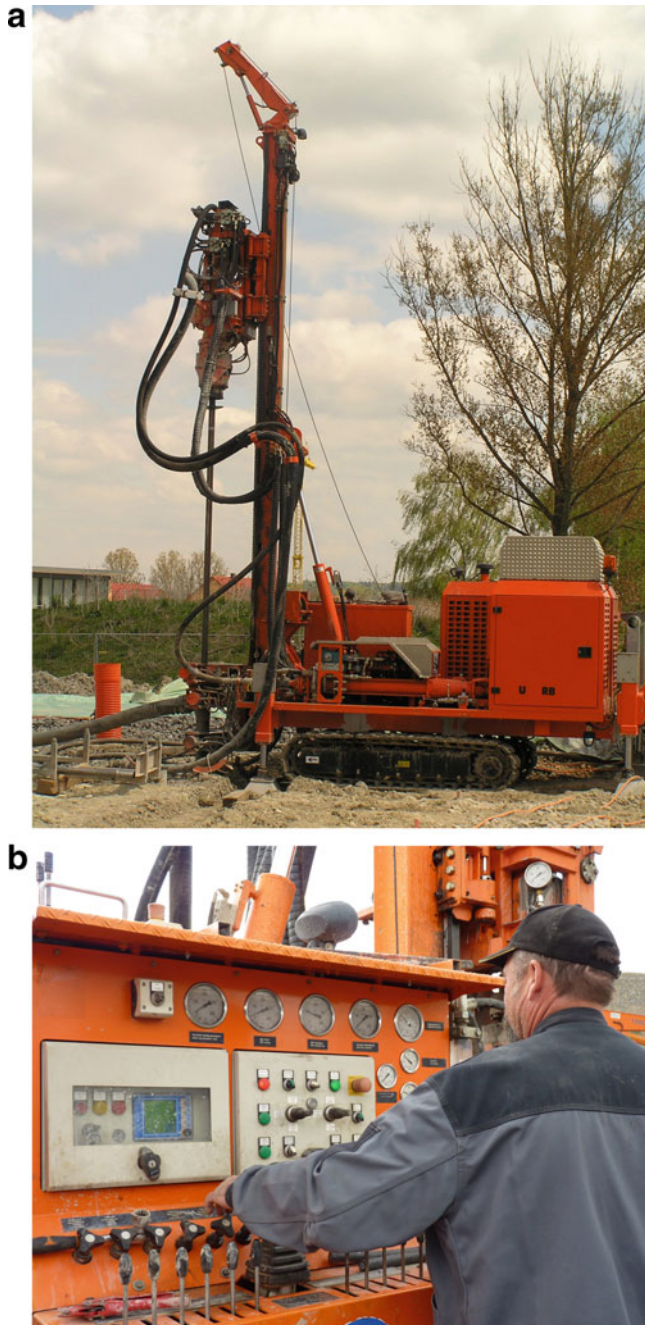


Fig. 6.9 **a** Drilling equipment for borehole heat exchangers. **b** Drillmaster at the operator panel of a drilling rig

drilling method used. The borehole must be sufficiently wide to lower the probe pipes and the grouting hose into the borehole without being damaged. Certain geological conditions may require the use of packers and several separate grouting hoses. The chosen borehole diameter also may require using spacers or centering aids (Sect. 6.2). A forceful insertion of the probes into the borehole may result in severe damage.

For budget reasons the small-diameter boreholes for geothermal probes are drilled by the direct rotary mud drilling technique rarely by dry drilling (e.g. percussion or cable drilling) (Fig. 6.10). In mud rotary drilling the cuttings are continuously hauled by the mudflow, in dry drilling intermittently with a tool. Indirect mud drilling pumps the cuttings through the drill string to the surface whereas direct mud drilling lifts the cuttings through the annular gap between the drill pipe and wall of the borehole. An installed casing ensures the stability of the borehole in dry drilling; a density-adjusted drilling mud stabilizes the borehole in mud drilling methods. Commonly, dry drilling methods are used for installing the standpipe for the mud rotary drilling subsequently used to complete the borehole (Fig. 6.11).

Two different types of rotary drilling methods can be distinguished depending on the drive used. Rotary mud drilling is mostly used in soil and unconsolidated sediments, the borehole being stabilized by the drilling mud. Rotary percussion drilling (down-the-hole-hammer) is used in hard rock. Because an air stream transports the cuttings in rotary percussion drilling, the borehole wall must be stable. Therefore, the borehole is cased to the depths where solid hard rock is reached (Fig. 6.12).

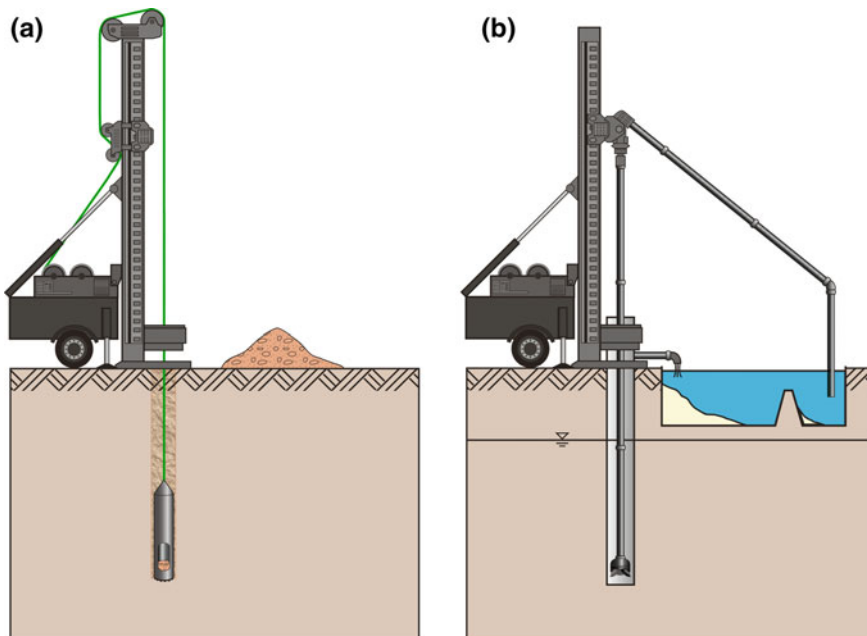


Fig. 6.10 **a** Cable drilling. **b** Direct-mud rotary drilling



Fig. 6.11 The picture from a drilling site shows the standpipe with the drill string and the down-the-hole hammer in place

A flushing flow of water and, if necessary, additives remove cuttings in mud rotary drilling methods. Rotary percussive drilling (pneumatic drifter drilling) produces the cuttings and drives the top hammer with compressed air.

An interesting variant of a rotary percussive method is the so-called Geothermal Radial Drilling. The method permits to drill a series of inclined boreholes radially from a fixed central drilling site. The resulting installation is a hybrid of ground heat collectors and vertical geothermal probes and is of advantage on smaller properties for utilizing all available land.

In unconsolidated cover material various **auger drilling** methods are also commonly used for emplacing geothermal probes (Fig. 6.13). Particularly hollow stem auger drilling is well suited for geothermal probe installation. The geothermal double U-tube can be installed together with the grouting hose inside the hollow stem auger that has been drilled to the desired depth. Auger drilling can also be performed in a standpipe (Fig. 6.13b). Probe and grouting tubes can be installed in the standpipe, which is later removed during grouting.

Direct push technology uses the weight of a carrier vehicle to drive geothermal loops into the ground by displacement and compaction of the soil particles only.



Fig. 6.12 Down-the-hole hammer used for geothermal probe installation



Fig. 6.13 Auger drilling for geothermal probes. **a** The geothermal probe can be installed inside a hollow stem auger that has been drilled to the desired depth. **b** Auger drilling in a standpipe (large diameter pipe to the right of the auger). The auger deposits drilled fine-grained material after being lifted out of the standpipe

The direct push devices can be mounted also directly on solid construction elements of the building. The hydraulic press can be combined with percussion. The direct push method is excellently suited for installing tools, measuring strings and monitoring instruments into soft near surface ground (Vienken et al. 2019). However, direct push machines can be used for inserting shallow geothermal probes into soft cover sediments. The method is rapid, clean, cost-effective, and straightforward. However, it requires ground with suitable mechanical properties. The probe loops reach maximum depths of some meters only, so that many loops must be installed for providing the thermal energy demand even of a single-family home. If the loops are installed without a backfill thermal connection to the ground may be weak depending on the groundwater table. If the probes must be operated with a working fluid containing anti-freeze, the system will be a potential threat to groundwater resources. In the absence of a tight backfill operating the loops with an anti-freeze bearing working fluid may be in conflict with legal regulations.

6.4.1 *Rotary Drilling*

Rotary drilling uses a top drive and the upwelling wash-fluid brings the cuttings through the annular space to the surface. The pumped fluid reaches an adequate flushing pool or settlement tanks or sedimentation ponds (Fig. 6.14). Samples of the cuttings for geological analysis need to be taken immediately from the washing-fluid before it reaches the tanks/pools. In the tanks, the cuttings settle from the drilling



Fig. 6.14 Example of a simple settling tank for drilling fluid from a geothermal probe installation site. Behind the tank: Geothermal probe with mounting aid ready for installation

fluid. After sedimentation, the clean fluid is pumped through the drill string back to the drilling tool where it picks up new cuttings. The pumping pressure needs to be high enough to overcome friction losses in the drillstring. Direct-wash rotary drilling uses typically piston or centrifugal pumps. Centrifugal pumps can generate large flow rates but depend on the delivery height, in contrast to piston and displacement pumps.

The stability of the borehole depends critically on the overpressure of the drilling fluid, which corresponds to the difference between the groundwater table and the drilling fluid table. Consequently, the density of the drilling fluid must be adequately adjusted.

The flow velocity of the drilling fluid in the annular space needs to be about $0.5\text{--}1.0 \text{ m s}^{-1}$ to produce the cuttings. Velocity depends on the density of the fluid and the size of the cuttings. The downward flow velocity of the drilling fluid in the drill string is much higher and the flushing jet forcefully hits bottom hole, where it loosens the cuttings and washes them into the annular space. The flow velocity of the drilling fluid in the drill string depends on the inner diameter of the string. A small diameter results in a high flow velocity, however friction losses increase considerably also. The upward fluid flow velocity in the annular space controls the maximum size of the cuttings that can be transported. Typical fluid ascending speeds of 0.5 m s^{-1} can transport cuttings not larger than about 8 mm.

Wash boring is a boring system to drill larger size holes in soft formations. Casing with a casing crown attached is rotated into the ground and water is used to flush out the drilled formation.

The drilling fluid has many functions in wash boring techniques. It stabilizes the wellbore, it produces the cuttings, it supports the drilling process and a clean bottom hole, it cools and lubricates drill bit and drill string and, in some techniques it drives the drilling tool (down-the-hole hammer, drilling turbine). Furthermore, a suitable fluid composition may help, to some degree, to control spontaneous variations of formation pressures.

Typical additives to the washing fluid in drilling boreholes for geothermal probes include: Bentonite clay powder, carboxymethyl cellulose (CMC) products and loading agents. Bentonite clay powder increases the viscosity of the drilling fluid and thus promotes the discharge of the cuttings, particularly if the fluid speed is low. Bentonite-bearing washing fluids tend to produce filter cakes in the wellbore. CMC products are polymeric additives that produce a thin filter cake grouting the borehole wall. The sealed wall facilitates the removal of the clay fraction from the borehole. The filter cake prevents loss of drilling fluid to aquifers and overburden. The seal stops infiltration of washing fluid into drilled clay layers thereby precluding clays from swelling. Because the additive bentonite cannot swell in a CMS fluid, CMC's must be added later to a bentonite fluid. Increasing the density of the drilling fluid with loading agents such as calcite or baryte powder is valuable in drilling artesian groundwater aquifers.

With this increased density of the drilling fluid many artesian aquifers or aquifers with slight hydraulic overpressure can be controlled. If, for example, an artesian aquifer with a hydraulic overpressure of 0.3 bar is drilled 60 m below surface,

adjusting the density of the drilling fluid to $\rho = 1.1 \text{ } 10^3 \text{ kg m}^{-3}$ will produce the necessary pressure of the drilling fluid:

$$\text{Pressure of drilling fluid: } 60 \text{ m} \times 1.1 \times 10^3 \text{ kg m}^{-3} \cong 6.6 \text{ bar.}$$

$$\text{Pressure of artesian aquifer: } (60 \text{ m} + 3 \text{ m}) \times 1.0 \times 10^3 \text{ kg m}^{-3} \cong 6.3 \text{ bar.}$$

$$\text{Overpressure of drilling fluid: } 6.6 - 6.3 \text{ bar} = 0.3 \text{ bar.}$$

The feed regulation of the drilling fluid depends on the ground to be drilled, on the planned drilling method, the power of the pump and the ascent rate of the fluid. The drilled solid materials need to settle sufficiently in the sedimentation tanks, for not to alter the density of the drilling fluid. Available standard methods can easily measure the density of the drilling fluid with hydrometers, the viscosity with a so-called Marsh funnel and the water release rate (water binding capacity) with a Ring apparatus.

In addition to the cuttings, several drilling parameters such as drilling progress, drilling (wash) fluid pressure; rotational speed and drill bit pressure give valuable information about geological changes at bottom hole during drilling. These parameters are in sight of the operator at the control panel of the drilling rig (Fig. 6.9b). The parameters can also been continuously digitally recorded and may serve as important legal proves if necessary and for the geological interpretation of the drilled stratigraphy.

6.4.2 Down-The-Hole Hammer Method

Rotary percussive drilling is mostly done with down-the-hole hammer (Fig. 6.12). The cuttings are brought continuously to the surface through the annular space by a powerful air stream. A top drive rotates via the drill pipe the down-the-hole hammer at speeds of several tens of revolutions per minute. At the same time, a compressor pumps air at 15–35 bar through the drill pipe to the down-the-hole hammer. The compressed air drives a plunger that causes the bit of the hammer to strike the bottom of the borehole at speeds up to 3000 times per minute. The compressed air leaving the hammerhead cleans the bottom hole and transports the cuttings trough the annular space to the surface.

Drilling with down-the-hole hammer is favorable in hard rock and hard cohesive soil. It is of limited use in loose sand and gravel. The great advantage of this method is that water influx to the wellbore from water conducting layers and structures can be recognized immediately during drilling.

Specially designed down-the-hole hammers can be operated with water instead of air or with a water-air mixture. Special down-the-hole hammers make it even possible to increase the diameter of the wellbore below a chosen depth.

Double head drilling is a further popular method for drilling boreholes for geothermal probes. Two separate top drives for the inner drill pipe and the outer casing work in tandem until the casing is put in place. After that, drilling is continued with the top drive for the inner drill pipe.

6.4.3 Concluding Remarks, Technical Drilling Risks

Drilling boreholes for geothermal probes is relatively rapid and short-lived, however, it suffers from cramped and limited space. Therefore compact and mobile drilling equipment is ideal. Space limitations make it essential to carefully plan and organize the drilling site. Before starting to drill, the exact location of existing pipework (water, gas), cables and other obstacles on the property must be cleared up.

We strongly recommend keeping details of the drilling progress with an appropriate drilling data recorder and documenting the data. Mechanical loggers record drilling progress, depth, drill bit pressure and drilling fluid pressure. These data give valuable information on the geological properties and structure of the ground. For example, drilling data from digital loggers can be combined with data from a gamma ray logger used to probe the borehole to considerably ease the geological interpretation of the drilled stratigraphy.

If several boreholes are to be drilled, minimum distances between the wells must be strictly observed (Sect. 6.3). If the individual geothermal probes that ought to be connected to the heat pump have different connection lengths or reach to different depths, then hydronic balancing is also necessary on the geothermal probe side.

If the borehole is exposed to water influx or even artesian water, natural gas etc., special measures are required to fight these threats. The procedures include protection by casing, increase of the density of the drilling fluid, installation of a packer or, in extreme situations, tight sealing of the borehole.

The most common **technical drilling risks** are briefly described in the following:

Swelling clays in clay-rich strata may represent a drilling risk. Drilling such strata requires a special drilling fluid that prevents swelling of clays (Sect. 6.4.1). After installation of the probe, the borehole must be professionally and permanently sealed excluding any water access to the clays in the future, otherwise swelling pressures may build up to where the installed probe may be destroyed or in the worst case may cause damage to nearby buildings.

Any geological formations that contain the mineral anhydrite (CaSO_4) must be drilled highly alert and attentive. Anhydrite reacts in contact with water to gypsum ($\text{CaSO}_4 \cdot 2\text{H}_2\text{O}$). The mineral transformation causes a volume increase of more than 60%. Extreme caution is required if aquifers are drilled in the footwall or hanging wall of the anhydrite rocks. Drilling should be aborted and the borehole should be firmly sealed when artesian aquifers are drilled in the footwall or aquifers with negative pressure in the hanging wall of an anhydrite layer (Figs. 6.15 and 6.16). Similar effects and challenges can be caused by any kind of other mineral in geological strata that react with water. Therefore, it is highly recommended to be aware of the problem and study available geological maps and other local geological stratigraphic information before drilling.

Drilling quicksand layers require casing of the respective sections to prevent sand loss to the borehole and potential erosion of the hanging wall and danger of subsidence of the surface. Wellbores without casing through strongly karstified ground beneath unconsolidated clastic sediments tend to draw material from the hanging wall

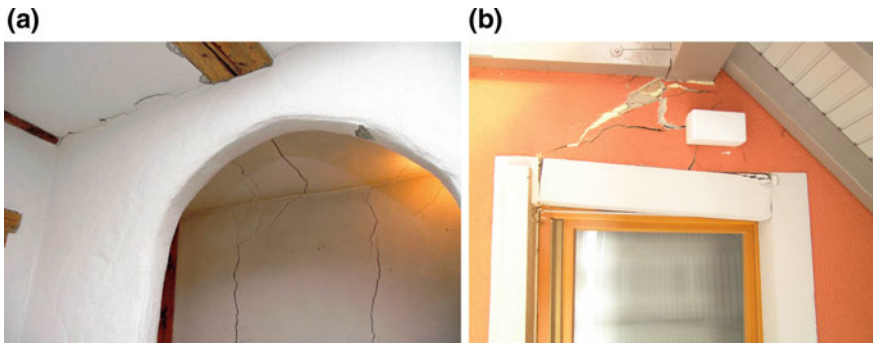


Fig. 6.15 Drilling risks: Structural damage of buildings caused by swelling layers in the ground. Here the differential surface movements have been caused by the reaction of anhydrite with water from a leaking aquifer to produce gypsum accompanied by a 60% volume increase (City of Staufen, SW Germany): **a** Damage pattern inside a building, **b** complex structure of damage around a window

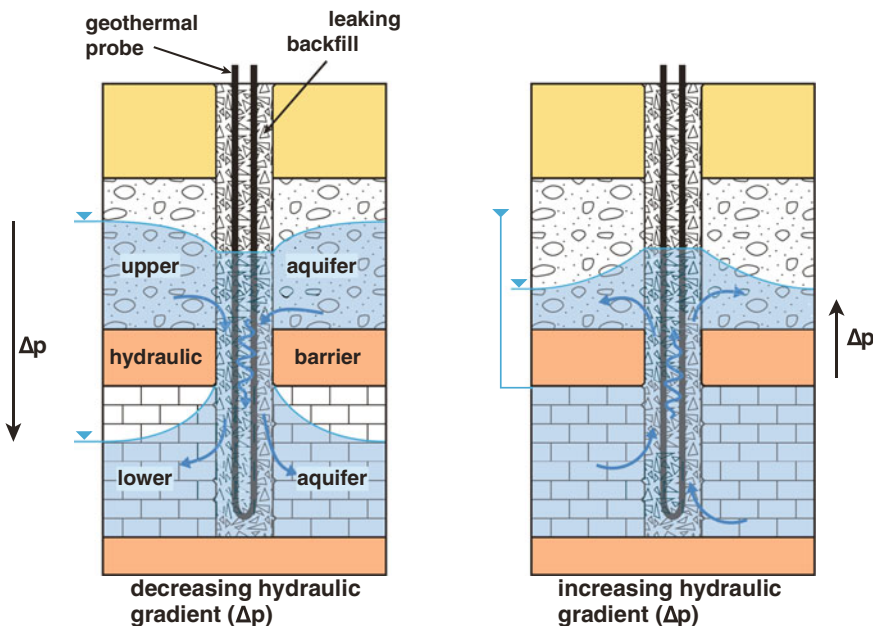


Fig. 6.16 Consequences of leaking backfill of a geothermal probe in stratified ground with aquifers increasing and decreasing hydraulic gradient

causing subsidence and sinkholes at the surface. Thus such drillholes should also be equipped with a standing pipe or a casing to the solid hard rock. Surface subsidence also may result from leaching and dissolution of soluble minerals in geologic strata such as halite and other salts by abundant water infiltration along hydraulic conduits

produced by drilling but also by other water conducting structures in the ground. It is strongly recommended to securely seal the wellbore under such circumstances.

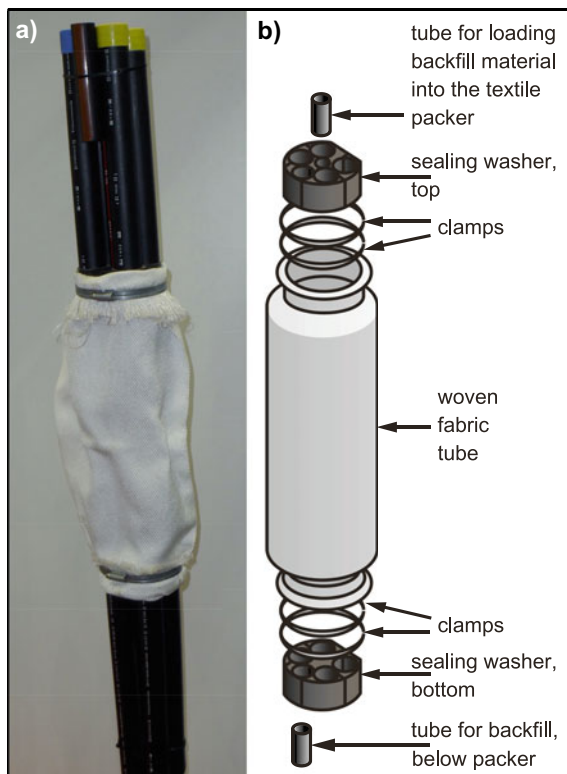
Serious drilling problems may occur if larger cavities or caves are drilled in susceptible rocks including karstified limestone, dolomite, salt- and gypsum-bearing strata, fault zones and coarse banked fractured hard rock aquifers. The drill pipe may break through and massive loss of drilling fluid may occur. Secondary problems resulting from this geological situation include difficulties with the backfill of the annular space. Special backfill materials and packers may be required. In the worst case the borehole can be lost and must be backfilled and firmly sealed.

During drilling through fault zones and other tectonically damaged ground the drill pipe may jam. The borehole crossing faults may close after its completion to where the geothermal probes cannot be installed. Commonly the only remedy is to over drill or drilling a new borehole.

Sections of the wellbore can be hydraulically separated using geothermal probe packers. Packers are also used to control weak artesian aquifers or separate aquifers at different hydraulic pressures. Specially designed hose-like geothermal probe packers (Fig. 6.17a) consist of two packer sealing elements, a fabric hose and mountings. Also the packer elements are made of textile fibers. The fabric hose is put over the

Fig. 6.17 Packer:

- a Geothermal probe packer (textile fabric packer).
 b Schematic assembly of a geothermal probe packer



geothermal probe and placed at the appropriate position. Both ends of the textile hose are then fixed to the probe by rubber sleeves and sealed (Fig. 6.17b). A grouting pipe is placed through the two rubber sleeves so that the section below the packer can be sealed. A second grouting pipe runs through the upper rubber sleeve and is used to fill the packer. A third grouting pipe is used to backfill the section above the packer. The assembly of geothermal probe, mounted packer and installed grouting pipes are lowered into the borehole and fixed at the desired position of the packer. After grouting the section below the packer, the packer itself can be inflated with backfill material in this way sealing the lower from the upper section of the borehole. Then follows backfilling of the upper section. In principle it is possible to install two packers for the isolation of a certain section of the borehole. In practice, however, placing the entire assembly of probes, packers and grouting tubes into a borehole against hydraulic overpressure can be challenging.

Drilling for a geothermal probe in certain regions may possibly expose layers with pressurized natural gas or artesian groundwater. Drilling into an artesian aquifer may cause large volumes of water to flow from the borehole causing additionally washout of fine-grained solid material. The occurrence may severely damage the borehole to where sealing is hindered later or made impossible. Moreover the ground around the borehole may subside or even collapse. Therefore it is necessary to plan with precaution when drilling in regions where artesian aquifers are known to exist. When drilling at sites where artesian aquifers pose a potential hazard the casing must be firmly anchored in the solid ground of the hanging wall. Because loaded high-density drilling fluid will become necessary if artesian aquifers are drilled, appropriate amounts and types of loading agents must be kept ready. Also a suitable packer system for reliably blocking the water ingress must be held in readiness. A weakly confined aquifer with low overpressure can perchance be sealed with a geothermal probe packer. We recommend sealing the lower section or the entire borehole using a “lost” packer if drilling into a stronger artesian aquifer or the borehole must be abandoned.

Natural gas may stream from the borehole under high pressure. Also possible are diffuse slowly developing gas seeps. If a gas reservoir is drilled, similar measures to the ones controlling an artesian aquifer are recommended. Additional precautions are of need, however, because gas may burn or explode (methane), it can be highly toxic (e.g. hydrogen sulfide) or it may cause a suffocation hazard (e.g. carbon dioxide, nitrogen). Therefore, the gas must be analyzed and identified before any decisions are made concerning the further procedure. If the gas is hazardous the geothermal probe cannot be installed and the borehole must be gas-tightly sealed and may not be overbuilt later.

Methane seeps are known particularly from coal-bearing strata (Carboniferous), from clays rich in organic material (e.g. middle Jurassic Opalinus Clay in central Europe) but also in other strata. 5 – 14 volume % CH₄ in air is explosive, higher concentrations can cause difficult to control fires.

In the Swiss village of Wilen (Canton Obwalden), natural gas has been drilled at 125 depth, which then streamed into the borehole at an overpressure of 3 bar (Wyss 2001). The judicious and rapid reaction of the drillmaster controlled the discharge.

The gas was burned. Later on the borehole was sealed and refilled. A geothermal probe has not been installed.

Groundwater may contain high amounts of dissolved gasses. The commonly used probe pipe material, PE pipes is permeable for gases. Carbon dioxide, for example, can easily diffuse through the walls of the PE pipes, due to the size and structure of the CO₂ molecules. Restart of the circulation pump of the primary circuit after extended downtime brings the gas-rich water to the surface where it degasses possibly with massive foam generation. Conventional air separators in the inlet line may get overcharged and cannot separate all of the large amount of gas exsolved from the pumped water. The foam may reach the evaporator of the heat pump and may considerably reduce the heat extraction power of the system and may eventually shutdown the heat pump. Considerable corrosion hazard can potentially be associated with CO₂-rich salty waters, which may damage the heat exchanger of the evaporator of the heat pump. Geothermal probe projects in regions with known free CO₂ gas in soil, strata or hard ground should use gas-proof probe material that is impervious to gas diffusion. Also, if the probe is being built nonetheless the plot should be kept free from installations or buildings.

6.5 Backfill and Grouting of Geothermal Probes

Backfill and grouting of a geothermal probe is an essential component for an efficient, ecologically meaningful operation, for the durability of the probe and for observing groundwater protection regulations. It must efficiently physically and chemically stably connect the probe with the surrounding ground. The backfill must be permanently impervious. It is important that the original hydraulic functionality of impervious layers separating aquifers remains intact (Fig. 6.16). The tightness of the grouted probe must be higher than that of the impervious layers in the stratigraphy. The hydraulic conductivity of the grouted probe is not exclusively determined by the backfill material. Other factors include the material of the probe including the surface texture of the tubes and the temperature variations during operation (freeze / thaw).

Whether or not inefficient grouting must be repaired or just reduces the efficiency of the probe depends on the geological situation underground. Repair work is mandatory if the wellbore penetrates complexly stratified ground particularly if artesian aquifers are part of the stratigraphy. However, inefficient grouting is very hard to repair and remediate. If a grouted probe with double U-tubes with an incomplete backfill must be repaired it can be attempted to fill in the cavities afterward. For this purpose one of the tubes can be cut open at the damaged depth and used for injecting backfill. The U tube is then lost for heating purposes though. The second and intact U tube can be used as heat exchanger. Also the necessary measurements controlling the success of the remediation can be made from the second U tube. If the described repair work was unsuccessful it can be attempted to remove the installed probes by drilling. This is a technically very difficult task and demanding for even

the best drillers. The plastic material and the contorted course of the four tubes make drilling a challenge. If the probe is lost the wellbore must be carefully sealed.

It must be kept in mind that the land owner and client is liable for any damage of any kind resulting from a unprofessional and incompetent construction of the ground source heat exchanger system. Nevertheless, in some countries backfill is not an authoritative requirement.

Immediately after drilling of the borehole, the probe pipes are taken from the reel and mounted in the borehole. Grouting must be started without delay. Backfill of the probe seals the different drilled layers of the ground against each other and thus is important for protecting groundwater horizons, preventing hydraulic short cuts along the borehole and restoring the sealing properties of aquitards/aquiclude (Fig. 6.16). A proper backfill represents also an additional barrier for leaking heat transfer fluid from damaged probe pipes to the groundwater. An appropriate backfill thermally connects the geothermal probe optimal to the surrounding ground. The backfill stabilizes the borehole, must fill it permanently and without settling. In continuous unconsolidated gravel series grouting is not necessary and perhaps should not even be attempted.

From the described function and requirements, optimal backfill material has the following properties:

- Low hydraulic conductivity ($k \leq 10^{-9} \text{ m s}^{-1}$), long-lasting tightness
- k of the grouted probe system should be lower than k of the aquitards separating aquifers
- Approved for use in aquifers, water-hygienic unproblematic, not hazardous for water
- Easy to use and secure workability at the construction site, easy to pump
- Sedimentation-stable, volume constant and low-shrinkage setting behavior
- Resistant to chemical attack (concrete-corrosive waters, sulphate-bearing rocks)
- Thermal and mechanical stability
- Excellent flow properties
- Void-poor structure of the set material
- Excellent thermal conductivity.

Many different products are used as backfill material. The components of backfill, normally cement, bentonite, clay or quartz sand, are mixed with water to a suspension. The different components have different functions. Cement provides compressive strength and sealing properties. The swelling properties of clay are responsible for volumetric stability of the suspension. The features of bentonite are similar to clay. It has a particularly high swelling capacity and a distinctly thixotropic behavior. Admixing quartz sand or quartz powder increases the thermal conductivity of the backfill. Cement makes operation of the geothermal probe at freezing temperatures possible. However, cement should be added sparingly to keep the backfill slightly plastic. Flexible backfill assists accommodation of the thermal expansion of the probe and averts water-conducting structures along the probe pipes to form.

Typical backfill materials have a high thermal conductivity in the range of 0.6–1.0 $\text{W m}^{-1} \text{ K}^{-1}$. Improved products may reach 1.6–2.2 $\text{W m}^{-1} \text{ K}^{-1}$ and enhance

transport of thermal energy to the heat transfer fluid in the probe pipes. Presently new pipe materials with high thermal conductivity are being tested (Sect. 6.2).

Factory-ready backfill materials should be used only. The backfill suspension needs to be mixed to the density specifications given by the provider within the limits of the accuracy of the measuring instrument (about $\pm 0.05 \text{ g cm}^{-3}$). Deviations can only be accepted for defensible exceptional cases. Otherwise the desired backfill material properties cannot be warranted. The components must be mixed at the construction site and the sealing slurry must be handled instantly. Special backfill and grouting mixers have been designed for geothermal probe installation (batch mixer, colloidal mixers, continuous mixers). Colloidal mixers proved to be appropriate tools for grouting geothermal probes (Fig. 6.18). After 90–120 s mixing time the backfill material tends to be colloidal and completely homogenized. The density of the suspension should be within 1.3 and 1.9 t m^{-3} (Fig. 6.19). The suspension may not unmix before and during curing, setting and drying. The Marsh funnel time, a practical measure related to the viscosity of the suspension should vary between 40 and 100 s L^{-1} (28 s L^{-1} for pure water). The backfill should achieve minimal settlements in the range of 0.5–1.0% and the strength should be $\geq 1 \text{ N mm}^{-2}$. The temperature during setting of the backfill materials must stay below the danger of heat damage to the probe pipe material.

In order to achieve a dense, void-poor backfill it is necessary to grout from bottom to top (Tremie process). Density and viscosity of the backfill material should be high enough to push remaining drilling fluid and water from the borehole during ascent. The backfilling work should not be interrupted and carried out without delay after



Fig. 6.18 Use of a colloidal mixer at the construction site

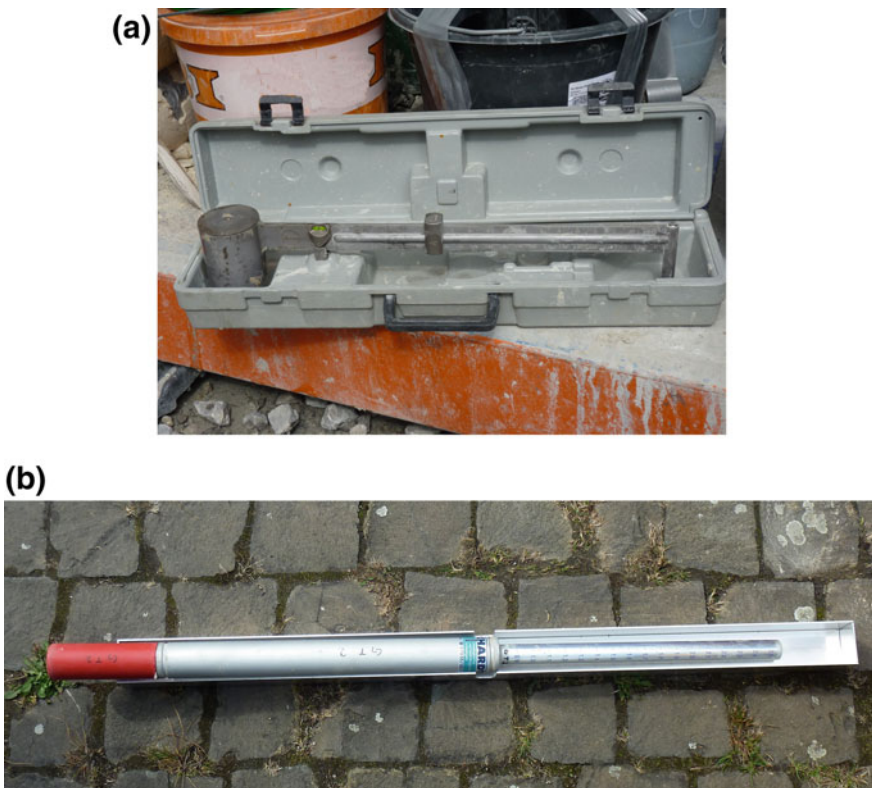


Fig. 6.19 Tools for measuring the density of the backfill slurry at the construction site: **a** Density balance, **b** hydrometer

completion of the borehole. The suspension-filled grouting line should remain in the borehole. If the grouting pipe is to be removed from the borehole, this should be done carefully and slowly and with re-injecting backfill material. The actual volume of the backfill material must be bigger than the difference between volumes of the borehole and the geothermal probe. Backfilling is not finished before the density of the suspension discharging from the top borehole has not reached the density of the original backfill slurry.

In practice, however, very often too “thin” low-density low-viscosity suspensions are being grouted because they are easier to pump. Such suspensions have a high water/solid ratio and thus produce an incomplete and short-lived backfill of the probe. This results in a reduced heat transfer capacity from the ground to the heat transfer fluid in the probe pipes and may potentially trigger more serious damages. The correct density of the backfill slurry must be measured on-site with a density balance or a hydrometer (Fig. 6.19) and should be documented. The density and the related viscosity of the slurry should be notably higher than that of water. On the other hand it should not be too thick either. Highly viscous backfill slurry tends to form voids

and other flaws particularly in wellbores with inserted U-tube probes. The viscosity of the suspension should be unconnected to the flow velocity because significant changes in flow velocity occur at different points in the system during grouting.

Centrifugal pumps build up relatively little pressure and thus can only be used for backfilling of geothermal probes with shallow depths. Positive-displacement pumps (worm pumps) are suitable for backfilling of deeper probes.

One of the important functions of an appropriate backfill is to prevent a permanent hydraulic connection of drilled aquifers at different levels. If aquifers at different levels have been connected by a borehole, several quantitative and qualitative effects may be triggered, particularly if the aquifers that were originally separated by groundwater barriers are at different hydraulic pressures (Fig. 6.16). Firstly, hydrochemical alteration and exchange of groundwater contaminants between aquifers become possible. For example, seepage of highly mineralized deep groundwater may deteriorate shallow fresh-water aquifers. Anthropogenic contaminants from shallow groundwater levels may gain access to deeper aquifers and nitrate, pesticides, bacteria and organic solvents can be transferred to unpolluted groundwater. Normally groundwater in different soil and ground layers is of distinctive chemical composition. Migration of water from one layer to another because of a hydraulic short-cut along an improperly grouted borehole may cause a multitude of chemical reactions between the water and the solid aquifer rock including dissolution of rock thus creating cavities and precipitation of minerals reducing the hydraulic conductivity of the aquifer. Furthermore, a short-cut of aquifers at different hydraulic potentials (water table) can cause hydraulic disturbance such as changes of the water tables including drying-up of springs or subsidence or uplift of the ground and related possible damages to buildings. Faulty grouting of wellbores through artesian aquifers below anhydrite-rich strata caused uplift of several 10 s and lateral displacements wreaking severe damages to buildings in some towns and villages in the Upper Rhine Valley (Staufen (Fig. 6.15), Böblingen, Rudersberg, Lochwiller). For this reason, if aquifers at different levels are drilled, water tables must be observed and regularly measured and if the hydraulic potentials are significantly different appropriate precautions need to be taken to isolate the aquifers.

On the background of damage cases new tube materials have been developed featuring a rough outer surface, which improves the tightness of the system in problematic stratified ground (Fig. 6.16). The rough surface of the tube enhances the contact of tube and backfill.

Drilling a borehole for a geothermal probe may, like any other drilling, cause turbidity and microbial contamination of groundwater. This possible danger is particularly relevant for neighboring groundwater wells, mineral water or thermal water developments. Experienced drilling companies should be aware of these vulnerabilities and with all associated legal aspects and responsibilities. They should be capable of performing the necessary tasks without affecting other uses of the ground at specified distances from the geothermal probe borehole.

Geothermal systems should not excessively heat or cool drilled aquifers, if present, which are kept for further utilization because this may lastingly alter the chemical and microbiological properties of the groundwater.

6.6 Construction of Deep Geothermal Probes

Conventional double U-tube geothermal probes that shall be installed to depths significantly below 150 m must consist of special probe materials resisting the higher pressure and the excessive stresses associated with standard installation. Special installation techniques for the overly long probe may be necessary for avoiding damages to the probe. The standard pipe material for deep probes is polypropylene random (PPR) and pipes PN20 are typically used. Because this special pipe material has much thicker walls the geothermal probe has a strongly increased thermal borehole resistance (Sect. 6.3) so reducing the efficiency of the system. This must be considered in planning the geothermal probe system. Therefore, pressure-resistant thick-wall pipes should be avoided whenever possible. Installing probes with standard materials and wall thicknesses in deep boreholes requires a more elaborate installation procedure for not compromising the pressure-stability of the probe pipes. More than 300 m long probes should not be built with conventional pipes, however.

Mounting a central tube helps to compensate buoyancy during installation of the probe. The extra tube can be used for grouting of the deeper sections of the probe. Very deep probes may require several grouting tubes.

If the deep probe system reaches distinctly elevated temperatures, e.g. in combination with solar thermal systems, the geothermal probe should be made of polyethylene (PE-RC) pipes or cross-linked polyethylene (PEX) pipes. Both materials are more resistant to crack formation than e.g. PE 100. The pipes withstand pressures of 15–16 bar during a 50-year lifetime. In addition to the thick walls the used pipes have a larger inner diameter leading to an increased flow rate and consequently to an enhanced heat extraction rate. A newly designed probe foot made of corrosion resistant stainless steel (Fig. 6.20) suited for deep probes connects the tubing.



Fig. 6.20 Specially designed probe foot for deep geothermal probes

The relevant pressurization of the probe pipe corresponds to the pressure difference between external pressure (fluid pressure of the saturated zone) at depth and the internal pressure in the pipe (hydrostatic pressure of the heat transfer fluid + system pressure of the geothermal probe loop). The pressure conditions need to be carefully examined for geothermal probes deeper than 150 m. Typical system pressures of the probe loops vary between 1.0 and 2.5 bar during operation.

The backfill material used for geothermal probes has a density (ρ_V) between 1.4 and $1.9 \cdot 10^3 \text{ kg m}^{-3}$; the density of the heat transfer fluid (ρ_w) is much lower around $1.0 \cdot 10^3 \text{ kg m}^{-3}$. The difference between hydrostatic pressures of the fluid-filled probe and the grouting suspension determines the maximal possible depth of the probe.

For example: With a density of the backfill suspension $\rho_V = 1.8 \cdot 10^3 \text{ kg m}^{-3}$ and a water-filled probe pipe the pressure difference reaches 16 bar ($=16 \cdot 10^5 \text{ Pa}$) at the probe foot in 200 m depth.

This follows from:

$$(\rho_V - \rho_w) \cdot 9.81 \text{ m s}^{-2} \cdot 200 \text{ m} = 16 \times 10^5 \text{ Pa} \quad (6.7)$$

Dimension: $1 \text{ Pa} = 10^5 \text{ bar} = 1 \text{ kg/(m s}^2\text{)}$.

The resulting pressure difference implies that for the densities used in the example, construction site practice advises that a quality-assured installation of a probe deeper than 200 m is not possible.

A reliable estimate for the maximum possible installation depth (D_{\max}) of a geothermal probe follows from the relationship:

$$D_{\max} = 15 \cdot 10^5 \text{ Pa} / [(\rho_V - \rho_w) \cdot 9.81 \text{ ms}^{-2}] \quad (6.8)$$

With the parameters used in the example above the resulting $D_{\max} = 191 \text{ m}$. The underlying assumption here is that the pipe material tolerates not more than 15 bar pressure difference.

The mounting and installation procedure for very deep geothermal probes depends on the planned depth and the water table in the borehole.

If the borehole is water-filled nearly to the top, the probe pipe must be filled with water already on the mounting reel and inserted to the borehole this way. The density of the anticipated backfill material must be in harmony with the planned depth of the probe (Eq. 6.8). For a 400 m deep geothermal probe the maximum tolerable density of the backfill is $\rho_V = 1.375 \cdot 10^3 \text{ kg m}^{-3}$. These considerations need to be coordinated with all other requirements for the backfill.

If the water table in the borehole is more than 150 m below surface, the installed geothermal probe should not exceed 300 m depth. In principle, deeper probes are possible but conventional conditions at typical construction sites may not warrant quality assured installation, which is considerably more intricate than at high water tables. Quality assured installation of deep probes into completely dry boreholes is likewise difficult and convoluted.

Moreover, the pressure losses for circulating heat transfer fluids in standard 32 mm diameter probe pipes gradually increase with length (depth) and become exceedingly high at lengths higher than 130 m, which seriously compromises the profitability of the installation.

The deepest geothermal probes using conventional design and double U-tubes reach down to about 800 m. Note however, that specially devised deep geothermal probes employing coaxial tubes may reach to 2000 m (Fig. 4.1). The installation of the heavier probe on larger reels requires a special mounting tool. For large diameter probes deeper than about 300 m the wellbore is drilled by mud rotary drilling.

The deep probes exploit ground at higher temperature thus passive cooling in the warm season is not possible in contrast to common near surface probes. However, also deep probes can successfully store excess solar thermal energy in the warm season for use in the cold season.

6.7 Operating Geothermal Probes: Potential Risks, Malfunctions and Damages

Ground source geothermal probes are established and mature systems for heating and cooling of buildings and other structures. These installations require a professional dimensioning, design and construction. Inappropriate construction and operation normally results in a case of damage. For this reason, official authorities in Switzerland released a damage catalogue addressed to all parties involved in planning, installation and operation of geothermal probes with the intention to reduce damage cases (Basetti et al. 2006). Several damage cases have been documented and analyzed (Greber et al. 1995; Wyss 2001; Grimm et al. 2014) (Fig. 6.15). In Switzerland and SW-Germany an institution called “heat-pump-doctor” assists concerned citizens in especially difficult instances including legal help. In Germany, as an example, drilling companies must take out a legally required liability insurance including a follow-up liability insurance for several years. Special risks related specifically to drilling have been discussed in Sect. 6.4.3 above.

A common problem results from excessive heat extraction from the geothermal probe causing the surroundings of the probe to freeze; resulting normally in reduced efficiency of the system and may finally lead to a complete failure of the system.

Cases of damage occasionally result from long operation times for the heat pump caused by a flawed control system for the heat pump – geothermal probe system and (or) by inadequate coupling to the heat distribution system of the building.

Commonly mistakes that lead to later damages on the geothermal system are already made in the planning phase of the project. Typical errors include wrong determination of the heat requirement of the building, ignoring the necessary continuous hot water demand, using inadequate thermal parameters and properties of the drilled ground, under dimension of the geothermal probe (too short probe) and not correctly considering the thermal effects of other nearby geothermal probes. Damage

cases occur also after installation and commissioning caused by incorrect adjustment of the heat pump or the hydraulic system. It is also problematic if the client adds further buildings, annexes, or installations to be heated by the geothermal probe for which it has not been designed.

During construction it is important to insist on a correctly emplaced backfill (Sect. 6.5). If the backfill is lacking or incomplete, or excavation or other improper material has been used as backfill then the system imposes a threat to groundwater safety. Moreover the stability of the geothermal probe is compromised resulting in poor extraction rates combined with involuntary operation at freezing conditions. Finally the response of the ground to a faulty probe may damage buildings in the nearby and more distant surroundings. In SW-Germany, as an example, the construction of geothermal probes induced various serious damages with financial losses for the client and third parties at nine construction sites. Damage to buildings has been caused by swelling and subsidence of the ground. Damages include also dry running wells, permanently reduced yield of springs, adverse connection of different aquifers resulting in impaired groundwater quality, polluted surface waters and more. The damage cases have been caused by faulty backfill in most cases. Faulty backfill in combination with connected aquifers with different hydraulic potentials (Fig. 6.16) is responsible for the most severe damage cases. Two cases of drilling artesian aquifers caused minor damage.

Operating a geothermal probe under freezing conditions (negative °C) may result in damages to the probe, the backfill and the ground itself because ice may form at the outer probe pipe surfaces and in the ground surrounding the probe. Related to the freezing–thawing cycles increasing numbers of fractures form together with ice in the backfill and the enclosing ground is concentrated at material boundaries between probe and backfill and backfill and ground. The fractures gradually increase in size. The ice cover steadily displaces the backfill around the probe pipes with the result that the seal for groundwater protection becomes broken. Ice formation may cause ground swell in the vicinity of the probe during the cold season. After thawing, the ground surface may subside and even collapse locally (sinkholes, cones around the probe, ground settling above the supply lines). Further damage in the probe environment slowly develops. Additionally, the electrical power requirement of the entire system gradually increases. However, not all damages become manifest at the surface (swelling, subsidence). Damage to the structure of the system grows to be visible first in performance deterioration of the installation. In extreme cases the entire system may break down.

If the thermal properties of the drilled ground layers or of deep groundwater tables have been considered for the design of the system incorrectly or insufficiently the danger exists that the probe may be too short and thus operated later under freezing condition with all the negative consequences for the entire system as previously explained.

Unprofessional and improper drilling of boreholes combined with unmindful supervision may lead to very serious or even catastrophic damage to structures and buildings of a large area as the example of Staufen (SW Germany) shows where 250 buildings have been damaged and the total cost of the reconstruction exceeds 200

millions of dollars (Fig. 6.15). These drilling risks, however, jeopardize any drilling and are not a risk exclusive to building geothermal probes.

The probe pipes can be defiled by forceful installation into the borehole, especially when the diameter of the borehole is too small or the ground unstable.

Installation of the probe in the cold season without prior warming of the pipes is difficult because of the stiff and inflexible probe plastic. The probes often develop damages during installation and consequently later the system suffers from leakages.

In case the geothermal probe is intended to be used for heating *and* cooling or it is planned to use the probe for storing excess heat in the warm season in the ground (e.g. heat from a solar-thermal installation) one must bear in mind that conventional probe material does not tolerate temperatures above 30–40 °C. Such applications require high-pressure cross-linked polyethylene pipes (PEX pipes).

Geothermal probes that are much longer than 150 m call for special stress and pressure resistant probe materials or a special installation protocol so that the probe is not damaged (Sect. 6.6).

6.8 Special Systems and Further Developments

6.8.1 Geothermal Probe Fields

If a geothermal probe in combination with a heat pump is used to heat a house this classic scheme is called a **monovalent** heating system. Only one energy source is used, therefore ground source heat pump, ground source heat exchanger, ground source loop and similar equivalent expressions are used. If many geothermal probes are installed in many boreholes to cover the larger heat requirements of a bigger building one speaks of a **geothermal probe field**.

If several geothermal probes are needed to cover the heat requirement of a building the mutual interferences need to be carefully evaluated. The usable heat reservoir per probe decreases with the number of geothermal probes installed in the available volume of ground. Geothermal probe fields require well-considered management plans to avoid the risk of continuously decreasing temperatures in the ground resulting from overexploitation. Dimensioning and planning of probe fields must utilize adequate modeling tools.

Commonly, geothermal probe fields are also used for cooling in addition to heating. Combining geothermal probes with solar-thermal systems is becoming increasingly popular. These **bivalent** heating systems consequently use two sources of thermal energy.

Many geothermal probes are typically required to cover the heat requirement of larger buildings. In contrast to single family homes with one or two installed geothermal probes and monovalent systems, bivalent or polyvalent systems are of interest for larger objects or buildings where air conditioning, cooling, utilization of process heat, utilization of other regenerative energies including solar and/or biomass,



Fig. 6.21 Geothermal probe field in an excavation pit: Wellheads with probes installed. After completion of the building the foundation slab will cover the geothermal probes

in combination may be of interest. Combined heating and power systems may be integrated into complex systems where a geothermal probe field is an integrated part. To meet the diverse requirements and all the individual profiles of the components and to deploy all the multifarious plant technologies an overall energy concept is utterly required. One must keep in mind that geothermal probes respond very slowly to changing conditions therefore they are not the right instruments for short-term storage of thermal energy.

The term geothermal probe field is used for groups of more than five closely arranged geothermal probes. Geothermal probe fields that also function as seasonal heat storage devices for solar-thermal installations or for cooling of larger buildings may involve ordered arrays of 100 or more geothermal probes (Fig. 6.21).

Examples of large geothermal probe fields include the installation at the Nye Ahus Hospital at Lørenskog near Oslo (Akershus University Hospital, Norway) with 350 geothermal probes each reaching to 200 m depth. The Umranije Shopping Center in Istanbul (Turkey) draws its thermal energy demand from 208 geothermal probes in a probe field.

Particular requirements must be complied for construction, installation and operation of geothermal probe fields. The design of large geothermal probe fields as heat reservoirs (sinks and sources) presupposes detailed knowledge of the thermal and hydrogeological structure and property of the ground. This necessitates the drilling of one or several test case geothermal probes at the planned site and collecting thermal and hydrogeological parameters of the ground. Thorough and detailed geological documentation of the drilled ground is compulsory. Water table, hydraulic conductivity and important hydrochemical parameters (e.g. concrete corrosive groundwater)

must be measured if aquifers have been drilled. Thermal-Response-Tests (Sect. 6.3.2) provide the project management the necessary data on the thermal properties of the ground. Local climatic conditions and variations must be known and implemented into the project planning.

With increasing number of geothermal probes in a probe field the individual probes interfere with each other and obstruct the transport of thermal energy through the ground. The typical specific performance of a solitary single probe can only be attained by a probe in the probe field if the ground is actively thermally regenerated in the warm season by transfer of excess heat to the ground. If properly designed the probe field can be operated with pure water as heat transfer fluid and no antifreeze chemicals are necessary, which increases the efficiency of heat transfer drastically.

Geothermal probe fields used for heating and cooling, particularly if sited in aquifers may create considerable thermal effects in the ground with remarkable cold or warm thermal plumes. The resulting temperature changes may cause local chemical or biological alterations in the groundwater. Increasing groundwater temperature, for example, can promote microbial activity in the ground that may cause chemical reactions between groundwater and the minerals of the solid ground thus changing groundwater composition. These changes may be inoffensive or harmful and toxic (mobilizing arsenic, cadmium, uranium for example). Stinted dimensioning of probe fields may generate the feared ice barriers in groundwater.

Heat storage in the ground changes the chemical composition of groundwater with the consequence that some minerals may dissolve and other minerals may precipitate from the water as the mineral-water equilibria adjust to the changed temperatures. Particularly critical is the supply of additional dissolved oxygen via the borehole to the aquifers, which typically results in precipitation of iron oxides and oxyhydrates and production of concrete corrosive sulphate. Even seemingly small temperature reductions from 10 to 2 °C cause feldspars to dissolve and clays and silica to form in sandy soils. These silicate-involving reactions are generally slow. However, reaction progress of dissolution-precipitation reactions rapidly increases with temperature. Various geochemical modeling tools are in use for analyzing groundwater composition data and for predicting the response to changing temperature, matrix minerals and chemical composition of the groundwater. The most popular of these tools is the code PHREEQC (Parkhurst and Appelo 1999) published and maintained by the USGS (Boulder, Co) (Sect. 15.3).

Geochemical and physical processes in the reservoir also rearrange the conditions for microbial prosperity. Population density and amount of biomass may dramatically change. High-temperature heat reservoirs may develop zoned microbial populations with thermophile microorganisms in the core region and mesophile microorganisms in an outer zone. The original population may be killed off. The adjustments to the biomass seem to be of local not regional extent (Ruck et al. 1990), however, the feature needs to be observed.

Several countries have issued strict legal constraints for minimizing the potential environmental impact on the ground or on groundwater. Such constraints may require that the temperature increase in the aquifer may not exceed 5 °C at 10 m distance from the nearest geothermal probe and must be less than 2 °C at 50 m from the probe field.

Therefore, it may be favorable computing or modeling the thermal consequences of the probe field in advance. The model calculations should reliably predict the temperature distribution in the ground during later operation of the probe field. Public authorities often request the installation of monitoring wells downstream for the reliable verification of the compliance with regulations.

Integrative solutions may combine different sources of thermal energy and use a district-heating grid for the distribution of the heat to several buildings or an entire settlement. In the following we describe an example of a successful integrative system located in the city center of Frankfurt Main (Germany), which has been built starting in 2013: The system is based on geothermal probe fields with a total of 382 probes. One probe field of 122 about 100 m deep probes provides heating and cooling of the apartments in the “Henninger Tower”. The new settlement “Stadtgärten” consists of 800 apartments in several blocks on 4 construction fields in close vicinity of the tower. The settlement is connected to a local heating grid divided into two components. One grid distributes hot water and a second grid at circulates water at lower temperature for heating and cooling. The core element of the system is a geothermal probe field with 260 probes reaching 100 m into the ground. The thermal output of the field is about $600 \text{ kW}_{\text{th}}$. The thermal energy extracted from the ground transferred to the grids via a heat pump. Additional heat is produced by an integrated gas fired condensing boiler. A cogeneration plant produces the electricity for the heat pump. A solar thermal collector linked to the geothermal probe field increases the efficiency of the heat pump. A local solar thermal collector on each building assists the hot water production. Each apartment has its own transfer point for hot water and heating energy. The entire settlement with its integrative thermal systems has been completed in 2019 (internet presentations in German only).

6.8.2 Cooling with Geothermal Probes

Air conditioning and cooling are typical planning issues for larger buildings. However, with climate change these subjects may also receive increasing attention for residential developments and family homes. Geothermal probes in $10\text{--}12^{\circ}\text{C}$ temperate ground are well suited for cooling tasks. In combination with a heating system interesting synergy effects may develop.

Geothermal probes can be used to transport excess thermal energy of the warm season to the ground where it can be stored for later use. The excess thermal energy may result from high room temperatures in the summer but also from technical facilities and production processes such as heat from IT equipment. Storage of excess heat in the ground accelerates recovery of the ground heat reservoir that has been exploited in the cold season for heating.

The operation of a geothermal heating system with a geothermal probe extracts thermal energy from the ground during the cold season. The ground cooled by some Kelvin at the end of the heating period. In the beginning of the warm season the building can be air-conditioned by pumping cold heat transfer fluid from the cooled

ground alone. The heat transfer fluid warmed by the excess heat of the building is piped back to the ground where it is cooled again (building heat source rather than ground heat source = reversed geothermal probe). The cool ground slowly warms and regenerates. Later in the warm season it will be often necessary to operate the heat pump of the loop as refrigerator to transfer the excess heat of the building to the ground. The ground continuously warms and recovers as a heat reservoir. The reversible heat pumps are needed for such kind of operational mode that reversibly heats and cools ground and building. Note, however, the portion of geothermal energy is a small fraction of the total energy budget in this mode of operation. The ground has predominantly the function of a heat storage device and not that of a heat source.

A geothermal probe can also be exclusively used for cooling purposes. Sustainable operation of such a cooling system requires that the stored thermal energy can be removed from the reservoir during the downtime e.g. in the cold season. In aquifers the stored thermal energy is dispersed by groundwater flow but also by heat conduction of the ground. Problems may arise if the probe is placed in clay or cohesive material with very low hydraulic conductivity.

6.8.3 Combined Solar Thermal – Geothermal Systems

The advantage of combining solar thermal with geothermal systems is easy to understand. In the warm season plenty of solar thermal energy can be harvested but there is no use for it in house or building heating. Thus solar thermal installations are primarily used for preparing hot water. If the solar installation is correctly planned then the furnace can be switched off during the warm season because the solar device produces sufficient heat for preparing hot water. If the solar heat source shall be used for house heating, a long-term heat reservoir is necessary. It makes it possible to store the solar summer heat and extract it when needed in the winter for heating. Geothermal probes can efficiently transfer the thermal energy to a ground reservoir. If the geology of the ground is favorable and if the environmental regulations can be respected, the combination of geothermal probes and solar devices can make very efficient bivalent heating systems.

As explained above, the bivalent system uses two different sources of renewable energy. The solar thermal energy that is transferred to the ground in the warm season improves regeneration of the heat reservoir. During the heating period thermal energy can be extracted from the ground and the lost heat is restocked in the warm season. The solar thermal system efficiently refills the used heat in the season when more solar energy is collected than is needed for hot water production. During this crucial period regeneration of the ground heat reservoir is efficiently enhanced and improved. It makes sense to elevate the reservoir temperature above its natural level prior to the heating period using the ground around the probe as a heat reservoir. At the beginning of the heating period, the ground source heat pump finds improved starting conditions. This results in a significantly improved annual energy efficiency of the heat pump

operation, giving rise to a distinctly increased seasonal performance factor. This is an important economic aspect for all systems with electricity-driven heat pumps.

The specific efficiency of the heat reservoir increases with its size because the volume grows with the cube of the size whilst the surface area of the reservoir where the heat losses occur increases merely quadratic with the size. Therefore, the large geothermal probe fields have a better efficiency. Heat storage in a subsurface reservoir is more efficient if the temperature difference between the reservoir and the surrounding ground is small. In favorable systems the reservoir temperature is only slightly above the surrounding ground thus minimizing heat losses.

The authorities of many countries require that near-surface aquifers may not be permanently heated to temperatures higher than 20 °C because of microbiological concerns.

A further emerging application is the seasonal heat storage in high-temperature ground reservoirs. The reservoirs operate with many, some with more than 100 bore-hole heat exchangers (Fig. 6.22). Large solar thermal systems collect thermal energy in the warm season that is continuously transferred to the ground reservoir via the installed geothermal probe field. The reservoir may be heated up to 90 °C. The thermal energy supports heating of buildings during the cold season that are connected to a local heating network. About 50% of the heat requirement of the connected buildings can be covered by renewable energy on a long-term average (Schmidt et al. 2003). For geothermal probe heat reservoirs, large numbers of closely spaced probes (1.5–4 m) must be installed in a circular array, hydraulically connected and padded with thermal insulations at the surface (Fig. 6.22). The optimal relation between surface and volume of the reservoir is for the probes to be arranged in a circular array and they should not reach very deep. For loading the reservoir the heat transfer fluid flows through the central probes first and then through the peripheral probes in order to optimize the temperature distribution in the ground. For the heat extraction the flow direction is being reversed.

These high-T thermal energy storage systems should not be confused with the bivalent geo-solar thermal systems described in previous paragraphs. The later systems use widely spaced geothermal probes in probe fields. The probes do not thermally influence each other and the reservoir is at a similar temperature as the untouched ground. The high-temperature heat storage (Fig. 6.22) is comparable to a hot water tank and function as an underground hot pot. The closely spaced vertical loops create a hot central area that loses thermal energy slow enough for cost-effective and beneficial operation of the system.

In the following we describe the ground probe heat reservoir at Crailsheim (Germany) in some detail as an example of a high-T thermal energy storage system. The heat reservoir is based on 80 geothermal probes (loops) drilled 55 m deep into upper Triassic limestone (Fig. 6.22a). The system stores thermal energy produced by a solar thermal system with 7300 m² collector surface (Germany's largest solar thermal installation). The thermally ideal circular reservoir has a 3 × 3 m orthogonal arrangement of the boreholes (Fig. 6.22b). The reservoir has a volume of 37,500 m³. The hottest region is in the center of the reservoir. The temperature resistant enforced polyethylene pipes must operate at 65 °C in the core of the reservoir but

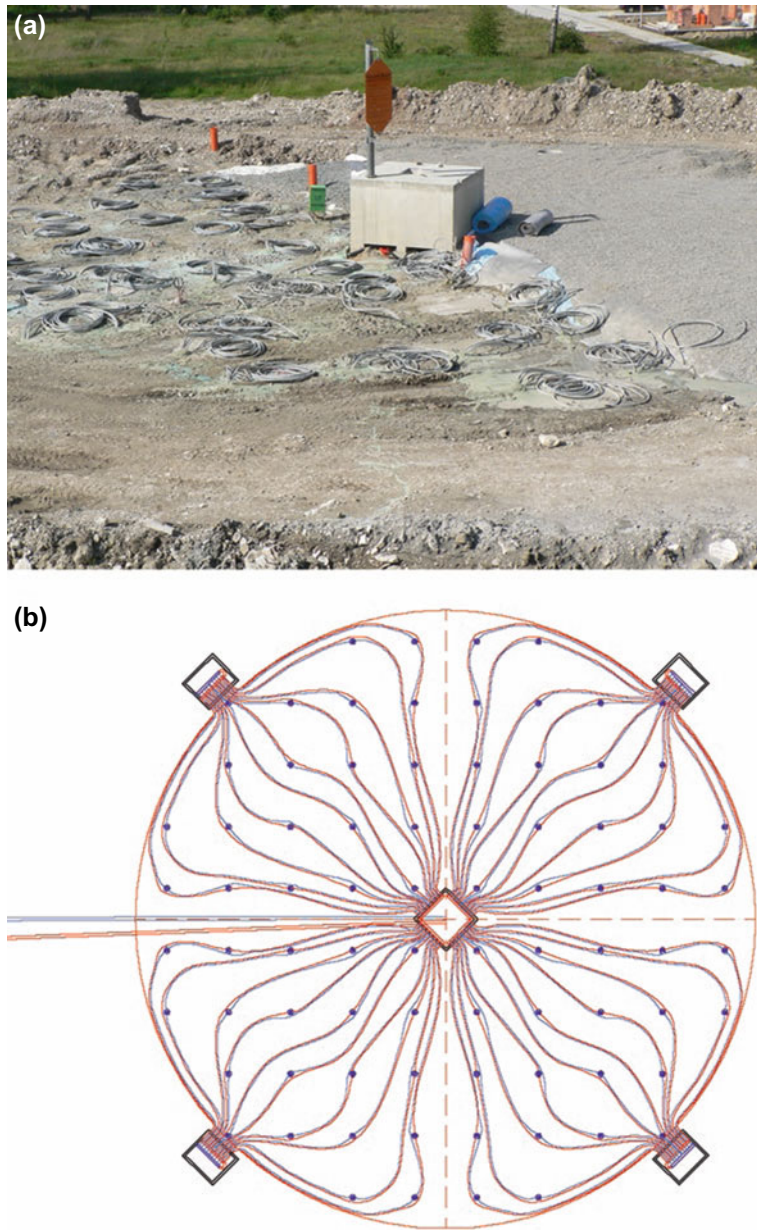


Fig. 6.22 The ground loop heat reservoir at Crailsheim: **a** Left: Probe pipes installed in closely spaced boreholes. Right: Probes already covered with thermally insulating material. **b** Map of the high-temperature heat storage system. The individual probes are marked with a blue dot. Heat transfer fluid is water (courtesy of Solites)

must withstand maximum loading temperatures up to 90 °C. The heat capacity and the thermal conductivity of the ground has been measured by a Thermal Response Test (Sect. 6.3.2) before construction of the reservoir (0–80 m: $2400 \text{ kJ m}^{-3} \text{ K}^{-1}$, $2.46 \text{ W m}^{-1} \text{ K}^{-1}$). Temperature resistant backfill material has been used for grouting. The reservoir is thermally insulated at the surface (Fig. 6.22a). The solar heat from the collectors is transferred to the heat central and can be used directly for heating and hot water supply or stored in the ground probe heat reservoir. The heat used by the buildings is distributed by a grid fed by the heat central with solar thermal energy or, if necessary, by an additional conventional boiler. The system presently (2019) supplies 260 apartments, a school and a coliseum with solar thermal energy. The final expansion stage will connect 211 new apartments to the system.

6.8.4 *Geothermal Probe: Performance and Quality Control*

Regardless of the large number of installed geothermal probes, some issues remain unsettled. Several important aspects of performance and quality control have not received the attention they deserve. Particularly the subjects related to the quality and durability of the backfill in the borehole and to its efficiency as hydraulic seal, the control of the thermal performance of the probe and also the actual precise position of the probe pipes at depths.

Related to these issues, measurement methods providing in-situ data from geothermal probes that allow for conclusions regarding the quality of the backfill would be highly desirable and welcomed. Technical problems include the small diameter of the boreholes and the coiled course of the probe pipes. Most probe pipes have an outer diameter of 32 mm. Therefore standard tools for geophysical borehole logging typically used for groundwater monitoring and production wells, do not work in geothermal probe pipes because of this size limitation. Recently, measuring equipment fitting narrow probe pipes has been developed.

At present (2019), the quality of the backfill is very difficult to examine. In addition to the space problem with the small pipe diameters, it is almost impossible to differentiate between the signals from inadequate and incomplete backfills and the nearby probe pipes next to the tested pipe. Also the grouting hose filled with backfill material is normally next to the probe pipes and adds additional complexity to the geometry and signal interpretation. The precise location and orientation of probe pipes and grouting hose may vary from central in the borehole to peripheral at the borehole wall over short vertical distances compounding the situation further. The problem is related to the utility and layout of spacers and centering aids. A rigorous interpretation of borehole data would require precise knowledge of the spatial position of all probe pipes. Data must then be collected in all probe pipes.

A **cable-free small-size data logger**, NIMO-T, which fits into 32-mm U-tube probes measures temperature and pressure in geothermal probes and records temperature as a function of depth (pressure) (Fig. 6.23). The temperature logs are measured in completed and installed probes that have not been operated yet. The data logger is



Fig. 6.23 Cable-free mini data logger for temperature and pressure down-pipe measurements (23 × 219 mm)

23 mm in diameter and 219 mm in length. The internal diameter of a 32 mm U-tube is 26 mm thus it is a bit fiddly to insert the logger into the probe pipe. The logger sinks in the probe pipe through its controlled and adjustable weight with a velocity of about 0.1 m/s to the probe foot and registers P and T. The sinking velocity can be adjusted to the needs at the specific site by changing the weight of the device. The measured pressure relates to the depths. The logger is recovered by flushing the device to the surface from the other side of the U-tube. The recuperation process disturbs the temperature profile. Because of this, the undisturbed temperature profile cannot be measured before a certain delay for thermal equilibration. The data can be downloaded and processed at the construction site immediately after recuperation of the logger. The logger operates to 350 m depth and the temperature resolution is 0.0015 °C (Forrer et al. 2008).

A follow-up model of NIMO-T is GEOsniff® (by enOware) used for the quality assurance and monitoring of near surface geothermal probes. The device contains the P-T sensors in a sphere of only 2 cm in diameter. The ball moves through the entire probe loop, sinks to the deepest point of the probe and continuously transmits pressure and temperature data to the surface station. The device may also be applied in thermal response tests.

Fiber-Optical Probe Measurements also produce temperature data with vertical resolution. The fiber-optic cables can be attached to the probe before installation or may be placed into the probe pipe after installation. Temperature is being measured every 0.5 m and interpolated in between. Optical fibers serve as temperature sensors because of their specific physical properties. The fibers produce simultaneous and synchronous temperature data with high temperature and depth resolution along the entire length of a geothermal probe. The simultaneous T measurement with distributed sensor technology is a significant advancement over measuring T with temperature sensors at discrete points along the vertical probe (Hurtig et al. 1997). Because the temperature sensor cable can be permanently installed with the probe pipe, the vertical temperature profile can be retrieved any time or even continuously. Fiber-optical temperature measurement can be ideally combined with thermal response tests providing detailed thermal conductivity data of a layered ground, which in turn helps to locate faulty backfill sections. The fiber sensor also enables

monitoring the backfill implementation of the geothermal probe borehole during and immediately after the termination of the grouting work.

Cable-Connected Temperature Sensor (ϕ 18 mm): The device can be lowered and hauled up in one of the probe pipe (Fig. 6.24). The collected temperature vs. depth data can be used to control the setting of the backfill. Under favorable conditions the gathered data also may show voids and faulty backfill. Deviations from the undisturbed vertical temperature profile (Fig. 6.25) may indicate an incomplete and faulty backfill. Vertical groundwater flow results from different hydraulic potentials in separate aquifers (Fig. 6.16). Local vertical groundwater flow induces a temperature signal at voids in the backfill that can be measured in the geothermal probe tube. $\Delta T = T_{\text{measured}} - T_{\text{undisturbed}}$ ($T_{\text{undisturbed}}$ = blue curve on Fig. 6.25). $\Delta T < 0$ indicates descending cool groundwater, $\Delta T > 0$ infers upwelling groundwater (see also Fig. 14.15). From the temperature vs. depth curves the velocity of the vertical groundwater flow component can be derived. Without significant vertical groundwater flow voids in the backfill may be detected with the temperature sensor only in exceptional cases.

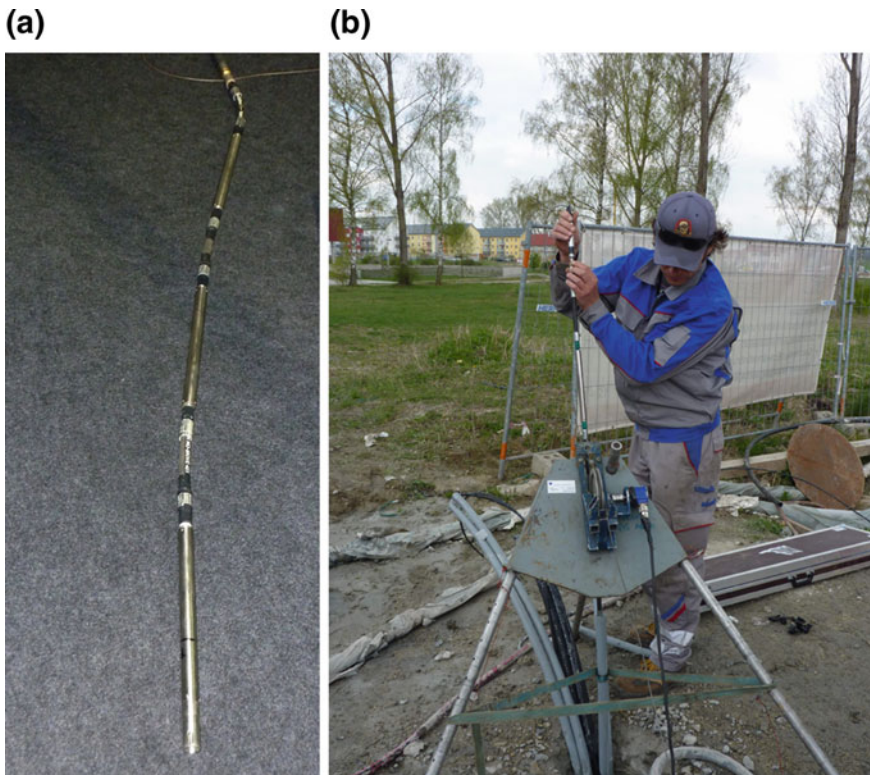


Fig. 6.24 **a** Flexible tool string for geophysical measurements in geothermal probes, **b** Inserting a gamma ray logger into a geothermal probe

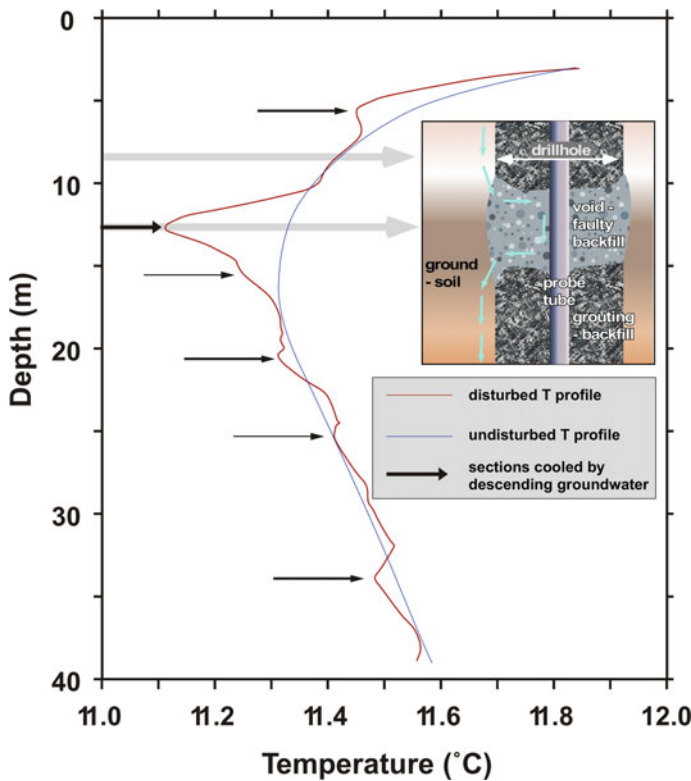


Fig. 6.25 Example of a disturbed temperature profile (red) with indications of strong and weak thermal effects of groundwater contact due to faulty backfill (arrows). The excursions from the undisturbed profile (blue) imply descending colder groundwater from above

The cable-connected temperature sensor can be extended and used as **Gamma Ray Logger** also. The method of measuring naturally occurring gamma radiation is used to characterize the geological strata in a borehole (Fig. 6.24b). The individual elements of the logger for temperature and gamma ray can be connected with flexible connectors so that the sensor chain can follow the coiled probe pipes. If the backfill has an added radiating tracer, the gamma ray logger can be used to control the backfill, in analogy to the classical borehole gamma logging in wells. Labeled grouting materials are presently being tested. As already mentioned, the presence of (three) additional probe pipes in the borehole contributes to the measured data and complicates the analysis and interpretation of the data. The variable spatial orientation of the probe pipes complicates the situation further. For the use of labeled backfill legal requirements may exist.

The flexible geophysical **Multi-Tool** (Fig. 6.20a) can be expanded by a magnetic inclinometer for precise measurement of the 3D-orientation of the probe pipes. A three-axis sensor measures inclination and orientation of the pipes. Separate flexible

inclinometer tools measure the dip and orientation of the geothermal probe pipes. Maximum length of these tools is presently about 100 m. With a diameter of 27 mm, the inclinometer tool fits into a standard probe pipe. Measurement precision is about 0.001 K. Testing the tool has shown that the pipes are too strongly twisted so that the inclinometer chain every so often got jammed and could not be lowered in the geothermal probe completely.

Gamma-Gamma Logging of geothermal probes measures density of the surrounding material and thus gives information about the completeness and quality of the backfill. The gamma-gamma method is based on nuclear physical interaction of gamma rays from a source in the sensor and the atoms that make up the rocks and backfill. The interaction processes absorb gamma ray energy when passing through the ground (rock, backfill). The detected remaining back-scattered gamma irradiation is thus inversely proportional to the density of the ground. The method measures density of the formation and detects incomplete backfill and other cavities in the wellbore. The device has a length of 80 cm and a diameter of 15 mm. Also with this method, the presence of other water-filled probe pipes in the borehole and their complicated spatial position complicate the processing and interpretation of the data. Measuring with a gamma-gamma logger may not be inoffensive at all sites and buildings.

Data from a **Magnetic Susceptibility Probe** (ϕ 16 mm) allow conclusions regarding the quality of the backfill of geothermal probes. The method requires that magnetically conductive material have been blended in with the backfill slurry. The probe is lowered with a cable in one of the geothermal probe tubes. The recorded data can be read and processed after the probe returned to the surface. The probe is also used for monitoring the sealing work during construction of the probe.

An **Ultrasonic Tool** detects irregularities regarding density, homogeneity and structure of the local environment of the geothermal probe and thus also controls the completeness of the backfill. The ultrasonic probe uses a pulse-echo technique. A further tool under development is the **Kappa Probe** measuring magnetizability of rocks and ground, indirectly permitting conclusions on the quality of the backfill.

Many tools and methods are currently being developed and tested. Several of these tools and methods have originally been developed and used in the oil industry, then adapted by the groundwater well industry and now being modified and tailored for the needs of the geothermal energy industry.

With further developments and increasing popularity of geothermal probe systems there is a growing demand for controlling the professional installation of the geothermal probe and to quantitatively measure its performance during operation. The future development is evident: For the approval and acceptance of geothermal probes and for the quality control of these systems quantitative data and measurement based investigation procedures will become standard and an integral part of the construction project.

The quality and the economic success of a geothermal probe system are closely related to the quality of the backfill. At present (2019) no generally recognized method exists that explicitly detects and localizes voids in the backfill.

A potentially helpful evaluation method uses temperature data collected with a fiber-optical sensor in the annulus during a thermal response test (Riegger et al. 2012). As described above fiber optical sensor strings are capable of continuously measuring the temperature in a tube of the geothermal probe at a large number of depth points simultaneously. During the thermal response test the tube is flushed with hot heat transfer fluid. At any given depth the sensors record the temperature increase with time. It increases first rapidly and then slowly approaching T_{\max} . Flushing the system with hot water is then stopped and the thermal attenuation recorded at every sensor point along the geothermal probe. The temperature initially falls rapidly and later asymptotically approaches its pre-test level. The temperature vs. time curves now available at closely spaced depth increments can then be analyzed. The T-t curves are analogous to P-t curves recorded during hydraulic pumping tests in hydrogeology. The T-t data can be analyzed using T-t Horner plots. These plots, which are commonly used in hydrogeology for deriving the hydraulic conductivity (k) (e.g. on Fig. 14.13), are used here for deriving thermal conductivity (λ). Since perfectly grouted sections and voids in the backfill produce significantly different λ signals, voids in the backfill can be precisely identified and localized even in the absence of groundwater flow as shown on Fig. 6.25.

6.8.5 Thermosyphon, Heat Pipe: Geothermal Probes Operating with Phase Changes

Geothermal probes may integrate the thermal effect of a phase transition such as boiling or condensation of a heat transfer fluid into the geothermal system (Sect. 4.1). The technique used in geothermal applications is known as thermosyphon or heat pipe. The principle is as follows: Instead of using a conventional heat transfer fluid for extracting heat from the ground, the thermosyphon uses a liquid with a low boiling temperature and directly evaporates the liquid in the geothermal probe by the geothermal heat added by the ground. The ground provides the reaction enthalpy of the liquid–vapor phase change, the latent heat of evaporation. At the surface the vapor is condensed to the liquid phase and the reaction enthalpy gained. This latent heat of condensation can be used for house heating or other purposes. Like in conventional geothermal probes also thermosyphons work in grouted boreholes. Thus the probe works independent of the geological structure and properties of the ground.

The thermosyphon has the evaporator at the bottom of the probe and the condenser at the wellhead. Inverse installations with the condenser at the bottom of the pipe and the evaporator at the top are known as wicked heat pipes. Wicked heat pipes have a wide range of technical applications (Reay and Kew 2013; Sabharwall 2009).

At present heat transfer fluids used for thermosyphons include propane, ammonia and carbon dioxide. Some important physical properties of these transfer fluids are listed on Table 6.3. Among these working fluids ammonia is toxic, difficult to handle and could be hazardous to the groundwater after a leakage. Propane is flammable and, if unprofessionally handled, explosive. Thus there are legal requirements for using

Table 6.3 Properties of heat transfer fluids used for geothermosyphons

	Ammonia	Carbon dioxide	Propane
Boiling temperature (°C) at 1 bar	-33	-78	-42
Density (10^{-3} kg m $^{-3}$) at boiling T	0.682	1.032	0.58
Vapor pressure (bar) at 0 °C	4.82	34.91	4.76
Enthalpy of phase change (kJ mol $^{-1}$)	21.4	23.2	19.0

both these fluids. In some countries their use in geothermal probes is not permitted at all. For these reasons, thermosyphons operating with carbon dioxide, so-called CO₂-probes have been further developed and improved. The temperature of CO₂ at the critical point is 31.1 °C at a pressure of 73.8 bar.

The liquid CO₂ flows along the walls of the probe pipe downwards evaporates because of the heat uptake from the ground. The warmed CO₂ gas flows in the interior of the probe to the surface and supplies heat to the heating loop by condensation (Fig. 6.26).

The great advantage of thermosyphons is that they do not require a pump for circulating of the heat transfer fluid in contrast to conventional geothermal probes. There is no heat loss like with U-tube probes where valuable heat is transferred between the probes transporting the working fluid in opposite direction. Therefore the seasonal performance factor of a CO₂ thermosyphon is considerably higher than for conventional geothermal probes.

Standard PE pipes used for geothermal probes are not CO₂ proof. Therefore, CO₂ based heat pipes are made from a flexible, pressure-resistant, corrugated high-alloy stainless steel or aluminum. Ordinary steel, iron or copper pipes are susceptible to corrosion. The deployed pipes have diameters in the range of 40 to 60.3 mm.

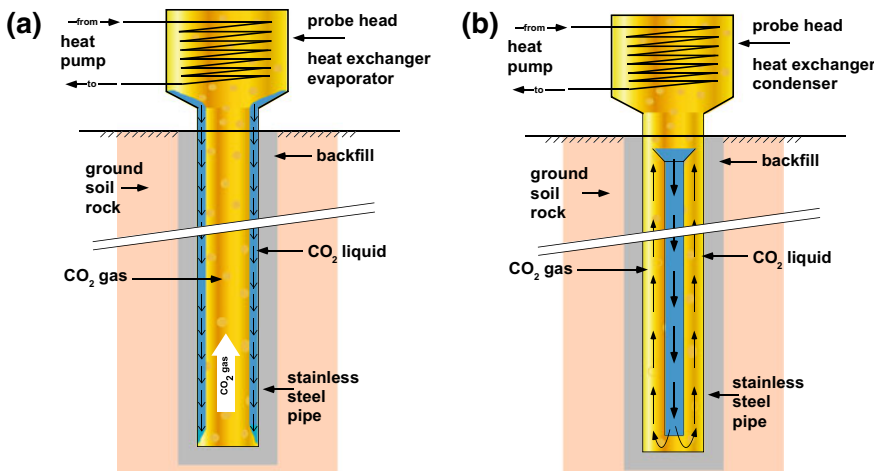


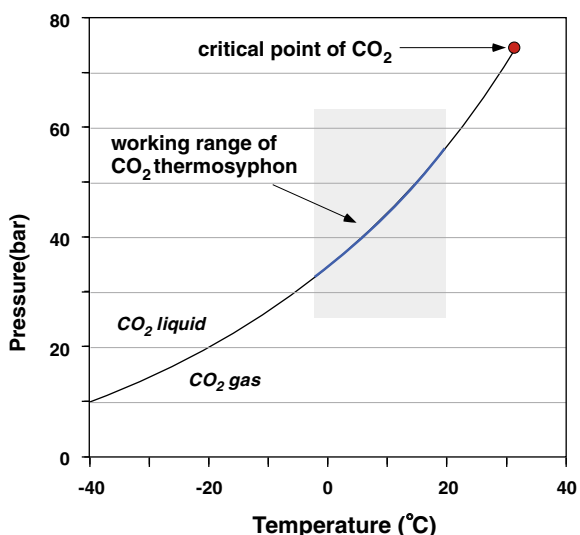
Fig. 6.26 Schematic diagram of geothermally driven thermosyphons: **a** Single pipe probe; **b** Two pipe probe

The thin film of liquid CO₂ flows downward in spirals along the corrugated pipe protected by the coil. After evaporation the gas rises in the free center of the pipe without obstructing the liquid film to the heat exchanger where it condenses. The heat exchanger disposes of copper coil tubing bundles in a pressure-tight strong housing (Fig. 6.26). The heat transfer fluid of the heat pump circulates to the probe head of the CO₂ heat pipe where it evaporates in the coil bundles (Fig. 6.26). The latent heat of evaporation is taken from the warm CO₂ gas. The thermosyphon is presently in the state of market launch. The technique certainly has a great potential for house heating applications also.

In addition to the described so-called single-pipe probe (Fig. 6.26a) CO₂ thermosyphons with two pipes have recently been developed (Fig. 6.26b). The two-pipe CO₂ probe separates the liquid and the gas phase by a coaxial pipe. The CO₂ gas streams upwards in the outer pipe to the heat exchanger where it condenses to liquid CO₂ that flows downward in the inner pipe. The design prevents obstruction of the CO₂ gas stream in small-diameter pipes by the downward trickling liquid CO₂. Two-pipe CO₂ thermosyphons can be used for cooling also, but this mode requires a pump for the liquid CO₂.

The boiling curve of CO₂ (Fig. 6.27) separates the pressure and temperature conditions where CO₂ is in a liquid phase from those where CO₂ is in a gas phase. The curve ends at the critical point above where CO₂ is in a supercritical state. In order to operate the thermosyphon in the temperature range relevant for near surface geothermal applications (about – 2 to + 20 °C) the probe needs to be run in a pressure range of 35 to 55 bar. It is fully possible to operate a CO₂ thermosyphon above freezing conditions of water by selecting an appropriate working pressure, thereby avoiding all undesired perils and troubles associated with freezing of the probe and the surrounding ground (Sect. 6.7). However, also CO₂ probes may suffer

Fig. 6.27 Phase diagram of CO₂, blue section of the boiling curve is the typical working range of a CO₂ geothermosyphon (CO₂ data from Weast and Selby 1967)



from heat losses in the cold season because the probe is exposed to the low ambient temperatures in the uppermost meters and may give off some of the collected heat to the near surface ground. Because a CO₂ thermosyphon is operated at comparatively high pressures it is mandatory that the backfill of annular space of the probe be absolutely and permanently impervious. Leakages may cause deformation of the corrugated pipe thereby drastically reducing the functionality of the probe.

Ammonia-driven heat pipes have a well-established range of applications and have been in use for years. With ammonia as refrigerant they are used for example to stabilize permafrost ground along the Trans Alaska Pipeline (Fig. 6.28). Inside the vertical support pillars two heat pipes filled with ammonia take up the heat from the ground, this causes the fluid to boil. NH₃ gas then flows to the condenser at the top of the heat pipe giving off heat of condensation through the finned radiators to the air. The liquid NH₃ condensate returns to the bottom of the heat pipe as thin liquid film along the pipe wall. The boiling reaction in the evaporator at the bottom of the heat pipe completes the cycle. It extracts heat from the ground thereby cooling the vulnerable permafrost. The liquid Heat pipes are also used for snow thawing on sidewalks and pedestrian zones and deicing of railroad track switches (Narayanan 2004; Reay and Kew 2013).



Fig. 6.28 Heat pipes stabilize permafrost soil along the Trans Alaska pipeline. The working fluid is ammonia. The evaporator is at the top of the heat pipe; the condenser at the bottom cools the pillar. 122,000 heat pipes are installed along the 1285 km long pipeline

References

- Acuña, J. & Palm, B., 2009. Local Conduction Heat Transfer in U-pipe Borehole Heat Exchangers, pp. 6, Excerpt from the Proceedings of the COMSOL Conference, Milan.
- ASHRAE Handbook, 1997. Ground source heat pumps - design of geothermal systems for commercial and institutional buildings. American Society of Heating, Refrigerating, and Air-Conditioning Engineers (ASHRAE), Atlanta, GA.
- Basetti, S., Rohner, E., Signorelli, S. & Matthey, B., 2006. Documentation of cases of damage of geothermal probes (in German), pp. 65, Schlussbericht Energie Schweiz, Zürich.
- Carslaw, H. S. & Jaeger, J. C., 1959. Conduction of Heat in Solids. Oxford at the Clarendon Press, Oxford, 342 pp.
- Diersch, H. J., 1994. FEFOLW, Finite Element Subsurface Flow & Transport Simulation System. Reference Manual.
- Eskilson, P., 1987. Thermal Analysis of Heat Extraction Boreholes. Department of Mathematical Physics, Lund Institute of Technology, Lund, Sweden.
- Eugster, W. J., 1998. Longterm behavior of the geothermal probes at Elgg (Zurich, Switzerland) (in German). In: Projekt 102, Polydynamics, pp. 38, Schlussbericht PSEL, Zürich.
- Eugster, W. J., 2001. Langzeitverhalten der Erdwärmesondenanlage in Elgg/ZH.- Schlussbericht DS-Projekt 42478, im Auftrag des Bundesamtes für Energie, 14 S., Zürich.
- Forrer, S., Mégel, T., Rohner, E. & Wagner, R., 2008. Better planning security for geothermal probe projects (in German). bbr Fachmagazin für Brunnen- und Leitungsbau, **5**, 42–47.
- Gehlin, S., 2002. Thermal Response Test, Method Development and Evaluation. Unpub. Doctoral Thesis, University of Technology, Luleå, Sweden.
- Gehlin, S. & Nordell, B., 1997. Thermal Response Test – a Mobile Equipment for Determining Thermal Resistance of Boreholes. In: Proc. 7th International Conference on Thermal Energy Storage Megastock '97.
- Greber, E., Leu, W. & Wyss, R., 1995. Erdgasindikationen in der Schweiz.- Schweizer Ingenieur und Architekt, **24**, 567–572.
- Grimm, M., Stober, I., Kohl, T. & Blum, P., 2014. Damage Analysis Drilling Geothermal Probes (Schadensfallanalyse von Erdwärmesondenbohrungen in Baden-Württemberg). Grundwasser, **19**/**4**, 275–286 (DOI <https://doi.org/10.1007/s00767-014-0269-1>).
- Gustafsson, A. M., 2006. Thermal Response Test – Numerical simulations and analysis. Unpub. Licentiate Thesis, University of Technology, Luleå, Sweden.
- Hellström, G., 1999. Thermal performance of borehole heat exchangers. In: The second Stockton International Geothermal Conference, 16/03.
- Hellström, G. & Sanner, B., 2000. EED Earth Energy Designer, pp. Computer Program for Borehole Heat Exchangers, Lund University Sweden.
- Huber, A., 2008. Code EWS, Comptuing Geothermal Probes (in German). Huber Energietechnik AG.
- Hurtig, E., Großwig, S. & Kasch, M., 1997. Fiberoptical temperature measurement: Monitoring the temperature field at geothermal probe sites. Geothermische Energie, **5**(18), 31–34.
- Kohl, T. & Hopkirk, R. J., 1995. "FRACTURE" a simulation code for forced fluid flow and transport in fractured porous rock. Geothermics, **24**, 345–359.
- Mogensen, P., 1983. Fluid to Duct Wall Heat Transfer in Duct System Heat Storages. Proc. Int. Conf. Subs. Heat Storage, 652–657.
- Pahud, D., 1998. PILESIM: Simulation Tool of Heat Exchanger Pile System, Laboratory of Energy Systems, Swiss Federal Institute of Technology, Lausanne.
- Parkhurst, D. L. & Appelo, C. A. J., 1999. User's guide to PHREEQC (version 2) – a computer program for speciation, batchreaction, one dimensional transport, and inverse geochemical calculations. In: Water-Resources Investigations Report 99-4259, pp. 312, U.S. Geological Survey, Denver, Colorado.
- Puttagunta, S., Aldrich, R. A., Owens, D. & Mantha, P., 2010. Residential Ground-Source Heat Pumps: In-Field System Performance and Energy Modeling. GRC Transactions, **34**, 941–948.

- Reay, D. & Kew, P., 2013. Heat Pipes: Theory, Design and Applications. Sixth edition, Butterworth-Heinemann, Elsevier, 288 p.
- Riegger, M., Heidinger, P., Lorinser, B. & Stober, I., 2012. Using fiberoptical temperature sensors for verifying the quality of grouting of geothermal probes (in German). *Grundwasser*, 17/2, 91–103, Springer Verlag (DOI <https://doi.org/10.1007/s00767-012-0192-2>).
- Ruck, W., Adinolfi, M. & Weber, W., 1990. Chemical and environmental aspects of heat storage in the subsurface. *Z. Angew. Geowiss.*(9), 119–129.
- Sabharwall, P., 2009. Engineering Design Elements of a Two-Phase Thermosyphon to Transfer NGNP Thermal Energy to a Hydrogen Plant. Idaho National Laboratory, Report prepared for DOE, INL/EXT-09-15383.
- Sanner, B. & Chant, V. G., 1992. Seasonal Cold Storage in the Ground using Heat Pumps. Newsletter IEA Heat Pump Center, 10(1), 4–7.
- Sanner, B. & Hellström, G., 1996. “Earth Energy Designer”, Software for Dimensioning Geothermal Probes. Tagungsband 4. Geotherm. Fachtagung in Konstanz (1996), S. 326–333.
- Sanner, B., Reuss, M. & Mands, E., 2000. Thermal Response Test – Experiences in Germany. In: Proceedings Terrastock 2000, 8th International Conference on Thermal Energy Storage, pp. 177–182, Stuttgart, Germany.
- Schmidt, T., Mangold, D. & Müller-Steinhagen, H., 2003. Central solar heating plants with seasonal storage in Germany. Elsevier Ltd. *Solar Energy*, 76 (1–3), 165–174.
- Signorelli, S., 2004. Geoscientific Investigations for the Use of Shallow Low-Enthalpy Systems. In: ETH No. 15519, pp. 157, Dissertation of the Swiss Federal Institute of Technology Zurich, Zurich.
- Theis, C. V., 1935. The Relation between the lowering of the Piezometric Surface and the Rate and Duration of Discharge of a Well Using Groundwater Storage. *Trans. AGU*, 519–524.
- VDI, 2001. Use of subsurface thermal resources (in German). Union of German Engineers (VDI), Richtlinienreihe, 4640.
- Vienken, T., Kreck, M. & Dietrich, P., 2019. Monitoring the impact of intensive shallow geothermal energy use on groundwater temperatures in a residential neighborhood. *Geothermal Energy*, 8, 14 p.
- Wagner, R. & Clauser, C., 2005. Evaluating thermal response tests using parameter estimation for thermal conductivity and thermal capacity. *Journal of geophysics and engineering*, 2, 349–356.
- Weast, R. C. & Selby, S. M. e., 1967. CRC Handbook of chemistry and physics (48th edition). CRC Press Cleveland, Ohio, USA.
- Wyss, R., 2001. The blowout at the geothermal probe wellbore at Wilen (Obwalden, Switzerland) (in German). *Bull. angew. Geol.*, 6(1), 25–40.
- Yu, X., Zhang, Y., Deng, N., Ma, H., & Dong, S., 2016. Thermal response test for ground source heat pump based on constant temperature and heat-flux methods. *Applied Thermal Engineering*, 93, 678–682.
- Zapp, F. J. & Rosinski, C., 2007. Effects of heat transfer fluid parameters on the transfer of thermal energy of thermal ground probes (in German). In: Der Geothermiekongress, Bochum.

Chapter 7

Geothermal Well Systems



Operator panel of a drilling rig

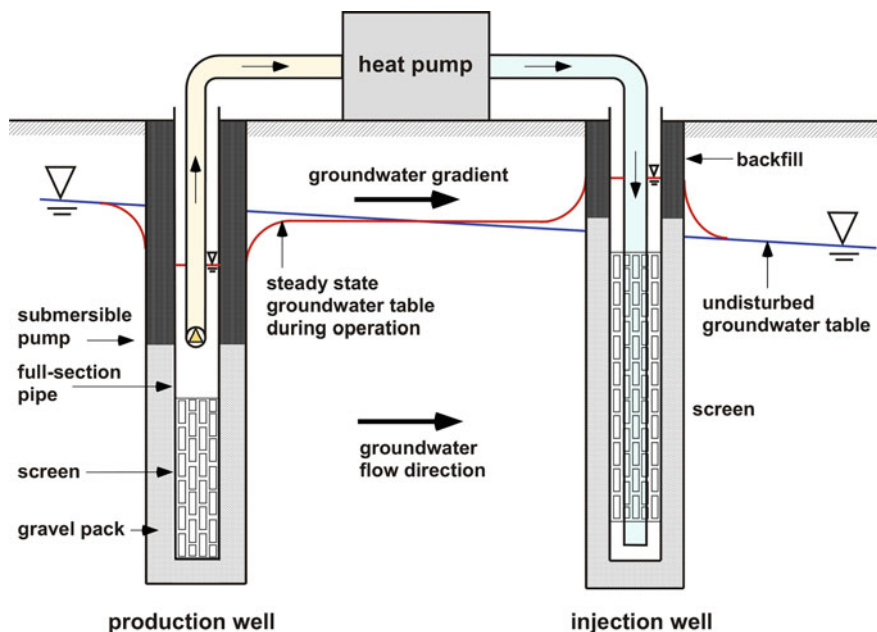


Fig. 7.1 Geothermal well system with production and injection well

Geothermal well systems utilize the thermal energy of clean groundwater of hydraulically highly conductive aquifers with water tables close to the surface (Fig. 7.1). The thermal energy of water produced from the well can be extracted by means of heat pumps (Sect. 4.1). Such systems are also called two-well-systems, water-water-heat-pump-systems, or groundwater heat pump. They can be used for both heating and cooling. Geothermal well systems are a form of direct-use systems of near surface groundwater. The use of geothermal energy from groundwater can be particularly energy efficient in these systems. The direct-use of groundwater as a heat transfer fluid minimizes energy losses in heat exchanger systems. The relatively constant temperature of the groundwater flow is ideal for heat extraction by heat pumps. The advective heat transfer by groundwater flow has clear advantages regarding efficiency and economy compared with the conductive heat transfer utilized in geothermal probes. Limitations of direct use of groundwater are imposed by the availability of sufficient volumes of groundwater and appropriate aquifer properties, technical feasibility of well system development and the admissible thermal impact of the well system on groundwater and aquifer.

Geothermal well systems used exclusively for heating are particularly efficient in regions with elevated groundwater temperature associated with big cities for example. The cooling of groundwater resulting from the operation of geothermal wells contributes appreciably to environmental protection.

Heating and cooling with geothermal wells has become increasingly popular in recent years. In Switzerland, as an example, the number of installed geothermal wells

doubled from 2007 to 2017 and reached 5802 systems in 2017. The systems generate 12% of all geothermally produced heating energy (Energieschweiz 2018). In many places extended systems with several production and injection wells provide heating energy for entire neighborhoods and are used for cooling in the warm season. An example for a multi-well system operates in March-Hugstetten near Freiburg (SW Germany): The heating energy for 38 three-storied blocks with 151 apartments is produced by a system of 7 production wells with a total flow rate of 42 l s^{-1} and 12 injection wells. The system also supplies domestic hot water and air conditioning in the warm season. Each apartment block is equipped with a separate heat pump. The annual performance factor (APF) of the complete system is APF = 4, some of the blocks reach even APF = 5 (Isele and Kölbel 2006).

Geothermal well systems are increasingly used in so called aquifer storage facilities or aquifer thermal energy storage systems (ATES) for storing excess heat particularly cropping up in the warm season in an aquifer. The stored thermal energy can be retrieved for heating purposes in the cold season (see Sect. 8.7.2 for more details).

7.1 Building Geothermal Well Systems

The geothermal utilization of shallow groundwater requires a production and an injection well on the property for small and medium-sized systems (homes, smaller buildings). Larger buildings entail a system of several two-well units (two-well gallery). The geometrical arrangement of the two-well units and the power of each unit must be evaluated with a numerical model. Prerequisite for a successful model is an expert knowledge of the subsurface. Numerical simulation of heat and cold storage in the ground permits an optimized design of the well system for long-term operation and reliable prediction of the effects on the surroundings.

Engineering of production and injection well is similar to normal standard groundwater wells or groundwater measuring points with full-section pipes and screens, with an adequate gravel bed and appropriate sealing in sections with aquitards and in the near-surface area. However, geothermal well systems have relatively small diameters because of small production rates compared to ordinary groundwater wells. Because of different flow patterns of production and injection wells (Fig. 7.1), the production well should be screened at greater depth than the injection well. The pump must be installed above the screened section because of the increased flow velocity close to the pump inlet. The screened section in the injection well should begin higher up to prevent overflow of the well particularly during periods with a high groundwater table. This also helps to retard ageing processes. Experience shows that injection wells age faster than production wells. To prevent early ageing, the return pipe must be placed and connected to the injection well deep below the undisturbed water table (Fig. 7.1) and the screens must be in the groundwater under all operation conditions.

The submersible pump (Fig. 7.1) produces groundwater of about 10°C (Central Europe) to the surface; a heat pump extracts thermal energy from the groundwater and cools it to about 5°C . The cool water is returned to the aquifer passing through

the injection well. Re-injection of the thermally depleted groundwater assures a quantitative mass balance and conserves the resource groundwater.

The two wells may not interfere thermally with each other. The re-injection of the cooled water should not be upstream of the production well, of course. Ideally, if space permits, the injection well is placed normal to the hydraulic gradient (normal to the groundwater flow direction) or, second best geometry, downstream from the production well. Furthermore, some waters tend to become critically oversaturated with respect to certain minerals when cooled. The chemical effects of cooling should be carefully considered and chemical composition data must be available for modeling mineral scaling processes during project planning.

Before starting the operation, the yield of the two wells needs to be evaluated by means of appropriate pumping tests to ensure a sustainable utilization (Chap. 14). If measured yield is insufficient for meeting the planned heat extraction needs, then the wells can be deepened or the well diameter increased. Well depths for two-well direct-use systems are typically in the range of 5–15 m. Two-well systems work best if groundwater-surface distances are small and the hydraulic conductivity of the aquifer is high. Two-well systems for single-family homes are operated with flow rates of less than 1 L s^{-1} .

The supply lines for the wells must be laid frost-proof. The supply pipes must have a gradual slope to the wells so that they can be emptied easily if necessary. It must be ensured that the line position is below the groundwater table at all times.

Temperature variations of groundwater are relatively small. The mean annual temperature of shallow groundwater is related to the annual mean air temperature and typically ranges from 7 to 12 °C in moderate climates. Groundwater temperature in the vicinity of bigger cities can be significantly above normal thus making the utilization of geothermal well systems for heating purposes particularly efficient. The constant temperature enables very efficient operation of the heat pump. Heat extraction should not cool the groundwater by more than about 6 °C. Monovalent operation is usually trouble-free. The seasonal performance factor (Sect. 6.3.1) of geothermal two-well systems should be near 5. The German legislator, for instance, prescribes seasonal performance factors of 4 or better for water-water heat pumps used for house heating to ensure the energy efficiency of the system. If the heat pump is also used for hot water preparation a minimum annual performance factor of 3.8 must be achieved.

Heat output of 7 and 10 kW respectively require groundwater abstraction in the order of 2 and 3 $\text{m}^3 \text{ h}^{-1}$ corresponding to 0.6 and 0.9 L s^{-1} flow rate respectively. The necessary flow rates are low so that 3" or 4" low-capacity submersible pumps are sufficient. The finished diameter of the production well should not be chosen to small despite the relatively small required extraction rates particularly in the upper section where the pump is installed. A generous well diameter minimizes hydraulic resistivity during pumping avoiding energy losses and uncontrollable power consumption during operation. The production well must be designed so that the pump can be installed deep enough for unproblematic operation also if groundwater table is low. Increasing the length of the screened section and the well diameter will improve, within limits, well performance. It is advised not to scrimp on the well diameter.

Large well diameters generate long-term performance reserves for balancing later ageing and degradation or in case of increased heat demand.

Attention must be paid to a sufficient distance between production and injection well (Eq. 7.1). This is important and avoids unwanted thermal interferences at the production well during operation. Typically, the distance between the two wells is some tens of meters, but shorter distances are possible depending on the conditions at the specific location. Possible long-range thermal effects on the groundwater by the operation of a two-well system must also be kept in mind and should be avoided. Specifically, the measured aquifer parameters from a qualified pumping test (Sect. 14.2) in the first drilled well can be used to determine the reach of the depression and injection cones. The model cones and the deduced minimum distance between the wells can then be verified by a properly devised pumping test in the second drilled well. If necessary, a third well must be drilled.

The necessary minimal distance (d) in meters between production and injection well can be estimated from Eq. 7.1:

$$d = 0.6 Q / (i k_f H) \quad (7.1)$$

assuming the aquifer has constant thickness (H) [m] and hydraulic conductivity (k_f) [m s^{-1}] and equally long filter sections and a continuous operation of the heat pump. Q [$\text{m}^3 \text{s}^{-1}$] represents the production and infiltration rate respectively and (i) is the dimension-less hydraulic gradient. The equation is valid if the wells are positioned normal to the direction of groundwater flow. An injection well should never be placed upstream of the production well.

It is important that the injection well has sufficient conductivity for trouble-free take up of the pumped and cooled water from the heat pump. Water injection produces a positive cone around the injection well, which may become problematic if the difference between surface and groundwater table is small. The dimensioning of the injection well should consider the typically highest groundwater tables of the year thus avoiding overflow from the well. Here also, skimping on well depth, well diameter and length of the filter section of the injection well may not be economically advisable.

The power reserves created by generous dimensioning of well depth, well diameter and length of the filter section at the two wells invariably increase the durability and lifetime of the wells significantly. They also delay potentially necessary regeneration work. An increased filter section or a larger final diameter of the well reduces water flow velocity in the production well substantially and slows down well ageing markedly. Like in any other well, the filter section in the production well of a geothermal well system must begin considerably below the depression cone also during periods of low groundwater table and during maximum extraction rates. Otherwise atmospheric oxygen enters the well past the filter section producing sinter and mineral scales (sedimentation of iron ochre).

7.2 Chemical Aspects of Two-Well Systems

Ageing of wells is a cumulative effect of a number of different processes including iron-manganese ochre formation, scaling, siltation, corrosion, and formation of biofilm (slime). Geothermal well systems typically have contact to atmospheric oxygen. This may support increased microbiological activity and resulting biofilms of bacteria and algae. Access of oxygen also promotes oxidation of iron and manganese to insoluble Fe- and Mn-oxides and oxyhydrates. The processes may also impair the aquifer itself. If the systems are also used for cooling, microbiological deterioration is to be expected.

Corrosion of casing, screen and other components of the system is mainly a consequence of access of atmospheric oxygen to the pumped water. The resulting oxidation of sulfide minerals in the soil and rock causes increased sulphate and low pH. These parameters are a secondary indication of oxygen access and ongoing corrosion. Also increased chloride and carbon dioxide support corrosion (Sect. 15.3). If hydrogen gas can be detected in the produced water then the system has a severe corrosion problem that needs to be fixed without delay.

Geothermal well systems should never be installed within the chemical plume of a waste deposit, a landfill, legacy assets and other groundwater damage areas. In aquifers with high natural sulphate concentrations sulphate-resistant materials must be used for constructing the well. Access of oxygen is typically the result of a drawdown cone in the production well reaching into the filter section.

Groundwater quality has a strong influence on the operation and lifetime of the geothermal well system. Biofilms, iron hydroxide scales and other deposits, particularly on heat transfer components reduce the efficiency of the system rapidly. The efficiency of the system is also compromised by scale deposits in the filter section, because of the required increase of pump pressure to maintain the flow rate.

It is recommended designing the geothermal well system with ample reserve capacity and planning drilling depth, screen section, well diameter and other well parameters accordingly. Like in any other groundwater well the start of the screened section must always lie below the groundwater table also at minimum water level and maximum abstraction of water after many years of operation. Otherwise oxygen may enter the well potentially resulting in severe corrosion, iron ochre sedimentation and clogging of the pump. The composition of the groundwater should be analyzed on a regular basis. Parameters that should be measured include: pH, electrical conductivity, total hardness, dissolved CO₂, iron, manganese and other parameters depending on the local situation.

The scaling and corrosion potential can be evaluated and modeled from chemical composition data and the temperature of the groundwater by using computer codes such as PHREEQC (Parkhurst and Appelo 1999). If conditions are very unfavorable, the project must be abandoned.

7.3 Thermal Range of Influence, Numerical Models

Computation of the thermal energy utilization must first distinguish between monovalent use for heating or cooling or for a combination of heating and cooling. After that, the energy need of the building or the facility determines the necessary amount of groundwater to cover these needs. The maximum annual groundwater demand controls the number of wells and their engineering details. These settings can then be used to model the thermal effects of operating the well system. These modeled thermal effects must be appraised and, if necessary, the array and spacing of wells must be adjusted and optimized as to minimize the effects on the aquifer.

Numerical models of geothermal utilization of near-surface groundwater have been computed already in the 80ties of the last century. Successful approximation solutions have been developed for small and medium size systems that are still valid and widely used. The layout of two-well systems, particularly the distance between the two wells should be assessed using approximation methods (e.g. Eq. 7.1).

During operation of the geothermal two-well system a thermal anomaly relative to the undisturbed temperature distribution gradually develops around the injection well. The temperature anomaly decays nearly exponentially along the groundwater flow direction. The outer limit of the created temperature anomaly may be defined by the boundary where the temperature difference to the undisturbed temperature field is smaller than one Kelvin. For stationary conditions in the one-dimensional case and by ignoring longitudinal dispersion the cooling distance L can be approximated by Eq. 7.2a (Söll and Kobus 1992):

$$L = \log_{10} (\rho_w c_w n_d H H_D u / \lambda_D) \quad (7.2a)$$

where L is the cooling length or length of the anomaly in meters, ρ_w stands for the density of water [kg m^{-3}], c_w for the heat capacity of water [$\text{J kg}^{-1} \text{K}^{-1}$], n_d is the flow porosity of the ground [-], H the thickness of the aquifer [m], H_D represents the thickness of the cover layer [m]. λ_D the thermal conductivity of the cover layer [$\text{W m}^{-1} \text{K}^{-1}$] and u the effective groundwater flow velocity [m s^{-1}].

The cooling distance L [m] for the case of radial flow caused by the injection rate Q [$\text{m}^3 \text{s}^{-1}$] can be estimated from Eq. 7.2b (Söll and Kobus 1992):

$$L = \sqrt{0.733 \frac{\sigma_w c_w Q H_D}{\lambda_D}} \quad (7.2b)$$

where ρ_w stands for the density of water [kg m^{-3}], c_w for the heat capacity of water [$\text{J kg}^{-1} \text{K}^{-1}$], H_D represents the thickness of the cover layer [m]. λ_D is the thermal conductivity of the cover layer [$\text{W m}^{-1} \text{K}^{-1}$].

Equation 7.2b is valid for very small hydraulic gradients corresponding to nearly stagnant groundwater. The cooling distance L characterizes the symmetrical circular anomaly around the injection after very long times of operation.

For appreciable hydraulic gradients and significant groundwater flow, the thermal anomaly at the injection well becomes oval shaped. The maximum length of the anomaly from the well to the <1 K boundary in flow direction can be estimated using an iterative procedure developed by Ingerle (1988).

The maximum lateral extent B_T of the temperature anomaly normal to the flow direction can be approximated by Eq. 7.3 for the hydraulic width B_H [m]:

$$B_H = Q / (i k_f H) \quad (7.3)$$

with Q being the flow rate in $\text{m}^3 \text{s}^{-1}$, i is the dimensionless hydraulic gradient [m m^{-1}], k_f the hydraulic conductivity [m s^{-1}] and H stands for aquifer thickness [m].

In many areas, the groundwater flow direction changes with periodic or irregular fluctuations of the groundwater table. From other areas data on dispersion coefficients of the aquifers have been determined experimentally. If such parameters change and the variability of aquifer properties are known and significant they can be considered in Eq. 7.4. The lateral extent of the thermal anomaly influenced by the seasonal variation of groundwater flow direction and dispersion effects can be considered by the propagation angle α . From experience the propagation angle α varies from about 5° for the pure dispersion case and 15° for dispersion and strong seasonal variations of the flow direction. The total width of the thermal plume B_T can be estimated as a function of the downstream distance x [m] from the injection well:

$$B_T = B_H + 2x \tan \alpha \quad (7.4)$$

where B_H [m] denotes the hydraulic width defined by Eq. 7.3.

Another approach for modeling the temperature changes in the aquifer around the injection well has been described by Kobus and Mehlhorn (1980). They consider four specific points on an isotherm around the injection well and compute the temperature changes using Eqs. 7.5 and 7.6. The flow trajectory through the injection well is defined as x-axis. The intersection of the isotherm ΔT representing a considered temperature difference relative to the undisturbed temperature field with the x-axis is given by:

$$x_0 = (4\pi \alpha_T)^{-1} (Q \Delta T_E / n_d u H \Delta T)^2 \quad (7.5)$$

where α_T stands for the transvers dispersivity [m], u for the effective flow velocity [m/s], n_d the dimensionless flow effective porosity, H the aquifer thickness [m], Q the flow rate [m^3/s] and ΔT_E the temperature difference of the water between the two wells [K]. The intersection of the isotherm ΔT with the y-axis that is normal to the flowline through the injection well is given by Eq. 7.6 for $x \leq x_0$:

$$y = \pm [4 \alpha_T x \ln \{Q \Delta T_E / n_d u H \Delta T (4 \pi \alpha_T x)^{0.5}\}]^{0.5} \quad (7.6)$$

The simple computing approaches presented above are supplemented by a large number of more or less user-friendly software for modeling geothermal two-well systems for home heating and cooling. The software ranges from relatively simple spreadsheets to sophisticated (and expensive) packages. Two examples: GED (Poppei et al. 2006); EGON (Rauch 2009). This kind of software does not provide the user with a general solution for the immense variety of possible well configurations, well operation conditions, variable groundwater and heat flow conditions, and parameters of technical equipment such as heat pumps. Computed model solutions are valid for simplified conditions and special settings such as for single two-well systems in ideal isotropic aquifers and special boundary conditions. The software Groundwater Energy Designer (GED) by Poppei et al. (2006) successfully computes, for example, the groundwater flow field and heat transfer in homogeneous isotropic aquifers for several well systems decoupled. It is, however, not designed to model transient conditions and variable and complex geological structure of the ground. The code EGON (Rauch 2009) models the heat plume in a vertical section along the flow trajectory through the injection well. The computation is done for a single well and solves for decoupled groundwater flow and heat transfer using analytical, numeric and empirical methods. The program handles transient flow and heat conditions.

Geothermal well projects for larger buildings with several wells used for heating and cooling definitively require groundwater flow models for planning the engineering details. Coupled groundwater flow and heat transfer can be modeled using numerical finite difference or finite element codes. For the direct vicinity of the well a 3-D model is needed. The results of decades of research and plentiful of experience is available for general simulation of heat- and mass-transfer. The basic physics of flow mechanics and of heat transfer has been outlined in classic books of e.g. Bear (2007) and Carslaw and Jaeger (1959). Heat transport in groundwater by combined conduction, convection and dispersion has been comprehensively treated by Sauty (1980). The models implemented in the codes cover a large variety of relevant processes. Well known program packages include FEFLOW by WASY (Diersch 1994), TOUGH2 of Lawrence Berkeley National Laboratory (Pruess 1987) and HST3D of the U.S. Geological Survey (Kipp Jr. 1997).

Meaningful system planning and decisions on the number of required wells, well dimensioning and layout requires a sound knowledge of hydrogeological parameters including hydraulic conductivity, storage coefficient, aquifer thickness, aquifer structure and hydraulic gradient and its temporal variations. Furthermore, serious models are based also on injection temperature, the pre-operation underground temperature and flow fields, hydraulic gradients, specific heat capacity and thermal conductivity of all rocks present in all strata, just to name the most important parameters. These derived data are input for the programs and can be used to compute the time-dependent temperature field, the temperature evolution in space and time related to the reinjection of the thermally depleted water, the range of the thermal effect during operation and, if applicable, a possible thermal breakthrough.

The relatively large specific area of highly porous or intensely fractured near-surface rocks and soil promote rapid heat exchange between ground and re-injected

water primarily by heat conduction. The resulting decrease of the temperature difference between rock and water reduces the thermal plume in space and time. The process has formal similarities to the process of mixing and distribution of a sorptive tracer. Therefore, indirect solutions for heat transfer can be gained from pure groundwater flow models such as MODFLOW (Harbaugh 2005) used for modeling contaminant transport and associated sorption processes.

The presented computational concepts, programs and models are also valid for deep aquifers and their hydrothermal systems (Chap. 8).

References

- Isele, N. & Kölbel, T., 2006. Thermal power supply of a housing development with “cold local heating” (in German). BBR, 12, 54-59.
- Parkhurst, D. L. & Appelo, C. A. J., 1999. User’s guide to PHREEQC (version 2) – a computer program for speciation, batchreaction, one dimensional transport, and inverse geochemical calculations. In: Water-Resources Investigations Report 99-4259, pp. 312, U.S. Geological Survey, Denver, Colorado.
- Söll, T. & Kobus, H., 1992. Modellierung des großräumigen Wärmetransports im Grundwasser.- In: Kobus H.: Wärme- und Schadstofftransport im Grundwasser, Bd. 1, S. 81–133, DFG, Deutsche Forschungsgemeinschaft, Weinheim/Basel/Cambridge/New York.
- Ingerle, K., 1988. Computation of aquifer cooling by heat pumps (in German). Österreichische Wasserwirtschaft, 40 (11/12).
- Kobus, H. & Mehlhorn, H., 1980. Approximative computation of the continuous operation of geothermal installations (in German). In: Gas und Wasserfach, 121, 261-268.
- Poppei, J., Mayer, G. & Schwarz, R., 2006. Groundwater Energy Designer (GED): Software for utilization of groundwater for heating and cooling. In: Colenco Power Engineering AG Report for the Swiss Federal Energy Agency, pp. 70, Baden, Switzerland.
- Rauch, W., 2009. EGON. In: User Manual, University of Innsbruck, Austria.
- Bear, J., 2007. Hydraulics of groundwater. Dover Publications Inc. 592pp. ISBN-13: 978-0486453552
- Carslaw, H. S. & Jaeger, J. C., 1959. Conduction of Heat in Solids. Oxford at the Clarendon Press, Oxford, 342 pp.
- Sauty, J. P., 1980. An analysis of hydrodispersive transfer in aquifers. Water Resour. Res., 16(1), 145-158.
- Pruess, K., 1987. TOUGH2, Transport of Unsaturated Groundwater and Heat. In: User’s Guide, Version 2.0 (1999), Lawrence Berkeley Laboratory Report LBL-43134.
- Diersch, H. J., 1994. FEFOLW, Finite Element Subsurface Flow & Transport Simulation System. Reference Manual.
- Kipp, K. L. J., 1997. Guid to the Revised Heat and Solute Transport Simulator HST3D. In: Water-Resources Investigations, pp. 149, U.S. Geological Survey.
- Harbaugh, A. W., 2005. MODFLOW-2005; The U.S. Geological Survey Modular Ground-Water Model—the Ground-Water Flow Process. Techniques and Methods. U.S. Geological Survey, 6-A16.

Chapter 8

Hydrothermal Systems, Geothermal Doublets



Production test at a geothermal power plant

Hydrothermal systems use the thermal energy of an aqueous fluid at greater depths. Depending on the heat content of the fluid, systems with high enthalpy can be distinguished from low enthalpy systems. High enthalpy systems produce electrical power directly from hot steam or from a high-temperature two-phase fluid (Sect. 4.2). Lowenthalpy systems use the warm or hot water directly or via a heat exchanger to feed local or district heating systems, for industrial or agricultural utilization or for balneological purposes. Profitable electrical power production is possible at fluid temperatures above 120 °C. The thermal water is produced from deep groundwater reservoirs (aquifers). In principle, thermal water may also be retrieved from water conducting faults and fault zones, however, hydrothermal systems typically connect to aquifers.

High-enthalpy hydrothermal systems are related to regions with extreme geothermal gradients and very high ground temperature at shallow depth typically found in volcanic active areas, young rift systems and similar geological conditions. Low-enthalpy systems can be developed in any region with average or slightly elevated geothermal gradient. Therefore, the potential for low-enthalpy systems is evident because they can be installed in normal continental crust. The present day situation is, however, strongly focused on high-enthalpy systems and most of the worldwide installed electrical power capacity from geothermal sources relates to high-enthalpy systems (Sects. 1.3, 3.4).

Deep aquifers that permit the installation of geothermal doublets may also be used as seasonal heat storage systems (ATES). This can be attractive if for example the (seasonal) excess heat from a cogeneration unit, a photovoltaic system or from industrial waste heat can be transferred to the deep ground for use in the cold season. An aquifer heat storage system (ATES) uses, in contrast to a geothermal probe storage system, the heat capacity of water and rock of a natural aquifer that is hydraulically sealed at the bottom and the top of the conductive layer (Sect. 8.7.2). Aquifer heat storage systems use a production and an injection well, similar to geothermal doublets. For charging the system, water is produced from one well, loaded with thermal energy in a heat exchanger and re-injected into the aquifer through the second well. The process is reversed for discharging the system (Hasnaina 1998a; b).

8.1 Exploration of the Geologic and Tectonic Structure of the Underground

Hydrothermal systems use natural deep groundwater residing in geological reservoirs with high hydraulic conductivity. The reservoirs are embedded in other geological units with different properties. Therefore detailed and thorough knowledge of the geological structure of the underground is absolutely compulsory for exploring and constructing hydrothermal systems. The prime exploration target is to prove

the existence of suitable geothermal reservoirs and determine the depth and thickness of the thermal aquifers. The exploration process involves a long series of data accumulation before the first exploration borehole is drilled. The pre-drilling exploration first collects all geological and hydrogeological data that are already known about an area. The general structure of the underground of a potentially interesting area is then explored with geophysical tools, primarily with seismic soundings, supported by gravimetric, geomagnetic and aeromagnetic measurements if necessary (Sect. 13.1). Collected seismic field raw data must be processed with complex mathematical tools and algorithms. The correctness of the modeled structure of the underground depends much on the sound assumptions about rock properties that have been used in converting time to depth data. Seismic data may image the geological structures along vertical Sects. (2D seismic survey) or in three-dimensional space (3D seismic survey). Remember that an exploration drillhole provides 1D information about the structure of the subsurface.

The deep and consequently hot aquifer used by a hydrothermal system should have a high hydraulic conductivity. The decisive aquifer parameters are temperature and yield. The attainable yield or flow rate results from an economically and technically manageable drawdown in the production well. The productivity index (PI) is defined as the ratio of flow rate and drawdown (Sects. 8.2 and 8.6). This crucial parameter for hydrothermal systems cannot be derived from geophysical pre-drilling data from the surface. However, the productivity index can be determined, like other hydraulic parameters (Sect. 8.2), from hydraulic test data from well tests in a borehole.

Nevertheless, geophysical prospection may find indirect clues for elevated hydraulic conductivity such as indications for faults and other major brittle deformation structures or gradual facies changes in sedimentary units. Seismic data also give hints on the stress regime of an area, if the region is under compression or extension. Even stress changes with time may be revealed. Generally, the chances for finding zones with elevated hydraulic conductivity increase if fractured units and fault zones are being drilled, although brittle deformation structures may be sealed by secondary minerals and the structures may not conduct hot fluids. Similarly, increased hydraulic conductivity may be associated with extensional stress regimes whereas originally water-conducting structures could be closed in compressional regimes. The pre-drilling prediction of the structure of the underground must finally be verified by an expensive drillhole. Because drilling is the most expensive part of a hydrothermal energy project, pre-drilling exploration is important and should be taken serious.

Figure 8.1 shows an example of a geologically interpreted seismic cross section through the upper Rhine river valley south of Strasbourg. The valley is a Tertiary rift structure with Paleozoic basement exposed east (Black Forest) and west (Vosges) of the graben structure. The existing 2D seismic section has been calibrated with data from several existing deep boreholes in the area (three are shown on Fig. 8.1). The borehole data have been projected onto the plane of the section. The seismic data show the depths and the thicknesses of the potentially valuable hydrothermal aquifers, Hauptrogenstein formation and Muschelkalk formation. The section also shows a general half-graben structure and the presence of a negative flower structure typical of extensional strike-slip tectonics in the western part of the section. Both

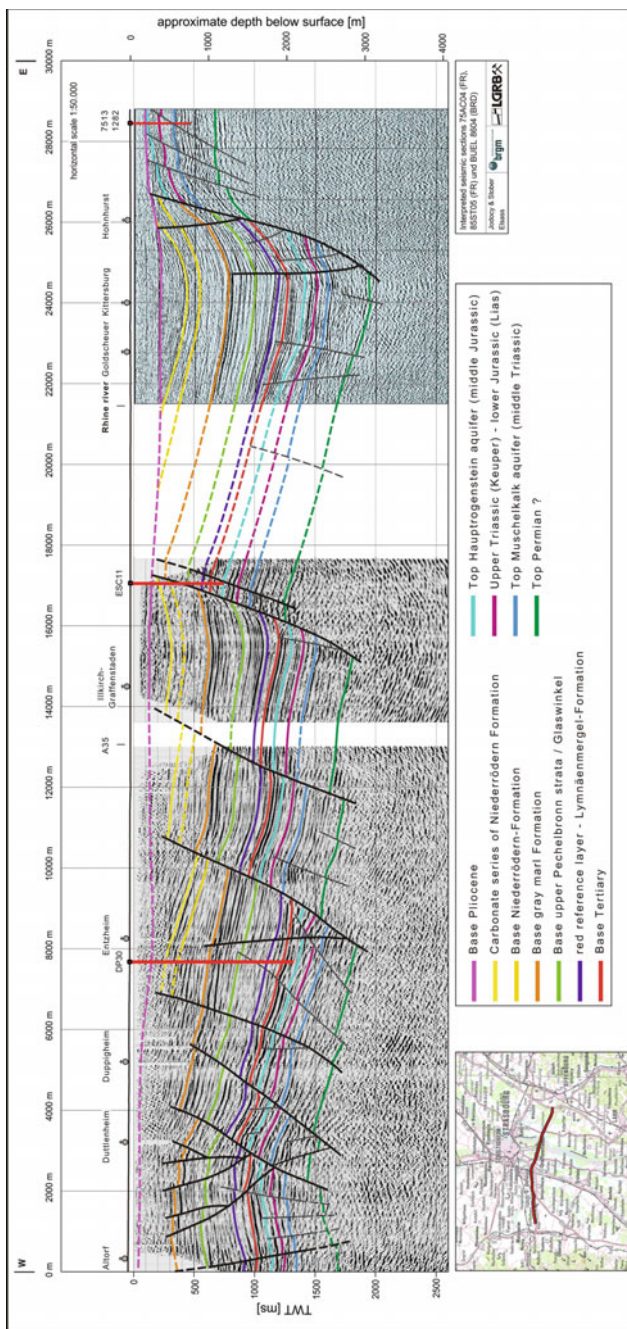


Fig. 8.1 Seismic section across the upper Rhine graben south of Strasbourg (France) with geological interpretation (Jodocy and Stober 2008). Depth axis in two-way travel time (TWT) in milliseconds [ms] on the left side, converted to approximate depth below surface [m]. Three projected drillholes in red. Note negative flower structure typical of extensional strike-slip tectonics in the western part of the section. Also note the fault system at m = 26,000 m (Hohnhurst) with a vertical displacement of ~1500 m forming the E-rim of the graben structure

structural features are evidence for an extensional regime. The section exhibits several faults with associated vertical displacements of strata (reflectors) in the deeper parts of the section. The faults are lacking in the upper part of the section and they are absent in the young deposits of the Pliocene (see at 24,000 m in Fig. 8.1). The structures are thus older faults that are no longer active. These brittle structures may have been sealed by deposition of secondary minerals and may not be associated with high hydraulic conductivity. Thus these structures may not be a prime exploration target.

The base of the Tertiary sequence of strata rests slightly discordant on the sediments of middle Jurassic age. In the Mesozoic sequence the top of the middle Jurassic Hauptrogenstein formation, the transition from the lower Jurassic (Liassic)—to the upper Triassic (Keuper group) and the top of the upper Muschelkalk formation (middle Jurassic) can be identified. Below follows the Permian to lower Triassic clastic sediments (Rotliegend formation and Buntsandstein formations). The two sedimentary sequences are separated by the seismic reflector associated with thin shales of the boundary clay formation marking the top of the Permian. The Buntsandstein formation represents a further potential fracture aquifer for geothermal utilization. In the Eastern part of the section the top of the Permian is at about 3000 m below surface, the deepest position in the half-graben structure. Given the thickness of 50–60 m of the Permian covering the pre-Permian basement, the top of the crystalline basement rocks, mostly gneiss, is at about 3050 m below surface in the deepest portion of the graben structure (at 24,000 m of Fig. 8.1).

The section (Fig. 8.1) shows the depth of the two prime target formations Hauptrogenstein and Muschelkalk for a potential geothermal development and installation of geothermal doublets. The top of the Hauptrogenstein formation varies from 1200 to 2400 m along the section. The approximate thickness of Hauptrogenstein is 50 m and upper Muschelkalk 80 m. Also the about 230 m thick lower Triassic Buntsandstein (above top Permian in Fig. 8.1) is a fracture aquifer with potential for geothermal utilization. The geothermal gradient in the upper Rhine rift valley is elevated and close to $44\text{ }^{\circ}\text{C km}^{-1}$. Thus the expected temperature of the water in the Hauptrogenstein formation is about 120 and 135 $^{\circ}\text{C}$ in the upper Muschelkalk formation at the deepest location of the two aquifers along the section. Perhaps as much as 150 $^{\circ}\text{C}$ can be expected at the base of the Buntsandstein aquifer.

From the example above it follows that already existing seismic data and data from deep boreholes need to be collected and carefully studied during the early stages of pre-drilling exploration. The research results from existing seismic exploration and from related boreholes enable a sensible decision on the necessity of further seismic investigations, if necessary including also 3D seismic models of the subsurface for better localization of fault zones. Reprocessing old seismic data may be possible and has proven to be very helpful in many cases. Existing deep boreholes greatly facilitate geological interpretation of seismic data (e.g. Fig. 8.1). Furthermore, seismic travel time data can be calibrated using borehole data (Sect. 13.1). If boreholes are not available within a suitable distance from the investigated new site, then seismic travel time data need to be converted to depth using uncertain model assumptions. The sound interpretation of seismic data establishes the stratigraphy, depths and thickness and

in some cases the sedimentary facies of the geological strata underground. A further important goal of the seismic data interpretation is the survey of deformation patterns and fault systems (Fig. 8.1). Fault mapping may show that large fault displacement disrupts hydrothermal target aquifers. Hydraulic connection of the displaced aquifer may be indirect through the fault. Surveying fault patterns is generally more difficult, if not impossible, in crystalline basement compared to sedimentary cover sequences. Identified and mapped faults in the cover can be extrapolated to the crystalline basement in some favorable cases. However, we strongly advise not regarding faults as such as target structures for hydrogeothermal systems. Faults may or may not have a higher hydraulic conductivity compared to their host rocks. Mylonitized and sheared faults and faults sealed by secondary mineral deposits in fact can essentially be impermeable (Stober et al. 1999). Fault systems often show a characteristic structure with an impermeable fault core and permeable zones of crushed material on both sides of the core (Choi et al. 2016). Therefore a fault zone can be simultaneously water conductive parallel to the fault and impermeable across the fault (Stober et al. 1999). Stressed fault zones in tectonically active regions may become seismically active under hydraulic loads (Sect. 11.1).

Recorded and stored (and available) data from borehole measurements collected from already existing boreholes of the area of interest are most useful and should be carefully gathered and studied. The data such as geophysical logs, well logs, lithology logs permit a predrilling prediction of the lithology profile, petrophysical properties, reservoir characteristics, and drilling properties of the ground at the site of interest (Sect. 13.2). Well logging has replaced the time consuming and expensive drilling of core samples. Data collected with acoustic borehole scanner tools (televiewer) provide information on the incidence and orientation of fractures. Large-scale data regarding the present regional stress field can be viewed on the World-Stress-Map (<https://www.world-stress-map.org/>). These stress field data are important input parameters for geomechanical modeling of the seismicity potential of the geothermal project (Sect. 8.3). The stress field data also may indicate the orientation of faults and fractures with elevated or reduced hydraulic conductivity respectively.

8.2 Thermal and Hydraulic Properties of the Target Aquifer

The most important thermal parameters in the context of hydrothermal system development are thermal conductivity λ [$\text{W m}^{-1} \text{K}^{-1}$] and the specific heat capacity c [$\text{J kg}^{-1} \text{K}^{-1}$] (Sects. 1.4 and 1.5) of the geological material and the fluid phase(s) contained in it.

The **thermal conductivity** refers to the ability of material to transport thermal energy; the heat capacity represents the ability to store thermal energy. The heat capacity of material is a particularly important parameter for characterizing the effects of time dependent systems and transient states.

The heat flow density q [W m^{-2}] is a further important parameter in the framework of hydrothermal system development. It quantifies the heat flow per surface area and contains the parameter time in the dimension Watt [J/s], energy per time. The heat flow density q relates to the product of thermal conductivity λ and the temperature gradient $\text{grad } T$ [K m^{-1}] and is defined by the Fourier equation of conductive heat transfer (Sect. 1.4; Eq. 8.1):

$$q = \lambda \text{ grad } T \quad (8.1)$$

The Fourier equation (Eq. 8.1) states that the driving force of a non-equilibrium temperature distribution $\{\text{grad } T\}$ causes the flow q of an extensive parameter, here thermal energy per time, to reduce the imposed driving force of the process. The magnitude also depends on material properties, here the heat conductivity λ . If λ is high, high heat flow results from the imposed driving force, if λ is low the same driving force decays over a much longer period of time. These simple relationships have significant consequences for hydrothermal projects.

Thermal conductivity λ varies between 2 and $6 \text{ W m}^{-1} \text{ K}^{-1}$ in hard rocks. Water has a very low λ of only $0.6 \text{ W m}^{-1} \text{ K}^{-1}$ at 20°C . Highly porous aquifers have a lower thermal conductivity than impervious rock units with a low porosity. The specific heat capacity c of hard rocks varies within the very narrow range of $0.75\text{--}0.85 \text{ kJ kg}^{-1} \text{ K}^{-1}$. However, the specific heat capacity of liquid water of $4.187 \text{ kJ kg}^{-1} \text{ K}^{-1}$ is five-times greater than that of rocks. Water poorly conducts thermal energy but it is highly capable of storing heat.

The thermal conductivity λ of water increases with temperature to a maximum at about $140\text{--}150^\circ\text{C}$ depending on pressure and then slightly decreases with further T -increase (Fig. 8.2a). λ also increases with pressure.

The **density** ρ [kg m^{-3}] of rocks ranges from 2000 to 3000 kg m^{-3} . Some rocks, peridotite and eclogites, may be as heavy as 3300 kg per m^3 , other rocks, for example coal, may weigh less than 2000 kg per m^3 . Typical continental basement rocks, granite and gneiss, weigh about $2700\text{--}2800 \text{ kg per m}^3$. Liquid water has a density of about 1000 kg m^{-3} at the temperature of $+4^\circ\text{C}$ and surface pressure of 1 bar (density anomaly of water). The density of rocks and water depends on the temperature and pressure. The P - T dependence of rock density can be normally ignored in planning hydrothermal facilities. The density of water as a function of temperature and pressure is shown in Fig. 8.2b. Density decreases with temperature regulated by the thermal expansibility of water and it increases with pressure controlled by the compressibility of water. Water under hydrostatic pressure at 7 km depth and 80°C has a density of $\sim 1000 \text{ kg m}^{-3}$, similar to surface water. However, in regions with normal geothermal gradients, the temperature effect slightly outweighs the pressure effect and, consequently, the density decreases slightly with depth. Decreasing hydraulic conductivity with depth and increasing mineralization and salinity of the deep water efficiently inhibits upwelling of deep hot water. The density of water depends also on the total amount of dissolved solids (TDS). At a given pressure and temperature the density increases with TDS. Deep water is commonly highly mineralized. Several hundred grams of dissolved solids per kg liquid is not uncommon. The density decrease of

pure water with depth in thermally normal areas is more than compensated by the concurrent density increase caused by the growing TDS with depth. The net-effect is a slight density-increase with depth under normal conditions. The boiling temperature of water increases with pressure and TDS buildup with depth.

The **dynamic viscosity** μ [Pa s] of a fluid describes the internal resistance to flow; it is a measure of fluid friction. It strongly depends on temperature (Fig. 8.2c)

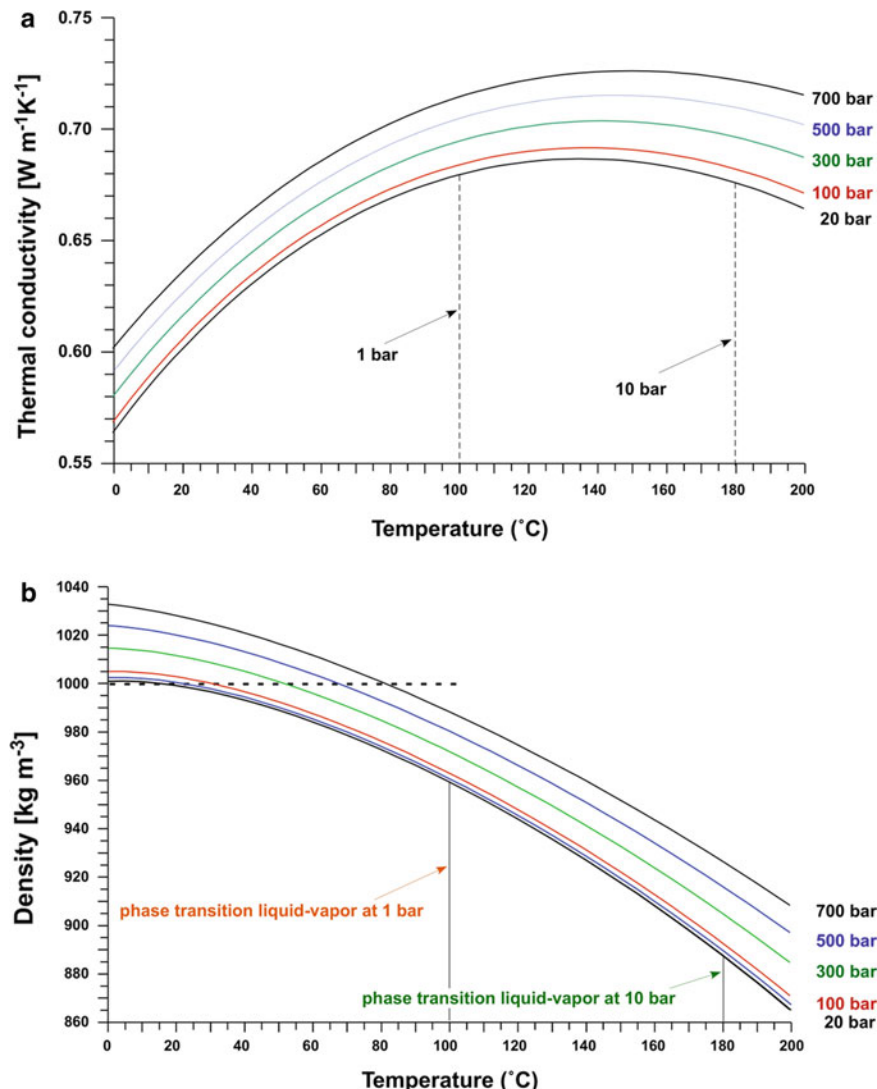
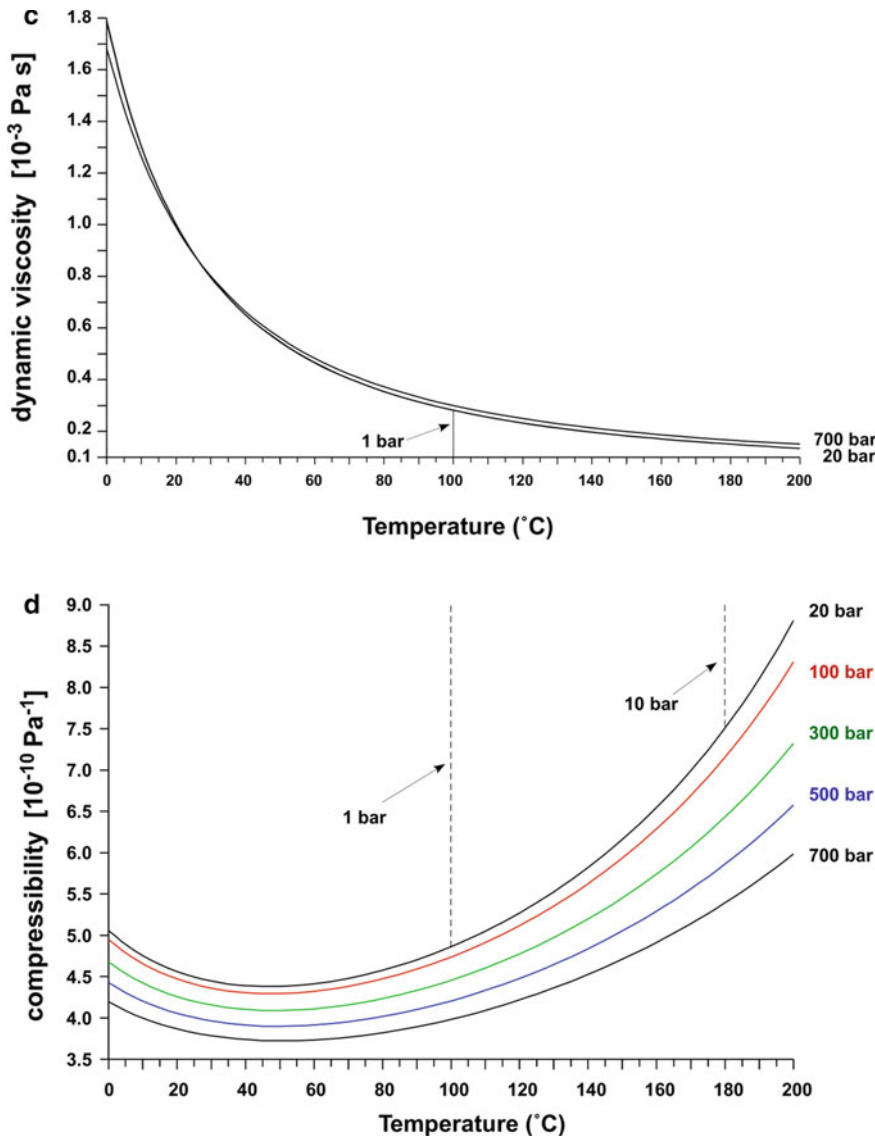


Fig. 8.2 Pressure and temperature dependence of important properties of water (Wagner and Kretschmar 2008): **a** Thermal conductivity λ ; **b** density σ ; **c** dynamic viscosity μ ; **d** compressibility β

**Fig. 8.2** (continued)

and decreases from 0.2 at 0 °C to 1.75×10^{-3} Pa s at 200 °C. The three orders of magnitude decrease of μ is in sharp contrast to the small variation of density with T. Viscosity largely regulates the flow properties of thermal groundwater. Kinematic viscosity ν [$m^2 s^{-1}$] is defined as the ratio of dynamic viscosity and density ($\nu = \mu/\rho$).

The **compressibility** β_F [Pa^{-1}] of a fluid describes the volume change with pressure at constant temperature normalized to the volume at a reference pressure (Eq. 8.2).

$$\beta_F = 1/V \Delta V / \Delta p \quad (8.2)$$

The compressibility of H_2O is inversely proportional to the pressure. At temperatures above 50 °C c_F increases with temperature, whereas c_F decreases with temperature below 50 °C (Fig. 8.2d). The compressibility generally varies from 4.0×10^{-10} to $5.5 \times 10^{-10} \text{ Pa}^{-1}$.

Permeability and hydraulic conductivity describe the ability of a system (rock) to let a viscous fluid pass through its pore space. The permeability characterizes the conductive properties of the rock matrix (soil, hard ground). Hydraulic conductivity characterizes the conductive properties of the system including both the porous solid and the flow properties of the fluid flowing through the pore space including fractures (fracture pore space). A rock with a given permeability has a low conductivity for “sticky” fluids and a high conductivity for “thin” fluids. Permeability and hydraulic conductivity should not be confused. Fluid flow in rock with a given permeability structure and for an identical flow force (hydraulic gradient) may differ considerably for aqueous fluids of different temperature, salinity, gas content, total of dissolved solids etc. **Hydraulic conductivity** k_f [m s^{-1}] represents the material related proportionality factor in the Darcy flow law, which relates fluid flow Q [$\text{m}^3 \text{ s}^{-1}$] through the area A [m^2] to a hydraulic gradient i [dimensionless], representing the driving force for fluid flow.

$$Q/A = k_f i \quad (8.3a)$$

$$k_f = Q/(i A) \quad (8.3b)$$

Equation 8.3a represents the phenomenological Darcy flow equation of the form $J = L X$, where J is the flow of a quantity per unit area depending on the material property L and driven by the force X . It has the same structure like the Fourier Eq. 8.1. Equation 8.3b defines the hydraulic conductivity.

Permeability κ [m^2] and hydraulic conductivity k_f are related by the Eq. 8.3c. The flow-relevant properties of the fluid (viscosity μ , density ρ) are contained in k_f whilst κ describes rock properties only and refers to the structure of the rock independent of the fluid contained in it.

$$k_f = \kappa(\rho g / \mu) \quad (8.3c)$$

where g is the acceleration due to gravity. It is evident from Eq. 8.3c that the hydraulic conductivity of the ground increases with temperature, because the viscosity of water strongly decreases with temperature (Fig. 8.2c).

The pressure and temperature dependence of physical and thermal properties of H₂O (Fig. 8.2) has consequences for developing and operating hydrothermal systems. The borehole drilled after termination of pre-drilling exploration needs to be extensively tested. A well test in a thermal aquifer first pumps the relatively cool water standing in the borehole. During later operation the temperature of the produced water gradually increases and, consequently, the density of the fluid decreases. Thus at early stages of a pumping test the density of the water is typically higher and consequently the water table is lower. This is reversed in later stages of the well test with the somewhat paradox effect that the water table raises during pumping because the density of the hydrothermal fluid decreases. This density effect is particularly prominent in highly conductive aquifers (Fig. 8.3).

The dependence of the hydraulic conductivity on the physical properties of water means in practice that the conductivity of an aquifer at 70 °C is about three times higher than at 10 °C, all other aquifer properties being the same (Fig. 8.4). The

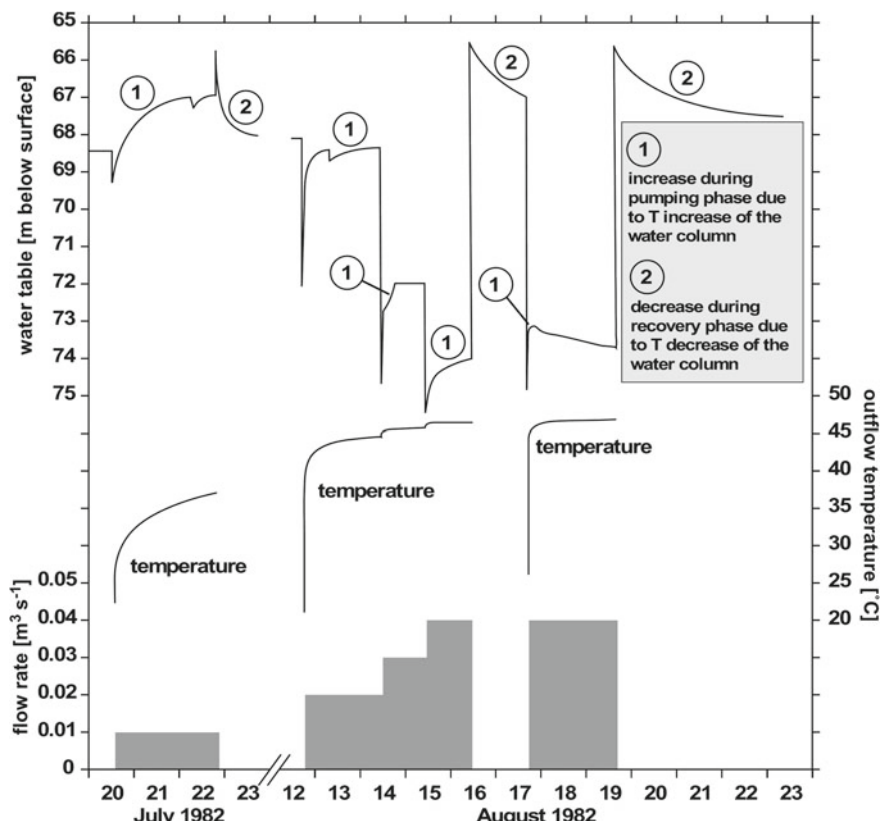


Fig. 8.3 Apparently paradox behavior of the water table during a pumping test in a thermal water well (Stober 1986). The figure shows the daily measurements of (from top to bottom): water table, outflow temperature, and the pumping rate

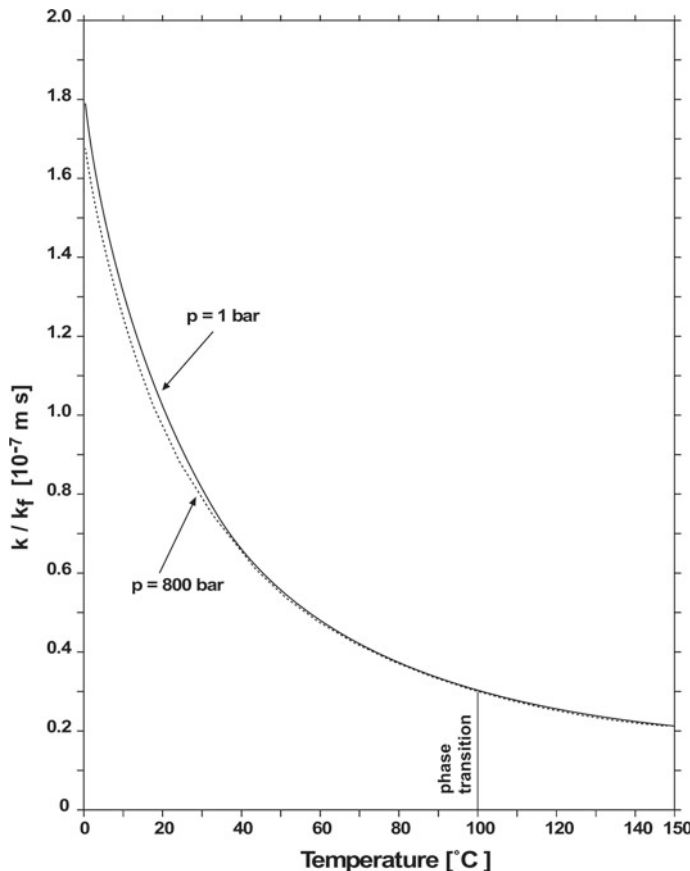


Fig. 8.4 Permeability κ /hydraulic conductivity k_f versus temperature at 2 isobars for pure water. The strong curvature of the relationship is mostly the result of the temperature dependence of the dynamic viscosity of water (Fig. 8.2c), which is incorporated in k_f but not in κ . The relationship shows that hydraulic conductivity k_f is extremely sensitive to temperature (at low to moderate temperature) for aquifer rocks with the same permeability κ

dynamic viscosity dominates the temperature variation of the hydraulic conductivity (Fig. 8.2c). The effect of density variations with changing $P-T$ on the hydraulic conductivity is negligible (Fig. 8.2a). In the temperature range 0–200 °C the changes in dynamic viscosity greatly exceed density changes. Therefore, the key parameter dynamic viscosity is of prime importance for the flow behavior of thermal groundwater.

The dependence of the hydraulic conductivity on the physical properties of water has direct consequences for the design of hydrothermal doublets. Extracting heat from the pumped hot deep water at the surface produces cool, heat depleted water that needs to be re-injected into the aquifer. Consequently, the hydraulic conductivity and the water uptake capability of the injection well decrease dramatically with a

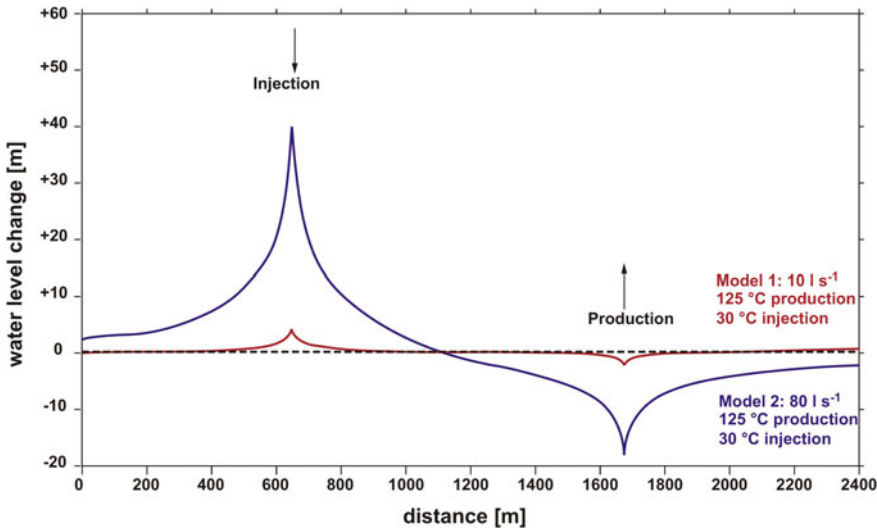


Fig. 8.5 Comparison of the cone of injection and depression at a hydrothermal doublet well. The cone at the injection well is much larger due to the injection of cooled water than the cone of depression at the production well

declining temperature of the injected water. This, in turn, has the consequence that the injection cone is much more prominent than the cone of depression at the production well (Fig. 8.5). These interrelations should be considered in the planning phase of a hydrothermal project. If ever possible the well with the highest conductivity should be used as injection well.

The physical and thermal properties of water depend, in addition to T and P , also on its chemical composition. The chemical composition is a complex property and includes the total amount of dissolved solids (TDS), the kind of dissolved solids and the amount and type of dissolved gases. The thermal power of a hydrothermal system depends on the chemical composition of the produced fluid and it is imperative to know and monitor the water composition in hydrothermal projects (Sect. 8.6, Eq. 8.6).

Hydraulic conductivity k_f is the central and decisive parameter controlling fluid flow rates in the underground. It is, together with the fluid temperature, the parameter that decides the economic success of the project. Hydraulic conductivity k_f is the material related factor in the phenomenological Darcy flow law (Eq. 8.3a). The total amount of water flowing through the aquifer cross section per unit time Q [$\text{m}^3 \text{ s}^{-1}$] follows from the Darcy equation if the flow relevant cross section [m^2] of the aquifer is known. The amount of hot water available for the hydrothermal system varies with pressure and, mostly, temperature because of the $P-T$ dependence of k_f . Fluid flow Q is clearly higher at high- T than in colder aquifers.

The Darcy flow law is valid for laminar and linear flow. Other, non linear, flow laws apply to conditions where the geological material has a very low hydraulic conductivity k_f and the hydraulic gradients are very low or of material with extremely high

hydraulic conductivity and ultra-high gradients (flow force). Both types of extreme conditions do not normally occur in hydrothermal system setups (Kappelmeyer and Haenel 1974).

Hydraulic well tests provide data on drawdown and relaxation or pressure build-up and decline for given water production and injection rates (pumping rates). The observed gradients i (drawdown, depression cones) and the pumping rates Q permit an insight into the conductivity of the examined (tested) geological unit (Chap. 14). The conductivity derived from the well test is a property of the tested unit as a whole. It describes the conductivity of the aquifer of thickness H [m] and is commonly referred to as **transmissivity T** [$\text{m}^2 \text{ s}^{-1}$]. Transmissivity characterizes the conductivity across the thickness of the tested section. For a homogeneous and isotropic aquifer of thickness H , the hydraulic conductivity k_f can be computed from the measured transmissivity T directly from Eq. 8.4a:

$$T = k_f H \quad (8.4a)$$

In layered ground, the measured transmissivity T is contributed by several layers j with different thicknesses H_j and hydraulic conductivities k_{fj} . Thus total transmissivity T is the sum of the transmissivities of all layers j (Eq. 8.4b):

$$T = \sum_j k_{fj} H_j \quad (8.4b)$$

A generalized formulation of the transmissivity-conductivity relation is given by Eq. 8.4c:

$$T = \int_0^H k_f dh \quad (8.4c)$$

The **productivity index PI** [$\text{m}^3 \text{ s}^{-1} \text{ MPa}^{-1}$] proved to be a very useful parameter for characterizing a hydrothermal system. PI is the production rate Q [$\text{m}^3 \text{ s}^{-1}$] per pressure decrease Δp [Pa]. It can be computed from the obtained production rate Q for a given fixed drawdown (expressed in Pa). The PI is particularly useful if no well test data have been obtained. The PI comprises well specific properties such as skin and wellbore storage in addition to the hydraulic properties of the aquifer (Chap. 14).

The **absolute porosity n** [dimensionless] is the total volume of all voids and pores of a rock unit per rock volume. A rock contains pores that are interconnected, pores that are isolated, fracture pore space, cavities and any other form of space that is not filled with minerals. The total volume of all these voids is the total pore space. The total volume of a rock contains all voids. The ratio of the total volume of voids and the rock volume is the porosity n ($n = V_v/V_r$; with V_v total volume of voids; V_r total volume of rock). The porosity n characterizes the storage capacity of an aquifer.

The water conducting features of hard rock aquifers are predominantly fractures and cavities. Conductivity and yield of the aquifer are mostly determined by the

fracture network and geometry of the cavity system. Fluid flow is strongly linked to the **flow effective porosity** n_f [-], which is the portion of the total porosity that is interconnected and where water can be freely transferred from one pore to the next. Water firmly attached to the grain surfaces and water in dead end pores is stagnant water and not part of the flow effective porosity even if this water resides in interconnected porosity. The effective porosity is the relevant porosity parameter for geothermal applications. n_f is always smaller than n . The difference between total and flow effective porosity is particularly significant in shales and marls. Clay and mica-rich rocks may have a high total porosity but a low flow effective porosity and, consequently, a low permeability. Suitable deep hardrock aquifers for hydrothermal system are thus mica-poor rocks with predominantly feldspar and quartz such as granite, sandstone, arkose and mica-poor gneiss or (karstified) limestone. High effective porosity generally relates to high permeability κ . However, the relation between n_f and κ is not simple and direct because permeability depends also on the size distribution, shape and connective structures. Both parameters can be derived from tracer tests and pumping tests in the wells (Chap. 14).

Hydraulic well tests may also provide the **storage coefficient** S [-] characterizing the tested aquifer (Chap. 14). The storage coefficient S relates to the volume change ΔV of the stored water (fluid) in response to a pressure change caused by a change in the height of the water column Δh in an aquifer per unit surface area A :

$$S = \Delta V / (\Delta h A) \quad (8.5a)$$

The storage coefficient S indicates how much water (ΔV) runs off an aquifer if the water column in the aquifer is lowered by Δh . S is a parameter derived from well tests and depends on the flow porosity n_f . In unconfined aquifers S is about $\approx n_f$. Deep confined aquifers used for geothermal doublets have $S \ll n_f$. This means that only a small portion of the water contained in the flow porosity can be released by changing the hydraulic pressure. The **specific storage coefficient** S_s [m^{-1}] normalizes the volume response to the volume of the aquifer, in contrast to the storage coefficient S where it is normalized to area. The relation between storage coefficient S and specific storage coefficient S_s is analogous to the relation between transmissivity and hydraulic conductivity. The relation is given by Eq. 8.5b for isotropic homogeneous aquifers of the thickness H [m]:

$$S = S_s \cdot H \quad (8.5b)$$

Storage coefficients of layered or inhomogeneous, anisotropic aquifers can be described by equations analogous to the Eqs. 8.4b, c.

Various methods and tools for hydraulic wells testing and for determination of hydraulic parameters of the deep ground will be presented in Chap. 13.

8.3 Hydraulic and Thermal Range of Hydrothermal Doublets, Numerical Models

Hydraulic or thermal short circuits between the production and injection wells must be absolutely avoided during operation of hydrothermal systems (see also Sect. 7.3). Appropriate seals must prevent hydraulic connections to another groundwater level. The schematic setup of an injection well is depicted in Fig. 8.6. The distance from the injection well to the production well at connection depth to the aquifer must be sufficiently large for safe operation during a period of about 30 years. During this time the temperature of the produced water should not be influenced by the injection of cooled water into the exploited aquifer. For a specific system, the minimal distance between the two connecting sections of the wells in the aquifer depends on

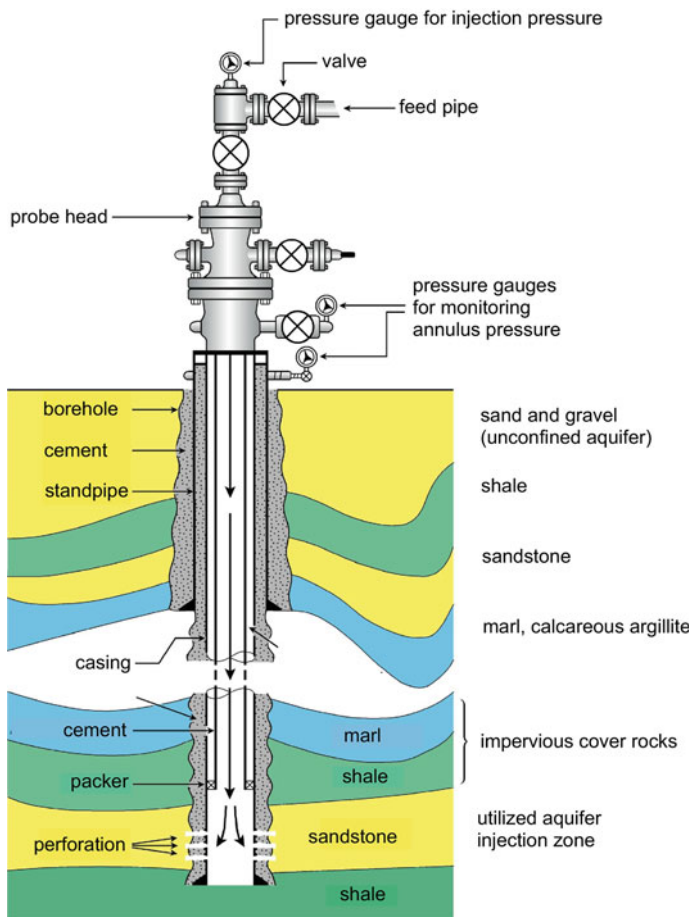


Fig. 8.6 Schematic structure of an injection well (from Owens 1975)

the geological structure and the properties of the ground but also on the technical conditions of the system such as well design and pumping rates. However, the well distance should not be too large because the sustainable yield of the production well depends on the recharge of the aquifer by the injection well.

Dimension and size of the geothermal reservoir is, of course, important for the utilization of the aquifer. The volume of stored hot water and the thermal energy it contains can be computed from the surveyed shape and dimension of the reservoir and the petro-physical reservoir properties including porosity and temperature distribution. For instance, greater aquifer thickness, for all other parameters and dimensions being the same, increases transmissivity and hence also the achievable fluid production rate (Sect. 8.2).

Starting point for a three-dimensional geological underground model is data from geophysical, typically seismic exploration and data from existing boreholes in the area (Sect. 8.1). Numerical models optimize the location of and the distance between the two wells. Predrilling models need to assume plausible values for a number of crucial parameters of the target aquifer and the geological structure of the underground and thus are prone to considerable uncertainty. The “known” geologic structure of the underground is based on the interpretation of seismic signals. Modeled depths of the target aquifer, details of the stratigraphy, fault and fracture patterns from seismic exploration are combined with data on hydraulic conductivity, temperature and water composition from existing wells and well tests. The reliability of model predictions improves greatly with drilling of the first well of the hydrothermal doublet. Still, the geology of the underground is always good for surprises and the true structure and properties of the target aquifer can only be captured in a very simplified manner by pre-drilling models.

Numerical modeling starts with a conceptual model that bundles all available geological, hydrogeological and thermal data and information about the underground. It is the task of the geologist to construct a three-dimensional geological model of the structure of the underground from irregularly distributed 1D borehole data and a limited number of 2D seismic sections (and if available data from 3D seismic exploration). The resulting geological 3D model contains the position and orientation of the different stratigraphic layers and their thicknesses. By assigning hydraulic conductivity, porosity and other parameter values to the layers and imposing geothermal gradients to the model area a learned hydraulic model can be developed. This model depicts the basic hydrogeological concept of the underground. The model converts the lithological and stratigraphical units of the geological 3D structure model to hydrostratigraphic units with associated hydraulic parameters. The thermal structure and properties of the underground follow from the assignment of thermal parameters to the individual strata and lithological units. This still relatively crude and simple model of the underground forms the basis for numerical models of heat and mass transfer. A preliminary stationary groundwater flow model can be further developed from the 3D underground model by assuming plausible geohydraulic boundary conditions and with quantitative estimates of groundwater recharge and vertical components of groundwater flow.

Numerical reservoir models are effective tools for developing, characterizing and optimizing hydrothermal projects (Fig. 8.7). Numerical 3D models based on finite differences (FD) or finite elements (EF) mathematical techniques are routinely generated using a number of different codes. Examples are: SPRING by Câmara

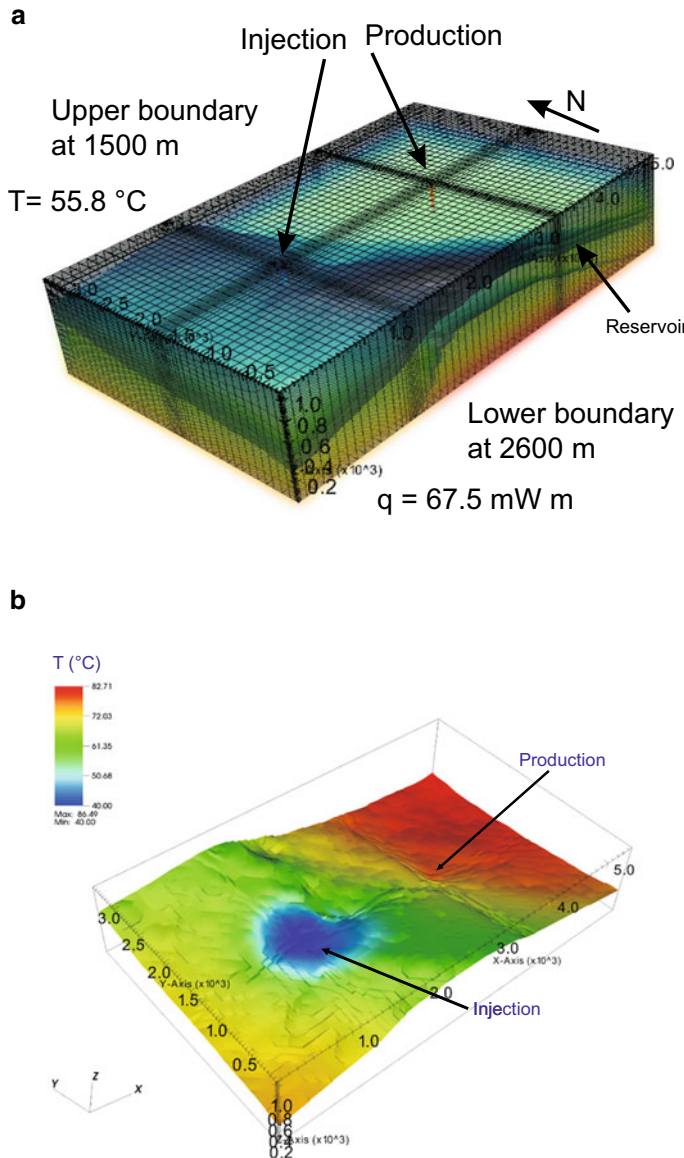


Fig. 8.7 Example of a numerical model for a hydrogeothermal doublet: **a** Geometry of the model, **b** model predictions for 50 years of operation (figure kindly provided by Geophysica GmbH)

et al. (1996), FEFLOW by Trefry and Muffels (2007), SHEMAT by Clauser (2003), MODFLOW by Harbaugh (2005). Temperature data and hydraulic conductivity data can be combined with data from hydrochemical surveys for the creation of a thermal–hydraulic-chemical model (THC model) of the project area. A THC model quantitatively predicts the hydraulic consequences of water extraction (pressure reduction) and re-injection (pressure increase), the reach of the thermal effects (cooling) and the alteration of the original chemical composition of the produced deep fluid during later operation of the plant. The prediction of the chemical consequences of P – T changes permits planning of countermeasures preventing scaling and corrosion (Sects. 8.4 and 15.3). Simpler TH models can be built if the expected chemical effects are believed to be relatively small.

Evidently a numerical thermal water flow model must be calibrated and validated. This is done by varying the geohydraulic aquifer parameters and the chosen boundary conditions until measured and computed groundwater potentials and potential distributions reasonably match and results in plausible groundwater balance. Chosen parameter values must be restricted to a plausible range for the investigated site. The calibration is typically associated with considerable uncertainties because of the limited number of data-backed grid points.

In the following step, the natural temperature field can be modeled using the calibrated stationary groundwater flow model. The typical result of the modeling effort is a rather simplified picture of the temperature distribution in the underground. Normally, the model does not even include heat transfer due to advection because of an insufficient database.

In addition to the model calibration, a thorough sensitivity analysis is a further important component of project planning. Thus hydraulic well tests producing quantitative test data are essential for a successful model calibration. Using numerical models, it is important to ensure internally consistent mass balance. For example, numerical circulation tests must be run with [kg s^{-1}] and not [L s^{-1}] because heat extraction changes the density of the hot fluid and hence more mass would be injected than produced when using [L s^{-1}]. It is important to carefully follow model instructions and handbooks (although it might appear old fashioned).

Numerical models of the conditions underground predictively deduce the suitability of the location for installing a geothermal plant. The models help optimizing the detailed underground position of production and injection wells in order to exclude thermal interference over the entire operating time. Models can predict pressure changes in the wells after yearlong operation of the plant. Negative consequences of predicted hydrochemical changes of the hydrothermal fluid can be prevented by taking appropriate countermeasures e.g. by installing the correct scale and corrosion inhibitor systems. A well-calibrated stable numerical model can be used for predictions of the later operation phase. Models assist in developing optimal utilization concepts thus optimizing the economic efficiency of the system.

Even if the pre-operation distribution of the hydraulic conductivity in the aquifer was relatively homogeneous, the water uptake capacity of the injection well may become problematic during operation (see Fig. 8.5). Injection of cool water leads to a strongly lowered hydraulic conductivity in the injection zone, because of the

viscosity increase with decreasing temperature (Sect. 8.2). Therefore it is advised to use the borehole with the highest hydraulic conductivity of the rock matrix as injection well.

The updated numerical model is also used to define the license area (claim). A well-structured numerical model shows the likely hydraulic and thermal range influenced by the planned geothermal installation. In many countries, the licensing authorities require a professionally derived model from the petitioner.

A geomechanical model of the site is standard for hydrothermal or petrothermal projects. It is based on the all geological data and information available particularly on a structural geological analysis and also includes the stress field data (Sects. 8.1 and 8.2). The model predicts the type of structures (fault zones, fracture systems) prone to activation of shearing at various injection or production rates. Thus the model predicts the potential for stress release and the likely magnitudes of induced seismicity. Numerical geothermal system models may be requested by licensing authorities for assessing seismic risks during construction and operation of geothermal systems (Sect. 11.1).

The quality of the model results depends strongly on the number (density) and quality of the measured hydraulic and thermal parameters. Also the scale of the model is crucial for the significance of the model predictions.

A numerical type model of a district heating system supplied by a geothermal doublet near Den Haag (Netherlands) is shown in Fig. 8.7. Target horizon of the doublet is the Delft Sandstone unit (upper Jurassic to lower Cretaceous) at 2200 m depth. Heat flow has been modeled by the three-dimensional finite difference code SHEMA that solves coupled heat, transport and flow equations. The integrated regional model has the dimension 22.5×24.3 km and a depth resolution of 5000 m. From this regional model local reservoir models have been developed such as the one shown in Fig. 8.7a for a field of 5.5×3.5 km and a depth range of 1500–2600 m. The number of nodes is about 170,000. Figure 8.7b shows the prediction of the T-distribution after 50 years of operation of the geothermal system at a production rate of $150 \text{ m}^3 \text{ h}^{-1}$, a temperature of the produced fluid of 79 °C and a temperature of the re-injected (cooled) fluid of 40 °C. The model predicts a significant decrease in temperature at a distance <1 km around the injection well after 100 years (Mottaghy and Pechtnig 2009).

8.4 Hydrochemistry of Hot Waters from Great Depth

The chemical composition of hot water from deep reservoirs has many significant effects on the operation of a hydrothermal system and it may be critical to the economic success of a geothermal project. The produced hot aqueous solutions contain typically a large amount of dissolved solids and gases. In the reservoir the fluids are under a high pressure promoting gas dissolution in the liquid phase. At temperatures below about 110 °C microorganisms are typically present in the

fluid-rock systems and add further complications particularly at the fluid reinjection wells. The gas-rich, saline, high-temperature fluids circulating in geothermal systems are extremely corrosive and aggressive and require appropriate materials and suitable anti-corrosion measures. Particularly vulnerable are production pump, heat exchanger, pipe and filter systems (Sect. 15).

Sampling of hot water is challenging. Samples may be taken downhole in the reservoir aquifer or at or near the wellhead. Downhole samples are taken at $P-T$ conditions of the reservoir. Sample containers can be sealed gas-tight at depth so that no gas-loss or contamination occurs when the samples are brought to the surface. Sampling at the wellhead is often affected by gas-loss and other alterations of the sampled fluid caused by depressurization. Sophisticated sampling techniques can avoid these problems (Fig. 8.8). Very gas-rich fluids may undergo phase-separation at the surface even in pressurized closed systems. The sample temperature at the wellhead is close to the reservoir temperature if production rate is high. The outflow temperature increases with production rate that is with the flow rate in the well. The production temperature depends on the flow rate (Fig. 8.9). Consequently, a small production rate produces a fluid with a higher density than at high production rates (Fig. 8.2a). These effects influence the productivity index PI defined by $Q/(\Delta p)$ (Sect. 8.2) also.

Some of the dissolved solids in the produced fluids may precipitate as a result of changing pressure and temperature in the production-injection cycle. The saturation state of the fluid with respect to many minerals may potentially change from undersaturated or saturated in the reservoir aquifer to strongly oversaturated if cooled and depressurized. Particularly critical is the situation if decreasing pressure and temperature is accompanied by gas-loss. As an example, CO₂-loss from the produced fluid very commonly leads to rapid formation of carbonate crusts and deposits (scales) in pipes and in surface installations that may dramatically reduce the efficiency of the entire system (Fig. 8.10). Geothermal systems should be operated under a certain minimum over-pressure and as closed systems in the near surface region to prevent gas-loss and scaling. Because it is the purpose of a geothermal system to extract thermal energy from the produced fluid, the fluid cools and the saturation index of most solids increases (more details in Sect. 15). Particularly problematic is supersaturation of the fluid with respect to several sulphate minerals. Sulphate scales are difficult to prevent, for example with inhibitors or with acidification, and difficult to remove if once formed. Ba- and Sr-sulphate precipitates have been observed in injection wells. Carbonate and iron scales are easier to deal with. Lead salts can be problematic because they accumulate ²¹⁰Pb a β-ray emitter in addition to ²⁰⁸Pb. Also other sulfides but some sulfates as well contain radioactive elements (e.g. ²²⁶Ra) and thus form radioactive scales that require special treatment, handling and disposal. Other challenging scales are briefly described in Sects. 11.3 and 15.3.

The chemical properties of the produced geothermal fluid may also make them aggressive to materials. The chemical reactions between the fluids and the mostly metallic system components may cause severe damage known as corrosion. Using corrosion resistant though expensive materials can prevent such damages. Damage



Fig. 8.8 Sampling of hydrothermal water for chemical analysis at the wellhead of Soultz-sous-Forêts (near Strasbourg, France). The 163 °C hot fluid is cooled under pressure by means of SC20 sample coolers from Spirax Sarco. The deep fluid then passes a flow through cell. Here a transparent cell with a fluid inlet and outlet and four inserted electrodes and sensors measuring temperature, pH, ORP, and conductivity (courtesy of GEIE EMC, photo Julia Scheiber)

analysis of failed submersible pumps showed various, partly massive corrosion related failures partly in combination with scales.

Chemical fluid-rock reactions also will take place in the reservoir aquifer itself. The cooled fluid enters the aquifer from the injection well and its altered saturation status may cause minerals to precipitate in the pore space and so reduce the permeability of the reservoir. Added chemicals such as inhibitors and inorganic acids may, on the other hand, also cause dissolution of minerals in the aquifer thus producing secondary porosity and improve permeability. Dissolution may also occur for some minerals that have a high solubility in the cooled fluid. Some hydrothermal

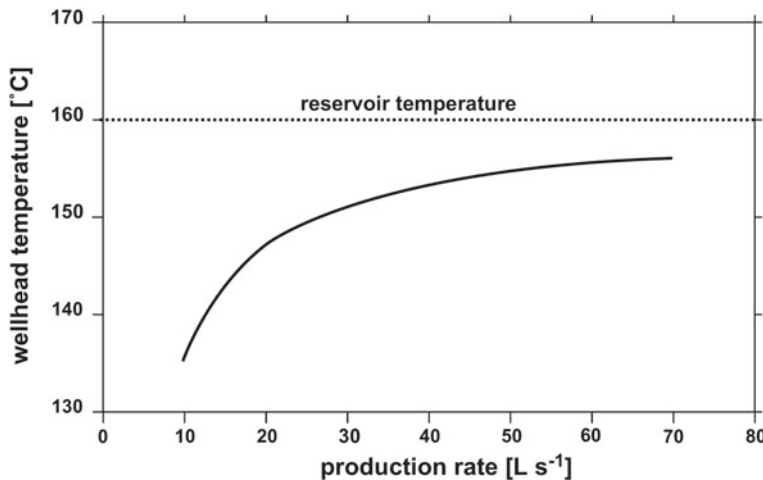


Fig. 8.9 Temperature of produced fluid versus production rate. Models for a 4000 m deep well of 7" Ø (Ramey 1962)



Fig. 8.10 Carbonate (calcite) scales in a pipe caused by pressure loss and degassing

systems are also impaired by microbial corrosion and alteration so that biogeochemical processes must be considered and adequate bio-remediation strategies must be developed (Amann et al. 1997; Dingh et al. 2004).

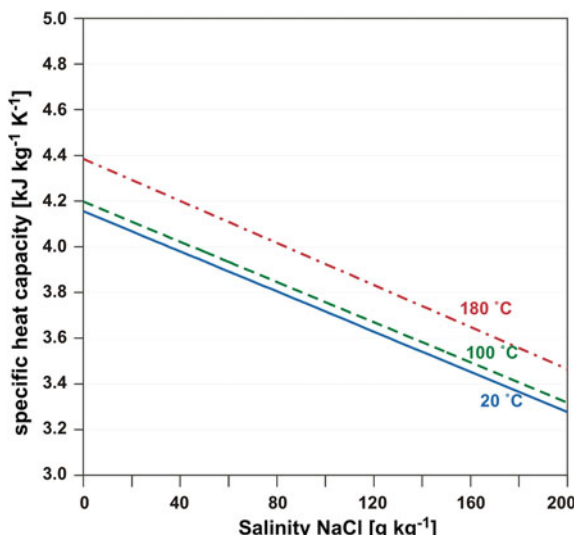
In any case, each reservoir system is chemically unique and its chemical peculiarities must be carefully evaluated and analyzed. Some parameters are transient and thus must be measured on site meaning at the wellhead (Fig. 8.8). These parameters include temperature, pH, oxidation-reduction potential (ORP) and electrical conductivity (EC). From the EC the total of dissolved solids (TDS) can be estimated. But also alkalinity titrations should be made on site.

The hydrochemical properties of the hot fluid also influence the heat content of the fluid. The heat content depends on density and specific heat capacity of the fluid. Depending on $P-T$ and fluid composition the heat content of highly mineralized water can be higher or also smaller than that of fresh water (Eq. 8.6; Fig. 8.2). Density of water increases, but the heat capacity decreases with increasing salinity (Fig. 8.11). Consequently the thermal performance decreases with increasing temperature in high TDS fluids compared to fresh water.

Hydrochemical analyses and microbiological examinations, also analysis of dissolved gasses should be made in the exploration phase and then in regular intervals during operation of the system. It is important to recognize changes in reservoir conditions as early as possible. The chemical-microbiological monitoring should be accompanied by a hydraulic monitoring that measures production rate, temperature and drawdown. The reaction of the reservoir on continuous system operation must be utterly documented. Purposeful reaction on changes in the reservoir is only possible if these data have been collected (Fig. 8.8).

In recent times it has been suggested that the extraction of strategically and economically attractive metals such as lithium (Li) from the produced hydrothermal fluid could potentially be a profitable business supporting the economy of the geothermal power plant. It has been proposed that the extraction of rare and valuable elements from a large fluid flow between production and injection well could be

Fig. 8.11 Specific heat capacity of water versus NaCl-concentration (Sun et al. 2008)



carried out with galvanic separation or selective adsorption methods (Friedrich et al. 2018). However, no pilot installation exists today and the feasibility of the procedure remains to be proven (2020). Of course it will be a major challenge to profitably extract 1 ton battery grade $\text{LiOH} \cdot \text{H}_2\text{O}$ worth 52,000 Yuan (7345 US\$ May 2020) from 5.7×10^5 L of thermal water (using the unusually high Li concentration of thermal water in the basement of the Upper Rhine Graben).

8.5 Reservoir-Improving Measures, Efficiency-Boosting Measures, Stimulation

Ideal sites for hydrothermal systems are deep aquifers with high hydraulic conductivity and high temperature, in contrast to petrothermal systems (EGS systems) where only temperature matters. If the first drilled well of a project does not open, against prediction and expectation, an aquifer with the required hydraulic conductivity for profitable circulation of hot fluid then several possible measures may keep the project within the moneymaking range.

The well can be deepened and additional and deeper aquifers may be accessed that produce fluid at a higher temperature. However, there must be some reliable evidence for success to justify the additional investments. The wells of most hydrothermal doublets are drilled as inclined boreholes resulting in increased contact with the target aquifer and an improved water extraction rate compared with vertical boreholes through a horizontally stratified geology. Inclined boreholes increase the chance of drilling through permeable fault and fracture zones. These often steeply dipping structures may function as water conducting channels and much of the water produced from a hydrothermal well can be contributed by high-permeability faults. However, keep in mind that many fault zones have a lower hydraulic conductivity than the rock matrix and are essentially watertight and form hydraulic barriers (Sect. 8.1; Stober et al. 1999).

If the optimal reservoir aquifer has been drilled and its key properties, hydraulic conductivity and temperature, are promising then drilled sidetracks from the wellbore into the target aquifer further increase the yield of the well.

The key parameter for economic success of a hydrothermal project is, in addition to reservoir temperature, the yield of the production well. The yield is the production rate per drawdown that is economically and technically tolerable. Open fractures and connected fracture networks control the hydraulic conductivity and thus the yield in hard-rock aquifers. If the drilled aquifer has a lower than expected hydraulic conductivity, the situation can, to a certain degree, be rescued by specific stimulation measures aimed at improving the hydraulic conductivity of the aquifer.

The classic and prime conductivity improving measure is pumping water to the aquifer under high pressure with the hope to extend existing fractures and so increasing the conductivity of the aquifer. This method is known under

various names including aquifer stimulation, conductivity-boosting methods and reservoir-improving measures.

However, reservoir improvement is first attempted by mildly increasing hydraulic pressures in the injection well in order to clean fractures and cavities from conductivity-reducing fine-grained material. Rapidly changing delivery heads may help to cleanse the aquifer rock around the production well. Both techniques are commonly used in near-surface hydrogeology. These are standard methods for obtaining sand-free wells and improving well yield.

Rock matrix treatment with acids is also a common standard method in well engineering for drinking, mineral and thermal water wells. It proved to be particularly successful in carbonate rock aquifers and carbonate deposits on fractures. Acidizing techniques are also routinely used in the oil industry. The reaction of acids with calcite of the carbonate rock matrix or calcite on fractures produces CO₂ gas. Acidizing is also used for wells in silicate rock aquifers such as clay-rich sandstones for example. Commonly used acids include hydrochloric acid (typically 15%), diluted formic acid, acetic acid, mixtures of HCl and HF and many others (Portier et al. 2007). Hydrofluoric acid (HF) in mixtures with HCl is used for dissolving silicate rocks. Its handling at the drilling site requires extreme safety precautions because direct contact with HF is fatal. If the aquifer rocks contain abundant swelling clay minerals the clays such as smectite the acid activation makes them swell thereby clogging the flow porosity rather than improving it. However, Portier et al. (2007) found in a study of U.S. oil wells that acid stimulation improved the productivity in 90% of the stimulated wells by a factor of 2–4.

The penetration depth of the acid into the rock matrix of the near wellbore depends on the pumping pressure and ranges from a few cm to dm at very low pressure to increasingly greater infiltration radius at higher pressure (usually up to 30 bar). The conductivity-improving effect of pressure acidizing also depends on the amount, concentration and type of acid. Type, intensity and degree of acidizing are adjusted to the type of casing and the well design, which must be efficiently protected from corrosion.

Flushing water conducting structures of the aquifer and increasing their permeability is the sole purpose of increased pumping pressures in combination with acids. The reservoir-improving measures in hydrothermal projects never aim at creating a new fracture network, in contrast to petrothermal systems (EGS). These methods try to establish an improved hydraulic connection from the wellbore to the existing fracture or karst aquifer.

Further aquifer stimulation measures such as massive hydraulic stimulation are not performed in developing hydrothermal systems. These brute force methods need to be applied in developing petrothermal EGS systems (Enhanced Geothermal Systems) for creating the underground heat exchanger (Sect. 9.4).

Massive hydraulic stimulation is routinely carried out by the oil and gas industry for improving the productivity and yield of wells in sedimentary rocks. Typically large amounts of water are injected under high pressure with the goal to expand existing water conducting features primarily fractures. Quartz sand or other proppants are

added to the injection water with the purpose of keeping the expanded fractures open (Liang et al. 2016).

8.6 Productivity Risk, Exploration Risk, Economic Efficiency

The economic success of a hydrothermal installation depends critically on the geological conditions at great depth (hundreds or thousands of meters underground). Project development rests on data and knowledge from old, often distant boreholes in the area and on data from geophysical exploration tools such as 2D and 3D seismic imaging. The pre-drilling exploration, however, does not provide reliable information on the crucial parameters, temperature, yield and injectivity that determine the future economic success of the hydrothermal project. Therefore, drilling the first borehole for a hydrothermal doublet system is always afflicted with some risk of opening unsuitable ground. The risk of drilling a very expensive borehole into a target horizon that is colder, less permeable and thinner than predicted from the exploration data is inherent in hydrothermal system development. The geological risks associated with hydrothermal projects greatly exceed that of near surface systems. The same geological exploration risks are also known in the oil and gas industry. However, the value of the produced product (oil versus hot water) and the associated rate of return are very different in the two industries and consequently also the economic risk associated with unsuccessful drilling. The geological risk can and must be reduced by an extensive exploration program and a careful, competent and rigorous analysis of the exploration data.

The pre-drilling exploration report is also used as a basis for obtaining exploration risk insurance. Various formats of risk insurances have become increasingly popular in the last years. The insurances may cover different aspects of the total risk associated with the development of a hydrothermal system. The economic overall risk is usually divided into risk groups (geological, exploration, productivity, drilling and so on). The risk groups are analyzed and evaluated separately and contracts are offered for the separate groups as insurance.

Insurance companies generally distinguish five different risk groups: Exploration risk, geological and geotechnical risks, economic risks, environmental and political risks. The individual risk groups cannot always be clearly separated.

Exploration risk: The main risk of hydrothermal projects is the exploration risk. It is the risk of drilling one or several boreholes into a hydrothermal aquifer of insufficient thermal productivity and inappropriate fluid composition.

Thermal power P ($J\ s^{-1} = W$) of a geothermal well is proportional to the production rate (Q) and the temperature (ΔT) and defined by Eq. 8.6:

$$P = \rho_F c_F Q(T_i - T_o) \quad (8.6)$$

where ρ_F denotes the density [kg m^{-3}] and c_F the specific heat capacity [$\text{J kg}^{-1} \text{K}^{-1}$] of the fluid, Q the production rate [$\text{m}^3 \text{s}^{-1}$], T_i the production temperature [K] and T_o the injection temperature [K]. The thermal power P of a typical hydrothermal doublet in e.g. the Molasse basin (near Munich, Germany) producing low-TDS water at a rate of $Q \sim 100 \text{ L s}^{-1}$ [$0.1 \text{ m}^3 \text{s}^{-1}$] is about 30 MW given by $\rho_F \sim 990 \text{ kg m}^{-3}$ and $c_F \sim 4300 \text{ J kg}^{-1} \text{ K}^{-1}$ (Fig. 8.11) and a temperature difference $\Delta T \sim 70 \text{ K}$ between production and injection temperature, respectively. P may increase to 40 MW if the production rate can be enlarged to 130 L s^{-1} or if ΔT can be expanded to 90 K. In contrast, the thermal power P of a plant producing a fluid at $120 \text{ }^\circ\text{C}$ with a TDS of about 100 g L^{-1} declines to 27 MW at the same Q and ΔT as a result of the decreasing specific heat capacity of high-TDS fluids ($c_F \sim 3.8 \text{ kJ kg}^{-1} \text{ K}^{-1}$ Fig. 8.11). The density ρ_F of the saline fluid at $120 \text{ }^\circ\text{C}$ on the boiling curve is near 1010 kg m^{-3} . Consequently the total mineralization (TDS) or salinity of the hydrothermal fluid has a significant effect on the thermal power. An increasing amount of dissolved solids reduces the thermal power considerably. This salinity effect increases with increasing temperature. Although the density of the fluid increases with salinity, this positive effect is overcompensated by the reduced specific heat capacity (Fig. 8.11).

Furthermore, it follows from Eq. 8.6 that the production rate Q and the related hydraulic conductivity k_f of the hydrothermal reservoir are the key parameters controlling the power output of the hydrothermal doublet. This is because ρ_F and c_F vary within restricted ranges and the maximum for $\Delta T = (T_i - T_o)$ is about $80 \text{ }^\circ\text{C}$, which can be achieved by a deeper well if necessary and permitted by the geometry of the aquifer. Consequently, if only 50 L s^{-1} can be pumped from the well instead of 100 L s^{-1} the thermal power P declines from 30 to 15 MW in the Molasse basin example above.

The exploration risk also relates to an unfavorable and damaging composition of the hydrothermal fluid. Dissolved solids or gasses may rule out a geothermal utilization or may make it difficult and cost-prohibitive. The fluid may be highly corrosive because of high salinity and high content of hydrogen sulfide. The fluid may precipitate radioactive or highly toxic scales. So far most hydrothermal wells produced fluids that were chemically controllable although at various levels of extra costs.

Accordingly a hydrothermal well is commercially viable if the hot water yield exceeds the project defined lower limit of the production rate Q_{\min} at the upper limit of drawdown Δs_{\max} and if the produced fluid has a temperature higher than that of the project defined lower T_{\min} limit. The project specific values of Q_{\min} , Δs_{\max} and T_{\min} are linked to economic considerations of the operator (Stober et al. 2009). The envisioned products of the hydrothermal system have a controlling effect on the parameter values. If the system should produce electrical power then T_{\min} is about $120 \text{ }^\circ\text{C}$ and production rate Q should be higher than 50 kg s^{-1} (limits in the year 2020). General site-independent geological and technical conditions set an upper limit of $\sim 200 \text{ }^\circ\text{C}$ to the production temperature T_i and about in Eq. 8.6. Likewise, the maximum production Q of hot water from a deep aquifer by a single well is about 150 kg s^{-1} . From these limits it follows that the maximum geothermal power for a hydrothermal doublet system is about $P \sim 50 \text{ MW}_{\text{th}}$.

The thermal energy E [J] extracted from a hydrothermal well can be computed from the thermal power P [W] of the system and the time of operation Δt [s] (Eq. 8.7):

$$E = P \Delta t \quad (8.7)$$

During the working life of the hydrothermal plant the crucial parameters production rate Q and temperature of the produced fluid T_i should not decrease noticeably. Precondition for this is a hydrothermal reservoir of a sufficiently large extent. Important is also to exclude impairment by other hydrothermal plants in the surrounding area.

Hydrothermal power plants require very large fluid mass fluxes Q for successful operation. Production rates Q exceed those common in the oil industry by many times. A production rate of 3 kg s^{-1} is considered an excellent oil well. Hydrothermal reservoirs and the production techniques must satisfy much higher requirements (Sect. 12) than in the hydrocarbon industry. Reservoir properties of a specific geologic unit that is interesting for the oil and gas industry may prove unsuitable for hydrothermal power systems.

The hydraulic conductivity of hard rock aquifers and the related yield of a hydrothermal well are controlled by the amount and shape of interconnected open fractures and other water conducting features of the rock matrix and the hydraulic properties of local fracture and fault zones. Hard rock aquifers can be categorized according to their predominant type of pore space into fractured aquifers and karst aquifers (Figs. 8.12 and 8.13).

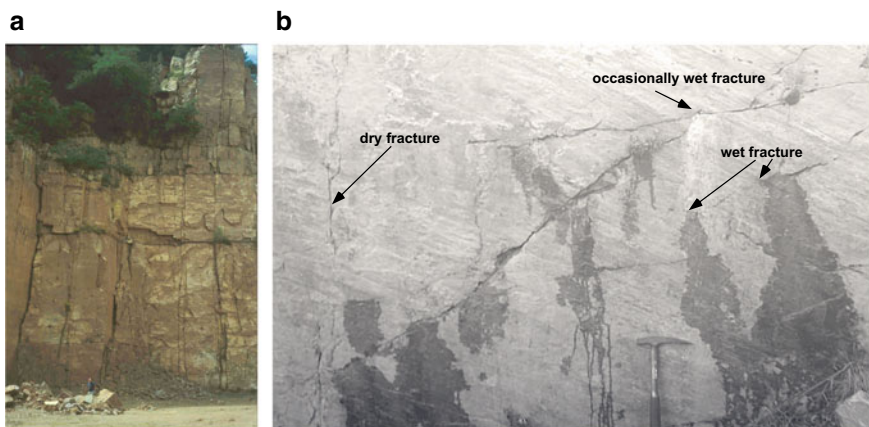


Fig. 8.12 Surface outcrops of typical fracture-dominated sandstone and quartzite aquifers. **a** Lower Triassic Buntsandstein unit in the Voeglinshofen quarry (Alsace, France). **b** Vendian quartzite with dry fractures, wet fractures and mineral-stained occasionally active water conducting fractures near Lom (Norwegian Caledonides) showing that water conduction depends on detailed fracture properties

Fig. 8.13 Example of a water producing karst channel underground in middle Triassic limestone (Muschelkalk) at Talmühle spring near Horb, SW-Germany



If the tested hydraulic conductivity of the aquifer in the first drilled wellbore is lower than expected and predicted by pre-drilling exploration stimulation measures need to be carried out to improve aquifer properties (Sect. 8.5). Specific possible actions include acidizing carbonate aquifers (limestone) and hydraulic stimulation, hydraulic fracturing in combination with acidizing techniques. Horizontally drilled sidetracks in the target aquifer may further improve yield (this is common practice in the oil industry).

Conditions for economic success or successful reservoir discovery (strike) are defined at project start by the investor or developer. The anticipated return defines the minimum value for the achievable production rate and the minimum temperature of the produced fluid to make the project an economic success. A hydrothermal well is successful if the parameter limits are achieved or topped.

A partially successful well failed to meet the criteria for strike, however utilization with a revised concept is technically feasible and, financed by the insurance benefit, economically viable.

The exploration risk may not be easily insured in regions of the world where limited or no experience with similar hydrothermal projects exist. Insuring projects that employ new technologies with experimental character or for research purposes such as EGS/HDR projects (Chap. 9) may not be insured at all.

Efficiency and work life of a hydrothermal system depends mainly on the hydraulic, thermal and chemical properties of the aquifer and the stored hot water.

These properties need to be explored and investigated best possible and the results, testing methods, and investigation tools should be carefully documented. The operator and investor are making the final decision on the economic efficiency of a hydrothermal plant based on business indicators. The consumer structure of the power consumers is central in the decision making process.

The exploration risk is the controlling factor of all the economic uncertainties. The first successfully drilled and thoroughly tested well greatly reduces the exploration risk of the project. Still, the second well to be drilled, usually the injection well, must be able to take up the produced hot water for a trouble-free hydrothermal fluid circulation (Sect. 8.2). The development costs (drilling, stimulation, hydraulic and other well tests) stand for about 50–70% of the total costs of a hydrothermal doublet project (exploration, surface installations, and plant being the other costs). Careful project development, a clearly defined agenda of project development phases, milestone scheduling and strict and rigorous termination criteria minimize the economic risk.

Regions with unusually high thermal gradients (thermal anomalies) are potentially attractive and may save investment costs because of short drilling depths. However, high temperature at shallow depth is only beneficial if achievable production and reinjection rates are also sufficiently high for profitable operation of the plant.

Regions with normal thermal gradients produce relatively low temperature fluids even from very deep drill holes (>4000 m). These low-enthalpy hydrothermal systems supply mostly energy for the heat market. For profitable operation of a hydrothermal doublet heating system it is necessary for the system to continuously provide heat for local and district heating networks all year around. The successful project provides heat at different temperature levels to a range of different heat clients. The produced thermal energy is distributed following a **cascade principle**. An example system shall produce hot water of 90 °C. The district heating system of the first user extracts heat and cools the water to 60 °C, which is then used by the second customer to warm a group of greenhouses. The water leaves the second customer with 30 °C and is used for fish farming by a third consumer (Fig. 8.14). The water from the fish farm with a temperature below 30 °C is re-injected into the subsurface reservoir by the hydrothermal doublet system. The uses of thermal energy are not limited to the examples described but further innovative concepts; designs and ideas for heat use wait to be developed by the ingenious entrepreneur. The produced heat can also be used for cooling.

Electricity can be commercially produced from fluids with more than 120 °C using an appropriate technology. The efficiency of electrical power production increases with temperature. However, low-enthalpy hydrothermal doublet systems draw fluid from aquifers with typical reservoir temperatures rarely exceeding 150–170 °C. Very important for the economic success of a system producing electrical power is the profitable marketing of the thermal energy leaving the electrical power plant (residual heat ~90 °C). This “waste heat” must be sold and customers must be integrated into the project development. Similar considerations also apply to EGS and HDR systems (Chap. 9).

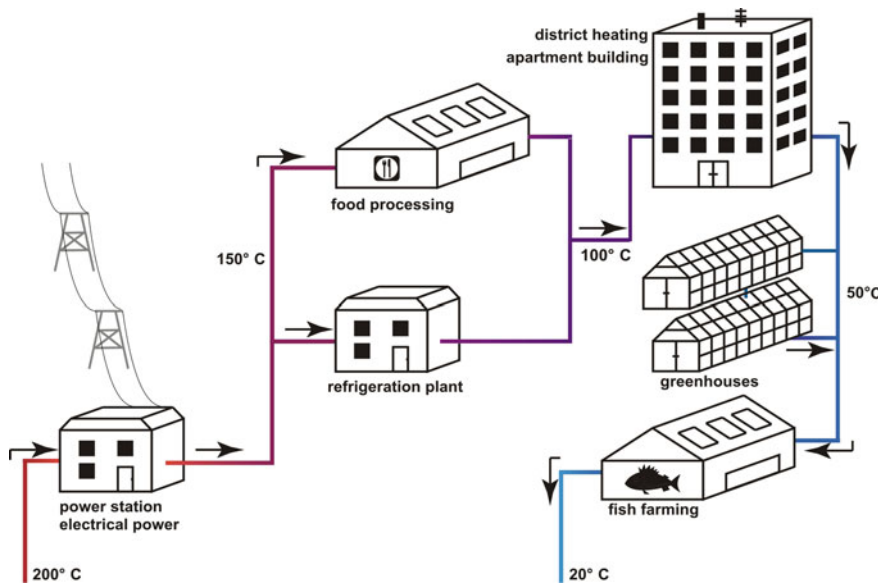


Fig. 8.14 Serial use of thermal energy produced by a hydrothermal doublet system. Cascade system (after Dickson and Fanelli 2004)

Geological and geotechnical risks refer to the general method-inherent uncertainty of geological predictions. The anticipated existence of geological structures and underground strata deduced during the pre-drilling exploration phase from geophysical data is prone to intrinsic fuzziness. Geological risks during drilling include the occurrence of unexpected geological strata, unpredicted pressure conditions or large amounts of fluids with potential erosion and collapse of the wellbore. Inadequately handled unexpected geological features usually also cause geotechnical and drilling technical problems.

Drilling risks are related to all technical problems linked to the drilling rig, drilling tools, and the drilling process. Drilling problems include lost tools, damaged casings, defective cementation, pipe sticking, hole deviation, pipe failures, mud contamination, borehole instability, blowout and more (Sect. 12). These drilling problems almost always cause a significant delay in drilling operations. Technical drilling problems may, in the worst case, cause the loss of the wellbore and of all investments up to that day. Drilling risks are borne by the drilling contractor. Drilling risks can be covered by insurances.

Operational risks are related to the power plant technology, the surface installed technical equipment and the plant operation. The operational risk related to the power plant technology can be insured. However, the operational risk related to the hydrothermal reservoir, specifically the constant temperature and production rate during the lifecycle of the system cannot be insured and must be borne by the

operator. All variations in temperature and production rate but also in the chemical composition of the fluid during the operation of the hydrothermal doublet are operator risks. This includes all alterations of technical installations that may be caused directly or obliquely by fluctuations in fluid properties. Also part of the operational risk is the changing energy market that causes uncertainties in price trends for electrical and thermal energy over the operation period of 30 years. Planning and developing the project can minimize some of these risks by inserting conservative economic parameters, limiting production rates and distances of the doublet wells in the reservoir.

Environmental risks: Hydrothermal systems can be afflicted by a risk to the environment in analogy to the near surface geothermal energy utilization also. Hydrothermal doublets can be hazardous to groundwater resources and to soil. Large projects and massive invasions to the deep underground require appropriate preventive measures and security precautions to minimize hazards. Drilling deep to ultra deep wells requires a mining law approval process in many countries, which also considers the interests of neighbors and local residents. Environmental consequences of and environmental risks associated with geothermal energy installations in general will be discussed in Sects. 11.2 and 11.3.

Induced seismicity: Reservoir stimulation measures may potentially induce seismic events particularly in areas with natural seismicity. Seismicity can be triggered also in hydrothermal plants during operation. The intensity of the trembling is usually small but in some reported cases strong enough to be felt at the surface. The occurrence of stimulation induced seismicity depends on the geological structure of the ground and the type of rocks present, on existing active tectonic stresses, level of applied injection pressures, magnitude and timeline of injection flow rate during stimulation and the structure and volume of the stimulated fracture system. A monitoring program that measures vibration velocities should therefore accompany deep drilling for geothermal systems. Vibration velocity data characterize the seismic energy of an induced seismic event that reaches the surface. Magnitude data used for characterizing seismic energy released at the site of a natural seismic event are not appropriate for assessing stimulation-induced seismicity in geothermal projects. The occurrence of induced seismicity can, to a certain point, be predicted from numerical models, evaluated and partially controlled. The keys to seismicity control are continuous measurement and monitoring of the injection pressure and a seismic monitoring program specifically designed for the specific hydrothermal project that measures vibration velocities in the near and far surroundings of the plant site. If the data indicate a growing risk for intolerable seismicity injection pressure and pumping rate must be reduced (Sect. 11.1).

Political risks: The utilization of low-enthalpy hydrothermal systems for electrical power production and thermal energy uses also depends on governmental subsidies in most countries, which represent a political risk that needs to be considered in project planning. Subsidies comprise for example direct public contributions to the price of electrical energy that is collected from all consumers of electrical energy, direct grants to specific projects, support for research and development, grants for experimental sites and many more. However, at present the majority of the

general public and politics favor supporting the expanding use of non-fossil energy in many countries (“renewable energy”, “renewables”). Political support for geothermal energy utilization adjusts to arising new technologies, to the evolving global energy market, to the national unemployment situation and other macroeconomic factors and their long-term variations. Low-enthalpy hydrothermal energy utilization is a relatively young player in the global energy market. Substantial progress in improving hydrothermal systems will make the technology more cost competitive in the future. In contrast, production of electricity and heat from fossil resources (coal, oil, gas and others) will inevitably experience long-term cost increases caused by dwindling resources and environmental regulations. The enduring trends on the energy market make geothermal energy more competitive and finally independent on subsidies in the long run.

8.7 Some Site Examples of Hydrothermal Systems

In the following we present some site examples of low-enthalpy hydrothermal power plants based on hot water extraction from deep aquifers and heat storage systems in aquifers. Typical reservoir temperatures of the utilized aquifers are below about 150 °C and few systems produce electrical power today. However, the existing systems supply local communities with reliable base load electricity. The experience collected during development and operation of the systems and the reported troubles that needed to be mastered can be valuable for developing hydrothermal systems elsewhere.

Paris Basin (N France): The first hydrothermal doublets for heating residential buildings in the Paris Basin have been installed near Melun l’Almont south of Paris in the late 1960ies (Ungemach 2001; Ungemach et al. 2005). Subsequently, many more wells were drilled as a result of sharply rising oil prices in the period 1980 to 1987. Of the total of 63 deep wells only two were complete failures and five wells were only partially successful. Today (2019), 37 hydrothermal doublet systems commercially produce thermal energy in the Paris basin. The produced thermal energy is used for direct house heating and hot water supply. The geothermal energy is transferred to secondary loops using heat exchangers and reaches the end-user through separate distribution networks. Since the end of 2010 the airport Paris-Orly uses the thermal energy produced by a geothermal doublet. It supplies about 1/3 of the total heating demand of the airport.

The first doublets have been drilled as vertical wells from two drilling sites; later inclined wellbores have been drilled from one site, today many doublets are installed using horizontal boreholes into the aquifers. From the beginning, numerical models optimized the management of the geothermal plants and helped avoiding unwanted interferences with neighboring systems and maximized the life cycle of the installations (Sauty et al. 1980; Antics et al. 2005). Most geothermal systems are designed as hydrothermal doublets, which assure sustainability by recycling the produced highly mineralized water into the reservoir. Some newer installations also

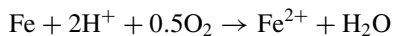
use 3 well systems. Since 2009 a resources management model for the Paris Basin optimizes the geothermal energy utilization with a focus particularly on mapping the cooling plumes.

The Paris Basin is a large concentric geological structure in northern France of several hundred km in diameter. The basin developed after the Triassic by central subsidence of the Paleozoic basement. The basin contains a complete stratigraphic succession from the Permian through the Mesozoic to the Tertiary. Tertiary strata are exposed in the center of the basin structure in the region of Paris. Thermal energy is extracted by hydrothermal doublet systems from several different thermal aquifers. The utilized aquifers are of lower Cretaceous, upper Jurassic, middle Jurassic and Triassic in age. Most of the wells are about 1700 m deep. The production rates range from 25 to 75 L s⁻¹. The temperature of the hot water varies between 58 and 83 °C. The waters are highly mineralized and contain 10–40 g L⁻¹ dissolved solids predominantly NaCl with a pH ~ 6. The hot water also contains appreciable amounts of dissolved CO₂ and H₂S gas. The waters comprise sulphate from evaporite leaching. Sulphate reducing bacteria produce hydrogen sulfide (H₂S) from sulphate, which caused severe corrosion and scales in the system components including the casing in the first systems installed. Sulfide scales form from the following (net) processes:

1. Sulphate to sulfide reduction



2. Pipe steel corrosion



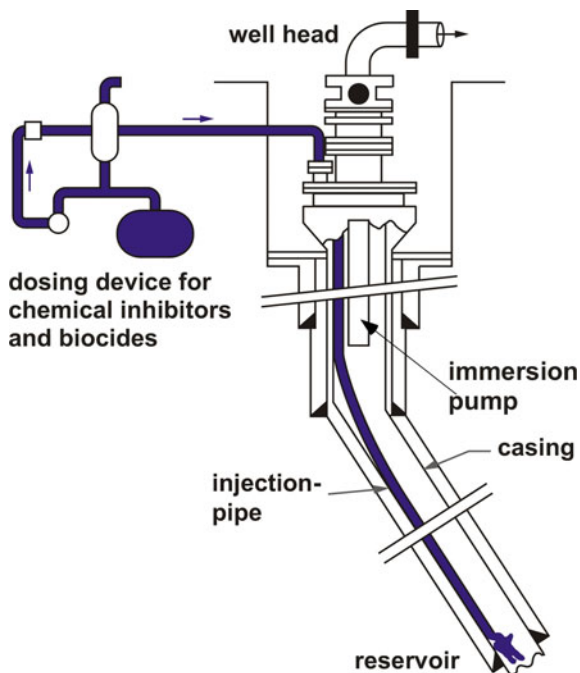
3. Pyrrhotite scale formation from the products of reaction 1 and 2:



Today, the entire doublet systems, production and injection well and the surface installations are routinely corrosion protected by injecting special inhibitors at bottom hole of the production well (Fig. 8.15). Some of the wells have been fitted with a corrosion protecting centered fiberglass liner in the grouted casing. Already in 1971 plate heat exchangers have been built using titanium alloys for corrosion protection. Tailored workover procedures rehabilitate geothermal well damages in the Paris Basin (Ungemach and Turon 1988).

Aquitanian Basin (SW France): Geothermal energy is utilized from a system of 18 single wells not from doublets. Three different aquifers of middle Eocene, upper Cretaceous and middle Jurassic (Dogger) age supply the thermal energy. Further geothermal heating installations in France using deep aquifers operate in the regions Languedoc, Lorraine, Bresse and Limagne.

Fig. 8.15 Schematic drawing of a production well in the Paris Basin showing the down hole injection tubing for injecting corrosion preventing inhibitor chemicals at bottom hole (redrawn from BRGM, France)



Upper Rhine Rift Valley (Germany, France, Switzerland):

Bruchsal Research Site (Germany): In the early 1980s two deep wells have been drilled in the city of Bruchsal (20 km N of Karlsruhe, Germany) with the purpose to produce geothermal energy. The system was not completed before 2008 because of various economic problems and is running with fairly small power output. Nevertheless, many important technical and other lessons have been learned from the Bruchsal site, which has been a research and test site rather than a commercial power plant.

The site is located in the N-S trending Tertiary (Oligocene) Rhine rift valley near the eastern main boundary fault (about at km 26 on Fig. 8.1). The main boundary fault is a major fault zone with a series of listric normal faults with westward dipping fault surfaces. The sedimentary cover sequence of the Variscan basement is downfaulted in the graben interior and several geological units with aquifer properties are present at sufficiently large depth to host thermal water with a great potential for geothermal applications. In addition, the local geothermal gradient is about 50 °C/km and thus significantly higher than the average gradient in central Europe of 33 °C/km.

The two vertical wells, 1874 and 2542 m deep, access the thermal water of the Buntsandstein reservoir, a lower Triassic sandstone. The yield of both wells is nearly identical. The transmissivity of the aquifer is $T = 3.6 \times 10^{-5} \text{ m}^2 \text{ s}^{-1}$ (Bertleff et al. 1988). The horizontal distance between the wells is 1.4 km and the wells are connected with an insulated thermal water pipeline. Highly saline thermal water is produced from the deeper well. It has a bottom hole temperature of 134 °C. The produced water is re-injected into the shallower wellbore after heat extraction. The

pumping rate is at modest 24 l s^{-1} (2012) limited by the capacity of the present pump (Fig. 4.11). Higher rates seem possible but have not been tested. Several earlier pumps with similar capacities broke down due to technical failures unrelated to the specifics of the Bruchsal site.

Water samples have regularly been chemically analyzed from the Bruchsal wells over a period of nearly 30 years. The chemical composition of the highly mineralized and CO_2 rich thermal water is remarkably constant. The main components are Na^+ and Cl^- (Table 8.1). The total of dissolved solids is 127 g L^{-1} . The water is effectively a mixture of in 1.6 mol L^{-1} NaCl , 0.3 mol L^{-1} CaCl_2 and 0.1 mol L^{-1} . Carbonate alkalinity is very low. However, the pressure decrease during production causes the thermal water to become oversaturated with respect to calcite. In order to prevent carbonate scales the system is kept under 22 bar pressure in surface installations. The high content of dissolved CO_2 gas requires a special gas separator (Fig. 8.16) that removes a large part of the CO_2 before the thermal water enters the power plant. The gas is re-dissolved in the water leaving the heat exchanger with $60\text{ }^\circ\text{C}$.

The conversion of the thermal energy from the produced thermal water into electrical power is accomplished by a binary loop Kalina plant using a mixture of water—ammonia as a heat transfer fluid. The thermal energy of the hot water is transferred to the working fluid of the secondary loop by plate heat exchangers. The plant is cooled by a wet cooling tower (Fig. 4.9). The wet cooling procedure atomizes the water to be cooled in the air and trickled over the tower packing. The water loses heat of evaporation to the air. Droplet separators compensate for the water losses. The thermal power of the system is about 7 MW_{th} . The electrical power of the plant is $550\text{ kW}_{\text{el}}$. Given an annual operating time of around 8000 h, the research and development plant produces about 4400 MWh electrical energy.

Rittershoffen (Alsace, France): The geothermal power plant at Rittershoffen about 40 km NE of Strasbourg is also based on a hydrothermal doublet. The Rittershoffen plant provides the starch plant Roquette at Beinheim (Alsace) 15 km east of Rittershoffen with thermal energy for steam production and for dryers.

Table 8.1 Chemical composition of water from the Bruchsal well GB2. $\text{pH} = 5.0$ at $134\text{ }^\circ\text{C}$

Component	Concentration (mg L^{-1})
Ca	7140
Mg	324
Na	37,400
K	3440
Fe	47
Mn	23
Cl	75,200
HCO_3	350
SO_4	586
SiO_2	83
CO_2 gas	~ 2000

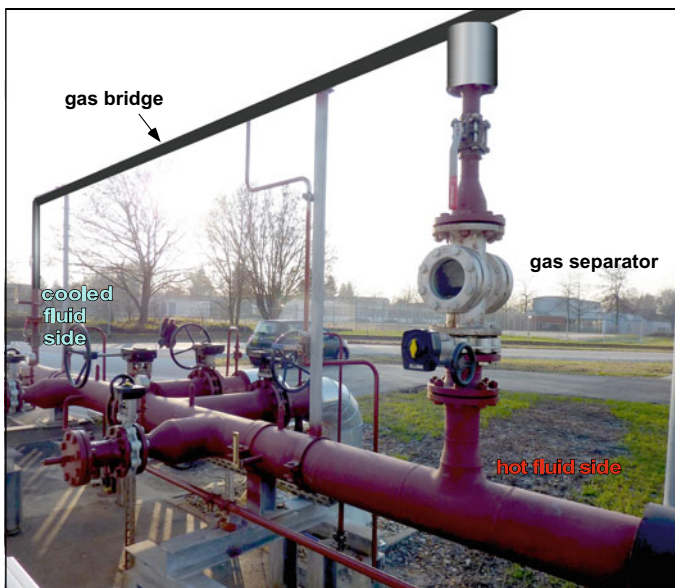


Fig. 8.16 CO₂ gas separator (gas bridge) for separation of excess dissolved CO₂ from the thermal water before entering the heat exchanger of the Kalina plant at the Bruchsal geothermal site (hot fluid side). The collected CO₂ gas is re-dissolved into the cooled water leaving the plant (cooled fluid side)

The geothermal doublet at Rittershoffen extracts the thermal energy from two aquifers, the lower Triassic Buntsandstein formation and the uppermost Variscan crystalline basement, which consists here of strongly altered and fractured granite. The aquifers are hydraulically connected by a highly permeable fault zone.

The first well GRT-1 has been drilled in 2012. It is a 2580 m deep vertical drillhole used as injection well. The production well GRT-2 is a 2708 m deep inclined borehole of 3196 m length. Both wells reach the granite in the same massive N-S trending Rittershoffen fault zone (dip W 45°). Both open holes have been drilled with $\varnothing = 8\frac{1}{2}''$. The open hole in GRT-1 measures 658 m and in GRT-2 1076 m (Vidal et al. 2017; Baujard et al. 2017). The temperature of the hydrothermal water is 177 °C at bottom hole of GRT-2 (163 °C in GRT-1). The deep water contains about 100 g kg⁻¹ dissolved solids, predominantly NaCl and CaCl₂ and is rich in dissolved CO₂ gas.

The thermal water reservoir required chemical and hydraulic stimulation. The development of the reservoir avoided perceptible seismicity of magnitude M_L > 1.7 (see Sect. 11.1). An elaborate large network of seismic monitoring stations precisely localized the micro seismic reaction of the reservoir and made a timely correction of the stimulation measures possible if necessary. The data collected by the monitoring system also served as preservation of evidence in potential conflict situations.

The chemical stimulation measures using GRT-1 as an example were carried out in packer-separated sections. During the subsequent hydraulic stimulation water was

injected with stepwise increasing injection rate in 8 steps with the final maximum flow rate reaching 80 L s^{-1} . The pressure release has also taken place in steps, avoiding the classical shut-in with the intention to prevent seismic aftershocks. The considerate procedure kept all seismicity below the critical value of $M_L = 1.7$ despite increased magnitude of the seismic activity during the decompression phase. The stimulation efforts resulted in an increase of the productivity index PI in GRT-1 by a factor of 5. It reached $\text{PI} = 25 \text{ L s}^{-1} \text{ MPa}^{-1}$ for the nominal value $Q = 70 \text{ L s}^{-1}$. PI of GRT-2 was slightly higher than PI of GRT-1. The hydraulic analysis of the stimulation measures showed that the aperture of existing fractures close to the wellbore increased and that no new fractures were created (see also Sect. 9.3). After completion of stimulation a circulation test of three weeks duration and a pumping rate of 28 L s^{-1} examined the hydraulic properties of the doublet. Two tracer tests resulted in a tracer breakthrough after 14 days demonstrating that the two wells are hydraulically connected (Sanjuan et al. 2016).

Commissioning of the geothermal plant was in 2016 with a thermal power of 24 MW_{th}. The highly mineralized water is produced by a line shaft pump at a rate of $70\text{--}75 \text{ kg s}^{-1}$. It reaches the wellhead with 168°C and flows through a series of 12 plate heat exchangers before it is returned to the aquifer by GRT-1 without a pump. The temperature of the water at the wellhead of GRT-1 is 70°C (Mouchot et al. 2018; Boissavy et al. 2019). Using $(T_i - T_o) = \Delta T = 98^\circ\text{C}$, $Q = 70\text{--}75 \text{ kg s}^{-1}$ and the proper values of ρ_F and c_F for mineralized water a computed thermal power $P \sim 24\text{--}26 \text{ MW}_\text{th}$ follows from Eq. 8.6 in agreement with the reported thermal capacity of the plant. An appropriate chemical inhibitor added to the water minimizes formation of Sr-rich barite $(\text{Sr,Ba})\text{SO}_4$ and galena PbS scales in the plate heat exchangers (see also Sects. 8.4, 11.2, 15.3). The inhibitor passes through the entire doublet system.

Bavarian Molasse Basin (Germany): A series of geothermal installations successfully produce thermal and electrical energy in the Munich region in southern Germany. 19 plants were in operation in 2019, several geothermal doublets and multiple-well plants are currently under construction and more projects will be realized in the near future. The 19 plants have a combined installed capacity of 280 MW_{th} and 35 MW_{el} from 7 cogeneration plants. Declared objective of the Munich municipal utilities company is the exclusive use of renewable energy for district heating by 2040. Utilization of deep geothermal resources started with the thermal power plant Unterschleißheim in 2003 producing thermal energy for a local district heating grid. The plant was followed by a cogeneration plant in Unterhaching close to Munich.

All geothermal systems in the larger metropolitan area of Munich pump hydrothermal water from the same massive upper Jurassic limestone aquifer (Fig. 8.17). The aquifer is characterized by an extremely high yield and a favorable water composition with very low TDS. The high yield of the limestone is related to the reef facies occurring in parts of the Molasse basin (Birner et al. 2012; Stober 2013). The reef limestone contains cavernous structures and is karstified. In other regions of the Molasse basin the upper Jurassic Malm limestone is more massive banked limestone and dolomite with low or very low permeability. The Malm aquifer in the Munich area is also strongly fractured and faulted, which further contributes to its high hydraulic conductivity. The reef limestone aquifer has a typical hydraulic

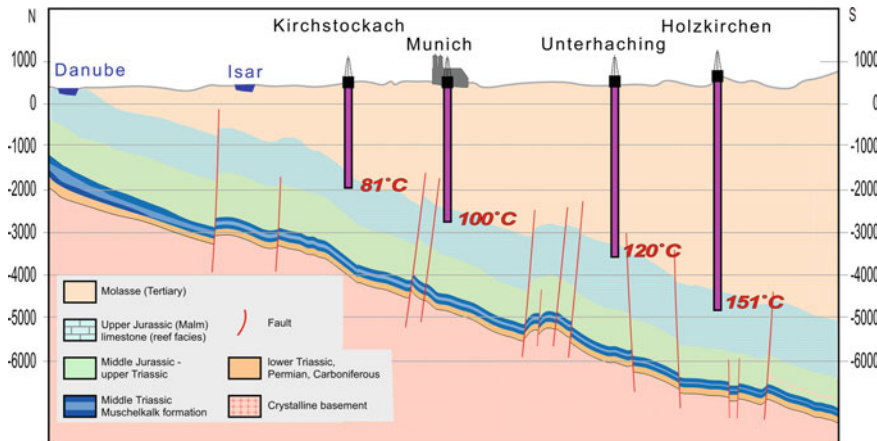


Fig. 8.17 Schematic geological N-S cross section of the Molasse Basin through Munich (Bavaria) showing the southward dip of the basement cover complex with the main aquifer of the upper Jurassic Malm limestone in highly permeable reef facies and the minor aquifer of the Triassic Muschelkalk formation. Schematic position of geothermal plants mentioned in the text with bottom hole temperatures in the limestone aquifer. The Holzkirchen temperature refers to the temperature at the pump

conductivity of 10^{-6} – 10^{-5} m s $^{-1}$ in the Munich area (Birner et al. 2012). The Malm limestone crops out at the surface in the north and its cover increases to several thousand meters thickness in the south (Fig. 8.17). The limestone varies in thickness with a maximum of 500–600 m. The Variscan basement and its cover sediments gently dip towards the south forming a strongly asymmetric basin created by the Alpine orogeny. The basin has been filled by Molasse type sediments during the Tertiary (Fig. 8.17). The entire sequence of rocks is covered by the frontal parts of the Alpine nappe system about 40 km south of Munich. The increasing depth of the limestone aquifer results in a gradual increase of the temperature and the total mineralization of the water residing in its pore space.

Unterhaching: The first of two vertical wells UH-1 reached the upper Jurassic limestone aquifer at 3350 m depth in the year 2004. The thickness of the aquifer at UH-1 is 380 m, the temperature at bottom hole \sim 120 °C and the yield $Q \leq 150$ L s $^{-1}$. UH-1 serves as production well. Two years later the second well UH-2 reached its final depth of 3864 m and the aquifer thickness is 650 m due to fault structures (Fig. 8.17).

The capacity of the plant is in the final stage of development about 70 MW_{th} thermal energy. The yield of the 3446 m deep production well is 150 L s $^{-1}$. After energy extraction the cooled water is pumped back to the same aquifer using a 3864 m deep injection well, which is at a higher temperature of 133 °C because of the greater well depth. The two wells are connected by a 3.5 km long thermal water pipe.

Electrical power was generated by a power plant working on the basis of the Kalina process (Sect. 4.2). The capacity of the plant was 3.36 MW_{el} electrical power

in 2009. In the mean time the Kalina plant has been decommissioned and the system is entirely used for district heating today.

Construction of the district heating grid started in 2006 and reached 35 km length in 2010 and measures 47 km in length (2019). The plant produced 58 MW_{th} in 2015 and the target for the final thermal capacity is 90 MW_{th}. The geothermal system supplies 7000 households with 108 GWh thermal energy per year (2017). After energy extraction the cooled water is pumped back to the same aquifer horizon using UH-2 as injection well. UH-2 is at a temperature of 133 °C because of the greater well depth. The two wells are connected by a 3.5 km long thermal water pipe.

The produced thermal water has a surprisingly low content of dissolved solids of only 600 to 1000 mg L⁻¹. The major dissolved components are Ca²⁺ and HCO₃⁻ and not NaCl like in most other deep waters from more than 3 km depth. The water also contains appreciable amounts of dissolved nitrogen, hydrogen sulfide and methane. Permanent excess nitrogen pressure imposed to the thermal water cycle prevents chemical precipitation of solids and access of atmospheric oxygen gas. The thermal water pipes are made from glass-fiber reinforced plastic for preventing corrosion problems.

Because of the extremely high yield of the aquifer and the low content of dissolved minerals in the deep water at the Unterhaching plant site a series of follow-up projects have been realized in the larger Munich metropolitan area (Birner et al. 2015; Stober et al. 2014). In 2014 a thermal power plant at Unterföhring uses a doublet doublet with two production and two injection wells all drilled from the same drilling site.

Kirchstockach is one of several geothermal power plants operated by Stadtwerke München (Munich municipal utilities company: [swm.de](#)). The doublet has a planned capacity of 33 MW_{th} and runs presently at 27 MW_{th}, the production well is 1981 m deep and yields 90 L s⁻¹ thermal water at 81 °C, the bottom hole temperature of the 2002 m deep injection well is 76 °C. Cooled water can be re-injected at a rate of 100 L s⁻¹.

Holzkirchen (Germany): The geothermal power plant Holzkirchen 25 km south of Munich is representative for similar installations in the Bavarian Molasse Basin. It is a cogeneration plant producing thermal energy for district heating and electrical energy from a hydrothermal doublet (Fig. 8.18). The total capacity is about ~30 MW. The political decision for building the plant was made in 2015. Drilling of the inclined well Th 1a started 2016 and drilling of the inclined well Th 2b was completed 2017. With 6084 m drilling length well Th 2b is longest and deepest well in the Molasse Basin. Drilling length of Th 1a is 5600 m. Bottom hole is at -4800 m b.s.l. and the top of the Malm limestone aquifer is at ~-4500 m. In 2017 a circulation test followed the final fitting of the wells with the pump, screens and casings with a pumping rate of 50 L s⁻¹. The electrical power is produced with binary cycle ORC plant (Sect. 4.2) from Turboden S.r.l. using isobutane as the heat transfer fluid in the turbogenerator system. The plant received the operating license July 4th 2019. Its capacity was 3.2 MW_{el} in 2019 as originally planned. However, the plant reached an output >4 MW_{el} in March 27th 2020. The temperature of the produced hydrothermal water is 149 °C at the wellhead and 151 °C in the wellbore Th 1a at position of the pump. The production rates Q have been varied in the range 65–80 kg s⁻¹. The

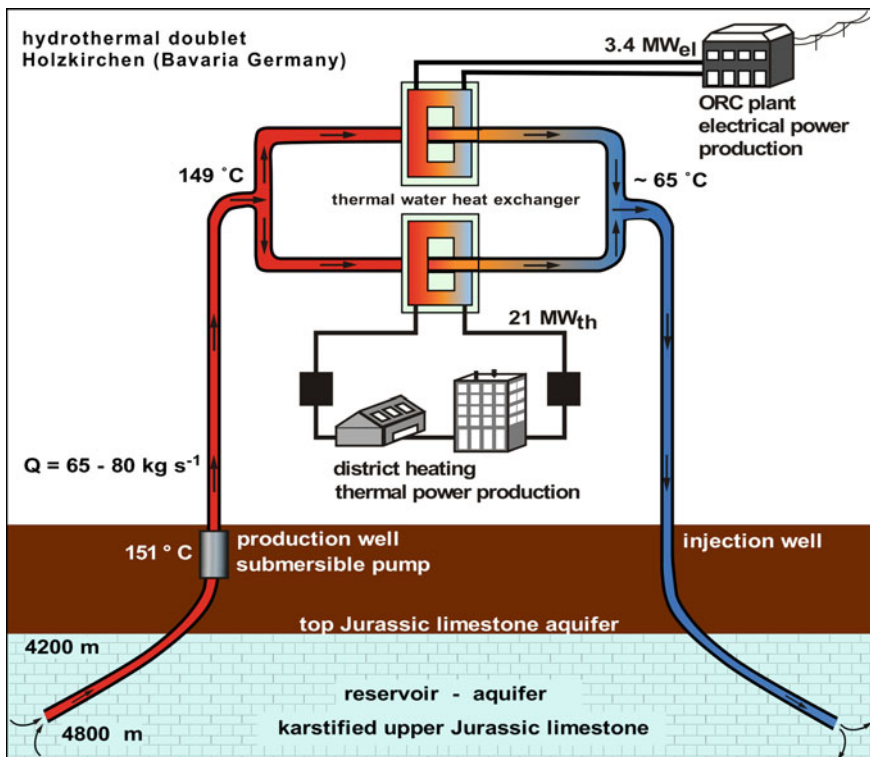


Fig. 8.18 Hydrothermal doublet at Holzkirchen south of Munich (Bavaria Germany). Data from gw-holzkirchen.de (Gemeindewerke Holzkirchen)

water contains dissolved organic carbon (DOC). The prime product of the plant is 21 MW_{th} thermal energy for district heating.

8.8 Project Planning of Hydrothermal Power Systems

Planning and developing a hydrothermal power plant is a complex undertaking requiring close collaboration of competent experts from many different fields and a clearly structured project management with well-defined responsibilities. The key themes are two fold: (1) the exploration risk, which encumbers all hydrothermal system projects, must be minimized by sound specialist analysis and model-based operation forecasts for the reservoir system. (2) Consumers for the produced thermal energy must be found. A hydrothermal doublet system should never be installed without consumer contracts with buyers for the produced thermal energy. The amount of thermal energy that can be converted to electrical energy is always a small fraction of the total thermal energy produced. Thus most of the energy produced must

be sold to heat customers. Consequently, the sites for potential hydrothermal plants are strongly determined by the location of existing or future heat consumers such as district heating grids or industry (in addition to geological conditions). If there are no consumers for the produced heat, the installed hydrothermal plant will essentially be an energy annihilation system (Sect. 8.6).

A hydrothermal doublet project begins with the evaluation of the geothermal potential of a location where nearby heat customers already exist or can be acquired. In low-enthalpy regions and for electrical power plants, there must be plausible potential for the existence of an aquifer at 2 to 4 km depth with a hot water reservoir temperature of 120 °C or more.

It is strongly recommended that project developers and the authorities discuss the project with affected parties in a public hearing prior to the first operations at the site. Public information and reliable citizen participation creates transparency, confidence and acceptance for the project.

A geothermal power plant receives not just once a general operation license. During project development approvals for partial steps are required from many different responsible authorities. It is recommended that the project developer seek assistance from an experienced and competent consulting company. Safe utilization of deep geothermal energy requires detailed planning und supervision of all works in view of environmental protection issues and consistent compliance of all related regulations.

The following checklist in bullet point form summarizes and structures the key work items for the development of a hydrothermal system.

Phase 1: Preliminary study.

The preliminary study defines and describes the aim and purpose of the project from which the type of geothermal utilization comes out.

1.1 Objectives of the project

1.2 Geological starting point

- Available data (data compilation; general geology, seismic profiles and wells, hydraulic tests, heat flow data)
- Geological structure of the underground (sections across the study area, interpretation of seismic sections)
- Depth and thickness of aquifers
- First estimate of temperature at potential target aquifers
- Hydraulic conductivity, possible yield
- Chemical composition of thermal water in different target reservoirs
- Local mining regulations, mining concessions, operation licenses

1.3 Energy utilization concept

- Planned and existing district heating (township, communities, local power company, definition of heat to be provided by the geothermal installation)
- Production of electrical energy (optional, if desired)

1.4 Rough technical concept of the geothermal power plant

- Different technical systems (doublet, distance of wellbores, side tracks)
- Well construction design (needed for a first cost estimate)
- Surface installation, power plant concept

1.5 Cost estimate, financial concept, economic responsibility

Phase 2: Feasibility study

2.1–2.4 Points 1.1–1.4 of the pilot study in more detail, decision on the alternatives to be planned

2.5 Analysis of costs, investment and financing

- Exploration
- Wellbores, underground installations
- Surface facilities, plant

2.6 Economy

- Operation costs
- Costs and expenditures, revenues
- Profitability analysis, cost-efficiency studies

2.7 Comprehensive risk analysis, quantification of exploration risk

2.8 Ecological analysis, ecological balance study

2.9 Project schedule, project flow

Phase 3: Exploration

3.1 Entrusting a consulting company, assigning the project management

3.2 Applying for the exploration rights at the local mining authority

3.3 Completing geophysical exploration with a competent specialist firm (if necessary)

3.4 Concept for drilling (following the legal requirements of the mining authorities)

3.5 Invitation to bid for the first wellbore, formulation of an operational plan

3.6 Drilling and testing the first well

3.7 If necessary executing stimulation measures

3.8 Decision on strike

Phase 4: Development

4.1 Invitation to bid for the second wellbore, formulation of an operational plan

4.2 Drilling and testing the second wellbore

4.3 If necessary executing stimulation measures

4.4 Building surface installations and a power plant (parallel to 4.1–4.3)

4.5 Securing the license area at the local mining authority

4.6 Operation of the plant, production of thermal water, thermal and electrical energy

Phases 1 through 3.5 involve all pre-drilling work items for developing a hydrothermal reservoir. Key steps include obtaining the exploration claim from the local mining authorities and deciding on the drilling position. Basis for both is a sound evaluation of the geothermal potential of the site of interest. This is centered around existing geological data and, equally important on developed concepts for the utilization of the geothermal energy to be produced in local and district heating grids and for electrical power production. Also, insurance agreements must be signed and, most important, a financial backer must be found.

Phases 3.6 to 3.8 decide on the strike of drilling within the means of the project target definition. If the well fails to meet the criteria for being successful according to the project conditions it still may be useful for a substitute geothermal project or other purposes. However, this utilization differs from the original concept because the geological and geothermal situation is different than predicted by pre-drilling exploration. Perhaps, the wellbore struck a gas or oil reservoir! Perhaps, and far more common, the yield or the temperature of the thermal water is lower than hoped for. Still, the produced water can possibly be used for feeding a thermal spa or as deep geothermal probe, however, not for electrical power production as originally intended.

If the first well is successful, the project continues with the invitation to bid for the second wellbore and with further geophysical, hydraulic and hydrochemical research (phase 4). It is important that the production and injection well obey the planned minimum distance in the aquifer so that the produced thermal water maintains its original temperature over the entire lifetime of the system. It is aimed to install a trouble-free working thermal water circulation (primary loop) with sufficient high yield and water temperature. For this, production tests, stimulation measures if necessary, and extensive hydrochemical investigations are needed. Where appropriate, special measures help preventing scaling and corrosion. The challenge of this project phase is also the strain on the drilling equipment and on the drilling technique, the requirements on the well engineering materials and the pump and pump equipment. Decisions on the optimal technology for the power plant and the engineering of the plant are also made on the basis of hydraulic data and hydrochemical properties of the thermal water.

The multifaceted tasks of a geothermal project require an efficient and unified collaboration of experts from very diverse fields. Engineers, geologists, lawyers, insurance and financing experts must work together hand in hand. Subcontractors must be commissioned and their work must be coordinated. A successful geothermal project requires a well-coordinated and efficient effort of all intermeshed actors.

8.9 Aquifer Thermal Energy Storage (ATES)

ATES open-loop systems use deep aquifers for temporary storage of excess thermal energy (“waste heat”) for later retrieval mostly for heating purposes. ATES is interesting for sensible usage of process heat from cogeneration units, gas or steam turbine

plants, power plants and other sources of “waste heat”. The systems utilize like geothermal doublets at least one production and one injection well (Doughty et al. 1982). ATES is operated on a seasonal basis. The system is usually loaded during the warm season by transferring the excess heat to aquifer water pumped from the production well at the surface heat exchanger. The hot water is then returned to the aquifer through the injection well. The procedure creates a heat ball around the screen of the injection well. The process is reversed during the cold season and the recuperated thermal energy is used for heating purposes typically in district heating systems. Because groundwater flow velocities in deep aquifers are very small the heat losses by the system are minimal.

The efficiency of ATES can be defined by the coefficient of heat recycling τ (level of storage use). It is the ratio of heat taken and heat added to the aquifer ($\tau = \text{heat out} / \text{heat in}$). The recycling coefficient τ is typically around 0.7. The value relates to one or several storage cycles. With increasing number of cycles the coefficient τ increases because the aquifer rocks gradually increase in temperature thus increasing the temperature of the total storage consisting of both water and rock. ATES can also be used for storage of cooled water, typically with a better efficiency $\tau = 0.8$.

Because ATES stores the thermal energy in both the groundwater and the aquifer rocks the product $\rho_F c_F$ in Eq. 8.6 becomes:

$$\rho c = \{\rho_S c_S\}(1 - n) + \{\rho_F c_F\}n \quad (8.10)$$

where the subscripts S and F denote the properties of the rock and the fluid, respectively and n stands for the porosity. ρc has the dimension $J \text{ m}^{-3} \text{ K}^{-1}$. If τ is significantly below 1 the stored heat accumulates in the aquifer during prolonged operation of the system.

Deep ATES require appropriate geological conditions with homogeneously high hydraulic conductivity k_F of the aquifer, unproblematic chemical composition of the groundwater, suitable temperature, and originally low groundwater flow velocity with hydraulic conductivity being the decisive parameter. The thermal interaction between the “warm” and “cold” side of the ATES depends on the distance of the two wells, the hydraulic conductivity and the production rate (Kim et al. 2010). The thermal and hydraulic properties of ATES can be modeled with numerical models such as TOUGH2, USGS, HST3D or FEFLOW (to name a few) sufficiently precise (e.g. Lee 2010; Gao et al. 2017). If the temperature changes in the aquifer are large geochemical and biological alterations may take place with the potential consequence of scale formation in components of the system.

ATES can potentially also be used in the warm season for cooling purposes depending on the temperature and depth of the aquifer storage. In this case the direction of water flow changes two times per year and each well must be equipped with a production pump and an injection string. However, the bi-directional application of ATES is a cost-effective technology for using summer heat in the cold season and winter cold for cooling in the warm season. Shallow ATES are likely more economical than deep ones because of lower drilling costs and higher storage

capacity related to the higher temperature difference between groundwater and the injected water.

On the other hand, deep ATES can be combined with solar thermal systems and other systems producing seasonal excess heat. ATES can be successfully used for greenhouse heating or for district heating systems; particularly if “waste heat” from industrial sources or combined heat and power (CHP) plants can be transferred seasonally to ATES. ATES can be combined with heat pumps producing water at a higher and constant. ATES is especially attractive in regions with existing combined heat and power (CHP) units or district heating grids. ATES are large-scale systems and require consumers with a high demand in thermal energy (>10 MW) and corresponding sources of “waste heat”.

Presently, more than about 2800 ATES operate worldwide producing 2.5 TWh thermal energy for heating and cooling. Most of these systems are near-surface systems with storage temperatures below 25 °C. 85% of aquifer heat storage systems operate in the Netherlands (dutch-ates.com) and 10% in Sweden, Denmark and Belgium (Fleuchaus et al. 2018). High-temperature ATES (>90 °C) have not been extensively tested and used so far (see site examples below) but have a great potential and are certainly a sustainable and future-oriented technology deserving support and promotion. The ATES in Neubrandenburg (Germany) and Utrecht (the Netherlands) inject water at 90 °C, in Zwammerdam (the Netherlands) water at 88 °C into the aquifer. Analysis of the deep ATES systems in the Netherlands has shown that the efficiency of the systems is controlled by the characteristics of the heat demand rather than by the properties of the storage installation.

The ATES Neubrandenburg (Germany) was an example of a deep high-temperature storage system (Kabus et al. 2005). The facility transferred seasonal excess heat (~20 MW) from a thermal power station to an aquifer at 1250 m depth. It injected water at 85–90 °C at a rate of 28 L s⁻¹ into a sandstone reservoir (Triassic Upper Postera Sandstone). The original groundwater residing in the sandstone had 55 °C and a TDS of 135 g kg⁻¹. The unloading temperature was at 70 °C thus the ATES operates at an efficiency of about $\tau = 0.75$. Unfortunately, the facility has recently been decommissioned. Rumors have it that the ATES has been successful technology but went dead because of disputes over respective areas of authority.

References

- Hasnaina, S. M., 1998a. Review on sustainable thermal energy storage technologies, Part I: heat storage materials and techniques. *Energy Conversion and Management*, 39, 1127–1138.
- Hasnaina, S. M., 1998b. Review on sustainable thermal energy storage technologies, Part II: cool thermal storage. *Energy Conversion and Management*, 39, 1139–1153.
- Stober, I., Richter, A., Brost, E. & Bucher, K., 1999. The Ohlsbach Plume: Natural release of Deep Saline Water from the Crystalline Basement of the Black Forest. *Hydrogeology Journal*, 7, 273–283.
- Choi, J.H., Edwards, P., Ko, K. & Kim, Y.S., 2016. Definition and classification of fault damage zones: a review and a new methodological approach. *Earth Sci. Rev.*, 152, 70–87.

- Kappelmeyer, O. & Haenel, R., 1974. Geothermics with special reference to application, pp. 238, E. Schweizerbart science publishers, Stuttgart.
- Câmara, G., Souza, R. C. M., Freitas, U. M., Garrido, J. & Ii, F. M., 1996. SPRING: Integrating remote sensing and GIS by object-oriented data modelling. Image Processing Division (DPI), National Institute for Space Research (INPE), Computers & Graphics, 20 (3), 395–403, Brasil.
- Trefry, M. G. & Muffels, C., 2007. FEFLOW: a finite-element ground water flow and transport modeling tool. *Ground Water*, 45 (5), 525–528.
- Clauser, C., 2003. Numerical simulation of reactive flow in hot aquifers using SHEMAT and Processing SHEMAT. Springer Verlag, Heidelberg/Berlin.
- Harbaugh, A. W., 2005. MODFLOW-2005; The U.S. Geological Survey Modular Ground-Water Model—the Ground-Water Flow Process. Techniques and Methods. U.S. Geological Survey, 6–A16.
- Mottaghy, D. & Pechnig, R., 2009. Numerical 3-D model and prediction of the temperature evolution of thermal reservoirs (in German). *BBR - Fachmagazin für Brunnen- und Leitungsbau*, 60(10), 44–51.
- Amann, R., Glöckner, F.-O. & Neef, A., 1997. Modern methods in subsurface microbiology: in situ identification of microorganisms with nucleic acid probes. *FEMS Microbiol. Rev.*, 20(3/4), 191–200.
- Dingh, H. T., Kuever, J., Mussmann, M., Hassel, A. W., Stratmann, M. & Widdel, F., 2004. Iron corrosion by novel anaerobic microorganisms. *Nature*, 427, 829–832.
- Friedrich, H.-J., Zschornack, D., Hielscher, M., Hinrichs, T. & Wolfgramm, M., 2018. Extraction of rare strategic metals from geothermal brines (in German). *Geothermische Energie*, 88/1, 22–23, Berlin.
- Portier, S., André, L. & Vuataz, F.-D., 2007. Review on chemical stimulation techniques in oil industry and applications to geothermal systems. In: *Engine*, pp. 32, CREGE, Neuchatel, Switzerland.
- Liang, F., Sayed, M., Al-Muntasher, G. A., Chang, F. F. & Li, L., 2016. A comprehensive review on proppant technologies. *Petroleum*, 2, 26–39.
- Ungemach, P., 2001. Insight into geothermal reservoir management district heating in the Paris Basin, France. *GHC Bulletin*, 22, 3–13.
- Ungemach, P., Antics, M. & Papachristou, M., 2005. Sustainable Geothermal Reservoir Management. Proceedings World Geothermal Congress 2005, Antalya, Turkey, 24–29 April 2005, 12 pp.
- Sauty, J. P., Gringarten, A. C., Landel, P. A. & Menjoz, A., 1980. Lifetime optimization of low enthalpy geothermal doublets. In: In: Strub, A.S. & Ungemach, P. (eds): *Advances in European Geothermal Research*, pp. 706–719, D. Reidel Publ. Co. Dordrecht, The Netherlands.
- Antics, M., Papachristou, M. & Ungemach, P., 2005. Sustainable Heat Mining, a Reservoir Engineering Approach. In: *Proceedings, thirteenth workshop on geothermal reservoir engineering*, pp. 14, Stanford University.
- Ungemach, P. & Turon, R., 1988. Geothermal Well Damage in the Paris Basin: A Review of Existing and Suggested Workover Inhibition Procedures. *SPE Formation Damage Control Symposium*, 8–9 February 1988, Bakersfield, California, 17 pp.
- Bertleff, B., Joachim, H., Koziorowski, G., Leiber, J., Ohmert, W., Prestel, R., Stober, I., Strayle, G., Villinger, E. & Werner, J., 1988. Data from geothermal wells in Baden-Württemberg (Germany) (in German). *Jh. geol. Landesamt Baden-Württemberg*, 30, 27–116.
- Vidal, J., Genter, A. & Chopin, F., 2017. Permeable fracture zones in the hard rocks of the geothermal reservoir at Rittershoffen, France.- AGU, *Journal of Geophysical Research: Solid Earth*, 122(7), 4864–4887.
- Baujard, C., Genter, A., Dalmais, E., Maurer, V., Hehn, R., Rosillette, R., Vidal, J. & Schmittbuhl, J., 2017. Hydrothermal characterization of wells GRT-1 and GRT-2 in Rittershoffen, France: Implications on the understanding of natural flow systems in the Rhine Graben. *Geothermics*, 65, 255–268.

- Sanjuan, B., Scheiber, J., Gal, F., Touzelet, S., Genter, A. & Villadangos, G., 2016. Inter-well chemical tracer testing at the Rittershoffen geothermal site (Alsace, France).-European Geothermal Congress, 7 p., Strasbourg, France.
- Mouchot, J., Genter, A., Cuenot, N., Scheiber, J., Seibel, O., Bosia, C. & Ravier, G., 2018. First year of Operation from EGS geothermal Plants in Alsace, France: Scaling Issues.- Proceedings, 43rd Workshop on Geothermal Reservoir Engineering, Stanford University, SGP-TR-213, 12 p., Stanford/California.
- Boissavy, Ch., Henry, L., Genter, A., Pomart, A., Rocher, Ph. & Schmidlé-Bloch, V., 2019. Geothermal Energy Use, Country Update for France. European Geothermal Congress, Den Haag, The Netherlands, 18 p.
- Birner, J., Fritzer, T., Jodocy, M., Savvatis, A., Schneider, M. & Stober, I., 2012. Hydraulic properties of the Malm aquifer in the S-German Molasse basin and their significance for geothermal energy development (in German). *Z. geol. Wiss.*, 40, 2/3: 133–156, Berlin.
- Stober, I., Wolfgramm, M. & Birner, J., 2014. Hydrochemistry of deep fluids in Germany (in German). *Z. geol. Wiss.*, 41/42 (5–6), 339–380.
- Doughty, C., Hellström, G., Tsang, C.F. & Claesson, J., 1982. A Dimensionless Parameter Approach to the Thermal Behavior of an Aquifer Thermal Energy Storage System. *Water Resources Research*, 18/3, 571–589.
- Kim, J., Lee, Y., Yoom, W.S., Jeon, J. S., Koo, M.-H. & Keehm, Y., 2010. Numerical modeling of aquifer thermal energy storage systems. *Energy*, 35/12, 4955–4965.
- Lee, K. S. 2010. A Review on Concepts, Applications, and Models of Aquifer Thermal Energy Storage Systems. *Energy*, 3, 1320–1334.
- Gao, L., Zhao, J., An, Q., Wang, J. & Liu, X., 2017. A review on system performance studies of aquifer thermal energy storage. *Energy Procedia*, 142, 2537–3545.
- Fleuchaus, P., Godschalk, B., Stober, I. & Blum, P., 2018. Worldwide application of aquifer thermal energy storage. *Renewable and Sustainable Energy Reviews*, 94, 861–871, (doi.org/https://doi.org/10.1016/j.rser.2018.06.057).
- Kabus, F., Möllmann, G. & Hoffmann, F., 2005. Speicherung von Überschusswärme aus dem Gas- und Dampfturbinen-Heizkraftwerk Neubrandenburg im Aquifer. Fachtagung Geothermische Vereinigung e.V., Landau in der Pfalz.
- Jodocy, M. & Stober, I., 2008. Development of a geothermic information system for Germany; State of Baden-Württemberg (in German). *Erdöl-Erdgas-Kohle*, 10, 386–393.
- Wagner, W. & Kretschmar, H.-J., 2008. International Steam Tables, Properties of Water and Steam, Springer, Berlin, Heidelberg.
- Stober, I., 1986. Strömungsverhalten in Festgesteinsaquifern mit Hilfe von Pump- und Injektionsversuchen (The Flow Behaviour of Groundwater in Hard-Rock Aquifers – Results of Pumping and Injection Tests) (in German). *Geologisches Jahrbuch, Reihe C*, 204 pp.
- Stober, I., 2013. Die thermalen Karbonat-Aquifere Oberjura und Oberer Muschelkalk im Südwestdeutschen Alpenvorland. *Grundwasser*, 18(4), 259–269, (DOI: <https://doi.org/10.1007/s00767-013-0236-2>).
- Owens, S. R., 1975. Corrosion in disposal wells. *Water and Sewage Works*, 10–12.
- Ramey Jr., H. J., 1962. Wellbore heat transmission. *JPT 435 Trans AIME*, 225.
- Sun, H., Feistel, R., Koch, M. & Markoe, A., 2008. New equations for density, entropy, heat capacity and potential temperature of a saline thermal fluid. *Deep-Sea Research*, 55, 1304–1310.
- Dickson, M. H. & Fanelli, M., 2004. What is Geothermal Energy? Download from International Geothermal Association.

Chapter 9

Enhanced-Geothermal-Systems (EGS), Hot-Dry-Rock Systems (HDR), Deep-Heat-Mining (DHM)



Equipment for hydraulic stimulation

Enhanced-Geothermal-Systems (EGS) use the deep underground as a source of heat for the production of electrical and thermal energy irrespective of the hydraulic properties of the deep heat reservoir (Sect. 4.2). In other words the rocks are hot at depth irrespective of whether or not they qualify as aquifers or aquitards. Weakly fractured granites at depth are best described as “hot dry rocks” (HDR). However, keep in mind that also the few fractures present are interconnected and filled with hot pore water (Ingebritsen and Manning 1999; Stober and Bucher 2007a, b). The term “hot dry rock” originates from the early-days of geothermal energy utilization where the concept was to drill a deep wellbore into hot but assumingly dry rocks for extraction of thermal energy. Later it was found that the fracture porosity of continental rocks is always saturated with hot water so that the term hot-dry-rock became rather misleading (Bucher and Stober 2007a, b). The upper continental crust is always fractured; its fracture density differs however. A saline, occasionally gas-rich fluid is typically present in the fractures. The geothermal utilization of the hot underground with low hydraulic conductivity is sometimes also referred to as “deep heat mining” (DHM). Because the continental crust is predominantly granitic or gneissic, HDR systems strongly focus on granitic heat reservoirs. Typical target temperatures for HDR systems are above 200 °C. This means that wellbores of 6 to 10 km have to be drilled in continental crust with an average geothermal gradient.

Some years ago, it has been proposed to use HDR technology also in deep sedimentary basins (Huenges 2010). Sedimentary rocks with low hydraulic conductivity at great depth may also provide thermal energy, of course. The systems yet to be developed may also be termed Engineered-Geothermal-Systems (likewise abbreviated as EGS). The HDR technology has originally been developed by the oil- and gas-industry. It is a well-established, decades old method of reservoir engineering and development of low-permeability sedimentary reservoirs, improving the production rates and inflow and hydrocarbon migration conditions. The concepts have been translated to geothermal energy applications, first expanded to the crystalline basement of the continental crust and recently returned to deep sedimentary successions and thereby closing the circle between the diverse industries.

The desired temperature of the target heat reservoir of EGS (typically > 200 °C) can be reached by adjusting the depth of the wellbore. However, the hydraulic conductivity of typical reservoir rocks is too low for circulating hot fluids for driving a geothermal power plant. For example, crystalline basement rocks at 5 km depth have a mean hydraulic conductivity of only 10^{-9} m s⁻¹ (Ingebritsen and Manning 1999; Stober and Bucher 2007a, b, Stober and Bucher 2015). The fundamental task of EGS development is the creation of a sufficiently large volume of the reservoir around the wellbores with a significantly higher hydraulic conductivity ($> 5 \cdot 10^{-5}$ m s⁻¹). Furthermore, the engineered high-conductivity volumes need to be connected so that sufficient fluid flow rates can be achieved and the fractured rock volume can function as a heat exchanger. Reservoir stimulation techniques are central to EGS development.

EGS development is quite different in distinct types of host rocks because of different natural fracture and porosity patterns and deformation behavior of igneous, metamorphic and sedimentary rocks. The fracture patterns of layered sequences of

sedimentary rocks are strongly influenced by post-sedimentary compaction, diagenesis and weak metamorphism. Fracture patterns in coarse-grained granites are mostly controlled by tectonic and thermal stresses. During stimulation measures, the water injected under high pressure migrates predominantly along fractures in quartz-feldspar dominated rocks (e.g. granites), however, in rocks rich in sheet silicates such as shale, slate, mica-schist and mica-rich gneiss the injected water may also migrate along the foliation in addition to fractures. Thus in schistose rocks the injection pulse is damped and consequently the potential for generating seismicity is reduced. Note that at the target temperature of about 200 °C all reservoir rocks classify by definition as metamorphic rocks. Thus granites are strictly sub-greenschist facies metagranites, clay and mudstones are low-grade metapelites, limestones are low-grade marbles (Bucher and Grapes 2011).

For improving the hydraulic conductivity of the reservoir rocks EGS are being developed by using both hydraulic and chemical stimulation techniques. These methods have been derived by the oil and gas industry and have been used for decades for improving production from hydrocarbon reservoirs. Stimulation in the context of EGS is a time limited process in the development phase of the system. Once the underground heat exchanger works as planned, no further stimulation measures are needed during regular operation of the plant. Typical hydraulic stimulation is of short duration and pumps fluid at high pressure with large injection rates into the well.

The U.S. Department of Energy (DOE) defines EGS as engineered geothermal reservoirs for the production of economically relevant amounts of thermal energy from low-conductivity or/and low-porosity geothermal resources. The EGS reservoirs need to be stimulated with efficiency-boosting methods irrespective of the type of the reservoir rocks (MIT 2007).

9.1 Techniques, Procedures, Strategies, Aims

EGS produce geothermal energy from weakly fractured hot rocks. The interconnected fractures in crystalline basement rocks such as granites and gneisses are saturated with hot fluids, typically saline brines. The water-conducting fractures in basement rocks of the continental upper crust are complex structures that control the hydraulic conductivity of the basement (Mazurek 2000; Caine and Tomusiak 2003; Stober and Bucher 2007a, b; Stober and Bucher 2015). Stimulation measures typically increase the aperture of existing fractures and thus improve the hydraulic conductivity of the reservoir rocks. High-pressure injection of water irreversibly widens the existing fractures. Rarely new fractures are generated, except perhaps in dense unfoliated metasediments (Huenges 2010).

The created EGS underground heat exchanger is then used in a fashion like in hydrothermal systems. Water is injected into the reservoir through an injection borehole. The water flows through the heat exchanger and extracts thermal energy from the hot rock at depth. After passage through the underground heat exchanger the heated water is pumped to the surface from a production well. The fluid advection

is driven by the potential difference between the injection and production well. The subsurface distance between the two wells measures several hundreds to thousand meters.

EGS are primarily built for the conversion of geothermal to electrical energy. Consequently, as mentioned above, the temperature should be 200 °C or higher, which means reservoir depths of 5 km and deeper in areas with moderately warm continental geothermal gradients (38 K km^{-1}). However, two 7 km deep wellbores must be drilled in areas with a typical average continental geotherm (27 K km^{-1}). Since EGS are independent of the presence of highly conductive aquifers at depth, the technology may be installed nearly anywhere. Because of this circumstance, EGS have a tremendous energy potential and the technology can be regarded as the future most important use of geothermal energy (MIT 2007; Lund 2007; Brown et al. 2012). EGS technology may have the capability for becoming the prime source of energy in the future.

The method to improve the hydraulic conductivity of the heat reservoir is also known under the misleading term “hydraulic fracturing”. The technique causes an increased conductivity of the rocks by hydraulically expanding fractures in the rock matrix. It always causes seismic noise when rocks are stimulated by injecting water into wellbores under very high pressure. The seismic noise proves that stimulation does what it is supposed to do, opening existing fractures thus increasing the hydraulic conductivity of the rock reservoir. The seismic noise associated with stimulation may be annoying or even scaring to uninformed people in densely populated areas; however, it has never caused damage to surface installations such as homes and other buildings (in sharp contrast to mining activities for example). The key point here is that the local residents should be educated about the possible “side effects” of possible hydraulic fracturing operations.

When using the hydraulic fracturing method (surface) water is injected into the heat reservoir with several hundred bar wellhead pressure. The purpose of the effort is to open and widen open fractures and re-fracture old fractures that have been sealed by younger mineral deposits. The fracturing affects volumes of reservoir rock around the uncased wellbore, the open hole or in a packer-isolated section of the wellbore. It is hoped that the efforts permanently increase the hydraulic conductivity of the bedrock. Usually water from a nearby river or lake (or similar) is used as injection fluid. However, the water may be charged with a series of additives such as Na_2CO_3 , HCl , NaOH , HF and many others that support the effort by chemically interacting with the bedrocks and the fracture minerals (e.g. Portier et al. 2007).

There are several types of stimulation techniques depending on the sharpness, the duration, the frequency, the chemical additives and the number and dimension of sections to be stimulated. One distinguishes between massive hydraulic stimulation, pulse stimulation, multi-frac, gel stimulation, water-frac, acid-frac and many more. If acid-frac is to be attempted on the basis of the bedrock mineralogy, it has to be decided what kind of acid and at what concentration it will be sufficient to obtain the desired result. The choice of “mild” and “strong” acidizing techniques depends of the mineralogy of the target formation. However, the protection of the casing from chemical attack needs to be considered also.

The minimum volume of heat exchanger rock depends on the temperature and conductivity of the accessed reservoir. However, rule of thumb estimates for an economically profitable heat exchanger volume vary from 10^8 m^3 (MIT 2007) to 2 10^8 m^3 (Rybäck 2004). The minimum surface area of a commercially useful heat exchanger is about $2 \cdot 10^6 \text{ m}^2$ (Rybäck 2004). If the open hole is assumed to be about 300 m, it follows that, for a doublet system, the distance between the wellbores at depth should be about 1000 m.

If the EGS technology ought to become a widely distributed source of renewable energy, mature reservoir engineering is the prime requirement. Many questions are still unanswered and subject to challenging research in the near future. The questions include: How can the hydraulic conductivity of the reservoir be significantly improved using hydraulic and chemical techniques as mild as possible; How can the flow paths of the fluid between the wells be controlled and engineered as desired; How does the hot fluid react with the rocks and what are the chemical consequences of the hot fluid circulation; What is the time evolution of the system and the associated cooling pattern?

9.2 Historical Development of the Hydraulic Fracturing Technology, Early HDR Sites

The oil and gas industry traditionally uses “HDR” techniques to improve the hydraulic conductivity of sedimentary rocks by fracturing low-conductivity sediments. From early on the industry also used chemical stimulation for reservoir improvement. The technique has been transferred from the oil and gas industry to the deep geothermal technology. Early efforts to extract thermal energy from the deep underground go back to the early 1970ies. The experiments at Fenton Hill (New Mexico, USA) by the Los Alamos National Laboratories have truly been pioneering and innovative research and efforts. The heat reservoir at the Fenton Hill research site was a biotite-granodiorite (Brown et al. 2012). Inspired by the ground-breaking Fenton Hill project, several follow-up projects have been initiated worldwide. The challenging pioneering early projects include: The Urach Deep Wellbore (UDW) in Germany (1970ies); Rosemanowes, Cornwall (UK) in the 1980ies, Le Mayet (France); Hijiori (Japan); Ohachi (Japan); Soultz-sous-Forêts (France). Later profound efforts further developed the EGS technology in Australia (Hunter Valley, Cooper Basin) and in the USA (Desert Peak in Nevada, Coso volcanic field near Los Angeles).

The pioneering project Soultz-sous-Forêts in the upper Rhine rift valley started officially in 1988 as an European HDR research cooperation. It followed French-German geological exploration studies. After an comprehensive feasibility study, two boreholes were drilled to 3500 m (GPK 1 and GPK 2) and a geological heat exchanger has been established by hydraulic stimulation in the years 1993–1997. Hot water was then pumped at a rate of 25 L s^{-1} and a temperature of 142 °C. Later GPK

2 has been deepened to 5000 m and two new boreholes were drilled to 5000 m (GPK 3 and GPK 4) into the granitic Variscan basement in 2001–2005. The temperature at this depth is 203 °C. The pumped highly mineralized fluid (96 g kg^{-1} Na-Ca-Cl) has a temperature of 150 °C at the wellhead of GPK 2. After heat extraction in the plant the saline fluid cooled to 70 °C and afterwards returned to the reservoir without using reinjection pumps (Mouchot et al. 2018). Since 2008, the pilot power plant based on Organic Rankin Cycle technology (ORC) produces 1.7 MW electrical power to the grid. The plant is in trouble-free continuous operation. The Soultz-sous-Forêts power plant is primarily an industrial research system that has produced invaluable and important knowledge for the advancement of the HDR technology (Dezayes et al. 2005; Gérard et al. 2006; Genter et al. 2010, 2012).

The highly mineralized deep fluid at Soultz-sous-Forêts has a gas to liquid ratio of $1.03 \text{ Nm}^3 \text{ m}^{-3}$ at reference conditions (273.15 K, 1.01325 hPa). 91% of the gas is CO₂. A pressure of 2.3 MPa is maintained in the surface installations to avoid CO₂ degassing. The pH of the fluid (25 °C) is 4.9–5.3 (Pauwels et al. 1993). Corrosion and scaling affecting the surface installations result from the *P-T* changes imposed on the deep fluid. The prime scaling material is Sr-rich barite ((Ba,Sr)SO₄), accompanied by some galenite (PbS) and a small amount of other sulfides (Fe, Sb, As sulfide). The barite contains radioactive lead and radium isotopes (e.g. ²¹⁰Pb, ²²⁶Ra). For operational and environmental reasons chemical inhibitors are added to the produced fluid. The inhibitors prevent or minimize scaling in the surface installations and in the injection well (Sects. 8.4, 8.7.1, 11.2, 15.3). The chemical composition of the produced fluid and the scale material is periodically monitored (Scheiber et al. 2015; Mouchot et al. 2018).

The common concept of all these projects has been the development of a geothermal heat reservoir in the crystalline basement for electrical power production. The fundamental feasibility of the concept has been demonstrated by the ground-breaking Fenton Hill project in New Mexico (USA) in the 1980ies. At Fenton Hill the heat exchanger has been created by hydraulic stimulation from two 3500 m deep wells. The temperature at depth is 234 °C and did not decrease during 11 month of flow testing the system. During the tests of one-year duration the output was 4 MW_{el} during continuous operation and 10 MW_{el} during 15 days at full power. However, the system was not commercially lucrative (MIT 2007; Duchane and Brown 2002; Brown 2009) mainly because of insufficient flow rates at low pumping pressures. Also, hydraulic experiments showed that fractures did not irreversibly open. Nevertheless, the Fenton Hill project produced unique and valuable data and experience for future EGS projects. The adventure of the Fenton Hill project has been documented and described in great detail by Brown et al. (2012). The EGS interested reader finds a wealth of information on all aspects of HDR system development.

In these early days of the EGS development during the 1970ies and the beginning of the 1980ies it was still assumed that the crystalline basement of the continents would be mostly free of water (dry) at great depth and that the rocks would be essentially unfractured. Consequently the developing technology has been named “hot-dry-rock” (HDR) and the term “hydraulic fracturing” has been transferred from the oil and gas industry to geothermal system development also. The term hydraulic

fracturing is a consequence of the concept that new vertical penny-shaped cracks must be created in the massive rocks (Smith et al. 1975; Duffield et al. 1981; Ernst 1977; Schädel and Dietrich 1979; Kappelmeyer and Rummel 1980; Dash et al. 1981). Today, it is common knowledge that the continental crust is fractured to the brittle ductile transition zone at about 12 km depth and that the fracture system is interconnected and water-saturated (e.g. Stober and Bucher 2005; Stober and Bucher 2007a, b, Stober and Bucher 2015). Still the hydraulic conductivity of the crystalline basement is normally insufficient for EGS and the geological heat exchanger at depth must be engineered by stimulation methods.

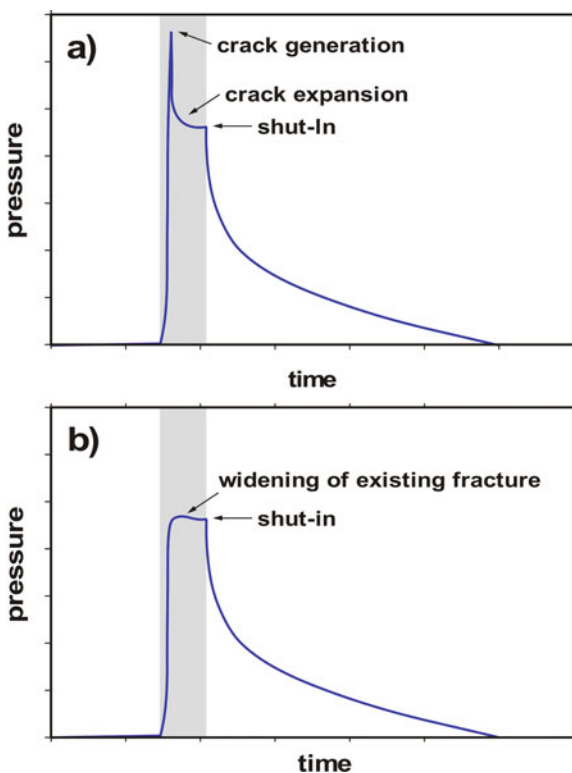
9.3 Stimulation Procedures

Hydraulic stimulation experiments have shown already in the 70 s and 80 s of the last century that the crystalline basement normally has a natural fracture network. The existing fracture network has been hydraulically activated during the experiments. No new artificial cracks and fractures have been opened by high-pressure water injection (Batchelor 1977; Stober 1986; Armstead and Tester 1987). The prime reaction of granite and gneiss on stimulation is that it just modifies the fracture geometry by first increasing the fracture aperture and then displacing the rocks due to shear stresses. The process results in a permanent and irreversible misfit of the two original fracture surfaces and as a consequence an increased average aperture and hydraulic conductivity (Pearson 1981; Pine and Batchelor 1984; Baria and Green 1989; MIT 2007). This mechanical behavior is different from that of unmetamorphic sediments where stimulation indeed creates new fractures and cracks.

Figure 9.1 shows recorded pressure versus time plots of (a) the process generating a new fracture and (b) the process of expanding an existing fracture. The pressure level and the shape of the pressure—time curve differ distinctly in the two experiments. Generating new cracks requires massively higher pressures and the pressure collapses suddenly when the crack forms. Pressure—time data discriminate stimulations that create new cracks from widening an existing fracture network.

Hydraulic expansion of fractures makes lateral displacement of locked uneven fracture surfaces possible by decreasing the shear strength of the fracture surface. Lateral displacement requires an existing stress component parallel to the fracture surface (Fig. 9.2). Fracture surfaces without a shear stress component open and close elastically without being displaced laterally (Stober 2011). Orientation and magnitudes of the principal stresses at reservoir depth can be derived from in-situ stress analysis using data from wellbore breakouts (Zobak et al. 2003) and micro-seismic events. Fractures with a high angle to the normal stress component will not or hardly open and will also not be displaced laterally because of minimal shear stresses. Thus hydraulic stimulation activates only a fraction of the fracture system. Improved hydraulic conductivity only results from fractures that are sheared during hydraulic stimulation. This also means that the fluid flow pattern during hydraulic standard well tests, for example pumping or injection tests, may differ totally from

Fig. 9.1 Pressure—time curves of stimulation experiments: **a** new crack forms, curve shows a distinct pressure spike, **b** expanding existing fractures



the fluid flow pattern caused by hydraulic stimulation. Stimulation generates directed fluid flow.

Shearing of two rough and jagged fracture surfaces causes small mismatches and gaps when the aperture decreases with phasing out the hydraulic pressure. The created misfits cause an increase of the fracture porosity and a permanently enhanced permeability. The effect is known under the term “self-propelling”.

The function of the injected water is to decrease the shear resistance of the fracture due to pore pressure increase enabling the displacement of the fracture surfaces. After relief of the hydraulic pressure the hydraulic conductivity is permanently and irreversibly improved. However, in the absence of anisotropic stresses in the underground the rocks deform just elastically and hydraulic stimulation does not permanently improve the hydraulic conductivity (Stober 2011) because hydraulic fracture dilatation does not create the required misfits. Furthermore, even if tectonic stresses are present shearing is possible only for those fractures with an appropriate orientation relative to the stress ellipsoid.

The small displacements and shear movements of rock blocks generate mechanical vibrations in the underground. Because of the similarity to seismic tremors the small mechanical vibrations are known as micro-seismicity. The development of EGS

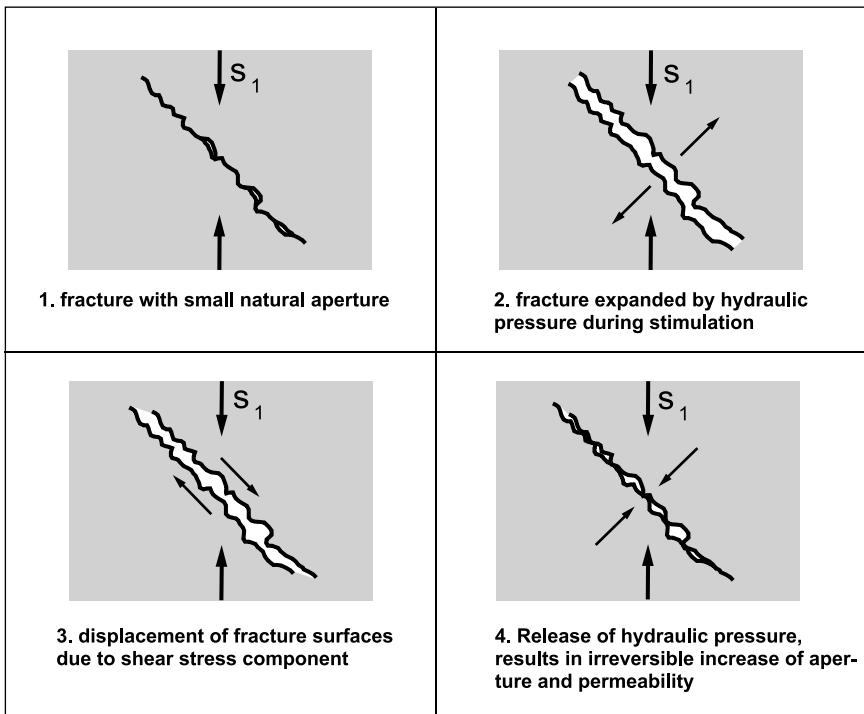


Fig. 9.2 Permeability increase as a result of hydraulic stimulation (self-propelling)

power plants inevitably requires reservoir stimulation, which is fundamentally associated with micro-seismicity. Micro-tremors are invariably coupled with successful stimulation measures. The natural stress-state of the underground in particular the magnitude of tectonic shear stresses controls the seismicity of an area. Hydraulic stimulation causes a stepwise relief and decay of naturally present stresses in the underground and micro-seismicity propagates slowly with the advancement of the pressure front of the injected water.

It is the objective of EGS development to keep the micro-seismic tremors at the surface as small as possible but the micro-structural effects in the reservoir maximal and hydraulic stimulation efficient. Chemical methods may be helpful in support of smooth deep geothermal system development. Experimental studies have been recently initiated, using new formulas for the chemical composition of the injection fluid and using various chemical additives to the surface fresh water normally used for reservoir stimulation (Portier et al. 2007). During the 1970ies so-called propping (usually quartz sand) have occasionally been added to the injection fluid during stimulation of crystalline basement reservoirs with the idea that the hard solid particles helped to keep fractures open (Smith et al. 1975; Schädel and Dietrich 1979). Today successful stimulation experiments have been carried out with inorganic acids (hydrochloric acid or mixtures of HCl and hydrofluoric acid, HF),

complexing substances (nitrilotriacetic acid, NTA) or organic acids (organic clay acid, OCA) (Genter et al. 2010). The purpose of the chemical stimulation is to remove or leach fine-grained mineral dust and carbonates from fracture surfaces. The method has been successfully used by the oil and gas industry for increasing well productivity for a long time. The first acidizing measures have been performed more than 100 years ago in limestone formations.

The hydrocarbon industry distinguishes between slickwater stimulation, stimulation with a high-viscosity fluid (additives: polymers or tensides) and acidization (Williams et al. 1979; Kalfayan 2008). Slickwater stimulation injects a large volume of a low-viscosity fluid ($\sim 1500 \text{ m}^3$) with about 100 t of suspended proppings (quartz sand, bauxite sand) to the reservoir. The wellhead pressures may reach about 700 bar. The proppings help to maintain the permeability improvement after stimulation. Proppings improve the hydraulic properties of fractures that have not undergone shearing during stimulation. The method is mainly used for slate. Stimulation with high-viscosity fluids requires much lower volumes of injected fluid (about 400 m^3). Also here about 100 t of proppings are usually suspended in the fluid for injection. The technique is mostly used for sandstones. Acid fracturing also applies up to 700 bar wellhead pressure but the fluid is injected with rapidly and strongly varying rates. The method aims to roughen the fracture surfaces and is used mainly in limestone and other carbonate rocks. The hydrocarbon industry uses stimulation techniques exclusively in sedimentary reservoir rocks in complete contrast to EGS development.

Stimulation of geothermal reservoirs can be carried out in sections of the wellbore and in separate isolated zones. The relatively new method helps avoiding hydraulic shortcuts and minimizes the chance to trigger unwanted seismic events.

Hydraulic stimulation techniques changed considerably over the last years. Currently the fluid injection rate is increased stepwise with a corresponding gradual increase of the injection pressure over an extended period of time. The procedure results in substantially larger volumes of injected fluids compared to the past. The subsequent shut-in is carried out stepwise with gradually decreasing injection rates and not as a sudden complete pumping stop. The procedures drastically reduce and control micro-seismicity associated with hydraulic reservoir stimulation.

Hydraulic stimulation measures must be accompanied by a monitoring program that records the micro-seismic signals at or close to the surface. Typically, geophones record ground movement in shallow monitoring wells that are placed around the deep stimulation well (Fig. 9.3). The seismic signals induced by the stimulation can be resolved in 3D and separated into the x–y–z components. The geophones record ground movements quantitatively. Interpretation of the data results in a 3D-image of the activated fracture volume.

This 3D-image of the seismic noise, however, includes only the fractures that experience shear movements. Open fractures without a shear stress component and other cavities that do not suffer shear displacement produce no seismic signal and remain quiet. Thus the geophones of the monitoring wells log merely the seismic active part of the entire fracture volume. The derived 3D-image may correspond to the real fracture volume but not necessarily. This condition is particularly evident

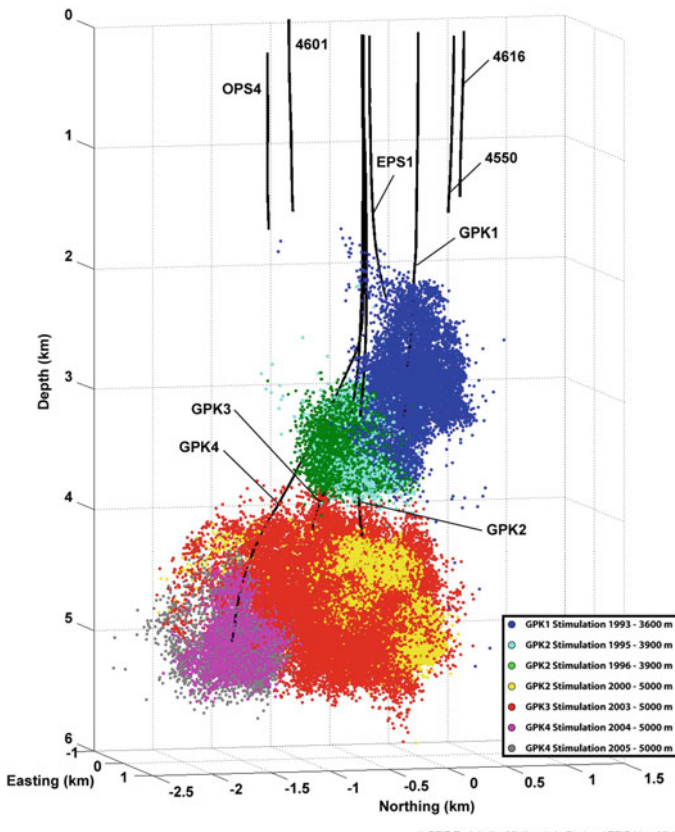


Fig. 9.3 Geophone recordings of seismic noise generated by hydraulic stimulation of the wells at Soultz-sous-Forêts. Note the position of four, about 1500 m deep monitoring wells (drawing by Nicolas Cuenot, with kind permission by A. Genter)

in wells that have been repeatedly stimulated. In this case the geophones receive seismic signals mostly from an outer zone around the previously stimulated fracture volume.

The created 3D-image of the activated fracture network is typically not spherical but anisotropic and ellipsoid shaped. The orientation of the created elongated fracture volume determines the target point for the second wellbore. For optimal hydraulic connection the second well is also stimulated (Fig. 9.3). The EGS development makes a great effort creating a zone of increased hydraulic conductivity, the heat exchanger, in the underground that is surrounded by low-conductivity rock. The longitudinal extent of the heat exchanger ranges over several hundred meters, the specific length depending on rock properties, the stress field, and the particulars of the injection procedures.

At the EGS project Soultz-sous-Forêts (Upper Rhine Rift) the natural fracture and fault system of the granitic reservoir rock is oriented parallel to the direction of the principal stress ($\sim 170^\circ$). The orientation of the stimulated fractures as recorded by geophysical borehole measurements excellently matches the direction of the regional stress field. The hydraulic stimulation has been very successful and massively increased the injectivity and the productivity of two wells. The well with the highest initial hydraulic conductivity showed the least response to stimulation. It is thought that the high primary conductivity was related to relatively few highly permeable fractures and faults (Baria et al. 2004; Tischner et al. 2007). The principal stimulation mechanism, fracture broadening followed by fracture displacement, is not efficient in this case.

Widening the natural fracture system for developing the underground heat exchanger requires very high pressures. The so-called opening pressure must be surmounted. Its magnitude depends on the lithostatic pressure and on the orientation of the controlling fracture system. Fluid flow rates do not significantly increase until the opening pressure is exceeded. An opening pressure of 170 bar wellhead pressure was required in gneiss at 4.4 km depth at the Urach EGS site. Slightly lower opening pressures were required in granite at 5 km depth at the Soultz-sous-Forêts EGS site.

At the Soultz-sous-Forêts EGS site maximum wellhead pressures of 180 bar resulted in injection flow rates of about 50 L s^{-1} . The maximum seismic response to the stimulation reached a magnitude of 2.9. Stimulation at the EGS site Basel, Switzerland, also located in the upper Rhine rift valley with injection flow rates of up to 63 L s^{-1} resulted in a wellhead pressure of 300 bar and a seismic response of up to a magnitude of 3.4. Stimulation of the well Habanero 1 at the EGS site in the Cooper Basin, Australia, with 350 bar wellhead pressure lead to injection flow rates of up to 40 L s^{-1} . The monitored seismicity reached maximum a magnitude of 3.7.

The summarized experience shows that reservoir stimulation in the deep crystalline basement with injection rates of some tens of L s^{-1} water and wellhead pressures of about 200–300 bar may cause seismic reactions above a magnitude of 3. The magnitude of the seismic reaction to stimulation depends on many factors and parameters including: The injection flow rate, the total volume of injected fluid (water), the properties of the initial natural fracture system, the maximum applied wellhead pressure, the duration of stimulation, the chemical composition of the injected fluid (water), the temperature and, critically, the rates of pressure changes (rates of pressure increase) (Nicholson and Wesson 1990; Bommer et al. 2006; Giardini 2009; Shapiro and Dinske 2009). However, the tectonic condition and the stress state of the underground are the key properties controlling micro-seismicity. How these many relevant properties and parameters interact at any given micro-seismic event is not yet fully understood. However, the concept of seismogenic permeability k_s defines an important derived parameter that relates the hydraulic properties of the reservoir to the chance of inducing seismicity by hydraulic stimulation (Talwani et al. 2007).

The reported stimulation related relatively high magnitudes of induced seismicity at some sites lead to the renouncement of some of these projects. The recent

procedures developed and used in hydraulic and chemical stimulation improved predictability and control of induced seismicity in EGS projects substantially (Sect. 11.1.6).

9.4 Experience and Coping with Seismicity

The stimulation efforts at Soultz-sous-Forêts required about 180 bar wellhead pressure for significantly improving hydraulic conductivity of the granitic reservoir rocks. The same efforts at the Basel EGS project, 150 km south of Soultz also in the Rhine graben, with 300 bar wellhead pressure triggered seismicity that scared the public and caused the abandonment of the project (Sect. 11.1.3). The EGS project Urach, about 170 km east of Basel, applied up to 660 bar wellhead pressure during stimulation experiments without causing perceptible seismicity (Stober 2011). The three very contrasting examples of seismic response to reservoir stimulation in the same region demonstrate the controlling importance of the existing stress field for the magnitude of triggered seismic events. In the Basel region differential stress is high, in the Urach region very low. Therefore seismic events, natural earthquakes, occur more often and with higher magnitude in the Basel region than in the Urach, or also the Soultz area. This can be seen on earthquake frequency maps, e.g. the European-Mediterranean Seismic Hazard Map.

The early (1993) stimulation efforts at the Soultz-sous-Forêts site triggered seismicity at 3600 m as shown on Fig. 9.3 (Cornet et al. 1997). The initial rock permeability was very low 10^{-17} m^2 (Evans et al. 2005). The permeability rapidly increased with increasing injection pressure and the first micro-seismicity was observed when the differential pressure exceeded 5 MPa. Seismicity increased dramatically above 6 L s^{-1} injection rate because permeability reached the critical values for seismogenic permeability k_s (Talwani et al. 2007). Further increase of injection rates was followed by decreasing seismicity. Finally the differential pressures stabilized at 9 MPa. The pressure did not further increase with increasing injection rates. The successful stimulation increased the injectivity, defined as flow rate per unit differential pressure, from 0.6 to 9.0 L s^{-1} per MPa (Evans et al. 2005). The high injectivity resulted in non-Darcian fluid flow (Kohl et al. 1997).

The reservoir at the Basel and Soultz sites is in granitic basement, at the Urach site in metamorphic gneissic basement. The rheology of granite is controlled by quartz and feldspar and it responds to stress predominantly by brittle deformation. The response of the mica-rich gneisses at Urach to stress has a strong ductile component even at temperatures of 200 °C and lower.

Hydraulic reservoir stimulation is a well-established method in the geothermal and hydrocarbon industry that has been applied for decades and worldwide (Bencic 2005). Seismic monitoring of stimulation efforts has not become standard routine for EGS development before the Basel incident in 2006. This is also a consequence of the necessity to build EGS power plants near the potential user and consumer of co-produced thermal energy (in contrast to the hydrocarbon industry that produces

oil and gas mostly in uninhabited areas). Thus geothermal EGS project must drill wellbores near cities and other densely populated regions where the public is alarmed and scared if transitory seismicity from stimulation measures can be sensed at the surface.

In regions with natural seismicity necessary stimulation works may interact with natural stress release processes. There induced seismicity is the result of the step-by-step reduction of stored stresses that may not have been released without the high-pressure fluid injection (or at least not at this time). The possibility for induced seismicity and its potential magnitude at a specific site can, to some degree, be assessed, predicted and partly controlled. Efficient seismicity control requires complete and constant readings and supervision of the injection pressure and a seismological monitoring in the close and further surroundings of the site. If observed seismicity increases above a site-specific threshold value injection pressure and flow rates, respectively, must be reduced. However, the details of interacting mechanisms for triggering seismic tremors by hydraulic stimulation are not yet fully understood and the topic requires further basic research (Sect. 11.1).

9.5 Recommendations, Notes

It is a great advantage if, during the reconnaissance survey of the selected site, an exploration well can be drilled to the crystalline basement that later needs to be stimulated. In areas where the reservoir rocks in the basement are covered with a sequence of sedimentary rocks geophysical exploration methods such as gravimetric, magnetic and magnetotelluric techniques cannot detect the presence, structure and orientation of fracture and fault systems in the basement. Even state-of-the-art seismic investigations may discriminate flow-relevant structures in the underground only vague and uncertain. Very prominent, thick and flat-lying fault zones may give a weak signal and can be imaged under favorable circumstances (Schuck et al. 2012).

The drilled exploration well may later be used as a monitoring well for seismic signals during stimulation works in the EGS deep wells and further on during operation of the plant to record and observe seismicity. Furthermore, the exploration well can be used for hydraulic tests in the crystalline basement, producing reliable and needed data of the hydraulic conductivity and the storage properties of the basement prior to stimulation. Water (fluid) samples collected in the exploration drillhole give valuable information on the composition of the deep fluid (Bucher and Stober 2010). The chemical data from the uncontaminated basement fluid permits prediction of possible scale formation and corrosion and facilitate development of prevention strategies at the very beginning of the project. Regrettably, most projects drill the first bore as future production well for economic reasons and forgo the exploration well. Unfortunately, after completion of the production well hydraulic reservoir stimulation is often the next work on the agenda. The natural hydraulic and hydrochemical reservoir conditions remain unexplored and unknown. The lack of these crucial data may later threaten the entire project or may cause unnecessary high extra costs.

The pretended savings from waiving the exploration well may change suddenly to economic disaster.

It is strongly recommended to set up a seismic monitoring network at a very early stage of EGS project development. The network should continuously record all seismic signals above a magnitude of 1.0 (Richter scale) in a 10 km range around the site of the planned power plant. The monitoring must continue during drilling of the boreholes, the stimulation measures and later during the operation of the plant. The focal mechanism of seismic events and the orientation and magnitude of the principal stresses can be derived from geophysical fault-plane solutions. These data help designing an optimal reservoir geometry. Increased induced seismicity typically occurs related to hydraulic injection and stimulation rather than in the later continuous operation of the plant. However, plant shutdown for maintenance or the subsequent resumption of operation may cause induced seismicity.

The underground in a wide range around the planned stimulation measures needs to be stable and major fault zones should be spacially avoided. Prominent fault zones may react preferentially on stimulation in regions with increased natural seismicity. They often contain abundant and thick zones of fine-grained crushed rock fragments and clay from cataclasis (brittle fracturing and shearing). Some of these materials may swell during stimulation thus sealing water-conducting structures and resulting in a decreasing hydraulic conductivity.

Drilling engineering and future stimulation measures benefit greatly from a good knowledge of the petrography and the mineralogical composition of the rocks. Deformation properties of rocks depend on rock type and type and modal amount of rock-forming minerals. The patterns of brittle deformation in granites are controlled by the properties of the dominant minerals quartz and feldspar. Granite is more regularly and more strongly fractured than metamorphic basement, predominantly gneiss. Gneisses are typically rich in mica and hornblende in addition to quartz and feldspar. The deformation pattern in gneiss is strongly influenced by the mechanical properties of mica and the mica-related gneissic fabric. Gneiss tends to form fewer though more pronounced fault zones parallel to the foliation (gneiss fabric).

Drilling of the wellbore and the upcoming planned hydraulic stimulation of the reservoir profit much from a profound knowledge of hydrostatic, lithostatic and anisotropic pressures in the subsurface. This requires extensive pressure gauging, investigation of in-situ stress indicators (wellbore deformation, wellbore breakouts, hydraulic fracturing) and recording natural pore pressures. These data and information must be ascertained before beginning with the systematic stimulation works. The data are essential for a rigorous assessment of the completed reservoir stimulation and also for the sound appraisal of the observed seismicity.

Oriented drillcores should be taken in the first EGS wellbore from the planned reservoir rocks. The cores give insight into micro-fracture orientation, water-conducting structures and into the macro-fracture network and fault zone properties. The cores can be used for determining mechanical and physical parameters of the rocks (Young's modulus, Poisson number, density, acoustic impedance data, thermal conductivity) and for mineralogical examination. Alternatively some of these data can be produced by optical or acoustic borehole deformability tests with borehole jacks.

Equally important is a qualified geophysical logging of the wellbore (e.g. gamma-log, temperature-log, electrical conductivity-logging, Caliper-log) (Sect. 13.2).

Temperature is of course a central parameter for EGS thus its reliable assessment critical. Measured temperature data from great depth are scarce. It is thus necessary to extrapolate existing temperature data from shallow ground to EGS reservoir depths. The temperature at depth can be computed from the thermal conductivity of the rocks and the known vertical heat flow. The extrapolation assumes that the hydraulic conductivity of the rock is low enough that advective heat transport by groundwater flow can be ignored. Temperature estimates can be improved by considering the internal heat production of the rocks also (Eq. 1.5b).

Water samples for hydrochemical analysis must be collected (with a downhole sampler if necessary) before the start of hydraulic stimulation and the injection of large volumes of fluid. Knowing the chemical composition of the original fluid residing in the fracture pore space of the reservoir is a precondition for planning efficient scaling and corrosion prevention (Sect. 15.1). If the reservoir is wasted with injection fluid first and the original fluid condition is unknown, system development can react to a difficult fluid composition after damage has already occurred. Water in the crystalline basement is normally highly saline at typical reservoir depths of some km. Total dissolved solids (TDS) range from some tens to some hundreds of g L⁻¹. The major solutes are sodium, calcium and chloride (Bucher and Stober 2000, 2010). Some fluids contain appreciable amounts of dissolved gasses (e.g. CO₂, N₂, CH₄, H₂S). Planning and construction of the surface installations require knowledge of the chemical composition and properties of the produced thermal fluid for efficiently coping with scaling and corrosion and handling the aggressive, saline and possibly gas-rich hot fluid.

The initial hydraulic tests should be of short duration and should be run with low flow rates. They should not cause substantial pressure changes. Therefore the slug test is the ideal choice of the first test method (Sect. 14.2). In the next step constant rate pumping or injection tests, depending on hydraulic conductivity, supply the necessary information on natural flow regime and the quantification of the natural hydraulic conductivity (Sect. 14.2). Pressure variations in these tests should be kept relatively small. A short step-drawdown test (step test) may follow. It gives first data on the well efficiency. Then pre-simulation tests can be designed using these derived test data. Pre-simulation tests provide extensive information and experiences on the reaction of the underground on fluid injection. With these hydraulic experiments the system developer is slowly and carefully approaching the concept of the actual site-optimized stimulation methods and putting them into practice.

Knowledge of the natural stress field and the orientation of fault planes in this stress field are indispensable for many activities at the drilling site (Sect. 11.1.6). The regional orientation of the present principal stress can be taken from the world stress map (world-stress-map.org). It must be kept in mind, however, that the local situation at the EGS site may differ from the information given on the map. Also the stress field varies with depth and its depth-dependence is not necessarily reflected by the data given on the world stress map. The orientation of open fractures may change with depth because of the depth-dependence of the stress field. With increasing depth open

fractures tend to be vertically oriented because of the increasing confining pressure at a constant or decreasing horizontal stress component (Brown and Hoek 1978; Stober and Bucher 2015) (Fig. 9.4). In the deep wellbores at Rittershoffen (Sect. 8.7.1) and Soultz-sous-Forêts (Sect. 9.2) the stress field changed significantly below 2000 m depth (Valley and Evans 2003; Hehn et al. 2016).

The success of stimulation measures depends on the existence of a suitable natural fracture network and an appropriate stress field. If nothing can be stimulated in a stress free reservoir an EGS project will crash. If stimulation was possible, the final hydraulic properties of the reservoir decide on the economic success of the project.

Hydraulic short cuts and an extreme stimulation of singular fractures or fault zones can be prevented or the danger minimized by section-by-section stimulation

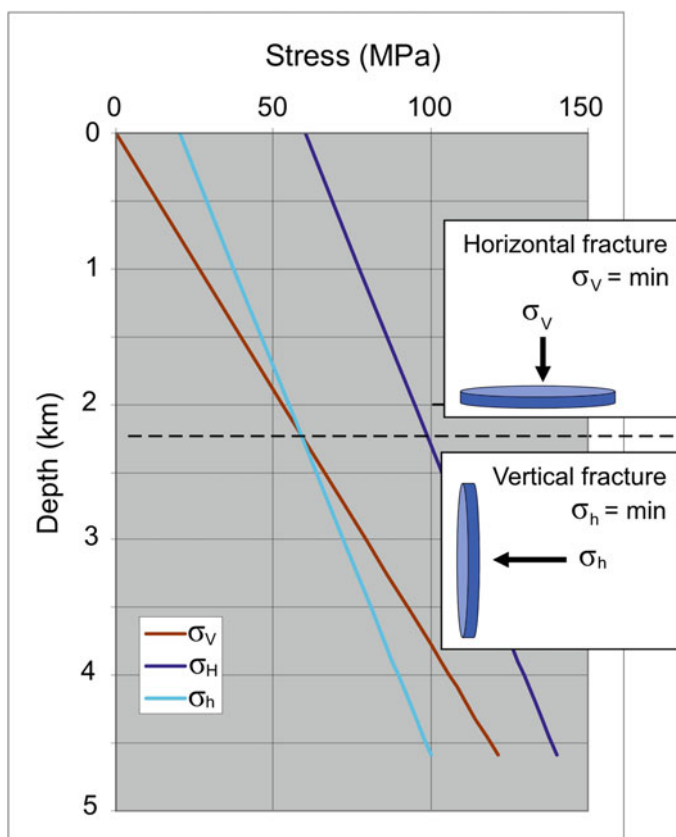
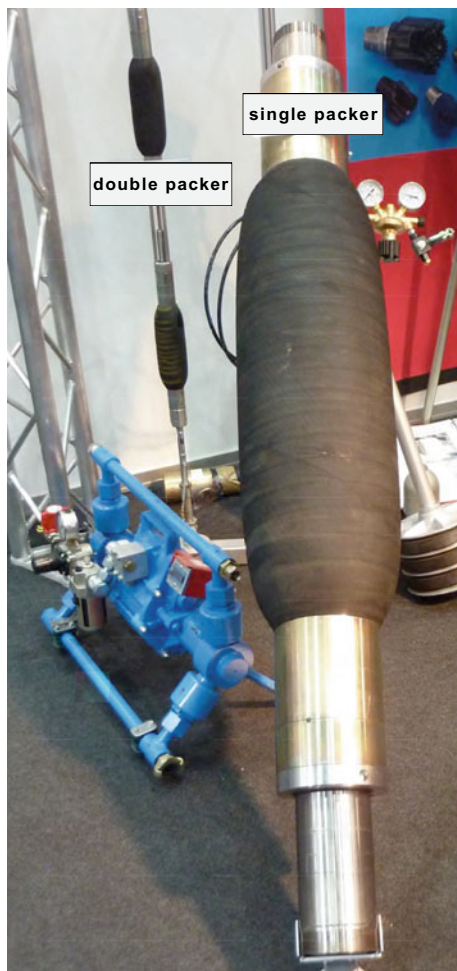


Fig. 9.4 Adjustment of the orientation of open fractures with depth resulting from a changing stress field after data from Brown and Hoek (1978). σ_V minimum principal stress (compressive stress) horizontal fracture, σ_h minimum principal stress vertical fracture, σ_H maximum principal stress (tensile stress). Changing from preferred horizontal to vertical fracture orientation at about 2.2 km depth

of isolated portions of the reservoir. Packer and cement bridges (concrete plugs) are used for the hydraulic isolation of defined rock volumes (Fig. 9.5, 14.2). A wide range of packer systems is available in all dimensions for different wellbore diameters and special applications and different needs.

Target points of the wells are planned in accordance with the natural stress field at reservoir depth. It can be expected that the stimulated rock volume, the future hot rock heat exchanger, develops in direction of the stress ellipsoid. The definition of the optimal distance of the bottom holes of the two wells, the quantification of the thermal range and the prediction of the life cycle and ageing of the system require knowledge of thermo-physical rock parameters (thermal conductivity, density, heat capacity, heat production rate).

Fig. 9.5 Examples of a single packer and a double packer. A packer consists of a central pipe and a rubber mantle. The rubber mantle can be pressed to the borehole wall after it has been positioned in the wellbore by inflating or by compressing it



If the EGS project uses exclusively vertical wellbores, the surface installation will be spread over distances of several hundreds of meters and these space requirements must be taken into account. An unrelated note: Vertical bores have the advantage that the handling of thermal casing expansion during production of thermal water is considerably simpler.

References

- Armstead, H. C. H. & Tester, J. W., 1987. Heat Mining, E. & F. N. Spon, London.
- Baria, R. A. & Green, S. P., 1989. Microseisms: A Key to Understanding Reservoir Growth. In: Baria, E. R. (ed.): Hot Dry Rock Geothermal Energy, Proc. Camborne School of Mines International Hot Dry Rock Conference, 363–377, Robertson Scientific Publications, London.
- Baria, R., Michelet, S., Baumgärtner, J., Dyer, B., Gerard, A., Nicholls, J., Hettkamp, T., Teza, D., Soma, N. & Asanuma, H., 2004. Microseismic monitoring of the world largest potential HDR reservoir. In: Proceedings of the 29th Workshop on Geothermal Reservoir Engineering, Stanford University, California.
- Batchelor, A. S., 1977. Brief summary of some geothermal related studies in the United Kingdom. In: 2nd NATO/CCMS Geothermal Conf. 22–24 Jun., Section 1.21, pp. 27–29, Los Alamos.
- Bencic, A., 2005. Hydraulic Fracturing of the Rotliegend Sst. in N-Germany - Technology, Company History and Strategic Impotance. In: SPE Technology Transfer Workshop, Suco, Zeit Bay Field.
- Bommer, J. J., Oates, S., Cepeda, J. M., Lindholm, C., Bird, J., Torres, R., Marroquin, G. & Rivas, J., 2006. Control of hazard due to seismicity induced by a hot fractured rock geothermal project. *Engineering Geology*, 83 (4), 287–306.
- Brown, D. W., 2009. Hot Dry Rock geothermal energy: Important lessons from Fenton Hill. Proc. Thirty-Fourth Workshop on Geothermal Reservoir Engineering, Stanford University, Stanford, Cal, USA, 4.
- Brown, E.T. & Hoek, E., 1978. Trends in relationships between measured rock in situ stresses and depth. *Int. J. Rock Mech. Min. Sci. Geomech. Abstr.*, 15, 211–215.
- Brown, D. W., Duchane, D. V., Heiken, G. & Hriscu, V. T., 2012. Mining the Earth Heat: Hot Dry Rock Geothermal Energy. Springer Verlag, Heidelberg, 657 p.
- Bucher, K. & Grapes, R., 2011. Petrogenesis of Metamorphic Rocks, 8th edition. Springer Verlag, Berlin Heidelberg. 428 pp.
- Bucher, K. & Stober, I., 2000. The composition of groundwater in the continental crystalline crust. In: Stober, I. & Bucher, K. (eds.). *Hydrogeology in crystalline rocks*, 141–176, KLUWER Academic Publishers.
- Bucher, K. & Stober, I., 2010. Fluids in the upper continental crust. *Geofluids*, 10, 241–253.
- Caine, J. S. & Tomusiak, S. R. A., 2003. Brittle structures and their role in controlling porosity and permeability in a complex Precambrian crystalline-rock aquifer system in the Colorado Rocky Mountain Front Range. *GSA Bulletin*, 115(11), 1410–1424.
- Cornet, F., Helm, J., Poitrenaud, H. & Etchecopar, A., 1997. Seismic and aseismic slips induced by large-scale fluid injections. *Pure and Applied Geophysics*, 150, 563–583.
- Dash, Z. V., Murphy, H. D. & Cremer, G. M., 1981. Hot Dry Rock Geothermal Reservoir Testing: 1978 to 1980. Los Alamos National Laboratory Report LA-9080-SR.
- Dezayes, C., Gentier, S. & Genter, A., 2005. Deep Geothermal Energy in Western Europe: The Soultz Project (Final Report). BRGM/RP-54227-FR, 51 pp.
- Duchane, D. V. & Brown, D. W., 2002. Hot Dry Rock (HDR) Geothermal Energy Research and Development at Fenton Hill, New Mexico. *GHC Bulletin*, 32, 13–19.
- Duffield, R. B., Nunz, G. J., Smith, M. C. & Wilson, M. G., 1981. Hot Dry Rock, Geothermal Energy Development Program, pp. 211, Los Alamos National Laboratory Report.

- Ernst, P. L., 1977. A Hydraulic Fracturing Technique for Dry Hot Rock Experiments in a Single Borehole, pp. 7, Soc. Petrol. Engineers of AIME, Dallas, Texas.
- Evans, K., Genter, A. & Sausse, J., 2005. Permeability creation and damage due to massive fluid injections into granite et 3.5 km at Soultz: 1- Borehole observations. *J. Geophys. Res.*, 110, 1–19.
- Genter, A., Keith, E., Cuenot, N., Fritsch, D. & Sanjuan, B., 2010. Contribution to the exploration of deep crystalline fractured reservoir of Soultz of the knowledge of enhanced geothermal systems (EGS). *C. R. Geoscience*, 342, 502–516.
- Genter, A., Cuenot, N., Goerke, X., Melchert, B., Sanjuan, B. & Scheiber, J., 2012. Status of the Soultz geothermal project during exploitation between 2010 and 2012. *Proc. Thirty-Fourth Workshop on Geothermal Reservoir Engineering*, Stanford University, Stanford, Cal, USA, 11.
- Gérard, A., Genter, A., Kohl, T., Lutz, P., Rose, P. & Rummel, F., 2006. The deep EGS (Enhanced Geothermal System) project at Soultz-sous-Forêts (Alsace, France).- *Geothermics*, pp. 473–483.
- Giardini, D., 2009. Geothermal quake risks must be faced. *Nature*, 462, 848–849.
- Hehn, R., Genter, A., Vidal, J. & Baujard, C., 2016. Stress field rotation in the EGS well GRT-1 (Rittershoffen, France). *European Geothermal Congress*, 10 p., Strasbourg, France.
- Huenges, E., 2010. *Geothermal Energy Systems: Exploration, Development, and Utilization*, pp. 486, Wiley-VCH Verlag GmbH & Co. KGaA, Berlin.
- Ingebretsen, S. E. & Manning, C. E., 1999. Geological implications of a permeability-depth curve for the continental crust. *Geology*, 27, 1107–1110.
- Kalfayan, L., 2008. Production enhancement with Acid Stimulation, 2nd Edition. PennWell Corp., 270 pp.
- Kappelmeyer, O. & Rummel, F., 1980. Investigations on an artificially created frac in a shallow and low permeable environment.- *Proc. 2nd. International Seminar on the Results of EC Geothermal Energy Research*, pp. 1048–1053, Strasbourg.
- Kohl, T., Evans, K. F., Hopkirk, R. J., Jung, R. & Rybach, L., 1997. Observation and simulation of non-Darcian flow transients in fractured rock. *Water Resources Research*, 33, 407–418.
- Lund, J. W., 2007. Characteristics, Development and utilization of geothermal resources. *Geo-Heat Centre Quarterly Bulletin*, 28, 1–9.
- Mazurek, M., 2000. Geological and Hydraulic Properties of Water-Conducting Features in Crystalline Rocks. In: Stober, I. & Bucher, K. (eds.). *Hydrogeology of Crystalline Rocks*. Kluwer Acad. Publ, 3–26.
- MIT, 2007. *The Future of Geothermal Energy, Impact of Enhanced Geothermal Systems (EGS) on the United States in the 21st Century*, Massachusetts Institute of Technology, U.S.A.
- Mouchot, J., Genter, A., Cuenot, N., Scheiber, J., Seibel, O., Bosia, C. & Ravier, G., 2018. First year of Operation from EGS geothermal Plants in Alsace, France: Scaling Issues.- *Proceedings, 43rd Workshop on Geothermal Reservoir Engineering*, Stanford University, SGP-TR-213, 12 p., Stanford/California.
- Nicholson, C. & Wesson, R. L., 1990. Earthquake Hazard associated with deep well injection - a report to the U.S. Environmental Protection Agency, pp. 74, U.S. Geological Survey Bulletin.
- Pauwels, H., Fouillac, C. & Fouillac, A. M., 1993. Chemistry and isotopes of deep geothermal saline fluids in the Upper Rhine Graben: Origin of compounds and water-rock interactions. *Geochimica et Cosmochimica Acta*, 57, 2737–2749.
- Pearson, C., 1981. The Relationship Between Microseismicity and High Pore Pressures During Hydraulic Stimulation Experiments in Low Permeability Granitic Rocks. *Journal of Geophysical Research*, 86(B9), 7855–7864.
- Pine, R. J. & Batchelor, B. A., 1984. Downward migration of shearing in jointed rock during hydraulic injections. *Int. J. of Rock Mechanics Mining Sciences and Geomechanical Abstracts*, 21(5), 249–263.
- Portier, S., André, L. & Vuataz, F.-D., 2007. Review on chemical stimulation techniques in oil industry and applications to geothermal systems. In: Engine, pp. 32, CREGE, Neuchatel, Switzerland.
- Rybach, L., 2004. EGS – State of the Art. In: *Tagungsband der 15. Fachtagung der Schweizerischen Vereinigung für Geothermie*, Basel.

- Schädel, K. & Dietrich, H.-G., 1979. Results of the Fracture Experiments at the Geothermal Research Borehole Urach 3. In: Haenel, R. (ed): The Urach Geothermal Projekt (Swabian Alb, Germany), pp. 323–344, Schweizerbart'sche Verlagsbuchhandlung, Stuttgart.
- Scheiber, J., Seibt, A., Birner, J., Genter, A., Cuenot, N., Moeckes, W., 2015. Scale Inhibition at the Soultz-sous-Forêts (France) EGS Site: Laboratory and On-Site Studies.- Proceedings World Geothermal Congress, 12 p., Melbourne, Australia.
- Schuck, A., Vormbaum, M., Gratzl, S., Stober, I. 2012. Seismische Modellierung zur Detektierbarkeit von Störungen im Kristallin.- Erdöl, Erdas, Kohle, 128 (1), S. 14–20, Urban-Verlag, Hamburg/Wien.
- Shapiro, S. A. & Dinske, C., 2009. Fluid-induced seismicity: Pressure diffusion and hydraulic fracturing. *Geophysical Prospecting*, 57, 301–310.
- Smith, M. C., Aamodt, R. L., Potter, R. M. & W., B. D., 1975. Man-made geothermal reservoirs. *Proc. UN Geothermal Symp.*, 3, 1781–1787.
- Stober, I., 1986. Strömungsverhalten in Festgesteinsaquiferen mit Hilfe von Pump- und Injektionsversuchen (The Flow Behaviour of Groundwater in Hard-Rock Aquifers – Results of Pumping and Injection Tests) (in German). *Geologisches Jahrbuch, Reihe C*, 204 pp.
- Stober, I., 2011. Depth- and pressure-dependent permeability in the upper continental crust: data from the Urach 3 geothermal borehole, southwest Germany. *Hydrogeology Journal*, 19, 685–699.
- Stober, I. & Bucher, K., 2005a. The upper continental crust, an aquifer and its fluid: hydraulic and chemical data from 4 km depth in fractured crystalline basement rocks at the KTB test site. *Geofluids*, 5, 8–19.
- Stober, I. & Bucher, K., 2007b. Erratum to: Hydraulic properties of the crystalline basement. *Hydrogeology Journal*, 15, 1643. (*See further correction in Stober & Bucher 2015*).
- Stober, I. & Bucher, K., 2007a. Hydraulic properties of the crystalline basement. *Hydrogeology Journal*, 15, 213–224.
- Stober, I. & Bucher, K., 2015. Hydraulic conductivity of fractured upper crust: insights from hydraulic tests in boreholes and fluid-rock interaction in crystalline basement rocks. *Geofluids*, 15, 161–178.
- Talwani, P., Chen, L. & Gahalaut, K., 2007. Seismogenic permeability, k_s . *Journal of Geophysical Research*, 112, B07309. <https://doi.org/10.1029/2006JB004665>.
- Tischner, T., Schindler, M., Jung, R. & Nami, P., 2007. HDR Project Soultz: Hydraulic and seismic observations during stimulation of the 3 deep wells by massive water injections. In: Proceedings, thirty-second workshop on geothermal engineering, Stanford University, pp. 7, Stanford, California.
- Valley, B. & Evans, K., 2003. Strength and elastic properties of the Soultz granite. – In: Zürich, E. (Hg.): Synthetic 2nd year report, Zürich, Switzerland: 6 S., Zürich (Eidgenöss. Techn. Hochsch.).
- Williams, B. B., Gidley, J. L. & Schechter, R. S., 1979. Acidizing Fundamentals. Society of Petroleum, 273 pp.
- Zobak, M. D., Barton, C. A., Brady, M., Castillo, D. A., Finkbeiner, T., Grollimund, B. R., Moos, D. B., Peska, P., Ward, C. D. & Wipurt, D. J., 2003. Determination of stress orientation and magnitude in deep wells. *International Journal of Rock Mechanics and Mining Sciences*, 40, 1049–1076.

Chapter 10

Geothermal Systems in High-Enthalpy Regions



Krafla flash steam power plant, Iceland

Most of the electrical power produced from geothermal resources originates from regions with extreme geothermal gradients and very high surface heat-flow (Sects. 1.3, 3.4). The regions reach high ground temperatures at shallow depth and are typically found in active volcanic areas, young rift systems and similar geological settings. These geothermal sources are also known as high-enthalpy reservoirs or high-enthalpy systems with reference to the high heat content of the reservoir fluid used as heat transfer substance. High-enthalpy systems produce electrical power directly from dry steam or from a high-temperature two-phase fluid in flash-steam plants (Sect. 4.2, 4.4).

10.1 Geological Features of High-Enthalpy Regions

High-enthalpy regions are typically related to a specific plate tectonic situation and to magmatism at plate boundaries. Fluid temperature may exceed 200 °C at depths of a few hundred meters or less. High-enthalpy geothermal regions are typically associated with active volcanism or recently active volcanism (Sect. 1.2). High-enthalpy regions with significant geothermal power production include:

- Destructive plate boundary, subduction related volcanism: Pacific Ocean (ring of fire): Japan, Philippines, California, New Zealand. Indian ocean: Malaysia. Other: Italy.
- Constructive plate boundary, extension rift: Oceanic: Iceland. Continental: Kenya, Ethiopia.

However, not every high-enthalpy region is suitable for geothermal utilization.

High-enthalpy fields are typically characterized by the presence of active or recently active volcanoes, young lava flows and surface phenomena including hot springs, fumaroles and mud pots, at some localities also geysers (Fig. 10.1). The geothermal surface activity relates to the transfer of thermal energy from molten rocks or solidified but still hot lava to infiltrating meteoric water (e.g. Henley and Ellis 1983; Clyne et al. 2013; Pope et al. 2016). The fluids, gases and liquids, expelled at the surface often change composition over short distances as a result of very heterogeneous subsurface conditions.

Most of the hot water expelled at the surface is heated meteoric water. Some magmatic water may be contributed to the fluid in andesitic volcanic systems, whereas basaltic volcanoes release not much magmatic H₂O steam. At shallow depth volcanic fluids are mostly various gasses, including CO₂, H₂S, HCl, HF and others. The volcanic gasses mix with steam and oxygen from the atmosphere in the near surface zones of the geothermal system resulting in a multitude of chemical reactions changing the composition of the fluids and altering the rock matrix. At greater depth the pore space of the volcanic rocks is saturated with liquid hot water of 200–300 °C. The water in the liquid zone has typically a low pH (5 or lower) and contains predominantly dissolved NaCl. The hot water is very rich in dissolved silica and tends to form silica sinter when it cools at the surface. The hot water may cool along its ascent

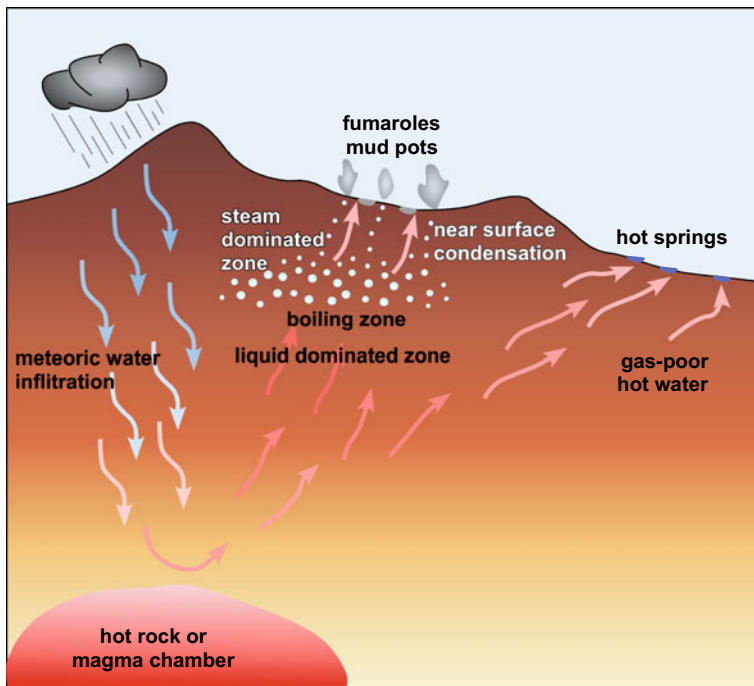


Fig. 10.1 Schematic high-enthalpy region showing the development of typical surface phenomena from heat transfer from volcanic heat source to infiltrating meteoricwater (inspired by Clyne et al. 2013)

path and may reach the surface in the liquid state at various temperatures forming hot springs. If the liquid water rises rapidly to the surface conserving its thermal energy it starts to boil at some depth in a liquid—steam transition zone (Fig. 10.1). Steam and volcanic gases dominate the zone above the boiling zone. The total dissolved solids in the residual liquid phase in the boiling zone increases passively. Most of the steam condenses to liquid water in the condensation zone near the cool surface. Some steam and gas reaches the surface and is expelled in fumaroles. If the ejected gasses contain predominantly H₂S the discharge vents are termed solfataras.

In contact with atmospheric oxygen the H₂S gas oxidizes to elementary sulfur and forms characteristic yellow vents with sulfur crusts and needles (Fig. 10.2). Reaction 10.1 describes this process:



Further oxidation of sulfur produces sulfur dioxide (SO₂), which dissolves in liquid water producing first sulfurous acid (H₂SO₃) and ultimately sulfuric acid (H₂SO₄) from the net-reaction H₂S + 2O₂ = H₂SO₄. The strong acid forms often together with HCl and HF contained in volcanic gasses a very aggressive low-pH

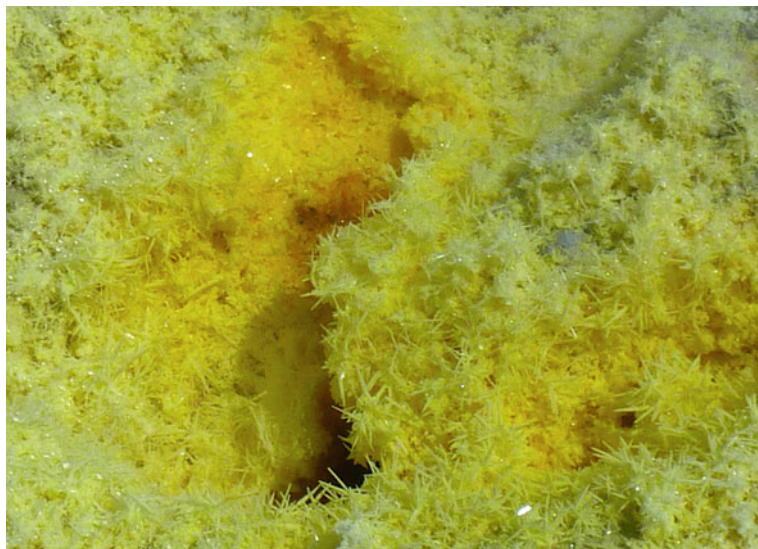


Fig. 10.2 Sulfur needles crystallized around a volcanic gas vent (solfatara), Volcano island, Italy. Size of needles 2–3 cm

liquid that reacts with the primary igneous minerals. The pH of condensation liquids is often below 2 and may be as low as 0 (1 m H⁺). The resulting solid Al-rich reaction products, mostly a variety of clay minerals, form the mud slurry present in and characteristic of mudpots (Fig. 10.3). Because of the very low pH of such hot waters in streams and ponds at the surface they often contain extremely high concentrations of Al and Fe. The various degassing processes in volcanic zones occur often side-by-side in vent fields with a large number of discharge vents (fumaroles, solfataras, mudpots, hot springs). In these fields the rock and soil surface is typically hydrothermally altered to colorful muddy patches ranging from red, orange, gray, yellow and bluish in color (Fig. 10.4).

Moffettes are a subtype of fumaroles with discharge vents producing CO₂ gas at temperatures below 100 °C occurring in the marginal areas of geothermal high-temperature fields. The CO₂ may be accompanied by other volcanic gases (e.g. H₂S, CH₄, He). Depending on the H₂O content moffettes range from dry gas vents to warm CO₂-rich mineral springs with (Ca)–Na–HCO₃ waters at pH at about 7. At the discharge point of the warm spring travertine is a typical deposit consisting of CaCO₃.

Hot gas-poor waters from the liquid zone may migrate over considerable distances to the surface where they discharge in hot springs. The mineralized pH-neutral waters still may reach 100 °C at the surface and the ascend paths can be followed to greater depth at some springs. The spring water is supersaturated with respect to several minerals and typically forms sinter deposits in the spring or at its rims (Fig. 10.5).



Fig. 10.3 Boiling mudpot at Námafjall, Iceland. Mudpots form from the reaction of very acid condensation liquids and the minerals of volcanic ashes and rocks. The resulting typically gray slurry contains the solid reaction products, mostly clay



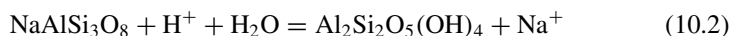
Fig. 10.4 Colorful surface alteration of rocks and volcanic ashes in a high-temperature geothermal field, Hveradalir, Iceland



Fig. 10.5 Hot spring with deposits of siliceous sinter. The ascend pipe connecting to the heat source is clearly visible. Yellowstone National Park, Wyoming/USA

Siliceous sinter deposits may contain amorphous silica, opal, or chalcedony. Sinter also may contain carbonate minerals in addition to silicates and oxide minerals.

In the liquid-dominated zone also alkaline hot water is often present ($\text{pH } 8\text{--}10$). It forms as a consequence of ongoing hydrolysis of silicate minerals and reactive volcanic glass. The saline Na-Cl waters are typically very Ca-poor, Mg may be extremely low, fluoride is often elevated and Al may be unusually high if pH is at 9 or above. The process leading to such high-pH waters can be pictured by the hydrolysis reaction of albite:



The reaction breaks down the albite component of the primary igneous plagioclase forming kaolinite or generally clay minerals. It consumes H^+ thus increasing the pH of the residual liquid and produces Na^+ thereby raising total dissolved solids.

Geysers are hot springs in volcanic high-temperature fields with intermittent discharge of steam and boiling water ejected from an underground reservoir. The phenomena occur relatively rarely in high-temperature geothermal field because the required suitable hydrogeological conditions and structures underground occur at only at a few places on the earth. Geysers need a 20–30 m deep discharge chimney, which narrows in the upper part and connecting to an underground water chamber. The chamber fills with cool groundwater, which is then heated by the hot rocks at depth. The water in the chimney remains at temperatures below boiling because of the



Fig. 10.6 Castle geyser with prominent sinter cone. Yellowstone National Park, Wyoming/USA

cooled rocks near the surface. After some time the water in the groundwater chamber starts boiling and the produced steam rapidly increases pressure. After reaching the critical threshold pressure the boiling water is ejected from the chamber through the chimney to the surface. The geyser erupts a column of water and steam into the air. The Strokkur geyser in Iceland typically ejects a 20 m high hot water column every 5–10 min. The Steamboat geyser at the Yellowstone National Park (USA) produces the highest eruptions worldwide. The frequent ejection of boiling mineralized water typically produces silica-rich deposits (geyserite) around the vent that may evolve to sinter cones (Fig. 10.6).

The interaction of hot aggressive fluids with lavas and ashes produces a large variety of alteration minerals. The type of produced minerals depends on the composition of the attacked volcanic rocks. In basaltic rocks a large variety of zeolites including stilbite, heulandite, mesolite, scolecite and others. The zeolites fill pores of lava thus reducing pore space. Clays are typical hydrothermal alteration products and occur in all types of volcanic rocks. The type of clay minerals depends on the type of altered volcanic rock, the alteration temperature and the composition of the fluid. At temperatures around 200 °C basaltic rocks may contain the zeolite wairakite as alteration product and epidote, prehnite and amphibole characterize high temperature alteration at 250–350 °C (e.g. Henley and Ellis 1983; Bucher and Grapes 2011).

Because of the heterogeneous structure of the underground in high-enthalpy fields, the composition hot water used for geothermal applications can differ considerably. However, fluids may vary also depending on external factors related to the specifics of the site location. Geothermal fluid can be derived from meteoric water

Table 10.1 Composition of geothermal fluids from two power plants in Iceland in mg L⁻¹. Hellisheiði is located inland, the fluid is derived from meteoric water. Reykjanes is located at the ocean, the fluid is seawater derived (data from Remorozza 2010; Giroud 2008)

	Hellisheiði	Reykjanes
SiO ₂	659	613
Na	201	9172
K	33	1294
Ca	0.4	1516
Cl	199	17,402
SO ₄	8	14

(e.g. Figure 10.1), however, at locations close to the ocean the fluid can be related to seawater infiltration (Table 10.1).

10.2 Development, Installation and Initial Commissioning of Power Plants

In volcanic geothermal regions the underground can be extremely heterogeneous regarding temperature distribution, rock type and structure, permeability, structure of pore space, liquid or gas present in the pore space, composition of the fluids present in the pore space, and other ground properties. This can make the development of geothermal installations in high-enthalpy regions challenging.

The considered geothermal application depends on the temperature and type of hot fluid present underground. In high-enthalpy fields high temperature fluids are at 250 °C or more. These fluids are typically used for electrical power production and for district heating. Intermediate temperature applications utilize fluids in the range of 150–250 °C. Fluids in the range of 100–150 °C are considered boiling low-temperature fluids and used mostly for district heating. 50–100 °C liquids are used for low-temperature applications such as greenhouse heating.

Geothermal power plants in high-enthalpy fields produce hot fluids, the heat-transfer medium, from a multitude of wells, at many sites from dozens of drillholes. Each of the wells typically provides about 5 MW_{el}. In large high-temperature fields like e.g. The Geysers (California, USA) electrical power is produced from several power plants each powered by many wells (Brophy et al. 2010).

Experience from several geothermal fields showed that continuous extraction of hot fluid from the ground might cause a gradual decrease of steam pressure in the fluid reservoir. This pressure loss gradually reduces power production. Today the produced geothermal fluids are reinjected into the reservoir along with additional water from distant sources at some sites (e.g. industrial wastewater) thereby supporting the natural recharge of the reservoir with meteoric water (Sect. 4.4, 10.3). Because of the typically high hydraulic conductivity of volcanic ground (Sect. 10.1) the number of drilled reinjection wells can be much lower than the number of production wells.

Injection wells are being drilled to relatively shallow depth just being sufficient for maintaining the required steam pressure for power production.

The use of thermal energy obtained from high-enthalpy fields typically follows the cascade principle (Sect. 8.6; Fig. 8.14). The primary purpose of extracting thermal energy from the ground is electric power generation. However, thermal energy is also distributed by district heating grids serving bigger settlements or urban quarters. Thermal energy is also produced for direct industrial use. The remaining thermal energy contained in low-T water is used for agricultural purposes or for greenhouse heating. Greenhouses also use geothermally produced electricity for powering artificial lighting extending daylight time (Sect. 4.4; Fig. 10.7).

All relevant material and data regarding the geology at the considered site must be compiled during the exploration phase prior to the development of a high-enthalpy field. The extensive exploration studies include geological, structural, hydrochemical, thermal and geophysical investigations. Hydrochemical studies for example provide data on reservoir temperatures from aqueous geothermometers (Sect. 15.2), thermal surveys supply ground temperature and heat flow density data. The collected data capture the structure, depth and extent of the thermal reservoir. Also the temperature distribution, porosity structure and fluid flow structure can be derived from the collected data. Important geophysical techniques (Sect. 13.1) used for the exploration of magmatic-volcanic systems include resistivity measurements (e.g. TEM,



Fig. 10.7 Greenhouses near Flúðir Iceland heated with geothermal hot water

transient electromagnetic method) and the magnetotelluric method (MT) (Björnsson et al 2005; Christensen et al. 2006; Rosenkjær 2011). The methods obtain the structure and extent of the reservoir from the distribution of the electrical resistivity underground. Gravity and aeromagnetic data further improve the detailed structure of the reservoir. The regularly recorded local and regional seismicity provide the necessary knowledge of ongoing tectonic and magmatic activity. Geophysical exploration techniques are indispensable for providing essential data on the properties of the subsurface (Barkaoui 2011; Árnason et al. 2000).

During the investigation of the site a few exploration wells drilled to shallow depths (< 350 m) grasp and confirm the presence and potential of the underground reservoir. If the survey is successful the exploration wells can be integrated into the plant system during development of the site as production wells for hot water used in district heating or as injection wells reinforcing the fluid reservoir at depth.

The further development of the geothermal site is based on the results of the exploration phase and typically takes place in steps of 10–30 MW_{el} so increasing the installed power every 2–3 years. Production wells are typically drilled to 1500–2500 depth, at some sites also to 3500 m depth depending on the structure of the hot fluid reservoir. After completion of each development step the plant reassumes operation with increased capacity. Many sites use the produced thermal energy according to the cascade principle (electricity, district heating, etc.) from the beginning.

The operating phase follows the commissioning of the plant. Typically further wells must be drilled during regular operation. The new wells replace wells with decreasing production rates resulting e.g. from scaling and mineral deposits in the reservoir. Also wells with massive corrosion damages must be exchanged. The replacement wells are often drilled to greater depth in the reservoir than the original wells. An increased knowledge of the structure of the reservoir during operation time may suggest different target points for new wells. Decreasing vapor pressure in the reservoir during operation of the plant may also require a deeper well position.

High-temperature wells are typically drilled in four sections in addition to the standpipe installation by rotary drilling (chapter 12). The first 50–100 m is drilled with a large diameter (20"–24") and with a cemented backfill casing (18" or 20"). Then drilling continues to 200–600 m depth with a smaller diameter (17½" or 20"). The casing (13½" or 18") should have a cemented backfill at least in the deeper portion. The third section from 600 to 1200 m depth is typically drilled with a diameter of 12½" or 17½". Finally the last section, the so-called production casing has a diameter of 95/8" or 133/8" and must be cemented. The final production section (8½" or 12½") is drilled into the target horizon of the reservoir. A perforated liner (7" or 95/8") (Fig. 12.1) installed from the production pipe stabilizes the drillhole. The liner ends 20–30 m above bottom hole compensating the thermal expansion during operation. Fluid production takes place across the liner and from there passing through the casing to the surface. The number of drilled sections may increase depending on the local geological conditions and the depth of the target horizon in the reservoir. Directional drilling is routinely used for sinking production wells in high-enthalpy fields (chapter 12). At a certain depth of the vertical borehole further drilling is directed sideways into the hot fluid reservoir. Directed drilling typically begins from

the production section with deflection angles increasing in 2° to 3° steps every 30 m until final 20° – 40° (e.g. Sveinbjörnsson 2014). At the surface the well is sealed and secured with a wellhead. The wellhead is covered and the installations protected by a wellhouse (Fig. 10.8a, b).



Fig. 10.8 Wellhead in the high-enthalpy field Nesjavellir, Iceland. **a** Wellhouse, **b** Wellhead inside a wellhouse together with wellhead equipment

A new well is extensively tested after completion for evaluating its yield. The drastic pressure drop during testing produces large volumes of hot steam, which escape from the wellbore with high speed accompanied by an enormous noise that can be heard several km away from the well. In order to reduce these noise emissions the hot steam leaving the well is directed from the wellhead to a muffler or silencer (Fig. 10.9a, b). The muffler is also required during cleaning of the wells after longer downtimes. The furiously bursting steam removes sinter deposits thus helping to maintain yield. Also steam separators of the plant are equipped with silencers (Thorolfsson 2010).

Wells in high-enthalpy fields may require yield improving stimulation measures. This may particularly become necessary if fluid conducting structures have been clogged by the drilling operation. Well stimulation may simply help improving the hydraulic connection to the reservoir. The applied procedures are similar to those presented in Sect. 8.5. An additional technique repeatedly injects cold water into the well. Occasionally stimulation of a certain section of the well is carried out using packers.

10.3 Main Types of Power Plants in High-Enthalpy Fields

10.3.1 Dry Steam Power Plant

If the well of a high-enthalpy field produces primarily dry hot steam the geothermal fluid free of liquid water can be guided directly to the steam turbine. The turbine drives a generator where the mechanical energy is converted to electrical energy (Fig. 4.14b). Water may be present at reservoir depth but not at the wellhead because of the pressure-dependence of boiling. For example the boiling temperature of pure water at 100 bar pressure (about 1000 m depth) is close to 300 °C compared to 100 °C at the surface. For salt-rich water or brines the boiling temperature is even higher. Therefore hot dry steam shoots out from the well with high velocity under decompression of a hot fluid reservoir (180–350 °C). Thus the production of the fluid does not require a pump. The hot steam arriving at the wellhead is conducted to the turbine, which is driven by the steam from a group of wells. Dry steam plants are the most efficient and simplest electricity-producing geothermal installations. However, not many geothermal sites are suitable for this kind of utilization globally. Examples for such systems are the high-enthalpy fields “The Geysers” in northern California (USA) (Sect. 4.4), Larderello (Italy), or the Ulubelo geothermal field (Indonesia).

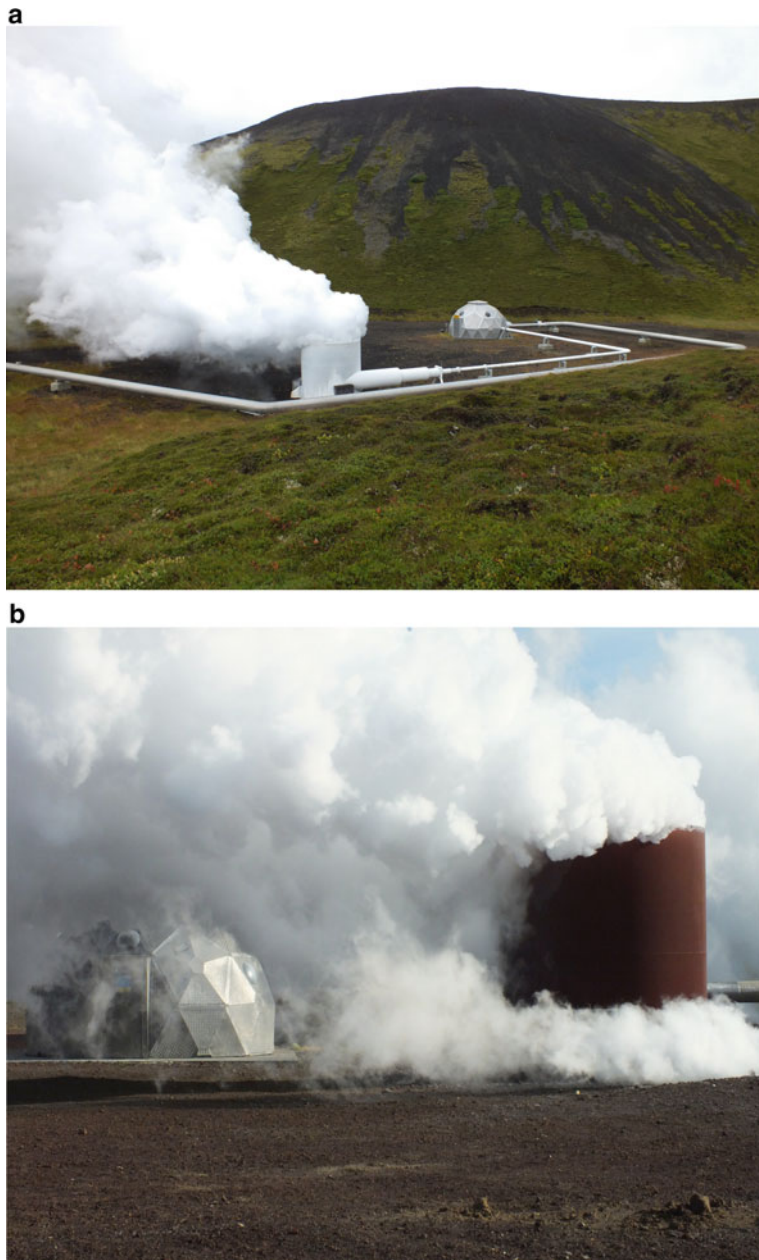


Fig. 10.9 Muffler (silencer) attached to the wellheads of geothermal wells. **a** Wellhouse and Muffler in use at the Nesjavellir plant, Iceland, **b** working muffler next to a wellhouse at the Krafla plant, Iceland

10.3.2 Flash Steam Power Plants

Most geothermal plants are flash steam plants (DiPippo 2012). This type of plant is used if the reservoir temperature and pressure is somewhat lower and the produced steam at the wellhead is wet rather than dry. This is the most common type of situation in high-enthalpy fields. In these plants the wet hot steam from the production well passes a separator unit (Fig. 10.10) where the hot steam is separated from the liquid phase, hot water or brine. The hot two-phase fluid of several production wells flows to one separator. From the separator the steam can be directed to the turbine (Fig. 10.11a). Usually the steam passes through an additional moisture separator just before it reaches the turbine house. Connected generators convert the mechanical energy produced by the turbines into electrical energy (Fig. 10.11b). As an example, the Krafla geothermal power plant (northern Iceland) uses 30 MW turbines serving 37.5 MVA electrical generators. In a high voltage substation the generated electricity at 11 kV is transformed to 132 kV for the transmission line.

The separated liquid phase is normally high-TDS brine locally with high concentrations of dissolved solids that are potentially harmful to the environment (toxic or radioactive for example). However, the liquids are reinjected into the reservoir thereby preventing gradual pressure loss over time and subsidence of the ground in the area above the geothermal reservoir.



Fig. 10.10 Steam separators at the flash steam plant Hellisheiði plant (Iceland)

Fig. 10.11 Turbine in plant hall at the Hellisheiði plant (Iceland). **a** Mitsubishi turbine 45 MW at 3000 rpm. Input 7.5 bar steam (out 0.1 bar). Steam at 168 °C. **b** Generator unit in the foreground at the Hellisheiði plant (Iceland). In the background a turbine (to the left)—generator (yellow) system in a plant hall housing 4 such units

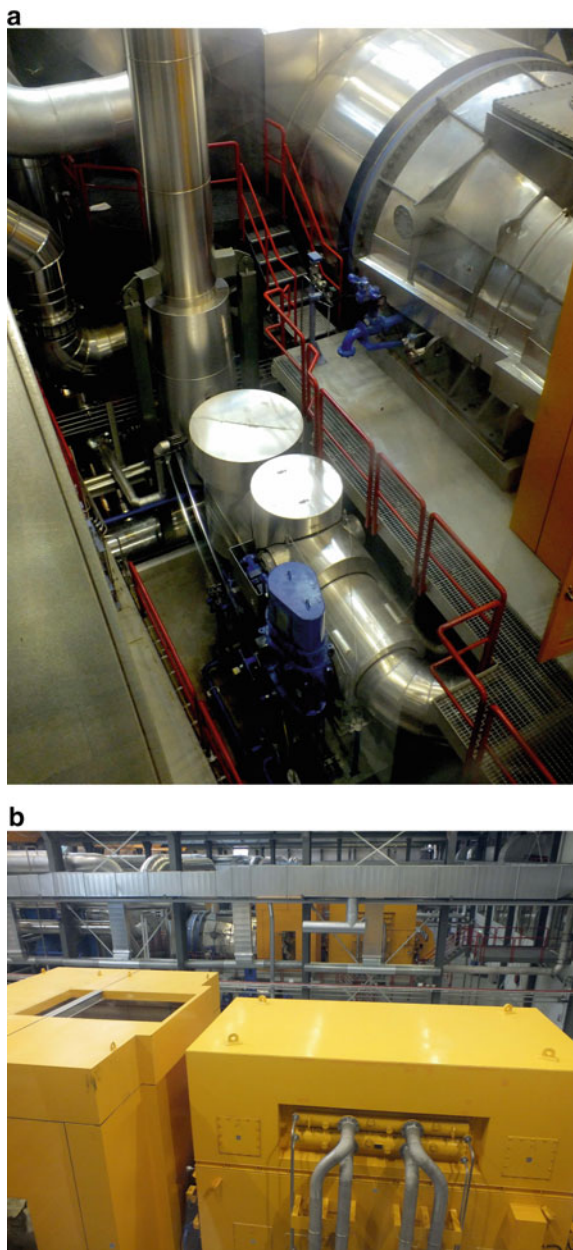




Fig. 10.12 Steam condenser and ejector towers at Nesjavellir (Iceland)

After leaving the turbine the hot steam passes through a condenser where is converted into the liquid phase (Fig. 10.12). The condensed still hot water is pumped to cooling towers (Fig. 10.13). Uncondensed steam in the condenser escapes via an ejector to the atmosphere (Fig. 10.12). At many plants the hot water from the condensers is used for district heating purposes after adjusting it to a preferred constant temperature. Water condensed from steam has low concentrations of dissolved solids but may contain problematic gases such as H₂S at some sites. Cold water from cold-water wells is needed for preparing district heating liquid together with water derived from the condensed steam.

The flash steam power plants described in Sect. 4.4 (Fig. 4.14a) are using the steam leaving the separator only. The plants can be characterized as single flash steam plants. Modern power plants produce additional steam from the liquid phase leaving the primary separator. The plants can be characterized as double or even triple flash steam plants if they produce steam from the liquid phase leaving the secondary separator. The installations are about 15–25% more efficient than single flash steam plants. However, they require additional investments and costly maintenance. An example for a double flash steam plant is the Hellisheiði geothermal power plant in Iceland (303 MW_{el}, 400 MW_{th}) the second largest geothermal plant in the world owned and operated by ON power, Reykjavik. 303 MW_{el} are produced by 6 turbines 45 MW and a 33 MW turbine. For the Reykjavik district heating grid the plant produces 133 MW_{th}.



Fig. 10.13 Cooling tower at the Hellisheiði plant (Iceland) with steam separators in the foreground

The Hellisheiði plant exploits of 500 kg s^{-1} hot steam of 180°C from 30 production wells 2000–3000 m deep in the reservoir of the Hengil central volcano. In the surroundings of the power plant more than 60 wells have been drilled in the rugged cavernous and caved underground of the volcano. Most wells were drilled as inclined holes. The produced fluid contains $\text{NaCl}-\text{NaHCO}_3$ at low concentrations ($\text{Cl} < 200 \text{ mg kg}^{-1}$). The total dissolved solids range from 1000 to 1500 mg kg^{-1} (Tab. 10.1). Depending on the location of the wells and its local fluid reservoir some fluids contain variable amounts of H_2S and CO_2 (Ármannsson 2016).

Cogeneration plants such as Hellisheiði or Nesjavellir in South-Iceland (Fig. 10.14) require cold-water wells producing cold groundwater that is stored in tanks. The cold water receives thermal energy from the steam leaving the turbines in the condenser unit associated with the turbine (Fig. 10.11). The water is heated to $85-90^\circ\text{C}$ and subsequently guided to low-pressure gas extractors where it boils and gives off dissolved oxygen gas. The procedure protects the pipes of the district heating grids from corrosion. The conditioned hot water leaves the power plant with 83°C and reaches the domestic and industrial consumer in Reykjavik ~20 km west of the plants after 27 h flow-time loosing only 1.8°C temperature. The pre-insulated underground pipeline from the hot water storage tank at the plant in Hellisheiði transfers thermal water at a rate of 2250 L s^{-1} to the city. Hot water from the wells produced from the geothermal field cannot be used directly for district heating grid because of its content of dissolved solids and gasses. The fluids are therefore prone

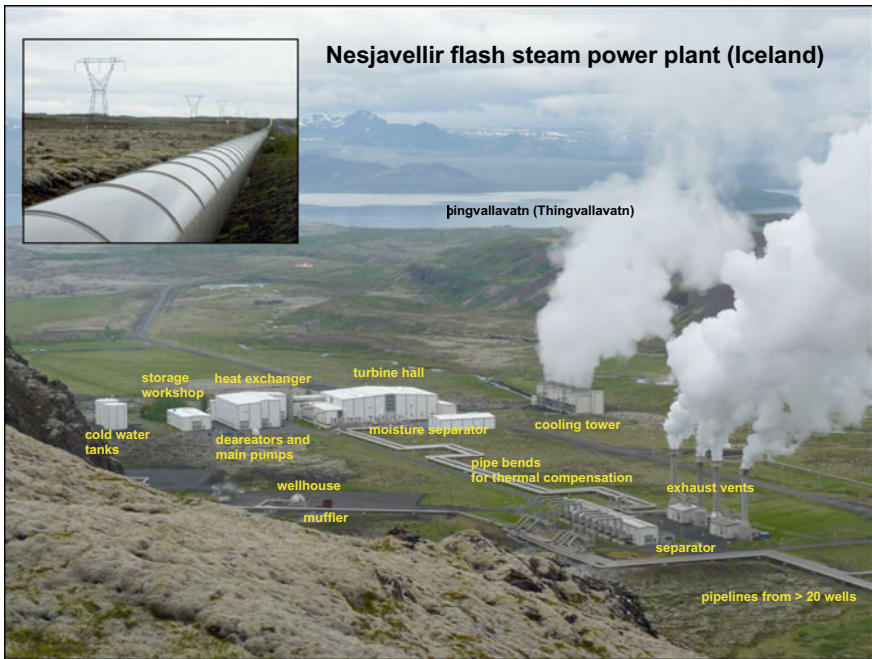


Fig. 10.14 Nesjavellir geothermal plant overview (Iceland). Note the extra pipe bends for compensation of temperature related length changes. Pipes are flexibly placed on rolls or slide rails. Inset: Power line and hot water pipeline transporting energy to Reykjavik

to scale formation and corrosion (Gunnlaugsson 2008a, b). Degassing of H₂S from the produced geothermal fluid requires an elaborate special treatment and reinjection of the toxic gas to the thermal reservoir (Gunnarsson et al. 2011).

10.4 Evolving Deficiencies, Potential Countermeasures

During operation of a geothermal power plant typical failings that may develop include: Loss of steam pressure in the reservoir, subsidence of the ground, increased seismicity, sinter formation and scales in the plant components, emission of poisonous and annoying foul-smelling gases, damages to the vegetation, and others. The cited flaws do not necessarily always occur, not automatically combined and not at each site. Geothermal energy installations in high-enthalpy fields are typically not located in the immediate vicinity of settlements. However, the defects may impair residents indirectly through increased costs for the energy consumed. In most volcanic areas the significant background seismicity is familiar to the residents. In

the following we present real defects that occurred at particular sites, the countermeasures undertaken and the interaction of various effects at these geothermal sites.

Steam pressure loss: The geothermal field “The Geysers” was hampered by a significantly reduced reservoir steam pressure from about 1987. Pressure loss resulted from steadily increasing steam extraction for additional plants producing progressively more electricity. As a consequence some of the plants decommissioned (Brophy et al. 2010). Detailed cause studies then showed that reservoir steam pressure decreased by about 1 bar per year already from as early as 1966. Planning countermeasures in 1991 suggested injection of external water into the reservoir for stabilizing reservoir steam pressure and ensuring sustainability of the field. From 1997 the plans were implemented and water from surface water bodies and treated wastewater brought into the reservoir. Presently treated urban wastewater from Santa Rosa and Clear Lake are injected at a rate of about 800 kg s^{-1} supporting the reservoir. The reservoir remediation retarded the decreasing energy production of the plants. Eventually production increased and decommissioned plants resumed operation (Brophy et al. 2010).

Seismicity: Active microseismicity has been observed from 1975 in the geothermal field “The Geysers”. In the early years of operation of the geothermal plants that is before the injection of external water to the reservoir commenced the seismic activity correlated with the steam extraction rate thus with power production although some of the cooled and condensed steam has been partly reinjected to the reservoir already at this time. The observed seismicity (Sect. 11.1) resulted mostly from subsidence caused by reduced fluid pressure in the reservoir as a consequence of high fluid extraction rates and to a smaller degree also from reinjection of cool fluids (condensed steam). Increasing volumes of injected external water in the late 1990s resulted in gradually increasing seismicity. Both the number of recorded seismic events and the maximum of measured magnitudes rose continuously. A seismic event of magnitude $M_L = 5.0$ has been recorded for the first time in December 2016. The increasing seismicity and the intensified magnitudes have been related to the thermal contraction resulting from reservoir cooling by the injection of external wastewater at high rates (Nicholson and Wesson 1990; Brophy et al. 2010).

Surface subsidence damages: Damages caused by surface subsidence resulting from yearlong extraction of geothermal fluids from reservoirs underground have been reported from several power producing geothermal fields. Besides “The Geysers” also the high-enthalpy field Larderello and the nearby Travale-Radicondoli field in northern Italy have been affected by surface subsidence. For the central area of the Larderello a subsidence of 170 cm has been documented (ENEL 1995). However, observed seismicity was not correlated with the injection rate (Batini et al. 1985).

Five geothermal fields of the seismically active Taupo volcanic zone on the North Island of New Zealand are used for geothermal power production (Rowland and Sibson 2004). The geothermal “Wairakei Power Station” near the high-enthalpy field Wairakei was in 1958 the first flash-steam power plant worldwide that got into operation (Thain 1998). Presently the Wairakei field has 55 production wells, 6 injection wells and 50 monitoring sites. All wells are distinctly less than 700 m

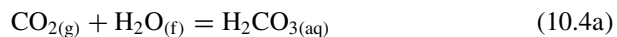
deep. Presently, the total electrical power output of the plant is 181 MW_{el}. Beginning in the early 1980s, the operation of the plant caused a significant decrease of steam pressure in the shallow reservoir with drastic negative commercial impact. Also the temperature of the produced fluid decreased slightly. The observed surface subsidence associated with the pressure loss caused no significant damages though. Subsequently new successful and profitable wells developed dry-steam reservoirs that compensated the lost power from the flash-steam field (Thain 1998). However, the produced fluids contained environmentally problematic components. At the surface new steam and gas vents opened and the near-surface ground temperature increased (Allis 1981). Like in other high-enthalpy fields increased fluid reinjections should stop or slow down the negative development. The fluid injections, however, also resulted in increasing microseismicity. The various experiences made in the Wairakei field were used for developing a new strategy for fluid reinjection that optimally considered the local properties of the field and all technical parameters including injection depth, location, temperature at depth, injection pressure, injection rates and many more (Mizuno 2013; Sherburn et al. 2015).

During operation of the geothermal plant on the Reykjanes peninsula in western Iceland an increase of the near-surface ground temperature and increased emission of CO₂ gas at the surface have been detected by monitoring measurements. It remained undecided if these manifestations were caused by loss of fluid pressure in the reservoir as a consequence of plant operation or if they had a natural cause (Óladóttir and Friðriksson 2015).

The geothermal power plant Hellisheiði, SW-Iceland, (Sect. 10.2) was planned and operated with sustainability in mind from the beginning. Reinjection of condensed steam thus avoiding fluid pressure loss in the reservoir was a prime objective. During progressive development and commissioning of the plant more than 60 wells have been drilled. 17 injection wells are used for maintaining the fluid pressure in the reservoir and for preventing surface subsidence. During well drilling seismicity with magnitudes M_L = 2 – 3 occurred at some locations. Other wells did not show seismic activity during drilling. The observed seismicity during the development stage was typically related to loss of drilling mud connected to drilling large cavities or open fractures or linked to high-pressure fluid injections during well tests after finishing well drilling. This induced seismicity was weak and confined to the development stage. Later, during operation of the plant and increased production and reinjection of fluid seismicity generally increased in the entire region and reached a magnitude M_L = 4.4 in 2011 (Hjörleifsdóttir et al. 2019). Hellisheiði then developed an elaborate strategy for fluid injection and successfully reduced seismicity.

Gas emissions: The steam produced for power production in high-enthalpy fields always contains some non-condensable volcanic gasses such as CO₂ and H₂S (Sect. 10.1). These gases are typically corrosive to the metals of the technical plant components, promote material fatigue and crack formation, or intensify scaling and sealing of conductive fractures in the reservoir (Sect. 15.3). The gas emissions are also of environmental concern and their release to the atmosphere compromises the environmental friendliness of geothermal power production.

In the year 2006 the CarbFix project started on the Hellisheiði geothermal field in SW Iceland with the objective of reducing the CO₂ gas emissions to the atmosphere. Shortly afterwards the SulFix project with the purpose of reducing H₂S emissions was initiated at Hellisheiði. The basic concept of both programs intends to separate the problematic gasses and reinject them to the fluid reservoir where they react with the rocks and precipitate as carbonate and sulfide minerals. The CO₂ and H₂S sequestration projects started with the installation of a pioneering gas separation unit (Gunnarsson et al. 2015). A special oxygen-free process dissolves the two gasses in liquid water from the plant. The efficiency of the process depends on *P*, *T* and the salinity of the water (Aradóttir et al. 2015). The two basic dissolution reactions produce uncharged complexes in the aqueous solution (aq):



The final distribution of carbon and sulfur to charged species depends on the pH of the aqueous solution at *P* and *T*:

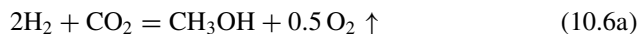


The process efficiently dissolves the two gasses in an aqueous solution (Eqs. 10.4, 10.5) and drastically reduces gas leakages. The two gases are captured in two different fluids. The carbon and the sulfur fluid are pumped to the reservoir separately preferably beneath sealing rocks. The dissolution of CO₂ and H₂S in water decreases the pH of the solution (Eqs. 10.4b, c; 10.5b, c) thereby increasing its reactivity with basaltic material in the reservoir. From 2014 on the CO₂-rich fluid was pumped to the basaltic rocks at 30–80 °C from 400 to 800 m deep wells. Data from a nearby monitoring station showed an outcome of the sequestration of 80–90% of the carbon fixed in carbonate minerals already in the first year of operation of the installation. Rock samples from cored wells showed that carbonate minerals (iron-bearing calcite, dolomite and magnesite) formed after short reaction times (Clark et al. 2020). The CarbFix program showed that CO₂ gas in fluid can be rapidly and permanently sequestered in reactive basaltic rock material.

The H₂S-rich aqueous solution from the plant (Eq. 10.5) has been pumped to deeper parts of the reservoir (>800 m) at a temperature of 270 °C starting from 2015 in the context of the SulFix program. Laboratory experiments and geochemical models

suggest that sulfide minerals (e.g. pyrrhotite FeS and pyrite FeS₂) should grow from dissolved H₂S by fluid-rock interaction in a basaltic reservoir considerably faster than the carbonate minerals from CO₂ (Aradóttir et al. 2015; Clark et al. 2020).

An alternative method for reducing CO₂ emissions from geothermal power plants has been established at Grindavík on the Reykjanes peninsula (SW-Iceland). CO₂ co-produced with steam by the Svartsengi geothermal power plant is transferred to the nearby George-Olah plant, the worldwide largest carbon dioxide—methanol plant. In operation since 2011 the plant produces 2 million liter methanol per year. It is planned expanding the production to 5 million liters per year. In addition to methanol (CH₃OH) the plant also produces hydrogen (H₂). Both products represent renewable fuels. Methanol is produced by the catalytically controlled reaction 10.6a.



and the required H₂ from the electrolysis of water (reaction 10.6b)



Water electrolysis requires a large amount of energy, which is supplied by the Svartsengi geothermal power plant. Oxygen produced by both reactions is released to the atmosphere. Both processes show that geothermal energy can be stored in fuels, here methanol and hydrogen, for later use (Garrow 2015). The innovative uses of energy from Svartsengi geothermal plant show that high-enthalpy fields have the potential for a commercially beneficial transformation of energy to renewable fuels.

Mineral scales: The most common minerals forming scales in high-enthalpy fields are various forms of silica (SiO₂) and Ca-carbonate (CaCO₃). Occasional deposits of heavy metal sulfides (Cu, Zn, Pb) have been observed (Sect. 15.3).

An impressive example of amorphous silica precipitation from geothermal waters is the geothermal spa “Blue Lagoon” on the Reykjanes peninsula in SW-Iceland (Fig. 10.15). The “Blue Lagoon” formed originally as an offshoot of the nearby geothermal power plant Svartsengi. The plant discharged warm, saline residual water in a highly permeable lava field for seepage. The seawater-derived water leaving the plant is highly supersaturated with respect to several solid phases including amorphous silica, chalcedony and quartz. The solids that precipitated from the water clogged the pore space and drastically reduced the permeability of the ground with the consequence that a permanent lake formed with turbid white warm water. Today the volume of discharge water is strictly limited thereby controlling the size of the lake. The main phase precipitating from the residual water is amorphous silica forming white crusts along the shore and white mud at the bottom of the lake. The lake water contains abundant floating white very fine amorphous silica particles giving the water its characteristic turbid whitish-blue appearance (Fig. 10.15).

Because heat extraction from the reservoir fluid in the plant the residual water cooled and its supersaturation with respect to amorphous silica drastically increases (SI_{as} ≫ 0). In addition, steam removed from the produced deep fluid in the separators of the flash-steam plant (Sect. 10.2) further increases silica concentration of the fluid



Fig. 10.15 Blue Lagoon on Reykjanes peninsula, SW-Iceland. The geothermal power plant Svartsengi in the background

and increases amorphous silica saturation in addition. For example: Separated steam from a high-enthalpy reservoir may contain 5 mg L^{-1} total dissolved solids (TDS) whereas the residual liquid may have a TDS of more than 45 g L^{-1} . The main dissolved components of the liquid are Na, Cl, Ca and K (Giroud 2008). Dissolved SiO_2 can be as high as $800\text{--}900 \text{ mg L}^{-1}$ (by comparison: 25°C water saturated with quartz contains 6 mg L^{-1}). The liquid phase of the geothermal fluid is also often enriched in B, F and Hg. Therefore the residual fluids are preferably returned to the reservoir also for disposal-related reasons.

Silica scales are a general and serious problem in high-enthalpy fields. For many geothermal plants the degree of supersaturation with respect to amorphous silica represents the limiting parameter for the attainable power production. If the geothermal fluid is cooled in the production process below a critical threshold value silica scales become uncontrollable with the exception of an indefensible effort. Ironically sinter material of amorphous silica is a sought-for resource.

The degree of supersaturation can be expressed by the saturation index (SI_{as}) for amorphous silica, which is the log of the difference of the concentration of silica in the actual fluid and its concentration at (metastable) equilibrium with amorphous silica (in mol kg^{-1}) at a given P and T . Consequently if $\text{SI}_{\text{as}} = 0$ the fluid has no driving force for scale formation. $\text{SI}_{\text{as}} = 0.3$ means that the solution is 2 times oversaturated with amorphous silica. The corresponding silica concentrations at 250°C and 100 bar are: $\text{SI}_{\text{as}} = 0$, $\text{SiO}_2 = 1174 \text{ mg kg}^{-1}$. If a fluid with $\text{SI}_{\text{as}} = 0$ at 250°C containing 1174 mg kg^{-1} dissolved silica is cooled to 100°C the fluid $\text{SI}_{\text{as}} = 0.45$. It is 2.8 times

oversaturated with silica. If the fluid is cooled to 80 °C the fluid in equilibrium with silica ($SI_{as} = 0$) contains 322 mg kg⁻¹ SiO₂ only. Thus 852 mg kg⁻¹ silica scales will form when the 250 °C reservoir fluid is cooled to 80 °C.

However, many factors control the effective amount of silica scales formed in the plant including the pH of the fluid. Silica solubility increases drastically in alkaline high pH fluids (Sect. 15.2). In addition to the thermodynamic limits to silica solubility the precipitation of silica scales is a dynamic also kinetically controlled irreversible process. If a fluid is oversaturated with respect to amorphous silica ($SI_{as} > 0$), the silica phase does not immediately and spontaneously form. First the silica colloids must be nucleated and the first very small colloids accrete to larger particles with a large active surface area and surface charge. Maturation and further increase of particle size by polymerization produce the final silica scale. Note that the stable solid silica phase is crystalline quartz and that amorphous silica is a metastable phase more soluble than quartz. A 250 °C hot liquid fluid in metastable equilibrium with amorphous silica has a $SI_{qz} = 0.51$, it is 3.24 times oversaturated with quartz. However, the stable phase quartz does not normally form because the kinetics of the quartz forming processes is much slower than that for amorphous silica. Silica scales in geothermal waters are also influenced by the presence of biomass at $T < \sim 110$ °C (Tobler et al. 2008).

Methods for avoiding or reducing silica precipitation commonly follow the lines (Brown 2011):

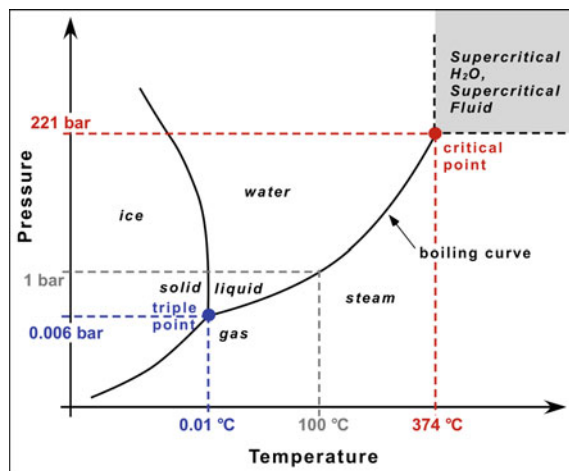
- Silica polymerization can be retarded by acids added to the fluid (e.g. HCl, H₂SO₄).
- Stabilizing the early-formed colloids by adding organic inhibitors.
- Increasing pH of the fluid thereby increasing silica solubility.
- Lowering fluid flow-rate in pipes reduces rate of silica precipitation.

In low-TDS fluids silica precipitation can be retarded by lowering fluid flow rates (Gunnlaugsson 2012a, b). Optimized steam separation with maximized revival of gases (e.g. CO₂) increases pH of the wastewater thereby at least reducing silica scales (Henley 1983). The processes related to silica scale formation are chemically complex and may vary considerably between locations. Strategies for scale prevention are typically developed after extensive site specific testing. Particularly the use of organic inhibitors for silica scale prevention requires comprehensive testing for finding the most effective formula for the site (Gallup 2009; Ikeda and Ueda 2017).

10.5 Use of Fluids from Reservoirs at Supercritical Conditions

Geothermal power production from high-enthalpy geothermal fields is strongly linked to the liquid–vapor transition of water. The *P-T* conditions of boiling in the geothermal reservoir underground and the technical installations of the plant,

Fig. 10.16 $P-T$ phase diagram for H_2O . The boiling curve terminates on the high- T side at the critical point of H_2O (374°C and 221 bar)



particularly in the steam separators represent fundamental operational parameters. With increasing pressure liquid water converts to steam at increasing temperature. The conditions of the phase transition are given by the boiling curve (Fig. 10.16). At 1 bar pressure water boils at about 100°C . At the 1 bar boiling point the liquid phase has a density of 959 kg m^{-3} and the density of steam is 0.6 kg m^{-3} . With increasing pressure along the boiling curve this large density contrast between the liquid and the steam phase gradually decreases. This is because liquid water is nearly incompressible in contrast to the steam, which is highly compressible. At 200°C and 15.55 bar along the boiling curve the density of steam reached 7.862 kg m^{-3} and liquid water 863 kg m^{-3} ; at 300°C and 85.92 bar the densities are: $\rho_{\text{steam}} = 46.21 \text{ kg m}^{-3}$ and $\rho_{\text{liquid}} = 712 \text{ kg m}^{-3}$ (data from: <https://www.pipeflowcalculations.com/tables/steam.xhtml>). The density ratio $\Delta\rho$ (liquid/steam) along the boiling curve decreases from 1600 at 100°C to 110 at 200°C and finally to 15.4 at 300°C . At 374°C and 221 bar the density of the two phases is equal ($\Delta\rho = 0$). At this point, the so-called critical point of water, the distinction of liquid water and steam becomes obsolete. Thus a fluid at $P > 221\text{ bar}$ and $T > 374^\circ\text{C}$ is referred to as a supercritical fluid. The compressibility of H_2O in the supercritical region is higher than that of liquid water (Sect. 8.2) (Suárez and Samaniego 2012). Surface tension and heat of evaporation of supercritical water is zero.

Supercritical water has a density like a liquid phase but a viscosity similar to gas. The relatively high density of supercritical water causes a correspondingly high specific enthalpy. At a supercritical pressure of $P = 250\text{ bar}$ H_2O has a specific enthalpy of 1790 kJ kg^{-1} at 370°C . It drastically increases to 2580 kJ kg^{-1} at 400°C . These properties suggest that supercritical water is a very energy-rich fluid substance and therefore potentially interesting for geothermal applications. Drilling a deep well into a fluid reservoir at supercritical conditions leads to a very high mass flux from the well because of the high pressure above 221 bar. Consequently the yield of systems producing from supercritical fluid reservoirs can be 10–20 times higher than that of

conventional high-enthalpy geothermal systems. These positive prospects motivate attempts for developing supercritical geothermal fields in a number of countries including Japan, New Zealand and Iceland (IDDP—Iceland Deep Drilling Project).

The high T and P of supercritical aqueous fluids with a high content of dissolved solids and gasses and the suspended solid particles make the production and handling of the fluid elaborate and expensive. Equipment and tools need special designs and require corrosion resistant material. Drilling wells to supercritical fluid reservoirs represents an enormous challenge. Even robust drill bits made of special steel alloys can resist the harsh conditions only thanks to massive injection of cooling water.

The first exploitation of a supercritical fluid reservoir has been made in Larderello (N-Italy) in the 1980s. A temperature of 380 °C at 3970 m depth has been documented for the well Sasso 22 (Bertini et al. 1980). The well San Pompeo 2 showed a temperature of > 400 °C at 2930 m depth and a pressure of about 240 bar (Batini et al. 1983). Well data with down hole temperature distinctly above 400 °C have been reported and documented from Japan, USA, Mexico, Kenya and Iceland (Reinsch et al. 2017). The well WD-1A in the high-enthalpy field Kakkonda (N-Japan) reached a temperature of 500–510 °C at 3710 m depth, probably the highest temperatures reached by a geothermal well worldwide (Ikeuchi et al. 1998). The well has been drilled in connection with the project “Deep Seated Geothermal Resources Survey”.

In Iceland some wells reached 360 °C at the shallow depth of 2200 m. The temperature was close to the critical T of 374 °C, the pressure has been clearly below P_{crt} . The fluids from the high-T wells were toxic, corrosive and strongly tended to form scales. The fluids were ecologically and economically difficult to handle and technically challenging to control. Furthermore, severe difficulties occurred during drilling including total loss of drilling mud along nearly the entire drilled section, collapse of the casing and rapid corrosion of the drill pipes.

The ongoing Iceland Deep Drilling Project (IDDP; see [iddp.is](#)) involves several Icelandic institutions and a number of international partners (Elders and Friðleifsson 2010). IDDP aims at developing supercritical fluid reservoirs for geothermal utilization. The first deep well IDDP-1 near the young volcanic fissure system Krafla in northern Iceland drilled into basaltic magma at 2104 m depth in the year 2009. The Krafla volcano produced the last massive eruptive basaltic lava flows from 1975 to 84 (Fig. 1.4). The eruptions are known as the Krafla fires and produced a 36 km² lava field. When the drill string hit the magma chamber it got stuck. However, cold-water circulation remained intact and some hydraulic tests were carried out. The well produced steam at a rate of 10–12 kg s⁻¹, a temperature of about 450 °C and pressure of 140 bar at the wellhead. At that time the well IDDP-1 was with its 36 MW_{el} the most powerful well that ever has been drilled. However, both the well and the surface installations corroded rapidly by the emitted acid gasses (HCl, HF, H₂S), further damaged by silica scales and silica erosion caused by suspended solid particles. The steam contained 90 mg kg⁻¹ HCl, 7 mg kg⁻¹ HF and 92 mg kg⁻¹ SiO₂. Steam condensation resulted in an acid liquid that precipitated amorphous silica. Several wet scrubber concepts were developed and tested for minimizing acid formation, corrosion and silica scales (Hauksson et al. 2014; Markusson and



Fig. 10.17 The drilling site of IDDP-1 in the Krafla volcanic field on Iceland with the black lava fields from the “Krafla Fire” 1984 in the distance. The IDDP-1 well drilled into a small active magma chamber at 2200 m depth

Hauksson 2015). The well IDDP-1 served exclusively as research well and never produced power for the grid. It was finally sealed for technical reasons (Fig. 10.17).

The second IDDP well (IDDP-2) is located on the Reykjanes peninsula in SW Iceland. Drilling started in August 2016 and in January 2017 at 4659 m depth successfully completed. The bore has a casing string and is cemented down to 3000 m depth. The temperature at bottomhole was 427 °C and the fluid pressure 340 bar. However, the well was not yet thermally equilibrated at the time of measurement. Alteration minerals present and extrapolation of T -gradients with the Horner method (Horner 1951) suggest that the temperature was as high as 535 °C (Friðleifsson et al. 2018). Thus at bottomhole the $P-T$ conditions were clearly in the range of supercritical H₂O. The well has been extensively tested (iddp.is) and is supposed to become operational in 2020 with an expected power of 30–50 MW_{el}.

Producing electrical power from supercritical fluid is a highly topical research and development subject at many high-enthalpy geothermal fields worldwide. Some significant projects include the “Japan Beyond Brittle Project” (JBBP), the DESCRAMBLE project of Europe developing new drilling technologies at the Larderello field, the “New Zealand Hotter and Deeper Project”, the “GEMex Project” of Mexico and the “Newberry Deep Drilling Project” (NDDP) of the USA. The functional exploitation of deep reservoirs of supercritical aqueous fluids is presently not

possible due to unresolved technical difficulties. For example the high-temperature stability of tools, equipment and drilling mud must be significantly improved. The hook load of conventional drilling rigs is limited to about 500 t, too small for the required new drilling technologies. The chemical composition of the produced fluid makes them extremely aggressive and corrosive, which represents a further challenge to the stability of the technical equipment (Reinsch et al. 2017).

References

- Allis, R. G., 1981. Changes in heat flow associated with exploitation of the Wairakei geothermal field, New Zealand. NZ Journal of Geology & Geophysics, 24, 1–19.
- Aradóttir, E., Gunnarsson, I., Sigrúnsson, B., Gíslason, S. R., Oelkers, E. H., Stute, M., Matter, J. M., Snæbjörnsdóttir, S. Ó., Mesfin, K. G., Alfredsson, H. A., Hall, J., Arnarsson, M. Th., Dideriksen, K., Júliusson, B. M., Broecker, W. S. & Gunnlaugsson, E., 2015. Towards Cleaner Geothermal Energy: Subsurface Sequestration of Sour Gas Emissions from Geothermal Power Plants. Proceedings World Geothermal Congress 2015, Melbourne, Australia, 19–25 April 2015.
- Ármannsson, H., 2016. The fluid geochemistry of Icelandic high temperature geothermal areas. Applied Geochemistry, 66, 14–64.
- Árnason, K., Karlssdóttir, R., Eysteinsson, H., Flóvenz, Ó. G. & Gunnlaugsson, S. Th., 2000. The resistivity structure of high-temperature geothermal systems in Iceland. Proceedings of the World Geothermal Congress, Kyushu-Tohoku, Japan, 923–928.
- Barkaoui, A.-E., 2011. Joint 1D inversion of TEM and MT resistivity data with an example from the area around the Eyjafjallajökull glacier, S-Iceland. Geothermal training program, report no. 9, Reykjavik, Iceland, 30 p.
- Batini, F., Bertini, G., Bottai, A., Burgassi, P., Cappetti, G., Gianelli, G. & Puxeddu, M., 1983. San Pompeo 2 deep well: a high temperature and high pressure geothermal system. In: Strub A, Ungemach P. (eds.): European geothermal update.- Proceedings of the 3rd international seminar on the results of EC geothermal energy research, p. 341–353.
- Batini, F., Console, R. & Luongo, G., 1985. Seismological study of Larderello – Travale geothermal area. Geothermics, 14/2–3, 255–272.
- Bertini, G., Giovannoni, A., Stefani, G. C., Gianelli, G., Puxeddu, M. & Squarci, P., 1980. Deep exploration in Larderello field: Sasso 22 drilling venture. Dordrecht: Springer, p. 303–311. https://doi.org/10.1007/978-94-009-9059-3_26.
- Björnsson, A., Eysteinsson, H. & Bebblo, M., 2005. Crustal formation and magma genesis beneath Iceland: magnetotelluric constraints. In: Foulger, G. R., Natland, J. H., Presnall, D. C. & Anderson, D.L. (eds): Plates, plumes and paradigms. Geological Society of America, Spec. Pap., 388, 665–686.
- Brophy, P., Lippmann, M. J., Dobson, P. F. & Poux, B., 2010. The Geysers Geothermal Field – update 1990–2010.- Geothermal Resources Council, Spec. rep. no. 20.
- Brown, K., 2011. Thermodynamics and kinetics of silica scaling. Proceedings International Workshop on Mineral Scaling 2011, Manila, Philippines, 25–27 May 2011.
- Bucher, K. & Grapes, R., 2011. Petrogenesis of Metamorphic Rocks, 8th edition. Springer Verlag, Berlin Heidelberg. 428 pp.
- Christensen, A., Auken, E. & Sorensen, K., 2006. The transient electromagnetic method. Groundwater Geophysics, 71, 179–225.
- Clark, D. E., Oelkers, E. H., Gunnarsson, I., Sigrúnsson, B., Snæbjörnsdóttir, S. Ó., Aradóttir, E. A. & Gíslason, S. R., 2020. CarbFix2: N and H₂S mineralization during 3.5 years of continuous injection into basaltic rocks at more than 250 °C. Geochimica et Cosmochimica Acta, Vol 279, 45–66.

- Clynne, M. A., Janik, C. J. & Muffler, L. J. P., 2013. "Hot Water" in Lassen Volcanic National Park – Fumaroles, Steaming Ground, and Boiling Mudpots. USGS Fact Sheet 173–98, 4 p.
- DiPippo, R., 2012. Geothermal Power Plants: Principles, Applications, Case Studies and Environmental Impact (3rd edition). Butterworth Heinemann, 600 pp.
- Elders, W. A. & Friðleifsson, G., 2010. The science program of the Iceland Deep Drilling project (IDDP): a study of supercritical geothermal resources.- Proceedings, World Geothermal Congress, 9 p., Bali, Indonesia.
- ENEL 1995. Geothermal energy in Tuscany and Northern Latium. ENEL Generation and Transmission, Relations and Communication Department, 50 p., Bagni di Tivoli, Roma.
- Friðleifsson, G. Ó., Elders, W. A., Zierenberg, R. A., Fowler, A. P. G., Weisenberger, T. B., Mesfin, K. G., Sigurðsson, Ó., Níelsson, S., Einarsson, G., Óskarsson, F., Guðnason, E. Á., Tulinius, H., Hokstad, K., Benoit, G., Frank Nono, F., Loggia, D., Parat, F., Cichy, S.B., Escobedo, D. & Mainprice, D., 2018. The Iceland Deep Drilling Project at Reykjanes: Drilling into the root zone of a black smoker analog. *Journal of Volcanology and Geothermal Research*, VOLGEO-06435; p. 19.
- Gallup, D. L., 2009. Production engineering in geothermal technology: a review. *Geothermics*, 38, 326–334.
- Garrow, T., 2015. A Methanol Economy based on Renewable Resources.- McGill Green Chemistry Journal, 1, 87–90.
- Giroud, N., 2008. A Chemical Study of Arsenic, Boron and Gases in High-Temperature Geothermal Fluids in Iceland. Dissertation at the Faculty of Science, University of Iceland, 110 p.
- Gunnarsson, I., Sigrúnsson, B., Stefánsson, A., Arnórsson, St., Scott, S. W. & Gunnlaugsson, E., 2011. Injection of H₂S from Hellisheiði power plant, Iceland. Proceedings, Thirty-Sixth Workshop on Geothermal Reservoir Engineering Stanford University, Stanford, California, January 31–February 2, 2011. SGP-TR-191
- Gunnarsson, I., Júlíusson, B. M., Aradóttir, E. S. P. and Arnarson, M. Th., 2015. Pilot scale geothermal gas separation, Hellisheiði Power Plant, Iceland, Proceedings, Proceedings World Geothermal Congress, 19–25 April 2015, Melbourne, Australia.
- Gunnlaugsson, E., 2008a. District Heating in Reykjavík, past – present – future.- United Nations University, Geothermal Training Programme, 12 p., Reykjavík, Iceland.
- Gunnlaugsson, E., 2008b. Environmental Management and Monitoring in Iceland: Reinjection and Gas Sequestration at the Hellisheiði Power Plant.- SDG Short Course I on Sustainability and Environmental Management of Geothermal Resource Utilization and the Role of Geothermal in Combating Climate Change, 8 p., Santa Tecla, El Salvador.
- Gunnlaugsson, E., 2012a Scaling in geothermal installation in Iceland. Short Course on Geothermal Development and Geothermal Wells, 6 p., Santa Tecla, El Salvador.
- Gunnlaugsson, E., 2012b. Scaling prediction modelling. Short Course on Geothermal Development and Geothermal Wells, 5 p., Santa Tecla, El Salvador.
- Hauksson, T., Markusson, S., Einarsson, K., Karlssdóttir, S.A., Einarsson, Á., Möller, A. & Sigmarsdóttir, P., 2014. Pilot testing of handling the fluids from the IDDP-1 exploratory geothermal well, Krafla, N.E. Iceland. *Geothermics*, 49, 76–82.
- Henley, R. W., 1983. pH and silica scaling control in geothermal field development. *Geothermics*, 12/4, 307–321.
- Henley, R. W. & Ellis, A. J., 1983. Geothermal Systems Ancient and Modern: A geochemical Review.- Earth-Science Reviews, 19, 1–50.
- Hjörleifsdóttir, V., Snæbjörnsdóttir, S., Vogfjord, K., Ágústsson, K., Gunnarsson, G. & Hjaltadóttir, S., 2019. Induced earthquakes in the Hellisheiði geothermal field, Iceland. Schatzalp, 3rd Induced Seismicity Workshop, p. 5, Davos.
- Horner, D. R., 1951. Pressure Build-up in Wells. In: Bull, E. J. (ed.): Proc. 3rd World Petrol. Congr., pp. 503–521, Leiden, Netherlands.
- Ikeda, R. & Ueda, A., 2017. Experimental field investigations of inhibitors for controlling silica scale in geothermal brine at the Sumikawa geothermal plant, Akita Prefecture, Japan. *Geothermics*, 70, 305–313.

- Ikeuchi, K., Doi, N., Sakagawa, Y., Kamenosono, H. & Uchida, T., 1998. High-temperature measurements in well WD-1A and the thermal structure of the Kakkonda geothermal system, Japan. *Geothermics*, 27, 5/6, 591–607.
- Markusson, S. H. & Hauksson, T., 2015. Utilization of the Hottest Well in the World, IDDP-1 in Krafla. *Proceedings World Geothermal Congress*, 6 p., Melbourne, Australia.
- Mizuno, E., 2013. *Geothermal Power Development in New Zealand Lessons for Japan*. Research Report, Japan Renewable Energy Foundation, 74 p., Tokyo, Japan.
- Nicholson, C. & Wesson, R. L., 1990. Earthquake Hazard associated with deep well injection - a report to the U.S. Environmental Protection Agency, pp. 74, U.S. Geological Survey Bulletin.
- Óladóttir, A. & Friðriksson, P., 2015. The Evolution of CO₂ Emissions and Heat Flow through Soil since 2004 in the Utilized Reykjanes Geothermal Area, SW Iceland: Ten Years of Observations on Changes in Geothermal Surface Activity. *World Geothermal Congress*, 10 p., Melbourne, Australia.
- Pope, E. C., Bird, D. K., Arnórsson, S. and Giroud, N., 2016. Hydrogeology of the Krafla geothermal system, northeast Iceland. *Geofluids*, 16, 175–197.
- Reinsch, T., Dobson, P., Asanuma, H., Huenges, E., Poletto, F. & Sanjuan, B., 2017. Utilizing supercritical geothermal systems: a review of past ventures and ongoing research activities. *Geothermal Energy*, 5:16, 26 p. <https://doi.org/10.1186/s40517-017-0075-y>.
- Remoroza, A. I., 2010. Cacite Mineral Scaling Potentials of High-Temperature Geothermal Wells. Thesis at the Faculty of Science School of Engineering and Natural Sciences, 97 p., Univ. of Iceland, Reykjavik.
- Rosenkjaer, G. K., 2011. Electromagnetic methods in geothermal exploration. 1D and 3D inversion of TEM and MT data from a synthetic geothermal area and the Hengill geothermal area, SW Iceland. University of Iceland, MSc thesis, 137 pp.
- Rowland, J. V. & Sibson, R. H., 2004. Structural controls on hydrothermal flow in a segmented rift system, Taupo Volcanic Zone, New Zealand. *Geofluids*, 4, 259–283.
- Sherburn, S., Bromley, C., Bannister, S., Sewell, S. & Bourguignon, S., 2015. New Zealand Geothermal Induced Seismicity: an overview. *Proceedings World Geothermal Congress*, 9 p., Melbourne, Australia.
- Suárez, M.-C. A. & Samaniego, F., 2012. Deep geothermal reservoirs with water at supercritical conditions. *Proceedings 37th workshop on Geothermal Reservoir Engineering*, Stanford University, SGP-TR-194, 9 p., Stanford, CA/USA.
- Sveinbjörnsson, B. M., 2014. Success of High Temperature Geothermal Wells in Iceland. ISOR Iceland Geosurvey, ISOR-2014/053, project-no. 13-0445, 42 p., Reykjavik, Iceland.
- Thain, I. A., 1998. A brief history of the Wairakei geothermal power project. *GHC Bulletin*, 4 p.
- Thorolfsson, G., 2010. Silencers for Flashing Geothermal Brine, Thirty Years of Experimenting. *Proceedings World Geothermal Congress*, 4 p., Bali, Indonesia.
- Tobler, D. J., Stefánsson, A. & Benning, L. G., 2008. In-situ grown silica sinters in Icelandic geothermal areas. *Geobiology*, 6, 481–502.

Chapter 11

Environmental Issues Related to Deep Geothermal Systems



Drilling rig for deep boreholes

The conversion of geothermal energy into electrical power or useful heat produces no CO₂ and no flue gas emissions such as soot particles, sulfur dioxide and nitrogen oxides. The operation of a geothermal power plant is deeply friendly to the environment. The risk for harmful environmental effects is extremely low during normal operation and even during accidents. The low-risk systems result from the use of high-quality structural materials and from the mature technology with numerous safety precaution installations.

Construction of geothermal systems and power plants causes CO₂ emissions related to manufacturing construction materials, transport of materials and equipment and service traffic, no different as with construction of other types of power plants. Careful planning of logistics helps to minimize these emissions.

Developing the underground heat exchanger of an enhanced geothermal system (Chap. 9) involves hydraulic stimulation measures that cause minor seismicity. Rarely the induced seismicity can cause irritation if physically sensed at the surface. Problems related to seismicity are dealt with in Sect. 11.1.

The geothermal fluid circulates in a closed system and cannot cause any damage to the environment. If a leak occurs in the surface installations, the fluid circulation can be stopped and the leaking section replaced. The working fluid in the secondary loop of the power production circulates also in a closed system. If leaks occur here, precautions on the construction and technical side help to minimize environmental pollution.

However, it may be necessary to test the thermal fluid circulation during the system development phase when the primary loop is not yet completely closed at the surface. It is only during these tests that the success of the entire effort can be visually seen from the rising white steam plumes (Fig. 11.1).

In binary geothermal power plants the working fluid of the secondary loop must be cooled below condensation conditions after leaving the turbines. The excess heat is released to the environment (Sect. 11.3), like in any other thermal power plant. The thermal emissions of geothermal plants are, however, orders of magnitude lower than those of thermal large-scale coal- and gas-fired plants and nuclear power plants. The emissions are considerably lower even if normalized to the power output of the units.

Several countries recommend the concept of combined heat and power or the technology may even be mandatory. Combined heat and power reduces energy loss related to the fluid cooling process and optimizes the use of the extracted geothermal energy. Integrated and cascade use of geothermal low-enthalpy resources also uses produced thermal energy rather than wasting it in the fluid cooling process (Chap. 8.6).

This book does not cover all potential environmental hazards that can be associated with the construction and operation of a low-enthalpy geothermal power plant. In the following sections, we present several environmental problems selected partly because of the topicality of the problems, partly because the hazards are sometimes unjustifiably ignored. Also geothermal projects can be plagued by very diverse failures and troubles during system development and later during operation. Careful planning, management, monitoring, educated and experienced personnel and adequate quality of used materials and equipment help reducing potential troubles



Fig. 11.1 Steam clouds at the Landau power plant during tests after successful development of the primary loop

and thus also minimize environmental effects. Finally, an open and straight communication philosophy that integrates all active parties in the project and a trusting working together is the best insurance against troubles and hazards.

11.1 Seismicity Related to EGS projects

Rock deformation caused by massive hydraulic stimulation of the planned EGS granite reservoir at 5 km depth has been physically sensed and acoustically recognized in the city of Basel (Switzerland). Ground shaking and thundering noises scared the local population (Kraft et al. 2009). The incident had disastrous effects for the public acceptance of deep geothermal projects, not only EGS projects but also for hydrogeothermal doublets. The “Basel incident” had extremely negative consequences for the further implementation of enhanced geothermal system. The question must be asked by anyone interested in geothermal energy development: Why did it happen? How can such incidents be avoided?

We explained in the previous Chap. 9 that the development of the underground heat exchanger of HDR systems requires massive hydraulic (and chemical) stimulation

Table 11.1 A selection of reported seismicity from geothermal projects

Geothermal system	Type ^a	Magnitude (M_L) ^b
Unterhaching, D	H	2.2
Landau, D	S	2.7
Insheim, D	S	2.3
Riehen, CH	H	—
Paris Basin, F	H	—
Gross Schönebeck, D	P	—
Horstberg, D	P	Minimal
Sankt Gallen, CH	S	3.5
Soultz (3.5 km depth), F	P	2.2
Soultz (5 km depth), F	P	2.9
Basel, CH	P	3.4
Urach, D	P	1.8
Fenton Hill, N.Mex. USA	P	<1.0
The Geysers, Calif. USA	D	4.0
Cooper Basin, AUS	P	3.7
Pohang, South Korea	P, S	5.4

^aType: Hydrothermal (H), petrothermal (P), fault system (S), dry steam (D)

^bMagnitude M_L :—below detection limit

Country abbreviations: D—Germany, F—France, CH—Switzerland, USA—United States of America, AUS—Australia

of the reservoir. The success of the stimulation process is expressed by microseismicity in the underground, which can be monitored and recorded by seismic monitoring programs. The data provide a 3D view of the stimulated rock volume that can be expected to have a significantly enhanced hydraulic conductivity compared with the original situation. The data derived from the observed microseismicity are fundamentally relevant for the location and detailed path of the second borehole.

The stimulation related seismicity is indispensable for the development of HDR/EGS project. However, it is absolutely essential to avoid any surface effects that can be sensed or heard (Chap. 9). We are firmly convinced that this is possible with prudent planning and conservative reservoir development strategies. It also should be kept in mind that in several documented geothermal projects massive hydraulic stimulation did not or barely result in recognizable and recordable microseismicity, but also making reservoir development difficult.

Seismic incidents are not exclusive to petrothermal systems (EGS, HDR). Deep geothermal systems that produce hot water from fault systems or inject fluids into faults have been exposed to problematic seismicity. There are also known incidents from hydrothermal systems. A selection of some incidents is listed in Table 11.1.

There are several possibilities to express the intensity of seismic events. A widely used conventional parameter is the logarithmic Richter magnitude scale, which

expresses the energy released by the seismic event. By definition any seismicity below magnitude 2 is microseismicity. Minor seismicity covers the magnitude range of 2–4. The infamous “Basel incident” reached a magnitude of 3.6 (Table 11.1). By definition of the Richter scale magnitude 3.6 characterizes an event that can be felt at the surface by most people but rarely causes structural damage. The listed magnitudes of seismic events related to geothermal projects (Table 11.1) refer to events caused by massive hydraulic stimulation of the geothermal reservoir. In some of the listed projects there were no predefined acceptable maximum magnitude, in other projects including Basel an upper limit has been part of the concession contract. The listed projects utilizing fault zones have massively stimulated the fault systems or injected the cooled fluid of the primary loop under high pressure into the fault systems.

The EGS related seismic incidents caused discussions about the cause for the unwanted seismicity above the magnitude two level and the potential risks for even stronger triggered seismicity that may cause major structural damage at the surface. Also social issues have been intensely discussed including improved communication with the local population at the project site. The general public acceptance of an EGS project varies strongly depending on complete transparency of the project and all its development phases. The perception of projects by the public depends a lot on the use of terminology. Instrumentally monitored microseismicity should definitely not be communicated to the public as “earthquakes”. For the layman the term earthquake is loaded by pictures of damage and death and prompts fears that are not backed by the physical nature of stimulation related microseismicity.

In Germany, the seismic incidents cause major insecurity at the involved authorities resulting in widely varying approval practices and processes. A major difficulty in this context is that a sound pre-drilling risk assessment of induced seismicity is impossible because of lacking data.

International research projects analyze induced seismicity and model geomechanical processes behind the seismicity. The results of the projects such as GEISER (Geothermal Engineering Integrating Mitigation of Induced Seismicity in Reservoirs: geiser-fp7.fr), PHASE (Physics and Application of Seismic Emission) and others clarified technical uncertainties and removed concerns. In-situ stimulation and other rock mechanical experiments are actively carried out in underground rock-laboratories for example the Grimsel Rock-Laboratory in Switzerland (Grimsel Test-Site: grimsel.com), the Äspö Hard Rock Laboratory in Sweden, and the Sanford Underground Research Facility (SURF: sanfordlab.org) in the USA thereby producing seriously needed data. The results clarify the detailed geomechanical processes behind seismicity. The dedicated ongoing research rapidly improves the strategies for minimizing induced seismicity.

11.1.1 *Induced Earthquakes*

Induced earthquakes are earthquakes that occurred as a direct or indirect consequence of human undertakings. The stress buildup in the underground can be entirely related

to constructional measures in the subsurface directly causing an earthquake. On the other extreme high sub-failure stresses may exist in the underground that any form of construction related actions releases as an earthquake. The difference is the different portions of pre-existing natural stresses (“autochthonous”) and added anthropogenic stresses (“induced”). This distinction is often difficult to quantify and a continuous range of direct and indirect causes exist.

Earthquakes are caused by spontaneous release of stored elastic deformation energy by friction-based sliding along pre-existing fault planes. Earthquakes are events where stored stresses are relieved by the displacement of rock masses. However, the terminology is strictly scale dependent. The displacement of the rock packets of the Earth crust occurs in general parallel to existing fault systems and may be active across the fault system on a cm to m scale.

The deformation processes in the earthquake hypocenter generate ground movements at the Earth surface. The intensity with which an earthquake is felt at the surface depends on the total strain energy released at the hypocenter (magnitude), the focal depth of the hypocenter below the epicenter and properties of the local hard ground and soil. The surface effects of a seismic event can be predicted and described from parameters including seismic intensity, vibration velocity and vibration acceleration (Sect. 11.1.2). These parameters characterize the earthquake at the surface; magnitude is a parameter that characterizes the earthquake at the hypocenter at depth.

Earthquakes suddenly release stored elastic deformation energy in rock masses at depth. Failure occurs when the stress state exceeds a certain threshold value (Nicholson and Wesson 1990). The high-pressure injection of fluids during reservoir stimulation does not significantly increase stored deformation energy. However, fluid injection lowers the threshold value for failure by reducing the effective frictional resistance on the critically stressed and loaded fault planes.

The hydrological and geological properties and the locally existing stresses at and around the injection zone of the reservoir control the reaction on fluid injection, in some situations an earthquake may be triggered in others high-pressure fluid injection may not result in an earthquake. The hydrological conditions for triggering earthquakes can be related to the seismogenic permeability (Talwani et al. 2007). It should be distinguished between factors that make earthquakes possible and factors that release them. It is not possible to quantitatively predict the probability for a triggered earthquake that may result from increased fluid pore pressure by fluid injection into a deep well (Nicholson and Wesson 1990).

The magnitude of an earthquake is proportional to the logarithm of the length of the activated fault (Wyss 1979; Wells and Coppersmith 1994). A magnitude 8 earthquake activates a fault system of several hundred km length and displaces the moved fault blocks by several meters. A magnitude 3 earthquake activates about some tens of meters of a fault and displaces fault blocks by some cm.

Anthropogenic seismicity is not exclusive to geothermal project development. It is also known from the oil and gas industry, from dammed lakes used as reservoirs for hydroelectric power systems, from underground storage of gas and compressed air, from the high-pressure injection of liquid waste in deep wells and also from

underground and open pit mining (Nicholson and Wesson 1990; Shapiro et al. 2007; McGarr 1991; Rutledge et al. 2004; Segall 1989; Cook 1976). Increasing seismic activity can also be triggered in exceptional cases by torrential rainfall events (Husen et al. 2007).

Production from oil and gas reservoirs may cause seismicity by decreasing pore fluid pressure from fluid extraction and increased loading. Isostatic compensation after massive reservoir exploitation can cause earthquakes even at large distances (Grasso 1992). As an example: High oil production from the Wilmington oilfield in the Los Angeles Basin (California, USA) subsequently caused subsidence of locally up to 8.8 m with subsidence rates of up to 0.71 m per year. Resulting from these ground movements several damaging earthquakes occurred from the 1940ies to the 1960ies with a maximum magnitude M_L of about 5.1 (Kovach 1974). At the end of the 1950ies massive water injection was started with the aim to bring subsidence to a halt and also to improve oil recovery from the field. The operations were successful. However, water injection triggered a series of small quakes ($M_L < 3.2$) (Nicholson and Wesson 1990). The example shows that water injection into an oil reservoir can reduce the effective load and may trigger quakes. Other examples of man-made, subsidence-related seismicity in oil and gas fields include the Goose Creek oil field quakes from 1925 in Texas (Davis and Pennington 1989), gas-extraction subsidence in the gas field of the Pau Basin near Lacq (SW France) (Segall et al. 1994) caused >1000 seismic events, 44 reaching magnitude >3.0, two of them magnitude >4. Further examples can be found, for example, in Grasso (1992).

The largest reported earthquake related to reservoir infill is probably the magnitude 6.5 earthquake of Koyna in India (Gupta and Rastogi 1976). Many earthquakes reported from dammed lakes have been summarized and analyzed by Talwani et al. (2007).

Liquids or gasses can be injected to the underground from deep wells for very diverse reasons including leaching salt from evaporites, disposing liquid toxic wastes, improving production from ageing oil and gas fields or fracturing reservoir rocks for improved hydraulic conductivity. Injected fluid volumes have been enormous at some sites so that fluid injection induced earthquakes. An infamous case of induced seismicity occurred at the Rocky Mountain Arsenal injection well near Denver (Colorado, USA). The 3671 m deep well was used around 1962 for disposal of hundreds of millions liters of toxic waste. The liquid was injected with wellhead pressures of about 72 bar into a reservoir that is cut by several sub-parallel faults. The resulting several hundred earthquakes reached a magnitude of 5.5 (Hsieh and Bredehoeft 1981; Nicholson and Wesson 1990).

A worldwide compilation of seismicity related to geothermal energy projects did not report any loss-producing damage quakes during drilling or during reservoir stimulation (Majer et al. 2008). The exception proves the rule: The $M_L = 5.4$ event in Pohang, South Korea (Kim et al. 2018, 2019). During operation of a geothermal system fluid injection is counterbalanced by fluid extraction, which is a fundamental difference to the other examples of injection-induced seismicity described above.

11.1.2 Quantifying Seismic Events

Seismic events can be characterized by the two quite different parameters magnitude and intensity. Magnitude is related to the strain energy released at the source of the event, the hypocenter at depth. The intensity of a seismic incident describes the effects and consequences of the event at a specific location at the surface. The empiric logarithmic magnitude scale (Richter Scale) derives the released energy from the vibration amplitude recorded by a seismometer. The amplitude relates to the seismic energy released by the ground rupturing process. Seismic events below magnitude 2 are referred to as microseismicity. It is not sensed at the surface. Magnitude 2–3 events are extremely light earthquakes and can be sensed at the surface only at very special conditions. A magnitude 3–4 event is a very light earthquake. Many people can feel such quakes, however, structural damages are very unusual. The Richter scale is open-ended and each succeeding scale unit represents ten times more seismic energy released. Since 1990, the planet Earth experienced five earthquakes with magnitude >9, magnitude 10 earthquakes have not been recorded yet.

The Richter magnitude has the symbol M_L where L stands for local. Other frequently used scales include the body wave magnitude M_b , surface wave magnitude M_s and the moment magnitude M_w . The moment magnitude indicates how much total energy is released in a seismic event. Thus it directly relates to rock displacement along faults and fractures and the total surface area along which the displacement occurred. The empirical relationship $M_w \sim 0.85 M_L$ indicates that the moment magnitude is somewhat smaller than the Richter magnitude (Ottemöller and Sargeant 2013).

The earthquake magnitude is not a measure for consequences and damages at the surface, the epicenter, above the hypocenter. The ramifications at the surface are influenced, as mentioned above, by the focal depth below the epicenter, by the type of rocks and soil and the structure and type of buildings.

The Gutenberg-Richter law relates the magnitude and the number of earthquakes in a given defined region during a certain time period with at least that magnitude (Eq. 11.1).

$$\log_{10} N = a - bM \quad (11.1)$$

where N is the number of events with at least magnitude $\geq M$. The parameters a and b are regional specific constants. The parameter a relates to the general seismicity of a considered region. The parameter b is close to 1 for tectonic earthquakes. Fluid injection may increase b, resulting in more but weaker seismicity. The Gutenberg-Richter law can be used to explore the possibility of high-magnitude events that have not occurred so far.

The macroseismic intensity is an empirical classification of local effects of an earthquake on residents and natural and man-made structures at the surface. The local near-surface structure of rocks and soil strongly influence the ground motion and thus the macroseismic intensity. The ground motion at the surface of loose soil can be

massively higher than on solid basement bedrock. Consequently an earthquake with the same magnitude and focal depth may have much higher macroseismic intensity on loose soil than on solid rock. The Mercalli scale expresses the macroseismic intensity by roman numerals from I (lowest) to XII (highest). Its highest value defines the location of the epicenter above the earthquake focal region. It declines with increasing distance from the epicenter.

In the context of induced seismicity related to geothermal projects robust quantitative predictions of local surface ground motions that may result from reservoir stimulation measures would be very helpful. The ground vibrations, ground movements and accelerations can be quantitatively characterized using methods of petrophysics and soil physics. The vibration velocity relates directly to the structural effects. Vibrations exceeding 5 mm/s may cause smaller damage and cracks of the plaster. Severe structural damage is not caused until vibration velocity exceeds much higher values.

The lower limit of sensing a seismic event at 5 km focal depth is about magnitude $M_L = 2\text{--}2.5$. Under special circumstances a magnitude 3.5–4.5 event may cause light damages to buildings at the epicenter. The US Geological Survey supposes that clear damages occur at magnitude M_L above 4.5 and ground vibration velocity clearly above 34 mm s^{-1} . Magnitude M_L 5 earthquakes may cause scattered severe structural damages to buildings. It follows that a maximum magnitude M_L of 2–2.5 should not be exceeded during massive hydraulic stimulation or operation of a geothermal system. For security reasons and for avoiding perceptible vibrations at any rate maximum acceptable magnitudes M_L of 1.7 are commonly required in recent projects.

11.1.3 *The Basel Incident*

The Swiss city of Basel is located at the southern termination of the upper Rhine rift valley in central Europe. The local high geothermal gradient and the geological structure of the rift valley and the potential for local buyers of produced thermal energy make Basel an optimal site for an EGS project. The valley has an infill of a thick succession of Mesozoic and Tertiary sediments covered with Quaternary deposits (Fig. 11.2). The top of the crystalline basement beneath the sediments is between 2640 and 2750 m below surface. The knowledge about the geological structure was limited to relatively shallow depth before project start. The Basel 1 wellbore reached 5009 m and drilled through 2300 m of basement rocks mostly granite. The basement and the older part of the cover are cut by numerous steeply dipping faults and form a complex pattern of fault blocks. The drilling site is located about 4.5 km from the surface outcrop of the eastern main border fault of the Rhine rift valley. The exact position of the border fault system at 5 km depth is not known. However, the fault system undoubtedly dips to the west and could be at close distance to the Basel 1 wellbore at 5 km depth. The natural seismicity in the Rhine rift valley decreases from Basel towards the north.

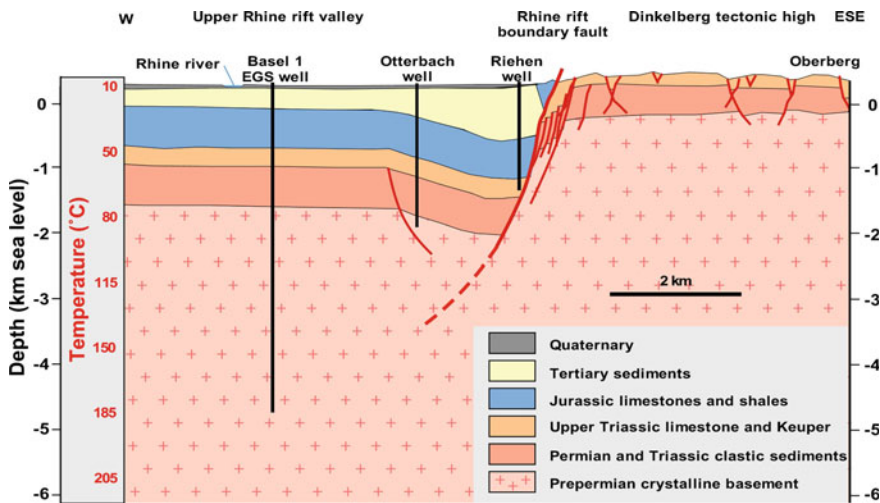


Fig. 11.2 Schematic E-W section across the Upper Rhine Rift Valley showing the geologic situation at the 5 km deep Basel-1 of the EGS project Basel, Switzerland. Modified from Häring et al. (2008)

December 2nd, 2006 was the beginning of massive hydraulic stimulation of the granite at 5 km depth by injecting river water at high pressure into the fractured granite at depth. The drilling site of Basel 1 is located within the city area of Basel. Six days later (Dec 8th) a seismic event with a magnitude of 3.4 and the epicenter at the drilling site of the geothermal project occurred. The measured ground vibration velocity was 9.3 mm s^{-1} . Three further seismic events with magnitude >3 occurred at January 6th, January 16th and February 2nd in 2007. The ground vibrations were accompanied by acoustic noise (bangs) and were felt and heard by many frightened people in the city.

The tremors have been caused by the hydraulic stimulation works by the geothermal project and are termed induced earthquakes following seismological terminology. Most of the monitored seismic events were in the range of microseismicity (Fig. 11.3). Microseismicity is the desired response of the fractured rocks to widening the aperture of joints and fractures for generating the underground heat exchanger. Some of the seismic events (Fig. 11.3) were above the tolerable microseismicity and represent accidentally induced stronger partly noticeable quakes. The transition between the two types of seismicity is continuous.

In the run-up to the stimulation works a pre-stimulation test had been carried out at November 25th, 2006. During the test water was injected to the wellbore at increasing rates starting with 3 L min^{-1} , then 6 L min^{-1} and finally 10 L min^{-1} . In the process the wellhead pressure increased from the initial 15 bar to 33 bar, 52 bar and finally 74 bar. The test reflects the natural hydraulic response of the granitic bedrock at conditions below the opening pressure and suggests that the hydraulic conductivity is about $10^{-10} \text{ m s}^{-1}$. This is a relatively low hydraulic conductivity

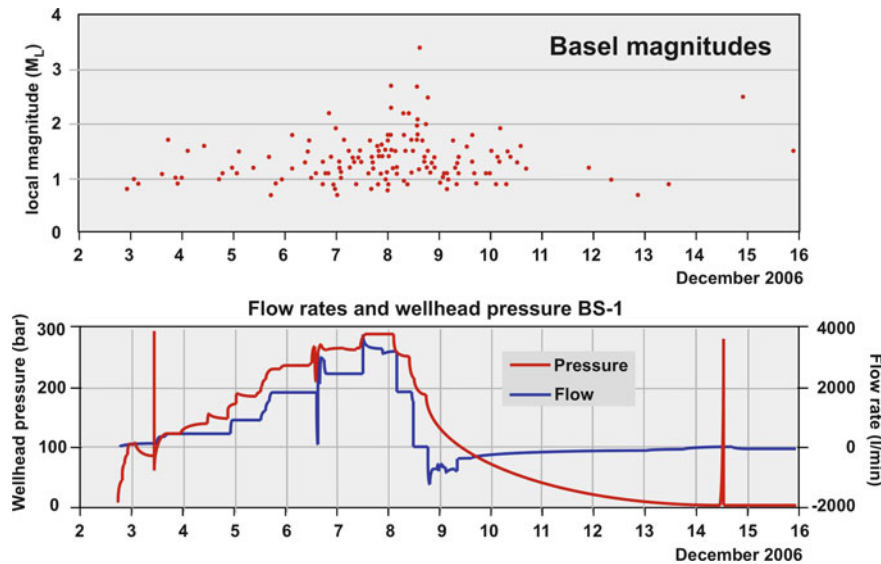


Fig. 11.3 Recorded seismic events induced by hydraulic simulation of granite at 5 km depth of the EGS project Basel, Switzerland. Kraft et al. (2009)

compared to other locations in crystalline basement at similar depths (Ingebritsen and Manning 1999; Stober and Bucher 2007a, b; Ladner et al. 2008).

Based on the results from the pre-stimulation test hydraulic stimulation of the granite started December 2nd, 2006. In the run-up, the procedural details have been hotly debated. Stimulation works ended December 8th, 2006. A total of $11,566 \text{ m}^3$ water was injected. The injection rate had been increased in 5 steps to a maximum of 3750 L min^{-1} . Towards the end of the injection procedure the wellhead pressure reached a maximum of 296 bar. Until about 2 o'clock local time of December 6th the injection rate of 1800 L min^{-1} and the generated wellhead pressure of 250 bar was not exceeded. Until then monitored seismic events were below magnitude 2 (Fig. 11.3). After increasing the injection rates to 3000 L min^{-1} and a corresponding wellhead pressure of 275 bar the first events with magnitude larger than 2 occurred. A further increase of the injection rate to 3750 L min^{-1} and pressures of close to 300 bar resulted in an increasing number of events with magnitudes greater than 2.5 (Fig. 11.3).

Injection has been gradually reduced and stopped at the 8th of December. The opened wellbore spewed a large amount of water and after a few hours the magnitudes of the quakes decreased considerably below 2.0. One event with a magnitude above 2.0 has been recorded at December 14th shortly after the well has been apparently closed (shut-in) and the wellhead pressure has again increased to 285 bar.

The data (Fig. 11.3) suggest a correlation between injection rate or injection pressure and the magnitude of seismic events. This observation in turn implies that properly adjusted hydraulic parameters may control induced seismicity. Critical for

answering the question of controllability of quakes by hydraulics is the understanding of quakes of magnitude 3 and more that followed in January and February 2007 at the Basel site.

The stronger earthquakes observed at the EGS project Basel (magnitude >3) were presumably caused by releasing tectonic shear stresses stored in existing shear zones by hydraulic stimulation. It is very unlikely to detect such a loaded shear zone during pre-drilling exploration or with hydraulic tests. However, during stimulation works is perhaps the best chance to detect potentially dangerous seismogenic shear zones in good time and sensibly react on the threat.

It has been suggested that the induced Basel earthquakes may have had a stabilizing effect in the sense that they may have prevented a much stronger natural earthquake in the future. However, the injected large volume of water that still resides in the ground may also have an opposite destabilizing effect. Fluid migration along pressure gradients may induce further quakes in the future, though probably with decreasing magnitudes. The hydraulic and seismic details of the Basel events suggest actually a destabilizing effect of the residual injection fluids (Langenbruch and Shapiro 2010). The observed late post-stimulation seismicity mirrors earthquake aftershocks following the law of Omori (1894) stating that the frequency of aftershocks decreases with the reciprocal time after the main incident.

The induced seismic events at the Basel EGS site did not cause special or unusual effects at the surface. The recorded seismic vibrations and the macroseismic perceptions were characteristic and typical of earthquakes with these magnitudes and focal depths. Also the sensed acoustic signal (bang) is a typical near-field earthquake phenomenon if high-frequency seismic signals are involved. Unique for the Basel incident was, however, that the epicenter was located in an extensive urban agglomeration, that the tremors were man-made and that the population has been caught off-guard and completely unprepared by the earthquakes.

After the perceptible seismic shocks beginning in December 2006 the project was stopped and later discontinued. The well remained open and the microseismicity evolved as anticipated. In 2011 the wellbore was sealed and in the following the pressure increased at the wellhead steadily and continuously. In the middle of 2016 observed seismicity increased markedly. In October 2016 the tremors reached magnitude $M_L = 1.9$. After sealing the well the seismicity occurred mainly along the northern and southern rims of the generated “reservoir”. The front of the fracturing zone created by the original stimulation measures resumed expansion. As a countermeasure against the increasing microseismicity the pressure at the wellhead was reduced in 0.5 bar steps from initially 8.5 bar. It is planned to keep the well open for some years in order to avoid a further pressure build-up (seismo.ethz.ch).

11.1.4 The St. Gallen Incident (E Switzerland)

The St. Gallen incident relates to another ill-fated geothermal project that finally has been abandoned as a result of unexpected difficulties in the underground. The

problems that hampered the project have been very different from those in Basel (see previous section). Therefore we briefly summarize the incident with the hope that the geothermal community learns from problems and mistakes.

The St. Gallen incident is a drastic warning for the existence of fluid over-pressure in frontal zones of alpine type thrust belts (Müller et al. 1988). The geologic situation in the St. Gallen underground is similar to the Alberta foothills of the Rocky Mountains (Jones 1982).

In the summer of 2013 a 4450 m deep geothermal well has been drilled in the context of an EGS project in the Sittertobel near the city of St. Gallen in E Switzerland. The well has a casing to 4002 m and a perforated casing from there to bottomhole. As planned the borehole reached a cavernous and fractured zone after drilling through hydraulically compact Upper Jurassic limestone (Malm limestone). However, an unexpected massive gas outbreak combined with a seismic shock of magnitude $M_L = 3.5$ ($M_W = 3.3$) occurred early morning of July 21. 2013. Some days before the incident (July 14.–19.) stimulation measures with hydrochloric acid produced the expected microseismicity ($M_L < 0.9$) near the base of the bore. July 20. 2013 the water level in the well suddenly increased as a result of methane gas influx at depth. Therefore the wellbore was sealed but the pressure at the wellhead increased steadily and reached 50 bar. In an effort to prevent an uncontrolled blowout a counter-pressure of up to ~90 bar was build up with a high-density mud well knowing that the measure fuels the risk of increased seismicity. Some increased microseismicity (M_L up to 1.4) resulted from the measures but the pressure at the wellhead slowly decreased. The surprising seismic event the next day ($M_L = 3.5$) was accompanied by acoustic noise (rumble). At the same time the pressure at the wellhead decreased rapidly. The gas has been successfully pushed back into the rock formation. No damages occurred at the surface.

The project was stopped and the well secured. In the fall 2013 one hydraulic well test, two acidification tests and four production tests were carried out with the intention to clarify if the opened rock formation can be used for geothermal purposes. A production rate of 5.9 L s^{-1} with peaks of up to 12 L s^{-1} was attained. Gas incursions repeatedly occurred at rates of $5000 \text{ Nm}^3 \text{ h}^{-1}$ (media release city of St. Gallen). The geothermal project was finally abandoned in 2014 because the inherent seismic risk at the well location troubled a productive utilization and because the yield was clearly below cost-effectiveness.

The wellbore St. Gallen reached the dense Malm limestone beneath the Tertiary Lower Marin Molasse at 3992 m MD. From 4404 m to bottom hole at 4450 m MD (4253 m TVD) Middle Jurassic Dogger was drilled. The temperature measured at 4000 m was 145°C . Pre-drilling extensive 3D seismic investigation was carried out. A massive NNE–SSW trending steeply dipping fault zone, the St Gallen fault zone, was evident on the seismic sections. The structure is visible in the Mesozoic and Paleozoic strata but not in the hanging wall and it is probably related to a Permian–Carboniferous Trough (Moeck et al. 2015). In the hope of high yield and sufficiently high flow-rates the fault zone in the Malm limestone was the declared prime target of the geothermal project. The undisturbed dense Malm limestone has a low hydraulic conductivity ($k_f \sim 1\text{--}5 \times 10^{-10} \text{ m s}^{-1}$), which is inappropriate for an EGS system. The

strike-slip fault system has a maximum horizontal stress S_H in NNW—SSE direction (Moeck et al. 2015). It is expected that the geothermal well connects hydraulically to the St. Gallen fault zone mentioned above particularly as the seismic events were located a few hundred meters from the open hole section of the well and also clearly lower than the well (Diehl et al. 2017). THOUGH2 numerical models suggest that the pressure wave rapidly propagates if a highly conductive fault zone connects the open hole section with a deeper fault zone in the crystalline basement or the predicted Permian—Carboniferous Trough (PCT) (Zbinden et al. 2019). It is presumed that the gas ingress originated from the PCT. The hydraulic procedures taken for preventing a threatening blowout reactivated the hidden inactive deep fault zone.

11.1.5 Observed Seismicity at Other EGS Projects

High hydraulic pressures are necessary to expand the natural fracture network for creating the underground heat exchanger. The so-called opening pressure depends on the lithostatic pressure and the orientation of the controlling fracture and fault system and must be surpassed. Significant increases of flow rates begin above the opening pressure. Much higher pressures are needed if a natural fracture network is not present and must be created by hydraulic methods. Prior to 2000, EGS projects created and stimulated the subsurface heat exchangers without seismic monitoring.

Stimulation work has activated fractures extending for several hundred meters. The strongest induced earthquake caused by geothermal system development reached magnitude $M_L = 3.7$. Personal or ponderable material damage is not known from any of the incidents (Majer et al. 2008). An exception is the geothermal project Pohang, South Korea, with an induced seismic event of $M_L = 5.4$ causing damages at the surface (see below).

At the EGS project Urach (SW Germany) the first stimulation experiments were carried out in the late 1970s in a 3300 m deep wellbore. 640 bar wellhead pressure and an injection rate of 1200 l min^{-1} were reached. Some years later maximum wellhead pressure even reached 660 bar during the continued stimulation experiments. Seismicity has not been monitored at that time. However, no reports on sensed tremors, acoustic signals or earthquakes have been recorded.

The thermal spa Bad Urach, in direct proximity of the EGS wellbore, produces hot water from the Triassic Upper Muschelkalk limestone strata at 650–700 m depth. No evidence for any impairments, damages or irregularities has been observed by the spa. During a further period with stimulation experiments (2002) wellhead pressures of about 350 bar and injection rates of 600 l min^{-1} have been applied. A seismological monitoring network has been established and observed microseismicity as a response to stimulation. Microseismicity was of low magnitude and reached a maximum magnitude of 1.8 in one single event. The opening pressure in the gneiss basement of the EGS project Urach is 176 bar (Stober 2011).

Injection experiments with very high wellhead pressures of 420 bar in the 4900 m deep drillhole Horstberg in the North German plains produced no impairments and caused no tremors with a measurable magnitude.

Stimulation experiments were also carried out in the 4421 m deep wellbore Habanero 1 in the Cooper Basin of Australia in 2003. More than 20,000 m³ water was injected at a flow rate of 40 L s⁻¹ and an overpressure of 350 bar. The resulting vigorous microseismicity was interpreted to originate from a sub horizontal 2.0 × 1.5 km sized structure of 150–200 m thickness. The seismic monitoring recorded a total of 12 macroseismic events with magnitudes between 2.5 and 3.7. The spatial distribution of the seismic events suggests a shear slip mechanism on an existing fault zone that has been released by fluid-reduced normal stress (Baisch et al. 2006). The interpretation has been confirmed by a new deep drill hole with a target 500 m distant point from Habanero 1. Habanero 2 drilled through a highly conductive fracture zone at 4325 m depth.

Habanero 1 was stimulated again in 2005. A total of 22,500 m³ water was injected at rates of up to 31 L s⁻¹ and a resulting overpressure of 270 bar (Baisch et al. 2009). This test was run with lower injection rates and consequently with lower overpressures at the wellhead. Only three stronger seismic events occurred and reached magnitudes of 2.5, 2.9 and 3.0. The early events of the 2005 stimulation occurred at the rims of the previously stimulated volume whereas the volume close to the wellbore has not been seismically reactivated and remained inactive (Chap. 9.3).

The EGS project Pohang, South Korea, drilled two about 4350 m deep wellbores (PX1, PX2) into Permian granodiorite. Massive hydraulic stimulation of both wells triggered a strong seismic event of M_L = 5.4 in November 2017. The earthquake occurred about two weeks after the last stimulation works at PX2. Repeated stimulation injected a total of 1970 m³ water at flow rates of 47 L s⁻¹ during a 2 weeks period. Subsequently very high pressures of up to 900 bar were measured at the wellhead (Kim et al. 2019; Alcolea et al. 2019). The static line pressure was therefore higher than vertical stress and the minimal horizontal stress (the later being smaller than the vertical stress in a strike slip stress regime). The foci of the seismic events clustered to a fault plane at some hundred meters away from the openhole section of the injection well. This seismically active surface probably belongs to a larger fault system (Alcolea et al. 2019). According to Kim et al. (2018) massive water injection was directly into the critically tension loaded fault zone. From the first stimulation works beginning in January 2016 the observed seismicity gradually increased and arrived at M_L = 3.1 in April 2017. The main event of November 2017 was located at 4.5 km depth. The hypocenters (foci) of the main quake and its pre- and aftershocks were located near the openhole of PX1. The distribution of the seismicity in space and time indicates that the fault zone consists of two segments, a SW main section and a NE subdivision. During all stimulation works a total of 12,800 m³ water was injected in the two wells (Kim et al. 2018). The earthquake of Pohang is the largest known induced seismic event related to an EGS project.

Stimulation measures at Soultz-sous-Forêts in the Rhine rift valley reached a maximum wellhead pressure of 180 bar at injection rates near 50 L s⁻¹ (Baria et al. 2006). The fluid injections resulted in a seismic reaction with a maximum magnitude

of 2.9 (by comparison Basel: Flow rate 63 L s^{-1} , pressure 300 bar, and magnitude 3.4). Stimulation experiments in wellbore GPK4 in 2005 with an incrementally increasing injection rate caused only about 200 seismic events.

In the Soultz EGS area there are 2 exploration drill holes (GPK1, EPS1), 3 bores for seismic monitoring (4550, 4601, OPS4), 3 deep (5000 m) geothermal wellbores (GPK2, GPK3, GPK4) and a large number of wellbores of the oil and gas industry. About 25 km of the total length of all these bores have been drilled in granite. In none of all these drillholes signs of seismicity induced by the drilling process have been observed.

The underground heat reservoir at the Soultz EGS site was hydraulically stimulated during several measures. The “upper reservoir” at 3500 m was stimulated in the wellbore GPK1 in 1993 and in the wellbore GPK2 in 1994 and 1995. The “deeper reservoir” at 5000 m has been stimulated in the borehole GPK2 in 2000, in GPK3 in 2003 and in GPK4 in the years 2004 and 2005 (Gérard et al. 2006). Hydraulic stimulation produced several thousand seismic events, generally with magnitudes <2 (up to a 2.9 maximum). All events with magnitude ≥ 2 occurred during the shut-in phase (Genter et al. 2010). Some data on the volumes of injected water and resulting magnitudes of seismic events are summarized for the stimulation works in the deeper reservoir in Table 11.2. The monitored seismicity can be related to shear slip on existing fault and fracture surfaces. No indication for extensional fractures was ever found.

At the Soultz EGS site several 1000 m of wellbores were drilled through “granite”. These granites, however, are rather variable in detail. Some varieties are fine-grained some coarse grained, some types contain strongly altered fractures and veins, some granites contain much biotite, some are rich in amphibole. Any significant analysis of seismicity induced by hydraulic stimulation works must take these diverse petrographic properties of the granites into account.

Table 11.2 EGS Soultz-sous-Forêts, hydraulic stimulation of the deeper reservoir and the resulting induced seismicity

Wellbore (year)	Injected volume (m^3)	Flow rate max. (L s^{-1})	Wellhead pressure max. (bar)	Number of induced seismic events	Magnitude (M_L)
GPK2 (2000)	~23,400	50	130	~14,000	$75 \times \geq 1.8$ 2×2.4 1×2.6
GPK3 (2003)	~34,000	50; 60; 90	180	~22,000	$43 \times \geq 1.8$ 2×2.7 1×2.9
GPK4 (2004)	~9300	45	170	~ 5800	$3 \times \geq 1.8$ 1×2.0
GPK4 (2005)	~12,300	45	190	~ 3000	$17 \times \geq 1.8$ 1×2.3 1×2.6

Table 11.3 EGS Soultz-sous-Forêts, combined chemical and hydraulic stimulation of the deeper reservoir (5 km)

Chemicals used	Date	Flow rate max. (L s ⁻¹)	Number of induced events	Magnitude (M _L)
RMA ^a	May 2006	28	~20	M \leq 1.9
NTA	October 2006	40	—	—
OCA	February 2007	55	~80	M \leq 1.5

^aRMA—regular mud acid; NTA—nitrilotriacetic acid (chelatant); OCA—organic clay acid

The induced seismicity during chemical stimulation is also clearly weaker than during purely hydraulic stimulation (Table 11.3). Three different types of chemicals are usually applied in chemical stimulation (Portier et al. 2007; Genter et al. 2010):

- Regular Mud Acid (RMA) is a chemical dissolving silicate minerals e.g. clay, feldspar and mica
- Nitrilo Triacetic Acid (NTA) dissolves calcite and some other carbonates
- Organic Clay Acid (OCA) is temperature resistant and is applied to clay-rich formations.

No seismic events occurred during the hydraulic circulation test of four month duration between GPK1 and GPK2 in the upper reservoir. Hydraulic circulation of several months duration in the deeper reservoir induced measurable seismicity, which was significantly weaker than during the stimulation phase. During circulation tests both flow rates and pressures were much lower, of course, than during stimulation. A few slightly stronger events (Table 11.4) with higher magnitudes have been recorded. They occurred always during the shut-in phase. All observed seismic events occurred within a distinct zone of the reservoir.

The extensive stimulation works carried out at the Soultz wells resulted in a permanently improved hydraulic conductivity of the basement rocks by a factor of up to 50.

Table 11.4 EGS Soultz-sous-Forêts, observed seismicity during circulation tests in the deeper reservoir (5 km)

	Jul.–Dec. 2005	Jul.–Aug. 2008	Nov.–Dec. 2008
GPK2 production rate (L s ⁻¹)	~12	~25	~17
GPK3 injection rate (L s ⁻¹)	~15 later ~20	~23	~12 later ~27
GPK4 production rate (L s ⁻¹)	~3	—	~12
GPK3 max. wellhead pressure (bar)	40 later 70	73	28 later 86
# seismic events	~600	~190	53
max. magnitude (M _L)	2.3	1.4	1.7

The Soultz-sous-Forêts geothermal power plant started out initially as a research project and converted to a commercial industrial facility with an installed power of 1.7 MW_{el} (Chap. 9.2) in the year 2016.

11.1.6 Conclusions and Recommendations Regarding Seismicity Control in Hydrothermal and Petrothermal (EGS) Projects

Seismic events may also occur at very shallow focal depths of 1–2 km in sedimentary sequences. This has been well documented in many studies. In sensible areas seismic events can be induced by very minor excursions of the stress field or the hydrogeological conditions. However, these kind of seismic events are relatively rare. Anyhow, the possibility for induced seismicity can never completely be excluded even if very “smooth” procedures are applied in developing a geothermal system.

Seismic risk assessment must strictly distinguish between the several phases of geothermal system development: (a) the drilling phase, (b) wellbore cleaning and hydrogeological efficiency-boosting measures, (c) massive hydraulic stimulation of the reservoir, (d) operation phase of the system.

The method of massive hydraulic reservoir stimulation is used routinely by the oil and gas industry (Chap. 9.2). During the many decades of wellbore drilling by the hydrocarbon industry induced seismicity has never been observed during the actual drilling process. To our knowledge, drilling related seismicity has not been reported or documented in the international literature.

Induced seismicity is unlikely to occur in typical hydrothermal systems at shallow depth (<1 km) and low temperatures. Microseismic events may inherently occur in hydrothermal reservoirs at greater depth and elevated temperature due to cooling by injection fluid or caused by pressure changes resulting from varying operating conditions. The seismicity originates on local fracture and fault zones. Fluid re-injection into the reservoir may alter the existing stress pattern in the underground and induce microseismic events. These events release very little energy, are of very short duration, have a high vibration frequency and a very low magnitude (Majer et al. 2008). Consequently the tremors remain unnoticed at the surface.

Production of thermal water from an aquifer may potentially induce seismicity after a long operating time. Fluid extraction reduces pore pressure in the aquifer and increases the effective load (e.g. Segall 1989; Dost et al. 2012; Robertsson and Chilingar 2017). Massive production of hydrocarbons from oil and gas fields or extensive freshwater extraction is often associated with severe local subsidence of the land surface. Furthermore, seismicity may also occur as a result of massive fluid injections into deeper reservoirs related to wastewater disposal or CO₂ underground storage (e.g. Healy et al. 1968; Ake et al. 2005; Segall and Lu 2015; Rutqvist 2012).

The problem is insignificant in geothermal doublets because the heat transfer fluid is routinely re-injected to the aquifer in a closed loop. Even if the transfer

fluid circulation is not completely closed the potential volume losses are small and insufficient to induce seismicity or subsidence. Still it cannot be completely excluded that under extremely unusual circumstances seismicity could be generated also in hydrothermal systems. Induced seismicity resulting from thermally induced stresses generated by injection of cold fluid into hot rock is potentially possible but has never been observed. It is also unknown in the oil and gas industry.

Well improvement measures in hydrothermal system development include well deepening, inclined drilling, deflected drilling (side tracks), directional boreholes, buildup of hydraulic overpressure, shocking and (pressure) acidizing (in limestone). The mature methods are routinely used in drinking water, mineral water and thermal water well development. In contrast to EGS development, the application of overpressure has the purpose to improve the hydraulic connection of the borehole to the aquifer and the fracture network respectively and not to generate a fracture network for the underground heat exchanger (Chap. 8.5). Consequently the applied overpressures are much lower for improving hydrothermal wells.

In recent years massive hydraulic stimulation has been used in some hydrothermal and fault system projects. Usually the stimulation attempts have been made as a last-ditch effort when the expected highly conductive aquifer proved to be an aquitard or when the drilled fault zone had a lower hydraulic conductivity than it was hoped for.

During ongoing operation at some plants very high injection pressures have been applied at injection wells into fault systems. The situation is analogous to massive hydraulic stimulation performed in EGS systems.

Assessing hydraulic stimulation in an aquifer is very different from considering stimulation in a fault zone particularly in regions with active natural seismicity. Massive hydraulic stimulation of a major fault and fracture zone bears the potential danger of spontaneously releasing stored stress that may possibly cause a significant seismic event. Failure of seismogenic faults causing a natural earthquake requires that shear stress exceeds a certain threshold value, which is given by the normal stress, the friction coefficient of the fault system and the shear strength of the rocks (Fig. 11.4). Fluid injection into a stress loaded fault zone may trigger a natural earthquake because the fluids alter the controlling parameters, cohesion, friction and normal stress and the system may prematurely fail (Fig. 11.4). It is therefore highly advised to avoid extra sensitive zones or treat them with great care and prudence. Continuous seismic monitoring and real-time modeling of the underground is strictly mandatory.

Slow migration of injected water in the fault zone and slow pressure build-up by heating of the injected cold water may favor retardation of abrupt stress release in the fault zone.

Furthermore a sensitive fault and fracture zone beneath a geothermally utilized aquifer can be seismically activated by operating of the geothermal plant particularly if re-injection rates are high. Therefore geologic and tectonic exploration and development programs should not exclusively focus on the aimed aquifer horizon.

The local stress field can be disturbed by pore pressure changes caused by the operation of hydrothermal doublets. The affected region depends on the position of the production and injection well relative to the orientation of the stress field. As

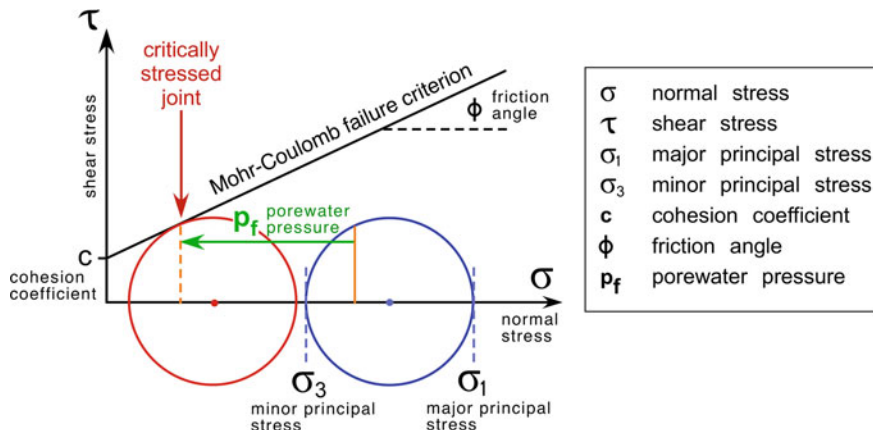


Fig. 11.4 Mohr–Coulomb failure criterion for rocks subjected to increasing porewater pressure (p_f). The Mohr stress circle is displaced to lower effective normal stress and intersects the failure criterion and the joint may slip

an example: The frequently utilized Upper Jurassic Malm limestone of the Bavarian Molasse Basin has a regionally low seismicity suggesting that faults are subcritically loaded in the N–S oriented stress field. The steeply dipping ENE–WSW oriented faults have only a minor potential for reactivation and many of the pairs of geothermal wells are oriented parallel to principal stress direction (Seithel et al. 2018).

Massive hydraulic stimulation has been used since the 1970s and it is the key method for developing a plant based on EGS (Chap. 9). The method has also been the subject of considerable research efforts. Still many physical processes and controlling parameters that influence the abundance, distribution and magnitude of induced seismic events are not yet fully understood (Kraft et al. 2009). During massive hydraulic stimulation injection rates of some thousand 1 min^{-1} water and wellhead pressures of several hundred bars are commonly applied. This opens and widens existing fractures in the reservoir rocks thereby increasing the hydraulic conductivity of the reservoir. The pore water pressure increases in the affected rocks during such a massive stimulation, which reduces the effective normal stress (Terzaghi law) on a joint surface. Increasing pore pressure reduces the friction on the joint and the critical shear stress decreases. According to the Mohr–Coulomb failure criterion the rock may fail along the existing joint (fracture, fault) (Fig. 11.4).

Critical for inducing seismicity is, however, the local tectonic shear stress at reservoir depth. The released seismic energy originates predominantly from stored natural deformation energy. The specific interactions between the controlling parameters are not precisely known, neither qualitatively nor quantitatively. Therefore, it is inherently impossible to reliably and quantitatively predict the risk for inducing seismicity already during the planning stage of an EGS project.

The widening of fractures and joints in the geothermal reservoir by stimulation works needs to be irreversible. The improvement of the hydraulic conductivity must

be permanent and stable. This fundamental demand requires shear slip during stimulation; pure elastic deformation is reversible (Stober 2011). Chemical stimulation and the use of proppings (Chap. 9.3) may keep fractures open in the absence of shear slip deformation.

Induced seismicity is also known from geothermal plants in high-enthalpy fields (Chap. 10). However, these plants are typically located in remote areas at some distance to other buildings and settlements in contrast to hydrothermal and petrothermal plants. Furthermore high-enthalpy fields have a characteristically active natural seismicity. The local population is used to frequent noticeable earthquakes. In the recent past increasing induced seismicity with mounting magnitudes some sensibility and worries developed in the surroundings of high-enthalpy plants.

The following recommendations for minimizing the risk for induced seismicity refer especially to projects enhanced geothermal (EGS) and hydrothermal systems (doublets). They also may be useful for some subfields of plants in high-enthalpy fields.

Geothermal reservoirs with high hydraulic conductivity and good storage capacity (hydrothermal projects) are capable of taking up injected fluids at relatively low well-head pressures. Consequently they are generally less susceptible to strong induced seismic events. Prominent geologically young fault zones in the vicinity of injections bear a significant potential for a strong induced seismic event, particularly if they have a low conductivity and a low storage capacity. The injected fluid then migrates preferentially along the fault zone and unlocks stored shear stresses. The likelihood of triggering an earthquake decreases if major fault zones are absent in the neighborhood of the wellbores. Generally regions with high natural seismicity are often also strongly faulted and fault zones are abundant. Thus such regions have clearly a higher risk for inducing seismic events during EGS development (Nicholson and Wesson 1990).

It is recommended to develop a geothermal energy project following methodically a structured succession of phases. The objectives of the phases include: Creating a risk assessment study, developing a risk mitigation and response plan, a seismic monitoring plan, an emission measurement network and a monitoring system for the hydraulic procedures. It must be strictly distinguished between planning for a geothermal project that requires hydraulic stimulation (petrothermal, EGS) and projects that do not e.g. hydrothermal systems.

The public should be provided with comprehensive, honest, serious and professional information about the project, particularly if it is near villages or towns. Information must be continuous from the initial planning, through development and operation.

Hydraulic fracturing (fracking): In compact little deformed rocks new fractures can be generated by especially powerful stimulation. Hydraulic fracturing, also known as fracking is a widespread and very successful technology for improving permeability of dense rocks used in the oil and gas industry. The fracking technique has been applied since the 1960s a million times particularly for mobilizing gas from “tight-gas” formations without causing environmental troubles.

Hydraulic fracturing of gas deposits fractures the dense rock formation behind the casing of the wellbore by high hydraulic pressures. A perforator (perforating gun) punches holes (20–35 mm) into the casing (or liner) and the cementation of a well (Fig. 12.12). High-pressure pumps press the frac-fluid through these holes into the compact rock creating a network of new conductive fractures. Wellhead pressures of 250–780 bar are typically applied and 300–600 m³ frac-fluid pressed into the formation during 1–2 h. The frac-fluid is a mixture of water (95–99%), proppants and additives. The proppants consisting of sand or ceramic pellets keep the generated fractures open. The chemical additives (biocides, solvents) inhibit growth of biofilms and reduce friction and corrosion. The total concentration of all additives in the frac-fluid is small and the fluids do not represent a threat to the environment. Low-permeability oil and gas reservoirs would not be accessible without the hydraulic fracturing technique.

However, some incidents of groundwater and surface water pollution with methane gas in the context of fracking in oil and gas fields in the USA made publics feel insecure and caused a general uncertainty regarding the use of the fracking technique. The general and common discomfort spread from hydraulic fracturing even to mild techniques of reservoir stimulation.

The geothermal industry may use analogous hydraulic fracturing techniques improving the hydraulic conductivity of compact unfractured rock reservoirs. In most countries today fracking is extensively regulated by law. Rigorous safety regulations and very detailed technical protocols set by the authorities minimize the risk for environmental damages or irritations. The legal assessment of project applications during approval procedures must clearly distinguish between the different techniques for permeability enhancement (fracking, hydraulic fracturing, massif hydraulic stimulation, chemical stimulation etc.), the type and composition of the used fluid, and considers all technical parameters including the applied pressure and volume of injected fluid, the local geology and hydrogeology and many more. Important is furthermore the proper development of the wellbore and the proper grouting prior and after the permeability improving measures (documented by geophysical well logs).

11.2 Interaction Between Geothermal System Operation and the Underground

Settling and subsidence effects in the land surface are occasionally associated with extraction of large amounts of fluids from the underground. The effects are well known in the hydrocarbon industry and also from drinking water withdrawal areas. Land surface subsidence is a slow process that usually affects a large area and is often partly reversible.

Several meters of surface subsidence resulted from high drinking water abstractions in the San Joaquin Valley near the city of Mendota in Fresno County (California,

USA). In the period 1925–1975 subsidence added up to nearly 9 m. Subsidence rates of up to 5 cm per year have been observed in several areas in the USA with high groundwater abstraction. Massive subsidence may go together with faulting (Johnson 1991). Decimeter to meter scale subsidence is commonly observed in the major oil and gas producing regions of the USA. An example is the Diatomite oil field in Kern County, California (Bondor and Rouffignac 1995). A further example is the Slochteren gas field in the Netherlands, which is in production since 1960. Settling of 30 cm in an area of 250 km² resulted from the long-term gas extraction. Natural gas production in the gas field Groningen (the Netherlands) caused subsidence of the land surface by about 30 cm since the 1970s and produced faults and fractures with associated seismicity of up to the magnitude M_L = 3.4 in January 2018.

One of the most sizable subsidence occurred in the Wilmington oil field, Long Beach (California), which came to nearly 9 m. Highest subsidence rates have been measured with >40 cm per year in San Joaquin Valley, California (Fielding et al. 1998). Subsidence is often accompanied by self-sealing of the wellbores and a resultant reduction of the production rate. Both effects are a consequence of the lowered pore pressure caused by fluid extraction. From this the subsequent increase of load reduces the pore volume (porosity), which results in subsidence. Subsidence is an unwanted incident. It has been combated in oil and gas fields by injecting water or gas (usually CO₂) into the reservoir. The method also stopped self-sealing of the wellbores and partly reversed the process. Subsidence halted and was partly compensated by subsequent uplift.

Subsidence is a potential threat also to geothermal systems where large amounts of thermal water are extracted from a deep reservoir for geothermal utilization. However, most geothermal systems are being planned as doublet systems with a quantitative recycling of the produced thermal water by reinjecting the fluid back to the reservoir. The closed primary fluid cycle regenerates the reservoir and prevents leaking of highly saline deep fluids to the surface environment. The closed primary fluid cycle requires a hydraulic connection between production and injection well. Therefore production-related pore pressure drop and injection-related pore pressure increase is typically restricted in doublet operation to the immediate vicinity of the respective wellbores. All together the hydraulic consequences are clearly more moderate than for pure production or injection only operation. Geothermal systems may cause land surface subsidence if the produced heat transfer fluids are not or only partially reinjected to the exploited reservoir as it is the case in many geothermal plants of high-enthalpy fields (Chap. 10). For example surface subsidence has been reported from the East Mesa geothermal field in California (USA) or the Euganean Geothermal Basin (N Italy) (Massonnet et al. 1998; Strozzi et al. 1999).

Radioactive elements are globally present in many minerals and rocks. Particularly granites and granite-derived gneisses contain minerals with abundant naturally radioactive elements such as uranium, thorium and potassium. In granites the zirconium silicate, zircon, incorporates U and Th in its structure (a favorable circumstance that allows isotopic dating of the granite). Decay of uranium in the structure of accessory zircon in granite produces a series of decay products including ²²⁶Ra, ²¹⁰Po and ultimately a series of stable lead isotopes. Typical subsurface heat exchangers in deep

EGS systems are developed in granitic reservoir rocks. Interaction of the fractured granite with the heat transfer fluid also transfers some of these “naturally occurring radioactive materials” (NORM substances) to the fluid in addition to the thermal energy. Consequently the thermal water pumped to the surface through the production well is naturally radioactive to variable degrees. In some cases the concentration of NORM in the fluid is critically high. Inappropriate disposal of NORM waste implies a significant risk for health.

Natural radionuclides are present in all deep waters of the upper continental crust. The total activity of the waters depends on the rock types building up the reservoir and varies over a wide range. As mentioned above granites and granite-derived rocks are typically relatively rich in radionuclides. The principal radioactive isotopes are: ^{226}Ra , ^{210}Pb , ^{228}Ra , ^{224}Ra , ^{40}K (Faure 1986). Radium 226 has a half live of 1600 years. From an environmental point of view the isotope is relatively long lived. It decays to radon (^{222}Rn), a radioactive noble gas (half live 3.8 days), which also may cause environmental troubles.

The risk of radioactive materials leaking to the surface environment is small in geothermal systems operated with a closed system primary cycle. Extracted radioactive elements either dissolved in the heat transfer fluid or as suspended solid particles in the fluid are reinjected into the reservoir in doublet systems. Precipitation and deposition of hazardous materials in the surface installations can be prevented by optimized operation of the system and by precipitation inhibitors added to the produced fluid (Chap. 8.4). However, there remains the potential that radioactive solid deposits and scales may form in surface installations, particularly in pressure shadows of pipe junctions and pipe bends, also in the heat exchanger, filters and pumps (Chap. 15.7).

Barite—celestite scales are relatively widespread (Chap. 15) and the $(\text{Ba}, \text{Sr})\text{SO}_4$ solid solution crystals may exchange Ra on the Ba sites of the crystal structure because of chemical similarities between the two elements. Thus deposition of low solubility barite may co-precipitate radioactive radium isotopes (^{226}Ra , ^{228}Ra , ^{224}Ra). Scales of galenite (PbS) and native lead (Pb) are also common and may incorporate the chemically identical radionuclide ^{210}Pb . To sum up, radioactive solutes of produced thermal waters can be considerably enriched in scales and become a serious disposal problem.

Scale deposits should be given serious attention. Scales in replaced pipe sections, pumps, filters and heat exchangers need to be analyzed and appropriately treated if necessary and responsibly disposed of.

Non-condensable gases dissolved in the produced heat transfer fluid, hot water and steam, include predominantly CO_2 and H_2S . The gases if released to the atmosphere by geothermal plants in volcanic high-enthalpy fields represent a serious environmental hazard (Olafsdottir et al. 2015; Óladóttir and Friðriksson 2015). In Iceland the SulFix and CarbFix research programs deal with the problem of properly disposing non-condensable gases (see Chap. 10).

11.3 Environmental Issues Related to Surface Installations and Operation

Geothermal system development considers potential environmental hazards well in advance and takes the necessary and suitable precautions. For instance, drilling mud containing commonly problematic organic components must be adequately and safely disposed. For collecting the commonly highly saline or even toxic deep fluids that have been brought to the surface during pumping tests appropriate collecting tanks must be made ready if they cannot be reinjected to the deep reservoir immediately. Cooling fluids contain softener, biocides and anti-corrosion chemicals and must be properly disposed.

During drilling but also later during regular operation the geothermal plant generates noise emissions. These must be carefully considered and mitigation measures should be planned particularly if the plant is close to inhabited places. Effective noise abatement measures reduce noise emissions efficiently. However, the improvements require investments into appropriate technical installations at extra costs.

Drilling with electrical motors is quieter than with fuel driven motors. Noise protection barriers and walls around the drilling site reduce noise efficiently. Air fin coolers are noisier than water-cooled systems (Fig. 11.5). If air-cooling is necessary, low-speed air fin coolers are more favorable with respect to noise emissions. Also running turbines make noise. Noise-induced annoyance can be reduced by thoughtful structural engineering and by creating green areas. Of some environmental concern is also the heat released by the heat transfer fluid during re-cooling of the fluid before re-injection. Anticipated noise emissions are one of the principal concerns of the public facing plans for a geothermal project.

Impact on landscape by pipelines can be avoided by putting them underground. This is more expensive than surface pipelines but it considerably increases the acceptance of the geothermal project in the public.

In the past dry-steam high-enthalpy geothermal power plants released steam to the atmosphere after the turbine unit with considerable odor nuisance. Today, the condensed and cooled steam is re-injected into the heat reservoir. This reduces or completely prevents obnoxious odors from reaching the air and improves the productivity of the reservoir by maintaining a sufficiently high fluid pressure in the reservoir. Re-injection of the produced thermal fluids is standard today in all geothermal power systems.

At temperatures below 200 °C special working fluids are used in the secondary cycles for the production of electrical power. Systems on the basis of the Organic Rankin Cycle (ORC) utilize organic working fluids, pentane for example. Kalina systems use an ammonia-water mixture as working fluid (Chap. 4.2). It is necessary to be prepared for a damage event and the appropriate security concepts, installations and equipment must be operational to prevent environmental hazard and hazards on the facility's grounds. Precautions against chemical hazards are routine in the chemical industry.

a)**b)**

Fig. 11.5 Air cooling systems: **a** Soultz-sous-Forêts EGS plant, Alsace, France. The village Kutzenhausen in the background, **b** Nesjavellir flash steam plant, Iceland

References

- Ake, J., Mahrer, K., O'Connell, D. & Block, L., 2005. Deep-injection and closely monitored induced seismicity at Paradox Valley, Colorado. *Bull. Seismol. Soc. Am.*, 95(2), 664–683.
- Alcolea, A., Meier, P., Vilarrasa, V., Olivella, S. & Carrera, J., 2019. Hydromechanical modelling of the hydraulic stimulation PX2-1 in Pohang (South Korea).- Schatzalp, 3rd Induced Seismicity Workshop, p. 73, Davos.
- Baisch, S., Weidler, R., Vörös, R., Wyborn, D. & de Graaf, L., 2006. Induced Seismicity during the Stimulation of a Geothermal HFR Reservoir in the Cooper Basin, Australia. *Bulletin of the Seismological Society of America*, 96, 2242–2256.

- Baisch, S., Vörös, R., Weidler, R. & Wyborn, D., 2009. Investigations of Fault Mechanisms during Geothermal Reservoir Stimulation Experiments in the Cooper Basin, Australia.- *Bulletin of the Seismological Society of America*, 99, 148–158.
- Baria, R., Jung, R., Tischner, T., Nicholls, J., Michelet, S., Sanjuan, B., Soma, N., Asanuma, H., Dyer, B. & Garnish, J., 2006. Creation of an HDR/EGS reservoir at 5000 m depth at the European HDR project. In: *Proceedings 31st Workshop on Geothermal Reservoir Engineering*, Stanford, California.
- Bondor, P. L. & Rouffignac, D. E., 1995. Land subsidence and well failure in the Belridge diatomite oil field, Kern county, California. Part II. Applications. *AHS Publ.*, **234**, 69–78.
- Cook, N. G. W., 1976. Seismicity associated with Mining. *Engineering Geology*, 10, 99–122.
- Davis, S. D. & Pennington, W. D., 1989. Induced seismic deformation in the Cogdell oil field of West Texas. *Bulletin of the Seismological Society of America*, 79, 1477–1495.
- Diehl, T., Kraft, T., Kissling, E. & Wiemer, S., 2017. The induced earthquake sequence of St. Gallen, Switzerland: Fault reactivation and fluid interactions imaged by microseismicity.- *Schatzalp*, 2nd workshop, Davos.
- Dost, B., Goutbeek, F., van Eck, T. & Kraaijpoel, D., 2012. Monitoring induced seismicity in the North of the Netherlands: status report 2010. Scientific report; WR 2012–03, Royal Netherlands Meteorological Institute, Ministry of Infrastructure and the Environment, 47 p., De Bilt.
- Faure, G., 1986. *Principles of Isotope Geology* (2nd edition). Wiley & Sons, 608 pp.
- Fielding, E. J., Blom, R. G. & Goldstein, R. M., 1998. Rapid subsidence over oil fields measured by SAR interferometry. *Geophysical Research Letters*, 25(17), 3215–3218.
- Genter, A., Keith, E., Cuenot, N., Fritsch, D. & Sanjuan, B., 2010. Contribution to the exploration of deep crystalline fractured reservoir of Soultz of the knowledge of enhanced geothermal systems (EGS). *C. R. Geoscience*, 342, 502–516.
- Gérard, A., Genter, A., Kohl, T., Lutz, P., Rose, P. & Rummel, F., 2006. The deep EGS (Enhanced Geothermal System) project at Soultz-sous-Forêts (Alsace, France).- *Geothermics*, p. 473–483.
- Grasso, J. R., 1992. Mechanics of seismic Instabilities induced by the Recovery of Hydrocarbons. *Pure Appl. Geophys.*, 139, 507–534.
- Gupta, H. K. & Rastogi, B. K., 1976. *Dams and Earthquakes*. Elsevier, Amsterdam, 229 pp.
- Häring, M. O., Schanz, U., Ladner, F. & Dyer, B. C., 2008. Characterization of the Basel 1 enhanced geothermal system. *Geothermics*, 37/5, 469–495.
- Healy, J., Rubey, W., Griggs, D. & Raleigh, C., 1968. The Denver earthquakes.- *Science*, 161, 1301–1310.
- Hsieh, P. A. & Bredehoeft, J. S., 1981. A Reservoir analysis of the Denver earthquakes-A case of induced seismicity. *Journal of Geophysical Research*, 86, 903–920.
- Husen, S., Bachmann, C. & Giardini, D., 2007. Locally triggered seismicity in the central Swiss Alps following the large rainfall event of August 2005. *Geophysical Journal International*, 171(3), 1126–1134.
- Ingebritsen, S. E. & Manning, C. E., 1999. Geological implications of a permeability-depth curve for the continental crust. *Geology*, 27, 1107–1110.
- Johnson, A. I., 1991. Land Subsidence. *IAHS Publication*, 200, 680.
- Kim, K.-H., Ree, J.-H., Kim Y.-H., Kim, S., Kang S. Y. & Seo W., 2018. Assessing whether the 2017 MW 5.4 Pohang earthquake in South Korea was an induced event. *Science*, 360, 1007–1009.
- Kim, K.-H., Ree, J.-H., Kim Y.-H., Kim, S., Kang S. Y. & Seo W., 2019. The 15 November 2017 Pohang earthquake. *Schatzalp*, 3rd Induced Seismicity Workshop, p. 7, Davos.
- Kovach, R. L., 1974. Source mechanisms for Wilmington oil field, California subsidence earthquakes. *Bull. Seismol. Soc. Am.*, 64, 699–711.
- Kraft, T., Mai, M. P., Wiener, S., Deichmann, N., Ripperger, J., Kästli, P., Bachmann, C., Fäh, D., Wössner, J. & Guardini, D., 2009. Enhanced Geothermal Systems: Mitigating Risk in Urban Areas.- *EOS, Transactions. American Geophysical Union*, 90(32 (11)), 273–274.
- Ladner, F., Schanz, U. & Häring, M. O., 2008. Deep-Heat-Mining-Project Basel: First Insights from the Development of an Enhanced Geothermal System (EGS) (in German). *Bull. angew. Geol.*, 13(1), 41–54.

- Langenbruch, C. & Shapiro, S. A., 2010. Decay rate of fluid-induced seismicity after termination of reservoir stimulations. *Geophysics*, 75(6), MA53–MA62.
- Majer, E., Baria, R. & Stark, M., 2008. Protocol for induced seismicity associated with enhanced geothermal systems. In: Report produced in Task D Annex I (9 April 2008), International Energy Agency-Geothermal Implementing Agreement (incorporating comments by C. Bromley, W. Cumming, A. Jelacic and L. Rybach).
- Massonet, D., Holzer, T. & Vandon, H., 1998. Correction to “Land subsidence caused by the East Mesa geothermal field, California, observed using SAR interferometry.- *Geophysical research letters*, 25/16, p. 3213.
- McGarr, A., 1991. On a possible connection between 3 major earthquakes in California and oil production. *Bull. Seism. Soc. Am.*, 81, 948–970.
- Moeck, I., Bloch, T., Graf, R., Heuberger, S., Kuhn, P., Naef, H., Sonderegger, M., Uhlig, S. & Wolfgramm, M., 2015. The St. Gallen Project: Development of Fault Controlled Geothermal Systems in Urban Areas.- *Proceedings World Geothermal Congress*, 5 p., Melbourne/Australia.
- Nicholson, C. & Wesson, R. L., 1990. Earthquake Hazard associated with deep well injection - a report to the U.S. Environmental Protection Agency, pp. 74, U.S. Geological Survey Bulletin.
- Óladóttir, A. & Friðriksson, P., 2015. The Evolution of CO₂ Emissions and Heat Flow through Soil since 2004 in the Utilized Reykjanes Geothermal Area, SW Iceland: Ten Years of Observations on Changes in Geothermal Surface Activity. *World Geothermal Congress*, 10 p., Melbourne, Australia.
- Olafsdottir, S., Gardarsson, S.M., Andradottir, H.O., Armannsson, H. & Oskarsson, F., 2015 Near Field Sinks and Distribution of H₂S from Two Geothermal Power Plants in Iceland. *World Geothermal Congress*, 9 p., Melbourne, Australia.
- Omori, F., 1894. On the aftershocks of earthquakes. *Journal of Colloid Science*, 7, 111–200.
- Ottemöller, L. & Sargeant, S., 2013. A Local Magnitude Scale M_L for the United Kingdom.- *Bulletin of the Seismological Society of America*, 103, 2884–2893.
- Portier, S., André, L. & Vuataz, F.-D., 2007. Review on chemical stimulation techniques in oil industry and applications to geothermal systems. In: *Engine*, pp. 32, CREGE, Neuchatel, Switzerland.
- Robertsson, J.O. & Chilingar, G., 2017. *Environmental Aspects of Oil and Gas Production*.- Wiley, 273 p., Hoboken, USA.
- Rutledge, J. T., Phillips, W. S. & Mayerhofer, M. J., 2004. Faulting induced by forced fluid injection and fluid flow forced by faulting. *Bull. Seism. Soc. Am.*, 94, 1817–1830.
- Rutqvist, J., 2012. The Geomechanics of CO₂ Storage in Sedimentary Formations. *Geotech. Geol. Eng.*, 30, 525–551.
- Segall, P., 1989. Earthquakes triggered by fluid extraction. *Geology*, 17, 942–946.
- Segall, P. & Lu, S., 2015. Injection-induced seismicity: Poroelastic and earthquake nucleation effects. *J. Geophys. Res. Solid Earth*, 120, 5082–5103.
- Segall, P., Grasso, J. R. & Mossop, A., 1994. Poroelastic stressing and induced seismicity near the Lacq gas field, southwestern France. *Journal of Geophysical Research*, 99, 15423–15438.
- Seithel, R., Müller, B., Zosseeder, K., Schilling, F. & Kohl, T., 2018. Betrachtungen der Seismizität um Geothermieanlagen im geomechanischen Kontext. *Geothermische Energie*, 89/2, 24–27, Berlin.
- Shapiro, S. A., Dinske, C. & Kummerow, J., 2007. Probability of a given-magnitude earthquake induced by a fluid injection. *Geophys. Res. Lett.*, 34, L22314.
- Stober, I., 2011. Depth- and pressure-dependent permeability in the upper continental crust: data from the Urach 3 geothermal borehole, southwest Germany. *Hydrogeology Journal*, 19, 685–699.
- Stober, I. & Bucher, K., 2007a. Hydraulic properties of the crystalline basement. *Hydrogeology Journal*, 15, 213–224.
- Stober, I. & Bucher, K., 2007b. Erratum to: Hydraulic properties of the crystalline basement. *Hydrogeology Journal*, 15, 1643. (*See further correction in Stober & Bucher 2015*).
- Strozzi, T., Tosi, L., Carbognin, L., Wegmüller, U. & Galgaro, A., 1999. Monitoring Land Subsidence in the Euganean Geothermal Basin with Differential SAR Interferometry. (researchgate.net/publication/228916258).

- Talwani, P., Chen, L. & Gahalaut, K., 2007. Seismogenic permeability, k_s . Journal of Geophysical Research, 112, B07309, doi:<https://doi.org/10.1029/2006JB004665>.
- Wells, D. L. & Coppersmith, K. J., 1994. New empirical relationships among magnitude, rupture length, rupture width, rupture area and surface displacement. Bull. seism. Soc. Am., 84, 974–1002.
- Wyss, M., 1979. Estimating maximum expectable magnitude of earthquakes from fault dimensions. Geology, 7, 336–340.
- Zbinden, D., Rinaldi, A. P., Diehl, T. & Wiemer, S., 2019. Induced seismicity during the St. Gallen deep geothermal project, Switzerland: insights from numerical modeling.- Schatzalp, 3rd Induced Seismicity Workshop, Abstract Book, p. 39, Davos.

Chapter 12

Drilling Techniques for Deep Wellbores



Top drive of a deep drilling rig

Drilling costs stand for about 70% of the total costs of a deep geothermal project. The drilling technique used in deep geothermal projects has been adopted for the most part from the oil and gas industry. The drilling technique used in geothermal projects, however, must satisfy higher requirements because of the combination of high temperatures, high volume fluxes and typically high concentrations of aggressive and corrosive solutes in the produced fluid. Borehole diameters are larger because of the high volume fluxes. In contrast to oil and gas wells, wellbores in the geothermal industry must provide evidence for an operation life of 30 years. Geothermal wells pump hot salty fluids directly along the casing to the surface. In contrast, oil wells produce hydrocarbons along a liner protecting the casing. The costs for a deep drill-hole in the geothermal industry are higher by a factor of 2–5 compared to boreholes in the oil and gas industry (Teodoriu and Falcone 2009).

Drilling and lining deep geothermal wellbores is a very complex and demanding affair. It requires interaction and cooperation of many different high-quality professionals and specialized service companies. Also the requirements to the pumping technique and equipment are extremely demanding because of the high temperature saline fluids that normally need to be pumped in geothermal systems (Sect. 15.3). In this book we try to give a brief overview over the subject only. Specialized textbooks dealing with drilling technique include: Bourgoyne et al. (1986), Aadony (1999), Skinner (2018). Useful definitions and explanation of drilling technology can be found at the Schlumberger Oilfield Glossary: glossary.oilfield.slb.com.

Deep boreholes are normally drilled in shift operation 24 h d⁻¹ without interruptions. An optimized logistics at the wellsite makes provisions for sufficient storage areas for drill pipes, casing, spare parts, cuttings, drilling mud and consumables. If the wellsite is located near inhabited buildings noise protection must be organized.

The type of lining of geothermal wells depends on the type of geothermal system (deep geothermal probe, hydrothermal well, EGS borehole) and on the actual lithological and hydraulic conditions. The well design differs between vertical and inclined boreholes. The drilling process of deep geothermal wells is subdivided into a series of drilling phases marked by the installation and cementing of the casing. The design details of the drill sections, casing and cementation follow the stratigraphy derived during the exploration stage. The diameter of the wellbore and the casing decreases step-by-step at each new drilling phase (Fig. 12.1). Deep drilling technology strictly uses the API (American Petroleum Institute) standard for all diameter measures for wells, drill bits and casings.

The structure of all deep wells is thus tapered. The planned final diameter of the wellbore at depth depends on the required or aspired flow rate. The needed final diameter at depth, the geological stratigraphy and the planned final depth define the initial diameter that needs to be started with at the surface. For a bore with four drilling phases typical diameters are for example: An 18^{5/8} inch surface casing is drilled with a 23 inch drill bit, a 13^{3/8} inch casing is drilled with a 16" drill bit, a 9^{5/8} inch liner with a 12^{1/4}" drill bit and a 8^{1/2}" drill bit is used for the open hole section. If the reservoir consists of stable rocks a casing is not needed in the reservoir section (open hole). Unstable rocks or rock fragments in the fluid require the installation of perforated liner or filter pipes (cased hole) (Fig. 12.2) (Devereux 2012; Bourgoyne

Fig. 12.1 Well design of a deep bore (example: Bad Saulgau, Germany)

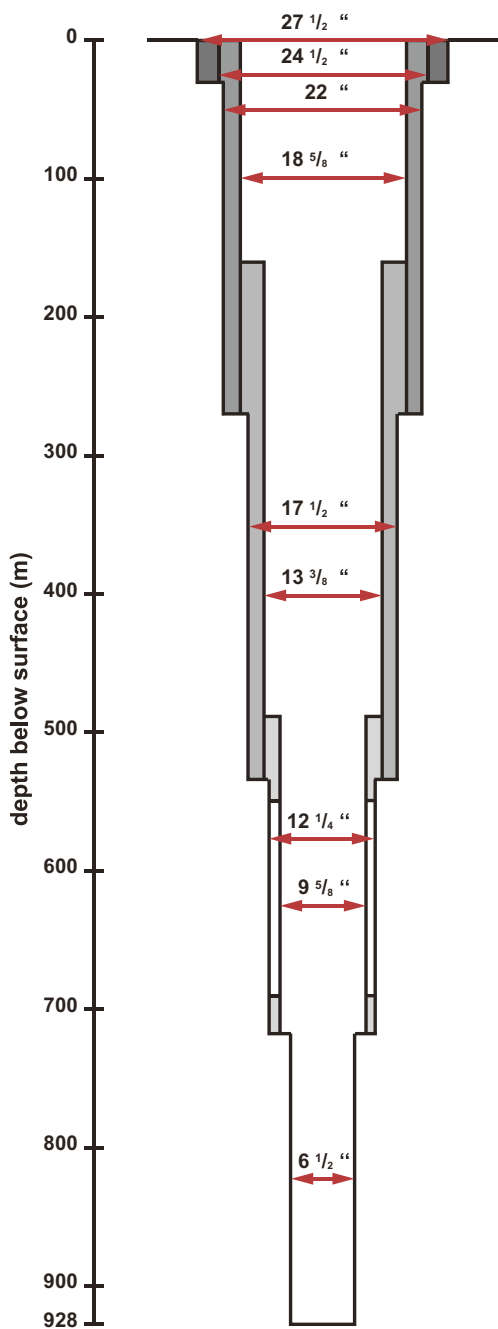




Fig. 12.2 Perforated liner (deep well at Hellisheiði plant, Iceland)

et al. 1986). It is very important that the hydraulic conductivity is not permanently and irreversibly reduced (skin) by the drilling operation or the drilling mud in the reservoir section (Chap. 14).

At the surface, drilling begins with a large diameter. The diameter successively tapers from phase to phase downward. The needed fluid flow rate, as mentioned, defines the minimum diameter of the openhole section and thus the overall structure of the wellbore. However, within these conditions some other aspects must be considered. The diameter must be large enough for trouble free installation of the casing and that sufficient space remains for a good quality cementation. Also the diameter should be large enough to minimize friction losses. On the other side, large diameter wellbores require larger drilling rigs and more energy and material resources. In short, they are more expensive. Drilling costs are roughly proportional to the volume of drilled rock.

Surface casing, conductor casing, casing and liner are needed to prevent instability of the wellbore. Liner are not installed to the surface but are mounted at a landed casing. The casing protects the wall of the bore and seals the well, together with the cementation, from fluid-bearing layers other than the target reservoir. This also makes it possible to separate possible layers with different hydraulic potential. The pipe material and the connectors must be pressure-resistant and must have a high tensile strength at the same time. Both properties drop off with increasing temperature. Therefore, careful pre-drilling consideration and engineering calculations of expected pressures on the casing (external and internal pressure), the anticipated loads such as the weight of the casing string, torsional loads from directional drilling

and sidetracks, grinding loads, compression loads and others are mandatory. The high temperature at the base of deep geothermal wells causes the casing of the production well to expand. The casing of the injection well tends to shrink during plant operation. The well engineering must consider the effect of the thermal parameters on the casing and cementation. Casing and the cementation should not be damaged during expansion or contraction. It must also be kept in mind that casing and cementation have considerably different thermal expansions. Frequent operation during short periods alternating with long downtimes seriously wears casing and cementation. Thermal cracking may damage the cementation and the backfill can become leaky. The damages will aggravate with increasing numbers of repeated starts (Teodoriu 2013).

After fitting the casing cement suspension is pumped into the annulus from bottom to top replacing progressively the drilling fluid. Cementation of a deep drill hole requires special cement properties and special preparation efforts. Cement is a powdered, hydraulic mineral binder that if mixed with water hardens to concrete (in air and in water). Deep drilling uses cements with fine powdered inert materials of similar grain size as fresh-water or salt-water suspensions. Bores of more than 3000 m depth require special mixtures of cement, inert materials and chemical additives and advanced recipes (Smolczuk 1968). The dry raw materials are delivered ready mixed to the drilling site. At the drilling pad the tempering water is prepared by adding NaCl, delayer and chemical additives in blending tanks. Then the powder mix is injected into the mixing water under continuous stirring.

The described mixing procedure results in homogeneous cement slurry with minimal air bubbles. The appropriate recipe for the cement grout and the proper technique of cement injection under the conditions of the bore are crucially important for the quality of the cementation. Quality criteria for deep well cementation are: high early strength, chemically resistant, impermeability to chemically aggressive fluids and excellent binding to both the casing and the rock. This also means that the cementation needs to remain at constant volume. Casing and cementation are the key elements for a safe and long-lasting plant operation. Very useful guidelines have been released by the American Petroleum Institute (API) (api.org).

The cemented casing also helps to safely proceed with the next phase of drilling and allows controlling geology-related over- and under-pressure relative to hydrostatic pressure. The position of the casing during cementation must be strictly centric in the bore thereby ensuring that it is completely surrounded by cement. Else the cementation may remain incomplete and cavities with drilling fluid persist. The centric positioning of the casing is brought about by centralizer elements if the annulus is sufficiently large. If the annulus is narrow centralizer fins made of e.g. carbon fibers are being mounted or painted directly on the pipes before placing in the bore. Special centralizing efforts are necessary for directional drilling and sidetracks.

The casing requirements are high; it must resist all stresses imposed by the regular operation of the plant for the entire life cycle of the system. It also must resist the enormous strains caused by chemical and hydraulic reservoir stimulation. If necessary, the casing of the production well must be protected from aggressive and

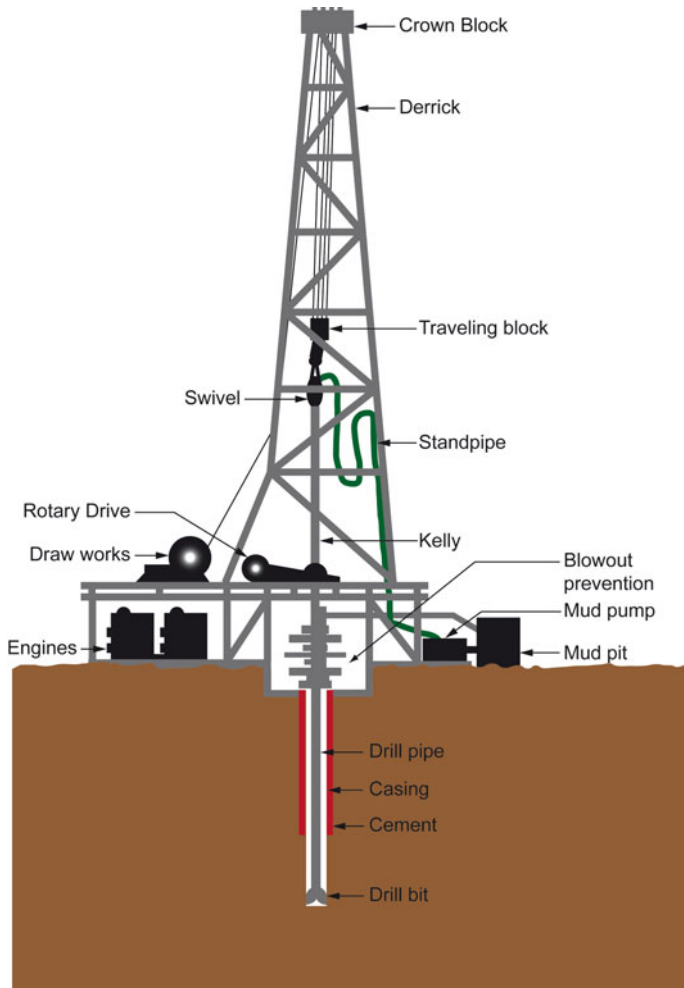


Fig. 12.3 Schematic view of a deep drilling rig with its major components

corrosive fluids by using (expensive) corrosion-resistant materials. At $T < 120 \text{ }^{\circ}\text{C}$ and $p < 250 \text{ bar}$, corrosion-prove fiberglass-enforced plastic pipes can be an option.

The hook load describes the size of operation of a drilling rig. It is the total load that can be held or lifted with the rig. The hook load limits the maximum drilling depth and the drilling and finished diameter of the bore. Hook loads of 150–500 t are required for 2000–6000 m deep wellbores. The essential components of a deep drilling rig are shown on Fig. 12.3. Figure 12.4 shows the some of the components (derrick, traveling block, drill lines, crown block) of Fig. 12.3 from a particular rig. Figure 12.5 shows an example of deep drilling operations from a very remote place



Fig. 12.4 Rig of the Basel EGS project (Switzerland) showing the components: derrick, yellow traveling block, crown block and drill lines

in western China. The central control room of a modern deep drilling rig is shown on Fig. 12.6.

The mast heights of the rigs are in the range of 30–45 m. Diesel-electric power generators or the local energy grid supplies the power for the system. The latter is quieter and environment-friendly but typically also more expensive. The generators can be enclosed for noise protection reasons.

Deep drilling rigs (Bjelm 2006; Hole 2006; Binder 2007) use the rotary drilling technique (Figs. 12.5, 12.6). Rotary drilling can only be used for drilling deep wellbores. Diesel-electric power supply drives the rotary table, the drill pipe and the drill bit at depth. The driving motor is located high up in the rig and drives the drill pipes from top.

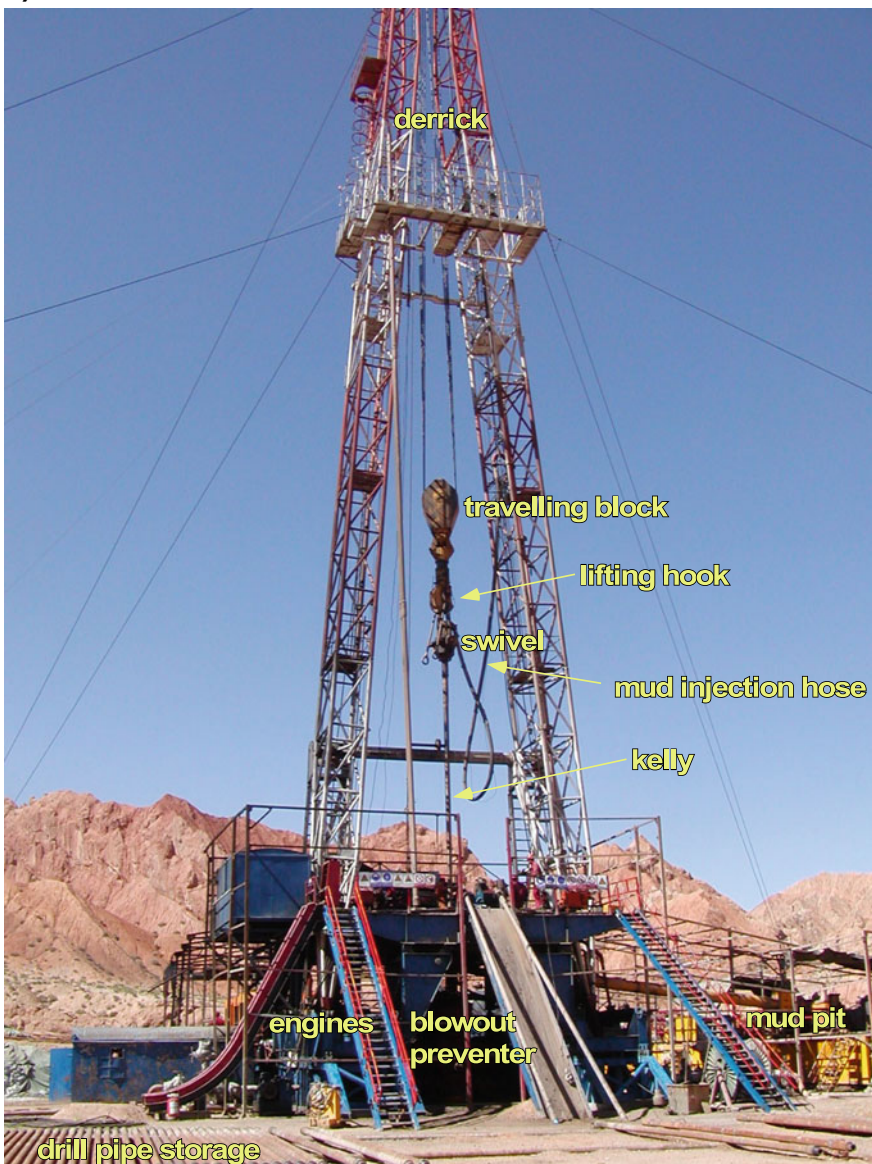
a)

Fig. 12.5 **a** Drilling rig in the Qilian Mountains (West China), **b** details of the platform of the rig, **c** drilling camp in a remote area without noise sensitive neighbors, **d** safety-first applies to drilling operations worldwide

b)**c)**

Fig. 12.5 (continued)

d)



Fig. 12.5 (continued)



Fig. 12.6 Central control room of a modern deep drilling rig (photo courtesy of Herrenknecht AG)



Fig. 12.7 Drill collars support the load on the drill bit

Another drilling technique is turbo drilling. In this technique a turbine drives a drilling bit at depth in the wellbore. This technique is mainly used in directional drilling.

The drilling string consists of drilling pipes of about 9 m length each (fitted by special connectors). The drilling string is permanently adjusted to the appropriate pressure by a qualified operator (Figs. 12.5b, 12.6). Immediately above the drill bit heavy weight drill pipes are typically mounted to increase the weight on the drill bits (Fig. 12.7).

Roller cones and diamond bits are used as cutting tools (Fig. 12.8a) in rotary drilling. The tools must be optimized for removing and transporting the cuttings in the respective geological formation. For coring the formation different bits must be installed (Fig. 12.8b). Diamond bits have a longer lifetime and no movable parts

compared to roller bits. Fine-grained sediments must be drilled with different bits than granitic basement (Fig. 12.8c).

Directional drilling is required if the wellbore needs to reach a well-defined target area such as a major fault zone that is expected to be highly water conducting. Typically drilling begins vertically. The wellbore deflection begins at a certain depth, at the so-called kick-off point (KOP). The slope then gradually decreases and the deviation from the vertical increases progressively. The length of the drilled section and the vertical depth differ steadily. The total length of the drilled section after completion of drilling is designated as “final depth” also measured depth (MD). This may cause confusion in regards to interpretation of temperature data, hydraulic tests

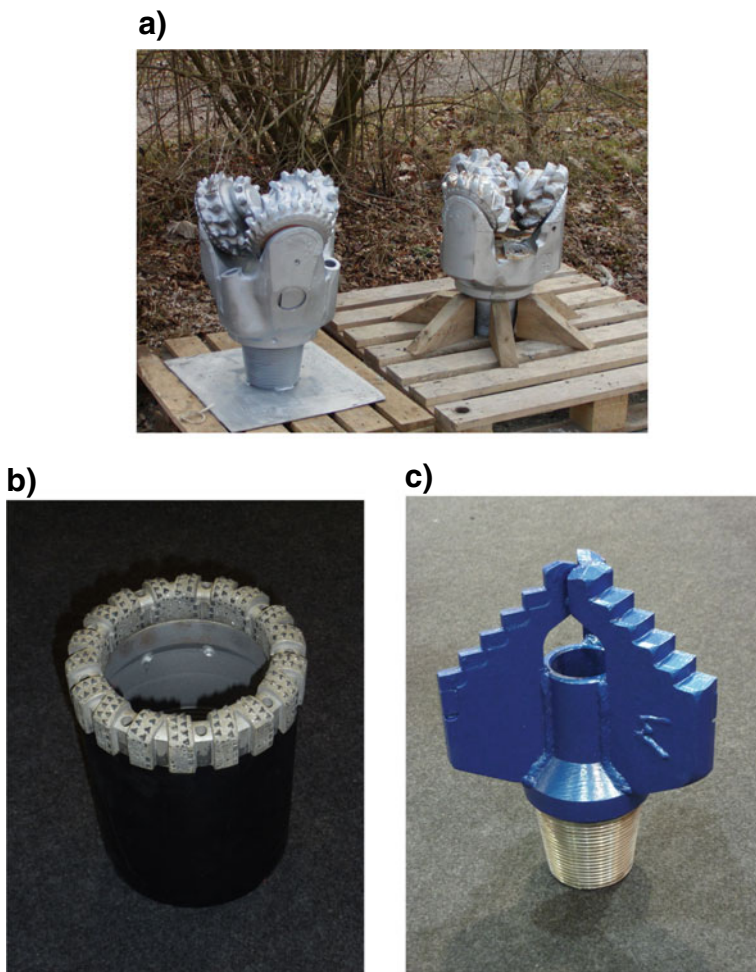


Fig. 12.8 Drilling tools: **a** Roller cones for deep drilling, **b** diamond bit for coring, **c** tool for drilling fine grained sediments (clays), **d** spent drill bits



Fig. 12.8 (continued)



Fig. 12.9 Tool for directional drilling ($8\frac{1}{2}$ ')

and other parameters and it needs to be correctly recognized that this is not a vertical depth (if drilling is not exclusively vertical). One must be aware that modern deep wellbores may have a drilled section that exceeds the vertical depth massively, that is measured depth (MD) is much larger than true vertical depth (TVD).

The drilling drive is placed below surface, as a downhole motor directly above the drilling bit. Directional drilling motors have an adjustable bend at the case. Deflected drilling operates without turning the entire drill string. Directional drilling uses special drilling tools (Fig. 12.9). The drill bit slowly and continuously deviates from the vertical drilling axis and it describes, because of the bend in the housing, a curved trajectory. Drives for directional drilling have a strong wear at the knee joint. The position of the drill bit is continuously recorded during drilling

and “measurement-while-drilling” devices (MWD) transmit the data to the surface (Inglis 2010). If the data analysis reveals a discrepancy between the actual and the planned drilling path, appropriate corrections are made. It is also possible to combine two motors: the downhole motor for the steering head to optimize the borehole placement and an additional second motor at the surface to optimize drilling efficiency. This relatively new technique enables to drill faster and deeper. Downhole motors are increasingly used also for drilling vertical bores because the drilling progress is substantially higher (Skinner 2018).

Rotary drilling turns the entire drill string including the drive. The drillmaster may influence the drilling path somewhat by varying the pressure on the drill bit. The drilling path can also be influenced by activating hydraulic fins. The control electronics sets hydraulically driven fins in motion and presses them against the wellbore thereby deflecting the drilling path into the opposite direction.

Planning the well drilling considers many bits and pieces including: planning details for directional drilling and defining a detailed drilling path, assigning appropriate casing materials, tailoring pipe wall thicknesses, choosing pipe connectors, specifying special thermally resistant cements, choosing appropriate down hole tools, reservoir-conserving drilling fluids, disposal of drilling mud and cuttings and choosing the right size (hook load) of the rig. The drilling location and the target point in the reservoir set the frame for the drilling path and the geologically controlled casing scheme. Planning of the drilling path, the details of tool selection and other technical equipment and installations are ultimately based on the geological underground model derived during the exploration phase (see e.g. Section 8.8).

In the upper 500 m of the bore, provision must be made for sufficient space for mounting the production pump. Continuous operation establishes a thermal steady state with a hot environment in the production well and a cooler setting in the injection well. Frequent operation interruptions create significant thermal stress on the material (casing, cementation, etc.). This must be considered in the planning stage and appropriate thermal resistivity of the installations is well-invested money. Generally, the casing in geothermal wells must resist extremely high mechanical, thermal and, as will be discussed later, chemical stresses. Compressive strength can be critical for large-caliber pipes, whereas tensile strength is limiting for small-caliber casing. Typically, however, the connectors are the vulnerable part for the tensile load (Australian Drilling Industry 1997).

Friction losses (Δp) in wells depend on flow rate and diameter of the casing (Fig. 12.10). The friction related pressure drop (Δp) is proportional to the flow rate (Q) squared. Thus doubling the flow rate (Q) leads to a four-fold pressure drop (Δp). Similarly, a 15% reduction of the flow cross-section amplifies Δp by a factor of two. Friction losses in wells with a 9^{5/8} inch casing and typical geothermal flow rates of 150 l/s are normally smaller than $p = 20$ bar. 7 inch casings, however, can be associated with friction losses of $\Delta p > 90$ bar, which may significantly threaten the profitability of the system. For flow-rates Q of about 100 l/s, expected Δp is correspondingly lower (10 and 45 bar for the considered casing diameters, respectively).

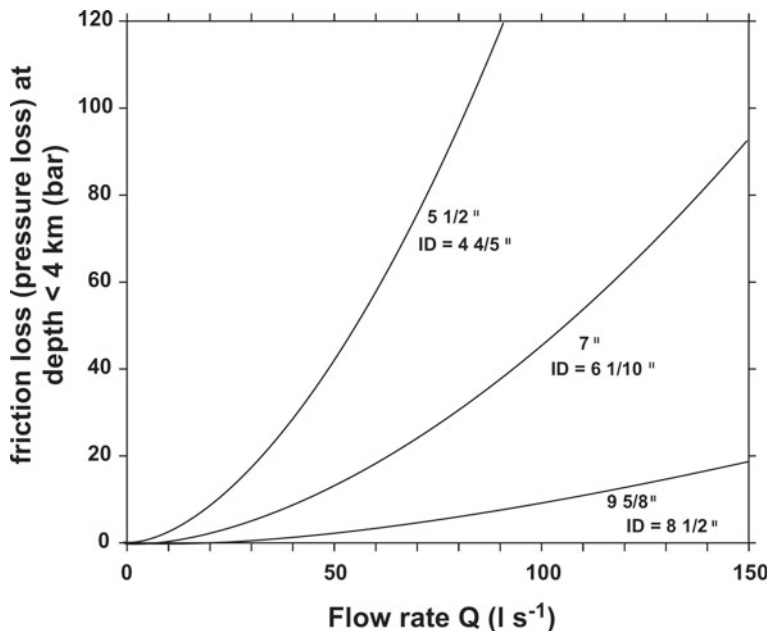


Fig. 12.10 Friction-losses Δp (bar) in a geothermal well as a function of flow-rate Q (L s^{-1}) for three casing diameters (inch '') and internal casing diameters ID (Cholet 2000)

Large diameter drilling, directional drilling and securing problematic and difficult drilling sections require the detailed study of active tectonic stresses, gas influxes and reservoir-conserving resource connection. The key devices preventing uncontrolled discharges of fluid and gas are blowout preventer, choke-manifold and drilling-spool (Fig. 12.11).

The very first action for the planned deep drilling is the selection of a drilling site (well site). It typically requires an area of 3000–5000 m^2 and access to water and electrical power. It is important that groundwater threatening fluids may not contaminate groundwater. Fluid- and waste-handling must be designed. Both standpipes for the planned doublet and the rig cellar should be defined decision of the drilling site foundation. Collection pools for drilling mud and cuttings need to be designed and brought into function. Collection tanks for the storage of highly mineralized and potentially toxic deep thermal fluids must be provided for hydraulic tests of several days of duration (Fig. 12.12). In most countries, the design and setting up of the drilling site must be coordinated and tuned with the responsible authorities.

Drilling mud performs many tasks. It cools the drilling tools, lifts the cuttings to the surface, stabilizes the bore and serves many other purposes. Deep geothermal drilling typically uses water-based drilling fluids. Special conditions may require oil-based drilling fluids or special foams. The complex site-specific requirements on drilling fluids require expert knowhow. Dedicated firms provide materials and



Fig. 12.11 a Blow-Out-Preventer waiting for installation, b blow-out preventer of the Qilian Rig shown in Fig. 12.5



Fig. 12.12 **a** Storage pond for highly mineralized and potentially toxic deep thermal reservoir fluids during hydraulic tests. **b** Storage pond with inflowing thermal fluid

chemicals that are mixed and added to the drilling fluid. An expert engineer supervises the operation and is responsible for optimizing the formula and monitoring changes in the produced mud. The appropriate formula for the drilling fluid also depends on the type of rock to be drilled. Clay-suspension in water is often used in the near-surface top hole because of groundwater protection concerns and because of optimal drilling progress with low-density fluids. Polymers are commonly added to increase the viscosity of the drilling fluid while drilling highly permeable formations. The filter cake from this drilling fluid helps to seal the permeable formation. Special inhibitor additives significantly reduce swelling of clay in drilled shales and mudstones. Still the viscosity of the fluid remains low and the clay-bearing cuttings are rapidly removed from the bore. Barite (BaSO_4) is a standard stabilizer for drilling formations under pressure. Drilling fluid reduces friction between drilling string and the bore in long and particularly in directional drilling sections (Van Dyke 1998; ASME 2005; Budi Kesuma Adi Putra 2008; Huenges 2010).

The drilling mud is pumped to mud tanks (pools) above ground, cleaned and reconditioned for reuse in the borehole. The drilling fluid is also used for transmitting pressure signals and data for the “measurement-while-drilling” (MWD) technology. The mud logging firm records important parameters, such as drilling progress, current depth and position of the drill bit, load on the drill bit, torque, speed, mud load, flow rate of drilling fluid among others. During drilling, geologically trained



Fig. 12.13 Well head

personnel examine the cuttings and identify the current drilled formation and compare the current data with the predicted profiles from the pre-drilling exploration phase. Specialized service firms carry out the precise maneuvers of the directional drilling. Other expert firms handle the fitting of the pipes and the subsequent cementation. Pipes, cement and additives must be ordered, delivered and stored on site in just sufficient amounts at exactly the right time. After drilling and completion the wellbore is securely sealed with a wellhead (Fig. 12.13).

During drilling and after completion of the wellbore, systematic hydraulic tests provide data on the hydraulic conductivity of the target horizon and the thermal reservoir (Sect. 14). Repeatedly collected fluid samples supply the necessary information on the hydrochemical properties of the formation fluid (Sect. 15) and methodical geophysical well logging makes physical and structural rock and formation properties available (Sect. 13.2). The type and duration of hydraulic tests depend on the typical prevailing hydraulic conductivity of the formation. If the initial natural conductivity is lower than required for a successful project it may be increased with engineered hydraulic and (or) chemical methods (Sect. 8.5, 9.3). If the two wellbores of a doublet and the reservoir design have been successfully completed then the two wells can be tightly connected above ground. The following circulation test of several weeks



Fig. 12.14 Blending device for high-density brine. The brine is injected into the production well to stop artesian over-flow after pump-switch-off

duration reveals the properties and conditions of the entire system. After switch-off of the production pump the well commonly keeps producing thermal water (Sect. 8.2). Injecting high-density salt water into the well may stop the unwanted artesian water. Some geothermal plants have been equipped with special auxiliary devices for this purpose (Fig. 12.14).

If the yield of the target layer is lower than expected or hoped for it is possible to gain access to additional layers that have been drilled and cased previously. The workover operation expectantly increases the total yield of the well. For this purpose the cased and cemented section of interest can be punched with a perforating gun or perforating system. The perforating gun contains a large number of removable charge carriers viz. metal cups filled with explosives (Fig. 12.15). It is lowered in the cased well to the desired depth. Varying the detailed design and assembly of the charge carriers, the type and amount of explosives and the firing sequence permits precise perforation of casing, cementation and the rocks close to the well. Penetration depths of more than 1 m can be realized with the technique. The design of the guns can be complex containing several units that can be fired separately. Perforation performance increases with new system designs and continuous development improves the functioning and precision of well perforation (Wan 2011).

Production pumps (submersible pumps, line shaft pumps) belong to the mechanically most strained assemblies of a geothermal power plant. Pump failures cause a

Fig. 12.15 Well perforating systems. Perforating gun with charge carriers



long-standing unplanned outage of the entire system. Pump and motor are combined in one unit in submersible pumps. The pump is submersed in the geothermal fluid at relatively large depth in the production well (several 100 m below surface). The pump operates in a chemically aggressive fluid at high pressure and temperature. The pump itself produces additional waste heat. Moreover desanding geothermal wells is not routinely performed in contrast to drinking or industrial water wells. The later wells are desanded by pumping at 50% higher capacity than later during the regular operation. As a consequence geothermal wells may later carry along solid sandy particles that represent a massive mechanical strain for the pump and can reduce its durability significantly. The electrical power supply requires a mechanically and chemically resistant cable leading through the wellbore from the surface to the pump at depth. Line shaft pumps have a pump unit that is placed in the production well at depth, the motor unit, however, is located above ground. The motor is thus not exposed to the high temperature of the produced fluid. Consequently, line shaft pumps can produce fluids with very high temperature (Fig. 12.16). Because pump and motor units are mechanically connected with a rod assembly the maximum depth for operating of line shaft pumps is about 300 m. Most geothermal plants produce geothermal fluid with submersible pumps. However, motor-failures of line shaft pumps can be fixed and repaired immediately, which is a significant advantage. Damaged submersible pumps must be recovered from depth, dismantled, repaired and finally re-installed. The repair is likely more time consuming and thus causes a longer full stop of the plant if no replacement pump is held at the site.

Submersible centrifugal pumps (Sect. 4.2, Fig. 4.11) have been in use for short operation periods down to 3000 m depth and volume flows of up to 280 l s^{-1} by the oil



Fig. 12.16 Line shaft pump

industry. Special submersible centrifugal pumps have been operated at temperatures of up to 232 °C and pumped highly viscous fluids, fluids with dissolved carbon dioxide, hydrogen sulfide and suspended solid particles. Such extreme conditions, however, reduce the working life of the pumps dramatically (Sect. 15.3).



Fig. 12.17 Injection pump

The efficiency of the submersible pumps depends not only on the critical components in the borehole including motor, seals and fittings, pump, sensors and cables but also on the above ground control systems. A diligent choice of fitting components optimized for the specific site conditions are crucial for the efficient, reliable and during operation of the pump system. Especially resistant materials must be used for pumping strongly corrosive fluids. At some sites a tubing string placed below the pump releasing acids or other chemicals helps increasing the durability of the pump (Fig. 8.15). The tubing string also provides access for gauges sending data to the surface.

At given hydraulic conditions the well yield decreases with increasing temperature. Most pump manufacturers define 180 °C as maximum temperature at which their pumps can be operated reliably and constantly. The actual operating conditions may later differ significantly from the predicted conditions forming the basis for the chosen pump design. If so, the efficiency of the system and pump durability may be appreciably reduced. Today most of the practical technical experience with submersible pumps draws on their use in oil fields. However, in the last years experience from specially designed pump systems for use in geothermal power plants is steadily growing (e.g. Ichikawa et al. 2000; Takács 2009; Qi et al. 2012).

Injection pumps (Fig. 12.17) for re-injecting cooled heat transfer fluid back to the underground reservoir can be placed above ground, in contrast to production pumps.

References

- Australian Drilling Industry, 1997. Drilling: The Manual of Methods, Applications, and Management. Crc Press, 624 pp.
- Aadony, B. S., 1999. Modern Well Design. Balkema, Rotterdam, 240 pp.
- ASME Shale Shaker Committee 2005. The Drilling Fluids Processing Handbook. ISBN 0-7506-7775-9.
- Binder, J., 2007. New technology drilling rig. Proceedings of the European Geothermal Congress 2007, 4 pp.
- Bjelm, L., 2006. Underbalanced drilling and possible well bore damage in low-temperature geothermal environment. Proceedings of the 31st Workshop on Geothermal Reservoir Engineering, Stanford, Ca, 6 pp.
- Budi Kesuma Adi Putra, I. M., 2008. Drilling practice with aerated drilling fluid: Indonesian and Icelandic geothermal fields. Geothermal Training Programme, UN University Reykjavik, Iceland, 11, 77–100.
- Bourgoyne, A. T., Millheim, K. K., Chenevert, M. E. & Young, F. S., 1986. Applied Drilling Engineering. In: Society of Petroleum Engineers (ed Series, S. T.), pp. 502, Richardson, TX, USA.
- Cholet, H., 2000. Well production. Practical handbook. Institut Français Du Pétrole Publications, 540 pp., Editions TECHNIP, Paris.
- Devereux, S., 2012. Drilling Technology in Nontechnical Language (2nd edition). PennWell Corp., 270 pp.
- Hole, H., 2006. Lectures on geothermal drilling and direct uses. UNU-GTP, Iceland, report 3, 32 pp.
- Huenges, E., 2010. Geothermal Energy Systems: Exploration, Development, and Utilization, pp. 486, Wiley-VCH Verlag GmbH & Co. KGaA, Berlin.
- Ichikawa, S., Yasuga, H., Toshia, T. & Karasawa, H., 2000. Development of downhole pumps for binary cycle power generation using geothermal water. Proceedings World Geothermal Congress 2000, Kyushu-Tohoku, Japan, 1283–1288.
- Inglis, T. A., 2010. Directional Drilling. Petroleum Engineering and Development Studies. Graham and Trotman, London (Kluwer, Springer), 274 pp.
- Qi, X., Turnquist, N. & Ghasripoor, F., 2012. Advanced Electric Submersible Pump Design Tool for Geothermal Applications. Geothermal Resources Council Transactions, 36, 543–548.
- Skinner, L., 2018. Hydraulic Rig Technology and Operations (Gulf Drilling Guides). Gulf Professional Publishing. 555 pp, ISBN 978-0128173527.
- Smolczyk, H. G., 1968. Chemical reactions of strong chloride solutions with concrete. Proceedings of 5. Intern. Symp. Chem. Cem., Tokyo, 274–280.
- Takács, G., 2009. Electrical Submersible Pumps Manual: Design, Operations, and Maintenance. Gulf Professional Publishing, Elsevier, Oxford, UK, 276 pp.
- Teodoriu, C. 2013. Why and when does Casing Fail in Geothermal Wells. OIL GAS European Magazine, 1, 38-40
- Teodoriu, C. & Falcone, G., 2009. Comparing completion design in hydrocarbon and geothermal wells: the need to evaluate the integrity of casing connections subject to thermal stress. Geothermics, 38, 238-246
- Van Dyke, K., 1998. Drilling Fluids, Mud Pumps, and Conditioning Equipment. Rotary Drilling Series, Unit 1, Lesson 7. University of Texas, Petroleum Extension Service, 235 pp.
- Wan, R., 2011. Advanced Well Completion Engineering 3rd edition. Gulf Professional Publishing, 736 pp.

Chapter 13

Geophysical Methods, Exploration and Analysis



Seismic exploration

Geophysical sounding and investigations provide an indirect view into the underground. Geophysical investigations collect data using instruments at the surface or placed in boreholes. Borehole geophysics and geophysical well logging can probe and research in cased and in uncased bores. In Chap. 13, we briefly present a selection of geophysical investigation methods. Detailed accounts on geophysical methods have been presented by e.g. Sheriff & Geldart (2006) and Telford et al. (2010).

13.1 Geophysical Pre-drilling Exploration, Seismic Investigations

Applied geophysics uses physical measuring systems for sensing the geological structure and the properties of the subsurface. The methods determine parameters and properties from diverse domains including the gravitational field, magnetic field, electrical conductivity, propagation of acoustic and electromagnetic waves. The methods are indirect, meaning that geological structure must be deduced from the collected data. The data must be geologically interpreted. The interpreted geophysical data portray the structure of the underground, the lithostratigraphy, the thickness and depth of the target formations and the position, orientation and thickness of fault zones. Under favorable circumstances the data even give evidence on the specific type of sedimentary facies of the target formation.

The very first step in geophysical exploration for a new geothermal power system is the careful and thorough search for all available geophysical data and direct and indirect information on the geology of the underground from previous exploration campaigns in the wider region of the new site. The compiled “old” data must be reviewed, evaluated and re-interpreted if necessary. The effort may make a new expensive seismic campaign obsolete or it can be significantly downsized. Digital reprocessing of “old” seismic data may significantly increase the conclusiveness of such data. New geophysical exploration data from the surroundings of the drilling site reduce localization errors viz. the difference between true and predicted position. Continuous improvement of the seismic exploration tools increases the resolution of the investigated geological structure at the site.

Reflexion seismology is a particularly important method for the geophysical investigation of deep geological structures. Other methods including gravimetry, geomagnetism, geoelectrics, magnetotelluric or combinations of these methods can be useful for cost-efficient reconnaissance investigations. They are sometimes needed for solving special local problems. For example for describing and evaluating recognized local seismic anomalies or seismic barriers.

Gravimetric measurements evaluate the intensity of the Earth gravitational field. A gravimeter is the standard instrument used by this geophysical method. It is an accelerometer specially designed for measuring the downward acceleration due to gravity. The local variations of the acceleration due to gravity reflect the density structure of the local geological underground but also the latitude and altitude of the

instrument position. The geological structure and nature of the underground can thus be deduced from the detected density variations (Telford et al. 2010). For example, the seismic exploration may have discovered an intrusive body crosscutting a well-stratified sequence of presumably sedimentary rocks. Gravimetric analysis can with certainty distinguish between intrusions of high-density igneous rocks such as gabbro and low-density salt domes. Gravimetry may also discover and localize larger caves in karstified formations in the subsurface. The method may also localize the depth of the basement-cover contact surface which separates dense basement rocks from lighter sedimentary cover rocks. There are many more potential useful applications of the powerful method.

Geomagnetic surveys measure deviations from the undisturbed geomagnetic field. The data relate to the magnetic susceptibility of the geological material forming the underground. Measurements can be made from the Earth surface or airborne. The magnetic susceptibility of near surface rocks (some km) and soil deform the natural magnetic field that has its origin in the deep Earth. The local deviations from the undisturbed magnetic field, so called magnetic anomalies, result from induced magnetization of Earth materials by the magnetic field. The size of the anomalies depends on the strength and direction of the Earth magnetic field at the location in question and on the magnetic properties of the geological material, the size of especially magnetizable geological units, strata or bodies. Typically, pronounced magnetic anomalies are caused by discrete perturbing rock bodies in the underground. The classic example: Lenses of iron ore cause strong magnetic anomalies. Iron oxides, iron sulfides and similar material display an inherited permanent remanent magnetization, independent of the present day magnetic field. Geomagnetic measurements try to relate observed anomalies to the nature, shape, size and depth of magnetic perturbations (Telford et al. 2010). Geomagnetic measurements have been successfully used to locate and characterize fault zones in the crystalline basement.

Magnetotelluric surveys for deep exploration use alternating electromagnetic fields for investigating the underground. Natural or technical sources can be used as stimulating primary magnetic fields. The geophysical method can be used to explore a wide range of depths from the near surface area to the deep underground because the range of periods of the alternating fields is very large and the penetration depth depends on the frequency. The applied magnetic fields induce electrical currents in conductive geological units and these currents in turn generate electromagnetic fields. From the recorded temporal variation of magnetic and electric fields follows, after appropriate data processing, the distribution of electrical conductivity in the geological units in the crust and down to the uppermost mantle. The frequency range of the currents defines the exploration depth (Vozoff 1987). The magnetotelluric methods used for geothermal site exploration use natural electrical currents in the subsurface as source. The method does not require an active transmitter station and is therefore economical. However, in densely populated areas the technique cannot be used because of continuously present electric noise. Magnetotelluric is mainly used as an exploration tool in high-enthalpy fields. Typical high-enthalpy reservoirs are capped and partly enclosed by a zone of alteration minerals (caprock) produced by the reaction of hot fluids with primary often chemically reactive volcanic rocks.

Typical caprock sealing volcanic reservoir rocks contain clay minerals, zeolites and hydroxides. Caprocks have a very low permeability and an electrical resistivity that is very different from the reservoir rocks. Thus the caprocks can be localized and the depth and size of the reservoir assessed. The use of magnetotelluric methods for the exploration in EGS and hydrothermal projects is still in the research and development stage.

In contrast to the geophysical exploration methods briefly described above, seismic exploration tools have a high resolution for the considered exploration depths of some 1000 m and produce realistic and detailed structural images of the underground. The exploration of geothermal reservoirs profited massively from the vast and comprehensive knowledge in the field of exploration seismics gathered by the oil and gas industry.

The prime exploration method for depths greater than 1000 m is reflection seismology. Compared with other geophysical methods, reflection seismology provides the clearest and most precise picture of the structure of the subsurface. The method sends acoustic waves from the surface to the underground. The acoustic waves are generated at the surface with truck-mounted vibrators (metal mass vibrating at high-frequency), falling weights or with detonating explosives in boreholes (Fig. 13.1). The waves propagate through the rocks and are being reflected and refracted at the boundaries of rock units with (highly) contrasting density (Fig. 13.2). A relatively small fraction of the wave energy reaches the surface where it is recorded by complex arrays of instruments, so-called geophones (Fig. 13.3). Geophones are highly sensitive microphones, which record the wave echoes from the various geological discontinuities underground. The reflected wave has travelled from the source at



Fig. 13.1 Reflection seismology. The illustrated vibrator is fitted to a truck (see front page of Chap. 13)

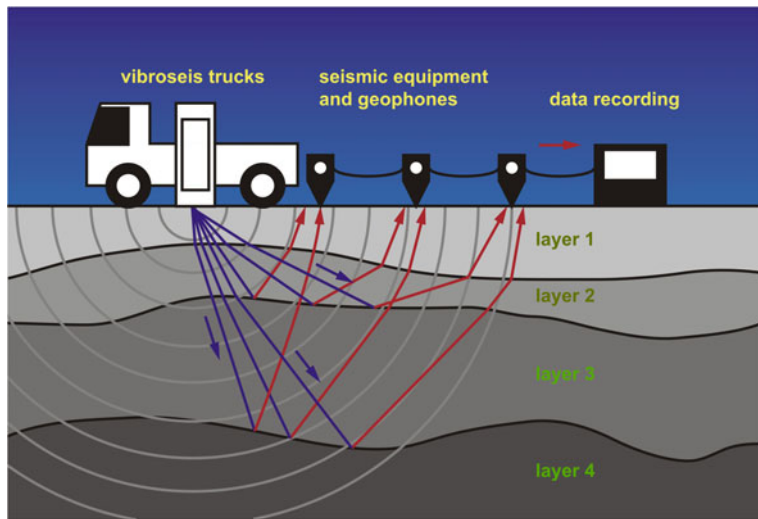


Fig. 13.2 Propagation of acoustic waves in the geological material underground



Fig. 13.3 Data recording during a reflection seismic survey

the surface to the reflecting geological surface underground and back to the geophone at the surface. The position of the reflector at depth is thus recorded as two-way travel time (in seconds). The two-way travel time depends on the depth of the reflector and the acoustic properties of all rock units that the wave has passed through.

Launching a seismic campaign starts with obtaining the necessary official permissions. Target areas and depth of the potential reservoir must be defined next. The layout of the seismic lines is fixed on the basis of topographic maps and on-site inspections. Experimental parameters such as point intervals; exsiccation energy, equipment, transducer channels and other must be determined. The details of the grid are finalized during the experimental fieldwork and the geophones are laid out and the vibro-lines are started to be run. The distance between the geophones controls the minimum resolvable wavelength. The total length of the line array defines the selectivity. The seismic resolution gradually decreases with depth. Higher frequency signals are being lost with increasing depth. The resolution at greater depth can be improved by signals from higher source energy. The measuring instruments, recording truck, the vibroseis trucks, the personnel and all necessary infrastructure must be moved to the exploration area. Preliminary data processing can be continuously performed during fieldwork. The major part of the data analysis and processing with sophisticated software is done post-fieldwork. The final travel-time to depth conversion requires a model of the geological structure of the underground or a known geological profile from an earlier nearby wellbore (Figs. 13.4, 13.5).

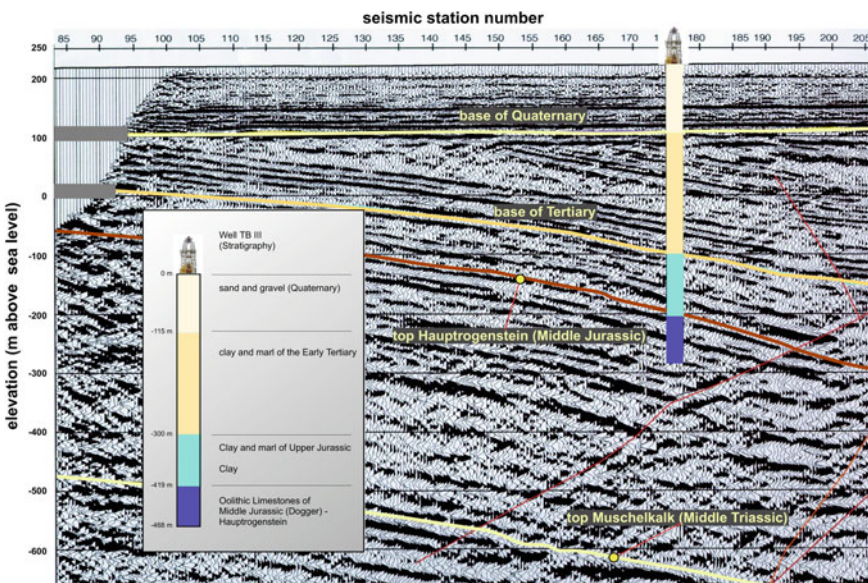


Fig. 13.4 An example of interpreted seismic data. Calibration of seismically recorded discontinuities using an existing drillhole

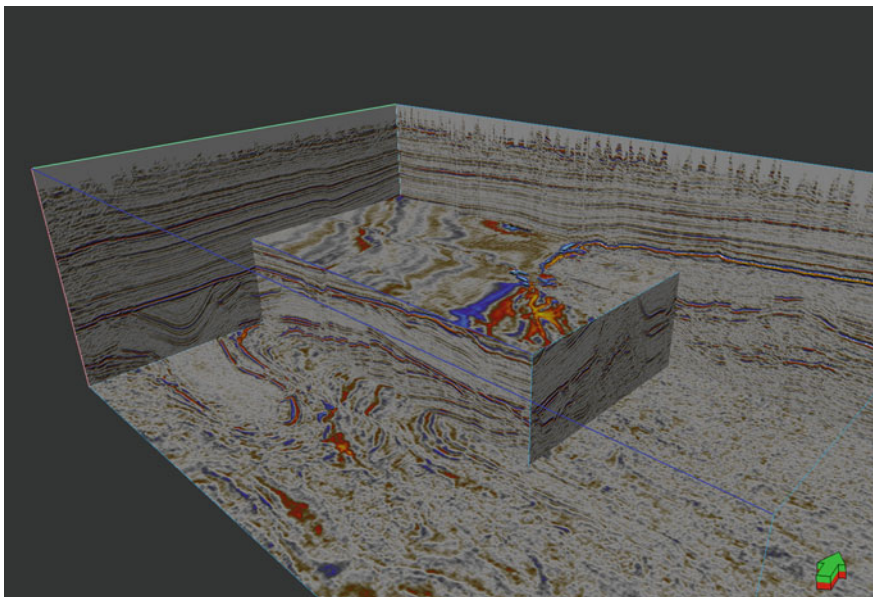


Fig. 13.5 3D seismic model. Note synformal structure below an erosion surface transgressively covered by undeformed strata visible on the vertical section on the l.h.s. (courtesy of DMT GmbH & Co.KG). Total height TWT \sim 1.6 s. Total area covered $\sim 4 \times 4$ km

Geological material boundaries (lithological boundaries) refract and reflect acoustic waves and partly convert them to other types of waves. The details of these processes at lithological boundaries bear valuable information on the geological nature of the boundary (Fig. 13.3). The processed data of the wave field result in a graphic display of the material (density) discontinuities along the seismic section.

The acoustic impedance Z controls the traveling velocity of seismic waves in a geological formation. The seismic wave velocity V is the ratio of the acoustic impedance Z and the density ρ of the rock ($V = Z/\rho$). The contact surface between two geological units can only be “seen” if there is an impedance contrast between the two units. If not then the reflection coefficient R at the interface is zero.

Seismic data processing copes with enormous quantities of data. The data are loaded with noise and must be filtered to make primary reflections visible. The information from single lines is then stacked. Skillful stacking of selected single lines enhances the visibility of important reflections from the underground. Processing distinguishes relevant geological signals from interfering signals and selectively eliminates the latter. Interfering signals include for example multiple reflections of primary signals.

Common-Midpoint staking (CMP) is the most widely used technique for seismic data processing. The installed geophone array receives energy from multiple source positions and the recorded tracks are then reordered according to common midpoints between source and geophone. After travel time correction the seismic signals appear

directly above the geological reflector. Further numerical data engineering improves the quality of the final seismic section. The final result is a graphic display of a seismic model section showing the geological reflectors at two-travel-time depth. The CMP technique distorts inclined or curved reflectors. In order to convert travel time in seconds to depth in meters specific seismic velocities need to be assigned to the different geological units and rock types. The final seismic section is a simplified lithostratigraphic model of the underground, showing lithological boundaries between geological units with an impedance contrast (Shaw et al. 2005; Sheriff & Geldart 2006; Telford et al. 2010). The model can be verified if accessible data from older drillholes exist from the same area. Processing and geological interpretation of the data from a seismic section (2D seismics) ultimately produce a geological cross-section (Fig. 13.4). If data from a number of intersecting seismic sections are available a 3D seismic model can be constructed. This can be further developed to a 3D block model of the geological structure of the underground, which may also be used as a basis for a geothermal simulation model (Fig. 13.5). The 3D model can be helpful for planning of the bore course (Chap. 12).

The hydrocarbon industry uses sophisticated and mature computer based techniques for reservoir characterization and optimization based on seismic data. Standard software applications such as PETREL and ECLIPSE (both from the company Schlumberger) help to develop an optimized picture of the geological underground and the potential hydrocarbon reservoir. PETREL is used to develop a geological and structural model from 2D/3D seismic data and for preparing a simulation model. ECLIPSE helps to analyze and predict the dynamic behavior of the reservoir over time and to model the evolution of pressure, temperature and flow rate during long-time operation. The economically critical decision on the exact position of the drillhole and the exact drill course for hitting the reservoir at the optimal location is ultimately based on the concept and picture of the geology of the underground derived from seismic data.

3D seismic attributes such as e.g. dip, azimuth, continuity or texture are used as interpretation tools and for refining geothermal reservoir characterization (Randen et al. 2000; Chopra & Marfurt 2006; Subrahmanyam & Rao 2008; Roden et al. 2015). The automated analysis of seismic attributes may help mapping structural features including fault systems, salt domes, and gas chimneys for example. One may distinguish signal related attributes correlating with two-dimensional features and structure related attributes correlating with the stratification and structure of geological bodies. The models are capable of uncovering the form and position of fault and fracture zones and even can be used for deducing the tectonic evolution and local deformation history. The 3D details of reflectors in sedimentary rocks bear information on the facies and facies distribution which can be relevant for geothermal reservoir exploration if e.g. facies changes are associated with significant changes in permeability (Shipilin et al. 2019).

Refraction seismic surveys analyze refracted seismic waves, in contrast to reflection seismology. The method uses travel times of waves from seismic sources that have been refracted along interfaces of geological layers with density contrasts. The wave that travels along the geological contact generates seismic signals that can be

recorded by the geophones (Telford et al. 2010). The seismic source is, like in reflection seismology, a shot (blasting explosives), vibrators (vibroseis trucks) or other sources. The sensors (geophones) are arranged in a regular spacing along a profile line and record the propagation of the wave field. Processing of the data is done using travel time diagrams. The resulting model shows the geological structure of the underground with layers with different seismic wave velocities (different densities of the material). The recorded travel time data relate to the depth of interfaces of geological units. Refraction seismology can be used to investigate the underground to a depth of about one third of the length of the geophone array. The velocity of acoustic wave in a layer is an important parameter because it relates to the density of the material. It can be derived directly from refraction seismology. Thus the rock material and geological identity of the layer can be directly deduced from refraction seismic travel time data (Stark 2008; Avseth et al. 2010; Reynolds 2011). Data from reflection and from refraction seismic surveys can be combined in hybrid systems improving the detailed recognition of geological structures.

13.2 Geophysical Well Logging and Data Interpretation

Geophysical well logging examines the wellbore, its immediate vicinity and the surrounding area of a wellbore. Well logging is the essential data collecting method in deep well drilling. A wide variety of physical principles are used for measuring methods including geoelectrical, magnetic, and acoustic techniques but also radar and methods using radioactivity. The measurements in wellbores produce data on geological, lithological, petrophysical, reservoir-relevant properties of rocks and materials. Also structural, textural and drill technical data can be routinely measured. State-of-the-art geophysical well logging has replaced or greatly reduced the necessity for time consuming and cost-intensive coring (Johnson 2002; Darling 2005; Ellis & Singer 2007; Liu 2017; Parker 2020). Well logging produces in-situ rock and material data in the natural environment, which is a great advantage over laboratory derived rock data (Ellis & Singer 2007).

The measurement of hydraulic and rock mechanical properties of the drilled rocks requires very robust instruments (borehole logging devices) that must resist high temperature, high pressure and chemically aggressive fluids. The probes and sensors are lowered or hauled in the borehole and record the data along the axis of the wellbore. The resulting depth versus parameter data and graphs are called logs. Cables connect the probes (instrument units) with a registration station above surface. The probes can be stopped and fixed at any depth and can so be used to measure parameter variation with time.

Well logging measures different groups of parameters: (a) physical parameters that characterize the immediate vicinity of the borehole, (b) measurements regarding the geometry and morphological details of the borehole, (c) properties of the fluid in the borehole (drilling fluid, formation water). The desired physical and chemical parameters can be collected with passive or active methods. A passive measurement

reacts on an external forcing, e.g. an electrical self-potential, magnetic field, natural radioactivity. Active measurements use engineered signals penetrating the rocks, e.g. electrical currents, radioactivity or acoustic waves. The active methods measure the interaction of the engineered external forcing with the rocks. The measurement of parameters of the wellbore geometry includes: Borehole diameter, borehole cross-section, borehole inclination and azimuth. The most important measurable parameters of the fluid phase present in the borehole are: Temperature, electrical conductivity (with a complex relationship to the salinity or the total mineralization of the fluid) and pH of the fluid (that can be measured to about 150 °C and 150 bar pressure, Midgley 1990).

The **borehole cable** serves as a mechanical mounting support for the probe. However, it also supplies the probe with electrical power, transmits the data to the surface recording unit and registers the vertical (depth) position of the probe and thus makes the log (depth versus parameter relation). Measurements in deep drillholes must consider and correct for the cable extension due to weight and temperature. The registration unit controls the measurement procedure, supplies the probe with energy via the cable, records measured parameters, stores the data and produces a real time graphic presentation of the log. The system also records formation parameters, the driving speed of the probe, the tensile stress on the cable and other crucial parameters. Most of the deployed probes are multi-channel probes that are able to transmit more than one parameter per probe run.

The **temperature log** records the temperature of the fluid in the wellbore. The drilling disturbs the thermal conditions around the borehole for some time. The undisturbed steady state temperature distribution can be accessed by repeated recording of the temperature log or measuring after longer periods of downtime. Significant changes in the steady state temperature versus depth profile may indicate major water inflow or outflow structures (Fig. 13.6). Consequently, temperature logs may also detect a leaking casing or back fill. Temperature data collected during a hydraulic pumping or injection test can be used for deriving thermal parameters of the subsurface materials (rocks). In addition, the temperature data can even be used to derive hydraulic conductivity of individual geological strata (Sect. 14.2; Figs. 14.10, 14.15).

The **electrical conductivity log** is important and interesting because it correlates easily measurable electrical conductivity (EC) with the total amount of ions present in the borehole fluid. The electrical conductivity of a fluid is related to the total amount of charged species (ions) dissolved in the fluid. The dissolved ions transport the electrical charges. Thus the EC can be used as a proxy for salinity (dissolved salt). The variations measured by an EC log correlates with the total mineralization of the fluid in the wellbore, it also helps to identify influx and outflow structures, and leakages in the casing and the cementation. Similar to the temperature logs, EC logs can recognize inflow and outflow structures only if they result in EC contrasts, which does not have necessarily to be the case. In other words, if for example the inflow water has the same temperature and salinity as the fluid present in the wellbore, the inflow cannot be recognized by the two methods. The electrical conductivity log is usually collected together with the temperature log. Because the EC depends on temperature, the EC data must be adjusted using the T data from the temperature log.

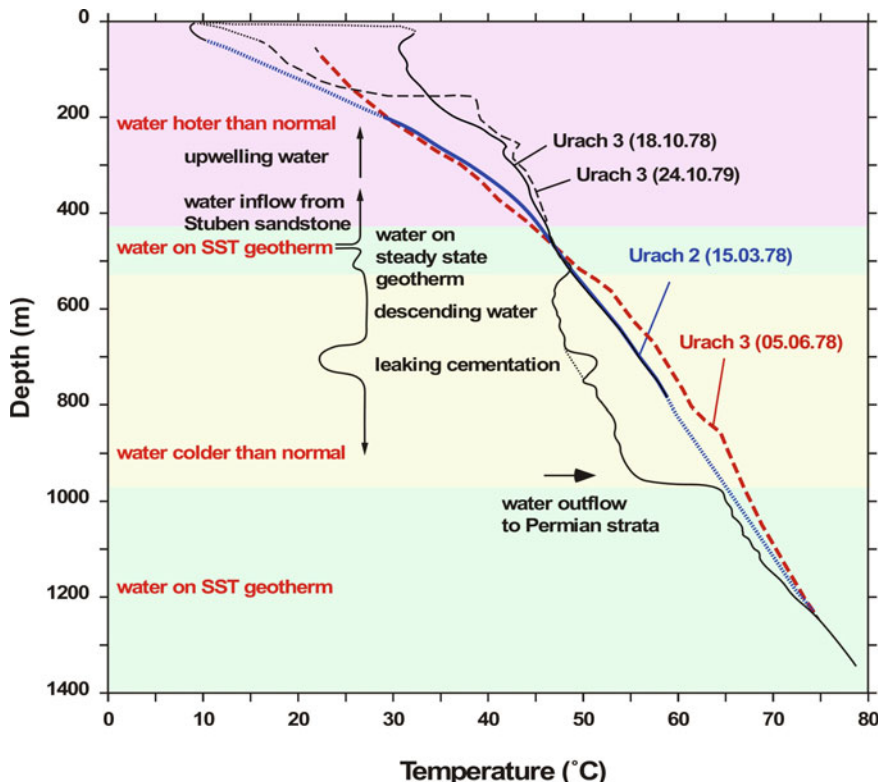


Fig. 13.6 Temperature log signaling water inflow and outflow structures. Urach 3 deep well, SW Germany (Stober 1986)

The **caliper log** is a geophysical well logging tool with extendable sensors that measures the geometrical details of the cross section of a wellbore along a depth profile. It is also used to measure the inside diameter of the casing. It shows wellbore breakouts and cavities and gives hints about the mechanical properties of the borehole wall. It is also an excellent tool for detecting mineral scales, corrosion of the casing or any other damage and deformation of the casing (Fig. 13.7). From caliper log data and the statistical analysis of the breakouts, the orientation of breakout fractures can be related to the local tectonic stress field and the direction of the principal stress in the regional tectonic context. However, better and more precise solutions can be obtained from optical or acoustic borehole scanners (see below).

Gamma ray logging measures the naturally occurring gamma radiation of the drilled geological formations in a borehole. The gamma rays originate from the radioactive decay of unstable isotopes such as ^{40}K in the structure of K-bearing minerals such as clays, micas and feldspar. Gamma rays are also emitted from uranium and thorium isotopes incorporated in various minerals including zircon,

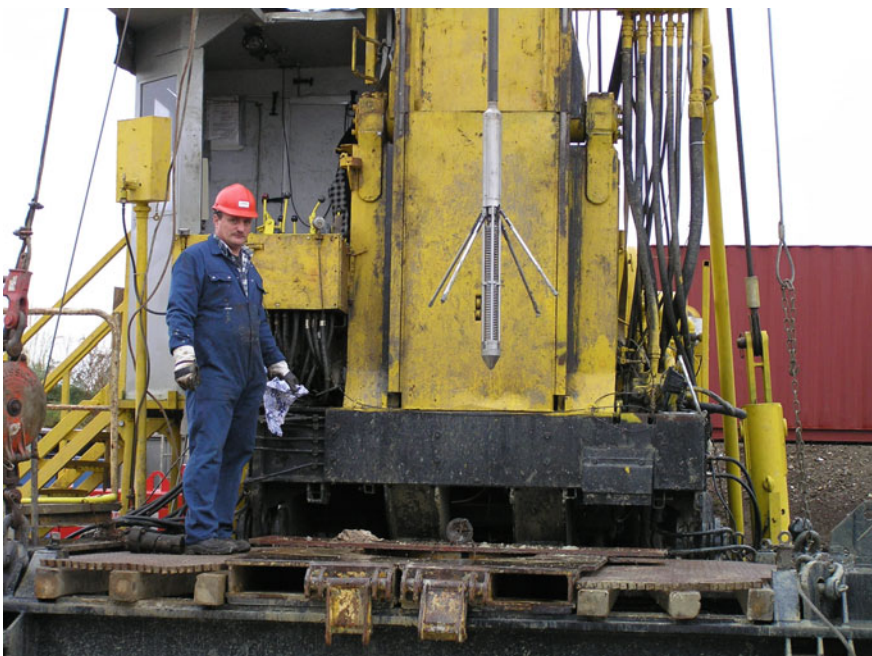


Fig. 13.7 Caliper log being removed from a deep well

monazite and others. Consequently, the gamma ray log detects lithological boundaries in the drilled profile if the fraction of minerals containing radioactive isotopes abruptly changes. Gamma ray logs are very useful in combination with cutting analysis for creating geological drill logs. They are helpful for locating the existence and position of planned doped clay barriers.

The density log measures a continuous record of the bulk density of the drilled formations (also gamma-gamma log). It uses an active gamma ray source and measures the density-dependent absorption and scattering of the gamma rays. The measured bulk density of the formation is related to the density of the rock matrix, the volume of pores and fractures and the density of the pore fluid. Thus knowing bulk density from density log and rock density from lab measurements the porosity of the formation can be deduced from: $\phi = (\rho_{\text{matrix}} - \rho_{\text{bulk}}) / (\rho_{\text{matrix}} - \rho_{\text{fluid}})$. For simple monomineralic rocks such as limestone, dolomite and sandstone ρ_{matrix} can be directly taken from tables.

Sonic logging measures the travel time difference Δt of a compressional wave in a borehole generated by a transmitter and picked up by two receivers at different distances to the transmitter (p-wave velocity). This time difference depends on the lithology, rock structure and the porosity of the formation. In the same rock matrix, Δt increases with porosity. Sonic logs can be used to generate a continuous porosity profile of the drilled section.

A **borehole-imaging log (scanning)** provides a detailed image of the wellbore from micro-resistivity or acoustic measurements. It shows the orientation of rock foliation, banding, veins, fractures, faults, breakouts and other conditions of the borehole. The borehole-imaging log can provide detailed information on the quality of the cementation and the casing. The images can be used to create a 3D picture of the geological structure in the wellbore. The data can also be used for obtaining quantitative information on the local stress field. Optical scanners require clear fluids in the well in contrast to the acoustic scanners.

A variety of further logging tools are routinely used for solving specific problems. Water inflow points and structures can be detected with **flowmeter logging**. The method uses a device with a spinner whose rotation relates to water flow rate in the borehole. Cement bond logging can assess the quality of cementation of the wellbore and the attachment to the formation and to the casing.

An important method for measuring hydraulic properties of the formation is **fluid logging**. It combines a hydraulic well test with geophysical well logging in an uncased wellbore. The resulting fluid log represents a hydraulic conductivity profile of the drilled formations. The method is particularly useful for aquitards (Sect. 14.2).

The so-called **fishing tool** is a useful piece of equipment for recovering objects that have been lost in or fallen into the bore. There are many differently designed devices for the purpose of fishing lost instruments and other tools from the drillhole (Fig. 13.8).

In addition to the highly developed well logging techniques a new development started in the 70s and 80s of the last century, **logging while drilling** (LWD). The methods measure relevant parameters during drilling by sensors integrated in the drill string. Also drilling paths can be measured directly during drilling (MWD) (Sect. 12). The data are being transmitted to the surface by pressure signals through the drilling fluid column. However, networked and wired drill pipes that transmit high-definition downhole data to the surface are increasingly used also. The real-time parameter data allow for instant decisions about the drilling direction and other well

Fig. 13.8 An example of a fishing tool that has been used for recovering a lost probe caused by a cable brakeage



management attributes. The rotating ultrasonic caliper sensor measures the geometry of the wellbore and the transmitted data provide information on the local stress field and instabilities of the bore (Elahifar 2013). The LWD tools tolerate formation temperatures of about 150 °C, some also up to 175 °C. For pure directional drilling procedures MWD tools for up to 200 °C are available. All measuring systems have a very limited formation penetration depth.

A special seismological technique has been developed which is used to explore the geology ahead of the bit whilst the well is being drilled. The technique is known as “**seismic while drilling SWD**” (Poletto & Miranda 2004). The technique produces a **vertical seismic profile** (VSP) and provides high-resolution data from the direct vicinity of the hot water reservoir. The receiver (geophone) is lowered during drilling and the seismic source (shotpoint) placed at the land surface. The technique is routinely used in directional drilling, horizontal drilling and drilling sidetracks in order to precisely monitor the drilling progress towards the target area.

References

- Avseth, P., Mukerji, T. & Mavko, G., 2010. Quantitative Seismic Interpretation: Applying Rock Physics Tools to Reduce Interpretation Risk. Cambridge University Press, 408 pp.
- Chopra, S. & Marfurt, K. 2006. Seismic Attributes- A Promising aid for geologic prediction, CSEG Recorder Special Edition, 110–121.
- Darling, T., 2005. Well Logging and Formation Evaluation (Gulf Drilling Guides), 2nd edition. Gulf Professional Publishing, 336 pp.
- Elahifar, B., 2013. Wellbore Instability Detection in Real Time Using Ultrasonic Measurements. PhD Thesis, Montan Universität Leoben, 125 p., Leoben/Austria.
- Ellis, D. V. & Singer, J. M., 2007. Well Logging for Earth Scientists (2nd edition). Springer Verlag, Heidelberg, 728 pp.
- Johnson, D. E., 2002. Well Logging in Nontechnical Language, 2nd edition. PennWell Books, 289 pp.
- Liu, H., 2017. Principles and Applications of Well Logging 2nd edition. Springer Geophysics, Heidelberg, 370 pp.
- Midgley, D., 1990. A review of pH measurement at high temperatures. *Talanta*, 37, 767–781.
- Parker, Ph. M., 2020. Field Well Logging Equipment. The 2021–2016 World Outlook for Oil and Gas. ICON Group International, Inc., 301 pp.
- Poletto, F. B. & Miranda, F., 2004. Seismic While Drilling: Fundamentals of Drill-Bit Seismic for Exploration. Elsevier, Amsterdam, 546 pp.
- Randen, T., Monsen, E., Signer, C., Abrahamsen, A., Hansen, J.O., Sæter, T. & Schlaf, J., 2000. Three-dimensional texture attributes for seismic data analysis. SEG Technical Program Expanded Abstracts, 2462 pp.
- Reynolds, J. M., 2011. An Introduction to Applied and Environmental Geophysics (2nd edition). Wiley-Blackwell, 712 pp.
- Roden, R., Smith, T. & Sacrey, D. 2015. Geologic pattern recognition from seismic attributes: Principal component analysis and self-organizing maps. *Interpretation*, 3, SAE59–SAE83
- Shaw, J. H., Connors, C. & Suppe, J. (eds.), 2005. Seismic interpretation of contractional fault-related folds. American Association of Petroleum Geologists Seismic Atlas, Studies in Geology #53, 152 pp.
- Sheriff, R. E. & Geldart, L. P., 2006. Exploration Seismology. Cambridge University Press, Cambridge, UK, 592 pp.

- Shipilin, V., Tanner, D. C., Moeck, I. & Hartmann von, H. 2019. Facies and structural interpretation of 3D seismic data in a foreland basin setting: A case study of the geothermal prospect of Wolfratshausen.- Geothermische Energie, 91/1, 24–25, Berlin.
- Stark, A., 2008. Seismic Methods and Applications: A Guide for the Detection of Geologic Structures, Earthquake Zones and Hazards, Resource Exploration, and Geotechnical Engineering. Brown Walker Press, 592 pp.
- Stober, I., 1986. Strömungsverhalten in Festgesteinsaquiferen mit Hilfe von Pump- und Injektionsversuchen (The Flow Behaviour of Groundwater in Hard-Rock Aquifers – Results of Pumping and Injection Tests) (in German). Geologisches Jahrbuch, Reihe C, 204 pp.
- Subrahmanyam, D. & Rao, P. H., 2008. Seismic Attributes - A Review. Proceedings 7th International Conference & Exposition on Petroleum Geophysics, Hyderabad, 398–405.
- Telford, W. M., Geldart, L. P. & Sheriff, R. E., 2010. Applied Geophysics (2nd edition). Cambridge University Press, Cambridge, UK, 792 pp.
- Vozoff, K., 1987. The magnetotelluric method.- In: Nabighian, M. N. (ed.): Electromagnetic methods in applied geophysics, vol. 2, Application. Society of Exploration Geophysicists, Tulsa, OK, 641–711.

Chapter 14

Testing the Hydraulic Properties of the Drilled Formations



Vortex on the river Rhine

Hydraulic tests provide the key data on the hydraulic conductivity of the reservoir formation and permeability structure of the reservoir. These hydraulic properties are fundamental for the success of a geothermal project. The first hydraulic tests are already made in the hanging wall of the intended reservoir formation during drilling of the deep well. After completion of the wellbore, the hydraulic properties of the reservoir formation must be extensively tested. This includes long-term tests, circulation experiments, or tracer tests in the intended target horizon. This chapter gives a brief overview over some standard hydraulic testing methods, the practical conductance of the tests and the processing and interpretation of measured data.

14.1 Principles of Hydraulic Well Testing

Hydraulic tests may solve very diverse problems. Therefore, the appropriate testing procedures depend on the specific data needed to answer the current question. However, all test methods monitor water pressure changes that result from an incurred excursion from the undisturbed pressure distribution in the reservoir. The excursion is being imposed by the testing method. A large variety of hydraulic testing schemes are currently used in groundwater exploration, by the oil and gas industry and in geothermal energy plant development (Kruseman and de Ridder 1994; Nielsen 2007; Zarrouk and McLean 2019). One type of test, the pumping tests and the production tests, produces water, whilst another type of test, the injection tests, introduces water into the formation to be examined. The details of the pressure to flow rate relationship are controlled by the sought-after hydraulic properties of the reservoir. Some tests use pressure pulses to get response signals from the reservoir. Some test require only a few minutes, other tests run for days. The duration of a hydraulic test depends on the type of test, the type of needed data and the hydraulic properties of the tested formation (Fig. 14.1). Some methods test the entire open-hole or the entire screened section of the wellbore, other experiments test specific sections of the formation that are of particular interest by separating the sections with packer or other systems (Figs. 9.5 and 14.2). Some tests continuously record the water pressure in the tested section of the bore, other tests measure water pressure near the surface, and some just monitor the groundwater table as a pressure response to extracting or injecting water. The tests also differ with respect to the water extraction rate. Some tests pump water at a constant rate from the reservoir and continuously monitor the pressure response. In other tests, the pumping rate increases stepwise. Tests may also be run at constant pressure so that the water flow rate gradually decreases during the test. Some tests are carried out concurrently with geophysical well logging (Sects. 13.2 and 14.2) others not. Some tests monitor the water temperature at the wellhead or near the pressure gauge in the tested section of the wellbore alongside with the pressure recordings.

The hydraulic properties of the reservoir measured and analyzed with the testing methods provide the conclusions on the yield of the well. This is the prime goal of hydraulic tests. Yield and temperature determine the commercial success of the geothermal project. However, hydraulic tests also provide water samples for

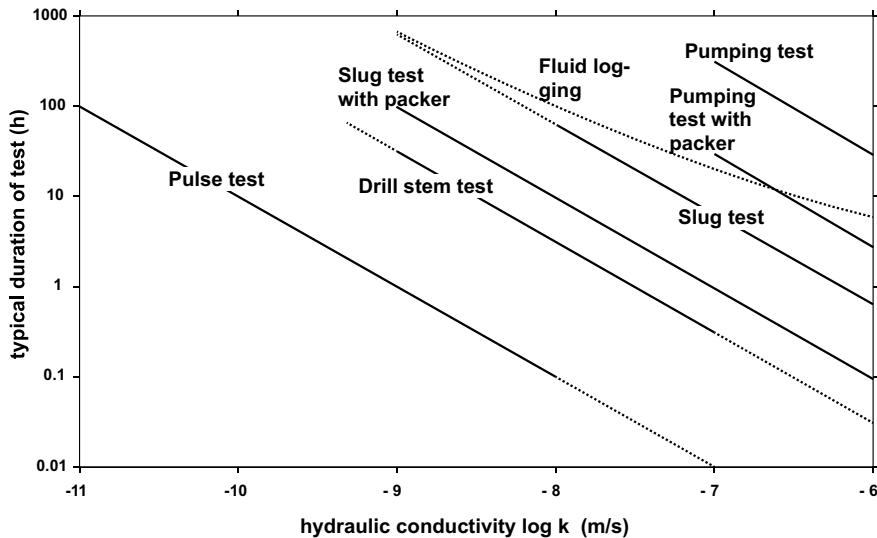


Fig. 14.1 Duration of various types of hydraulic tests in formations with different hydraulic conductivity (Stober et al. 2009; Hekel 2011)

the necessary hydrochemical analysis and isotope studies (Chap. 15). The well yield depends not exclusively on the hydraulic properties of the reservoir formation (hydraulic conductivity, storativity) but to some degree also on the hydraulic properties of the wellbore itself (skin, wellbore storage). Some testing methods are suitable to separate properties of the formation and properties of the wellbore. Appropriately designed well tests provide data on the hydraulic potential, the pre-testing pressure of the tested formation and give clues on the structure of the thermal aquifer (or aquitard) and the flow properties of the formation. The hydraulic response to the tests may indicate hydraulic interaction and communication with the formations above and below the reservoir (leakage). The tests may provide insights into the interaction between fractures and porous rock matrix or into the hydraulic significance of major fractures and faults. The tested volume of the reservoir formation increases with the duration of the test. Long-term tests may therefore provide information on the extent of the reservoir and the nature of hydraulically active borders (Kruseman and de Ridder 1994; Stober et al. 1999; Stober and Bucher 2005a).

The known hydraulic signal or stimulus imposed on the reservoir formation during the test by extracting or injecting water or by sending a pressure pulse triggers a response or reaction of the unknown hydraulic system. The reactions, pressure drop or pressure increase (or water table changes) are continuously recorded. Thus input and response signals are known and must be analyzed and interpreted in the context of the known geological situation, the structure of the underground known from seismic studies and plausible hydrogeological properties of the tested formation. Solving the mathematical inverse problem and finding the sought-after hydraulic parameters of the formation requires a sharp model concept of the tested formation or the wellbore

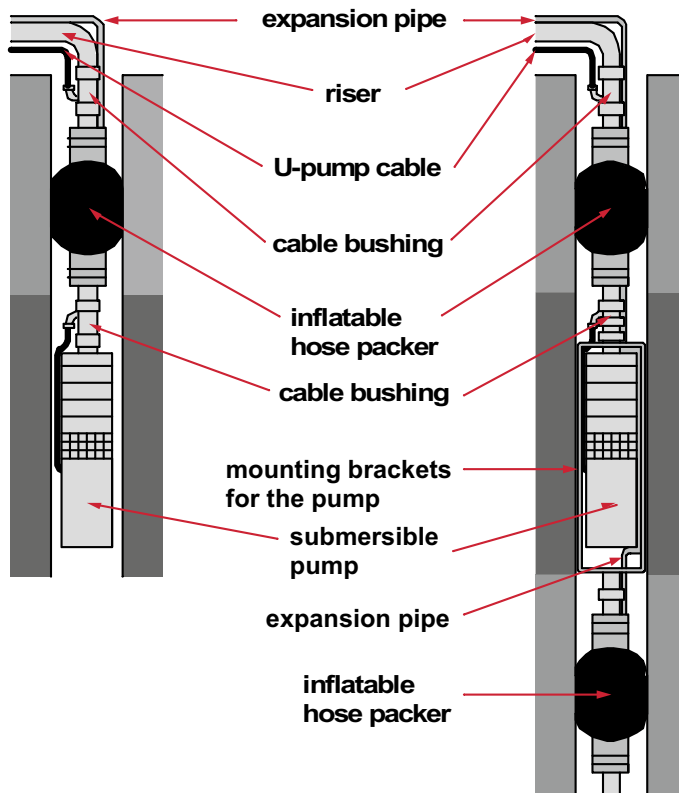


Fig. 14.2 Schematic illustration of single and double packer systems used in hydraulic tests

that is as close as possible to the real structure and properties of the system. This well-defined and well-founded model of the underground is required to react with the same response signals on the input signals like the tested system (Fig. 14.3). Figure 14.3 shows six different geological model concepts of the hydraulic situation in the tested formation. The six systems respond characteristically on the imposed external signal, in this case pumping water at a constant rate from a well. The hydraulic reaction of the system is monitored as drawdown and plotted against time elapsed since pumping started. The data are conventionally represented on double-log or semi-log plots. After pumping stops the drawdown slowly recovers and the recovery versus time after pump-stop also reflect the hydraulic properties of the tested underground. The recovery data can be displayed on so-called Horner plots (Fig. 14.3). The detailed shape of the drawdown versus time curves in pumping tests depends on many possible geological structures and features that may influence the hydraulic behavior of the tested formations. The graphical evaluation of the measured drawdown versus time data requires the choice of a model concept that best represents the hydraulic situation of the underground as stated above. The choice must be made among many model

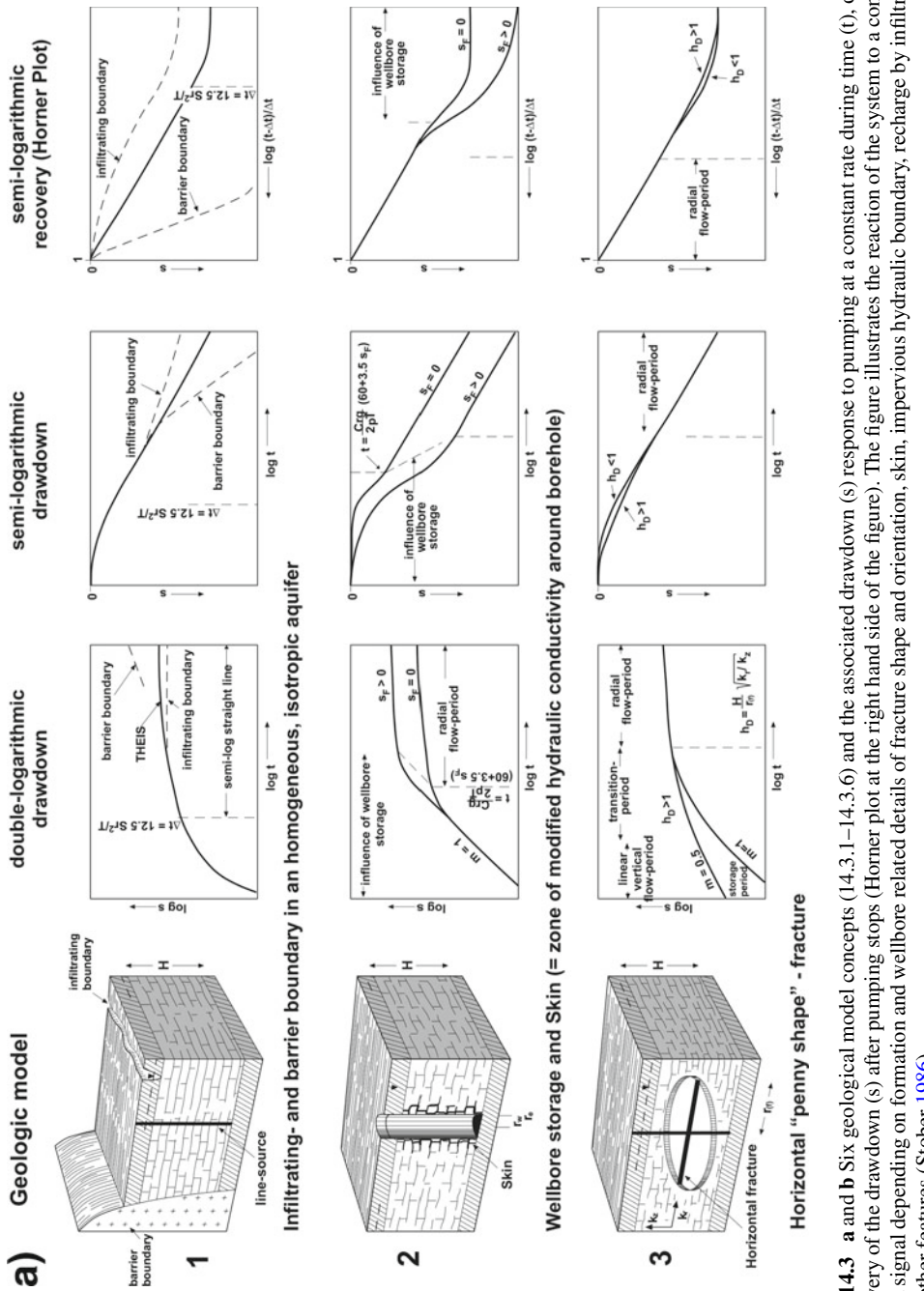


Fig. 14.3 a and b Six geological model concepts (14.3.1–14.3.6) and the associated drawdown (s) response to pumping at a constant rate during time (t), or the recovery of the drawdown (s) after pumping stops (Horner plot at the right hand side of the figure). The figure illustrates the reaction of the system to a constant input signal depending on formation and wellbore related details of fracture shape and orientation, skin, impervious hydraulic boundary, recharge by infiltration and other features (Stober 1986)

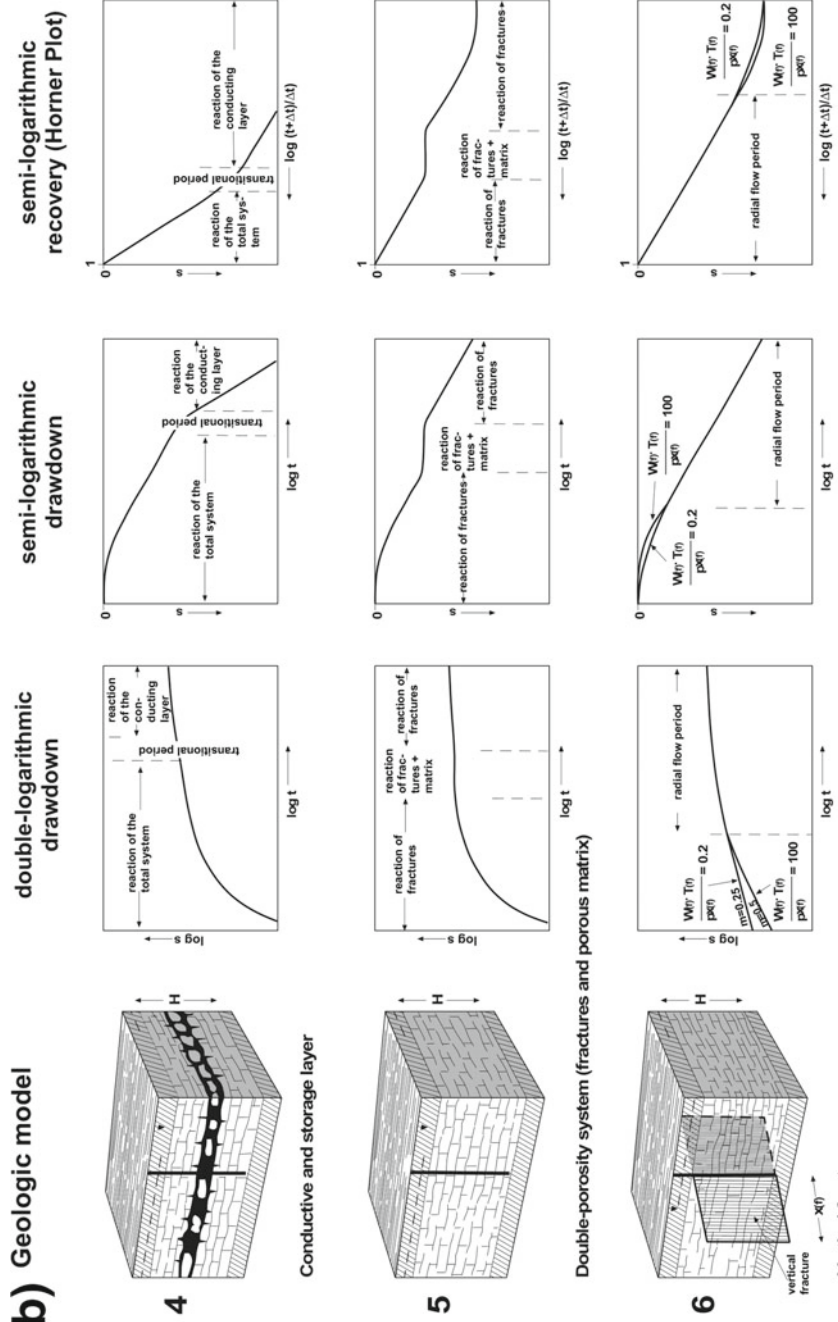


Fig. 14.3 (continued)

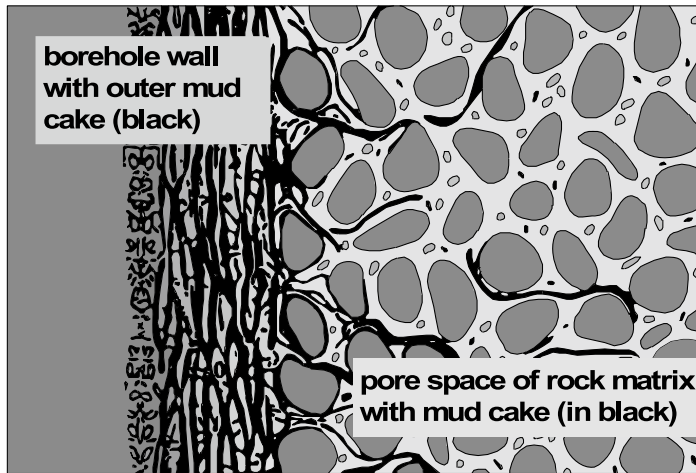


Fig. 14.4 Rock structure across a wellbore: Next the wall of the bore a damage zone with severely altered hydraulic conductivity (so-called skin) typically exists, the consequences of the drilling operations reach beyond the skin, however (mud cake in the porosity of the rock matrix)

concepts, which may prove difficult because of vague knowledge of the real situation. The number of feasible concepts can be drastically reduced by careful planning and implementation of the hydraulic tests. Critical is particularly the duration of the test. Very short tests may trigger response signals from the immediate vicinity of the wellbore (skin, wellbore storage). The hydraulic conductivity of the formation close to the wellbore is typically severely altered by the drilling operation (drilling mud, fracturing, acidization a.m.) and by technical efforts in the borehole (Fig. 14.4). Many experiments in crystalline basement rocks prove the presence of a zone of increased hydraulic conductivity near the wellbore (Stober 2011).

The skin, the zone of altered conductivity near the wellbore, influences the pressure response in the course of a hydraulic test. If the conductivity of the skin is lower than that of the tested formation pumping is accompanied by an additional pressure drop (increased drawdown in Fig. 14.3.1). The pressure response on pumping is smaller (decreased drawdown) if the skin has a higher conductivity than the formation. The skin related additional pressure change can be expressed as contribution to the drawdown Δs_{skin} (in meters):

$$\Delta s_{\text{skin}} = s_F Q / (2\pi T) \quad (14.1)$$

where s_F denotes the skin factor (dimensionless), Q is the production rate (pumping rate) in $\text{m}^3 \text{ s}^{-1}$ and T ($\text{m}^2 \text{ s}^{-1}$) stands for the transmissivity. The dimensionless skin factor can be positive or negative depending, as mentioned, on the hydraulic conductivity of the altered zone around the wellbore compared to that of the undisturbed formation (van Everdingen 1953; Hawkins 1956; Agarwal et al. 1970). For fully impervious wellbores $s_F = +\infty$ and for highly stimulated, acidized or fractured

zones near the wellbores s_F may be as low as $-\infty$. A simple procedure to derive a dependable value for the skin factor from pressure-time test data can be found in Matthews and Russel (1967).

At the beginning of a hydraulic pumping test the fluid in the wellbore is produced. Later fluid from the formation flowing to the wellbore due to the imposed pressure gradient by pumping is being produced gradually also. The reaction of the tested formation is delayed. This effect is called wellbore storage (C). It corresponds to the volume change ($\Delta V = r_w^2 \pi \Delta h$) in the wellbore per pressure difference (Δp), thus it has the dimension $m^3 Pa^{-1}$. The wellbore storage can be computed from Eq. 14.2:

$$C = \Delta V / \Delta p \quad (14.2)$$

Equation 14.2 illustrates that the wellbore storage depends on the diameter of the borehole ($2 r_w$) controlling ΔV . The duration of the wellbore storage t_B (s) is furthermore controlled by the transmissivity (T) of the tested formation and by the skin factor.

$$t_B = [r_w^2 / (2T)] \cdot [60 + 3.5 s_F] \quad (14.3)$$

It follows from Eq. 14.3 that the duration of the wellbore storage t_B increases with the skin factor and the square of the radius of the well and that it increases with decreasing transmissivity of the formation (Fig. 14.5). Consequently, tests in large-caliber wells drilled in aquitards are affected by the wellbore storage for the longest period of time.

If hydraulic tests in confined aquifers are carried out with dedicated testing tools, then the size of the tool and the compressibility of the fluid are the important parameters controlling the wellbore storage.

A network of monitoring wells is needed to record the spatial pressure distribution during pumping or injection in the tested well. However, in deep drilling a network of monitoring wells is not available. Evaluation of hydraulic tests in the first well is totally restricted to pressure data (drawdown) collected in that single deep borehole. In the early phase of the test the pressure signals are dominated by the geometry of the wellbore, the casing and cementation (if present) and the size of the testing tools. The hydraulic properties of the formation become visible in the data after a minimum duration of the test that must be longer than the duration of the wellbore storage (Eq. 14.3).

When testing non-thermal groundwater wells, the measured water table corresponds directly to the hydraulic pressure in the tested formation. Testing thermal water reservoirs, the pressure data must be corrected for the temperature related density differences. Because the density of water depends on temperature and pressure, water columns of equal weight but at different temperature have different length. The relatively small density difference results in length differences of several meters if the water columns are several hundred or even thousands of meters in a deep well (Sect. 8.2).

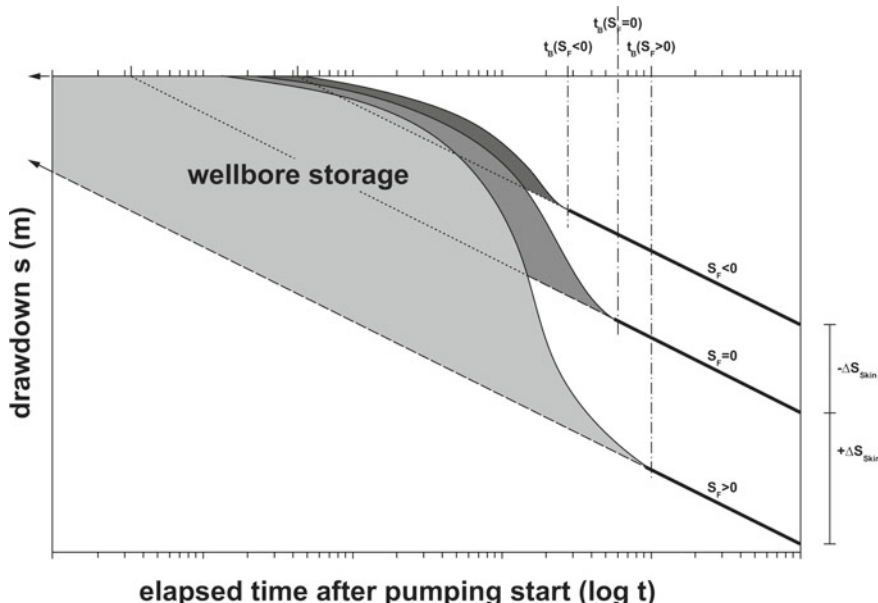


Fig. 14.5 Drawdown versus time plot showing that the early phase of the test is absolutely dominated by the wellbore storage, it gradually decreases (middle of diagram) and fades out at different times depending on the skin factor s_f . Note the constant slope of the straight-line relationship of the drawdown—time data (heavy solid lines) reflect the “true” hydraulic conductivity of the tested formation. The slope of these straight-line sections is a direct measure of the conductivity of the aquifer (this is what one wants to know!). Therefore, it is evident from the figure that tests running for a too short period of time will result in erroneous (high) hydraulic conductivities of the formation

Under quiescent conditions, the water column thermally equilibrates with the rock. It is cool near the surface and hot at depth. If water is pumped from the well, warm or hot water from depth flows upward and the entire water column increases in temperature controlled by the pumping rate, duration of pumping, the thermal conductivity of the rocks and other parameters. Because of this thermal effect, the water table paradoxically increases during the initial phases of a pumping test instead of reacting with the expected drawdown. After shut-in the water column reacts with a thermally induced drawdown instead of the expected water table recovery (Fig. 8.3). The inverse effects can be observed in injection tests pumping cool surface water into a deep thermal well. For the evaluation of pumping or injection tests in thermal reservoirs the measured drawdown (or recorded near surface pressures) must be normalized to a reference temperature. Each data point for the length of the water column (drawdown) in the wellbore must be density corrected to a reference temperature and pressure.

Straightforward and unproblematic is the direct pressure measurement in the wellbore at the depth of the tested formation. This avoids troubles with intricate and error-loaded temperature and density corrections that ignore further complications

caused by temperature anomalies, increased salinity or high gas concentrations in the fluid.

The water conducting structures of hard rock aquifers are typically single fractures or fracture zones, in contrast to rocks with a porous matrix. Thus the distribution of water conducting structures is heterogeneous. The orientation and geometry of these structures varies widely in fractured hard rock formations. In contrast to porous aquifers, they represent hydraulic discontinuum by nature. Many diverse model concepts have been developed especially by the oil and gas industry for the quantitative analysis and interpretation of hydraulic well test data (type curves, approximate solutions, specialized software). The models can be grouped into the following categories (Stober 1986; Kruseman and de Ridder 1994):

Type 1 models: The water conducting fractures are randomly oriented and regularly distributed in the formation. On a sufficiently large scale the formation behaves like homogenous continuous aquifer. The hydraulic properties can be modeled and interpreted with the concepts of Theis (1935). In this case the test data also can be interpreted by the approximation of Cooper and Jacob (1946). Typical example is regularly fractured crystalline basement (Fig. 14.3.4).

Type 2 models: The tested formation contains local domains (zones, horizons) of preferred high conductivity and high fracture porosity (Fig. 14.3.4). There are two endmember types of such domains: Conductive zones dominate the flow properties of the entire formation and have minimal storage capacity. Storage zones, in contrast, behave hydraulically the opposite way (e.g. Berkaloff 1967). Most discontinuities are mixtures of both endmember type domains. Classic example is a karstified zone in a limestone formation.

Type 3 models: The tested formation can be comprehended as double-porosity system, matching a fractured porous rock (Fig. 14.3.5). This model concept assumes the existence of two continuous homogeneous regimes of flow property, one characterizes the pore space of the rock matrix the other the regular random fracture pore space like in model type 1 (e.g. Barenblatt et al. 1960). Classic example: Fractured sandstone with matrix porosity.

Type 4 models: In the tested formation a prominent vertical fracture of limited extension strongly influences the hydraulic behavior of the system (Figs. 14.3.3 and 14.3.6). In strongly stimulated wells, it was found that hydraulic test data required the presence of a fracture (Dyes et al. 1958). The effects of fractures of different orientation on the pressure-time data in well tests have been further explored by e.g. Russel and Truitt (1964), Gringarten and Ramey (1974) and Cinco et al. (1975).

To what extent such models adequately represent the geological and hydraulic structure of the tested formation needs to be decided for each tested formation and each well anew. It is principally impossible to assign a certain model a priori to the formation of interest because the geometric details of the voids (general pore space) and their hydraulic interaction cannot be predicted beforehand. The right way for finding an appropriate model compares the measured with theoretical model pressure-time data (Fig. 14.3). Figure 14.3 presents six common example situations. It proved to be helpful for the model-finding process to also consider graphs of the derivatives of the pressure (drawdown, water table) time data (Fig. 14.6) and other

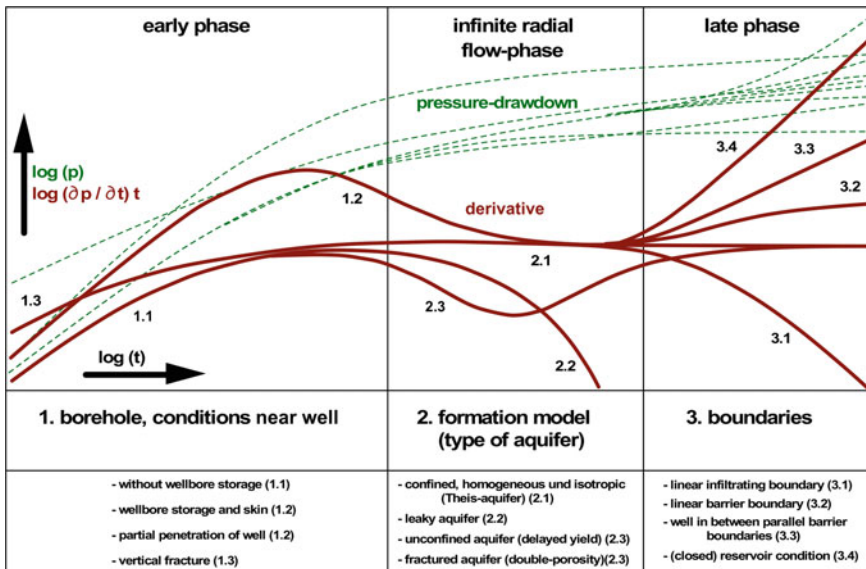


Fig. 14.6 Theoretical model curves for the draw down(s), the first derivative of the drawdown [$(\delta s/\delta t) t$] during a pumping test at constant rate and for different formation structures (Odenwald et al. 2009)

special functions (e.g. Bourdet et al. 1989). It is immediately obvious from Fig. 14.6, that derivative plots are graphically much more distinctive than pressure-time plots alone.

For finding an appropriate hydraulic model that best describes the properties of the formation, the data (pressure, drawdown) are plotted against time on a log–log graph or on a linear–log graph as shown on Figs. 14.3 and 14.6. The pressure recovery behavior after shutdown of the pump can be displayed on a Horner-plot (s vs. $\log(t + t')/t'$, t = pumping time, t' = recovery time). The diagnostic power of Horner plots is demonstrated by the example cases shown on Fig. 14.3. If many data have been recorded per unit time, the derivative of the pressure (drawdown) per unit time can be plotted (e.g. Fig. 14.6). The graphical representation of these data ($\log[(\delta s/\delta t) t]$ vs. $\log t$) is a very powerful tool for the diagnosis of the hydraulic behavior of the tested geothermal formation.

Radial flow towards a well (linear sink) results in a straight-line relationship of the data on a [s vs. $\log t$] plot (radial flow period). Volume flow towards an imperfect (heterogeneous) well can be recognized on a linear relationship between [s vs. $t^{-0.5}$] data. If fluid flow from the fracture pore space is followed by fluid flow from the porous matrix, the bilinear flow behavior can be identified by a linear relationship on a [s vs. $t^{0.25}$] plot.

14.2 Types of Tests, Planning and Implementation, Evaluation Procedures

Hydraulic tests must have lasted long enough to give the right answers. The correct hydraulic model can only be chosen for meaningful data interpretation if the duration of the test was sufficiently long. Implementation of **pumping and injection tests** follows a well-established standard procedure today (Fig. 14.7). The test is subdivided into several sub-tests, beginning with tests that explore the properties of the wellbore. The tests are being run using at least three different constant pumping (injection) rates. The future fluid production rate will be based on these test results. The following tests investigate the properties of the formation. After these testing procedures the system is left at sleep without pumping or injecting fluid. During the formation test water is pumped at a constant rate. It lasts for an extended period of time, typically substantially longer than the experiments testing the properties of the wellbore. The formation test explores the flow properties of the formation for finding the appropriate hydraulic concept model as explained in the previous section (Figs. 14.3 and 14.6). The volume of the formation that responds to the pressure signal imposed by the test increases with the duration of the test. Thus the extension of a hot water reservoir and its distant hydraulic boundaries can only be investigated in tests of sufficient duration (Sect. 14.1). Short-term tests do not provide hydraulic information on the distant regions away from the wellbore. In the worst case it is not even possible to derive hydraulic parameters of the formation because the tested volume remains within the wellbore storage and skin (Eq. 14.3).

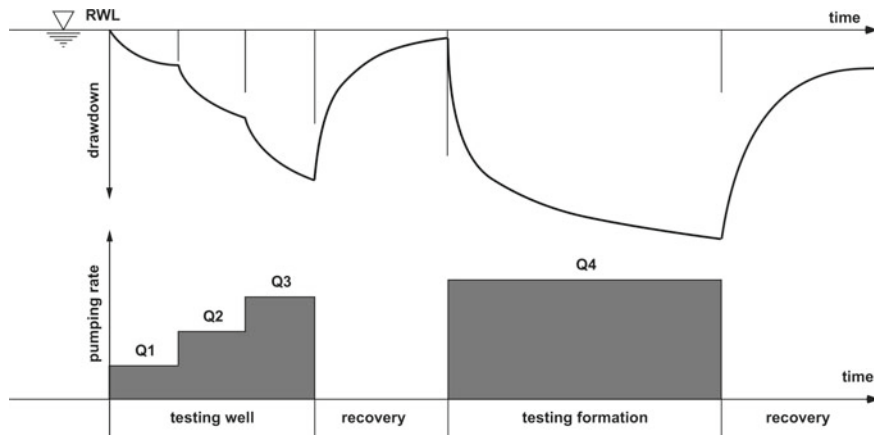


Fig. 14.7 Example of a hydraulic test design. RWL = groundwater level at-rest. Q = extraction rate (pumping rate), the first test series pumps at 3 different rates Q1, Q2 and Q3 and investigates the properties of the well, the following test is of longer duration and pumps at a higher rate Q4 exploring the properties of the formation

Following a model concept of a homogeneous isotropic formation of infinite extension, the transmissivity and the storage coefficient of the tested formation can be derived during the radial flow period. The measured drawdown (pressure) can be graphically plotted against the logarithm of time. From the slope of the straight line on a semi-log plot [s vs. $\log t$] (e.g. Fig. 14.3) the transmissivity T ($m^2 s^{-1}$) of the formation can be computed from Eq. 14.4 (Cooper and Jacob 1946). T follows from data recorded during radial flow period (slope = $\Delta s / \Delta \log t$, at $\Delta \log t = 1$, $Q =$ pumping rate $m^3 s^{-1}$).

$$T = 2.303 \cdot Q / (4 \cdot \pi \cdot \Delta s) \quad (14.4)$$

The storage coefficient S (dimensionless) can be computed from Eq. 14.5, taking the skin factor s_F , the transmissivity T (Eq. 14.4), and the radius r of the well into account:

$$S = [2.25 \cdot T \cdot t] / [r^2 \cdot (e^{2s_F})] \quad (14.5)$$

A typical example of the evaluation of pumping test data is shown for the 4000 m deep pilot hole of the continental deep drilling project in Germany (Fig. 14.8) (Stober and Bucher 2005a). The borehole is cased to 3850 m; the open-hole has a length of 150 m. The open-hole is in Variscan crystalline basement with exposed amphibolite and metagabbro. The temperature at bottom hole is 120 °C. The pumping rate was held constant at nearly one liter per second. The measured data, plotted on a semi-log pressure versus log time graph (Fig. 14.8), reflect the wellbore storage at about 0.2 days from test start. From then on, the data follow a straight-line relationship. This test phase signals the radial flow period and shows the hydraulic reaction of the formation, here the crystalline basement on pumping. The slope of the radial flow period can be converted to the transmissivity of the formation $T = 6.10 \cdot 10^{-6} m^2 s^{-1}$

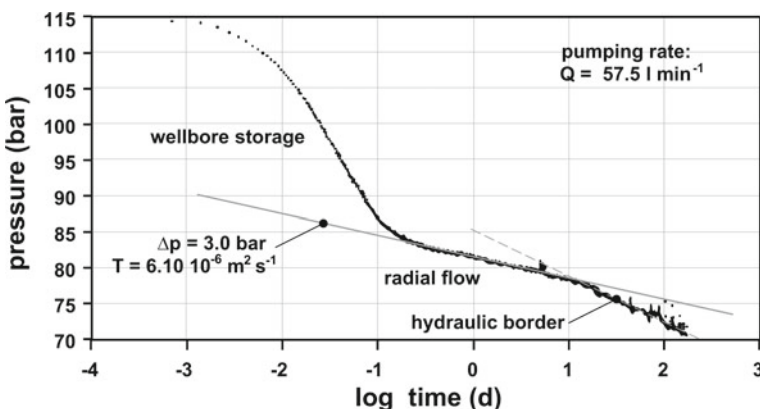


Fig. 14.8 Well test data and evaluation from the 4000 m deep pilot hole of the continental deep drilling project (KTB) in Germany (Stober and Bucher 2005a)

with help of Eq. 14.4. After 12 days of pumping, pressure decreases markedly and tends to follow a linear trend with a steeper slope. The feature causing the change in slope at $t = 12$ days is located at an estimated distance of about 1.2 km from the well. This feature is caused by a hydraulic boundary with lower conductivity than the tested formation, in the example case it is caused by an impervious fault zone, the “Franconian Lineament” (Stober and Bucher 2005a).

From the computed transmissivity, the geometry of the wellbore and the observed wellbore storage (Fig. 14.8) follow the skin factor $s_F = 1.35$ from Eq. 14.3. The skin causes an additional pressure difference (drawdown) of 3.5 bar (from Eq. 14.1). The storage coefficient $S = 5 \cdot 10^{-6}$ can be computed from Eq. 14.5. The example shows that elaborate well testing can provide the geothermal project with a large amount of critical and important data on the hydraulic properties of the wellbore, the target formation and the hydraulic structure of the reservoir.

Long-term pumping or **injection tests** are indispensable before operation of a geothermal doublet. The hydraulic testing must be accompanied by a hydrochemical research lineup (Chap. 15). After that long-term circulation or production tests must prove the functionality of the system. Also these tests must be backed with diverse supporting experiments.

Utilization of hydrothermal reservoirs taps thermal water from deep wells almost exclusively drilled in confined hardrock aquifers. Pressure or drawdown data from these confined aquifers commonly display the effect of the tides (Fig. 14.9). This clearly indicates that the fractures and other porosity of the formation are interconnected and hydraulically communicate over large distances. The effect of the tides changes the shape and geometry of the voids of the formation. Thus pressure (drawdown) drops and rises in the borehole depending on the position of sun, moon

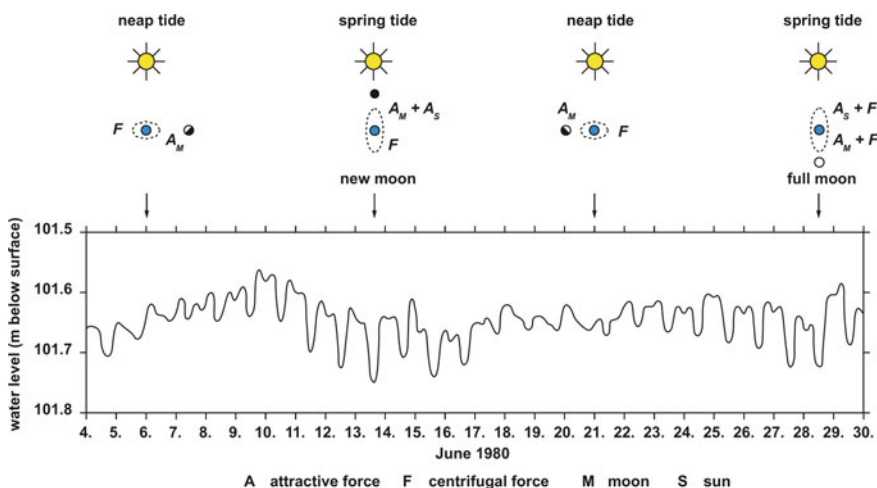


Fig. 14.9 Variation of pressure (water level) in the deep well Saulgau TB1, Germany, (in karstified upper Jurassic limestone, 650 m) caused by the tides (Example of tidal effects from: Stober 1992)

and Earth (Ferris 1951; Todd 1980). The hydraulic effects of the tidal forces permit obtaining the Young's Modulus (E), the specific storage coefficient and the porosity (Bredehoeft 1967; Langaas et al. 2005; Doan and Brodsky 2006).

Hydraulic tests may be of little significance, despite a sophisticated test scheme, if distinct formations with different hydraulic properties are jointly tested and the properties cannot be separated. By using packer systems (Figs. 9.5 and 14.2) and a proper well engineering, drilled formations can be hydraulically isolated and tested separately one-by-one, so that the derived parameters refer to a distinct and well defined tested formation.

Hydraulic tests can be combined with geophysical well logging techniques. For example, data from flow meter, electrical conductivity or temperature logs can be used to assess the contribution of separate formations that have been tested together in a pumping test, permitting assignment of hydraulic conductivity values to the individual but jointly tested formations. An example for such a combined technique is the fluid-logging method (Fig. 14.10), which repeatedly measures the electrical conductivity of the pumped fluid at depth during a long-term aquifer test (Tsang et al. 1990). The hydraulic evaluation of the aquifer test provides the total transmissivity of the tested section. The relative temporal changes of the electrical conductivity in the different formations can be used for a proportional distribution of the inflow rates from which the transmissivities of the discrete inflow sections follow. Precondition

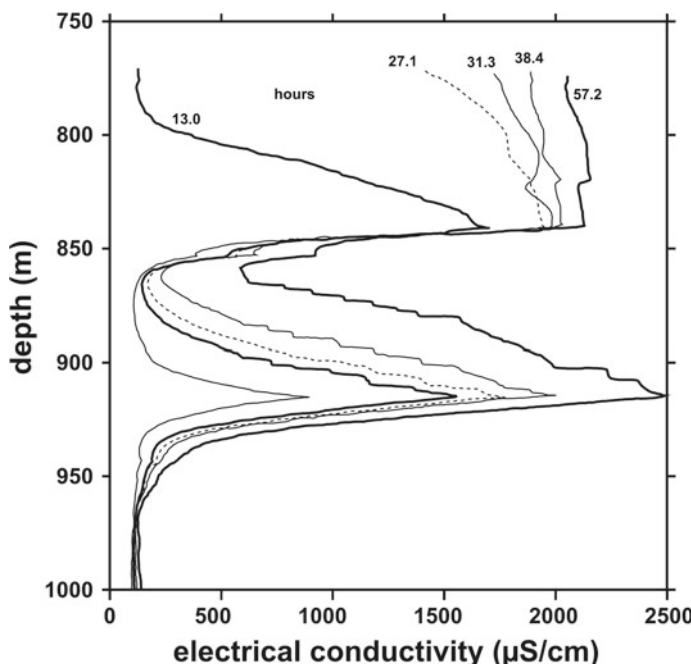


Fig. 14.10 Fluid-Logging in a 1690 m deep drillhole, data from the test section 770–1000 m (from Tsang 1987)

for the success of the method is fluid mixing in the tested section before the start of the pumping test.

The technical equipment for performing **packer tests** consists of a rod assembly with a valve and one or two packers (single, double packer, Fig. 14.2). The packer is a 0.5–1 m long enforced rubber sleeve, which can be mechanically or hydraulically pneumatically deformed, to where the mounted and inflated device seals the section to be tested. The tested section of the borehole is normally 1.5–5 m in length. During the hydraulic test, the temperature and the pressure in the tested interval are continuously monitored for detecting leaks and infiltrating water. The principle of the test is the same like in any other hydraulic test. The pressure measured in the test section at the beginning of the test serves as reference pressure, like the water level at-rest (RWL) in open wells. The initial pressure in packer tests is measured after mounting and inflating the packers. After a so-called compliance period external disturbances decline and disappear (exception are the tides, Fig. 14.9). The first step of the test changes the pressure in the test interval by extracting or injecting water (in very dense rock: gas). Withdrawal causes a pressure decrease, injection a pressure increase. In a second step, the pump is stopped and the pressure recovers slowly to the undisturbed formation pressure (Fig. 14.7). Pre-test pressure and final formation pressure should be equal.

For **packer tests** there exists a large number of hydraulic testing procedures also. The selection of the appropriate method is determined by the objectives of the testing and the expected hydraulic conductivity of the formation. The fields of application of diverse test methods are primarily related to the hydraulic conductivity of the target formation (Fig. 14.1).

Slug tests are used in formations with low to intermediate hydraulic conductivity (Butler 1998). In slug tests the pressure in the borehole or the tested interval is suddenly changed and the pressure response of the system monitored. Opening the test valve of a packer test installation transfers the pressure pulse instantly to the test interval (Fig. 14.2). During the induced flow period the pressure balances by water flowing from the formation (slug-withdrawal test) or water flowing to the formation (slug-injection test) depending on the imposed pressure gradient. Slug tests can also be used in open boreholes. Slug tests of very short duration that just send a pressure pulse to the tested section are called pulse tests. The pressure signal applied in slug tests is created by very rapid withdrawal or injection of a large amount of water or mechanically inserting a displacement body. The later type of test is also called a **bail-down test**.

Slug tests can provide transmissivity, storage coefficient, storage and skin factor. The analysis of the pressure vs. time data is typically done by means of type curves (Fig. 14.11) (e.g. Cooper et al. 1967; Ramey et al. 1975; Papadopoulos et al. 1973; Black 1985). Numerical methods are also available. The derived transmissivity data can be converted to formation permeability and hydraulic conductivity (Eqs. 8.3b and 8.4a–c).

Drill Stem testing (DST) uses the drill pipe as a testing tool where the DST equipment with packer systems replace the drill bit. The packers hydraulically isolate the section to be tested. Opening a valve imposes a pressure drop in the tested interval

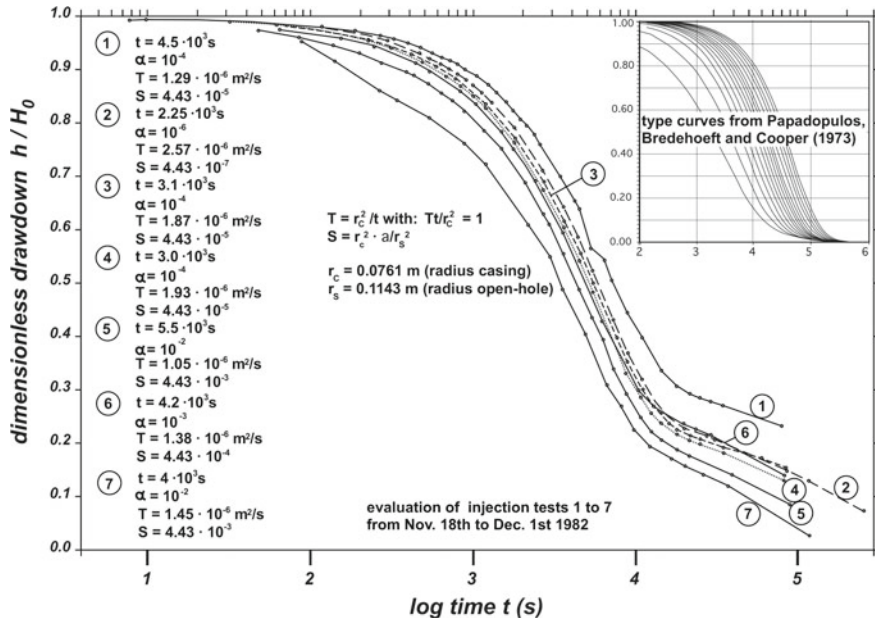


Fig. 14.11 Example of a slug test analysis from the 4440 m deep geothermal Urach 3 (Germany). Data derived from 7 test cycles. Evaluation with type curves (inset) from Papadopoulos et al. (1973)

causing water (fluid) flowing to the drillhole. Closing the valve causes the pressure to relax to the at-rest formation pressure. The standard procedure of a Drill-Stem test begins with a first short flow phase (valve open), followed by a first recovery phase (valve closed). The test continues with a long-term flow period and a long-term recovery period (Fig. 14.12). The name of the test relates to the drill stem being part of the test equipment. Depending on the test configuration, some of the test periods can be analyzed and interpreted like slug tests (Fig. 14.11), the recovery periods can be evaluated with the Horner method (Fig. 14.13; Horner plot, Horner 1951). Drill Stem tests supply transmissivity, possibly also wellbore storage and skin factor.

14.3 Tracer Experiments

Tracers are chemicals and substances that are deposited at one location (borehole) in the underground and then their migration is traced at other locations (boreholes) in the subsurface. Tracers are substances that can be detected at very low concentrations and high-degree of dilution with confidence and low-cost routine techniques. From the travel time of the tracer between the injection and the monitoring location follows a flows velocity and the scattering of the measured data reveals mixing and distribution processes, summarized by the dispersion. Tracer tests are routinely used

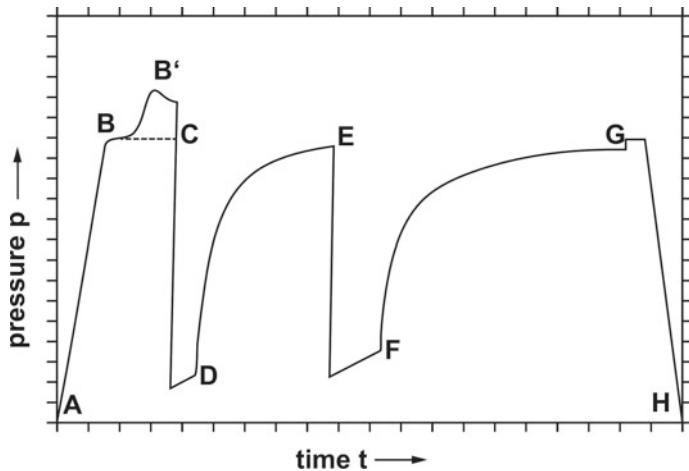


Fig. 14.12 Schematic pressure-time relationship of a Drill Stem Test. A-B) Mounting the DST drill pipe, B-C positioning and mounting the packers, B-B'-C expansion-related pressure response in low-permeability formations and subsequent relaxation, at C opening test valve, C-D first flow phase, D closing valve, D-E first recovery period, E opening valve, E-F second flow phase, F closing valve, F-G second recovery period, G-H deflating the packers and unmounting the DST equipment

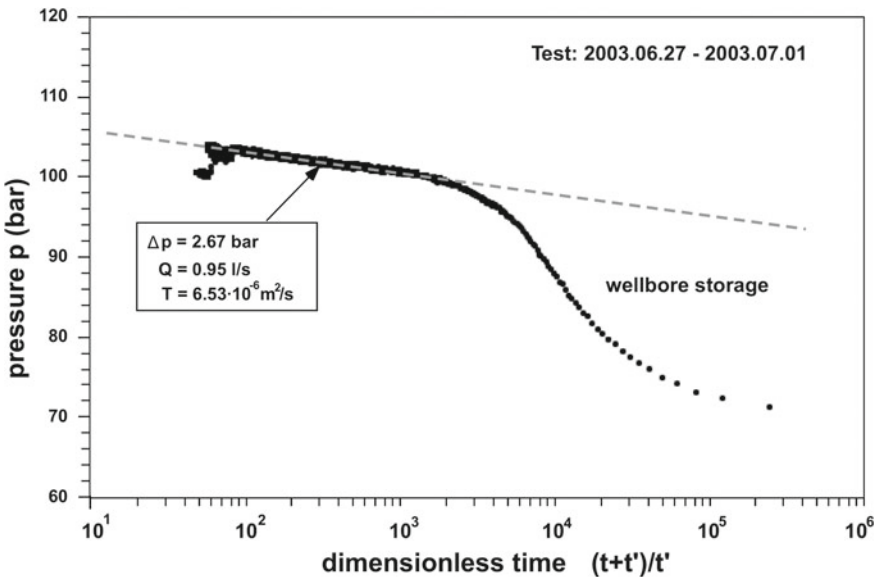


Fig. 14.13 Example of an evaluation of pressure buildup during a recovery phase with a Horner plot from test data collected in the deep geothermal well Urach 3 (Stober 2011). See also Fig. 14.11

in groundwater engineering (hydrogeology). They are being used to gain qualitative information about water flow paths. Tracer test data can also be quantitatively analyzed and reveal flow velocity, hydraulic conductivity, flow porosity, dispersion D ($m^2 s^{-1}$) and other parameters (Sauty 1980; Käss 1998; Leibundgut et al. 2011).

Thus tracer experiments are also very interesting and useful testing methods for developing geothermal doublets. Tracer experiments can show how re-injected cooled water from the plant spreads and migrates in the reservoir. For example, if a tracer arrives after a short period of time and with little dispersion that is with a sharp peak in the breakthrough curve at the production well then the thermal energy flux will behave in a similar way also. With the help of tracer experiments it can also be shown that geothermal wells may be hydraulically connected. Thus tracer experiments should be run in concert with the first long-term circulation tests.

The tracer substance used should be a non-reactive passive chemical that interacts with the minerals of the tested formation as little as possible. The inert behavior greatly facilitates the mathematical evaluation of tracer data and the interpretation of tracer concentration vs. time plots. The ideal tracer should not be toxic; it should be stable and not decay or decompose in the formation. Ideally it has properties similar to that of water. The synthetic organic chemical fluorescein, also known as uranium, specifically the sodium salt of fluorescein is a water-soluble fluorescent tracing dye that can be detected down to 10^{-9} g l^{-1} (=1 mg Uranine in 1000 m³ water). Uranine comes close to the ideal tracer and is often used in groundwater engineering applications.

A quantitative rigorous and reliable evaluation of tracer data requires a careful and firm planning and realization of the test. The test should be, in view of the later mathematical description of the test data using either analytical solutions (e.g. type curves) or numerical modeling, as simple as possible. For this purpose, tracer injection should be either instantaneous (Dirac pulse) or continuous over a well defined input-period. The tracer should preferably be injected directly into the tested formation. Samples must be taken at intervals close enough to fully cover the complete tracer transit in the observation well. Theoretically, it is necessary to sample in logarithmically equal time intervals as described in the standard tracer test text book (Käss 1998; Leibundgut et al. 2011) or general groundwater text books (Freeze and Cherry 1997; Schwartz and Zhang 2003).

Analytical solutions for tracer transport equations are available in the literature. These are solutions for the differential equations of mass transfer, for a number of different experimental arrangements. The analytical solutions can be recast in terms of dimensionless solutions that can be graphically displayed as type curves. The tracer transit on these type curves is displayed as the dimensionless tracer concentration ($C_D = C/C_{\max}$) versus the logarithm of the dimensionless time ($t_R = u^2 t / D_L$) for a series of hydraulic parameters (where u stands for the flow velocity and D_L represents the longitudinal dispersivity). For the analysis of the test data, the tracer concentration (C), normalized to the measured tracer peak concentration (C_{\max}) is plotted against log time (t). The resulting curve from the data is then matched with the type curve that fits best. The sought-after parameters are taken from the curve with optimal fit.

An example of tracer test data are shown for the thermal aquifer of karstified upper-Jurassic limestone near Saulgau (Germany) at about 650 m depth and at 42 °C (Fig. 14.14). For the tracer test, 2 kg Uranine have been injected into the geothermal well GB3 Saulgau. During the experiment, water has been pumped at a constant rate of $Q = 29 \text{ l s}^{-1}$ from the geothermal well TB1 at a distance of 450 m from the injection well GB3. This assured a radial-convergent flow regime. The first traces of Uranine arrived at the production well TB1 already after 22 days. The maximum tracer concentration, $1.4 \mu\text{g l}^{-1}$, was measured after 125 days. After 250 days, the pumping rate has been changed and water also was pumped from GB3, so that only the first part of the three year long series of measurements could be analyzed with the type-curve method (Fig. 14.14). The geo-hydraulic analysis of the data yielded a value for the flow porosity of 2.7%, a flow velocity of $u = 10^{-5} \text{ m/s}$ (0.86 m/d) and a longitudinal dispersion $D_L = 10^{-3} \text{ m}^2 \text{s}^{-1}$ using the type curve for Péclet number = 5 (for details of the analysis see Stober 1988). During a follow-up circulation test between the two geothermal wells two additional tracer chemicals have been injected into the formation, Eosine and di-tritium oxide (very heavy water). All injected tracers could be detected in the production well, however, the temperature of the produced water was not lowered by the injection of cooled water into the injection well.

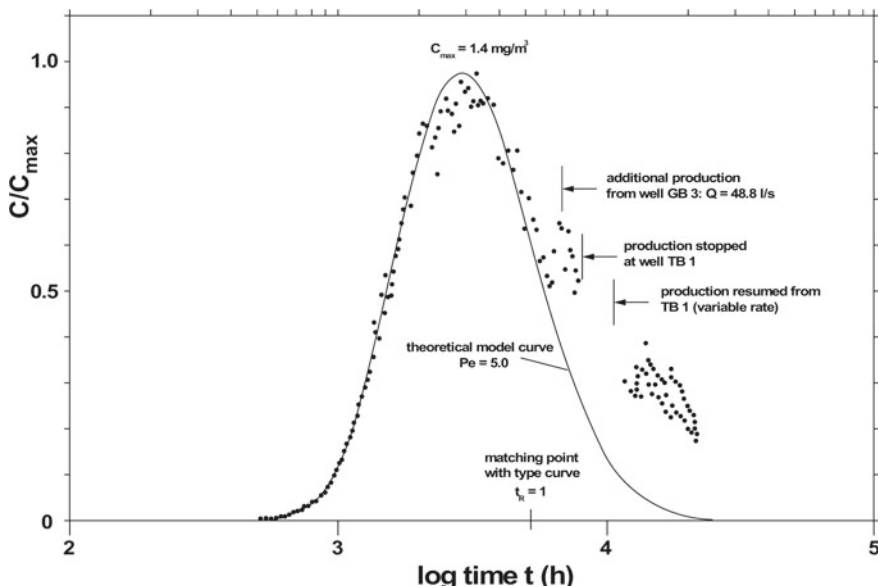


Fig. 14.14 Analysis of a tracer test with type curves. The data are from a tracer test implemented between the two 650 m deep geothermal wells Saulgau TB1 (production well) and GB3 (injection well) 430 m away from each other (Stober 1988). The data show the normalized tracer concentration C/C_{\max} at the time t (h). The best fit type curve for $Pe = 5.0$. Note that from $t \sim 7000$ h water also was pumped from the injection well GB3 (see text)

Tracer tests were carried out in the “Hot-Dry-Rock” geothermal wells at Fenton Hill near Los Alamos, New Mexico USA, during circulation tests as early as 1976 (Sect. 9.2). The first tracer tests at the site used Uranine, ^{82}Br and NH_4^+ for migration between the 3000 m deep wells GT-2(B) and EE-1 in Precambrian granite at 185 °C (reservoir depth at 2600 m, phase 1) (Tester et al. 1982). Further tracer tests were performed from 1985 on in phase II between the considerably deeper wells EE-3(A) and EE-2 that opened a reservoir at 3800 m depth and at more than 200 °C (e.g. Rodrigues et al. 1993). Tracer experiments were also carried out in the deep EGS wells at Soultz-sous-Forêts, France (Sects. 9.2 and 11.1.5). The first experiments in 1997 were performed in the 3500–3900 m deep upper granite reservoir between the wells GPK1 and GPK2 at about 160 °C. Between 2003 and 2009 experiments in the 5000 m deep granite reservoir performed between the deep wells GPK2 and GPK3 at a temperature of about 200 °C. Uranine was the tracer mainly used but experiments with benzoic acid ($\text{C}_7\text{H}_6\text{O}_2$) sulfur hexafluoride (SF_6) and other substances were also carried out (e.g. Sanjuan et al. 2006, 2015). Uranine proved to be a suitable non-resorbing tracer at the high temperature of the experiments. The tracer experiments produced breakthrough data and information on the dimension of the subsurface heat exchanger.

Tracer test data can also be used for the prediction of the thermal breakthrough in geothermal doublet systems (Shook 2001). The concentration of radioactive tracers such as tritium (^3H) can be continuously measured with appropriate instruments at the wellhead in contrast to other tracer substances that require laborious analytical work in the laboratory (Gulati et al. 1978; McCabe et al. 1981).

Other partially exceedingly sophisticated tracer tests are occasionally being used in geothermal system development. The goal of the tests is the detailed characterization of the geothermal reservoir. The complicated tests include multi-tracer tests and dual-scale push-pull tests for the characterization of the water-rock contact surface and the change of the properties of this surface in stimulation experiments. These testing methods are under development and belong to the category of research efforts rather than being mature methods of the applied sciences (e.g. Ghergut et al. 2007).

14.4 Temperature Evaluation Methods

Large volumes of ascending or descending waters leave a distinct thermal signature on the rock formation at depth. The thermal effects of vertical fluid migration can be used for deriving hydraulic parameters of the formation simply by monitoring the thermal imprint of fluid migration. The method is called temperature at-rest monitoring. Assuming that the fluid in basement fractures thermally equilibrates with the host rock, and knowing some other thermal parameters of rock and fluid such as the density of water ρ_w , the compressibility of water, the thermal conductivity of the rock (λ) and the vertical component of the flow velocity (v_z) several parameters can be derived from temperature measurements in the wellbore (Bredehoeft and Papadopoulos 1965; Mansure and Reiter 1979). Upwelling waters are displayed in

vertical temperature profiles as convex curves, descending waters as concave curves in the temperature versus depth profile (Figs. 14.15 and 14.6). The analytical solution of the differential equation to the problem is given by the Eqs. 14.6, 14.7, and 14.8:

$$(T_z - T_0)/(T_H - T_0) = f(\beta, z/H) \quad (14.6)$$

$$f(\beta, z/H) = [\exp(\beta(z - z_0)/H) - 1]/[\exp \beta - 1] \quad (14.7)$$

$$\beta = \rho_w c_w / \lambda v_z H \quad (14.8)$$

where

T_z temperature at depth from z_0 to $z_0 + H$ (measured temperatures).

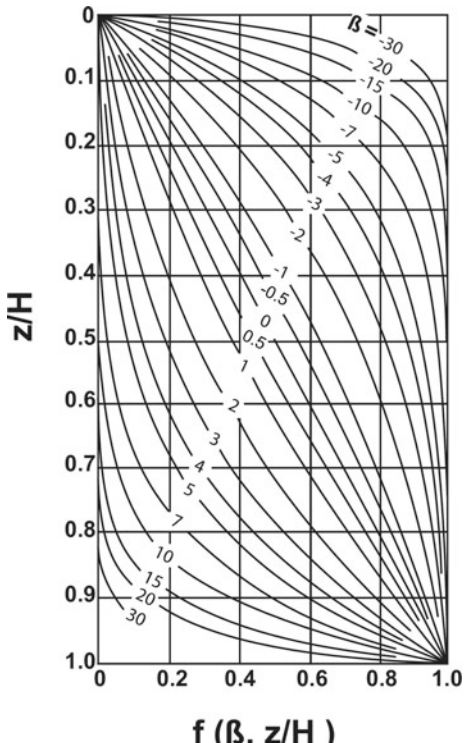
T_0 temperature measured at z_0 (reference depth $z_0 = 0$).

T_H temperature measured at depth $z_0 + H$.

H zone thickness of upwelling or downwelling fluids.

From the measured temperature profiles and with the help of type curves for the function f (Eq. 14.7; Fig. 14.16) the parameter β and thus the vertical component (v_z) of the flow velocity can be computed from Eq. 14.8.

Fig. 14.15 Type curves for deriving vertical water flow from temperature logs (Bredehoeft and Papadopoulos 1965)



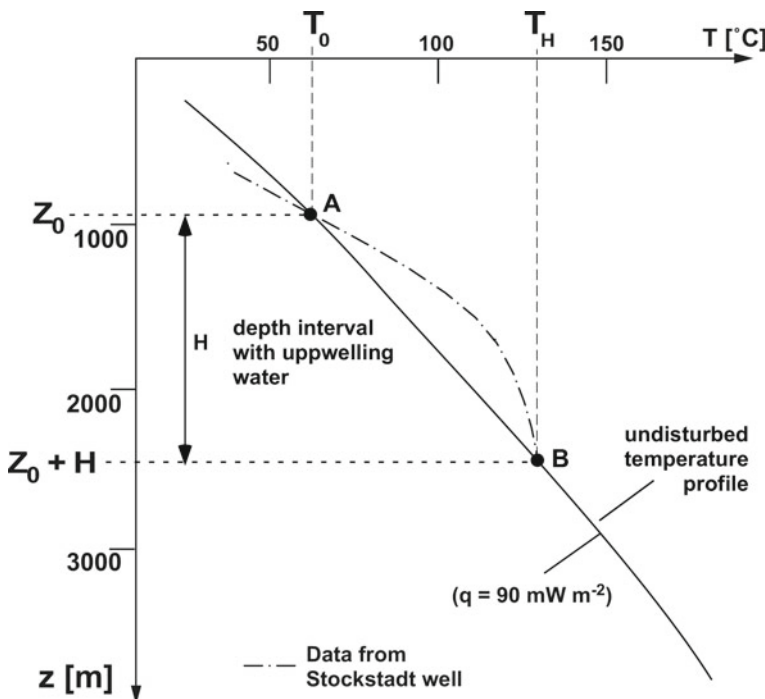


Fig. 14.16 Vertical water flow inferred from temperature logs. Measured T data from a deep well deviate from the undisturbed temperature profile between points A and B. The convex deviation of the measured temperature over the interval H implies a thermal effect from upwelling water. At the reference depth z_0 (set to 0) at temperature T_0 the anomaly begins (depth of point A) and it ends at $z_0 + H$ (depth of point B). The normalized depth variable z/H needed for the type curves on Fig. 14.15 varies between 0 (z_0) and 1 ($(z_0 + H)/H$). From the parameter β (Fig. 14.15) the vertical flow velocity v_z can be computed from the equations given in the text

Thermal modeling is an important tool for predicting the thermal structure developing in production and injection wells during operation (e.g. Nowak 1953; Pourafshary et. al. 2009; Al Saedi et al. 2018; Moradi et al. 2020).

References

- Agarwal, R. G., Al-Hussainy, R. & Ramey Jr., H. J., 1970. An Investigation of Wellbore Storage and Skin Effect in Unsteady Liquid Flow: I. Analytical Treatment. SPE Journal, 10(3), 279–290.
 Al Saedi, A. Q., Flori, R. E. & Kabir, C. S., 2018. New analytical solutions of wellbore fluid temperature profiles during drilling, circulation, and cementing operations. Journal of Petroleum Science and Engineering, 170, 206–217.
 Barenblatt, G. E., Zeltov, J. P. & Kochina, J. N., 1960. Basic Concepts in the Theory of Homogeneous Liquids in Fissured Rocks. Journ. appl. Math. Mech. (USSR), 24(5), 1286–1303

- Berkloff, E., 1967. Interprétation des pompages d'essai. Cas de nappes captives avec une strate conductrice d'eau privilégiée. Bull. B.R.G.M. (deuxième série), section III: 1, 33–53.
- Black, J. H., 1985. The interpretation of slug tests in fissured rocks. Quarterly Journal of Engineering Geology and Hydrogeology, 18(2), 161–171.
- Bourdet, D., Ayoub, J.A. & Pirard, Y.M., 1989. Use of Pressure Derivative in Well-Test Interpretation. Soc. Petrol. Engineers, SPE, p. 293–302.
- Bredehoeft, J.D. 1967. Response of well-aquifer systems to Earth tides. Journal of Geophysical Research, 72/12, 3075–3087.
- Bredehoeft, J. D. & Papadopoulos, I. S., 1965. Rates of vertical groundwater movement estimated from the earth's thermal profile. Water Resour. Res., 1, 325–328.
- Butler, J. J., Jr., 1998. The Design, Performance, and Analysis of Slug Tests. Lewis Publishers, New York, 252 pp.
- Cinco, L. H., Ramey, H. J. & Miller, F. G., 1975. Unsteady-State Pressure Distribution Created by a Well with an Inclined Fracture. Soc. Petrol. Engineers of AIME (SPE 5591), 18.
- Cooper, H. H. & Jacob, C. E., 1946. A Generalized graphical method for evaluating formation constants and summarizing well-field history. Trans. Am. Geoph. Union, 27, 526–534.
- Cooper, H. H. J., Bredehoeft, J. D. & Papadopoulos, I. S., 1967. Response of a finite-diameter well to an instantaneous charge of water. Water Resources Research, 3(1), 263–269.
- Doan, M.-L. & Brodsky, E. E., 2006. Tidal analysis of water level in continental boreholes. Tutorial, version 2.2, University of California, Santa Cruz, 61 p.
- Dyes, A. B., Kemp, C. E. & Caudle, B. H., 1958. Effect of Fractures on Sweep-Out Pattern. Trans. AIME, 213, 245–249.
- Everdingen, van, A. F., 1953. The Skin Effect and its Influence on the Productive Capacity of a Well. Petrol. Trans. AIME, 198, 171–176.
- Ferris, J. G., 1951. Cyclic fluctuations of water level as a basis for determining aquifer transmissivity. Intl. Assoc. Sci. Hydrology Publ., 33, 148–155.
- Freeze, K. A. & Cherry, J. A., 1997. Groundwater. Prentice Hall, 604 pp.
- Ghergut, I., Sauter, M., Behrens, H., Rose, P., Licha, T., Lodemann, M. & Fischer, S., 2007. Tracer-assisted evaluation of hydraulic stimulation experiments for geothermal reservoir candidates in deep crystalline and sedimentary formations. In: EGC Proceedings European Geothermal Congress, Unterhaching, pp. 1–12.
- Gringarten, A. C. & Ramey, H. J., 1974. Unsteady-State Pressure Distributions created by a Well with a single Horizontal Fracture, Partial Penetration, or Restricted Entry. Soc. Petrol. Engineers Journ., 413–426.
- Gulati, M. S., Lipman, S. C. & Strobel, C. J., 1978. Tritium Tracer Survey at The Geysers. Geothermal Resources Council Transactions, 2, 237–239.
- Hawkins, M. F., 1956. A Note on the Skin Effect. Trans. AIME, 207, 356–357.
- Hekel, U., 2011. Hydraulische Tests.- In: Bucher, K., Gautschi, A., Geyer, T., Hekel, U., Mazurek, M., Stober, I.: Hydrogeologie der Festgesteine, Fortbildungsveranstaltung der FH-DGG, Freiburg.
- Horner, D. R., 1951. Pressure Build-up in Wells. In: Bull, E. J. (ed.): Proc. 3rd World Petrol. Congr., pp. 503–521, Leiden, Netherlands.
- Käss, W., 1998. Tracing Techniques in Geohydrology. A. A. Balkema, Rotterdam, Netherlands, 581 pp.
- Kruseman, G. P. & de Ridder, N. A., 1994. Analysis and Evaluation of Pumping Test Data, pp. 377, International Institute for Land Reclamation and Improvement ILRI, Wageningen, The Netherlands.
- Langaas, K., Nilsen, K.I. & Skjaeveland, S.M., 2005. Tidal Pressure Response and Surveillance of Water Encroachment.- Society of Petroleum Engineers, SPE 95763, 11 p.
- Leibundgut, C., Moaloszewski, P. & Külls, C., 2011. Tracer in Hydrology. John Wiley & Sons, New York, 432 pp.
- Mansure, A. J. & Reiter, M., 1979. A vertical groundwater movement correction for heat flow. J. Geophys. Res., 84(7), 3490–3496.

- Matthews, C. S. & Russel, D. G., 1967. Pressure Buildup and Flow Tests in Wells. In: AIME Monograph 1, H.L. Doherty Series SPE of AIME, New York, 167 pp.
- McCabe, W. J., Barry, B. J. & Manning, M. R., 1981. Radioactive Tracers in Geothermal Underground Water Flow Studies. *Geothermics*, 12(2–3), 83–110.
- Moradi, B., Ayoub, M., Bataee, M. & Mohammadian, E., 2020. Calculation of temperature profile in injection wells. *Journal of Petroleum Exploration and Production Technology*, 10, 687–697.
- Nielsen, K. A., 2007. *Fractured Aquifers: Formation Evaluation by Well Testing*. Trafford Publishing, Victoria, BC, Canada, 229 pp.
- Nowak, T. J., 1953. The estimation of water injection profiles from temperature surveys. *Journal of Petroleum Technology*, 5, 203–212.
- Odenwald, B., Hekel, U. & Thormann, H., 2009. Groundwater flow - groundwater storage (in German). In: Witt, K.J. (Hrsg.): *Grundbau-Taschenbuch, Teil 2: Geotechnische Verfahren*, pp. 950, Ernst & Sohn.
- Papadopoulos, S. S., Bredehoeft, J. D. & Cooper, H. H., Jr., 1973. On the analysis of ‘slug test’ data. *Water Resources Research*, 9(4), 1087–1089.
- Pourafshary, P., Varavei, A., Sepehrnoori, K. & Podio, A., 2009. A compositional wellbore/reservoir simulator to model multiphase flow and temperature distribution. *Journal of Petroleum Science and Engineering*, 69, 40–52.
- Ramey, H. J. J., Agarwal, R. G. & Martin, I., 1975. Analysis of ‘slug test’ or DST flow period data. *Journal of Canadian Petroleum Technology*, 3(37), 47.
- Rodrigues, N. E.V., Robinson, B. A. & Counce, D. A., 1993. Tracer Experiment Results During the Long-Term Flow Test of the Fenton Hill Reservoir.- Proceedings, 18th Workshop on Geothermal Reservoir Engineering Stanford University, SGP-TR-145, 199–206, Stanford, California.
- Russell, D. G. & Truitt, N. E., 1964. Transient Pressure Behavior in Vertically Fractured Reservoirs. *Journ. Petrol. Technol.*, 1159–1170.
- Sanjuan, B., Pinault, J. L., Rose, P., Gérard, A., Brach, M., Braibant, G., Crouzet, C., Foucher, J. C., Gautier, A. & Touzelet, S., 2006. Geochemical fluid characteristics and main achievements about tracer tests at Soultz-sous-Forêts (France).- Final Report BRGM/RP-54776-FR, 67 p., Orléans, France.
- Sanjuan, B., Brach, M., Genter, A., Sanjuan, R., Scheiber, J. & Touzelet, S., 2015. Tracer testing of the EGS site at Soultz-sous-Forêts (Alsace, France) between 2005 and 2013.- Proceedings World Geothermal Congress, 12 p., Melbourne, Australia.
- Sauty, J. P., 1980. An analysis of hydrodispersive transfer in aquifers. *Water Resour. Res.*, 16(1), 145–158.
- Schwartz, F. W. & Zhang, H., 2003. *Fundamentals of Ground Water*. Wiley & Sons, New York, 592 pp.
- Shook, G.M., 2001. Predicting Thermal Breakthrough in Heterogeneous Media from Tracer Tests. *Geothermics* 30(6), 573–589.
- Stober, I., 1986. Strömungsverhalten in Festgesteinsaquiferen mit Hilfe von Pump- und Injektionsversuchen (The Flow Behaviour of Groundwater in Hard-Rock Aquifers—Results of Pumping and Injection Tests) (in German). *Geologisches Jahrbuch, Reihe C*, 204 pp.
- Stober, I., 1988. Geohydraulic Results from Tests in hydrogeothermal Wells in Baden-Württemberg (in German) (eds Bertleff, B., Joachim, H., Kozirowski, G., Leiber, J., Ohmert, W., Prestel, R., Stober, I., Strayle, G., Villinger, E. & Werner, J.), pp. 27–116, Jh. geol. Landesamt Baden-Württemberg, Freiburg i.Br.
- Stober, I., 1992. The tides and their hydraulic effects on groundwater (in German). *DGM*, 36(4), 142–147.
- Stober, I., 2011. Depth- and pressure-dependent permeability in the upper continental crust: data from the Urach 3 geothermal borehole, southwest Germany. *Hydrogeology Journal*, 19, 685–699.
- Stober, I. & Bucher, K., 2005a. The upper continental crust, an aquifer and its fluid: hydraulic and chemical data from 4 km depth in fractured crystalline basement rocks at the KTB test site. *Geofluids*, 5, 8–19

- Stober, I., Richter, A., Brost, E. & Bucher, K., 1999. The Ohlsbach Plume: Natural release of Deep Saline Water from the Crystalline Basement of the Black Forest. *Hydrogeology Journal*, 7, 273–283.
- Stober, I., Fritzer, T., Obst, K., Schulz, R., 2009. Nutzungsmöglichkeiten der Tiefen Geothermie in Deutschland.- Bundesministerium für Umwelt, Naturschutz und Reaktorsicherheit, 73 S., Berlin.
- Tester, J.W., Bivins, R. L. & Potter, R. M., 1982. Interwell Tracer Analyses of a Hydraulically Fractured Granitic Geothermal Reservoir. *Society of Petroleum Engineers*, 22, 537–554.
- Theis, C. V., 1935. The Relation between the lowering of the Piezometric Surface and the Rate and Duration of Discharge of a Well Using Groundwater Storage. *Trans. AGU*, 519–524.
- Todd, D. K., 1980. *Groundwater Hydrology* (2nd edition). Wiley, New York, 535 pp.
- Tsang, C.-F., 1987. A Borehole Fluid Conductivity Logging Method for the Determination of Fracture Inflow Parameters. In: *Report of the Earth Science Division*, pp. 53, Lawrence Berkley Laboratory, University of California.
- Tsang, C.-F., Hufschmied, P. & Hale, F. V., 1990. Determination of Fracture Inflow Parameters With a Borehole Fluid Conductivity Logging Method. *Water Resources Research*, 26(4), 561–578.
- Zarrouk, S. J. & McLean, K., 2019. *Geothermal Well Test Analysis: Fundamentals, Applications and Advanced Techniques*. Academic Press, 366 pp.

Chapter 15

The Chemical Composition of Deep Geothermal Waters and Its Consequences for Planning and Operating a Geothermal Power Plant



Silica sinter at Mammoth hot spring, Yellowstone NP, Wyo, USA

The fracture porosity of continental crust is normally saturated with an aqueous fluid (Ingebretsen and Manning 1999; Fritz and Frape 1987; Stober and Bucher 2005b; Bucher and Stober 2010). This fluid is used for transferring thermal energy from the hot depth to the cold surface for various uses. The chemical composition of this natural heat transfer fluid depends on the predominant (reactive) rock type of the thermal reservoir and its changes along the circulation pathway. Most deep fluids are saline brines with the major components NaCl and CaCl₂. Typical deep fluids contain between 1 and 4 molal NaCl equivalents corresponding to a total of dissolved solids (TDS) in the range of 60–270 g L⁻¹ (Kozlovsky 1984; Nordstrom et al. 1985; Pauwels et al. 1993; Banks et al. 1996; Stober and Bucher 2005b). The chemical composition of the fluid has a number of consequences for geothermal exploration and also for the later operation of a power plant that will be briefly explored in this chapter.

The pre-drilling conditions are usually unknown, but the aqueous fluid residing in the fracture porosity of crystalline basement (for example) at some thousand meters depth typically has a complex composition with a high salinity and locally high amounts of dissolved gases. The natural solutes have quite different origins that can be separated into locally derived components from reaction with the rock matrix and externally derived components that have been introduced by migrating fluids (Kharaka and Hanor 2005). Natural fluid migration velocities tend to be very small at several km depth because of decreasing natural hydraulic conductivity with depth (Stober and Bucher 2007a; b; Ingebretsen and Manning 2011) and because of decreasing head gradients driving fluid migration. Consequently, natural deep fluids have a composition that is not very far from equilibrium with the host rock and thus chemical interaction between fluid and rock is slow and weak.

Once the fluid becomes accessible after the first wellbore has been drilled, the fluids must be sampled and its chemical composition carefully analyzed and interpreted. Later, during operation of the plant and the associated fluid circulation, chemical changes of the fluid must be precisely monitored because they may reflect changing reservoir conditions and alteration of the reservoir structures. The hydrochemistry is a very sensitive monitor for subtle developments in the reservoir during the years of operation. Long-term operation of a system requires an excellent knowledge and understanding of chemical processes in the reservoir that are reflected in the composition of the produced fluid.

The situation described above does explicitly not include high-enthalpy volcanic environments where infiltrating surface fluids may chemically interact vigorously with highly reactive rocks (Giggenbach 1981; Nicholson 1993). High-enthalpy fields in active volcanic regions are typically associated with hot springs, steam vents and other surface structures expelling hot deep fluids. Therefore, the hot fluid from the geothermal reservoir can be sampled and analyzed pre-drilling in contrast to the situation in deep hydrogeothermal and EGS projects. The fluid composition gives valuable insight into reservoir conditions including the temperature and depth of the reservoir. However, the ascending fluid is often chemically modified after it left the geothermal reservoir. Chemical reaction with cooler rocks at shallow depth, mixing with fluids from other levels and dilution with low-TDS surface water may conceal

the original composition of the deep fluid. Some aspects of fluid chemistry in active volcanic fields are briefly presented in the different sections of this chapter.

15.1 Sampling and Laboratory Analyses

Some hydrochemical parameters must be measured at the wellhead of a borehole or at a hot spring. However, it is not a trivial matter to sample a fluid at 200 °C and 500 bar. Normally, fluids are being cooled and decompressed at the wellhead and then sampled. Electrical conductivity, pH and redox potential should be measured immediately after sampling. Alkalinity should also be titrated at the site, particularly for high-pH waters. Conservative composition parameters can be measured later after shipping to the service laboratory. Sampling and analysis of dissolved gasses requires special techniques and a certified laboratory with the appropriate expertise. Additional analysis, especially isotope composition analyses, can be helpful for solving special problems.

Because, deep fluids may contain relatively high concentrations of toxic or otherwise harmful components such as heavy metals including lead, zinc, cadmium, arsenic, mercury and others consequently the pumped deep fluid must be handled with care and should not be mistaken for drinking water.

Two-phase fluids from high-enthalpy reservoirs should generally be sampled at the same pressure for the gas and the liquid phase for example by means of a small separator. The enthalpy of the produced fluid must also be measured during fluid sampling. The gas and liquid phase analyses can later be combined resulting in the composition of the reservoir fluid.

Sampling requires special techniques that isolate the fluid from contact with the highly oxidizing atmosphere. Some solutes remain stable after cooling and transport. Other components may chemically interact in various ways at low temperature and change concentration. The most common situation is that some solids may become oversaturated and start to precipitate from fluid during cooling, degassing and oxidation. Some components can be kept in solution by acidifying a part of the sampled material. This can be done with e.g. nitric acid because nitrate is not a typical component of deep fluids. However, the appropriate method of sample conservation depends on the parameters to be analyzed and the planned analytical methods, which should be known before sampling. It may not be possible to analyze for a certain helpful extra parameter if the samples have been stabilized with chemicals that precludes this (Arnórsson et al. 2006; Nicholson 1993).

The hot salty fluid is chemically rather aggressive and tends to react with materials it comes in contact with, including steel tubing. Cooling loops from stainless steel may rapidly corrode in contact with certain brines adding metals to the solution and changing its REDOX state during sampling (Hewitt 1989; Parker et al. 1990). Sampling hose may be penetrable for oxygen and even CO₂, which may cause severe alteration of the original composition of the deep fluid.

Sampling bottles and any other equipment that has contact to the fluid to be sampled must be carefully pre-cleaned. Polybottles with tight locks are standard. Glass bottles should be avoided because they may release certain components to the fluid, although the glass contribution to high TDS fluids is probably negligible in most cases. However, polybottles loose H₂O from the sample by diffusion during long-time storage. This must be considered if some additional components of interest should be later analyzed in stored fluid samples. Sample bottles (e.g. polybottles) are typically not gas-prove so that atmospheric oxygen may contaminate the sample (Ármannsson and Ólafsson 2010). Light-sensitive components must be protected by dark colored sample bottles. Thus for sampling geothermal fluids different types of sample bottles must be utilized depending on the requirements of the components of interest. Sampling gas-rich thermal water requires absolutely gas-tight sample bottle. Some of the dissolved components can be reactive and unstable demanding an appropriate chemical conservation. Therefore fluid sampling may produce a number of sub-samples that have been chemically and physically (e.g. filtered, acidified, diluted, frozen) treated differently and stored in a series of different sample container. An excellent overview of the conservation methods for geothermal fluid samples can be found in Ármannsson and Ólafsson (2010).

Flow cells are typically used to measure the on-site parameters temperature, electrical conductivity, redox potential, pH and dissolved oxygen gas (Fig. 8.8). High dissolved oxygen may reflect gas leaks in the sampling devices and the flow cell. In addition to the abovementioned transient dissolved carbonate species some other solutes are unstable as well and need to be analyzed at the sampling site. This includes NH₄⁺ (ammonium), NO₂⁻ (nitrite), HS⁻ (hydrogen sulfide), thiosulfate and others. Dissolved silica can cause problems if saturation with amorphous silica is exceeded during sample cooling. This can be critical in high-enthalpy systems. In low enthalpy systems it is not normally necessary to analyze for dissolved silica at the sampling site directly. SiO₂-rich high-T fluid samples (SiO₂ > 100 ppm) can be diluted with a fixed amount of distilled or deionized water thereby effectively preventing precipitation of dissolved silica.

Analysis of the samples for major and trace components requires a laboratory equipped with a few specialized instruments. Most labs use ion chromatography (IC) for analyzing anions and photometry for uncharged solutes such as silica and boron. Cations can also be analyzed by ion chromatography but most labs use one of the several forms of ICP (inductively coupled plasma) spectroscopy (ICP-AES atomic emission spectroscopy = ICP-OES optical emission spectroscopy). The ICP instruments can be combined with a mass spectrometer (ICP-MS). In our lab at the University of Freiburg, the cations are being analyzed by atomic absorption spectroscopy (AAS) with a flame AAS (major components) or a graphite furnace AAS instrument (trace components). Titration methods are normally used for carbonate species and dissolved sulfide species. The quantitative analysis of elements present in a number of species and in different oxidation states such as Fe(II) and Fe(III) or As(III) and As(V), the various sulfur species, dissolved chromium, uranium and many more is analytically demanding and prone to alteration during fluid ascent from the reservoir, during sampling, handling and analysis (Arnórsson et al. 2006). Of course,

knowing the precise redox state of the fluid at depth would be very helpful for making predictions about its behavior upon production, decompression and cooling (in short during later operation of the plant).

Samples that are used for cation analysis are acidified with HNO_3 and also filtered through a 45 μm acetate filter at the sampling site. Samples for anion analysis by IC are normally being filtered only. Samples for later pH and carbonate measurement, if on site analysis is not possible, need to be kept in gas-tight containers and contact to the atmosphere must be excluded.

Recommendations and technical advice for sampling and analyzing hot, highly mineralized and often gas-rich geothermal fluids including high-temperature sulfur geochemistry can be found in: Ball et al. (1976), Thompson et al. (1975), Thompson and Yadav (1979), Giggenbach and Goguel (1989), Nicholson (1993), Cunningham et al. (1998), Ármannsson and Ólafsson (2010).

The downhole-sampler is a special device that allows collection of water samples at depth thus providing in situ properties of the fluid including dissolved gasses and gas composition at depth under pressure and at reservoir temperature.

Sampling the various fluids associated with volcanic high-enthalpy fields such as fumaroles, dry-steam and wet-steam wells requires experience, expertise and special equipment (Sutton et al. 1992; Arnórsson et al. 2006; Ármannsson and Ólafsson 2010). A treatise on analytical methods in addition to sampling techniques for fluids of high-enthalpy fields can be found in Giggenbach and Goguel (1989). Excel spreadsheets for the analysis and interpretation of liquid and gaseous geothermal fluids have been presented by Powell and Cumming (2010). The knowledge of the composition of the gas phase is particularly important for planning anti-corrosion and appropriate environmental protection measures. The following gases should be routinely analyzed: CO_2 , H_2S , NH_3 , also data for CH_4 , H_2 , N_2 , Ar and O_2 can be very helpful. For some purposes additional gases must be analyzed, including: He, CO, Ne, SO_2 , and the stable isotopes ^3He and ^4He , which require special sampling techniques. The concentration of SO_2 as an example can be useful for distinguishing volcanic (magma related) fluids from hydrothermal meteoric waters. The gases, particularly in fluids of high-enthalpy fields, can be collected in a NaOH solution under vacuum; NH_3 can separately be trapped in an acidified solution. Steam from fumaroles should be condensed and cooled below 40 °C (Powell and Cumming 2010).

It proved to be valuable collecting also samples for stable isotope analysis of oxygen (^{16}O , ^{18}O) and hydrogen (^1H , ^2H , ^3H) isotopes. Particular precautions must be taken if sampling for stable oxygen isotopes in H_2S rich fluids.

15.2 Chemical Parameters Characterizing Deep Fluids

A key parameter characterizing aqueous fluids is the pH value defined as the negative decimal logarithm of the activity of the hydrogen ion H^+ ($\text{pH} = -\log a_{\text{H}^+}$). It is a dimension-less quantity but numerically equal to the H^+ molality of solution because of the chosen standard state $a_{\text{H}^+} = 1$ for a $m_{\text{H}^+} = 1$ solution. Acid solutions have a low

pH (high H⁺ concentration); alkaline solutions have high pH (low H⁺ concentration). Neutral solutions are characterized by equal amounts of H⁺ and OH⁻ ions in the solution. At 25 °C pure water is neutral at pH = 7, at 108 °C the neutral point is at pH = 6.0 and at 200 °C a neutral solution has a pH = 5.5. The decrease of neutral pH is a consequence of the decreasing self-ionization constant K_w of water with temperature. Geothermal waters from crystalline basement reservoirs tend to be slightly acidic or close to neutral. pH values of deep waters at 150–200 °C tend to be in the range of 5–6 (Pauwels et al. 1993; Fritz and Frape 1987; Stober and Bucher 1999a; Bucher and Stober 2000). The parameter is difficult to assess for high-TDS fluids at high temperature and pressure. However, reliable predictions for potential risks for scaling and corrosion strongly depend on the precise knowledge of the pH of the produced fluid under reservoir conditions. Because pH is a logarithmic value the H⁺ concentration in a pH = 5.5 and a pH = 5.8 solution differs by a factor of 2 (there is twice as much H⁺ in a pH = 5.5 solution than in pH = 5.8 solution). Thus the numbers after the decimal point matter.

The oxidation state of the produced fluid can be characterized with the value defined as negative decimal logarithm of the activity of the electron e⁻ ($p_e = -\log a_e^-$) in analogy to the pH value. It is also a dimensionless quantity. Neutral surface waters in equilibrium atmospheric O₂ have a p_e value of about 13. Water of pH = 6 is stable in the range $p_e = 15$ (highly oxidizing) to $p_e = -5$ (very reducing). The presence of sulfate sulfur (SO₄²⁻) in most deep geothermal fluids rather than sulfide sulfur (H₂S, HS⁻) implies that p_e must be in the stable field for sulfate at the given pH of the fluids. Most deep fluids in crystalline basement reservoirs are relatively oxidized with sulfate as the dominant sulfur species in solution, with CO₂ rather than methane (CH₄) as the dominant carbon gas dissolved in the fluid and with carbonate carbon (C^{IV}) in the solution.

The solubility of many minerals depends on the oxidation state of the rock-fluid system. Particularly iron-bearing minerals may dissolve in highly reducing fluids and Fe²⁺ concentration of such fluids may be very high. On the other hand, iron-bearing minerals may not dissolve in oxidizing fluids and the concentration of Fe³⁺ in the fluids is extremely small. In most primary rock-forming Fe-bearing minerals (e.g. biotite) in granite and gneiss iron is present in its reduced divalent form. The mineral biotite is unstable at most reservoir conditions for geothermal applications (<350 °C). It dissolves in the pore fluid and re-precipitates as secondary minerals such as clay. The iron is insoluble at oxidizing high p_e conditions and precipitates as iron oxide or oxide-hydroxide mineral (goethite, ferrihydrite, hematite). Thus pumped hot deep fluids may contain measurable amounts of dissolved iron only if p_e is low and the conditions reducing. This is not normally the case, however. Trivalent iron (Fe³⁺) is soluble in very acid low pH fluids, which can be present in some volcanic environments, but the moderate pH of deep fluids in granite and gneiss typically precludes the presence of dissolved iron even under moderately oxidizing conditions. Thus very low Fe in geothermal deep-water at moderate pH indicates rather oxidizing conditions in the reservoir formation.

Generally, oxidation-reduction reactions transfer electrons from the reduced state to the oxidized state. For the important iron example: Fe²⁺ (reduced) =

Fe^{3+} (oxidized) + e^- (electron). If the reaction progresses to the right-hand-side it produces electrons and divalent iron is oxidized to trivalent iron. If the reaction runs to the left it consumes electrons or reduces iron from its trivalent to the divalent state. Thus if there is a source of electrons, the environment is reducing and (like pH) p_e is low (negative). Vice versa, if p_e is high (e.g. 15), electrons are rare and the environment is oxidizing.

The REDOX state of geothermal fluids is measured as the REDOX potential using an electrode system (millivolt mV electrode). Usually the mV electrode can be connected to a pH meter. The measured REDOX potential E_H (in Volt or mV) depends on temperature, which must be recorded together with the E_H measurement. The REDOX potential can be directly used as a parameter for fluid interpretation and risk prognosis. It must be converted to the parameter p_e for use in various hydrochemical software models or analyzing data on p_e versus pH diagrams:

$$p_e = E_H \{ \mathfrak{F} / (2.303 R T) \} \quad (15.1)$$

where E_H represents the measured REDOX potential $[J/C] = [V]$ with J = Joule and C = Coulomb (charge), \mathfrak{F} is the temperature dependent Faraday constant $[96485 \text{ C mol}^{-1}]$, R the universal gas constant $[8.314 \text{ J K}^{-1} \text{ mol}^{-1}]$ and T temperature [K]. The factor 2.303 converts to decimal log scale. The expression in {} has the dimension $1/V$, together with E_H in V results in the dimensionless p_e . At 25 °C the conversion is: $p_e = 16.9 E_H$ (in V). H_2O at pH = 6 is stable between $p_e = 15$ (strongly oxidizing) and $p_e = -5$ (strongly reducing). Deep water in the crystalline basement is typically relatively oxidized with sulfate (SO_4^{2-}) being the dominant sulfur species, with dissolved CO_2 gas, negligible CH_4 , and very low dissolved iron.

Dissolution of minerals in aqueous fluids releases electrolytes to the fluid. The ions resulting from the dissociation of the electrolytes make the solution electrically conductive. The contribution of a specific electrolyte in the solution to the total electrical conductivity (EC) depends on the charge of the ion, the degree of dissociation, the concentration of the electrolyte, TDS and other factors. The electrical conductivity (S m^{-1}) of the geothermal fluid results from the combined contributions of all ions present in the fluid. Therefore, measured EC is proportional to the TDS of the fluid. Natural near surface waters have EC in the range of 2–100 mS m^{-1} , the EC of seawater is about 4.5 S m^{-1} and the saline fluid (62 g L^{-1} TDS) from the 4000 m deep thermal fluid (120 °C) from the pilot hole at the German Continental Deep Drilling site (KTB) has a measured EC of 6.8 S m^{-1} . Because deep geothermal fluids are typically concentrated Na-(Ca)-Cl brines, EC is closely related to salinity. The EC is measured with an electrical conductivity meter, a resistance probe that can be attached to a hand-held instrument. The electrical conductivity depends on the temperature, which must be reported with the EC measurement. The EC can be measured as part of geophysical well logging. EC logs, also referred to as salinity logs, may identify and localize inflow structures of fluid with contrasting TDS (Sect. 13.2).

The measured concentration of dissolved solids is reported as mass of solute per unit volume of solution (g L^{-1}). If the amount of solute is expressed in mole

(millimole) units the concentration (mol L^{-1}) is termed molarity. Another commonly used concentration unit is mass of solute per kg of water (g kg^{-1} ; mg kg^{-1}). Using number of moles of solute per kg of pure water (solvent), the unit (mol kg^{-1}) is called molality. Molarity and molality should not be confused. Concentrations given in the two different units are very similar for low-TDS fluids; however, they differ for brines and other high-TDS fluids. As an example: A saturated NaCl solution at 25 °C contains 343 g NaCl per one liter solution (molarity = 5.86) and 358 g NaCl per one kg of water (molality = 6.13). Note also that solubility information is commonly given in molality that is number of moles of a substance dissolve in one kg of pure water.

The number and type of solutes to be analyzed in a water sample depends on the scope of investigation and the relative importance of the solute for understanding the chemical behavior of the rock-water system. Most saline deep fluids contain, in the order of importance, sodium (Na), calcium (Ca), potassium (K) and magnesium (Mg) as the dominant cations. It may be useful to analyze also for strontium (Sr), ammonium (NH_4^+) and lithium (Li). Critically important are the concentration of iron (Fe) and manganese (Mn). The two elements are present in detectable amounts only in reduced waters. Their concentration gives valuable information on the REDOX state of the fluid. Note, however, that in normal relatively oxidized waters, Fe is below 1 mg L^{-1} or even below 1 $\mu\text{g L}^{-1}$. Reported Fe concentrations above these levels must skeptically viewed. Aluminum (Al) is also present at very low concentration levels ($\mu\text{g L}^{-1}$) in most deep fluids although the fluids are in contact with Al-rich minerals, such as micas and feldspars, at depth. It should always be attempted to measure Al in the sampled deep fluids, because without Al-concentration data the saturation state of the fluid with respect to the minerals of the formation cannot be modeled.

The major anions of geothermal deep waters are chloride (Cl), carbonate or bicarbonate (CO_3^{2-} , HCO_3^-) and sulfate (SO_4^{2-}). It is recommended to analyze for fluoride (F^-) and bromide (Br^-) because Cl-rich waters and brines also contain the other halogens and because they are of diagnostic value. It is also recommended to analyze for iodide (I^-) in high-salinity fluids. The halogen data can give valuable hints about the origin of the salinity and thus the origin of the deep fluid. Other anions common in near surface waters such as nitrate (NO_3^-), nitrite (NO_2^-) and phosphate (PO_4^{3-} , HPO_4^{2-} , H_2PO_4^-) are less prominent in deep fluids and need not necessarily be analyzed. In reducing waters it may be necessary to analyze for sulfide (HS^-).

Because some trace elements may potentially form scales it is helpful for the assessment of the associated risks to analyze for lead (Pb), barium (Ba) and arsenic (As). Some trace elements are valuable for interpreting the origin of the fluids and the interaction processes between the fluids with the reservoir rocks, including: lithium (Li), rubidium (Rb), cesium (Cs), boron (B), bromide (Br) and fluoride (F).

In the pH range of typical deep fluids silica (Si) and boron (B) are present as uncharged complexes in the fluid. Most geothermal fluids are pumped from formations made of silicate rocks. The solubility of quartz is low at low temperature (~6 mg kg^{-1} at 25 °C) but rapidly increases with temperature. The concentration

of SiO_2 in the water bears important information on the reservoir temperature and depth. Thus dissolved silica in water can be used as a geological (geochemical) thermometer (Sect. 15.4.1). Boron may give indications on the origin of the fluids; however, it may not be necessary to analyze the parameter.

The total of dissolved solids (TDS) is the sum of all dissolved constituents (cations, anions, uncharged species). Because TDS is the total amount of solids remaining after evaporating one liter of the fluid to dryness it is common usage to convert analyzed bicarbonate to carbonate. TDS is given in g L^{-1} or mg L^{-1} . Analytical concentration data are typically reported as mg L^{-1} of the solute. The mass per volume data need to be recalculated to mmol L^{-1} and meq L^{-1} data for further research and quality tests including the charge balance of the analysis. An example analysis is given in Table 15.1.

The amount of a gaseous component (i) dissolved in a fluid c_i (mol L^{-1}) is proportional to the partial pressure p_i (Pa) of the gas (in the gas phase). This behavior of gases is known as Henry's law:

$$c_i = K_{H_i} p_i \quad (15.2)$$

The gas distribution coefficient K_{H_i} (Henry constant) depends on the type of gas, the temperature and the composition of the fluid (TDS). Gas solubility decreases with increasing temperature. It also decreases with increasing salinity (TDS). The most important and abundant gas in deep fluids is carbon dioxide (CO_2) followed by nitrogen (N_2). In very reducing environments methane (CH_4) and hydrogen sulfide (H_2S) may become important. The presence of high amounts of H_2S may cause serious environmental problems during plant operation. The gas must be removed from geothermal steam in high-enthalpy steam-driven power plants before releasing the steam to the atmosphere (Sect. 10.4). Very gas-rich fluids have properties that deviate significantly from those of gas-poor geothermal water. These properties influence the thermal power of the system and the hydraulic properties of the reservoir including hydraulic conductivity, transmissivity, and storage coefficient (Sects. 8.2 and 8.6).

Plausibility checks help to evaluate the trustworthiness and reliability of hydrochemical data purchased from a commercial laboratory. The first control parameter is the charge balance. The total of positive charges from the cations and negative charges from the anions must match in an electrically neutral solution. The calculated total of dissolved solids should be consistent with the measured electrical conductivity. The measured pH must be consistent with the analyzed concentrations of the carbonate species. Some concentration levels of specific solutes are implausible under certain conditions if the waters are reasonably close to equilibrium. As explained above, for example, high concentrations of iron in pH 6 waters are implausible if the REDOX potential or dissolved oxygen is high. Another example, if fluoride is high, calcium cannot be high at the same time because the concentrations of the two solutes are tied to the solubility of the mineral fluorite.

Table 15.1 Chemical composition of water from the Muzhaerte hot spring in the Tian Shan mountains of NW China (Bucher et al. 2009b)

Date	18 August 2005		
Temp °C	55		
pH	8.29 (at 25 °C)		
EC (mS/cm)	1.38		
	mg L ⁻¹	mmol L ⁻¹	meq L ⁻¹
Ca	38.80	0.97	1.94
Mg	0.69	0.03	0.06
Na	248.00	10.78	10.78
K	7.60	0.19	0.19
Sr	1.23	0.01	0.03
Rb	0.11	0.00	0.00
Li	0.39	0.06	0.06
Fe	<0.02		
Al	0.020	0.0007	0.0022
Alk (HCO ₃)	57.36	0.94	0.94
SO ₄	318.00	3.31	6.62
Cl	168.00	4.74	4.74
NO ₃	1.52	0.02	0.02
F	7.38	0.39	0.39
Br	0.11	0.0014	0.0014
SiO ₂	66.57	1.11	1.11
HBO ₂	6.04	0.14	0.14
TDS	921.82		
Cl/Br	1527	3443	
Na/Cl		2.28	
Ca/SO ₄		0.29	
X _{An}		0.08	
log a _{SiO₂}		-2.98	
Cations			13.05
Anions			12.71
EN			1.33

Stable isotope composition: $\delta^{18}\text{O} = -11.72\text{‰}$; $\delta^2\text{H} = -82.5\text{‰}$

15.3 Graphical Representation of Deep Fluid Composition

In the course of project development and operation of a power plant a large number of chemical fluid composition data accumulate. The data are collected in tables but for the evaluation and comparison of data graphical display and representation of data is very helpful. The type of graphical data representation primarily depends on the water

composition and its variation with time but also on the aspects of fluid geochemistry one wants to illustrate. It follows from the general chemical composition of deep fluids that the diagrams must display the major component Ca, Mg, Na, K, Cl, Alkalinity and SO₄. The four major cations cannot, unfortunately, be displayed on a two dimensional diagram. Therefore, the alkalis Na and K are displayed as the sum of the alkali metals with the disadvantage that Na–K variations remain invisible on the diagrams. However, the relative proportions of the major ions in most fluids can be adequately displayed on **ternary diagrams** one for cations (Ca-Mg-(Na + K)) and one for anions (Cl-SO₄-(carbonate alkalinity)) in % meq L⁻¹ (Fig. 15.1). The ternary cation and anion diagrams are well suited to represent a large quantity of data since a single point on each triangle represents one analysis. The major disadvantage of the graphs is that TDS cannot be discriminated. It only shows the relative proportion of cations and anions. Very diluted near surface water and highly concentrated brines plot to the same point in the diagrams if the ion proportions of the two fluids are the same.

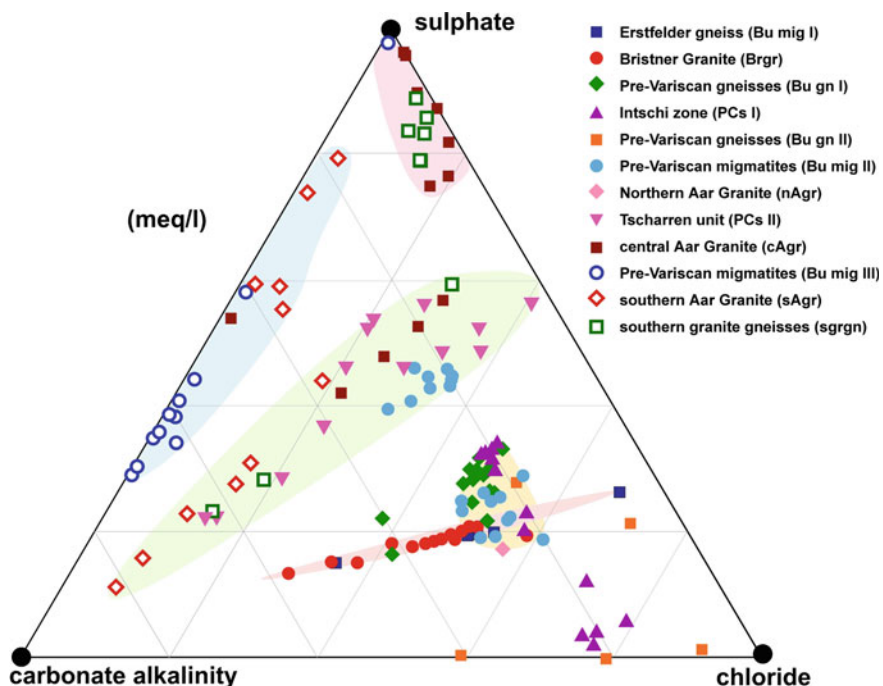


Fig. 15.1 Ternary diagram showing the anion concentration of water samples from the Gotthard rail base tunnel (Bucher et al. 2012). The tunnel has an overburden of up to 2200 m and the temperature of water on the fracture porosity reaches 45 °C. The tunnel cuts through basement rocks, predominantly granite and gneiss. Note the dramatic variation of anion concentration in waters from standard basement rock types

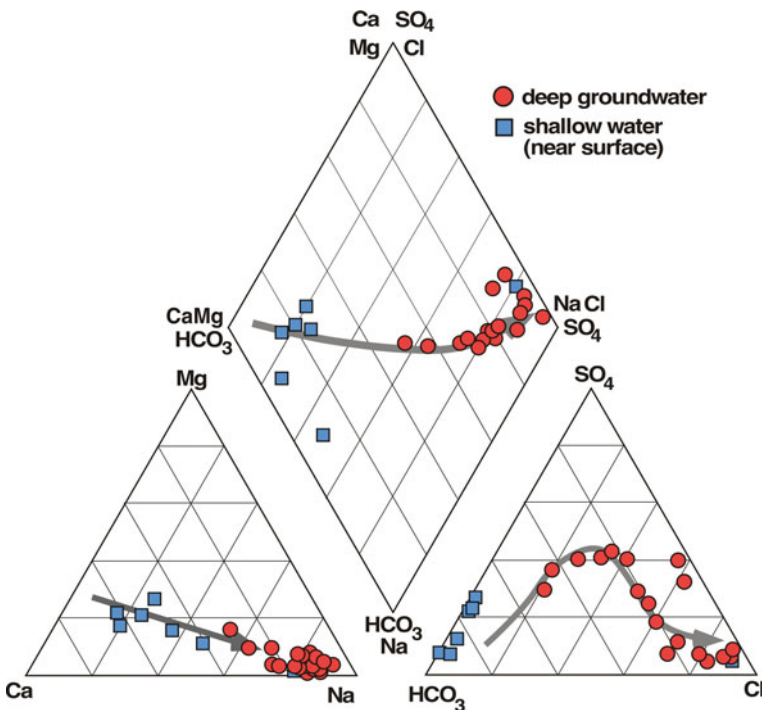


Fig. 15.2 Piper Diagram: Chemical composition of shallow and deep groundwater of the Black Forest basement (Stober and Bucher 1999a). The diagrams illustrate the evolution of near surface Ca-HCO₃ waters to Na-Cl deep waters with an intermediate sulfate-rich zone related to sulfide oxidation

An extension of the cation and anion triangle is the so-called **Piper diagram** (Fig. 15.2). The extra value added by the quadrilateral that combines information already displayed on the cation and anion triangle is minimal may not be worth the effort.

Schoeller-Diagrams avoid some of the shortcomings of the ion-triangles and derivatives (Piper). The Schoeller-Diagram is a histogram-type of diagram showing the concentration in meq L⁻¹ of a solute on a logarithmic scale. The solute and the order of the solutes on the diagram are arbitrary in principle. However, the great advantage of Schoeller-Diagrams is the pattern recognition potential, which only takes effect if a strict order of solutes and combination of solutes is obeyed. We strongly recommend displaying the following solutes in the strict original order on Schoeller-Diagrams: Mg, Ca, Ca + Mg, Na + K, Cl, Alk, SO₄ (all in log meq L⁻¹). The pattern distinguishes high-TDS clearly from low-TDS fluid. The amount of data that can be reasonably displayed depends on the variability of the data. However, even if data are similar more than 20 analyses typically lead to graphically quite chaotic figures. Note that the pattern recognition potential is destroyed if, for example, Mg and Ca are put into the reversed order Ca then Mg. Schoeller-diagrams are not in

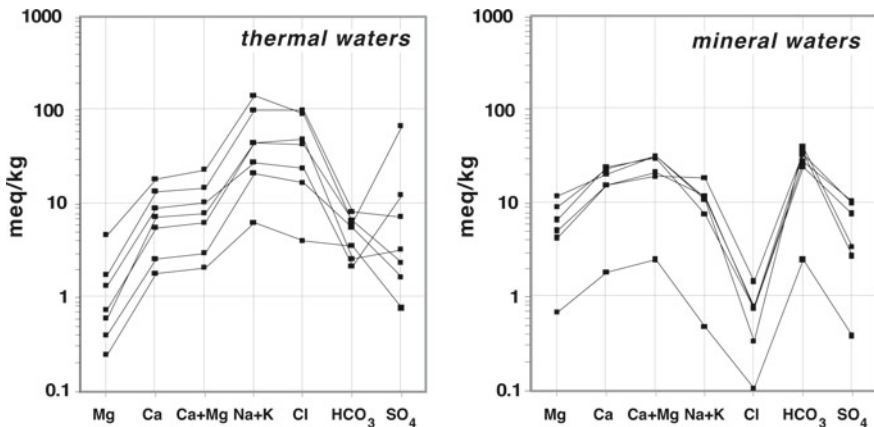


Fig. 15.3 Schöller Diagram: Chemical composition of thermal and mineral waters from the crystalline basement of the Black Forest area (fractured granite and gneiss) (Stober and Bucher 1999a)

common use in the US science community. However, we recommend trying this, in our opinion, useful type of diagram (Fig. 15.3).

The compositional characteristics of waters (Table 15.1) can be displayed on many different types of diagrams depending on the type of produced waters and the compositional features of the produced waters. It is important to realize that interesting compositional properties can be displayed on many different kinds of graphical diagrams including ionic-ratio diagrams (e.g. Na/K ratio, Ca/Mg ratio, Na/Cl ratio and many others).

The composition of steam or the gas phase of fluids in high-enthalpy fields can be displayed on **ternary plots** showing three gasses in % p_i on each diagram: H₂O-CO₂-H₂S, H₂O-CO₂-N₂, H₂S-CO₂-CH₄. The gas diagrams are useful for exploring the effect of steam separators on the composition of the gas phase (steam).

15.4 Estimating Reservoir Temperature from the Composition of Deep Fluids

The chemical composition of deep fluid reflects the temperature of the geothermal reservoir. It is therefore worth the effort deducing reservoir temperatures and with a given geothermal gradient the depth of the geothermal reservoir. The chemical composition of deep fluids residing at depth in a particular reservoir rock is controlled by the minerals making up the rock. The geothermal reservoir consists mostly of rock and contains very little fluid per total mass. After long fluid residence time in the deep reservoir fluid composition tends to reflect chemical equilibrium between rock and fluid. The equilibrium fluid composition is unique for the reservoir rock

and the $P-T$ conditions at the reservoir. Therefore, the reservoir temperature can be deduced from the fluid composition if the type of rock dominating the reservoir is known. The method for deriving fluid-rock equilibrium temperatures is known under the term **geothermometry** and the tools used are **hydrothermal geothermometers**. The temperature at depth can be derived from an empirical calibration or from computed equilibrium conditions using thermodynamic models and data. An empirical calibration correlates fluids from a known rock type with measured temperatures from the fluid sampling depth in deep wells. Examples of thermodynamic models of three widely used geothermometers are presented in the following. Inference of a meaningful reservoir temperature from temperature to composition relationships is fundamentally based on the assumption of chemical equilibrium of a considered chemical fluid-rock reaction.

15.4.1 The Quartz Thermometer

The most important example of a geothermometer widely used in geothermal applications is the solubility of quartz in water. Quartz is an abundant mineral in many reservoir rocks. Hot aqueous fluids dissolve quartz until the saturation concentration of $\text{SiO}_{2\text{aq}}$ in the fluid is reached. Thus from the analyzed silica concentration an equilibrium saturation temperature can be derived.

Quartz dissolution can be described by the simple reaction:



where $\text{SiO}_{2\text{aq}}$ is the uncharged respective SiO_2 complex in the fluid at P and T (see Walther and Helgeson (1977) for details). Equilibrium of reaction 15.3 requires that:

$$\log K_{PT} = \log a_{\text{SiO}_{2\text{aq}}} \quad (15.4)$$

Because the activity–composition relationship ($a = f(m)$) for uncharged silica species is close to $a_{\text{SiO}_{2\text{aq}}} = m_{\text{SiO}_{2\text{aq}}}$ and because the solubility depends predominantly on temperature and not much on pressure, the amount of dissolved SiO_2 in water (c_{SiO_2}) in equilibrium with quartz is a simple and easy to use geothermometer.

The silica geothermometer has been calibrated and improved for equilibrium with all three SiO_2 solid phases occurring in geothermal environments (Fournier 1977; 1981; Fournier and Potter 1982; Arnórsson 1983; Verma and Santoyo 1997; Verma 2000; Walther and Helgeson 1977). With the equilibrium constant (Eq. 15.4) for the dissolution equilibrium (Eq. 15.3) computed from data for quartz given by (Holland and Powell 2011) and for aqueous silica from Walther and Helgeson (1977) using the code SUPCRTBL (Zimmer et al. 2016) the rearranged $T - c_{\text{SiO}_2}$ function is given in Eq. 15.5:

$$T = \left\{ 1114.4 / (4.76713 - \log c_{\text{SiO}_2}) \right\} - 273 \quad (15.5)$$

where T is the temperature in degree C and c_{SiO_2} denotes the silica concentration in mg L^{-1} SiO_2 analyzed in the lab.

Figure 15.4 is a graphical display of Eq. 15.5. Figure 15.4 shows that SiO_2 dissolved in water in equilibrium with quartz rapidly increases with temperature from 11 mg L^{-1} at 25°C to 665 mg L^{-1} at 300°C . The SiO_2 dissolved in the produced fluid can be analyzed and the equilibrium temperature with quartz can be read from the diagram. The influence of the pressure is very small and can be neglected. As shown on Fig. 15.4, most of the displayed deep fluids have quartz equilibrium temperatures close to the measured bottomhole temperatures. This is convincing evidence that the silica thermometer represents a reliable instrument for deriving reservoir temperature estimates.

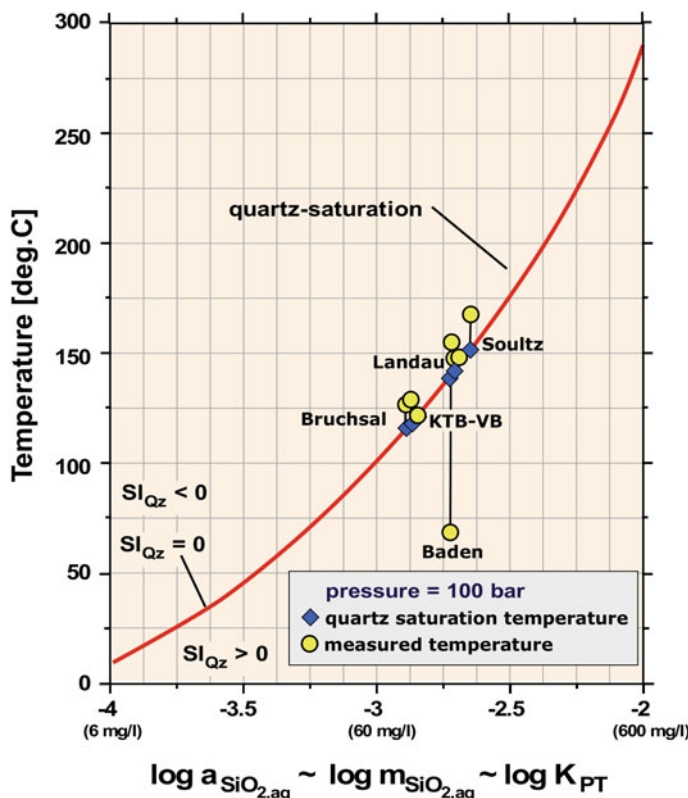


Fig. 15.4 Temperature dependence of quartz solubility (Eq. 15.5). Water data from various deep geothermal reservoirs in Central Europe. SI refers to saturation index (Eq. 15.17)

However, there is an example of thermal fluid with a large mismatch between measured and silica temperatures. The Baden-Baden fluid has a measured temperature that is much lower than the quartz-saturation temperature. The silica temperature suggests that the water is in equilibrium with quartz at ~ 130 °C. This may represent a temperature closer to the true reservoir temperature corresponding to a depth of ~ 4.5 km assuming a gradient of 30 °C km $^{-1}$. The water is an artesian spring and may cool on the paths to the surface.

Furthermore the silica thermometer is vulnerable to dilution by low-silica surface waters and to precipitation of solid SiO₂ along the ascent path. Thus the quartz geothermometer produces minimum temperature estimates. Also remember that the thermometer does not work in the absence of quartz-rich rocks. It cannot be used for hot springs with water from reservoirs with limestone or basaltic rocks.

The stable form of solid SiO₂ in geothermal formations is normally quartz. Thus quartz has the lowest solubility of all forms of SiO₂. Chalcedony is a metastable phase of SiO₂ and has a higher solubility than quartz. Amorphous silica has a much higher solubility than both quartz and chalcedony. A geothermal fluid in equilibrium with quartz at 150 °C contains about 150 mg L $^{-1}$ dissolved SiO₂ (Fig. 15.4). If pumped to the surface and cooled in a power plant the fluid will be oversaturated first with respect to quartz and below 125 °C also with respect to chalcedony. In principle, the stable solid quartz should precipitate in order to maintain equilibrium. However, reaction kinetics of quartz formation is slow and the fluid remains oversaturated with quartz and its SiO₂ concentration reflects the reservoir conditions. If the fluid would be cooled to below of about 40 °C, amorphous silica would spontaneously and rapidly precipitate. The silica crusts formed this way would age and slowly recrystallize to the more stable solid chalcedony. A 200 °C quartz-saturated fluid can be cooled to about 70 °C before amorphous silica deposition begins. In high-enthalpy systems where 300 °C fluids may be loaded with 665 mg L $^{-1}$ SiO₂ (Fig. 15.4) silica precipitates during extraction of the thermal energy and silica scales are a permanent and serious problem (Sect. 15.3). Silica scale prevention can be attempted with various scale inhibitors, typically organic chemicals added to the fluid (Frenier and Ziauddin 2008; von Hirtz 2016).

Note that the SiO₂ geothermometer is independent of the pH in acid and neutral fluids. In high-pH fluids the solubility of quartz rapidly increases with increasing pH because negatively charged silica species become predominant. The effect must be taken into account in dealing with high-pH fluids.

The code SUPCRTBL (Zimmer et al. 2016) stands for the Bloomington version of SUPCRT (Johnson et al. 1992) and has also been used for the two geothermometers given below. The code is accessible online at: (https://models.earth.indiana.edu/applications_index.php).

15.4.2 The K-Na Exchange Thermometer

A number of popular geological thermometers are based on cation ratios rather than absolute concentrations. The cation ratios are controlled by exchange reactions between minerals and the fluid rather than on the solubility of a mineral in the fluid like the quartz thermometer.

If the geothermal water resides in crystalline basement formations such as granite or gneiss, the rocks typically contain K-feldspar ($KAlSi_3O_8$) and plagioclase that is normally rich in Na-feldspar component ($NaAlSi_3O_8$). A fluid in contact with the two feldspars may reach equilibrium of the exchange reaction:



$$\log K_{PT} = \log(a_K^+ / a_{Na^+}) + \{\log a_{Ab} / a_{Kfs}\} \quad (15.7)$$

The equilibrium constant (Eq. 15.7) can be simplified to $\log K_{PT} = \log(m_K^+/m_{Na^+})$ if activity is approximated with the molality of the two cations. Log K_{PT} is mainly a function of temperature and does not depend much on the pressure. Thus the cation (m_K^+/m_{Na^+}) ratio can be used as a geothermometer (e.g. Santoyo and Díaz-González 2010). The temperature dependence of log K can be expressed as: $\log K = - (a/T) + b$ with a and b two temperature independent parameters and the temperature in [K]. Using the software SUPCRTBL (Zimmer et al. 2016) and the latest thermodynamic data collection (see references given above) the rearranged equation for the K-Na geothermometer is given in Eq. 15.8:

$$\text{Temperature } (^{\circ}\text{C}) = \{-1216.7 / (\log(c_{K^+}/c_{Na^+}) - 1.42125)\} - 273 \quad (15.8)$$

approximating $\log K$ by $\log(c_{K^+}/c_{Na^+})$ where c_{K^+} and c_{Na^+} are the analyzed concentrations of K and Na in the geothermal fluid in mg L^{-1} and assuming that all potassium and sodium exclusively occurs as K^+ and Na^+ species respectively. The expression in curly brackets of Eq. 15.7 represents the contribution of the solids to $\log K$. It is close to zero for low-T granites and gneiss containing microcline and albite. Figure 15.5 is a diagrammatic display of the Na-K exchange thermometer (Eq. 15.8).

The major uncertainty related to the Na-K exchange equilibrium is the actual alteration assemblage present in the reservoir rocks. The required assemblage for the geothermometer to work is microcline (low-T K-feldspar) and albite. Another assemblage in granitoid rocks such as granodiorite or tonalite is potassium white mica (muscovite, phengite) and albite. For this kind of reservoir rock the K-Na thermometer must be modified. For basaltic reservoir rocks the thermometer cannot be used because these rock lack K-feldspar (and also phengite/muscovite).

The K-Na thermometer is an excellent and robust tool for deriving T-estimates from the composition of hot water residing in granitic reservoirs. Because it is based on a cation ratio dilution of the deep high-TDS water with near surface water does

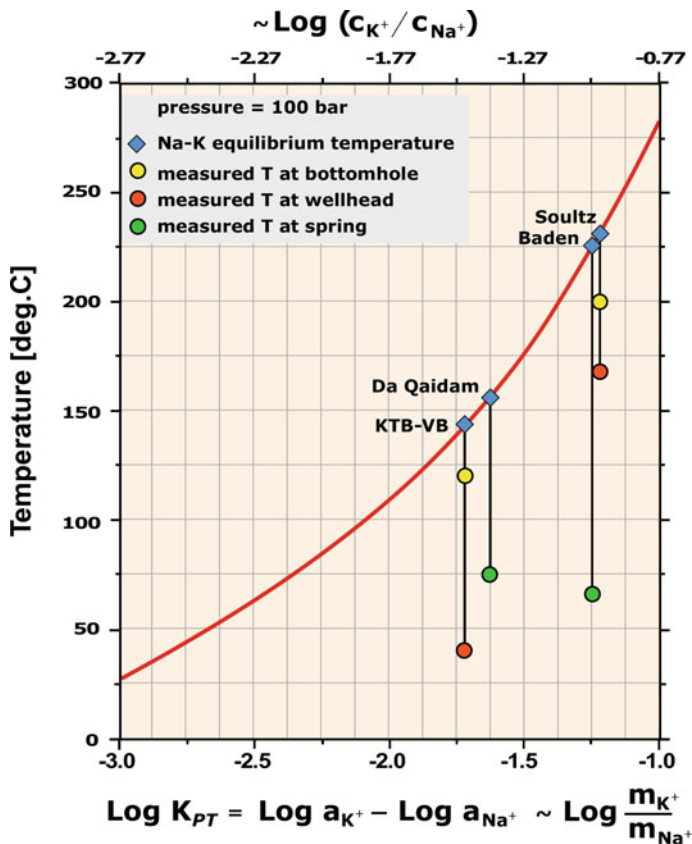


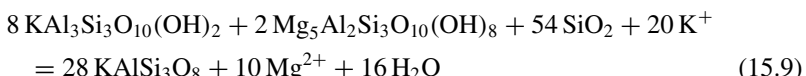
Fig. 15.5 Temperature dependence of the equilibrium constant of the K-Na exchange reaction (Eq. 15.6). Water data from deep geothermal reservoirs in Central Europe and from Da Qaidam hot springs (China) mentioned in the text. Note difference between K-Na, bottomhole and wellhead temperature at the GPK3 well at 5000 m (Soultz-sous-Forêts power plant, France) and the KTB-VB well at 4000 m (Continental Deep Drilling site, Germany) (explanation of the effect see Fig. 8.9)

not usually alter the K/Na ratio of the fluid during ascent. Also the cooled fluid emerging at the spring or other vents is not likely precipitating K- or Na-bearing alteration minerals. The cation-exchange behavior at mineral surfaces is relatively similar for the two alkalis and thus does not alter the K/Na ratio. Consequently the derived temperatures reliably indicate the temperature at the source region of the aqueous fluid.

15.4.3 The Mg–K Thermometer

The most common types of granite and gneiss typically making up continental basement reservoirs contain the major minerals quartz, K-feldspar, plagioclase and biotite in addition to small amounts of a number of accessory minerals. If these basement rocks reach the temperature range 200–500 °C in the presence of water new, so called alteration minerals form mostly at the expense of biotite (e.g. Fig. 5 in Bucher and Seelig 2018). The characteristic assemblage of altered basement rocks in the T-range of deep geothermal applications is phengite (K white mica, muscovite) and chlorite (Bucher and Grapes 2011). Below 200 °C phengite occurs as a component in clay, specifically smectite. The original biotite contains Mg and Fe and transfers the two components to chlorite upon alteration. Therefore it is plausible that the content of Mg and K of deep geothermal fluid is controlled by the minerals chlorite and muscovite. The Fe-component is less useful for deriving T-estimates because it depends on the REDOX state of the system in addition to $T\text{-}P$.

The Mg–K exchange in quartz-rich K-feldspar-bearing rocks containing the alteration assemblage phengite + chlorite at equilibrium requires equilibrium of the Al-balanced reaction: phengite (white mica) + chlorite + quartz = K-feldspar



for which an expression for $\log K$ can be written:

$$\log K_{PT} = 10 \log a_{\text{Mg}^{2+}} - 20 \log a_{\text{K}^+} + \{28 \log a_{\text{Kfs}} - 2 \log a_{\text{Chl}} - 8 \log a_{\text{Ms}}\} \quad (15.10)$$

with the contribution of the Kfs, Chl and Ms composition given in curly brackets. For pure solid phases the expression for $\log K$ reduces to $10 \log a_{\text{Mg}^{2+}} - 20 \log a_{\text{K}^+}$. With the simplification $a = m = c/M$ with c the concentration of K and Mg in the fluid in mg L⁻¹ and M the atomic mass in mg mol⁻¹ the temperature dependence of the equilibrium constant of reaction 15.9 can be expressed as:

$$T = 34853 / ((10 \log c_{\text{Mg}^{2+}} - 20 \log c_{\text{K}^+}) + 134.51) - 273 \quad (15.11)$$

The isobaric T versus Log K diagram (Fig. 15.6) is a graphical display of Eq. 15.11. Temperatures derived from the Mg–K thermometer are subject to many worries. Generally Mg–K temperatures tend to be lower than K-Na- or Qz-temperatures even if strictly derived for hot water upwelling from granitic basement. One uncertainty is related to the unknown and ignored contribution from the mineral composition (curly bracket in Eq. 15.10). Chlorite, muscovite and K-feldspar in altered granite may significantly deviate from the endmember composition given in Eq. 15.9. A second source of error is the simplification activity equals molarity, which is particularly problematic for Mg. Thirdly the analyzed total concentration of Mg can be

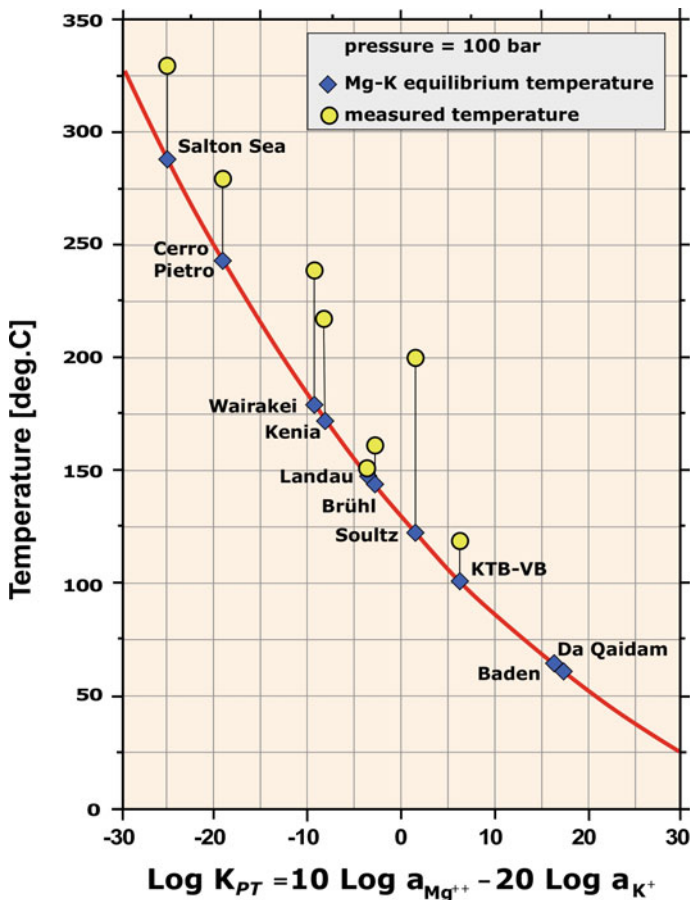


Fig. 15.6 Temperature dependence of the equilibrium constant of the Mg–K reaction (Eqs. 15.9 and 15.11). Water data from various deep geothermal reservoirs in Central Europe and from Da Qaidam hot springs (China) from the authors publications referenced in text. Data from Wairakei, Cerro Pietro and Salton Sea from Giggenbach (1988), Kenia from Malimo (2003)

massively different from the amount present as Mg²⁺ in the fluid because other Mg-species are important. The most important source of error is probably the very low concentration of dissolved Mg in many geothermal fluids. Deep fluids often contain less than 1 mg L⁻¹ Mg. In fluids residing in granite reservoirs at 200–300 °C typical Mg concentrations are on the order of 0.1–0.3 mg L⁻¹ or even lower. This low Mg content presents a serious source of error. It is susceptible to analytical errors. Typical detection limits for Mg in water are about 20 µg L⁻¹ in standard laboratories. Consequently equilibrium Mg in geothermal waters is frequently close to the detection limit. Secondly, if the fluid flows through sedimentary or other non-granitic rocks before emerging at the hot spring it likely takes up Mg from near surface water thereby drastically reducing derived temperatures. Particularly if seawater infiltration

is important at the geothermal site Mg–K temperatures may not be useful. Seawater contains about 1300 mg L⁻¹ Mg.

15.4.4 Other Cation Thermometers

Other cation thermometers use for example measured concentrations of Na and Li (Kharaka et al. 1988) or Mg and Li (Nordstrom et al. 1985) for deriving temperature estimates. The thermometers involving Li may give plausible and consistent results from very low to high temperatures (0–350 °C). Example calibrations of Li thermometers (Kharaka et al. 1988):

$$\text{Mg} - \text{Li} : T = 2200 / (5.47 + \log \sqrt{c_{\text{Mg}} - \log c_{\text{Li}}}) - 273 \quad (15.12)$$

$$\text{Na} - \text{Li} : T = 1590 / (0.779 + \log c_{\text{Na}} / c_{\text{Li}}) - 273 \quad (15.13)$$

with temperature T in °C and concentrations mg L⁻¹. The two calibrations were derived and tested having deep brines of sedimentary basins in mind. They need to be applied to geothermal fluids in granitic basement with great care. Note that Eq. 15.12 is incorrectly reproduced in Kharaka and Hanor 2005 resulting in massively erroneous temperatures for certain concentration combinations of Li and Mg. The two Li-thermometers have strictly been derived for brines in sedimentary basins (Kharaka and Hanor 2005). However, they work reasonably well with basement fluids from granite and gneiss.

Two examples: The T-estimates for granite water from the EGS plant at Soultz-sous-Forêts (France) using data from Bächler (2003) for a wellhead fluid sample at 165 °C are for Mg-Li = 226 °C (Eq. 15.12) and Na-Li = 243 °C (Eq. 15.13). The K-Na thermometer suggests 233 °C (Eq. 15.8). The measured temperature at 4950 m depth was 200 °C and the estimated fluid reservoir temperature is >200 °C. For the basement water from the KTB-VB well at the German Continental Deep Drilling site the corresponding T-estimates are: Mg-Li = 175 °C and Na-Li = 143 °C. The K-Na thermometer (Eq. 15.8) 147 °C (126 °C including rock contribution in curly brackets in Eq. 15.7), Mg-K = 104 °C from (Eq. 15.11) using endmember mineral compositions (123 °C if correcting for mineral compositions; expression in curly brackets in Eq. 15.10), and 116 °C from quartz solubility (Eq. 15.5). The measured temperature at bottomhole is constant 120 °C during one year of pumping (Stober and Bucher 2005a). The derived temperature data suggest that the K-Na, Mg-K and Qz thermometers produce temperature estimates that are a few degrees C within the measured bottomhole fluid temperature at 4000 m depth of the KTB-VB well.

15.4.5 The Ternary Giggenbach Diagram

A particularly widely used ternary diagram for geothermal fluids has been devised by Giggenbach (1988). Measured concentrations of Mg, K and Na are shown on a ternary plot together with the empirically derived data points for “fully equilibrated water” at temperatures ranging from 80 to 300 °C (Fig. 15.7). In a geothermal reservoir at depth infiltrating meteoric water evolves from the Mg corner through a field of “immature waters” and later through a field of “partially equilibrated waters” to “mature waters” before reaching the curve of full equilibration. The waters collected from hot springs or other vents of a geothermal field tend to define an evolution line that points towards a temperature on the “full equilibration curve”. This temperature is thought representing the reservoir temperature. Examples of the **Giggenbach triangle** can be found in: Gemici and Tarcan 2002; Stober et al. 2016; Fan et al. 2019; Li et al. 2020.

The Giggenbach diagram is based on the two temperature sensitive reactions presented and discussed above (Eqs. 15.6 and 15.9). The well-developed and rapidly established K-Na equilibrium causes the water composition from very many reported geothermal fields to lie on a linear array simply reflecting the K-Na equilibrium temperature (Eq. 15.8). The linear array intersects the curve “fully equilibrated

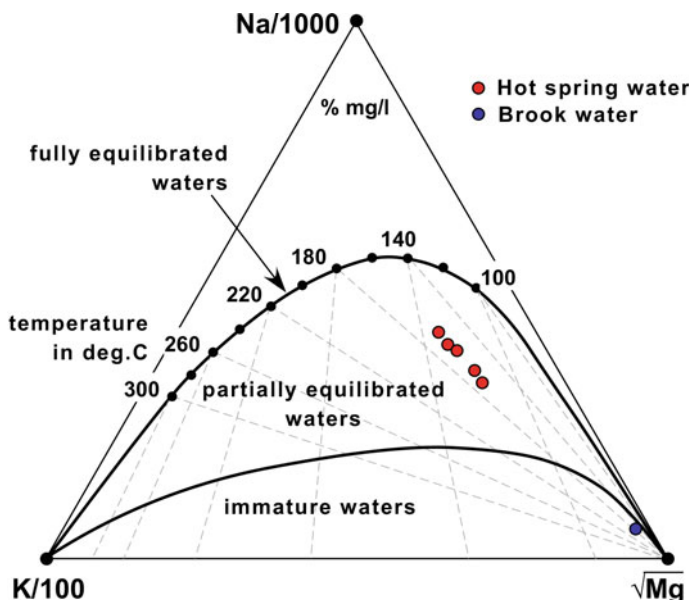


Fig. 15.7 Giggenbach diagram showing geothermal water from hot springs at Da Qaidam, W-China (SW rim of Qilian mountains). Water temperature at the hot springs = 72 °C, estimated temperature of the hot water reservoir = 130–150 °C (Stober et al. 2016)

waters” (Fig. 15.7) where the fluid would be in equilibrium with chlorite, phengite and K-feldspar in the granitic reservoir rocks. Most hot waters, however, do not represent full Mg–K equilibrium with altered granite. The various problems related to the Mg–K thermometer have been presented above (Sect. 15.4.3). The consequence of non-equilibrium Mg–K distribution is that the waters form a linear array given by the K–Na exchange reaction involving K-feldspar and albite (Fig. 15.7). The temperature along the K–Na isotherm represents a reliable estimate of the reservoir temperature (~160 °C for the waters from DaQaidam shown on Fig. 15.7).

From the comments above it follows that the Giggenbach diagram can be usefully applied to geothermal fluids in contrast to expressed doubts regarding this issue (Romano and Liotta 2020). Derived temperatures are meaningful simply because they represent K–Na exchange temperatures. It is useful also for fluids at T below 200 °C.

The field labels “partially equilibrated waters” and “immature waters” must be seen with great reservation (Fig. 15.7). These labels suggest that the waters incompletely reacted and equilibrated with the reservoir rocks. The position away from the “fully equilibrated water” curve basically reflects the kinetics of the reactions in the reservoir. However, the disturbance of the Mg–K composition of the waters is not exclusively internally created but rather has analytical and/or external reasons (see Sect. 15.4.3).

Fluids from some geothermal fields scatter irregularly on the Giggenbach diagram and form a data cloud of data points rather than a linear array along a K–Na isotherm. These fluids failed to reach equilibrium of both reactions (Eqs. 15.5 and 15.9). Meaningful reservoir temperatures cannot be derived from these fluids using hydrochemical geothermometers.

Also, for geothermal fluids in basaltic reservoir rocks the Giggenbach diagram cannot be used. Below 200 °C and above 300 °C the alteration assemblage does not contain chlorite (Weisenberger et al. 2020). In addition altered basaltic rocks do not contain K-feldspar and K-mica and smectite present below 200 °C contains very little K-mica component. The K–Na–Mg thermometers on which the Giggenbach diagram is based fail in basaltic systems.

15.4.6 *Multiple Equilibria Models for Equilibrium Temperature*

Temperature estimates can also be derived from multiple-equilibria models simultaneously solving for the equilibrium conditions of several (many) dissolution reactions (e.g. Chatterjee et al. 2019). At perfect equilibrium between fluid and rock in the reservoir the saturation index (SI) versus temperature curves for assumed or known minerals of the reservoir rocks must intersect at one unique temperature. The meaning of the variable saturation index (SI) is explained below (see Sect. 15.6 and

Eq. 15.17). If the fluid composition remains unchanged during production, the reservoir temperature can be modeled from the fluid composition at the wellhead. One serious difficulty of the method is the concentration of Al in the fluid. Typical basement rocks contain Al-bearing silicates such as feldspar and mica. The concentration of Al in the fluid in equilibrium with Al-minerals, however, is very low and poses an analytical challenge. In addition, the Al-concentration that is typically measured in fluids includes colloidal Al, which is often very high and massively higher than the true Al in solution. In most fluids the true reservoir concentration of dissolved Al remains unknown, which seriously limits multi-component temperature models. Note that K-Na and Mg–K equilibria presented above are not hampered by the Al problem since both reactions conserve Al.

For the computation of SI versus T diagrams we recommend using the code PHREEQC (Parkhurst and Appelo 1999) or the Bloomington codes SUPCRTBL and PHREEQC ONLINE (Zimmer et al. 2016) and SUPPHREEQC (Zhang et al. 2020). Link: https://models.earth.indiana.edu/applications_index.php.

Models based on chemical thermodynamics can also be used to study complex fluid-gas–solid reactions. However, chemical thermodynamic can predict the possibility of processes but cannot make predictions regarding when, how fast or if at all these reactions will occur. Kinetics of reactions, disequilibrium or metastable states may occur in natural systems that are in conflict with the conditions of stable equilibrium. Some of the chemical modeling codes (e.g. PHREEQC ONLINE) permit reaction kinetics to be considered and therefore can predict the evolution of water composition with time in systems undergoing active fluid-rock interaction. Nevertheless, the conditions of stable equilibrium set the reference frame for all chemical processes in hydrothermal and geothermal systems.

15.5 Origin of Fluids

The composition of deep fluids produced by a geothermal power system has many different aspects. One aspect is the ultimate origin of the saline fluid being pumped to the surface. A very useful tool in analyzing fluid origin is the Cl/Br ratio of the fluid. Seawater has a Cl/Br mass ratio of 288. This number, therefore, is the absolute reference number for seawater origin of salinity. Any Cl/Br ratio significantly above 288 suggests that the salinity of the fluid is derived from the dissolution of evaporitic NaCl sediments. Any number massively below 300 suggests that the salinity originates from crystalline basement (Trommsdorff et al. 1985; Stober and Bucher 1999b).

The ratio of the concentrations of chloride and bromide can give valuable information on the origin of the salinity and on mixing of different fluids. In the literature halogen data are given as Cl/Br or Br/Cl ratios on a mass or mole basis. We use here Cl/Br ratios on a mass basis (mg L^{-1}). The planetary reference fluid, standard mean ocean water has a Cl/Br = 288. If seawater mixes with low-TDS surface water

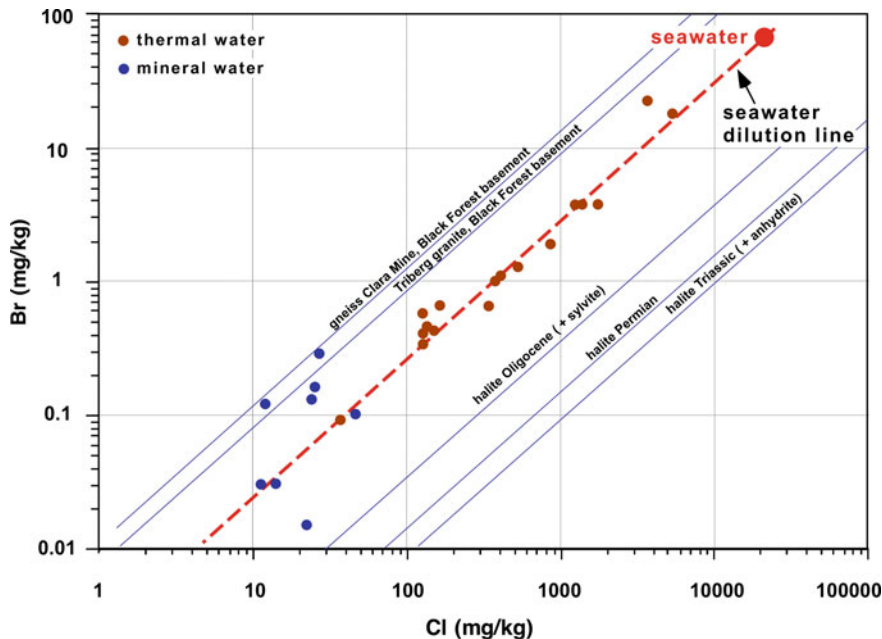


Fig. 15.8 Cl/Br ratio of deep water in the crystalline basement of the Black Forest region (Germany) (Fig. 15.2). Thermal waters: filled circles, mineral waters: open circles. The seawater dilution trend is given as dashed line, data from experimentally leached granite and gneiss and various evaporitic halites: full lines (Stober and Bucher 1999b)

the Cl/Br ration does not change and the mixtures follow the seawater dilution line (Fig. 15.8).

Granite and gneiss are the predominant reservoir rocks of the thermal waters of the Black Forest region in Germany (Fig. 15.3). Leaching experiments with powders of these crystalline basement rocks readily produced leachates with considerable chloride and bromide concentrations. The average measured Cl/Br mass ratio of about 100 is significantly lower than that of seawater (Bucher and Stober 2002). The chloride and bromide in granite and gneiss is mostly released from salty deposits on the grain boundaries of the silicate minerals and from fluid and solid inclusions in the silicate minerals (mostly in quartz) (Stober and Bucher 1999b). Dissolution of evaporitic salt deposits produces saline waters with extremely high Cl/Br ratios because halite (NaCl) cannot accommodate bromide in its structure. Dissolution of Triassic to Tertiary halite from upper Rhine valley resulted in Cl/Br ratios ranging from 2400 to 9900 (Stober and Bucher 1999b). If sampled deep geothermal fluids have Cl/Br ratios along the seawater dilution line (Fig. 15.8) fossil seawater is the probable origin of the water. The original seawater may have been diluted by near surface waters of low salinity. However, the salinity also may increase above that of seawater as a result of hydration of primary minerals a retrogression process that consumes water and desiccates the fracture porosity and passively increases the

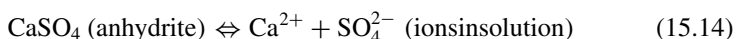
salinity of the residual water. The Cl/Br ratio does not change during the process until the brine becomes saturated with halite. Further desiccation and concurrent halite precipitation decreases Cl/Br ultimately to very low values. In crystalline basement Cl/Br is typically very low, which may indicate an origin of the salinity from salty fluid and solid inclusions and from alteration of Cl-bearing silicate minerals. The Cl/Br ratio may also be affected by other processes including evaporation, cryogenic processes and others (Frape and Fritz 1982; Frape et al. 2005). Also the ratio of Na/Cl may provide hints on the origin of the salinity of the reservoir fluid. Seawater has a molar Na/Cl ratio of close to 0.8 whereas brine deriving from halite dissolution has a molar Na/Cl ratio of close to 1.0 (e.g. Stober et al. 2017). Typical deep water from the basement has $\text{Na}/\text{Cl} > 1$ indicating a rock internal origin of the salinity, which can be further supported by low Cl/Br ratios.

15.6 Saturation States, Saturation Index

Each dissolved component, e.g. calcium, in the thermal water is distributed among a typically large number of charged and uncharged species (e.g. Ca^{2+} , CaOH^+ , $\text{Ca}(\text{OH})_2$, CaCl^+). For the evaluation of saturation states and thus the potential for scale formation it is necessary to compute the distribution of species in particular analyzed water samples at the temperature (and pressure) of interest. The specification must be computed with hydrochemical software such as WATEQ (Ball and Nordstrom 1991), PHREEQC (Parkhurst and Appelo 1999), Bloomington PHREEQC (Zimmer et al. 2016) and SOLMINEQ (Kharaka et al. 1988). With the help of the software, saturation states can be explored for different operating conditions at the plant and for the reservoir itself. Meaningful models require a full analysis of the major components but also of some critical trace components. Some of these codes are powerful tools for generating transport and mixing models and allow for sophisticated numerical hydrochemical modeling. The models are, however, sensitive to input pH and temperature (Parkhurst and Appelo 1999).

The code PHREEQC, for example, can be used to compare sampled geothermal water with hypothetical water that has been equilibrated with a chosen set of selected minerals. This way, it can be shown to what extent the composition of the thermal water is controlled by the solubility of the primary and secondary minerals of the reservoir rock.

Between a mineral of the rock formation and the thermal water in the fracture porosity a reaction relation exists. For example, if anhydrite (CaSO_4) in an evaporite formation is in contact with water the reaction can be written as:



If anhydrite is a pure solid phase its activity can be defined as $a_{\text{Anh}} = 1$. If the anhydrite and the fluid coexist at equilibrium, the following mass-action equation must hold:

$$K_{PT} = a_{\text{Ca}^{2+}} \cdot a_{\text{SO}_4^{2-}} \quad (15.15)$$

The dimension-less equilibrium constant is a function of pressure and, here, mostly of temperature. A sampled thermal water must be chemically analyzed (e.g. for calcium and sulfate sulfur) and the data be used for a distribution of species calculation using e.g. PHREEQC. The product of the computed ion activities of Ca^{2+} and SO_4^{2-} represents the ion activity product (IAP) and can be written as:

$$\text{IAP} = a_{\text{Ca}^{2+}} \cdot a_{\text{SO}_4^{2-}} \quad (15.16)$$

IAP is derived from the actual analyzed fluid of interest. It can be compared to the equilibrium condition K_{PT} . The logarithm of the ratio IAP/K is defined as the **saturation index SI**:

$$\text{SI} = \log_{10}(\text{IAP}/K) \quad (15.17)$$

If IAP exactly matches the equilibrium condition K, $\text{SI} = 0$ and the water is at equilibrium with the considered mineral (here anhydrite). If $\text{IAP} > K$, $\text{SI} > 0$ and the water is oversaturated with the mineral and has the potential to precipitate the mineral. If $\text{IAP} < K$, $\text{SI} < 0$ and the water is undersaturated with respect to the considered mineral and has the potential to dissolve the mineral.

An example: A deep water contains 190 mg L^{-1} dissolved silica ($\text{SiO}_{2\text{aq}}$) corresponding to $\log m_{\text{SiO}_{2\text{aq}}} = -2.5$. This value relates to the ion activity product IAP ($\text{IAP} = \log m_{\text{SiO}_{2\text{aq}}}$). This may appear somewhat confusing because SiO_2 is a single and uncharged species in the fluid (see Eq. 15.3). The measured temperature at bottomhole in the granite is 200°C . It follows from Eq. 15.5 and the graph representing quartz solubility (Fig. 15.4) that $\log K = -2.365$ at 200°C and the fluid at equilibrium with quartz contains 259 mg L^{-1} dissolved silica. Therefore the saturation index $\text{SI} = -0.135$ (Eq. 15.17). This means that the fluid is undersaturated with respect to quartz at 200°C . The fluid would be at equilibrium with quartz at 175°C .

15.7 Mineral Scales and Materials Corrosion

The hot geothermal fluid interacts at depth with the minerals of the reservoir formation. Typically, the fluid is not in an overall chemical equilibrium with the reservoir rock because of slow reaction kinetics and slow diffusion under most reservoir conditions and temperatures of 200°C and lower. However, the fluids are normally not far from equilibrium and reaction progress of fluid-rock interaction is small. This means the fluid composition does not change much over long periods of time.

The installation and operation of a geothermal power plant fundamentally changes this situation. The deep fluid is pumped to the surface, partly decompressed and substantially cooled. This may, and normally does change the saturation states of the fluid. As a consequence the fluid may become oversaturated with respect to one

or several minerals. The minerals may be deposited as scales in the borehole and in the surface installations. Particularly exposed to mineral scales and crusts are heat exchangers, steam separators, filter systems and pipes. However, the re-injected cool fluid may cause increased chemical interaction in the reservoir formation with potential consequences for the porosity and the hydraulic conductivity of the reservoir formation.

The hot water pumped to the surface in a production well does not change in temperature much, however, the pressure on the fluid is greatly reduced. Reducing the pressure by 500 bar reduces the solubility of calcite by 20% (at constant T). The resulting calcite or aragonite scales massively impair the operation of the geothermal plant (Figs. 15.9, and 15.10). For slowing down or preventing carbonate scale formation most geothermal plants are operated at elevated internal pressure in surface installations.

Another important chemical aspect is the generally high corrosion potential of the hot saline deep fluids. The corrosive fluids chemically attack the casing of the borehole, the submersible pump and all materials of the surface installations it comes in contact with.

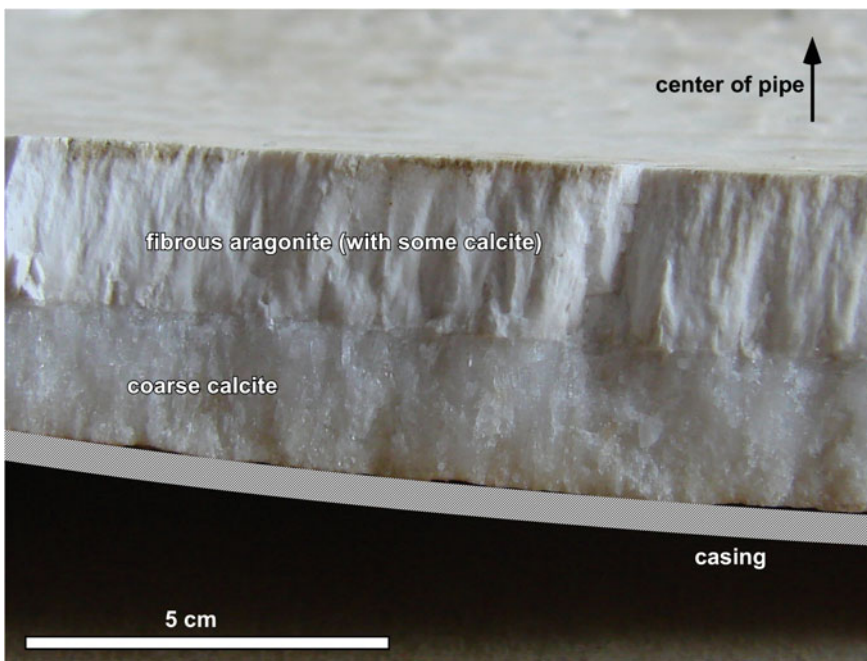
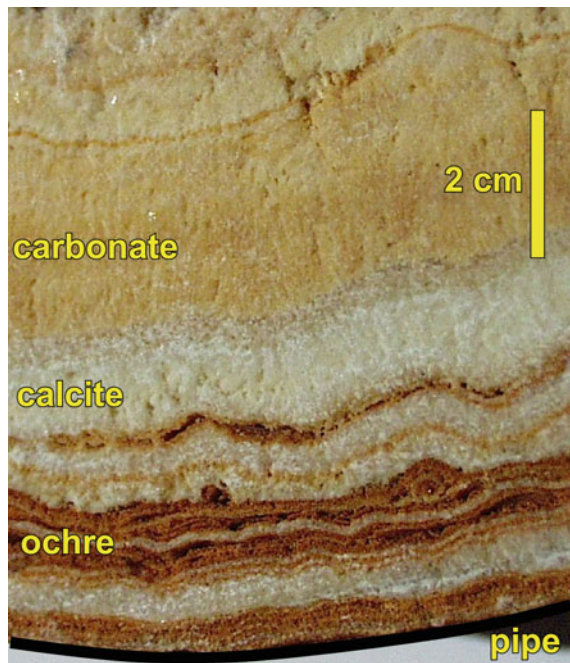


Fig. 15.9 Carbonate scales from a pipe used in a geothermal plant: aragonite and calcite on top, pure calcite below along the casing

Fig. 15.10 Carbonate scales clogging a pipe of a geothermal plant. The scales show a complex layering of mineral zones of differing thicknesses. Ochre zones contain various Fe-oxide-hydroxide minerals together with calcite. The calcite zones contain pure coarse-grained calcite, carbonate zones consist of more than one carbonate mineral including calcite, ankerite, aragonite



The geothermal water (fluid) alters the surface installations that come in contact with the pumped deep fluid including the fluid pump and the re-injection pipe. Dimensioning the system typically considers physical parameters such as pressure, temperature and production rate. These parameters define pipe diameters, pressure ratings and thermal properties of the materials. However, the thermal water system must be operated at a minimum pressure that prevents outgassing and unmixing dissolved gaseous components from the fluid. CO₂-loss from the decompressed fluid is the major cause of carbonate (calcite) scales in the installations. The potentially created gas-fluid mixture may result in a two-phase flow system in the installations with difficult to handle pressure variations in the installations. In special environments chemical inhibitors may help to prevent carbonate scales and still run the system at degassing conditions if degassing can be prevented at uneconomical high pressures only. Dimensioning and design of the heat exchanger must consider supply and return temperature, pressure gradient between primary and secondary loop, temperature and pressure of the secondary loop fluid, gas-content and composition of the produced thermal fluid and the heat capacity and viscosity of the fluids of the primary and secondary loop.

At the injection side of geothermal doublet systems boiling must be prevented. Ideally, the return flow pipe to the injection borehole is placed clearly below the dynamic water table. Filter systems at the production and injection well prevent solid particles from entering the installations of the power plant. This reduces abrasion and may restrict scales to the filter units and protect heat exchangers and pumps from

scale formation. The most typical scales include carbonates (calcite, aragonite) and sulfates (anhydrite).

Significant precipitation reactions in the reservoir will reduce the hydraulic conductivity of the fractured rock system. The resulting increase of the necessary injection pressure may require more powerful (and more costly) pumps. The uptake capacity of the return flow by the injection well can be greatly reduced with disastrous economic consequences.

It is therefore highly recommended to consider, predict and model possible chemical processes in the reservoir as soon as chemical data on the composition of the deep fluid become available. Injection of cold fluid into the fracture system of the heat reservoir causes a number of chemical processes to run simultaneously and for the entire duration of the plant operation (Fig. 15.11). The chemical effects of re-injecting cooled fluids into the reservoir include dissolution/precipitation reactions (typically involving carbonate and sulfate), ion-exchange and adsorption reactions, chemical consequences of mixing of fluids of different composition and temperature, solubility effects of fluid flow along temperature gradients (vertical flow), REDOX processes in low-flow fractures with stagnant fluids (that also may be coated with biomass at low temperature <110 °C) (Fig. 15.11).

The produced fluid comes in contact with many different installations and materials including the casing of the production and injection borehole, the pumps installed in each of the production wells and the filters, heat-exchangers, steam separators, turbines, pipes and other surface installations of the power plant. Many of the

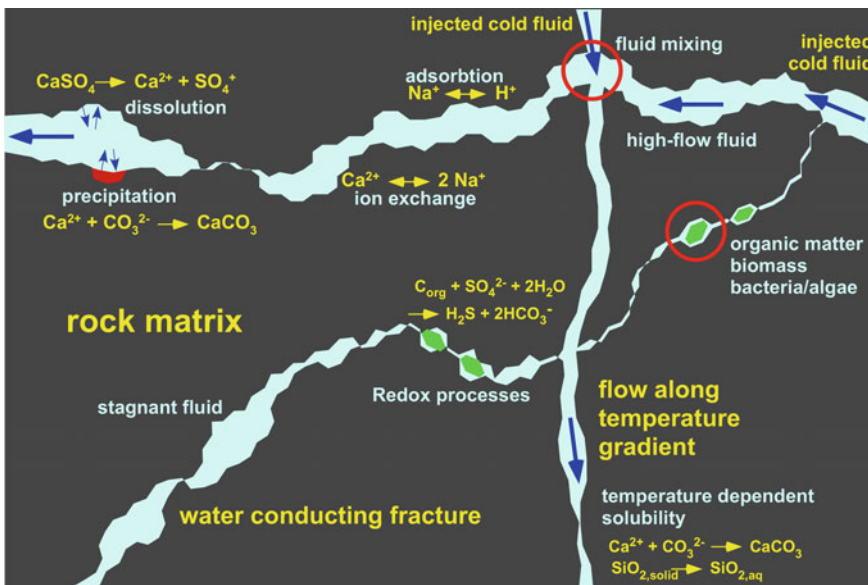


Fig. 15.11 Chemical processes along water conducting fractures of a geothermal reservoir resulting from injection of cool fluid in a hot reservoir formation (fluid-rock interaction)

components of the produced fluid may however cause severe corrosion of the materials used in the geothermal system. Corrosion-relevant chemicals in the geothermal fluid include: Oxygen, hydrogen sulfide, carbon dioxide, sulfate, and chloride. The origin of the trouble makers can be related to contamination with near surface fluids (leaks), the presence of abundant sulfide minerals in the geothermal reservoir formation, deep thermal CO₂ sources (metamorphic, magmatic), oxidation of primary sulfides by oxygen-rich surface fluids and resident fossil seawater at depth (Lund et al. 1976; Ellis and Conover 1981).

It is important to realize that corrosion is not an exclusive problem of deep geothermal systems but that also near surface systems can be affected by serious material corrosion problems (Sect. 7.2). The origin of dissolved gases in near-surface groundwater is normally the atmosphere or modified soil gasses.

If a geothermal fluid equilibrates with the atmosphere the dissolved gasses readjust their concentrations according to the partial pressure of the gas in the atmosphere (Sect. 15.2). A fluid that has been saturated with CO₂ at high temperature and pressure releases CO₂ to the atmosphere until an equilibrium concentration is reached. The fluids will essentially lose all gases with very low partial pressures in the atmosphere (H₂S, H₂, CH₄). However, it will gain gasses that have a very low partial pressure in the reservoir formation (e.g. O₂). Dissolved gasses in the fluid must be analyzed reliably and regularly. The reported concentration units must be clearly specified (recalculation to other units must be possible, clear and easy) and the analytical procedures must be documented.

Decreasing the concentration of the dissolved carbon dioxide in the fluid by degassing CO₂ as a result of contact to the atmosphere or of decompression of the fluid may cause precipitation of carbonate (calcite). The process of carbonate scale formation can be understood from the reaction:



If the CO₂ on the right hand side of Eq. 15.18 escapes (indicated by arrow), the reaction will progress to the right hand side according to Le Chatelier's principle and precipitate the mineral calcite or the metastable form aragonite (Fig. 15.9). Note that aragonite is the metastable form of CaCO₃ at all *P-T* conditions of geothermal plant operation. It is thus more soluble than the stable form calcite. Carbonate scales can be massive and must be prevented or minimized (Figs. 15.9 and 15.10). The most important measure follows from Eq. 15.18, namely that CO₂ loss must be barred. This can be realized by strictly operating in a closed system at about 10–20 bar pressure and under isolation from the atmosphere (geothermal doublet systems). The necessary minimum pressure for preventing carbonate scales for a specific system and fluid composition can be computed from thermodynamic models or it can be experimentally determined. In both methods, exact data on the composition of the produced geothermal fluid are needed.

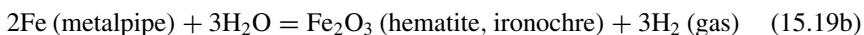
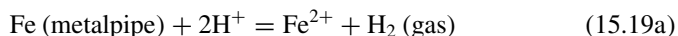
Other solids such as many scale-forming sulfates cannot be stopped from precipitating from cooled fluids by supporting measures on the gas-side. A good example is the solubility of anhydrite as described by Eq. 15.14. It follows from the inverse

temperature dependence of the reaction that anhydrite may not precipitate from the fluid if the fluid is saturated with anhydrite at high-T and then being cooled in the heat exchanger. However, from Eq. 15.14 and from Chatelier's principle it also follows that anhydrite will precipitate from an anhydrite-saturated fluid if Ca^{2+} is increased (e.g. by on-going calcite dissolution) or SO_4^{2-} is increased (e.g. by sulfide to sulfate oxidation due to contact to the atmosphere). Other frequently observed sulfate scales such as barite (BaSO_4) form by similar mechanisms. Scale prevention is difficult in the case of sulfates. Inhibitor chemicals may help. If not, mechanical cleaning of the system as long as the scales are soft is the only remedy.

Some scales may contain high concentrations of toxic or radioactive substances (e.g. As, Cd, Pb, Hg, ^{210}Pb , ^{224}Ra). Therefore, exposed equipment and the scales must be handled with great care and disposed of in a legally correct manner.

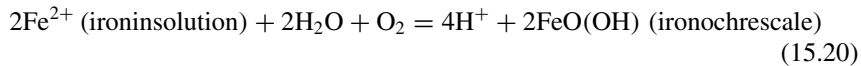
The occasionally high concentrations of CO_2 or H_2S in deep waters may corrode C-steel pipes. The degree of corrosion damage depends strongly on pH of the fluid. Therefore, pH and fluid composition must be known for a reliable evaluation of the corrosion risk. If corrosion resistance of C-steels is insufficient at a particular site, Cr-Ni steels or Ni-based materials need to be considered.

Steel pipes and casing can be corroded by direct interaction with hot low-pH fluids according to the overall reaction that dissolves the steel into the aqueous fluid:



Reaction 15.19a depends on pH and is favored by acid fluids. The produced $\text{Fe}(\text{II})$ in solution is no major problem as long as no atmospheric oxygen gains access to the fluid, in which case $\text{Fe}(\text{III})$ oxides, hydroxides and sulfates may cause severe scaling problems (iron ochre sedimentation). This situation is described by reaction 15.19b. If H_2 can be measured in the produced fluid, casing corrosion is likely to be in progress.

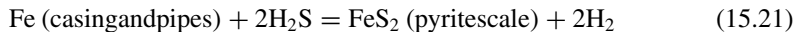
The iron oxidation process can be described by the reaction:



It oxidizes dissolved iron in the fluid (e.g. from pipe corrosion) by dissolved O_2 of typically atmospheric origin. Other oxidizing agents may also play an important role at some sites. CO_2 for example is a potential oxidizer that will be reduced to elementary carbon or to methane gas in the process. Because Fe^{3+} is essentially insoluble at moderate pH it precipitates as various minerals including goethite (FeO(OH)), hematite, schwertmannite, ferrihydrite and many others. It follows from Eq. 15.20 that the oxidation process produces protons and decreases pH, which in turn promotes the corrosion reaction 15.19a.

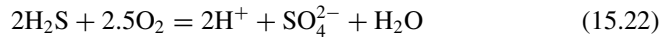
Reaction 15.19a dissolves metal from casing and other pipes and gradually reduces wall thickness. However, the co-produced hydrogen gas diffuses into the metallic materials and causes embrittlement of the steel (pitting corrosion). Corrosion velocity strongly depends on pH (Eq. 15.19a) and increases dramatically with decreasing pH. If pH is below 4 steel corrosion becomes a severe problem. Increasing dissolved CO₂ also decreases pH, however, carbonic acid is a relatively mild acid.

Hydrogen sulfide (H₂S) occurs as gas dissolved in reduced geothermal fluids. The gas, if present, may cause corrosion and scaling problems combined. The gas may react with the metals of casing and pipes according to the reaction (15.21):



The reaction corrodes the steel of the casing and produces difficult to remove pyrite scales and hydrogen gas that worsens corrosion.

If H₂S meets an oxidizing environment (e.g. atmospheric oxygen), sulfide sulfur is transferred to sulfate sulfur by the reaction:



The reaction produces sulfuric acid thereby decreasing pH and promoting the corrosion reaction 15.19a. So H₂S in the geothermal fluid is a notorious troublemaker. Continued corrosion at a hole or crack (welded connections) is self-accelerating. Pitting corrosion can be best prevented by selecting (expensive) corrosion resistant materials. Other measures include increasing the pH, decreasing fluid temperature, increasing flow velocity, adding scaling inhibitors and installing cathodic protection equipment.

The scaling-potential can be predicted from the composition of the produced fluid and its temperature changes during cycling through the surface installations, quantitative data on gas unmixing in the operation cycle and from thermodynamic or experimental models (e.g. Brown 2011). The evaluated scaling-potential indicates a tendency or possibility that mineral scales may form during operation of the plant. The thermodynamic analysis also suggests sensible procedures for scale prevention. However, the actual active scaling processes that must be expected at a given site are very difficult to predict reliably. This is because thermodynamics states if a precipitation reaction is possible but it cannot predict the velocity of its progress (kinetics). It may, in fact, not run at all because no crystal nuclei can be formed. In this context, the texture and roughness of surfaces of the used materials is important for nucleation and thus also influences scale formation. Along the fluid flow path, with its abrupt changes in flow direction and flow velocity, local zones of supersaturation for a certain mineral may develop even if the fluid is undersaturated with respect to that mineral in the reservoir or in most other zones on the system.

Laboratory testing of materials may help to select the best corrosion-resistant steels for the particular site. This requires, of course, knowledge of the composition of the produced fluids. Corrosion and scales can also be minimized or prevented by avoiding sharp 90° turns in the flow direction and massive fluid flow velocity

variations in the pipe system by using large radius pipe bends (minimizing zones of turbulent flow). Thus choosing the materials used for components of the thermal water loop must be made with great care. Pressure control, fluid filtration, and optimizing the operation management are further aspects of corrosion and scaling control.

At temperatures below about 120 °C microbial processes may bring additional complexity to the scaling problem (Magot et al. 1992). Microbial biomass may form at the low-temperature side of the heat exchanger and may pose a particular problem at the injection borehole. Microbial metabolism may produce scales and may promote, support and accelerate inorganic scaling. Dissolved organic carbon (DOC) in the fluid can be analyzed in the laboratory. DOC can originate from the decay of biomass or from its metabolic processes. DOC may also originate from technical products used in the system such as lubricants, grease, oil and other organic technical substances. The biomass may use these technical organic substances as nutrients.

The described chemical aspects of geothermal plant development show that chemical studies on the composition of the fluids and the secondary interaction products are indispensable. The data should be collected as early as possible in order to develop strategies for scaling prevention. Later, during operation of the plant, a chemical monitoring program should be established that recognizes upcoming troubles and failures rapidly. This will enable the plant management to devise appropriate protective measures.

Once mineral scales have formed in wellbores chemical and mechanical removal measures will be the appropriate remedy (Crabtree et al. 1999; McClatchie and Verity 2000). Scale removal techniques must be applied as soon as possible. The techniques should cause no damage to the pipes and wellbore and should preferably hinder future scale formation. Carbonate scales can be removed with acids; other soluble scales may also be removed with a variety of inorganic and organic dissolver chemicals. Mechanical removal of scales is performed with a large variety of workover tools such as casing scrapers.

References

- Ármannsson, H. & Ólafsson, M., 2010. Collection of geothermal fluids for chemical analysis. ISOR, Report No. 830566, 17 p., Reykjavík, Iceland.
- Arnórsson, S., 1983. Chemical equilibria in Iceland geothermal systems. Implications for chemical geothermometry investigations. *Geothermics*, 24, 603–629.
- Arnórsson, S., Bjarnason, J. Ö., Giroud, N., Gunnarsson, I. & Stefánsson, A., 2006. Sampling and analysis of geothermal fluids. *Geofluids*, 6, 203–216.
- Bächler, D., 2003. Coupled Thermal-Hydraulic-Chemical Modelling at the Soultz-sous-Forêts EGS Reservoir (France). PhD thesis, ETH-Zurich, Switzerland, 151 p.
- Ball, J. W. & Nordstrom, D. K., 1991. WATEQ4F, current version 4.00 2012: First release 1991 as User's manual for WATEQ4F, with revised thermodynamic data base and test cases for calculating speciation of major, trace, and redox elements in natural waters. Open-File Report 91-183; U.S. Geological Survey, 10 pp.
- Ball, J. W., Jenne, E. A. & Burchard, J. M., 1976. Sampling and preservation techniques for waters in geysers and hot springs, with a section on gas collection by A.H. Truesdell. In: Workshop on

- Sampling Geothermal Effluents, 1st, Proceedings, Environmental Protection Agency 600/9-76-011, pp. 218–234.
- Banks, D., Odling, N. E., Skarphagen, H. & Rohr-Trop, E., 1996. Permeability and stress in crystalline rocks. *TERRA Nova*, 8, 223–235.
- Brown, K., 2011. Thermodynamics and kinetics of silica scaling. Proceedings International Workshop on Mineral Scaling 2011, Manila, Philippines, 25–27 May 2011.
- Bucher, K. & Grapes, R., 2011. Petrogenesis of Metamorphic Rocks, 8th edition. Springer Verlag, Berlin Heidelberg. 428 pp.
- Bucher, K. & Seelig, U., 2018. Bristen granite: a highly differentiated, fluorite-bearing A-type granite from the Aar massif, Central Alps, Switzerland. *Swiss Journal of Geosciences*, 111, 317–340.
- Bucher, K. & Stober, I., 2000. The composition of groundwater in the continental crystalline crust. In: Stober, I. & Bucher, K. (eds.). *Hydrogeology in crystalline rocks*, 141–176, KLUWER Academic Publishers.
- Bucher, K. & Stober, I., 2002. Water-rock reaction experiments with Black Forest gneiss and granite. In: Stober, I. & Bucher, K. (eds.). *Water-Rock Interaction*. Water Science and Technology Library, 61–96, Kluwer Academic Publishers, Dordrecht.
- Bucher, K. & Stober, I., 2010. Fluids in the upper continental crust. *Geofluids*, 10, 241–253.
- Bucher, K., Zhang, L. & Stober, I., 2009b. A hot spring in granite of the Western Tianshan, China. *Applied Geochemistry*, 24, 402–410.
- Bucher, K., Stober, I. & Seelig, U., 2012. Water deep inside the mountains: Unique water samples from the Gotthard rail base tunnel, Switzerland. *Chemical Geology*, 334, 240–253.
- Chatterjee, S., Sinha, U.K., Biswal, B.P., Jaryal, A., Patbhaje, S. & Dash, A., 2019. Multi-component Versus Classical Geothermometry: Applicability of Both Geothermometers in a Medium-Enthalpy Geothermal System in India.- *Aquatic Geochemistry*, 25, 91–108.
- Crabtree, M., Eslinger, D., Fletcher, P., Miller, M., Johnson, A. & King, G., 1999. Fighting Scale - Removal and Prevention. *Oilfield Review*, Autumn, 30–45.
- Cunningham, K. M., Nordstrom, D. K., Ball, J. W., Schoonen, M. A. A., Xu, Y. & DeMonge, J. M., 1998. Water-Chemistry and On-Site Sulfur-Speciation Data for Selected Springs in Yellowstone National Park, Wyoming, 1994–1995. U.S. Department of the Interior, Open-File Report 98, 40 pp.
- Ellis, P. F. & Conover, M. F., 1981. Material Selection Guideline for Geothermal Energy Systems. NTIS Code DOE/RA/27026-1. Radian Corporation, Austin, TX.
- Fan, Y., Pang, Z., Liao, D., Tian, J., Hao, Y., Huang, T. & Li, Y., 2019. Hydrogeochemical Characteristics and Genesis of Geothermal Water from the Ganzi Geothermal Field, Eastern Tibetan Plateau. *Water*, 11, 1–28.
- Fournier, R. O., 1977. Chemical geothermometers and mixing models for geothermal systems. *Geothermics*, 5, 41–50.
- Fournier, R. O., 1981. Application of water geochemistry to geothermal exploration and reservoir Engineering. In: Rybach, L. & Muffler, L. I. P. (eds.). *Geothermal systems: Principles and case histories*. Wiley & Sons, New York, 109–143.
- Fournier, R. O. & Potter, R. W., 1982. An equation correlating the solubility of quartz in water from 25°C to 900°C at pressures up to 10,000 bar. *Geochim. Cosmochim. Acta*, 46, 1969–1973.
- Frape, S. K. & Fritz, P., 1982. The chemistry and isotopic composition of saline waters from the Sudbury Basin, Ontario. *Canadian Journal of Earth Sciences*, 19, 645–661.
- Frape, S. K., Blyth, A., Blomqvist, R., McNutt, R. H. & Gascoyne, M., 2005. Deep Fluids in the Continents: II. Crystalline Rocks. In: *Surface and Ground Water, Weathering, and Soils* (ed. J. I. Drever) Vol. 5 *Treatise on Geochemistry* (eds. H. D., Holland and K. K. Turekian), 541–580, Elsevier-Pergamon, Oxford.
- Frenier, W. W. & Ziauddin, M., 2008. Formation, Removal, and Inhibition of Inorganic Scale in the Oilfield Environment. Society of Petroleum Engineers, 240 pp.
- Fritz, P. & Frape, S. K., 1987. Saline water and gases in crystalline rocks. *GAC Special Paper* 33, The Runge Press Limited, Ottawa, 259 pp.

- Gemici, Ü. & Tarcan, G., 2002. Hydrogeochemistry of the Simav geothermal field, western Anatolia, Turkey. *Journal of Volcanology and Geothermal research*, 116, 215–233.
- Giggenbach, W. F., 1981. Geothermal mineral equilibria. *Geochimica et Cosmochimica Acta*, 45, 393–410.
- Giggenbach, W. F., 1988. Geothermal solute equilibria. Derivation of Na-K-Mg-Ca geoindicators. *Geochimica Cosmochimica Acta*, 52, 2749–2765.
- Giggenbach, W.F. & Goguel, R.L., 1989. Collection and analysis of geothermal and volcanic water and steam discharges.- Department of Scientific and Industrial Research, Chemistry Division, Report No. CD 2401, Petone, New Zealand.
- Hewitt, A. D., 1989. Leaching of metal pollutants from four well casings used for ground-water monitoring. In: Special Report 89–32, USA Cold Regions Research and Engineering Laboratory.
- Holland, T. J. B. & Powell, R., 2011. An improved and extended internally consistent thermodynamic dataset for phases of petrological interest, involving a new equation of state for solids. *Journal of metamorphic Geology*, 29, 333–383.
- Ingebretsen, S. E. & Manning, C. E., 1999. Geological implications of a permeability-depth curve for the continental crust. *Geology*, 27, 1107–1110.
- Ingebretsen, S. E. & Manning, C. E., 2011. Dynamic Variations in Crustal Permeability: Possible Implications for Subsurface CO₂ Storage. American Geophysical Union, Fall Meeting 2011, abstract id. H32B-04.
- Johnson, J. W., Oelkers, E. H. & Helgeson, H. S., 1992. SUPCRT92: A software package for calculating the standard molal thermodynamic properties of minerals, gases, aqueous species, and reactions from 1 to 5000 bar and 0 to 1000°C. *Computers and Geosciences*, 18, 899–947.
- Kharaka, Y. K. & Hanor, J. S., 2005. Deep Fluids in the Continents: I. Sedimentary Basins. In: *Surface and Ground Water, Weathering, and Soils* (ed. J. I. Drever) Vol. 5 *Treatise on Geochemistry* (eds. H. D., Holland and K. K. Turekian), 499–540, Elsevier-Pergamon, Oxford.
- Kharaka, Y. K., Gunter, W. D., Aggarwal, P. K., Perkins, E. H. & DeBraal, J. D., 1988. SOLMINEQ.88: A Computer Program for Geochemical Modeling of Water-Rock Interactions. U.S. Geological Survey, Water-Resources Investigations Report 88-4227, 420 pp.
- Kozlovsky, Y. A., 1984. The world's deepest well. *Scientific American*, 251, 106–112.
- Li, X., Huang, X., Liao, X. & Zhang, Y., 2020. Hydrogeochemical Characteristics and Conceptual Model of the Geothermal Waters in the Xianshuihe Fault Zone, Southwestern China. *Int. J. Environ. Res. Public Health*, 17(2), 500.
- Lund, J. W., Silva, J. F., Culver, G., Lienau, P. J., Svanevik, L. S. & Anderson, S. D., 1976. Corrosion of Downhole Heat Exchangers, Appendix A. DOE Contract E(10-1)-1548, Oregon, Institute of Technology, Klamath Falls, OR.
- Magot, M., Caumette, P., Desperrier, J. M., Matheron, R., Dauga, C., Grimont, F. & Carreau, L., 1992. *Desulfovibrio longus* sp. nov., a Sulfate-Reducing Bacterium Isolated from an Oil-Producing Well. *International Journal of Systematic Bacteriology*, 42, 398–403.
- McClatchie, D. W. & Verity, R., 2000. The Removal of Hard Scales From Geothermal Wells: California Case Histories. Society of Petroleum Engineers. SPE-60723-MS, 7 pp. doi.org/<https://doi.org/10.2118/60723-MS>.
- Nicholson, K., 1993. *Geothermal Fluids: Chemistry and exploration techniques*. Springer Verlag Berlin Heidelberg, Berlin, 263 pp.
- Nordstrom, D. K., Andrews, J. N., Carlsson, L., Fontes, J.-C., Fritz, P., Moser, H. & Olsson, T., 1985. Hydrogeological and Hydrogeochemical Investigations in Boreholes. In: Final report of the phase I geochemical investigations of the Stripa groundwaters, 85–106, Technical Report STRIPA Project, Stockholm.
- Parker, L. V., Hewitt, A. D. & Jenkins, T. F., 1990. Influence of casing materials on trace-level chemicals in well water. *Ground Water Monitoring Review*, 10(2), 146–156.
- Parkhurst, D. L. & Appelo, C. A. J., 1999. User's guide to PHREEQC (version 2) – a computer program for speciation, batchreaction, one dimensional transport, and inverse geochemical calculations. In: Water-Resources Investigations Report 99-4259, pp. 312, U.S. Geological Survey, Denver, Colorado.

- Pauwels, H., Fouillac, C. & Fouillac, A. M., 1993. Chemistry and isotopes of deep geothermal saline fluids in the Upper Rhine Graben: Origin of compounds and water-rock interactions. *Geochimica et Cosmochimica Acta*, 57, 2737–2749.
- Powell, T. & Cumming, W., 2010. Spreadsheets for geothermal water and gas geochemistry.- Proceedings, 35. Workshop on Geothermal Engineering, Stanford University, SGP-TR-188, 10 p., Stanford, USA.
- Romanò, P. & Liotta, M., 2020. Using and abusing Giggenbach ternary Na-K-Mg diagram. *Chemical Geology*, 541, 1–18.
- Santoyo, E. & Díaz-González, L., 2010. Improved Proposal of the Na/K-Geothermometer to Estimate Deep Equilibrium Temperatures and their Uncertainties in Geothermal Systems. *Proceedings World Geothermal Congress*, pp. 7, Bali, Indonesia.
- Stober, I. & Bucher, K., 1999b. Origin of salinity of deep groundwater in Crystalline rocks. *Terra Nova*, 11(4), 181–185.
- Stober, I. & Bucher, K., 1999a. Deep groundwater in the crystalline basement of the Black Forest region. *Applied Geochemistry*, 14, 237–254.
- Stober, I. & Bucher, K., 2005a. The upper continental crust, an aquifer and its fluid: hydraulic and chemical data from 4 km depth in fractured crystalline basement rocks at the KTB test site. *Geofluids*, 5, 8–19.
- Stober, I. & Bucher, K., 2005b. Deep-fluids: Neptune meets Pluto. In: Voss, C., (ed.). *The Future of Hydrogeology*. *Hydrogeology Journal*, 13, 112–115.
- Stober, I. & Bucher, K., 2007a. Hydraulic properties of the crystalline basement. *Hydrogeology Journal*, 15, 213–224.
- Stober, I. & Bucher, K., 2007b. Erratum to: Hydraulic properties of the crystalline basement. *Hydrogeology Journal*, 15, 1643. (*See further correction in Stober & Bucher 2015*).
- Stober, I., Zhong, J., Zhang, L. & Bucher, K., 2016. Deep hydrothermal fluid–rock interaction: the thermal springs of Da Qaidam, China. *Geofluids*, 16, 711–728.
- Stober, I., Teiber, H., Li, X., Jendryszczyk, N. & Bucher, K., 2017. Chemical composition of surface- and groundwater in fast-weathering silicate rocks in the Seiland Igneous Province, North Norway. *Norwegian Journal of Geology*, 97(1), 63–93. (<https://dx.doi.org/https://doi.org/10.17850/njg97-1-04>)
- Sutton, A. J., McGee, K. A., Casadevall, T. J. & Stokes, B. J., 1992. Fundamental volcanic-gas-study techniques: an integrated approach to monitoring. In: Ewert, J. W. & Swanson, D. A. (eds.) *Monitoring volcanoes: techniques and strategies used by the staff of the Cascades Volcano Observatory*, 1980–90, pp. 181–188., U.S. Geological Survey.
- Thompson, J. M. & Yadav, S., 1979. Chemical Analysis of Waters from Geysers, Hot Springs, and Pools in Yellowstone National Park, Wyoming, from 1974 to 1978. In: U.S. Geological Survey Open-File Report 79–704, 49 pp.
- Thompson, J. M., Presser, T. S., Barnes, R. B. & Bird, D. B., 1975. Chemical Analysis of the Water of Yellowstone National Park, Wyoming from 1965 to 1973. In: U.S. Geological Survey Open-File Report 75–25, 59 pp.
- Trommsdorff, V., Skippchen, G. & Ulmer, P., 1985. Halite and sylvite as solid inclusions in high-grade metamorphic rocks. *Contributions to Mineralogy and Petrology*, 24–29.
- Verma, M. P., 2000. Revised Quartz Solubility Temperature Dependence Equation along the Water-Vapor Saturation Curve. *Proceedings World Geothermal Congress*, pp. 1927–1932, Kyushu-Tohoku, Japan.
- Verma, S. P. & Santoyo, E., 1997. Improved equations for Na/K, Na/Li, and SiO₂ geothermometers by outlier detection and rejection. *Journal of Volcanology and Geothermal Research*, 79, 9–23.
- von Hirtz, P., 2016. Silica scale control in geothermal plants - historical perspective and current technology. In: DiPippo, R. (ed.): *Geothermal Power Generation. Developments and Innovation*. Woodhead Publishing, 443–476.
- Walther, J. V. & Helgeson, H. C., 1977. Calculation of the thermodynamic properties of aqueous silica and the solubility of quartz and its polymorphs at high pressures and temperatures. *Am. Jour. Sci.*, 277, 1315–1351.

- Weisenberger, T. B., Ingimarsson, H., Hersir, G. P. and Flóvenz, Ó. G., 2020. Cation-Exchange Capacity Distribution within Hydrothermal Systems and Its Relation to the Alteration Mineralogy and Electrical Resistivity. *Energies*, 13, 1–19.
- Zhang, G. R., Lu, P., Zhang, Y. L., Tu, K. & Zhu, C., 2020. SupPHREEQC: A program to generate customized PHREEQC thermodynamic database based on Supcrtbl. *Computer and Geosciences*, 143:164560.
- Zimmer, K., Zhang, Y., Lu, P., Chen, Y., Zhang, G., Dalkilic, M. & Zhu, Ch., 2016. SUPCRTBL: A revised and extended thermodynamic dataset and software package of SUPCRT92. *Computers & Geosciences*, 90, 97–111.